UNIVERSIDAD NACIONAL AUTÓNOMA DE MÉXICO

Maestría y Doctorado en Ciencias Bioquímicas

Estudio de la cadena respiratoria de *Wolbachia pipientis*

TESIS

QUE PARA OPTAR POR EL GRADO DE:

Doctor en Ciencias

PRESENTA:
M. en C. Cristina Uribe Alvarez

TUTOR PRINCIPAL: Dr. Antonio Peña Díaz
Instituto de Fisiología Celular

MIEMBROS DEL COMITÉ TUTOR

Dr. Diego González Halphen
Instituto de Fisiología Celular

Dr. Juan Pablo Pardo Vázquez
Facultad de Medicina

Ciudad de México. Agosto, 2018.

CIENCIAS Bioquímicas
Programa de Maestría y Doctorado

PMDCB/1030/2018

Uribe Alvarez Cristina
Estudiante de Doctorado en Ciencias Bioquímicas
P r e s e n t e

Los miembros del Subcomité Académico en reunión ordinaria del día 21 de mayo del presente año, conocieron su solicitud de asignación de **JURADO DE EXAMEN** para optar por el grado de **Doctorado EN CIENCIAS**, con la réplica de la tesis **"Estudio de la cadena respiratoria de Wolbachia pipientis"**, dirigida por el/la Dr(a). **Peña Díaz Antonio**.

De su análisis se acordó nombrar el siguiente jurado integrado por los doctores:

PRESIDENTE	Chávez Cossío Edmundo
VOCAL	Flores Herrera Oscar
VOCAL	Pérez Martínez Xochitl
VOCAL	García Trejo José de Jesús
SECRETARIO	Camarena Mejía Rosa Laura

Sin otro particular por el momento, aprovecho la ocasión para enviarle un cordial saludo.

A t e n t a m e n t e
"POR MI RAZA, HABLARÁ EL ESPÍRITU"
Cd. Universitaria, Cd. Mx., a 21 de mayo de 2018.
COORDINADORA

Dra. ANA BRÍGIDA CLORINDA ARIAS ÁLVAREZ

contacto: mdcbq@posgrado.unam.mx Tel. 5623 7006

RECONOCIMIENTOS

Esta tesis se realizó bajo la asesoría del **Dr. Antonio Peña Díaz** en el laboratorio 306-Oriente, Departamento de Genética Molecular, Instituto de Fisiología Celular, UNAM.

El jurado del examen estuvo conformado por:

Dr. Edmundo Chávez Cosío, Departamento de Farmacología, Instituto Nacional de Cardiología Ignacio Chávez.

Dr. Oscar Flores Herrera, Departamento de Bioquímica, Facultad de Medicina, UNAM.

Dra. Xóchitl Pérez Martínez, Departamento de Genética Molecular, Instituto de Fisiología Celular, UNAM.

Dr. José de Jesús García Trejo, Departamento de Biología, Facultad de Química, UNAM.

Dra. Rosa Laura Camarena Mejía, Departamento de Biología Molecular y Biotecnología, Instituto de Investigaciones Biomédicas, UNAM.

El Comité Tutoral que asesoró el desarrollo de este trabajo estuvo formado por:

Dr. Antonio Peña Díaz, Departamento de Genética Molecular, Instituto de Fisiología Celular, UNAM.

Dr. Diego González Halphen, Departamento de Genética Molecular, Instituto de Fisiología Celular, UNAM.

Dr. Juan Pablo Pardo Vázquez, Departamento de Bioquímica, Facultad de Medicina, UNAM.

El Jurado del examen de candidatura estuvo integrado por:

Dra. Rosa Laura Camarena Mejía, Departamento de Biología Molecular y Biotecnología, Instituto de Investigaciones Biomédicas, UNAM.

Dr. Juan Pablo Pardo Vázquez, Departamento de Bioquímica, Facultad de Medicina, UNAM.

Dr. Diego González Halphen, Departamento de Genética Molecular, Instituto de Fisiología Celular, UNAM.

Dra. Marietta Tuena Sangri, Departamento Bioquímica y Biología Estructural, Instituto de Fisiología Celular, UNAM.

Dra. Emma Cecilia Saavedra Lira, Departamento de Bioquímica, Instituto Nacional de Cardiología, Ignacio Chávez.

Dra. Bertha María Josefina González Pedrajo, Departamento de Genética Molecular, Instituto de Fisiología Celular, UNAM.

El jurado del examen de ingreso estuvo integrado por:

Dra. Bertha María Josefina González Pedrajo, Departamento de Genética Molecular, Instituto de Fisiología Celular, UNAM.

Dra. Xóchitl Pérez Martínez, Departamento de Genética Molecular, Instituto de Fisiología Celular, UNAM.

Dra. Sobeida Sánchez Nieto, Departamento de Bioquímica, Facultad de Química, UNAM.

Dr. Rogelio Rodríguez Sotres, Departamento de Bioquímica, Facultad de Química, UNAM.

Dr. José de Jesús García Trejo, Departamento de Biología, Facultad de Química, UNAM.

Se reconoce la colaboración, asesoría y asistencia del **Dr. Salvador Uribe Carvajal** y de la **Dra. Natalia Chiquete Félix** del Departamento de Genética Molecular, Instituto de Fisiología Celular, UNAM; de la **Dra. Martha Calahorra Fuertes** y de la **M. en C. Norma Silvia Sánchez** del Departamento de Genética Molecular, Instituto de Fisiología Celular, UNAM; de la **Dra. Martha Lucinda Contreras Zentella** del Departamento de Biología Celular y del Desarrollo, Instituto de Fisiología Celular, UNAM; del **Dr. Luis Vaca** y la **Dra. Arlette Bohórquez Hernández** del Departamento de Biología Celular y del Desarrollo, Instituto de Fisiología Celular, UNAM.

Se reconoce el apoyo de la **Dra. Laura Ongay Larios** de la Unidad de Biología Molecular del IFC**;** del **Dr. Fernando García Hernández** y el **Sr. Rodolfo Paredes Díaz** de la Unidad de Microscopía del IFC; de **Ramón Méndez Franco**, Auxiliar del laboratorio 305-Ote. Departamento de Genética Molecular, Instituto de Fisiología Celular; de **Leticia García Gutiérrez**, Asistente de procesos, Programa en Ciencias Bioquímicas, UNAM; de **Adelina González Pérez**, Asistente de procesos, Programa en Ciencias Bioquímicas, UNAM; de **Gabriela Valdés**, Secretaria ejecutiva, Coordinación del Departamento de Genética Molecular, Instituto de Fisiología Celular, UNAM.

Se agradece al **Dr. Juan Carlos González Hernández** del Instituto Tecnológico de Morelia por la donación de los oligonucleótidos ITS1 y ITS4. Se agradece a Bei Resources por la donación del anticuerpo anti-wsp.

La sustentante gozó del apoyo CONACyT **No. 344726** para realizar los estudios de doctorado (CVU No.288969).

El proyecto fue financiado por los proyectos para SU: CONACyT 239487 y DGAPA-PAPIIT IN204015; y para AP CONACyT238497 y DGAPA-PAPIIT IN2114.

Se agradece al **Posgrado en Ciencias Bioquímicas** y al **Programa de Apoyo a los Estudios de Posgrado (PAEP)** por los apoyos recibidos para la asistencia a Congresos Nacionales e Internacionales.

Dedicatorias

A mi mamá, por ser mi amiga, mi consejera y por cuidarme. Gracias por estar siempre a mi lado.

A mi papá, gracias por compartir tanto conmigo, por enseñarme a ser una mejor persona y por enseñarme a hacer ciencia durante los últimos cinco años. Gracias por exigirme, por apoyarme y por festejarme. Todo lo que soy se los debo a ustedes dos, los amo.

A Rodrigo, Shaista y María Luisa, aunque hay muchos kilómetros de distancia, siempre están en mi corazón y mis pensamientos. Gracias por estar en mi vida, por hacerla más feliz y divertida.

A Robin, gracias por haber llegado, por haber regresado, por haberte quedado y porque estoy segura que seguirás a mi lado. Amo ser tu familia y compartir todos los días contigo. Sin duda llegaste a mejorar mi persona y mi vida.

Al recuerdo de los mejores abuelos del mundo.

A mi familia académica:

Al Dr. Peña, por tantas enseñanzas, que van desde bioquímica hasta como hacer tus propias balas y hacer tu propio hidromiel. Por compartir las mejores anécdotas conmigo y por siempre apoyarme en el laboratorio.

Al Lab. 306 Ote, Martha, Norma y Kari, gracias por hacer todo más divertido, por su apoyo incondicional y por sus críticas en el trabajo, sin duda sirvieron para mejorar mi proyecto.

A Natalia, por enseñarme la mayoría de lo que aprendí durante el doctorado, por tanta paciencia, por festejarnos los cumpleaños y por hacer la vida en el lab. más entretenida.

A Dany por ser mi hermana mayor no-sanguínea. Por marcarme un camino a seguir en la ciencia, por darme tantos consejos, por entender mis miedos y ayudarme a afrontarlos.

A Mónica, Ale, Neus y Mau por ser mis hermanas no-sanguíneas desde hace 11 años, por todas las experiencias y las anécdotas de la FQ y las que siguieron. Siempre habrá un lugar especial en mi corazón para ustedes.

A Natalia Pavón, por empezar como una colaboración científica y acabar como amigas. Por ser tan positiva, por siempre ponerme más trabajo y por compartir muchos ideales conmigo.

A todos los miembros del Lab. 305 Ote, Lili, Emilio, Gerardito, Isa, Félix, Ulrik y Ramón porque he aprendido mucho a su lado y han enriquecido mi experiencia académica. Por los seminarios y por las convivencias.

A mi familia del IBT, Poncho, Checho, Ori, Marel, Hippie, Gigi, Sandy y Fabs, por madurar conmigo, por compartir los problemas y las frustraciones de ser un adulto y de titulación. Nunca me dejen.

A todas las personas del Rugby, que a pesar de que ayudaron a alargar mi estancia en el doctorado, seguro lo hicieron más divertido. Una vez puma, siempre puma. 1, 2, 3 Coyotas Awww!

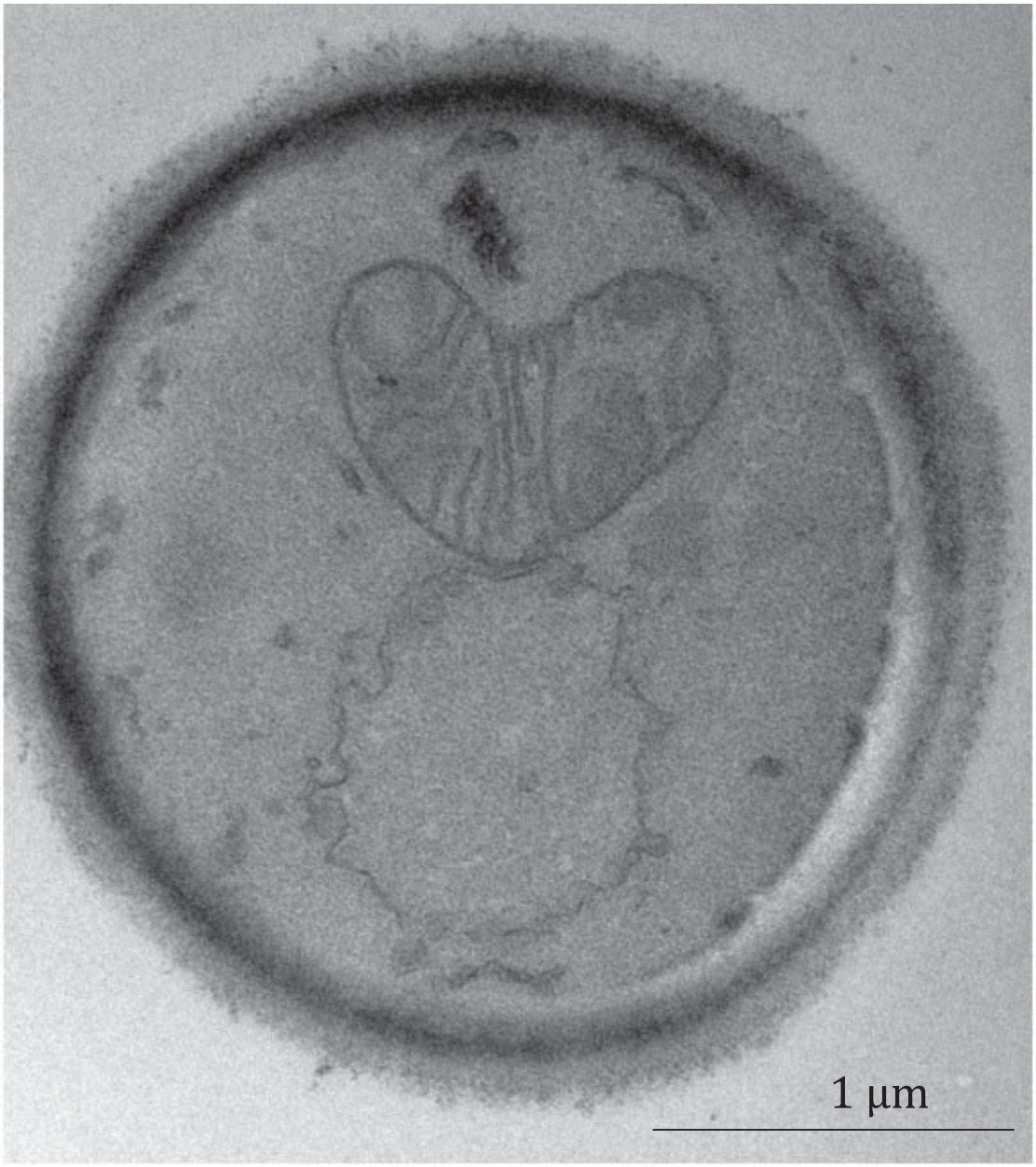

Microscopía Electrónica de Transmisión de *S. cerevisiae* W303.

Unidad de Microscopía del Instituto de Fisiología Celular

ÍNDICE

ÍNDICE DE TABLAS

ÍNDICE DE FIGURAS

1. Resumen

Wolbachia es una bacteria Gram negativa endoparasita/endosimbionte que coloniza a más del 65% de las especies de insectos. Influye sobre la proporción machos-hembras, la fertilidad, la expresión de proteínas, el metabolismo y la esperanza de vida de sus hospederos. Actualmente *Wolbachia* se utiliza como una herramienta para el control de enfermedades transmitidas por vectores. Por razones desconocidas a la fecha, *Wolbachia* no crece *ex vivo* y su cultivo en animales o en líneas celulares requiere una gran inversión y se recuperan pocas bacterias.

Estudios previos de los genomas de *Wolbachia* y sus hospederos reportan una posible simbiosis mutualista, dónde *Wolbachia* podría donar riboflavina, grupos hemos y/o energía en forma de ATP al hospedero. A la fecha estas hipótesis no han sido comprobadas con experimentos bioquímicos debido a la escasez de biomasa obtenida al cultivar *Wolbachia* en líneas celulares. En esta tesis se creó un endoparasitismo artificial utilizando a *Saccharomyces cerevisiae* como hospedero alterno aumentando dos órdenes de magnitud la cantidad de bacterias obtenidas.

Se estudiaron los efectos de *Wolbachia* sobre el metabolismo aerobio del hospedero ya que la riboflavina, que es el precursor de la síntesis de los grupos FAD y FMN; y los grupos hemo que forman parte de los citocromos respiratorios. Heddi et al. (1999), reportó que la actividad de las enzimas del metabolismo aerobio del hospedero *Sitophilus oryzae* están aumentadas cuándo alberga un endosimbionte que suplementa riboflavina conocido como SOPE. Al eliminar al endosimbionte con antibióticos las actividades enzimáticas disminuyen a la mitad.

Acorde a lo reportado en dicho sistema, en las levaduras infectadas con *Wolbachia*, la fosforilación oxidativa se encuentra acoplada por más tiempo; sin embargo, al aislar a la bacteria se observó que no consume oxígeno indicando que *Wolbachia* podría no expresar una cadena transportadora de electrones funcional. Los complejos respiratorios detectados en la fracción mitocondria-bacteria eran de *S. cerevisiae* y únicamente se encontraron algunas subunidades de la F_1F_0-ATPasa de *Wolbachia*. El análisis por BLAST del genoma reportado para *Wolbachia* (*w*AlbB) mostró la ausencia de algunas subunidades de los complejos transportadores de electrones, lo que indica que *Wolbachia* no tiene una cadena transportadora de electrones funcional.

Finalmente, observamos que el endoparásito provoca la muerte prematura de la levadura, efecto similar al observado en los mosquitos del género *Aedes* que los hace menos eficientes como vectores de enfermedades virales.

En esta tesis se logró construir un novedoso sistema de endosimbiosis artificial utilizando a *S. cerevisiae* como hospedero alterno. La metodología de infección de la levadura *S. cerevisiae* es relevante en el campo biotecnológico, en dónde podría facilitar la generación de microbio-reactores.

Nosotros utilizamos este sistema para estudiar la interacción del endosimbionte obligado *Wolbachia pipientis* con su hospedero y encontramos que, contrario a lo reportado, *Wolbachia* no posee una cadena transportadora de electrones capaz de suministrar ATP al hospedero. Sin embargo el aumento en la actividad de las enzimas del metabolismo aerobio podría indicar que hay una suplementación de grupos hemo y/o de riboflavina por parte de la bacteria. *S. cerevisiae* es una de las levaduras preferidas para manipular genéticamente, por lo tanto, la evaluación del efecto de la infección en mutantes de *S. cerevisiae* es una posibilidad novedosa. En el campo de infectología, *S. cerevisiae* podría utilizarse como modelo para estudiar la infección y propagación de otras bacterias como *L. monocytogenes.*

2. Abstract

Wolbachia is an endoparasitic/endosymbiotic gram-negative *Rickettsiae*-like bacterium. It has colonized over sixty five percent of insect species. *Wolbachia* efficiently manipulates fertility, protein expression, lifespan and metabolism in the host, thus constituting a potential tool for the management of insect vector-borne diseases. However, attempts to culture *Wolbachia* ex-vivo have been unsuccessful; unfortunately cell culture yields are low, thus precluding biochemical studies.

Previous studies of the *Wolbachia* available genomes indicate a possible mutualistic symbiosis, where *Wolbachia* donates riboflavin, heme groups and/or ATP to the host. To date, these hypotheses have not been tested with biochemical experiments due to the low culture yields. Here, an artificial endoparasite relationship was created using *Saccharomyces cerevisiae* as an alternative host, increasing bacterial yield by two orders of magnitude.

The effects of *Wolbachia* on the hosts aerobic metabolism were studied since riboflavin, which is the precursor of the synthesis of FAD and FMN groups; and heme groups are essential components of the electron transport chain. Heddi et al. (1999) reported that *Sitophilus oryzae* aerobic metabolism enzymes activities are increased when it harbors an endosymbiont (SOPE) that supplements riboflavin. When eliminating the endosymbiont with antibiotics the enzymatic activities are diminished by 50%.

In *Wolbachia*-infected yeast, mitochondrial respiratory-chain enzyme activities and respiratory controls were preserved for longer periods. However, no respiratory proteins or oxygen consumption from *Wolbachia* were detected. Only some F_1F_0-ATPase subunits were expressed. A BLAST analysis of the *Wolbachia* (*w*AlbB) genome showed that some subunits of the electron transport complexes were not present, which indicates that the organism may not be capable of generating its own functional respiratory proteins. In addition, we observed that *Wolbachia* causes premature death in yeast as it does in *Aedes* mosquitoes.

In this work an artificial endosymbiosis system was constructed using *S. cerevisiae* as alternate host. The infection methodology of *S. cerevisiae* is relevant in the biotechnological field, where it could facilitate the generation of one-cell microbe reactors.

We use this system to study the interaction of the obligate endosymbiont

Wolbachia pipientis with its host and we found that, contrary to some reports, *Wolbachia* does not have an electron transport chain coupled to the synthesis of ATP. However, the increase in the activity of aerobic metabolism enzymes could indicate that *Wolbachia* contributes with heme and / or riboflavin groups. *S. cerevisiae* is one of the preferred yeasts to manipulate by means of molecular biology; therefore evaluating the effect of infection on mutants of *S. cerevisiae* is a possibility that was very limited in insect cells. In the infectology field, *S. cerevisiae* could be used as a model to study the infection and spread of other bacteria such as *L. monocytogenes*.

3. Introducción

3.1 Simbiosis

Se denomina simbiosis a la asociación íntima entre dos especies que habitan un mismo nicho ecológico y que comparten actividades o requerimientos en común. Se puede presentar en tres formas: mutualismo, comensalismo o parasitismo. En el mutualismo ambas especies resultan beneficiadas; en el comensalismo, una especie se beneficia de otra sin perjudicarla ni beneficiarla; y en el parasitismo, la presencia del huésped daña al hospedero. Además, las relaciones simbióticas pueden clasificarse en ectosimbiosis cuando uno de los seres vive sobre el cuerpo del otro o endosimbiosis cuando uno vive dentro del otro, ya sea en sus órganos o células; también, dependiendo de si pueden vivir independientemente o no, los organismos se dividen en facultativos y obligados (Dimijian, 2000; Winner, 1969).

Las bacterias endosimbiontes obligadas pasan por un proceso de inactivación de genes y reducción de genomas (McCutcheon y cols., 2012; Stepkowski y cols., 2001) (ver Tabla 1). Generalmente, los genomas de bacterias de vida libre son mayores que los de las bacterias endosimbiontes. La bacteria de suelo *Sorangium cellulosum* tiene el genoma más grande, de 13 Mpb (Schneiker y cols., 2007), mientras que la bacteria de vida libre con el genoma más pequeño es la α-proteobacteria *Bartonella quintana*, con 1.5 Mpb (Alsmark y cols., 2004). Los endosimbiontes obligados bacterianos poseen genomas menores a 1.1 Mpb (ver Tabla 1) por lo que dependen del hospedero para sobrevivir (McCutcheon y cols., 2012).

Tabla 1.Características de algunas bacterias endosimbiontes y de vida libre.

Bacteria	Gen. (Mpb)	Hospedero	t (h)	Relación y papel para el hospedero	Ref.
Buchnera aphidicola	0.425-0.650	Pulgón (Bacteriocito)	36	Endosimbionte obligado: provee aminoácidos	(Lamelas y cols., 2011)
Wigglesworthia glossinidia	0.7	Mosca Tse-tsé (Citoplasma)	36	Endosimbionte obligado: provee vitamina B6, aminoácidos y es necesario para la fecundación.	(Akman y cols., 2002)
Blochmania sp.	0.7	Hormiga carpintero (Citoplasma)	36	Endosimbionte obligado: provee aminoácidos, compuestos nitrogenados, azufrados e hidroliza la	(Degnan y cols., 2005; Gil y cols., 2003; Vieira-Silva y cols.,

				urea.	2010)
Blattobacteria sp.	0.59-0.63	Cucaracha (micetocitos)	-	Endosimbionte obligado: provee aminoácidos y recicla nitrógeno.	(Sabree y cols., 2009)
Carsonella ruddii	0.16	Psílidos *Pachpylla venusta*	-	Endosimbionte obligado: se cree que provee aminoácidos al hospedero.	(Nakabachi y cols., 2006; Tamames y cols., 2007)
Tremblaya princeps	0.14	Cochinilla *Planococcus citri* (bacteriocito)	-	Endosimbionte obligado: a su vez posee otro endosimbionte llamado: *Candidatus moranella endobia*. Ambos proveen aminoácidos al hospedero.	(Lopez-Madrigal y cols., 2011; McCutcheon y cols., 2011)
Sulcia muelleri	0.19-.27	Saltamontes (bacteriocito)	-	Endosimbionte obligado: a su vez posee otro endosimbionte llamado *Arsenophonus* Ambos proveen aminoácidos al hospedero.	(Chang y cols., 2015; Kobialka y cols., 2016; Wu y cols., 2006)
Baumannia cicadellinicola	0.68	Cigarras (bacteriocito)	-	Endosimbionte obligado: provee vitaminas B1, B2, B3, B5 and B6.	(Wu y cols., 2006)
Hadgkinia cicadicola	0.14	Cigarras *Diceroprocta semicincta* (bacteriocito)	-	Endosimbionte obligado: puede proveer aminoácidos	(McCutcheon y cols., 2009)
Candidatus endoecteinascidia frumentensis	0.63	Tunicado *Ecteinascidiat urbinata* (bacteriocito)	-	Endosimbionte obligado: produce ecteinascidin 743, un agente quimioterapéutico.	(Moss y cols., 2003; Schofield y cols., 2015)
Wolbachia subgrupos C y D	0.95-1.08	Filarias nemátodos (Citoplasma)	-	Endosimbionte obligado: provee riboflavina y grupos hemo.	(Darby y cols., 2012; Fenn y cols., 2004; Foster y cols., 2005)
Sodalis glossinidus	4.1	Mosca Tse-tsé (Bacteriocito)	26	Endosimbionte facultativo: se cultiva en Mitsuhashi-Maramarosch suplementado con 20% de eritrocitos de caballo en 5 a 10% de CO_2.	(Belda y cols., 2012; Dale y cols., 1999; Matthew y cols., 2005)
Burkholderia rhizoxinica	3.75 Mb	*Rhizopus microsporus* (Citoplasma)	0.75	Endosimbionte facultativo: Crece en medio TSB.	(Partida-Martinez y cols., 2005)

Wolbachia subgrupo A, B, E y F	1.48-1.26	Artrópodos (Citoplasma)	-	Parásito reproductivo obligado intracelular: provoca feminización de machos, partenogénesis e incompatibilidad citoplasmática.	(Klasson y cols., 2008; Mavingui y cols., 2012; O'Neill y cols., 1997; Salzberg y cols., 2009; Wu y cols., 2004)
Coxiella brunetti	2.1	Garrapatas, macrófagos y neutrófilos (lisosomas)	20	Parásito intracelular obligado: cultivado en huevos de gallina fertilizados.	(Elliott y cols., 2013; Omsland y cols., 2013; Weiss, 1973)
Chlamydia sp.	1	Monocitos (fagosoma)	20-24	Parásito intracelular obligado. Cultivado en líneas celulares	(Moulder, 1991; Omsland y cols., 2014; Vieira-Silva y cols., 2010)
Rickettsia sp.	1.11	Garrapatas, piojos, pulgas, ácaros y mamíferos (citoplasma)	12-13	Parásito intracelular obligado. Cultivados en líneas celulares y huevos de gallina fertilizados	(Andersson y cols., 1998; McLeod y cols., 2004; Wood y cols., 2012)
Helicobacter pylori	1.66	Macrófagos, células dendríticas y epiteliales (vacuolas)	2.4	Patógeno facultativo intracelular: cultivado como bacteria libre en medios suplementados.	(Dubois y cols., 2007; Lamarque y cols., 2003; Siavoshi y cols., 2005a)
Escherichia coli	4.6	Células epiteliales, macrófagos y monocitos.	.35	Patógeno facultativo intracelular	(Levine, 1987; Sukumaran y cols., 2003)

Gen: tamaño del genoma; Mpb: Mega pares de bases; t (h): tiempo de duplicación en horas; - no reportado.

Los endosimbiontes obligados bacterianos realizan funciones específicas para el hospedero, como sintetizar nutrientes (Buchner, 1965; Dale y cols., 2006; Douglas, 2015), reciclar productos nocivos de excreción tales como urea o ácido úrico (Malke, 1964), sintetizar compuestos tóxicos que el hospedero utiliza como defensa y/o para facilitar el parasitismo de otras especies (Partida-Martinez y cols., 2007a; Partida-Martinez y cols., 2005) (ver Tabla 1).

3.2 *Wolbachia* sp

Wolbachia sp es un α-proteobacteria (Gram negativa) que infecta del 65 al 70% de los insectos que habitan la Tierra; es la bacteria intracelular más común reportada a la fecha

(Foster y cols., 2005; Jeyaprakash y cols., 2000; Werren y cols., 2008). Se transmite a la progenie por herencia materna (Bandi y cols., 2001) y mide de 0.02 μm a 1 μm de largo[58,59] (Figura 1), no presenta flagelos, fimbrias ni pili, sin embargo no se considera inmóvil, ya que existe la posibilidad de que utilice el citoesqueleto de actina del hospedero para desplazarse (Foster y cols., 2005). En artrópodos *Wolbachia* puede transmitirse horizontalmente. Los mecanismos sugeridos incluyen alimentarse con insectos previamente infectados con *Wolbachia*, canibalismo y transmisión de la bacteria en el alimento (planta) (Ahmed y cols., 2016; Chrostek y cols., 2017; White y cols., 2017).

Dependiendo del hospedero, *Wolbachia* puede considerarse un parásito reproductivo o un endosimbionte mutualista (Tabla 1). En artrópodos, esta bacteria ha desarrollado mecanismos de parasitismo reproductivo para facilitar la invasión de poblaciones provocando en sus hospederos incompatibilidad citoplasmática, feminización de machos y partenogénesis (Werren y cols., 2008). En *Drosophila melanogaster*, aumenta la longevidad, la capacidad reproductiva y suministra nutrientes durante periodos de estrés por exposición a dietas bajas o altas en hierro (Brownlie y cols., 2009a). En *Aedes aegypti* se ha observado que confiere protección contra la colonización del insecto por *Plasmodium*, virus del Nilo, chikungunya, zika, dengue, etc. evitando que dichas enfermedades se propaguen (Brownlie y cols., 2009b; Dutra y cols., 2016; Glaser y cols., 2010; Hedges y cols., 2008; Hoffmann y cols., 2011; Johnson, 2015; Moreira y cols., 2009; Mousson y cols., 2010; Pan y cols., 2012; Walker y cols., 2011).

En los nemátodos, la relación bacteria-hospedero ha evolucionado hacia una endosimbiosis obligada: *Wolbachia* es esencial para el crecimiento, desarrollo, cambio de estadio larvario, fecundación y supervivencia del parásito (Fenn y cols., 2004; Langworthy y cols., 2000; Taylor y cols., 1999). Ambos organismos poseen genomas complementarios; es decir, los genes de ciertas vías metabólicas y de síntesis de cofactores esenciales se encuentran únicamente en el genoma de la proteobacteria o en el del hospedero (Bandi y cols., 2001; Foster y cols., 2005; Rao y cols., 2002; Taylor y cols., 1999). Al ser esencial en el desarrollo de las filarias, *Wolbachia* se ha convertido en un posible blanco terapéutico contra las filariasis causadas por *Wuchereria bancrofti, Brugia malayi* y O*nchocerca volvulus* (Bandi y cols., 2001; Johnston y cols., 2010).

Los genomas de *Wolbachia* secuenciados a partir de hospederos artrópodos son más grandes que los obtenidos de especies de *Wolbachia* de nemátodos (ver Tabla 1) en

los que la bacteria es un endosimbionte obligado (Darby y cols., 2012; Foster y cols., 2005; Mavingui y cols., 2012; Metcalf y cols., 2014; Salzberg y cols., 2009; Wu y cols., 2004). Esto puede deberse a que en los artrópodos la bacteria no es necesaria y debe mantener sus mecanismos de parasitismo para garantizar su permanencia en la población.

Basándose en un análisis filogenético del gen ftsZ, *Wolbachia* se ha clasificado en 6 subgrupos dependiendo del hospedero en donde habita. Los subgrupos A y B corresponden a *Wolbachia* endosimbionte de artrópodos. Los subgrupos C y D corresponden a *Wolbachia* endosimbionte de filarias. El grupo E corresponde a endosimbiontes de colémbolos, que son artrópodos hexápodos y el grupo F corresponde a *Wolbachia* endosimbionte de termitas (Lo Nathan, 2002).

Como todos los endosimbiontes obligados, *Wolbachia* no puede cultivarse fuera de un hospedero por lo que se mantiene en animales vivos infestados con nemátodos, en artrópodos o en cultivos celulares. La primera línea celular infectada con *Wolbachia* fue obtenida a partir de huevos de mosquito tigre *Aedes albopictus* naturalmente infectados con *Wolbachia (w*AlbB) (O'Neill y cols., 1997) a esta línea celular se le conoce como Aa23 (Figura 1 a y b). Actualmente se ha logrado cultivar en neuroblastos y fibroblastos humanos (Noda y cols., 2002; White y cols., 2017), células L929 de ratón(Noda y cols., 2002)' mariposa Sf9 (Dobson y cols., 2002; Noda y cols., 2002) y derivados de líneas de insecto como la línea C6/C36 (Baldridge y cols., 2014).

Se h reportado que *Wolbachia* no puede establecer infecciones en mamíferos debido a sus propiedades antigénicas (Shiny y cols., 2009). *Wolbachia* posee un grupo de proteínas conocidas como *Wolbachia surface proteins* (wsp) localizadas en la cara externa de la membrana bacteriana. Aunque no se sabe la función exacta de estas proteínas, se cree que están involucradas en las interacciones bacteria-hospedero y en la distribución de *Wolbachia* durante los estadios de crecimiento del hospedero. Se ha propuesto la función de dos de estas proteínas en *Wolbachia* de *Brugia malayi*: *wBm*0432 interactúa con varias enzimas glucolíticas incluyendo a la aldolasa y la enolasa y *wBm*0152 interactúa con la actina y la tubulina del hospedero (Melnikow y cols., 2013). Las proteínas wsp evocan una respuesta inmune innata en mamíferos a través de la activación de TLR1 Y TLR4 en humanos y en ratones (Brattig y cols., 2004) que culmina con la eliminación de la bacteria del hospedero mamífero.

En 2015, en el Hospital "Peking University First Hospital" en Beijing, China, se amplificaron los genes 16S rRNA y *fbp*A de *Wolbachia* a partir de las muestras de

sangre de un paciente con linfoma de Hodgkin (Chen y cols., 2015). Las secuencias obtenidas de dichos genes indicaron una infección con *Wolbachia* del subgrupo B. Este caso sugiere que *Wolbachia* puede transmitirse a humanos inmunodeprimidos por medio de picadura de mosquito.

En 2017 se demostró que *Wolbachia* no es un endosimbionte exclusivo del reino animal, este puede colonizar de manera transitoria plantas de algodón (Figura 1 c y d), pepino y frijol, lo que facilita su transmisión de insecto a insecto (Chrostek y cols., 2017; Li y cols., 2017).

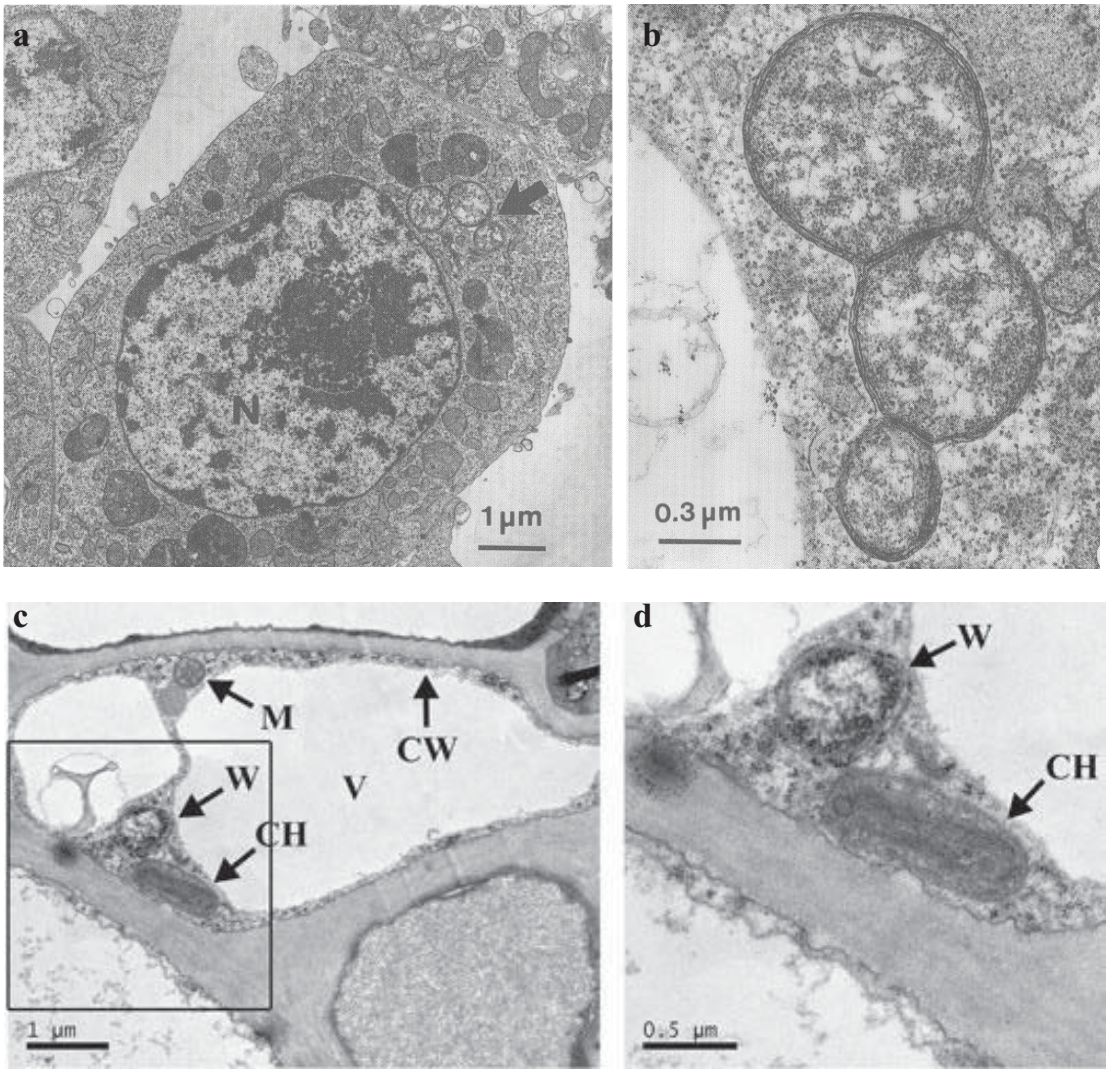

Figura 1. Microscopía de transmisión electrónica (MET) de *Wolbachia.* a y b) en la línea celular Aa23 infectada naturalmente. *Wolbachia* se señala con una flecha. Imagen tomada de (O'Neill y cols., 1997); c y d) y en el tubo del tamiz del floema de una hoja de algodón. CW, pared celular del floema de la planta; CH, cloroplasto; M, mitocondria; V, vacuola de la célula vegetal; W, *Wolbachia*. Imagen tomada de (Li y cols., 2017).

3.2.1 *Wolbachia* evitan la propagación de enfermedades transmitidas por vectores

Dos de las enfermedades con mayor relevancia epidemiológica a nivel mundial son el paludismo y el dengue. Según la OMS (Organización Mundial de la Salud), las enfermedades transmitidas por un vector artrópodo representan el 17% de las enfermedades infecciosas a nivel mundial, con 1,000 millones de casos y un millón de defunciones anuales (WHO, 2016; WHO, 2017). Varios grupos de investigación han reportado que los mosquitos infectados con *Wolbachia* disminuyen su capacidad de propagación de enfermedades (Blagrove y cols., 2013; Dutra y cols., 2016; Evans y cols., 2009; Hughes y cols., 2011; Hughes y cols., 2012; Hussain y cols., 2013; Kambris y cols., 2010; McMeniman y cols., 2009; Moreira y cols., 2009; Mousson y cols., 2010; Pan y cols., 2012).

Un mosquito hembra madura a los dos días de eclosionar y debe ingerir sangre para poner huevos fértiles. Si la sangre consumida estaba contaminada con algún patógeno, estos requieren un período de incubación que dura de 10 a 17 días para dengue y malaria, en dónde se replican en el intestino del mosquito para después migrar a las glándulas salivales (WHO, 2017). Normalmente, un mosquito hembra vive entre 40-50 días, lo que implica que por lo menos la mitad de su vida podrá ser contagiosa si consume sangre contaminada en su primera alimentación. *Wolbachia (w*MelPop*)* aislada de *Drosophila melanogaster* e introducida en *Aedes aegypti* acorta la vida media del mosquito en un 50%, disminuyendo el tiempo en el que el mosquito actúa como vector (Evans y cols., 2009; McMeniman y cols., 2010).

Wolbachia impide la colonización de hospedero por otros patógenos. Se ha observado que *Wolbachia* confiere protección contra la colonización del insecto por *Plasmodium* y virus de Dengue, virus del Nilo, Chikungunya, Zika, etc., evitando que dichas enfermedades se propaguen (Blagrove y cols., 2013; Dutra y cols., 2016; Evans y cols., 2009; Hughes y cols., 2011; Hughes y cols., 2012; Hussain y cols., 2013; Kambris y cols., 2010; McMeniman y cols., 2009; Moreira y cols., 2009; Mousson y cols., 2010; Pan y cols., 2012). El mecanismo por el que *Wolbachia* inhibe la colonización del patógeno no ha sido elucidado pero se piensa que compite por nutrientes como aminoácidos y colesterol (Caragata y cols., 2013; Caragata y cols., 2014), y que mantiene activado el sistema inmune del hospedero (Amuzu y cols., 2016; Terradas y cols., 2017).

Finalmente, *Wolbachia* causa incompatibilidad citoplásmica que puede utilizarse

como herramienta para prevenir la propagación de enfermedades (Loreto y cols., 2016). Ésta consiste en una modificación en el DNA del mosquito que provoca que los machos infectados únicamente puedan tener una descendencia viable si se aparean con hembras infectadas, si se aparean con hembras no infectadas la descendencia no es viable. La descendencia de una hembra infectada será 100% viable y portadora de *Wolbachia*. (Werren, 1997; Werren y cols., 2008). La estrategia sugerida sería disminuir la población total de mosquitos infectando a una población de machos con *Wolbachia*, pero no a las hembras, promoviendo la muerte de la mayoría de la progenie.

En Australia, Colombia, Estados Unidos y algunos países de Asia se han infectado mosquitos con *Wolbachia* (*wMel*) y se han introducido en zonas endémicas de dengue y se ha observado una disminución de casos reportados.

3.3 El genoma de *Wolbachia* y la relación endosimbionte-mitocondria

Wolbachia y sus hospederos tienen vías metabólicas complementarias. Por ejemplo, el genoma de *B. malayi* carece de las vías metabólicas para la síntesis de riboflavina y del grupo hemo, mientras que el genoma de *Wolbachia* de *B. malayi* (*wBm*) contiene los genes completos para ambas vías. Por otro lado, *B. malayi* tiene la capacidad de sintetizar aminoácidos *de novo*, mientras que *wBm* no tiene las vías metabólicas para producirlos, pero tiene simportadores de aminoácidos. Además, posee sistemas de translocación de proteínas, sistemas de secreción Tipo IV y sistemas de secreción ABC (Foster y cols., 2005; Klasson y cols., 2008; Wu y cols., 2004).

Todos los subgrupos de *Wolbachia* carecen de los genes que codifican para las enzimas de la glucólisis: glucosa-6-fosfatocinasa (HK), fosfofructocinasa (PFK) y sólo tiene los genes a partir de fructosa-1,6-bifosfato aldolasa. No tiene genes codificantes para la piruvato cinasa (PK), pero la sustituyen con una piruvato fosfato dicinasa. Dichas bacterias tienen todos los genes que codifican para las proteínas del ciclo de ácidos tricarboxílicos y la vía completa de gluconeogénesis necesaria para la vía de las pentosas (Foster y cols., 2005; Klasson y cols., 2008; Wu y cols., 2004).

Al ser un α-proteobacteria se espera que *Wolbachia* posea los genes necesarios para codificar cadenas respiratorias similares a las de, rickettsias y mitocondrias (Emelyanov, 2003). Cada genoma de *Wolbachia* posee diferentes genes para formar una cadena respiratoria (ver anexo B). Dependiendo de la especie, pueden incluir NADH: ubiquinona oxidorreductasa, succinato deshidrogenasa, glicerol-3-fosfato deshidrogenasa, glicerol deshidrogenasa, PQQ deshidrogenasa, ubiquinol oxidasa-citocromo *c* reductasa, citocromo *c* oxidasa soluble, citocromo *c* oxidasa, citocromo *d*

oxidasa y nitrato reductasa (Figura 2, anexo B). Según el genoma de *Wolbachia wAlb*B (Mavingui y cols., 2012) analizado en la plataforma MycroScope (Vallenet y cols., 2009) (http://www.genoscope.cns.fr/agc/microscope) esta posee 11 subunidades de Complejo I, tres subunidades de complejo II, una subunidad de complejo III y tres subunidades de complejo IV (ver Anexo B). Todos los genomas poseen las unidades a, b, c, α, β, γ, δ, ε de la F_1F_o-ATP sintasa (Foster y cols., 2005; Klasson y cols., 2008; Wu y cols., 2004).

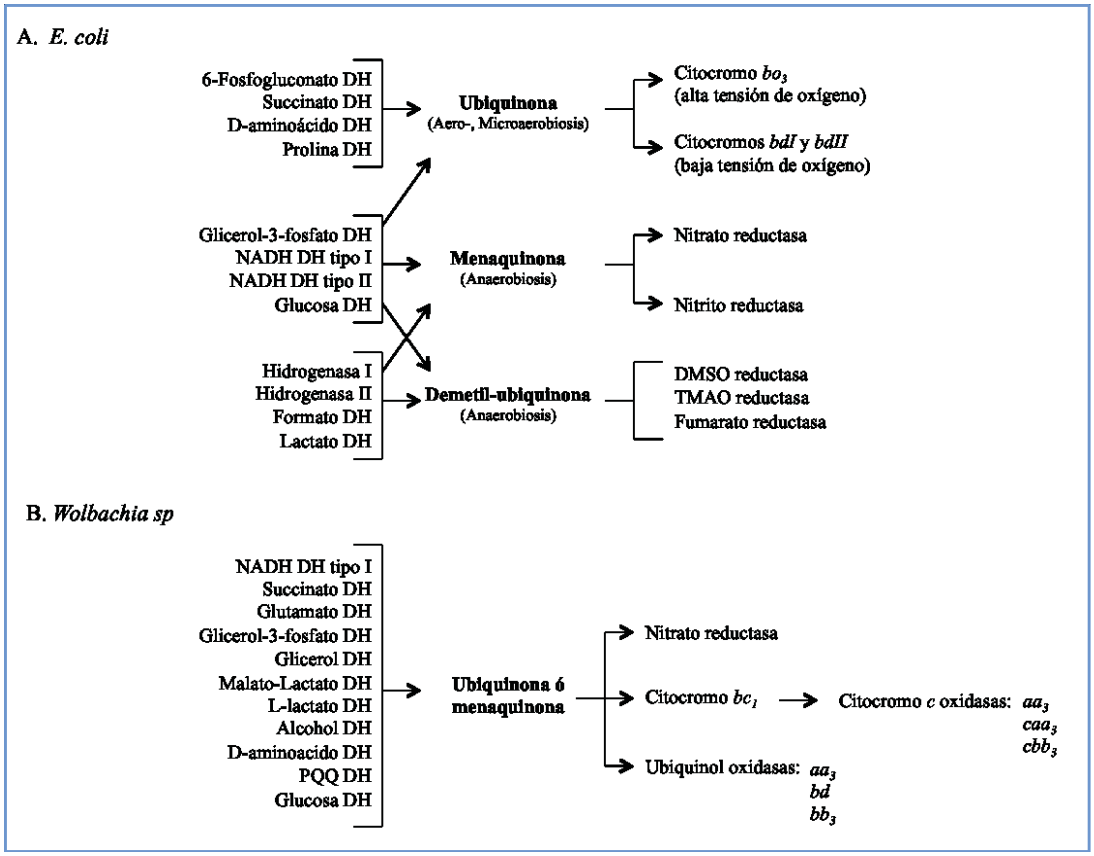

Figura 2. Diversidad de la cadena transportadora de electrones de bacterias. Imagen modificada de (Rosas-Lemus, 2016). A) La cadena respiratoria de *E. coli* ofrece una gran diversidad de deshidrogenasas y oxidasas que se expresan dependiendo de la disponibilidad de sustratos y de la concentración de oxígeno a la que está expuesta. *E. coli* no posee complejo III ni complejo IV por lo que los electrones pasan directamente de las pozas de ubiquinol a los citocromos bo_3 o *bd*; o a las reductasas que utilizan aceptores de electrones diferentes al oxígeno (Ingledew y cols., 1984; Trumpower, 1990; Unden y cols., 1997). B) La cadena respiratoria de *Wolbachia* incluye una cadena respiratoria similar a la mitocondrial, además de numerosas posibles deshidrogenasas (Foster y cols., 2005; Klasson y cols., 2008; Wu y cols., 2004).

Baldrige y cols. (2014) purificaron *Wolbachia* a partir de cultivos de líneas celulares de *Aedes albopictus* C7-10 mediante un gradiente de sacarosa y caracterizaron

su proteoma. Dentro de estas secuencias, no se encontraron las de complejo I, III o IV, únicamente subunidades de la succinato deshidrogenasa y de la ATP sintasa (Baldridge y cols., 2014). Darby y cols., 2012 sugieren que *Wolbachia* dona ATP a su hospedero lo que parece ser contradictorio, ya que para generar suficiente energía para el hospedero y para la bacteria, las proteínas de la cadena transportadora de electrones deberían ser fácilmente detectables. El grupo del Dr. Sullivan sugiere que *Wolbachia* no dona ATP al hospedero y únicamente le suplementa con riboflavina y grupos hemos (Pietri y cols., 2016).

Otras vías presentes en *Wolbachia*, pero no en Rickettsias incluyen la degradación de treonina, la biosíntesis de riboflavina, la síntesis de pirimidinas y la presencia de transportadores de hierro (Foster y cols., 2005; Wu y cols., 2004). En contraste, *Wolbachia* ha perdido la capacidad de biosíntesis de lipopolisacáridos y lípido A, pero puede sintetizar peptidoglicanos (N-acetilglucosamina y N-acetilmuramato), ácidos grasos, fosfolípidos e isoprenoides (Foster y cols., 2005).

El efecto de *Wolbachia* sobre el metabolismo de sus hospederos se ha estudiado utilizando a la filaria patógena de ratas de algodón, *Litomosoides sigmodontis*. Se observó que al eliminar *Wolbachia* con tetraciclina, había un aumento en la expresión de los genes de la cadena respiratoria que están codificados en el genoma mitocondrial (ND1-5 de la NADH deshidrogenasa, citocromo b, COX I, II y III y la subunidad ATP6 de la ATP sintasa). En ese estudio proponen que al eliminar *Wolbachia*, la filaria no es capaz de sintetizar enzimas funcionales que contengan grupos hemo y derivados de riboflavina, lo que resulta en una pérdida de energía que el organismo trata de compensar (Strubing y cols., 2010). Darby y cols. (2012) evaluaron mediante RNA-seq las vías metabólicas que aumentaron al tratar al hospedero con tetraciclina, observando mayor expresión de la subunidad 3 de la citocromo *c* oxidasa y de la ATP sintasa, por lo que proponen que *Wolbachia* sustituye a la mitocondria donando energía al hospedero (Darby y cols., 2012).

Otro endosimbionte que favorece el metabolismo energético del hospedero es una γ-proteobacteria conocida como SOPE (Endosimbionte Principal de *Sitophilus oryzae*); es un endosimbionte de *S. oryzae* (gorgojo de arroz). En larvas se ha reportado que el SOPE aumenta la fosforilación oxidativa al suministrar riboflavina y ácido pantoténico al hospedero, optimizando las actividades de la succinato citocromo *c* reductasa, glicerol-3-fosfato deshidrogenasa, citocromo *c* reductasa, piruvato deshidrogenasa y α-cetoglutarato deshidrogenasa. La adición de estas vitaminas a las

larvas aposimbiontes restaura las actividades de dichas enzimas en un 70-80% (Heddi y cols., 1999).

El protozoario *Strigomonas culicis* posee una bacteria endosimbionte no identificada, cuya eliminación disminuye el consumo de oxígeno del hospedero en un 76% (de 1.2 a 0.3 nmolO_2/min*10^6 células) (Loyola-Machado y cols., 2017).

3.4 Cadena transportadora de electrones (CTE) y fosforilación oxidativa

La respiración es un proceso que crea la energía protón motriz transmembranal que se utiliza para la síntesis de ATP por la ATP-sintasa (Mitchell, 1966) y para energizar el transporte secundario transmembranal. Mediante el flujo de electrones a través de los complejos de la cadena respiratoria se cataliza la translocación de protones al espacio intermembranal (EIM) generando una diferencia en el potencial transmembranal que se acopla a la síntesis de ATP, la principal molécula energética en los seres vivos.

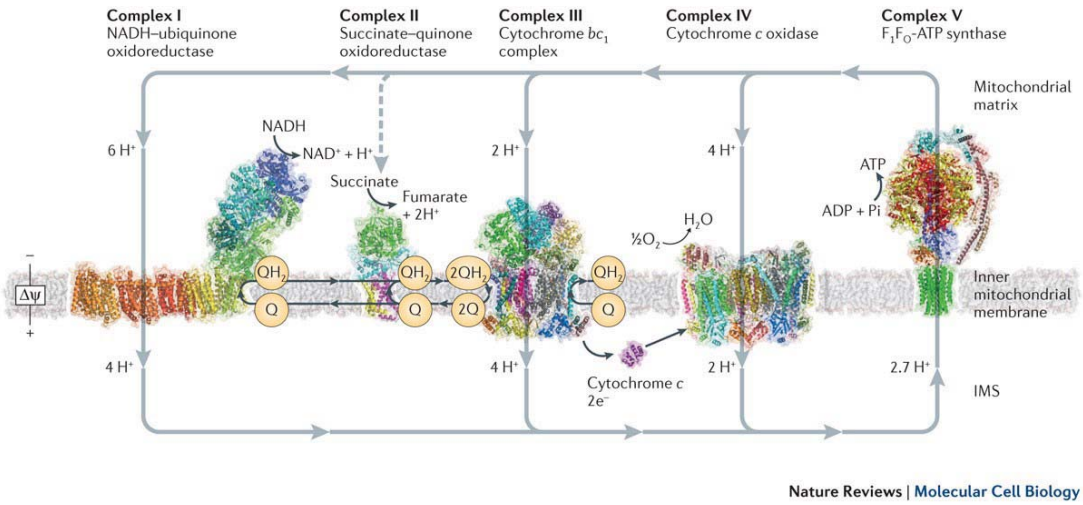

Figura 3. **Esquema de la cadena respiratoria clásica mitocondrial.** Tomada de (Sazanov, 2015). La cadena respiratoria mitocondrial clásica está formada por cuatro complejos. El complejo I (NADH-ubiquinona óxidorreductasa) y el complejo II (Succinato-ubiquinona óxidorreductasa) catalizan la transferencia de electrones producto de la oxidación del NADH y del succinato a la poza de ubiquinona (UQ) que se reduce a ubiquinol. Posteriormente, el complejo III (Ubiquinol ferrocitocromo *c* oxidorreductasa o citocromo bc_1) toma los electrones del ubiquinol y a través del citocromo *c* soluble transfiere los electrones al complejo IV (Citocromo *c* oxidasa) que finalmente reduce al O_2 formando agua. Los complejos respiratorios bombean 4/0/4 y 2 protones al espacio intermembranal (EIM o IMS en esta figura) generando un gradiente de pH que a su vez se convierte en el potencial eléctrico transmembranal. Esta fuerza protón-motriz es utilizada por el complejo V (ATP sintasa) para fosforilar ADP y producir ATP. Por cada molécula de NADH oxidada se bombean 10 protones (Lehninger, 2013; Sazanov, 2015) y en una ATPasa con diez subunidades c, se requieren 2.7 protones para

sintetizar una molécula de ATP. Para la imagen se utilizaron las estructuras de complejo I de *Thermus thermophilus* (PDB id. 4HEA), complejo II de *Sus scrofa* (PDB id. 1ZOY), complejo III de *Bos taurus* (PBD id. 1OCC), ATPasa de *B. taurus* (J.E. Walker, Medical Research Council, Mitochondrial Biology Unit, Cambridge, UK).

En una cadena respiratoria clásica (de mamífero), los electrones provenientes de intermediarios del metabolismo son transportados de la matriz mitocondrial (Mat) a través del Complejo I (NADH-ubiquinona oxidorreductasa) o del Complejo II (Succinato-ubiquinona oxidorreductasa) a la poza de ubiquinona (UQ), que se reduce a ubiquinol. Enseguida, el ubiquinol dona sus electrones al complejo III (Ubiquinol ferrocitocromo *c* oxidorreductasa o citocromo bc_1), el cual, a través del citocromo *c* soluble transfiere sus electrones al complejo IV (Citocromo *c* oxidasa) que finalmente reduce al O_2 formando agua. Los complejos I, III y IV sirven como bombas de protones transfiriendo 4, 4 y 2 protones, respectivamente, al espacio transmembranal generando una diferencia en el potencial eléctrico transmembranal (Figura 3)(Lehninger, 2013). Finalmente, el complejo V (F_1F_o ATP sintasa) aprovecha el gradiente de protones generado por la CTE disipándolo en un proceso acoplado a la producción de ATP.

3.4.1 NADH: ubiquinona óxidorreductasa (Complejo I)

La NADH: ubiquinona óxidorreductasa es el primer complejo multi-proteico de la CTE. Este complejo acopla la transferencia de un par de electrones del NADH producido durante la oxidación de los diferentes intermediarios del ciclo de Krebs y de la β-oxidación a la translocación de cuatro protones a través de la membrana interna mitocondrial, catalizando la siguiente reacción:

$$NADH + H^+ + Q + 4H^+_{Mat} \rightarrow NAD^+ + QH_2 + 4H^+_{EIM}$$

Esta enzima tiene una estructura de "L" formada por un brazo periférico (N) que posee como grupo prostético un flavín mononucleótido (FMN) y el sitio de unión a NADH del lado de la matriz mitocondrial. Posee además 8-9 centros Fe-S unidos covalentemente que conectan el FMN con el módulo Q, que es donde se encuentra el sitio de unión a la quinona. Finalmente, el brazo de membrana (P) se encuentra embebido en la membrana interna mitocondrial y se encarga de la translocación de los protones al espacio intermembranal (Figura 3). El complejo I de mamíferos y levaduras está formado por 42-43 subunidades de las cuales 7 están codificadas en genoma mitocondrial (Carroll y cols., 2003; Degli Esposti, 1998; Walker, 1992; Zhu y cols.,

2016). El complejo I de *E. coli* está formado por 13 subunidades, mientras que los de *Thermus thermophilus* y *P. denitrificans* poseen 14 subunidades (Carroll y cols., 2003; Sazanov, 2015; Stolpe y cols., 2004; Walker, 1992; Zickermann y cols., 2015) (Tabla 2).

El mecanismo de acción del complejo I es el mismo para todos los organismos: el NADH se oxida a NAD^+ en la subunidad Nqo1/NuoF del brazo N y dona sus electrones al FMN localizado en la misma subunidad. Después los electrones pasan de manera individual a través de 7 centros Fe-S colocados a una distancia igual o menor a 14 Å que forman una cadena que va desde el FMN hasta el sitio de unión a la quinona en el módulo Q donde los electrones reducen la ubiquinona a ubiquinol. El paso de los electrones del brazo N al módulo Q genera un cambio conformacional en el brazo de membrana que permite la translocación de cuatro protones al espacio intermembranal (Walker, 1992). La rotenona, el amital y la piericidina A inhiben la actividad del complejo I al bloquear el sitio de unión de la ubiquinona en el sitio Q (Degli Esposti, 1998). La función de las subunidades supernumerarias aún no ha sido elucidada, aunque se cree que pueden funcionar como chaperonas ayudando a ensamblar el complejo.

3.4.2 Succinato: ubiquinona óxidorreductasa (Complejo II)

El segundo complejo de la cadena transportadora de electrones se localiza en la membrana interna mitocondrial. Esta enzima también cataliza un paso del ciclo de Krebs por lo que es un punto de unión entre el ciclo de ácidos tricarboxílicos y la cadena respiratoria. Este complejo no bombea protones y no contribuye a la generación del potencial transmembranal. Cataliza la siguiente reacción:

$$\text{Succinato} + Q \rightarrow \text{Fumarato} + QH_2$$

El complejo está formado por cuatro subunidades: dos hidrofílicas que se encuentran del lado matricial, sdhA y sdhB; y dos membranales, sdhC y shdD. La subunidad sdhA es una flavoproteína que tiene el sitio de unión al succinato y una molécula de FAD^+ unida covalentemente. El succinato interactúa con el sitio de unión y dona sus electrones reduciendo el FAD^+ a $FADH_2$. Los dos electrones del $FADH_2$ pasan de manera independiente por los centros Fe-S hasta el sitio de unión de la ubiquinona, formado por las subunidades sdh B, C y D. Se cree que el hemo *b* que se localiza en la subunidad sdhB sirve para mantener al primer electrón atrapado entre la semiubiquinona y el hemo *b*. Posteriormente, cuando llega el segundo electrón se

reduce la ubiquinona y así se evita la producción de especies reactivas de oxígeno (EROs) (Cecchini, 2003; Sun y cols., 2005). Existen dos tipos de inhibidores: los que funcionan como análogos del succinato, como el malonato, malato y oxaloacetato y los que interfieren en el sitio de unión de la ubiquinona como la carboxina y la fenoiltrifluoroacetona (Hagerhall, 1997; Mowery y cols., 1977; Ramsay y cols., 1981).

3.4.3 Ubiquinol ferrocitocromo *c* óxidorreductasa (Complejo III)

El complejo III cataliza la transferencia de electrones del ubiquinol al citocromo *c* soluble, transfiriendo cuatro protones al EIM. El complejo III es un dímero: cada monómero está constituido por 11 subunidades en mamífero, 9 en levadura y 3 en bacterias (Iwata y cols., 1998; Lange y cols., 2002; Solmaz y cols., 2008; Trumpower, 1990; Wittig y cols., 2010; Xia y cols., 1997; Yang y cols., 1986; Zhang y cols., 1998). Las 3 subunidades codificadas en bacteria son el citocromo *b*, que en eucariotas es codificado en el genoma mitocondrial y que contiene los sitios Q_0, Q_i y dos grupos hemo *b*: b_L y b_H; la subunidad citocromo *c* que tiene un citocromo c_1; y la proteína Rieske que tiene un centro Fe-S. El complejo III tiene dos sitios de unión al ubiquinol, el sitio Q_0 que se encuentra cerca del EIM y el Q_i que se encuentra cerca de la matriz mitocondrial (Trumpower, 1990) (Figura 4).

El funcionamiento del complejo III requiere dos vueltas al llamado ciclo Q para completar la siguiente reacción:

$$QH_2 + 2 \text{ citocromos } c^{3+} + 2H^+_{Mat} \rightarrow Q + 2 \text{ citocromos } c^{2+} + 4H^+_{EIM}$$

En el primer ciclo, una molécula de ubiquinol se oxida en el sitio Q_O transfiriendo uno de sus electrones a los centros fierro-azufre de la proteína Rieske, de donde pasa al citocromo c_1 y de ahí al citocromo *c* soluble, colocando dos protones en el EIM. La semiquinona resultante dona su segundo electrón al sitio Q_O y reduce al hemo b_L, convirtiéndose en ubiquinona. El electrón pasa del hemo b_L al b_H y al sitio Q_i, en donde se encuentra unida una ubiquinona que al recibir el electrón se reduce a semiquinona. En la segunda parte del ciclo, otra molécula de ubiquinol se oxida en el sitio Q_O, transfiriendo de la misma manera un electrón al citocromo *c* soluble y bombeando dos protones al EIM. El electrón restante pasa hasta la semiquinona que quedó en el sitio Q_i por el mismo camino que el anterior, regenerando una molécula de ubiquinol. Así, por cada molécula de ubiquinol se transfieren cuatro protones al EIM y se reducen 2 moléculas de citocromo *c* soluble (Osyczka y cols., 2005).

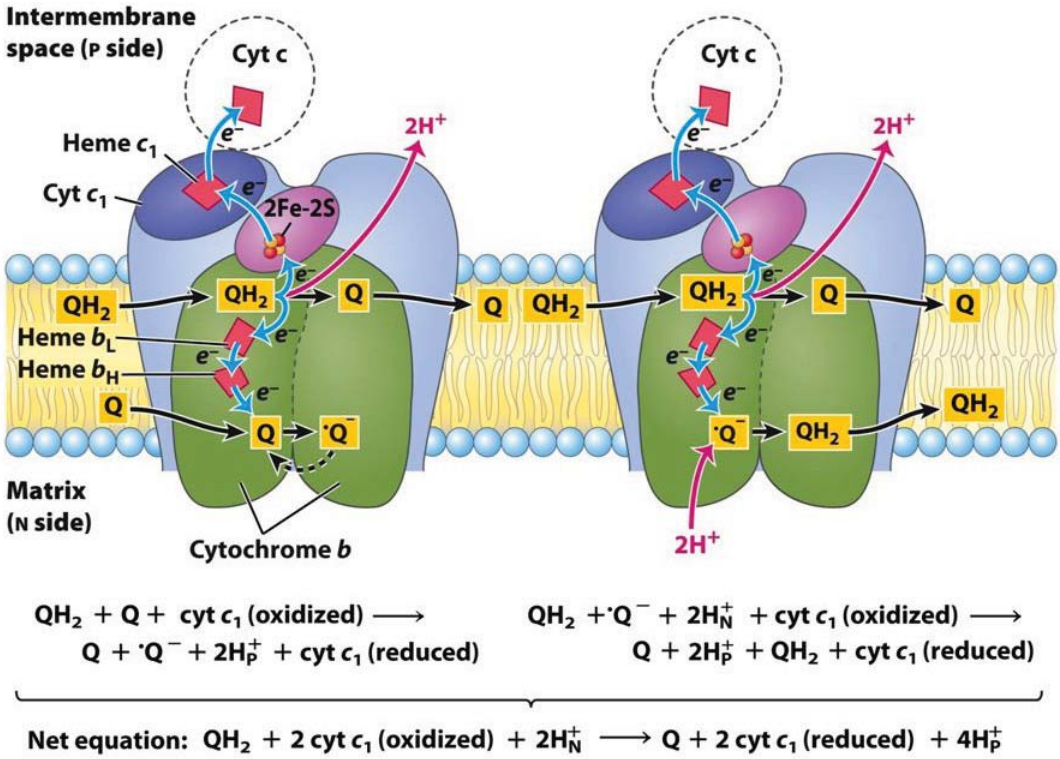

Figura 4. Esquema de reacciones químicas que se llevan a cabo durante el ciclo Q en el complejo III de la cadena transportadora de electrones. El complejo III de la cadena transportadora de electrones se forma por la subunidad citocromo *b* (verde) que posee dos grupos hemo de tipo *b* (b_L y b_H), la subunidad citocromo *c* que posee un grupo hemo de tipo *c* (azul) y la proteína de hierro azufre de Rieske (morada) que posee una agrupación formada por dos átomos de hierro y dos de azufre (2Fe•2S). El complejo III cataliza la reducción del citocromo *c* por medio de la reducción de la ubiquinona (QH2) a ubiquinol (Q) acoplado a la transferencia de 4 protones hacia el espacio intermembranal. Imagen tomada de (Lehninger, 2013).

La antimicina A es un inhibidor de complejo III que al unirse al sitio Q_i impide el transporte de electrones del citocromo b_H a la ubiquinona unida en este sitio (Drose y cols., 2008). Otros inhibidores del complejo III son el mixotiazol y la estigmatelina. Estos se unen al sitio Q_0 impidiendo la transferencia de electrones del ubiquinol a la proteína Rieske (Uribe-Carvajal, 2008).

3.4.4 Citocromo *c* oxidasa (Complejo IV)

El complejo IV es el último complejo de la cadena respiratoria y se encarga de reducir el oxígeno molecular a agua utilizando los electrones provenientes de cuatro citocromos *c* solubles:

$$4\ \text{citocromos}\ c^{2+} + O_2 + 8\ H^+_{Mat} \rightarrow 4\ \text{citocromos}\ c^{3+} + 2H_20 + 4H^+_{EIM}$$

Los monómeros activos de esta proteína están formados por 11-13 subunidades en eucariotes y 3-4 subunidades en procariotes. Las unidades conservadas entre reinos son COX I, II y III, que en eucariotes están codificadas en el genoma mitocondrial. En las subunidades COX I y COX II se encuentran 2 grupos hemos aa_3; y dos cobres Cu_A y Cu_B (Iwata, 1998; Steffens y cols., 1987; Yang y cols., 1986).

Un electrón proveniente de cada citocromo *c* soluble pasa de manera individual al primer cobre (Cu_A). Después, los electrones pasan al hemo *a* y finamente al centro binuclear hemo a_3-Cu_B donde se reduce una molécula de oxígeno a dos de agua. La reacción requiere 8 protones: 4 para la formación del agua y 4 que se bombean al EIM. Se cree que por cada electrón que se deposita en el centro binuclear un protón se bombea al EIM. El cianuro, la azida y el monóxido de carbono inhiben al complejo IV al bloquear el sitio de unión del oxígeno (Yoshikawa y cols., 1990).

3.4.5 ATP sintasa (Complejo V)

El complejo V (F_1F_o ATP sintasa) es una enzima transmembranal que se encarga de la producción de ATP a partir de ADP y Pi. Está formada por dos segmentos principales unidas por interacciones no covalentes: el segmento F_o que está embebido en la membrana mitocondrial interna y a través de la cual pasan los protones expulsados por la CTE al EIM; y el segmento F_1, que es la porción catalítica que se proyecta hacia la matriz mitocondrial y en coordinación con la rotación de las subunidades c, γ y ε de la porción F_o experimenta cambios conformacionales que fosforilan al ADP (Figura 5). La ATP sintasa actúa independientemente de la CTE, pero depende del potencial transmembranal generado por la translocación de protones. La síntesis del ATP acoplada a la respiración celular se denomina fosforilación oxidativa (Bakhtiari y cols., 1999; Jonckheere y cols., 2012).

El segmento F_0 está formado por las subunidades a-g en mamíferos, a-h en levaduras y a-c en bacterias. Constituye el grueso del motor rotatorio pudiendo variar de 8 a 15 subunidades: la mitocondria de bovino posee un anillo con 8 subunidades c, las levaduras poseen un anillo de 10 subunidades c y *E. coli* puede tener entre 10 y 14 subunidades. Los protones acumulados en el EIM pasan a la matriz mitocondrial a través de un canal formado entre las subunidades a y c de la subunidad F_0 ocasionando la rotación del anillo c. Las subunidades a y b de la subunidad F_0 forman el brazo periférico de la enzima y no giran (estator). Del otro lado del tallo central y del lado de la matriz mitocondrial se encuentra anclado el segmento F_1. Este segmento se encuentra

unido a este anillo rotatorio por medio de un eje central (subunidades γ, ε) que rota con el anillo c. Esta está formada por 3 subunidades α y β alternadas de manera circular. Los sitios de unión de ADP, Pi y ATP están localizados en las interfaces de las subunidades α/β. En un giro de 360° cada sitio activo pasa por tres estados: abierto que permite la entrada y salida de productos; relajado, en donde se encuentran el ADP y el fosfato en un espacio cerrado; y cerrado, donde se induce la formación del enlace fosfodiéster entre el ADP y el fosfato. El rendimiento teórico indica que por cada NADH que entra a la CTE se producirán entre 2.5 y 2.7 ATPs, mientras que por cada succinato, se producirán 1.5 a 1.6 ATPs (Lehninger, 2000).

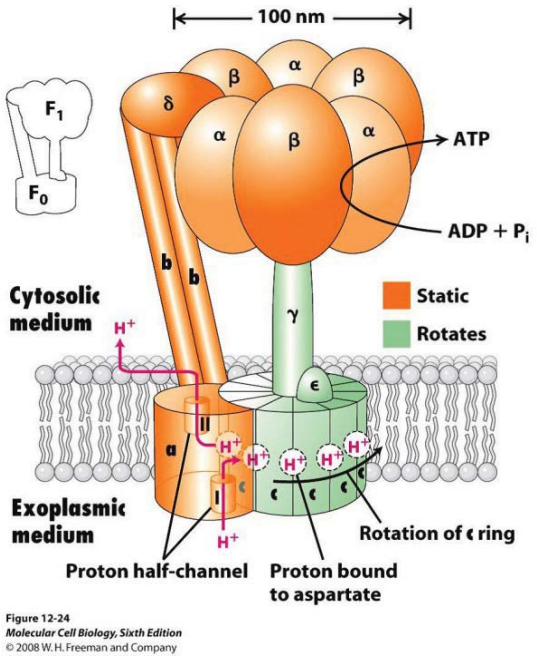

Figura 5. **Estructura de la ATP sintasa.** Estructura de la ATPasa, tomada de Molecular Cell Biology, 6ª edición, 2015. La ATPasa está formada por la unidad F_0, formada por las subunidades estáticas (naranja) a y b y la subunidades móviles (verde) conocidas como ``anillo c´´, un brazo periférico estático (naranja) constituido por las subunidades a y b; un tallo central móvil (verde) que

conecta las subunidades F_0 y F_1 formado por las subunidades γ, δ, ε, y la subunidad F_1 o unidad catalítica que se encarga de fosforilar el ADP y está formada por 3 dímeros de subunidades α/β.

3.4.6 Cadenas ramificadas de levaduras y bacterias

Las bacterias y las levaduras son organismos cosmopolitas, su metabolismo ha evolucionado para poder obtener energía a partir de diferentes fuentes. Como consecuencia, las cadenas respiratorias de dichos organismos son ramificadas, es decir, pueden estar formadas por diferentes deshidrogenasas, quinonas y oxidasas expresadas en función de la especie, los sustratos disponibles, la concentración de oxígeno en el ambiente y los requerimientos energéticos de la célula (Anraku, 1988).

Las NADH deshidrogenasas alternas o de Tipo II (NDH2), presentes en bacterias, hongos y plantas, están formadas por una cadena sencilla de aminoácidos con una masa entre 43 y 60 kDa y que tiene como grupo prostético un FAD unido no covalentemente. Estas se codifican en el genoma nuclear y no tienen segmentos transmembranales. La levadura *S. cerevisiae,* que no tiene complejo I, codifica para tres NDH2, una interna que cumple con la función de donador de electrones a la poza de ubiquinonas para surtir a la cadena transportadora de electrones, y dos externas cuya función es reoxidar el NADH citosólico. En bacterias, las NDH2 siempre se encuentran del lado citosólico de la membrana plasmática (Kerscher y cols., 2008; Kerscher y cols., 1999; Uribe-Alvarez y cols., 2016). Las NDH2 se inhiben con compuestos derivados de flavonas (Juarez y cols., 2004).

Los donadores de electrones adicionales que una bacteria puede utilizar dependen de la naturaleza de ésta: si es organótrofa, consumirá moléculas orgánicas y si es litótrofa utilizará donadores de electrones inorgánicos como hidrógeno, amoníaco, sulfuro, fierro, etc. En las bacterias se han reportado la formato deshidrogenasa, las D y L-lactato deshidrogenasas, la gliceraldehído-3-fosfato deshidrogenasa, la glucosa deshidrogenasa, la D-aminoácido deshidrogenasa, la hidrogenasa, etc. como donadores de electrones de la CTE. Al igual que la NDH2, estas deshidrogenasas no bombean protones al espacio intermembranal y transfieren sus electrones a la poza de quinonas, que en el caso de bacterias puede ser ubiquinona, menaquinona o dimetilmenaquinona, dependiendo del potencial redox de los sustratos y de la oxigenación del medio (Rosas-Lemus, 2016).

En las cadenas ramificadas bacterianas, existen diferentes tipos de oxidasas terminales: las citocromo *c* oxidasas (tipo I) y las quinol oxidasas (tipo II). Las oxidasas tipo I, reciben los electrones del citocromo *c* soluble y reducen el oxígeno a agua; pueden ser tipo IA, como el complejo IV y tener hemos *a* (aa_3 o caa_3) y cobre tipo IB y tener hemos *b* u *o*. Las oxidasas de tipo II o quinol oxidasas reciben electrones del

ubiquinol y los transfieren directamente al oxígeno. Estas pueden tener hemos *a*, *b* u *o* con cobre (IIA) o hemos *b* y *d* (IIB) (Anraku, 1988). Las oxidasas terminales de las cadenas ramificadas se expresan dependiendo la concentración de oxígeno del medio. *E. coli*, que no tiene complejo III ni complejo IV (Trumpower, 1990), bajo diferentes condiciones aeróbicas usa dos quinol oxidasas terminales: citocromos b_o en medios oxigenados y citocromos *bd* cuando la tensión de oxígeno baja (Figura 2) (Anraku, 1987).

Además de las oxidasas terminales (con citocromos) existen las oxidasas alternas (AOX). Estas enzimas toman electrones del ubiquinol y los transfieren directamente al oxígeno (Storey, 1976). Las AOX están compuestas por una sola cadena polipeptídica de ~40 kDa localizada del lado de la matriz mitocondrial o el citoplasma bacteriano (Cabrera-Orefice y cols., 2014). Esta enzima no contribuye a la formación de un potencial transmembranal y es codificada en genoma nuclear (Cabrera-Orefice y cols., 2014; Stenmark y cols., 2003). La respiración de la oxidasa alterna es insensible a inhibidores de los complejos III y IV (Tabla 2), pero es inhibida por alquilgalatos y derivados del ácido hidroxámico (Schonbaum y cols., 1971).

En medios aeróbicos, las oxidasas terminales tienen preferencia por el oxígeno como aceptor terminal. Sin embargo, en medios anaeróbicos en donde no hay oxígeno, se pueden utilizar nitratos, nitritos, fierro, óxidos de azufre, dióxido de carbono, fumarato, etc. como el aceptor final de electrones (Anraku, 1988; Zannoni, 2008).

Tabla 2. Componentes de la cadena respiratoria clásica de mamífero, levadura y bacteria.

	Especie	**T/M**	**Peso molec. (≈kDa)**	**Grupos prostéticos**	**Inhibidores**	**Referencias**
C I	Mamífero (BHM)	43/7	1000	FMN/ 7(Fe-S)	Rotenona, amital, piericidina A	(Carroll y cols., 2003; Degli Esposti, 1998; Walker, 1992; Zhu y cols., 2016)
	Y. lipolytica	42/7	960			(Kerscher y cols., 2001; Zickermann y cols., 2015)
	E. coli *T. thermophilus*, *P. denitrificans*	13-14	550			(Sazanov, 2015; Sazanov y cols., 2006; Stolpe y cols., 2004; Zickermann y cols., 2000)

C II	Mamífero (BHM)	4	123	FAD/ 3(Fe-S)/hemo tipo *b*	Malonato, carboxina.	(Hagerhall, 1997; Sun y cols., 2005; Wittig y cols., 2010)
	S. cerevisiae	4	120			(Hagerhall, 1997)
	E. coli	4	360 (T)			(Cecchini, 2003; Yankovskaya y cols., 2003)
C III	Mamífero (BHM)	11/1	482 (D)	2 hemos tipo *b* (b_H-b_L)/ 1 hemo *c1* y 1 Fe-S	Antimicina A, mixotiazol, estigmatelina	(Iwata y cols., 1998; Trumpower, 1990; Wittig y cols., 2010; Xia y cols., 1997; Zhang y cols., 1998)
	Y. lipolytica *S. cerevisiae*	9/1 10/1	458 (D) 533 (D)			(Lange y cols., 2002; Smith y cols., 2012; Solmaz y cols., 2008)
	P. denitrificans	3	122 (M)			(Yang y cols., 1986)
C IV	Mamífero (BHM)	13/3	205 (M)	-	Cianuro, CO, NO, NO_2	(Tsukihara y cols., 1996)
	Y. lipolytica *S. cerevisiae*	11/3 11/3	189 (M) 190 (M)			(Capaldi, 1990; Geier y cols., 1995; Mason y cols., 1973)
	P. denitrificans	4	130(M)			(Iwata, 1998; Schagger, 2002)
C V	Mamífero (BHM)	16/2	597 (M)		Oligomicina	(Jonckheere y cols., 2012; Watt y cols., 2010)
	Y. lipolytica *S. cerevisiae*	16/2 16/2	543 (M) 600 (M)			(Bakhtiari y cols., 1999; Davies y cols., 2012; Jonckheere y cols., 2012; Robinson y cols., 2013)
	P. denitrificans	9	530 (M)			(Garcia-Trejo y cols., 2016; Jonckheere y cols., 2012; Morales-Rios y cols., 2010; Morales-Rios y cols., 2015; Schagger, 2002; Zarco-Zavala y cols., 2014)

Abreviaciones: T/M, Subunidades totales/ subunidades codificadas en el genoma mitocondrial; (M), monómero; (D), dímero; (T), trímero; FMN, flavín mononucleótido; FAD, flavín adenin dinucleótido; CO, monóxido de carbono; NO, monóxido de nitrógeno; NO_2, dióxido de nitrógeno. BHM (Mitocondria de corazón de bovino), *Y. lipolytica* (*Yarrowia lipolytica*), *E. coli* (*Escherichia coli*), *T. thermophilus* (*Thermus thermophilus*), *P. denitrificans* (*Paracoccus denitrificans*), *S. cerevisiae* (*Saccharomyces cerevisiae*).

3.5 Cultivo de endosimbiontes/endoparásitos en hospederos artificiales

La construcción de ecosistemas artificiales análogos a relaciones simbióticas se han propuesto como modelos para estudiar la ecología y evolución de las simbiosis (Hosoda y cols., 2011b; Momeni y cols., 2011), construir sistemas endosimbionte/hospedero que faciliten la producción de compuestos útiles industrialmente (Brenner y cols., 2008; Mee y cols., 2012) y como hospederos de bacterias no cultivables como *Treponema pallidum*, el agente causal del sífilis (Stewart, 2012).

La diferencia entre un microorganismo obligado y un facultativo se define por su capacidad de crecer fuera de una célula huésped. Algunos endosimbiontes obligados se cultivan en animales infectados, y cuando se necesita cosechar, el animal muere y la bacteria se recupera. En algunos casos específicos, las bacterias se pueden alojar dentro de animales parasitados por filarias o directamente en moscas o mosquitos (artrópodos) que necesitan alimento con sangre. A pesar de que este tipo de cultivo es lo más cercano a la realidad, el cultivo de bacterias en animales ha traído muchos problemas éticos, además de altos costos de mantenimiento, bajos rendimientos bacterianos y altos riesgos de contaminación. A la fecha, muchas de las investigaciones de endosimbiontes se realizan en líneas celulares, donde no se sacrifican animales. Las líneas celulares también ofrecen la ventaja de que la variabilidad biológica es mínima en comparación con los animales, y las líneas celulares infectadas con endosimbiontes pueden almacenarse en nitrógeno líquido. Lamentablemente, las líneas celulares son sensibles a los cambios de temperatura, las concentraciones de oxígeno en la atmósfera, requieren medios suplementados costosos y una gran cantidad de material plástico desechable. Las líneas celulares tienen bajos rendimientos de biomasa en comparación con las bacterias o levaduras de vida libre, lo que significa que los rendimientos son aún más bajos.

3.5.1 Bacterias endosimbiontes de hongos

En los últimos años, el número de bacterias endosimbiontes ya sea mutualistas, comensales o parásitas encontradas en hongos ha aumentado notablemente; sin embargo, existen pocos estudios sobre la relación que puedan tener. Los casos más reportados de bacterias endosimbiontes son *Helicobacter pylori* como endosimbionte/endoparásito de *Candida sp*. (Bjorkholm y cols., 2000; Dubois y cols., 2007; Salmanian y cols., 2008; Saniee y cols., 2013a; Siavoshi y cols., 2005b;

Zendehdel y cols., 2005) y *Burkholderia sp* como endosimbionte de *Rhizopus* (Partida-Martinez y cols., 2005).

3.5.1.1 *Helicobacter pylori* como endosimbionte/endoparásito de *Candida sp*

Helicobacter pylori es una bacteria Gram negativa que coloniza la mucosa del estómago y se multiplica en los macrófagos y las células epiteliales y dendríticas. Dado que la bacteria se considera un factor importante en enfermedades como gastritis, úlcera péptica, adenocarcinoma y linfoma MALT, su infección y mecanismos patogénicos han sido ampliamente estudiados (Dubois y cols., 2007; Lamarque y cols., 2003; Montecucco y cols., 2001; Siavoshi y cols., 2005a). Se han amplificado fragmentos de los genes específicos *16S* rRNA, *cag*A, *ahp*C, *vac*A y *ure*AB de *H. pylori*, a partir de colonias de *Candida sp* aisladas de exudados faríngeos tomados de pacientes con úlcera gástrica y resultado positivo en la prueba bioquímica de la ureasa (Salmanian y cols., 2008; Saniee y cols., 2013a; Saniee y cols., 2013b; Siavoshi y cols., 2005b). El cultivo ex-vivo de *H. pylori* requiere una gran cantidad de suplementos, mientras que *Candida sp* es fácil de cultivar en condiciones de laboratorio. Si la bacteria persiste en cultivos de *Candida* en condiciones de laboratorio, se pueden cultivar grandes cantidades de bacterias.

3.5.1.2 *Burkholderia sp* como endosimbionte/endoparásito de *Rhizopus microsporus*

Un caso de una endosimbiosis mutualista bacteria-hongo es el de la bacteria *Burkholderia sp* que vive en el citoplasma del hongo *Rhizopus microsporus* (Partida-Martinez y cols., 2005) que es un parásito de las plantas de arroz. En este caso, la bacteria se encarga de sintetizar una toxina llamada rizoxina con la que facilita el parasitismo de la planta de arroz por *Rhizopus*. La rizoxina se une a la β-tubulina de las células de la planta de arroz inhibiendo la mitosis y deteniendo el ciclo celular. El tratamiento de la planta con el antibacteriano ciprofloxacina elimina a la bacteria e inhibe la producción de la toxina[30]. Si la planta es infectada por una cepa de *Rhizopus* carente de *Brukholderia*, no se observa el fenotipo infectado en la planta de arroz. Sorprendentemente, *Rhizopus microsporus* es insensible a la rizoxina, lo que sugiere que ha habido una co-evolución de estos organismos para lograr parasitar a un tercero que les dará sustento (Partida-Martinez y cols., 2007a; Partida-Martinez y cols., 2005; Partida-Martinez y cols., 2007b).

4. Planteamiento del problema

Las enfermedades transmitidas por vectores han sido poco estudiadas porque en su mayoría afectan países de tercer mundo. Estas enfermedades incluyen entre otras, a las ocasionadas por los virus del dengue, de la fiebre amarilla, del zika y del chikungunya que son transmitidas por moquitos del género *Aedes*. Como resultado del cambio climático y la facilidad de desplazamiento en el planeta, las enfermedades transmitidas por vectores están aumentando su cobertura mundial, lo que ha provocado un aumento en gastos médicos y una inversión en las estrategias para combatir dichas enfermedades. Las tres principales propuestas para erradicar estas enfermedades incluyen la creación de vacunas; la exterminación de los vectores con insecticidas, que podría causar un desequilibrio ecológico; y la posibilidad de infectar a los vectores con *Wolbachia* y evitar que los patógenos puedan colonizarlos.

A pesar de se han liberado mosquitos infectados con *Wolbachia* en diferentes regiones del mundo, no existe una legislación sobre el proceso. Sin embargo, los mecanismos de infección y permanencia de la bacteria en los hospederos permanecen desconocidos. Esto se debe a que *Wolbachia* no crece en medios axénicos. *Wolbachia* se cultiva en nemátodos que infectan conejos o en líneas celulares. Ambos cultivos son caros, difíciles de mantener y de bajo rendimiento.

Siguiendo el ejemplo de el cultivo axénico de *Coxiella*, estudiar los genomas reportados de *Wolbachia* podría ayudarnos a generar un medio de cultivo axénico constituido por elementos que sean especialmente requeridos por esta bacteria. Es decir si esta bacteria carece de las vías de síntesis de aminoácidos, se agregan estos al medio. Además los medios pueden suplementarse con elementos aerotolerantes y se pueden incubar los cultivos en atmósferas con bajas concentraciones de oxígeno para simular la atmosfera intracelular. Otra opción para aumentar la biomasa de *Wolbachia* es hacer cambios de hospedero a otras líneas celulares que crezcan mejor como la C6/C36 o a otro hospedero ya sea en huevos fecundados de pollo, que es la manera en que se crece Rickettsia o en hongos y levaduras como se ha sugerido recientemente.

Estudiar a *Wolbachia* nos facilitará el diseño de estrategias científicas viables para controlar las viremias y nos permitirá anticipar las repercusiones sobre el medio ambiente, lo que hace aún más urgente el estudio de esta bacteria.

Estudiar la interacción con su hospedero y cultivando a *Wolbachia* en mayores cantidades nos permitirá observar sí, como ha sido sugerido por varios grupos de

investigación, *Wolbachia* puede donarle ATP a su hospedero sustituyendo o suplementando la actividad de la mitocondria o si únicamente, y similar al SOPE, suplementa la actividad mitocondrial, ya sea mediante el control de la expresión mitocondrial en fases anormales del crecimiento o bien al donarle riboflavina o grupos hemo, como otros grupos han sugerido.

5. Hipótesis

Si *Wolbachia* emula las funciones de la mitocondria y es capaz de crecer y multiplicarse en el interior de un hospedero modificando el patrón de fosforilación oxidativa del sistema, debe de tener un metabolismo aerobio propio o bien debe manipular la fosforilación oxidativa del hospedero.

6. Objetivos

Determinar la actividad respiratoria de *Wolbachia* y estudiar sus efectos sobre el metabolismo aerobio del hospedero.

6.1 Objetivos particulares

- Optimizar el cultivo de *Wolbachia pipientis* ya sea en cultivos axénicos o cambiando el hospedero a una levadura.

- Estudiar la actividad respiratoria de *S. cerevisiae* en levaduras infectadas con *Wolbachia pipientis*.

- Determinar si *Wolbachia* posee una cadena respiratoria.

7. Materiales y métodos

7.1 Reactivos

Los reactivos ácido etilendiaminotetracético (EDTA), glucosa-6-fosfato, gliceraldehído-3- fosfato, glicerol, piruvato, malato, succinato, citocromo *c* de corazón de caballo, NAD^+, NADH, NADPH, ATP, n-dodecil β-D-maltósido, cloruro de azul de nitrotetrazolio (NBT), fluoruro de fenilmetilsulfonilo (PMSF), desoxicolato de sodio, ditionita de sodio, dodecil sulfato de sodio (SDS), trizma base, medio mínimo de Eagles, penicilina-estreptomicina, aminoácidos y vitaminas para MEM, L-glutamina, glucosa, perlas de vidrio, HEPES, trietanolamina, manitol, ácido 2-(N-morfolino)etanosulfónico (MES), CCCP, rotenona y antimicina A se adquirieron de Sigma Chem. Co (St. Luis Missouri, EUA). El etanol, sulfato de magnesio, cianuro de potasio, carbonato de potasio, hidróxido de potasio, cloruro de potasio, fosfato de sodio, bicarbonato de sodio y ácido succínico se adquirieron de JT Baker (Center Valley, PA, EUA). El 3,3′-hidrato de tetracloruro de diaminobenzidina (DAB) se adquirió de Fluka (Buchs, Switzerland). El persulfato de amonio, la glicina, la acrilamida y la bis N,N′-metilen-bis-acrilamida se adquirieron de BioRad (California, EUA). El imidazol y el ácido amino-caproico se adquirieron de MP (Santa Ana, CA, EUA). El sulfato de amonio se adquirió de Merck (Darmstadt, Germany); la triptona se adquirió de Difco (Franklin Lakes, NJ, EUA); y la peptona se adquirió de Bioxon (Edo de México, México). El PCR Master mix (2X) se adquirió de Thermo Scientific (Waltham, MA, EUA). La Taq polimerasa utilizada fue de Fermentas (adquirida por Thermo Scientific, Waltham, MA, EUA). La leche en polvo sin grasa se adquirió de Santa Cruz Biotechnology (Dallas, Texas, EUA). El suero bovino fetal (SBF) se adquirió de Biowest (Riverside – MO, EUA). El citrato férrico y el hidróxido de sodio fueron de Meyer (Vallejo, CA, EUA). El azul de Coomassie G se adquirió en Serva (Heidelberg, Alemania).

7.2 Anticuerpos Primarios

Los anticuerpos Anti-wsp (Proteína de superficie de *Wolbachia*) monoclonales producidos *in vitro* en ratón, NR-31029 fueron donado por BEI Resources, NIAID, NIH. La dilución empleada fue de 1:1000 en TBS-T (Tris 50 mM, NaCl 150 mM, Tween 20 0.1%, pH 7.4). Los anticuerpos Anti-VDAC monoclonales producidos en

ratón fueron comprados a Jackson Immunoreasearch (West Grove, PA, EUA). La dilución empleada fue 1:1000 en TBS-T.

7.2.1 Anticuerpos Secundarios

Los anticuerpos secundarios anti-IgG de ratón acoplados a peroxidasa de rábano fueron de Jackson ImmunoResearch (West Grove, PA, EUA) y se empleó en una dilución 1:10,000 en TBS-T.

7.3 Material Biológico

La línea celular Aa23 (*Aedes albopictus* infectada con la cepa de *Wolbachia w*AlbB (O'Neill y cols., 1997)) fue donada por la Dra. Ann Fallon de la Universidad de Minnesota, EUA.

Las cepas de *Saccharomyces cerevisiae* utilizadas en este trabajo fueron: BY4741 (*Sc*BY) (MATa; his3 Δ1; leu2 Δ0; met15 Δ0; ura3 Δ); W303 (*Sc*W303) (MATα; ura3-1; trp1Δ 2; leu2-3,112; his3-11,15; ade2-1; can1-100), donada por el Dr. Michel Rigoulet, del Institut de Biochimie et Génétique Cellulaires (IBGC), Université Victor Segalen; Bordeaux 2, Bordeaux, Francia. La cepa W303 rho^0 (*Sc*W303 rho^0) (MATα; ura3-1; trp1Δ 2; leu2-3,112; his3-11,15; ade2-1; can1-100; rho^0) donada por el Dr. Gabriel del Río, del Departamento de Bioquímica y Biología Estructural del Instituto de Fisiología Celular, UNAM. Las cepas 273-10B (MATα; leu2, arg8::hisG, ura3-52; leu2-3,112) y 273-10B rho^0 fueron donadas por la Dra. Xóchitl Pérez Martínez, del Departamento de Genética Molecular del Instituto de Fisiología Celular, UNAM.

La línea celular C6/C36 fue donada por el Dr. Cuauhtémoc Juan Humberto Lanz Mendoza del Instituto Nacional de Salud Pública, Cuernavaca, Morelos, México.

Las mitocondrias de corazón de bovino (BHM) fueron donadas por la Dra. Marietta Tuena Sangri del Departamento de Bioquímica y Biología Estructural del Instituto de Fisiología Celular, UNAM.

7.4 Mantenimiento y cultivo de las líneas celulares Aa23 y C6/C36

Las líneas celulares se cultivaron en medio mínimo de Eagle (MEM) de Sigma Chemical Co (M0643) complementado con aminoácidos no esenciales, L-glutamina, vitaminas, D-glucosa, antibióticos y bicarbonato de sodio (Shih y cols., 1998), pH 6.8 (HCl o NaOH). Los medios se esterilizaron por filtración (Millipore, 0.22 μm) y se

guardaron en alícuotas de 200 mL a 4°C. Previamente a ser utilizados, el medio se descongeló y se agregó 10% de suero bovino fetal (SBF) inactivado (30 min a 56°C) (Shih y cols., 1998). Las líneas celulares se cultivaron en cajas Petri True Line TR 4003 de 150 mm a 27°C en una atmósfera de 5% de CO_2 (incubadora de cultivos celulares ESCO). Las líneas se resembraron con una dilución de 1:10 cada vez que se alcanzaba el 100% de confluencia. La cantidad de células se cuantificó con azul de tripano 0.4% (1:1) en una cámara de Neubauer. Las células vivas no se tiñen, mientras que las células cuya membrana está dañada se tiñen de azul.

Alícuotas de las líneas celulares concentradas a 1 x 10^8 células/mL se mantuvieron a -80°C en MEM adicionado con 20% SBF y 40% DMSO estéril. El glicerol, comúnmente utilizado para congelar la levadura, no mantiene las líneas celulares viables. Para resembrar las células a partir de una alícuota en congelación, deben descongelarse en agua tibia y colocarse en un frasco de Roux con MEM y SBF al 20%. Después de 5 horas de incubación a 27°C en una atmosfera de 5% CO_2, el medio debe cambiarse, ya que el DMSO puede ser tóxico (Scientific, 2017).

Al principio del proyecto no se tenía incubadora de CO_2, por lo que se adicionó 20 mM de HEPES y se disminuyó la concentración de bicarbonato de sodio del 0.22% al 0.085% para evitar la alcalinización del medio. El MEM tiene rojo neutro como colorante: en un medio alcalino se torna morado, mientras que en un medio ácido se torna amarillo. El pH ideal se mantiene entre color naranja y anaranjado.

Para transportar las líneas celulares, deben resembrarse 1:2 en un frasco de Roux de 25 cm^2 de tapa no ventada. Las células se incuban a 27°C por un día en MEM, 20% SBF. Al día siguiente se adiciona un volumen de MEM, 5% SBF que llene el frasco, se cierra, se sella con parafilm y está listo para transportarse. Se reduce la cantidad de SBF para limitar el crecimiento de la línea celular.

7.4.1 Aa23Δw: Eliminación de *Wolbachia* de la línea celular Aa23

Wolbachia se eliminó de la línea celular Aa23 mediante pases seriales utilizando 10 μg/mL de tetraciclina (Dobson y cols., 2002) en el medio de cultivo Eagles. Los pases de la línea celular se realizaban cada semana en un volumen final de 6 mL (caja petri de 60 mm de diámetro) y se incubaban igual que la línea celular Aa23. A partir del décimo pase el cultivo se considera libre de *Wolbachia*. La eliminación de *Wolbachia* se confirmó por PCR y Western blot. Para realizar experimentos con esta línea celular, se

debe eliminar la tetraciclina por dos pases por lo menos, ya que este antibiótico afecta el metabolismo de la célula (Ballard y cols., 2007).

7.5 Infección de *Saccharomyces cerevisiae* con *Wolbachia* extraída de la línea celular Aa23

Se infectaron diferentes cepas de la levadura *Saccharomyces cerevisiae* con *Wolbachia* extraída a partir de la línea celular Aa23. Todos los procedimientos se realizaron en esterilidad y a temperatura ambiente. La línea celular Aa23 se cultivó en frascos de Roux (Corning, 225cm^2) en medio Mínimo de Eagle (MEM) complementado con 10% SBF durante 20 días a 27°C y una atmósfera de 5% CO_2. Las células se resuspendieron manualmente y se centrifugaron a 3,000 x g por 5 minutos. El paquete celular (1 x 10^7 células) se resuspendió en 10 mL de MEM con perlas de borosilicato estériles de 0.710-3 mm y se lisó agitando en el vórtex por 10 minutos. El lisado se centrifugó a 3,000 x g por 5 min para remover las células intactas. El sobrenandante se filtró por una membrana de 2.7 μm y se centrifugó a 16,500 x g por 10 minutos (Rasgon y cols., 2006). El botón se resuspendió en medio Mitsuhashi-Maramorosch (MM) (Dale y cols., 1999) suplementado con 20% SBF (MMS) y se agregó directamente a un botón de la levadura deseada cultivada en 50 mL de YPD durante 3 horas, a 250 rpm, 30°C. La levadura se concentró por centrifugación a 3,000 x g por 3 min (aprox. 60 mg). El botón de levadura se resuspendió con la bacteria y se centrifugó a 700 xg durante una hora a temperatura ambiente para favorecer el contacto entre la bacteria y la levadura(Noda y cols., 2002). El botón se resuspendió en el mismo medio, se plaqueó en MMFeS adicionado con 2% agar y 25% de eritrocitos de humano (MMSS) y se incubó a 27°C en una atmósfera de 5% CO_2 por 14 días. Posteriormente la levadura infectada se pasó a cajas de YPD suplementadas con 1 mM citrato de amonio férrico. La levadura se congeló en MM con 20% SBF y 40% glicerol y se mantuvo a -80°C.

7.5.1 Infección de *Saccharomyces cerevisiae* con *Wolbachia* extraída de levadura

Se cultivó la levadura infectada con *Wolbachia* en cajas Petri de 245 mm en MMSS (sólido) a 27°C en una atmosfera de 5% CO_2 por 14 días. Las células se concentraron a 3,000 xg por 5 minutos, se lavaron 2 veces con agua destilada y se resuspendieron en MM. Las células se lisaron con perlas de borosilicato de 0.5-3 mm; se centrifugaron a 3,000 xg por 10 minutos, el botón se filtró a través de membranas de

0.8, 0.65 y 0.45 μm, y se centrifugó a 16,500 x g por 10 minutos. El botón se resuspendió en 2 mL de MMSS y se agregó a un botón de *S. cerevisiae* previamente incubado por 3 horas en YPD, 250 rpm, 30°C. El protocolo de infección continuó como el indicado en el inciso anterior (7.5). El MM puede sustituirse por YPD y *Wolbachia* es incapaz de mantenerse en la levadura si el medio no está adicionado con al menos 1% SBF.

Se usaron paquetes de sangre caduca donados por el Instituto Nacional de Cardiología. El paquete de eritrocitos de humano se obtuvo centrifugando la sangre a 3,000 x g por 2 minutos.

7.6 Mantenimiento de diferentes cepas de *Saccharomyces cerevisiae* infectadas con *Wolbachia*

Las diferentes cepas de *S. cerevisiae* infectadas con *Wolbachia* se mantuvieron en cajas de YPD con 2% de agar a temperatura ambiente en una atmosfera de 5% de CO_2. El inóculo de las cepas infectadas se realizó en un mL de YPD, 1 mM citrato férrico amoniacal y 20% de suero bovino fetal. La levadura infectada se resembró cada mes agregando 2 mL de YPD adicionado con 20% SBF. La infección es estable entre 4 y 6 meses. Para un litro de medio MMSS se utilizaban 200 mL de SBF y 250 mL de paquete de eritrocitos humanos, lo que elevaba el costo de los cultivos. Se redujo la cantidad de SBF a 10, 5 y 1% gradualmente. Los medios no suplementados con SBF no mantienen el crecimiento de *Wolbachia*. Se agregó al medio 1 mM de Citrato Férrico amoniacal, este no debe exceder de 4 mM ya que es tóxico.

7.7 Cultivo de *Saccharomyces cerevisiae* en medio líquido (infectadas y no infectadas con *Wolbachia*)

Los precultivos se sembraron a partir de una asada del cultivo sólido (YPD con 2% agar) en 100 mL de YPDS (YPD , 1% SBF, 1 mM citrato férrico amoniacal) estéril y se incubaron a 30°C, 130 rpm por 48 horas. Los precultivos se trasvasaron a un litro (1:10) de YPDS que se incubó a 30°C, 130 rpm por 14 días.

7.8 Comprobación de la presencia de *Wolbachia* en los diferentes tipos celulares

Una vez cultivada la línea celular y las distintas cepas de *S. cerevisiae* la presencia de la bacteria se monitoreó siguiendo los siguientes protocolos:

7.8.1 Confirmación de la presencia de *Wolbachia* por PCR del gen *wsp*

Para obtener una mejor amplificación de los fragmentos del gen *wsp* a partir de las líneas celulares y de los cultivos de levadura, se obtuvo el DNA de *Wolbachia* de la siguiente manera: Se concentraron el equivalente a 50 mL de *wSc*W303 y por lo menos 1 x 10^8 células (línea de insecto Aa23). Éstas se resuspendieron en buffer SPG (Sacarosa 218 mM, KH_2PO_4 3.8 mM, K_2HPO_4 7.2 mM, L-glutamato 4.9 mM, pH 7.2) y se rompieron en el vórtex utilizando perlas de 0.5 mm para la levadura o 3 mm para la línea celular. Se realizaron dos ciclos de 5 minutos. Posteriormente se centrifugaron a 3,000 xg 5 min. para eliminar las células intactas. Se incubaron durante 30 minutos a 37°C con 30 µg/mL de DNAsa para remover el DNA del hospedero. La bacteria se concentró a 16,000 x g durante 5 minutos y se lavó dos veces en buffer SPG para remover la DNAsa (Iturbe-Ormaetxe y cols., 2011). Las muestras se calentaron durante 5 minutos a 95°C para inactivar cualquier DNAsa remanente. Finalmente se extrajo el DNA utilizando el Quick-gDNA MiniPrep (Zymo Research, D3025) siguiendo las instrucciones del proveedor.

Se utilizaron los oligonucleótidos para la proteína de superficie de *Wolbachia* sp: wsp81f (5′ TGGTCCAATAAGTGATGAAGAAAC 3′) y wsp691r (5′ AAAAATTAAACGCTACTCCA 3′) (Zhou y cols., 1998). El fragmento se amplificó usando una Taq polimerasa (Fermentas/Thermoscientific) bajo las siguientes condiciones: un ciclo de desnaturalización inicial a 94°C por 2 minutos; 30 ciclos de desnaturalización a 94°C por un minuto, hibridación a 52°C un minuto y extensión a 72°C un minuto; un ciclo de extensión final a 72°C por 5 minutos. Se cargaron las muestras en un gel de agarosa al 1% y se corrieron a 90 mV en medio TAE (1 lt de TAE 50X: se prepara con 242 g de Tris base, 18.61 g de EDTA, 57.1 mL de ácido acético glacial y se afora a un litro con agua destilada) en una cámara de electroforesis de BIO-RAD hasta que el frente de corrida alcanzara el final del gel

Se utilizaron 3 µL de la escalera 1 Kb plus (Invitrogen) como marcador de pesos moleculares. Se tiñó con bromuro de etidio. La banda debe corresponder aproximadamente a 590-632 pb dependiendo de la especie (Zhou y cols., 1998). Los productos de PCR se purificaron utilizando el GeneJET PCR Purification kit, (ThermoScientific), se resuspendieron en agua libre de DNAsas y RNAsas y se secuenciaron en la unidad de Biología Molecular del Instituto de Fisiología Celular, UNAM.

7.8.2 Western Blot para la proteína wsp

Se resuspendió una asada de levadura a partir de medio sólido en 200 µL de agua, o se tomaron directamente 200 µL de muestra de cultivo y se centrifugaron a 3,000 x g por 5 minutos. Se lavó dos veces y se solubilizó con 200 µL de buffer RIPA (Tris•HCl 25 mM pH 7.6, NaCl 150 mM, nonidet P40 1%, deoxicolato de sodio 1%, SDS 0.1%) suplementado con el inhibidor de proteasas complete 1X y PMSF 1 mM. Las muestras se sonicaron en un sonicador Sonics VibraCell a 80% de amplitud por 10 segundos y se agitaron 30 minutos a 4°C. Las muestras se centrifugaron a 12,700 x g por 5 min. Se recuperó la fracción soluble y se cuantificó la concentración de proteína por el método de Bradford en un PolarStar Omega (BMGlabtech) (ver Sección 7.13.2). Se agregó buffer de carga a la muestra (Buffer de carga 3X, ver sección 7.19) y se calculó el volumen necesario para aplicar 20-30µg de proteína por carril. Las muestras deben hervirse durante 5 minutos antes de cargarse en el gel (ver Sección 7.8.2.1). Se realizó una SDS/PAGE en un gel de poliacrilamida al 10% y se corrió a 100 mV en buffer de corrida.

Las proteínas del gel se transfirieron a una membrana de fluoruro de polivinilideno (PVDF) previamente activada en metanol y lavada en buffer de transferencia (fosfato de potasio 25 mM, fosfato de sodio 25 mM, Tris 12 mM, glicina 192 mM, ajustado a pH 7.0) con 20% metanol, por 10 min. Las membranas se bloquearon con 5% de leche en polvo sin grasa Blotto en TBS-T por 1 h, y se dejaron incubando toda la noche a 4°C con el anticuerpo primario anti-wsp. Las membranas se lavaron con TBS-T tres veces por 5 minutos y se incubaron a 37°C por 1 h con el anticuerpo secundario de ratón. Las membranas se lavaron tres veces por 10 minutos con TBS-T con un kit de quimioluminiscencia ECL (Chiquete-Felix y cols., 2009).

7.8.2.1 Geles para SDS-PAGE

Para cada gel SDS-PAGE al 10% se prepararon 10 mL de la siguiente solución: 4 mL de agua destilada, 3.3 mL de acrilamida/bisacrilamida al 30%/1%, 2.5 mL de Tris 1.5 M pH 8.8, 0.1 mL de SDS 10%, 0.1 mL de persulfato de amonio 10% y 0.004 mL de TEMED (Laemmli, 1970; Schägger, 1994). La solución se agitó y se vertió en medio de los vidrios previamente montados. Se agregó 1 mL de etanol lentamente para que la superficie quedara uniforme. Después de polimerizado (aprox. 15 min.), se retiró el etanol y se agregó la solución concentradora previamente preparada. Se agregó para 3 mL de volumen final, 2.1 mL de agua destilada, 0.5 mL de acrilamida/bisacrilamida al

30%/1%, 3.8 mL de Tris 1 M pH 6.8, 0.03 mL de SDS 10%, 0.03 mL de persulfato de amonio 10% y 0.003 mL de TEMED previamente mezclados en un tubo Falcon.

Preparación de las soluciones necesarias para los geles SDS-PAGE:

Tris/HCl 1.5 M pH 8.8. Para 100 mL, se disolvieron 18.15 g de Tris en 50 mL de agua destilada. Se ajustó el pH a 8.8 con HCl y se aforó a 100 mL.

Tris/HCl 1 M pH 6.8. Para 100 mL, se disolvieron 12.1 g de Tris en 50 mL de agua destilada. Se ajustó pH a 8.8 con HCl y se aforó a 100 mL.

Acrilamida/bisacrilamida 30%/1%. Para 100 mL, se disolvieron 29.2 g de acrilamida y 0.8 g de bisacrilamida en 100 mL de agua destilada. La acrilamida es neurotóxica por lo que se usaron guantes de nitrilo durante toda la manipulación.

Persulfato de amonio 10%: Para 5 mL se disolvieron 0.5 g de persulfato de amonio en agua destilada y se alicuotaron en volúmenes de 1 mL. Esta solución se guardó en congelación.

Buffer de muestra 3X: Para 10 mL se pesaron 0.36 mL de Tris/HCl 1M pH 6.8 (36 mM), 3 mL de glicerol 50%, 1.2 mL de SDS 10%, 0.3 mL de β-mercaptoetanol, 0.06% de azul de bromofenol y se aforó con 5.14 mL de agua destilada.

Buffer de corrida: Para 1 litro 10X, se pesaron 30 g de Tris, 144 g de glicina, 10 g de SDS y se aforó a un litro.

Tabla 3. Soluciones para preparar los geles SDS-PAGE (Laemmli, 1970; Schägger, 1994)

Gel separador

	5ml	10 ml	15 ml	20 ml	25ml	30 ml	40 ml	50 ml
6%								
H_2O	2.6	5.3	7.9	10.6	13.2	15.9	21.2	26.5
Acril/bisacril 30%/1%	1	2	3	4	5	6	8	10
Tris 1.5 M pH 8.8	1.3	2.5	3.8	5	6.3	7.5	10	12.5
SDS 10%	0.05	0.1	0.15	0.2	0.25	0.3	0.4	0.5
APS 10%	0.05	0.1	0.15	0.2	0.25	0.3	0.4	0.5
TEMED	0.004	0.008	0.012	0.016	0.02	0.024	0.032	0.04
8%								
H_2O	2.3	4.6	6.9	9.3	11.5	13.9	18.5	23.2
Acril/bisacril 30%/1%	1.3	2.7	4	5.3	6.7	8	10.7	13.3
Tris 1.5 M pH 8.8	1.3	2.5	3.8	5	6.3	7.5	10	12.5
SDS 10%	0.05	0.1	0.15	0.2	0.25	0.3	0.4	0.5
APS 10%	0.05	0.1	0.15	0.2	0.25	0.3	0.4	0.5
TEMED	0.002	0.004	0.006	0.008	0.01	0.012	0.016	0.02

10%								
H_2O	1.9	4	5.9	7.9	9.9	11.9	15.9	19.8
Acril/bisacril 30%/1%	1.7	3.3	5	6.7	8.3	10	13.3	16.7
Tris 1.5 M pH 8.8	1.3	2.5	3.8	5	6.3	7.5	10	12.5
SDS 10%	0.05	0.1	0.15	0.2	0.25	0.3	0.4	0.5
APS 10%	0.05	0.1	0.15	0.2	0.25	0.3	0.4	0.5
TEMED	0.002	0.004	0.006	0.008	0.01	0.012	0.016	0.02
12%								
H_2O	1.6	3.3	4.9	6.6	8.2	9.9	13.2	16.5
Acril/bisacril 30%/1%	2	4	6	8	10	12	16	20
Tris 1.5 M pH 8.8	1.3	2.5	3.8	5	6.3	7.5	10	12.5
SDS 10%	0.05	0.1	0.15	0.2	0.25	0.3	0.4	0.5
APS 10%	0.05	0.1	0.15	0.2	0.25	0.3	0.4	0.5
TEMED	0.002	0.004	0.006	0.008	0.01	0.012	0.016	0.02
15%								
H_2O	1.1	2.3	3.4	4.6	5.7	6.9	9.2	11.5
Acril/bisacril 30%/1%	2.5	5	7.5	10	12.5	15	20	25
Tris 1.5 M pH 8.8	1.3	2.5	3.8	5	6.3	7.5	10	12.5
SDS 10%	0.05	0.1	0.15	0.2	0.25	0.3	0.4	0.5
APS 10%	0.05	0.1	0.15	0.2	0.25	0.3	0.4	0.5
TEMED	0.002	0.004	0.006	0.008	0.01	0.012	0.016	0.02

Gel concentrador (5%)

	1 ml	2ml	3 ml	4 ml	5 ml	6 ml	8 ml	10 ml
H_2O	0.68	1.4	2.1	2.7	3.4	4.1	5.5	6.8
Acril/bisacril 30%/1%	0.17	0.33	0.5	0.67	0.83	1	1.3	1.7
Tris 1 M pH 6.8	0.13	0.25	0.38	0.5	0.68	0.75	1	1.25
SDS 10%	0.01	0.02	0.03	0.04	0.05	0.06	0.08	0.1
APS 10%	0.01	0.02	0.03	0.04	0.05	0.06	0.08	0.1
TEMED	0.001	0.002	0.003	0.004	0.005	0.006	0.008	0.01

7.8.2.2 Western Blot para VDAC

Los extractos, los geles y la transferencia se realizaron de la misma manera que en la sección 7.8.2. La cantidad de anticuerpos primarios y secundarios se ajustó según lo recomendado por los proveedores, reportado en la sección 7.2. Para poder utilizar varios anticuerpos en una misma membrana y poder estandarizar los datos, se desnudaron (eliminar los anticuerpos) y se re-probaron las membranas.

7.8.2.3 Desnudar y reutilizar membranas

Las membranas se desnudaron y se reutilizaron de acuerdo con el protocolo de Abcam. En resumen, las membranas se lavaron tres veces de 5 a 10 minutos a temperatura ambiente con buffer de desnudamiento (glicina 1.5%, SDS 0.1%, Tween 20 1%, pH

2.2). Posteriormente se realizaron dos lavados de 10 minutos con PBS y dos lavados de 5 minutos con TBS-T. Las membranas sin anticuerpos se bloquearon de nuevo (1 h con leche en polvo sin grasa) antes de agregar el nuevo anticuerpo primario.

7.8.3 Hibridación *in-situ* con sondas fluorescentes

Wolbachia se visualizó utilizando sondas específicas de oligonucleótidos diseñadas contra el gen 16S rDNA marcadas con Quasar 670 (Abs 647 nm, Em 670 nm) : W1, 5´-AATCCGGCCGARCCGACCC-3´ (Heddi y cols., 1999). Un mililitro del cultivo de levadura se centrifugó a 3,000 x g por 5 minutos. Para las líneas celulares se ajustó la concentración a 1 x 10^6 células/mL y se lavaron dos veces con PBS. Las células se resuspendieron en 3% de p-formaldehído en PBS y se incubaron una hora a 4°C. Las muestras se lavaron tres veces con PBS y se mantuvieron a 4°C para su posterior hibridación. En caso de hacer la hibridación en un portaobjetos, se colocó una alícuota (10 µL) de las muestras en portaobjetos y se dejó secar entre 24 y 48 horas. Los portaobjetos estaban recubiertos de poli-L-lisina. La muestra se esparció en el portaobjetos tratando de hacer una monocapa, si estaba muy concentrada no podía observarse correctamente. Después de fijar las muestras, se deshidrataron durante 3 minutos con etanol 50%, 80% y 90% consecutivamente. Se agregaron 50 µL de cada sonda (30 ng/µl) en buffer de hibridación (NaCl 0.9 M, formamida 35%, Tris-HCl 20 mM, pH 8, triton X-100 al 0.01%) y se incubó 2 horas en un cuarto obscuro a 46°C. Las muestras se lavaron dos veces durante 15 minutos con Tris-HCl 20 mM, NaCl 70 mM, EDTA 5 mM pH 8 y tritón X-100 al 0.01% en un cuarto obscuro a 48°C (Genty y cols., 2014). Las muestras se observaron en un microscopio confocal Olympus FV-10000 con una potencia del 5% de láser (rojo). Quasar 670 es un fluoróforo cuyos máximos de emisión/excitación se encuentran a 640/670 nm respectivamente.

7.9 Tinción de las levaduras con calcoflúor y FISH

Después de hibridar las muestras con la sonda 16S rDNA marcada con Quasar 670, las muestras se tiñeron con 0.05 mM de calcoflúor en DMSO-20% y bicina 20 mM. El espectro de excitación/emisión del calcoflúor se encuentra en 380-440/500-520 nm respectivamente. El calcoflúor se une al quitosano de la pared celular de la levadura. Se realizaron cortes en Z de las muestras en un microscopio Olympus-FV1000 o FV-3000. Las imágenes se reconstruyeron usando el software Imaris 7.2.1 e Image J.

7.10 Microscopía Electrónica de Transmisión

Se colectaron las células a partir de 500 µL de cultivos de levadura infectada y control a 14 días, y se tomó una pequeña muestra del aislado de *Wolbachia*. Las células de levadura se lavaron dos veces en agua destilada a 3,000 x g por 5 min, mientras que la muestra de bacteria aislada se lavó a 16,000 x g por 5 min y se trataron de acuerdo a (Sun y cols., 2015). Las muestras se fijaron en 2% de $KMnO_4$ a 4°C durante toda la noche. Al día siguiente se lavaron durante 15 minutos con agua desionizada 6 veces y se deshidrataron con lavados secuenciales de 10 minutos con etanol 50%, 70%, 80%, 90% y tres lavados con etanol 100%. Posteriormente la muestra se lavó con etanol-acetona (1:1) durante 8 minutos, después con acetona anhidra durante 5 minutos, después con acetona-EPON 821 (3:1) durante 1 hora y se dejaron en acetona -EPON 821 (1:3) toda la noche.

Al siguiente día, las muestras se concentraron y se resuspendieron en acetona - EPON 821 (1:1) durante 1 hora. Las muestras se concentraron de nuevo y se dejaron en la resina pura durante 24 horas. Después de este período, se incubaron durante 12 horas a 37°C y después por 36 horas a 60°C. Las muestras se cortaron a 70 nm en un ultra-microtomo (Ultracut Reicheit-jung) y se observaron en un microscopio electrónico de transmisión JEOL JEM-1200 EXII . Las fotografías se procesaron utilizando el Software Gatan Digital Micrograph.

Ningún protocolo que implicara la fijación de las levaduras con p-formaldehído o glutaraldehído permitió la clara observación de las mitocondrias y las bacterias.

7.11 RT-qPCR

Se tomaron 0.5 mL de muestra de cultivos de levadura a diferentes días. La muestra se concentró a 3,000 x g por 5 min y se lavó dos veces en agua destilada libre de RNAsas y DNAsas. Se obtuvo el RNA de la muestra utilizando el kit Quick-RNA MiniPrep Kit (Zymo Research). El cDNA de sintetizó a partir de 1 µL de RNA con el kit Revert Aid First Strand cDNA (ThermoFischer).

El qPCR para el gen *wsp* de *Wolbachia* se realizó de acuerdo con (Tortosa y cols., 2008): 50 ng de cDNA se corrieron con 0.5 µM de cada oligonucleótido utilizando 2X SYBR Green PCR Master Mix en un termociclador BioRad CFX96 Real-Time System. Los oligonucleótidos utilizados fueron específicos para *w*AlbB: 183F (5′-AAGGAACCGAAGTTCATG-3′) y QBrev2 (5′-AGTTGTGAGTAAAGTCCC-3′). El programa del termociclador incluía un paso de desnaturalización inicial de 10 minutos a

95°C para activar la enzima; 40 ciclos de 15 s a 95°C, 1 min a 60°C y 30 s a 72°C (Zouache y cols., 2012).

Para el gen 18S rRNA de *S. cerevisiae* se siguió el siguiente protocolo (Lu y cols., 2003): 50 ng de cDNA se corrieron con 0.3 μM de cada oligonucleótido en presencia de 2X SYBR Green PCR Master Mix en un termociclador BioRad CFX96 Real-Time System. Los oligonucleótidos empleados fueron: 18f (5′-CGGCTACCACATCCAAGGAA-3′) y 18r (5′-GCTGGAATTACCGCGGCT-3′). El programa incluye un paso a 95°C por 10 minutos, 40 pasos a 95°C por 15 s y 60°C por un minuto. Se corrieron duplicados de tres experimentos independientes. Todos los oligonucleótidos fueron sintetizados por Sigma-Aldrich Co (Saint Louis, MO). El cambio de fluorescencia del SYBR Green I Dye de cada ciclo se monitoreó en el software y se utilizó el Cq para calcular el número de transcritos de *Wolbachia wsp* y de *S. cerevisiae*. El kit 2X SYBR Green PCR Master Mix posee una enzima que necesita un ciclo de 10 minutos a 95°C para evitar que los oligonucleótidos dimericen.

7.12 PCR para el gen 5.8S rDNA de levadura

De las diferentes cepas de levadura se extrajo el DNA con el kit quick-gDNA mini-prep, Zymo Research. Se utilizaron los siguientes oligonucleótidos específicos ITS1 (5′ TCCGTAGGTGAACCTGCGG 3′) y ITS4 (5′ TCCTCCGCTTATTGATATGC 3′) (White, 1990). El fragmento se amplificó usando Taq polimerasa (Fermentas/Thermo Scientific) bajo las siguientes condiciones: un ciclo de desnaturalización inicial a 94°C por 5 minutos; 40 ciclos desnaturalización a 94°C por un minuto, hibridación a 52°C por 2 minutos y extensión a 72°C por 2 minutos; un ciclo de extensión final a 72°C por 10 minutos. Se corrieron las muestras en un gel de agarosa al 1% usando el marcador 1Kb plus (Invitrogen), teñido con bromuro de etidio. La banda debe pesar aproximadamente 800 pb para *S. cerevisiae* (White, 1990). El producto de PCR se purificó (GeneJET PCR Purification kit, ThermoScientific), se resuspendió en agua y se secuenció en la unidad de Biología Molecular del Instituto de Fisiología Celular, UNAM.

7.13 Determinación de proteína

Para determinar la cantidad de proteína presente se utilizaron dos métodos:

7.13.1 Determinación de proteína por Biuret

La concentración de proteína de una muestra de células o de mitocondrias se determinó por medio del método de Biuret (Gornall y cols., 1949). Para prepara el reactivo de Biuret se prepara la solución A: 100 mL de solución de $CuSO_4$ al 17.3% en agua caliente; y la solución B: 17.3 g de citrato sódico y 100 g de Na_2CO_3 disueltos en 800 mL de agua caliente. Posteriormente se mezclan las soluciones y se guardan en obscuridad.

En un tubo de vidrio se añaden 62.5 μL de desoxicolato de sodio 5%, 175 μL de agua, un mL de solución de Biuret y 12.5 μL de la suspensión de mitocondrias o células. El cambio de absorbancia se determinó a 540 nm en un espectrofotómetro Beckman DU-50. El cambio en la absorbancia se debe a que la interacción del ion Cu^{2+} con los enlaces peptídicos de la proteínas genera una coloración violeta, proporcional a la concentración de la proteína en la muestra.

7.13.2 Determinación de proteína por Bradford

La concentración de proteína de una muestra de células lisadas o de un extracto proteico se determinó por el método de Bradford. A diferencia del método de Biuret, este método no posee ningún agente para solubilizar las membranas celulares como el desoxicolato de sodio. Las determinaciones se realizaron en placas de Elisa de 96 pozos. Primero, se realizó una curva patrón de 0, 2, 3, 4 y 6 μg de proteína utilizando un patrón de 1mg/ml de γ-globulina y se llevó a un volumen final de 20 μL. En los siguientes pozos se adicionaron 2.5-5μL de la muestra problema y se llevó a un volumen final de 20 μL. Después se adicionaron 180 μL de reactivo de Bradford (1:5). Se incubó la placa 15 minutos a temperatura ambiente y se leyó la absorbancia a 590 nm en un PolarStar Omega (BMG labtech) (Bradford, 1976). Se obtuvieron los valores de proteína de las muestras haciendo una regresión lineal de la curva patrón.

7.14 Curvas de crecimiento de *Saccharomyces cerevisiae* W303 y BY4741

Se sembraron precultivos de 48 horas de *Saccharomyces cerevisiae* en 30 mL de YPD (2%) o YPgal (2%), agitando a 130 rpm. Se determinó la densidad óptica del cultivo y se resembró en 100 mL a una densidad óptica final de 0.05 aproximadamente. Los medios se incubaron a 28°C, 130 rpm. Se determinó la absorbancia a 600 nm con un espectrofotómetro Beckman DU-50. Se utilizó la cepa BY4741 como control, porque en comparación con la cepa W303, presenta una fase diáuxica más clara.

7.15 Viabilidad celular

La viabilidad de la línea celular Aa23 y de las levaduras se evaluó usando el kit BacLight live-dead staining (Molecular Probes, Carlsbad, CA), que utiliza fluoróforos para distinguir la integridad de las membranas: el SYTO9 (verde) se une al DNA de todas las células tiñéndolas de verde mientras que el yoduro de propidio (rojo) únicamente tiñe aquellas que tengan las membranas dañadas. Por lo tanto, todas las células vivas aparecen verdes mientras que las muertas adquieren una coloración roja. A 10 µL de una suspensión celular se le agregaron 0.5 µL de SYTO9/IP preparado como indica el fabricante. Las células se visualizaron con un microscopio de epifluorescencia NIKON. El porcentaje de células vivas equivale a 100- (células muertas rojas/ total de células verdes). Filtro B-3A-Verde, excitación (420/490), emisión 520. Filtro G-2A-Rojo, excitación (535±50), emisión 590.

7.16 Ensayos de fermentación en levaduras

Se realizaron los precultivos y cultivos como se describió en la sección 7.7. A las 6, 8 y 10 horas se tomó una muestra de 5 mL del cultivo y se centrifugó a 3,000 x g por 5 minutos. Las células se resuspendieron a un volumen final de 50%. Se incubaron 0.5 mL de células en 1 mL de MES-TEA 0.1 M pH 6.0, 0.2 mL de glucosa 1 M y 2 mM de cianuro en un volumen final de 10 mL (completar con agua destilada). Las muestras se incubaron 10 minutos en agitación a 30°C. Se centrifugaron 30 s a 10,000 xg y se guardó el sobrenadante tapado y congelado.

La concentración de etanol se cuantificó con un ensayo acoplado a alcohol deshidrogenasa siguiendo la reducción del NAD^+ a 340 nm en un espectrofotómetro Aminco-Olis. La reacción se lleva a cabo en 2 mL de volumen final que contienen 0.2 mL de buffer de pirofosfato de sodio 0.1 M pH 9.0, 0.1 ml de NAD^+ (20 mg/mL), 0.1 mL de muestra y 1.8 mL de agua. La mezcla de reacción se agregó a la celda y se tomó el punto inicial (A1). Después se adicionaron 10 µL de alcohol deshidrogenasa (30 mg/mL) y se agitó durante 10-15 min. Se registró la absorbancia A2. Los cálculos se realizan como reglas de tres con la DO de una curva estándar de etanol. Como controles se cuantificaron blancos sin muestra.

7.16.1 Consumo de glucosa

Se realizaron precultivos y cultivos como está descrito en la sección 7.7. Se tomaron muestras de 1 mL a diferentes horas de cultivo y se centrifugaron a 3,000 x g por 5 minutos. Se separó el sobrenadante y se mantuvo en congelación a -80°C. Las muestras se descongelaron en hielo y la concentración de glucosa en el medio se cuantificó con un kit D-Glucose HK Assay Kit de Megzyme.

7.17 Aislamiento de la fracción mitocondrial

Después de cultivar las levaduras, se lavaron con agua destilada dos veces por centrifugación a 3,000 x g por 5 minutos y se resuspendieron en medio de extracción (Manitol 0.6 M, MES 5 mM, pH 6.8 ajustado con TEA). Se homogenizaron empleando un homogenizador (Bead beater Biospec Products) en una camisa de hielo y perlas de vidrio de 0.5 mm mediante tres pulsos de 20 segundos, con intervalos de 40 s de descanso (Gutierrez-Aguilar y cols., 2014). Posteriormente las mitocondrias se aislaron por centrifugación diferencial (Pena y cols., 1977) a 4°C utilizando una centrífuga Beckman con un rotor JA 25.5. Las muestras se centrifugaron, a 3,000 x g por 5 min para eliminar las células intactas; después el sobrenadante se centrifugó a 10,900 x g por 10 min. El botón de todos los tubos, ligeramente rojizo, se resuspendió en medio de extracción con un pincel y se concentró en un solo tubo hasta llegar a ¾ partes del volumen. Se centrifugó de nuevo a 5,000 rpm por 5 min y finalmente el sobrenadante se centrifugó a 12,000 rpm por 10 minutos. El sobrenadante se desechó y el botón se resuspendió en el sobrante de medio del tubo (700 µL).

7.18 Mediciones del consumo de oxígeno

7.18.1 Oximetría de fracción mitocondrial de *S. cerevisiae*

La concentración de oxígeno se cuantificó con un OROBOROS (Innsbruck, Austria) con un electrodo tipo Clark inmerso en una cámara de 1.5 mL con agitación a 750 rpm y 30°C. El experimento se llevó a cabo en el medio de respiración (MES 5 mM, manitol 0.6 M, ácido fosfórico 4 mM pH 6.8, KCl 10 mM, pH 6.8). Se utilizó una concentración de células de 0.5 mg/mL. Dependiendo del experimento, se añadió una concentración de 2 mM de diferentes sustratos respiratorios: NADH, etanol, succinato, glicerol-3-fosfato, piruvato-malato, glutamato. Todos los sustratos se ajustaron a un pH de 7.4-7.6. El estado fosforilante (estado III) se estimuló añadiendo ADP 400 µM. Para inducir un estado desacoplado se añadió 6 µM CCCP. Como inhibidores de los diferentes

complejos respiratorios se utilizaron para complejo I, rotenona 0.1 μM en DMSO; para NADH deshidrogenasas alternas 20 mM flavona; para complejo III, 0.1 μM Antimicina A en DMSO; y para complejo IV, 1 mM cianuro de sodio. Los valores de control respiratorio (CR) se obtuvieron calculando el cociente de la velocidad del consumo de oxígeno en estado III sobre estado IV utilizando etanol como sustrato. El análisis de los datos se realizó con el software DatLab Oroboros.

7.18.2 Actividad de la citocromo *c* oxidasa

La cuantificación de la actividad de la citocromo *c* oxidasa se realizó en las mismas condiciones que los trazos de oximetría. El ensayo se realizó en presencia de 2 μM antimicina A para inhibir al complejo III. Como donador de electrones se adicionó ascorbato 5mM (pH 7.4)-TMPD 50 μM. El ascorbato mantiene al TMPD en un estado reducido y esté último dona sus electrones al citocromo *c* soluble que es el sustrato del complejo IV. Al final del trazo se agregó 1 mM de cianuro de sodio.

7.18.3 Oximetría de la línea celular C6/C36

La respiración de la línea celular C6/C36 y *w*C6/C36 se cuantificó en un OROBOROS con un electrodo tipo Clark inmerso en una cámara de 1.5 mL con agitación a 750 rpm y 28°C. La reacción se llevó a cabo en un medio de respiración para líneas celulares (manitol 75 mM, sacarosa 25 mM, KCl 100 mM, KH_2PO_4 10 mM, $MgCl_2$ 5 mM, Tris-HCl 20 mM, pH 7.4). Las líneas celulares se incubaron 20 días, se despegaron por agitación, se cuantificaron en una cámara de Neubauer y se utilizaron 5 millones de células por cámara. Las células se resuspendieron en el medio de respiración para líneas celulares y se permeabilizaron con digitonina al 0.025% y se agregó citocromo *c* 10 μM y ADP 2 mM. Se añadió al trazo NADH 2 mM, rotenona (DMSO) 0.1 μM, succinato 2 mM, Antimicina A (DMSO) 2 μM, Ascorbato 5mM (pH 7.4), TMPD (Tetrametil-fenilen-81 diamina) 50 μM y cianuro de sodio 1 mM. El análisis de los datos se realizó con el software DatLab Oroboros.

7.19 Electroforesis en geles Nativos

Se realizó la electroforesis en geles de poliacrilamida (PAGE) (Wittig y cols., 2006) para separar y analizar las proteínas de la membrana de las mitocondrias y de *Wolbachia.* La electroforesis en geles nativos separa proteínas entre 10 kDa, hasta 10 MDa. En la electroforesis nativa las proteínas retienen su actividad enzimática, sus

estados oligoméricos y las interacciones proteína-proteína. Existen tres tipos de geles nativos: nativos azules (BN-PAGE), nativos claros (CN-PAGE) y nativos claros de alta resolución (hrCN-PAGE).

Para hacer una BN-PAGE se utiliza azul de Coomassie (Serva-blue G-250) en el amortiguador del cátodo y en la muestra. El azul de Coomassie se une a las proteínas de membrana confiriendo una carga negativa y provocando que las proteínas migren hacia el ánodo, evitando la formación de bandas barridas. La migración de las proteínas queda en función de su peso molecular. En la CN-PAGE, las proteínas migran de acuerdo con su peso molecular y su carga intrínseca, por lo que no se puede calcular el peso molecular de las proteínas, sin embargo, este tipo de electroforesis nos permite ver las interacciones proteína-proteína que no se mantienen en la BN-PAGE. La hrCN-PAGE tiene desoxicolato de sodio en el amortiguador del cátodo por lo que las proteínas migraran con carga de manera similar a los obtenidos en la BN-PAGE, con mayor resolución que los CN-PAGE y sin la coloración conferida por el azul de Coomassie de los BN-PAGE.

7.19.1 Preparación de los geles

Se realizó un gel en gradiente de acrilamida del 4 al 12%. Para poder secuenciar las bandas, todos los buffers y los geles se prepararon con agua miliQ (MilliQ®Biocell) y se utilizaron guantes para evitar contaminación por queratina.

Para un gel de 13.3 x 8.7 cm de Biorad con 1.5 mm de espesor se necesita:

Tabla 4. Preparación de geles de gradiente BN o hrCN-PAGE

	Acrilamida H 12%	**Acrilamida L 4%**	**Concentrador**
Solución AB	1.11 mL	0.39 mL	0.25
Amortiguador 3X	1.50 mL	1.50 mL	1
Glicerol 80%	1.14 mL	0.29 mL	-
Agua destilada	0.73 mL	2.30 mL	1.74
TEMED*	4.4µL	4.4µL	4.5µL
Persulfato de amonio 10%*	12µL	12µL	16µL
Volumen final	4.5	4.5	3.02

* Se añaden al final.

Solución AB: acrilamida al 48.5% y bis-acrilamida al 1.5%

Amortiguador 3X nativo: ácido ε-aminocaproico 1.5 M, bis-Tris150 mM/imidazol 75 mM, pH 7.0 (ajustado con HCl)

Glicerol al 80%

Persulfato de amonio al 10%

Para un gel de 20 x 18 cm se consideraron 18.57 mL de cada solución. La mezcla de acrilamida H se agregó en el contenedor más cercano a la salida del gradientero y la acrilamida L se agregó en el contenedor lejano a la salida del gradientero. El agitador mecánico se colocó en el lado de la acrilamida H. El agitador se colocó en velocidad 4. El TEMED y el persulfato de amonio de agregaron a cada contenedor y se abrió primero la válvula que comunica ambos compartimentos (con agitación) y después se abrió la válvula de salida. Al terminar el vaciado de los contenedores, se agregó etanol a la superficie del gel y se esperó a que polimerizara. Cada gel se realizó por separado. Finalmente se agregó la mezcla de gel concentrador en la parte superior y se dejó polimerizar con el peine necesario.

Dependiendo del tipo de gel son los amortiguadores necesarios.

7.19.2 Amortiguadores para BN-PAGE

- Amortiguador de cátodo para BN (1): tricina 50 mM, bis-Tris 15 mM (o imidazol 7.5 mM), azul de Coomassie de Serva 0.02%
- Amortiguador de cátodo para BN (2): tricina 50 mM, bis-Tris 15 mM (o imidazol 7.5 mM), azul de Coomassie de Serva 0.002%
- Amortiguador de ánodo: bis-Tris 50 mM (o imidazol 25 mM), pH 7.0 (ajustado con HCl).

Durante la corrida se utilizó primero el amortiguador BN(1) y cuando las muestras iban a la mitad del gel, se cambió por el amortiguador BN(2).

7.19.3 Amortiguadores para hrCN-PAGE

- Amortiguador del cátodo para CN: tricina 50 mM, imidazol 7.5 mM (ó bis-Tris 15 mM).
- Amortiguador del cátodo para hrCN: tricina 50 mM, imidazol 7.5 mM (ó bis-Tris 15 mM), laurilmaltósido 0.01%, desoxicolato de sodio 0.05%.

- Amortiguador el ánodo: imidazol 25 mM (ó bis-Tris 50 mM, pH 7.0 ajustado con HCl).

A diferencia de los geles azules, en los geles claros, las proteínas migran según su peso molecular y su carga intrínseca. Se prefieren los geles CN cuando las interacciones proteína-proteína son más débiles y no pueden observarse en un gel BN.

Los geles claros nativos de alta resolución (hrCN) son similares a los BN ya que al darle una carga negativa al amortiguador del cátodo con el desoxicolato, las proteínas migran de acuerdo con su peso molecular. Las ventajas de estos geles sobre los BN pueden apreciarse al medir actividades enzimáticas; al no tener un tono azulado, las actividades se observan más claras.

7.19.4 Preparación de muestras y corrida de los geles

Para los tres tipos de electroforesis nativas, las mitocondrias se solubilizaron con laurilmaltósido (LM) (2g / mg de proteína) para poder analizar los complejos mitocondriales individuales. A diferencia de la digitonina (4g / mg de proteína), el LM tiene una mayor capacidad de remover lípidos, por lo que elimina las interacciones entre complejos.

El detergente se disolvió en amortiguador de muestra (ácido ε-aminocaproico 750 mM, bis-Tris 50 mM / imidazol 25 mM pH 7.0 ajustado con HCl). Después de agregar la cantidad de detergente correspondiente, las muestras se incubaron en agitación en el cuarto frío durante 30 minutos y se centrifugaron a 17,500 rpm durante 75 minutos, o 100,000 x g durante 20 minutos. Se colectó el sobrenadante en un tubo limpio y se cuantificó la proteína por Bradford. Dependiendo del tamaño del gel y de la concentración de proteína se varío la cantidad de volumen de muestra a cargar para evitar la transferencia de muestras entre pozos. Para un gel grande se cargó un máximo de 200 µl de volumen, mientras que para un gel chico se cargó un máximo de 80 µl.

Para preparar una muestra para gel BN-PAGE, se agregó 1µl de solución de azul de Coomassie (Serva Blue-G250) al 5% en amortiguador de muestra por cada 100 µl de muestra.

Una vez preparada la muestra se cargó en los geles y se corrió a un amperaje constante de 30 mA por gel a 4°C.

7.20 Actividades en gel

Se utilizaron los geles nativos (BN, CN y hrCN-PAGE) para identificar bandas que presentaran actividad enzimática. Las determinaciones permiten distinguir cambios cualitativos en la cantidad de los complejos cuando provienen de diferentes condiciones.

7.20.1 NADH deshidrogenasa

La actividad de NADH deshidrogenasa se determinó utilizando bromuro de nitro-azul de tetrazolio o NBT que se precipita y cambia de coloración amarilla a morada al reducirse. Se utiliza para detectar actividad de complejo I, supercomplejos que tengan complejo I o NADH deshidrogenasas alternas. Para detectar la actividad se incubó el gel en un volumen de 15-30 mL (que cubriera completamente el gel) de amortiguador Tris 10 mM pH 7.0 con una concentración final de NADH de 1 mM y de 0.5mg/mL de NBT (60 mg NBT disueltos en 2.8 mL de formamida y 1.2 mL de agua) en agitación a temperatura ambiente. La actividad es visible después de 30 min. En caso de que el gel fuera BN, se destiñó después de detectar la actividad con una solución acético-metanol 1:1. Si el gel se pone en contacto con la solución desteñidora antes, la actividad desaparece.

7.20.2 Succinato deshidrogenasa

Esta tinción utiliza el mismo principio que el empleado para la NADH deshidrogenasa. En vez de utilizar NADH como sustrato se utilizó succinato a una concentración final de 5 mM (pH 6.8). Esta tinción comienza a revelarse después de varias horas en agitación.

7.20.3 Citocromo *c* oxidasa

La actividad de complejo IV se determinó utilizando 3´,5´-diaminobencidina (DAB) y citocromo *c* de corazón de caballo como donador de electrones. La forma oxidada de la diaminobencidina es color rojo; al oxidar al citocromo *c* y reducirse, se precipita y como una banda de color café. Para detectar la actividad se incubó el gel en un volumen de 15-30 mL (que cubriera completamente el gel) de amortiguador de fosfatos 50 mM pH 7.4 con 10 mg/mL de citocromo *c* y 20 mg/mL de DAB. La reacción tarda horas en ser detectada.

7.20.4 ATPasa

La actividad de hidrólisis de ATP del complejo V se detectó mediante la aparición un precipitado de fosfato de plomo. El ATP agregado se hidroliza a ADP y Pi, el cual reacciona con el nitrato de plomo formando fosfato de plomo que forma un precipitado blanco. Para detectar la actividad, el gel se incubó durante una hora en un amortiguador de incubación (glicina 270 mM, Tris 35 mM pH 8.4). Después se cambió al amortiguador de actividad (glicina 270 mM, Tris 35 mM pH 8.4, $MgSO_4$ 14 mM, $Pb(NO_3)_2$ 0.2%) y se añadió ATP 8 mM gota a gota. La reacción tarda aproximadamente media hora. En este caso, no es necesario que el complejo V se encuentre completamente ensamblado, por lo que se pueden observar muchas bandas.

7.21 Espectros diferenciales de los citocromos

Se obtuvieron los espectros de absorción de las muestras de 500 a 630 nm usando el espectrofotómetro Clarity, Olis spectrofotometer a 20°C y 900 rpm. Se utilizaron muestras de 200 µL finales a una concentración de 15 mg/mL de extracto. La primera muestra se oxidó con persulfato de amonio, se incubó 30 segundos en agitación y se cuantificó la absorbancia. La segunda muestra se incubó sin agitación, con ditionita. Después de obtener ambos espectros, el espectro oxidado se restó del espectro reducido.

El contenido de citocromos por mg de proteína se calculó utilizando los coeficientes de extinción molar. Para el citocromo $a+a_3$ (Steffens y cols., 1987), $\Delta\varepsilon_{604-630\ nm} = 24\ mM^{-1}\ cm^{-1}$; para el citocromo *b* (Berden y cols., 1970), $\Delta\varepsilon_{563-577\ nm} = 28\ mM^{-1}\ cm^{-1}$; y para el citocromo $c+c_1$ (Green y cols., 1959), $\Delta\varepsilon_{553-539\ nm} = 19.1\ mM^{-1}\ cm^{-1}$.

Concentración de citocromo (nmol/mg) = (Abs/0.8) / (Concentración de la muestra en mg/mL)(ε)(Volumen de la muestra).

7.22 Secuenciación de las bandas de proteína

Las bandas indicadas de los geles hr-CN PAGE o BN-PAGE se cortaron, se digirieron con tripsina, se separaron en una columna de HPLC Ekspertnano LC 425 (Eksigent, Redwood City CA) y se analizaron en un espectrómetro de masas MALDI-TOF/TOF 4800 Plus (ABSciex, Framingham MA) (Shevchenko y cols., 2006) en la Unidad de Genómica, Proteómica y Metabolómica, del CINVESTAV-IPN. Los espectros MS/MS generados se compararon usando el software Protein Pilot v. 4.0 (ABSciex, Framingham MA) contra las bases de datos de *Saccharomyces cerevisiae* ATCC

204508 (Uniprot, 6721 secuencias de proteína) y de *Wolbachia* (Uniprot, 47781 secuencias de proteína) usando el algoritmo Paragon.

7.23 Separación de *Wolbachia* de la fracción mitocondrial

7.23.1 Aislamiento de *Wolbachia* por gradientes

Se rompieron las células infectadas con *Wolbachia* por sonicación en buffer SPE (Baldridge y cols., 2014). Las bacterias se filtraron por membranas de 5 a 1.5 μm y se centrifugaron 10 minutos a 16,000 xg. El paquete se resuspendió en SPE y se colocó en un gradiente de sacarosa del 60 a 30%. Las células se centrifugaron a 210,000 xg por 90 min. Las fracciones se separaron, se les agregó aproximadamente 30 mL de agua y se centrifugaron a 14,000 rpm para concentrar las fracciones.

7.23.2 Aislamiento de *Wolbachia* por incubación ex vivo

El protocolo de aislamiento de *Wolbachia* se adaptó a partir de (Rasgon y cols., 2006). Un cultivo de 14 días de 100 mL de *wSc*W303 se centrifugó a 3,000 xg durante 5 minutos. El botón se lavó dos veces con agua estéril y se lisó con perlas de borosilicato estériles de 0.425-0.6 mm durante dos ciclos de 5 minutos con intervalos de 5 minutos. El lisado se centrifugó a 3,000 xg a 4°C durante 7 min para remover las células que no se rompieron. El sobrenadante se transfirió a un tubo limpio y se centrifugó a 18,400 xg por 5 minutos. El botón se resuspendió en un mL de medio mínimo de Eagle, SBF al 20% y se centrifugó a 5,000 xg por 5 minutos. El sobrenadante se filtró a través de filtros de jeringa de 2.7, 0.8, 0.65 y 0.45 μm y se incubó hasta 7 días a 27°C en una atmosfera de 5% de CO_2. Se agregaron 300 μg/mL de G418 para evitar el crecimiento de levaduras en el medio. Todos los procedimientos se realizaron en condiciones de esterilidad. Se empleo como control un cultivo de 14 días de *S. cerevisiae* cultivado en las mismas condiciones.

7.24 Hidrólisis de ATP en *Wolbachia* aislada

Se detectó la cantidad de fosforo inorgánico presente en el medio siguiendo el método de (Dryer RL, 1956). Se agregaron 50 μg/mL de *Wolbachia* aislada cuantificada por Biuret a un buffer de succinato 2 mM, $MgCl_2$ 2.5 mM en 10 mM de HEPES pH 6.8 en un volumen final de 110 μL. Dónde se indica, se agregaron 3 μg/mL de oligomicina. Las muestras se incubaron 10 minutos para permitir la acción de la oligomicina. La

reacción se inició con 2.5 mM de ATP y se agitó 10 segundos en un vórtex. Las muestras se incubaron 15 minutos en agitación a 27°C, se centrifugaron 5 minutos a 14,000 rpm y se recuperaron 100 µL del sobrenadante. Estos se agregaron a una placa de Elisa junto con 41 µL de Molibdato de Amonio 25 mM y se incubó por 10 minutos en agitación a temperatura ambiente. Posteriormente se agregaron 41 µL de ELON y se incubó la placa durante 10 minutos en obscuridad. Se midió la absorbancia en un POLAR Star Omega a 530 nm. La concentración de fosfatos se calculó utilizando una curva estándar.

7.25 Infección de la línea celular C6/C36

Las línea celular C6/C36 se cultivó en medio mínimo de Eagle (MEM) de Sigma Chemical Co (M0643) suplementado con aminoácidos no esenciales, L-glutamina, vitaminas, D-glucosa, antibióticos y bicarbonato de sodio(Shih y cols., 1998), pH 6.8 (HCl o NaOH). Previamente a ser utilizado se agregó 10% de suero bovino fetal (SBF) inactivado (30 min a 56°C)(Shih y cols., 1998). Las líneas celulares se cultivaron en cajas de Petri True Line TR 4003 de 150 mm a 27°C en una atmósfera de 5% de CO_2 (incubadora de cultivos celulares ESCO). La infección de la línea celular se realizó con la técnica de infección ¨Shell vial¨ descrita por (Dobson y cols., 2002).

8 RESULTADOS

8.1 Crecimiento, adaptación y transporte de la línea celular Aa23

La línea celular Aa23 infectada con la cepa *w*AlbB de *Wolbachia pipientis* fue donada por la Dra. Ann Fallon del Departamento de Entomología de la Universidad de Minnesota. La línea celular se mantuvo en MEM que contiene rojo de fenol como indicador de pH: el color del medio debe mantenerse (rojo) para que las células no se despeguen; si el medio presenta un color morado indica un medio alcalino, mientras que un medio amarillo indica un pH ácido y en ambos casos la viabilidad celular disminuye. Al principio del proyecto no teníamos incubadora de CO_2 por lo que se adicionó al medio 20 mM de HEPES y se redujo la concentración de bicarbonato de sodio del 0.22% al 0.085%. La línea celular crece en monocapa y puede mantenerse en este estado hasta 60 días agregando medio fresco cada 30 días, ya que tiende a evaporarse. La línea celular no crece en agitación. Si se utiliza la incubadora con 5% CO_2, la concentración de bicarbonato de sodio debe ajustarse.

El rendimiento de la línea celular es de ~3 millones de células por frasco de Roux grande (225 cm^2)/75 mL. Para despegar la línea celular hay tres opciones: la primera es agitando vigorosamente durante 15 segundos. En este caso, después de extraer las células, puede agregarse medio fresco al frasco de Roux y la línea celular crece de nuevo. También se puede despegar la línea celular con tripsina o despegándola mecánicamente con jaladores pequeños (scrappers), en estos casos el rendimiento es mayor, pero el cultivo no puede crecer de nuevo en la misma caja.

8.2 Infección por *Wolbachia* en la línea celular Aa23

Se comprobó la presencia de *Wolbachia* en la línea celular de *Aedes albopictus* Aa23 de tres maneras. La primera fue amplificando un fragmento del gen *wsp* de *Wolbachia*. (Figura 6a). La línea celular Aa23 amplifica un fragmento de ADN de aproximadamente 600-650 pb, mientras que la línea celular tratada con tetraciclina durante 9 pases (Aa23Tet) no amplifica dicho fragmento. La secuencia del fragmento amplificado se encuentra anotada en el Anexo A.

El segundo método empleado para comprobar la infección de la línea celular fue hibridar el gen 16S rDNA de *Wolbachia* con una sonda marcada con Quasar 670 (Figura 6b). En dichas imágenes, se observan cúmulos de células Aa23 de

aproximadamente 5 μm con marcas de hibridación (rosa) que confirman la presencia de la bacteria.

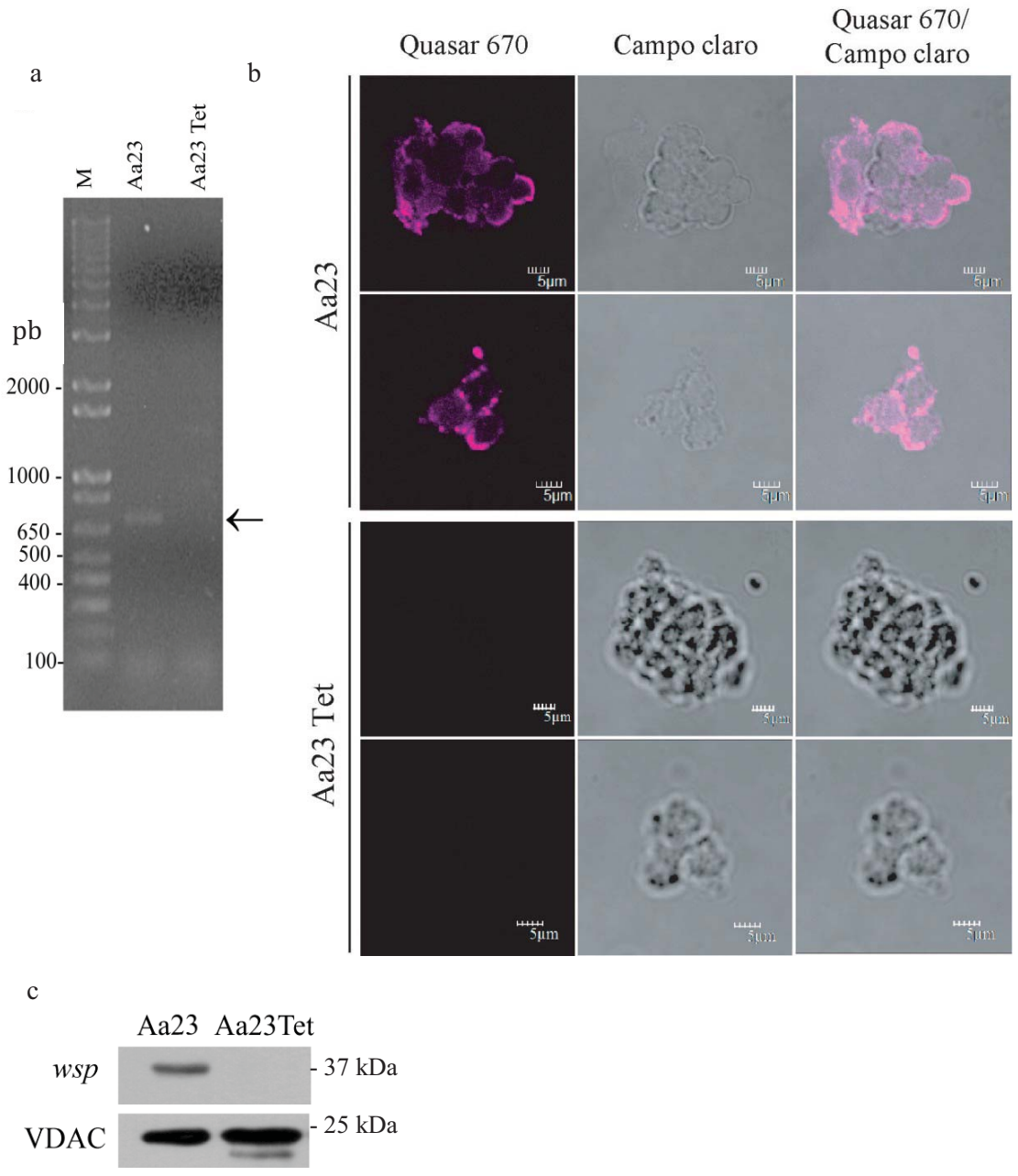

Figura 6. Infección de la línea celular Aa23 con *Wolbachia*. (a) El fragmento amplificado del gen *wsp* de *Wolbachia* pesa 650 pb. Carril 1, marcador 1kb plus (Invitrogen); carril 2, Aa23; carril 3, Aa23Tet. (b) Microscopía confocal de dos campos observados de la línea celular Aa23. En la primera columna se muestra la fluorescencia obtenida por la hibridación del gen 16S rRNA de *Wolbachia* con una sonda marcada con Quasar 670 (rosa); la segunda columna muestra el campo claro y la tercera es una sobreposición de las imágenes, donde se observa la sonda dentro de la línea celular. (c) Western blot contra la proteína wsp de *Wolbachia*: carril 1,

Aa23; carril 2, Aa23Tet; línea 1, proteína wsp detectada a 37 kDa; línea 2, VDAC utilizado como control de carga detectado a 25 kDa.

El tercer método para comprobar la infección con *Wolbachia* fue identificando la proteína wsp por Western Blot (Figura 6c). De acuerdo con el proveedor, el anticuerpo primario monoclonal contra la proteína wsp da una señal a 37 kDa. En la placa revelada se observa una banda en 37 kDa en la muestra de Aa23. Esta señal no se observó en la línea celular tratada con tetraciclina (Aa23Tet). Se utilizó como control de carga la proteína VDAC (Canal aniónico dependiente de voltaje) cuya señal se detecta a 25 kDa. El anticuerpo anti-wsp puede dar una banda inespecífica a 70 kDa.

8.3 Cultivo de *Wolbachia* en diversos medios

Para aumentar el rendimiento de *Wolbachia* y dado que la línea celular Aa23 tiene un crecimiento limitado en la superficie donde se coloque, se intentó cultivar la bacteria ex-vivo. Se utilizaron como base medio corazón-cerebro (BHI), MEM y Mitsuhashi-Maramarosch adicionados con diferentes concentraciones de sustratos compatibles (trehalosa, sacarosa, manitol y glicerol), SBF, catalasa, eritrocitos, y se cultivaron a concentraciones bajas de oxígeno. También se intentó cultivar la bacteria en un medio con lisado de la línea celular y otro con lisado de *Drosophila* sin lograr incrementar de manera significativa la cantidad de biomasa y comprometiendo el monocultivo de *Wolbachia* en algunos casos. Previamente, (Rasgon y cols., 2006) reportaron que *Wolbachia* puede permanecer viva, infectiva y sin aumentar su biomasa en MEM suplementado con 20% SBF en una atmósfera de 5% CO_2. Nosotros observamos que *Wolbachia* es capaz de sobrevivir en medio BHI y en Mitsuhashi-Maramarosch con 20% de eritrocitos y 20% de SBF en una atmósfera de 5% de CO_2. Sin embargo, al no lograr un aumento de la biomasa bacteriana, ninguno de estos cultivos nos acercaba a nuestro objetivo. Otra opción para aumentar el rendimiento de la bacteria fue cambiarla a un hospedero artificial. Recientemente se han encontrado diversas alfa y gamma proteobacterias como endosimbiontes de amibas, hongos filamentosos y levaduriformes (Bianciotto y cols., 1996; Bianciotto y cols., 2002; de Boer y cols., 2004; Hoffman y cols., 2010; Kang y cols., 2009; Lumini y cols., 2007; Partida-Martinez y cols., 2005; Saniee y cols., 2013a; Sato y cols., 2010). Se ha propuesto utilizar a estos hongos como posibles hospederos alternos para el cultivo de endosimbiontes obligados (Hosoda y cols., 2011a; Hosoda y cols., 2011b; Momeni y cols., 2011).

8.4 Cultivo de *Wolbachia* como endosimbionte de la levadura *Saccharomyces cerevisiae*

Decidimos infectar a la levadura no patógena *S. cerevisiae*, ya que es de fácil manejo y su manipulación genética es sencilla. Además *S. cerevisiae* es aerobia facultativa lo que, en caso de ser necesario, nos permitiría mantener al sistema en concentraciones bajas de oxígeno. A diferencia de BY4741, la cepa W303 posee una pared celular más débil que el resto de las cepas de *S. cerevisiae* (Aguilar-Uscanga y cols., 2003; Avrahami-Moyal y cols., 2012; Smith y cols., 2000) y tiene una alta resistencia a las especies reactivas de oxígeno, que aumentan en presencia de *Wolbachia* (Fallon y cols., 2013; Pan y cols., 2012).

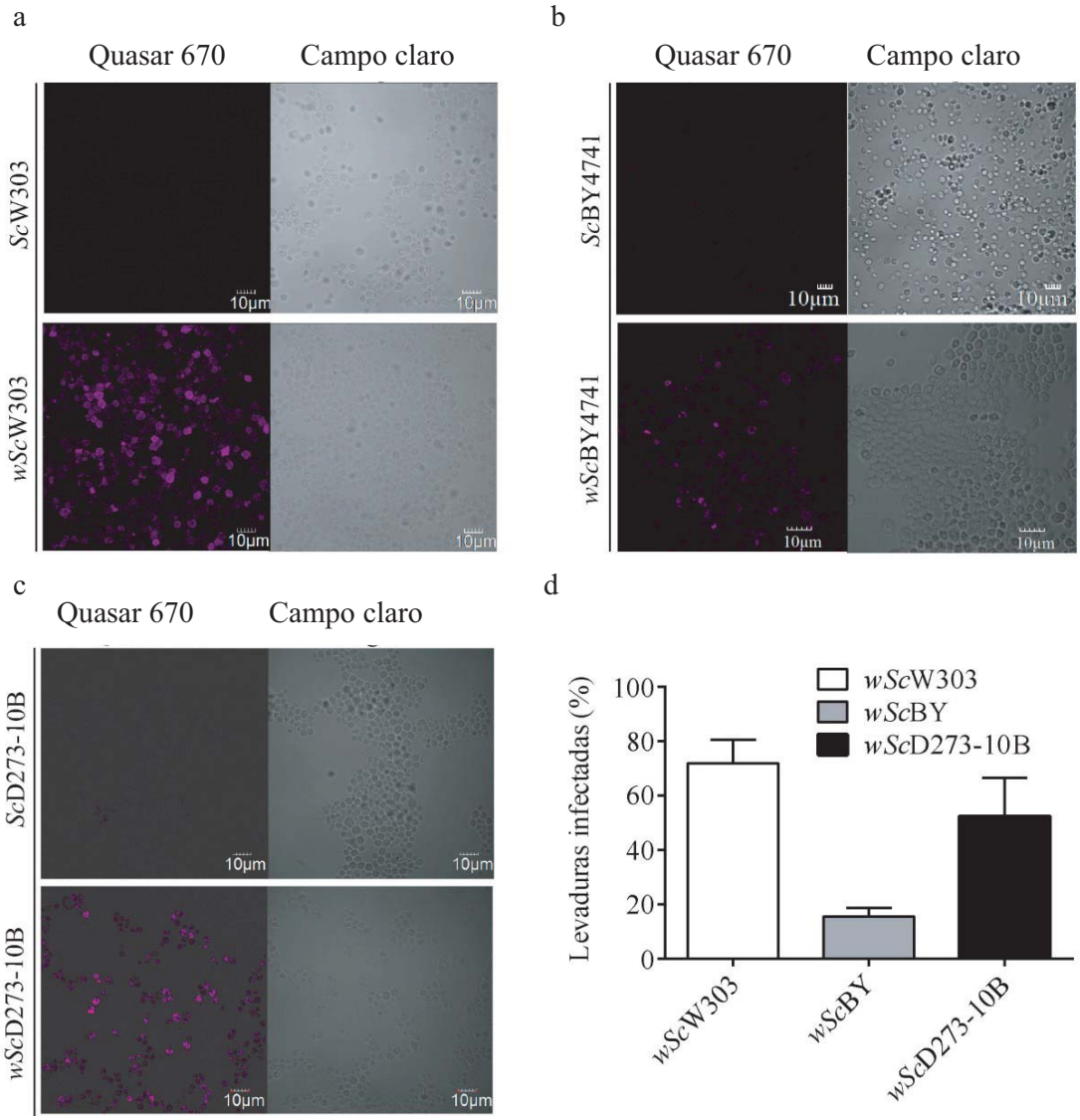

Figura 7. Infección de la cepas *Sc*W303, *Sc*BY y *Sc*D273-10B con *Wolbachia w*AlbB de la línea celular Aa23. FISH utilizando una sonda específica contra el gen 16S rDNA de

Wolbachia marcada con Quasar 670 (rosa) en cultivos control (primera línea) e infectados (segunda línea) para (a) *Sc*W303, (b) *Sc*BY, (c) *Sc*D273-10B e infectados (segunda línea) para (a) *wSc*W303, (b) *wSc*BY, (c) *wSc*D273-10B). (d) Porcentaje de células infectadas considerando positivas aquellas con hibridación (marca rosa) contadas en un microscopio epifluorescente Olympus.

Se infectaron las cepas *Sc*W303, *Sc*BY y *Sc*D273-10B siguiendo el protocolo modificado de (Dobson y cols., 2002). Después de 14 días de cultivo en medio sólido, se realizó una hibridación *in-situ* utilizando una sonda contra el gen 16S rDNA de *Wolbachia* marcada con Quasar 670 y se observó que menos del 20% de las levaduras de la cepa *wSc*BY presentaban marca de hibridación (Figura 7b, d). En comparación, en la cepa *wSc*W303 se encontró marca en el 71.8 ± 8.7% (Figura 7a, d) de las células, mientras que *wSc*NB40 presentó marca en el 52.3 ± 14.3% (Figura 7c,d).

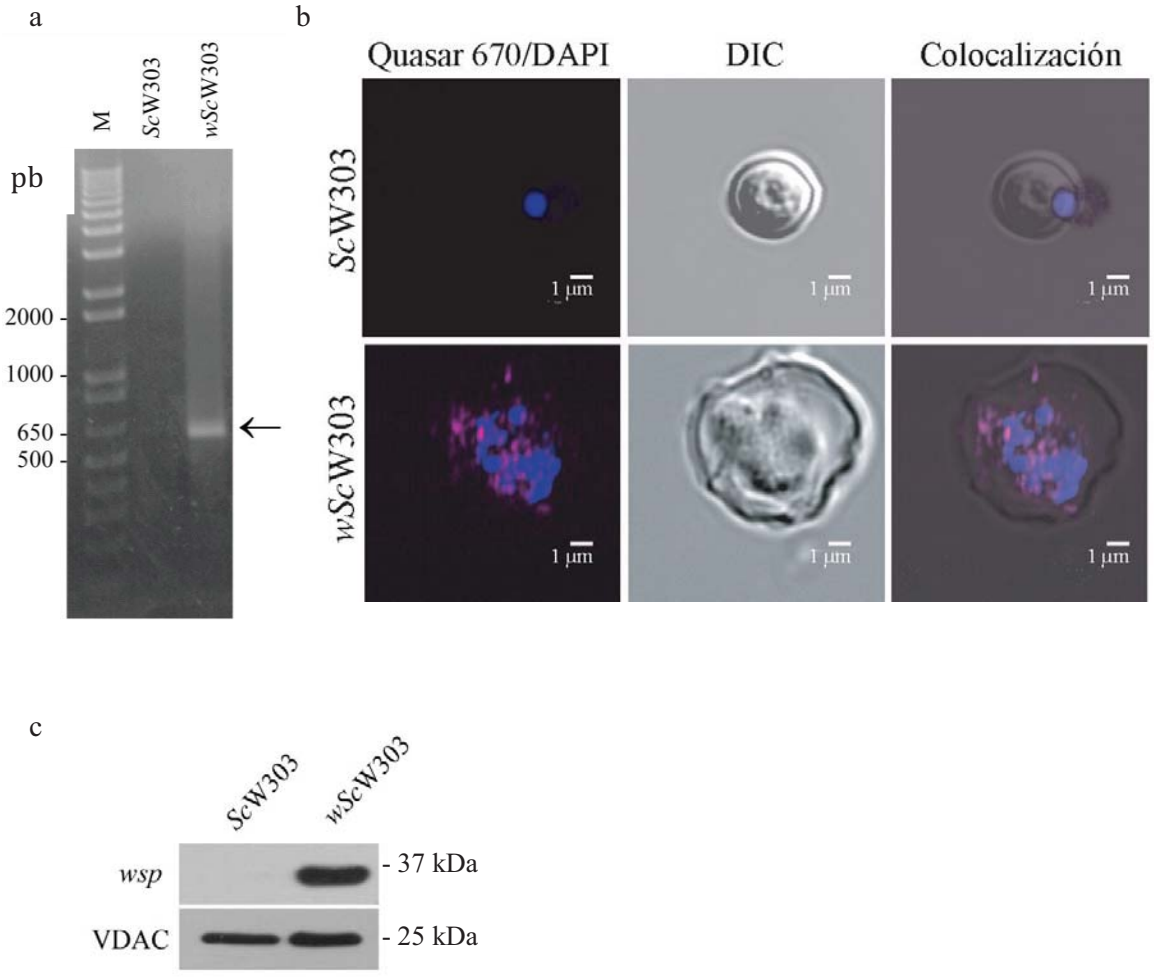

Figura 8. Infección de la levadura *S. cerevisiae* con *Wolbachia.* (a) PCR del gen wsp de *Wolbachia* de una infección artificial en *S. cerevisiae*. Carril 1, marcador 1 kb plus (Invitrogen);

carril 2, *Sc*W303; carril 3, *wSc*W303 infectada. (b) Microscopía confocal de *Saccharomyces cerevisiae* W303 (*Sc*W303) y de levadura *Saccharomyces cerevisiae* W303 infectada (*wSc*W303). En la primera columna se muestra la fluorescencia obtenida por la hibridación del gen 16S rRNA de *Wolbachia* con una sonda marcada con Quasar 670 (rosa) y DAPI (azul); la segunda columna muestra el campo claro con óptica Nomarski (DIC) y la tercera es una sobreposición de las imágenes donde se observa la sonda dentro de la célula. La microscopía fue realizada en un microscopio confocal Leica en la UBIMED, FES Iztacala, UNAM. (c) Western Blot contra la proteína wsp de *Wolbachia*: carril 1, *Sc*W303; carril 2, *wSc*W303; línea 1, proteína wsp detectada a 37 kDa; línea 2, VDAC utilizado como control de carga detectado a 25 kDa.

La infección de la cepa de *S. cerevisiae* W303 se analizó con los mismos métodos empleados para comprobar la infección de la línea celular Aa23 (Figura 6). El PCR (Figura 8a) del gen *wsp* de *Wolbachia* amplificó una banda similar a la obtenida de la línea celular Aa23. Las imágenes de microscopía confocal muestran la hibridación de la bacteria dentro de la levadura. Además al agregar DAPI y teñir el ADN dentro de la levadura se observó que a diferencia de los controles donde únicamente se tiñó el núcleo de la levadura, se tiñeron varios puntos dentro de la célula señalando el DNA bacteriano (Figura 8b). En el Western Blot contra la proteína wsp, la levadura infectada mostró una banda en 37 kDa (Figura 8c, *wSc*W303). Esta señal no se observó en la levadura control (*Sc*W303). Se utilizó como control de carga la proteína VDAC (Canal aniónico dependiente de voltaje) cuya señal se detecta a 25 kDa.

El medio de cultivo empleado para infectar a la levadura fue Mitsuhashi-Maramarosch suplementado con 10% Suero Bovino Fetal. Una vez infectada, la levadura crecía en YPD con 1% SBF y 1 mM de citrato férrico amoniacal, y la infección se perdía al omitir dichos suplementos (Figura 9).

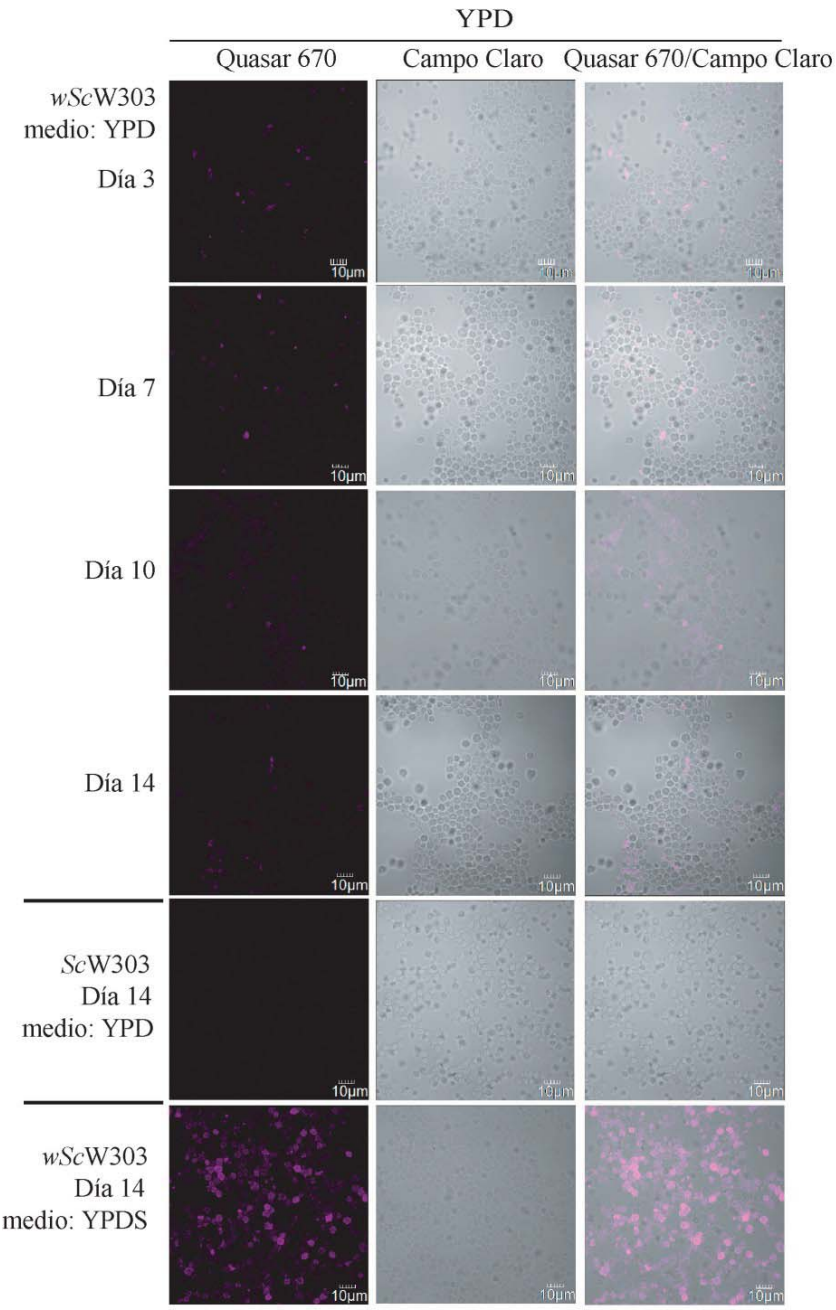

Figura 9. La infección de *Wolbachia* en *Sc*W303 depende de la correcta suplementación del medio. Microscopía confocal de la levadura *Saccharomyces cerevisiae* W303 infectada con *Wolbachia* (*wSc*W303) cultivada en un medio sin Suero Bovino Fetal ni citrato férrico amoniacal a días 3, 7, 10 y 14. En la primera columna se muestra la fluorescencia obtenida por la hibridación del gen 16S rDNA de *Wolbachia* con una sonda marcada con Quasar 670; la segunda columna muestra el campo claro y la tercera es una sobreposición de las imágenes. Se utilizó como control negativo a *Sc*W303 (sin infectar) de 14 días cultivada en medio YPD y como control positivo a w*Sc*W303 de 14 días cultivada en medio YPDS: YPD suplementado con 1% de Suero bovino fetal y 1 mM de citrato férrico amoniacal. El inoculo de los cultivos infectados (*wSc*W303, líneas 1, 2, 3, 4 y 6) fue tomada de la misma caja petri, la diferencia radica en que no se agrego SBF y citrato férrico amoniacal a los precultivos y a los cultivos del cultivo de las líneas 1, 2, 3 y 4.

A pesar de que la cepa de levadura fue tomada del EuroScarf, se comprobó su identidad para descartar la contaminación por otra levadura (Figura 10). Se amplificó un segmento de del gen 5.8S rRNA. La secuencia del fragmento amplificado se encuentra en el Anexo 1 y el análisis por BLAST coincide con la secuencia de *S. cerevisiae.* Se utilizaron los mismos oligonucleótidos para amplificar el fragmento de 350 pb del gen 5.8S rRNA de *Yarrowia lipolytica E129.* Se utilizó esta levadura porque amplificaba un fragmento de diferente peso molecular al amplificado por *S. cerevisiae.* Se utilizó *Escherichia coli* DH5-α como control negativo ya que al ser un procarionte no posee los mismos genes ribosomales que una eucarionte.

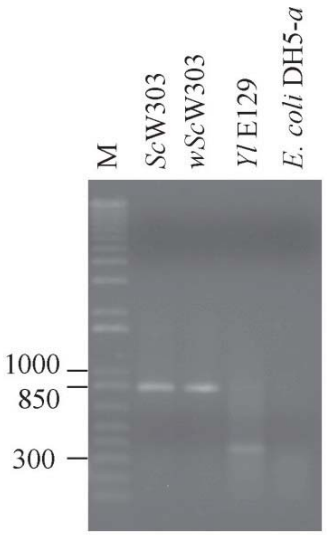

Figura 10. Comprobación de la identidad de *S. cerevisiae*. PCR del gen 5.8S rRNA de *S. cerevisiae*. Carril 1, marcador 1kb plus (Invitrogen); carril 2, *Sc*W303; carril 3, *wSc*W303, carril 4: *Yarrowia lipolytica*, Carril 5: *Escherichia coli* DH5-α.

Con el fin de comprobar que *Wolbachia* se encontraba dentro de la levadura y no adherida a su pared celular, teñimos la pared de las levaduras *Sc*W303 y *wSc*W303 previamente fijadas e hibridadas con la sonda 16S rDNA con calcoflúor y la observamos en un microscopio confocal (Figura 11 y 12). El calcoflúor es un colorante que se une a la celulosa y a la quitina de la pared celular de las levaduras. Las bacterias no tienen estos componentes en sus membranas, por lo que no se tiñen con el calcoflúor. Se realizaron cortes en Z y al hacer una reconstrucción de las imágenes se observó a la bacteria dentro de la levadura (Figura 12, Películas S1 y S2).

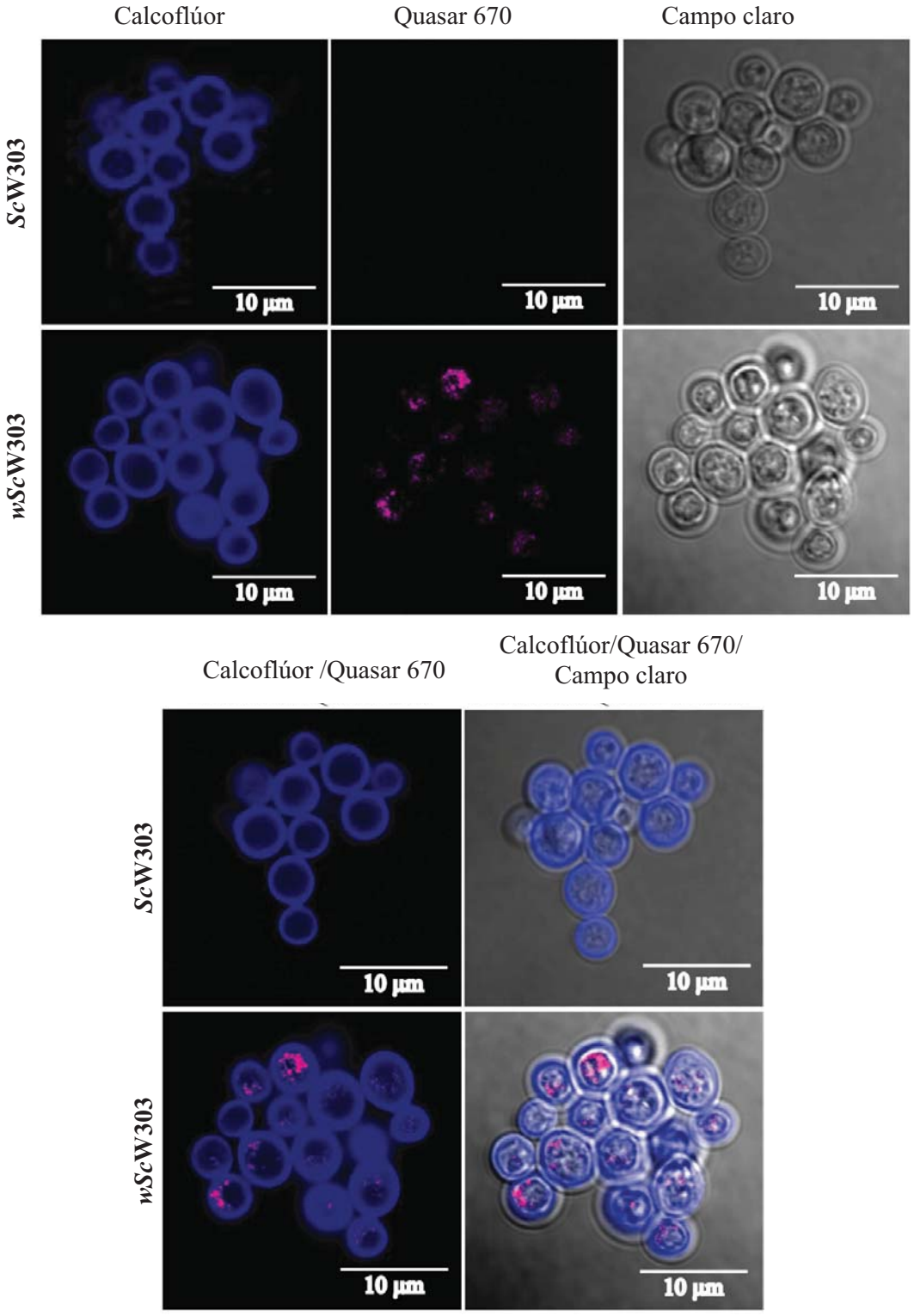

Figura 11. La levadura *wSc*W303 teñida con Calcoflúor e hibridada contra la sonda 16Sr DNA de *Wolbachia*. Microscopía confocal de *Saccharomyces cerevisiae* W303 (*Sc*W303) y *S. cerevisiae* W303 infectada (*wSc*W303) hibridadas con la sonda 16S rDNA de *Wolbachia* y teñida con calcoflúor. En la primera columna se observa la pared celular de la levadura teñida con calcoflúor. En la segunda columna la fluorescencia obtenida por la hibridación del gen 16S

rDNA de *Wolbachia* con una sonda marcada con Quasar 670. En la tercera columna se muestra el campo claro. Las siguientes columnas muestran la sobreposición de las imágenes de calcoflúor con Quasar 670 y calcoflúor con Quasar 670 y campo claro.

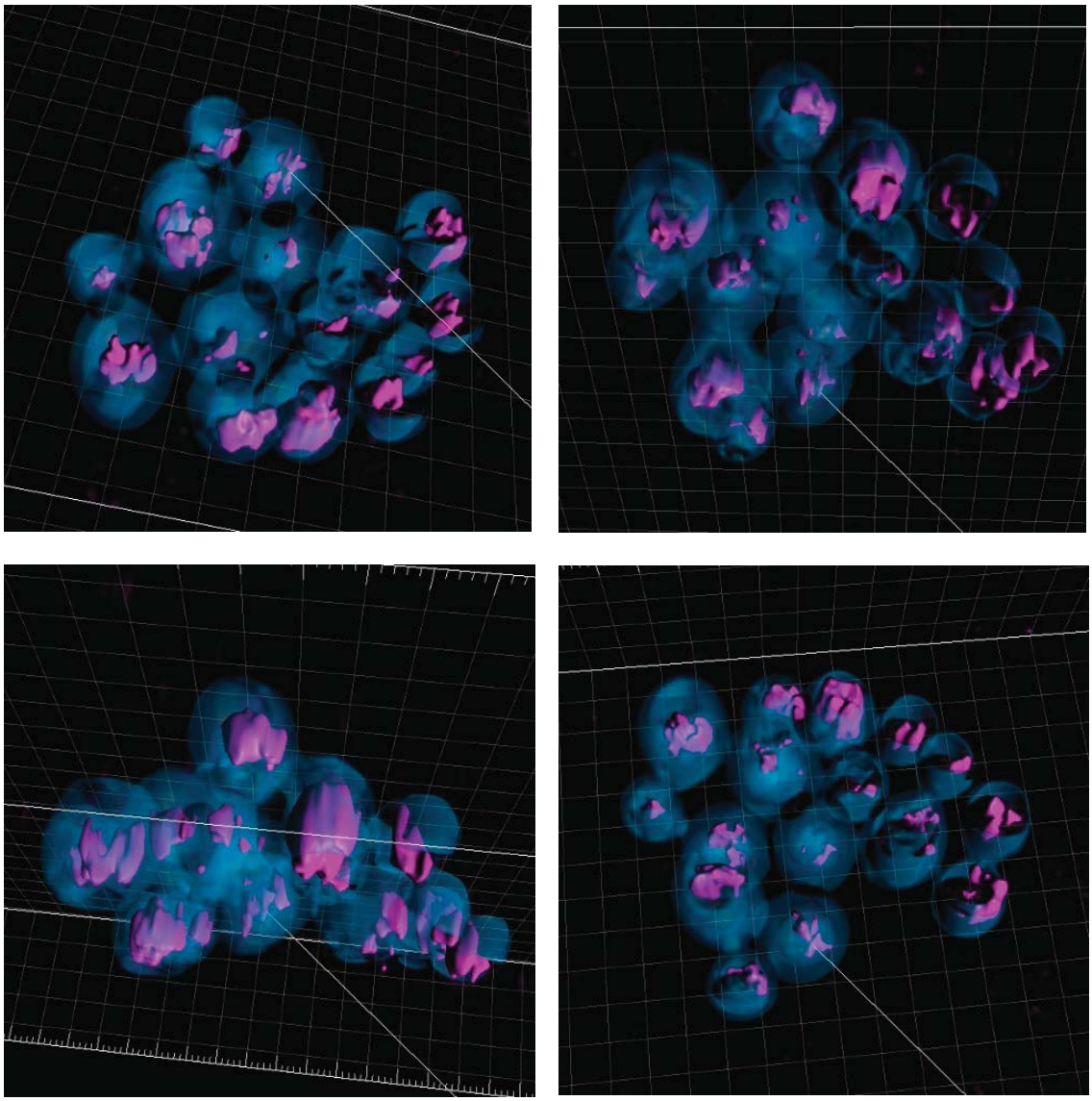

Figura 12. Reconstrucción de los cortes en Z de la levadura *wSc*W303 teñida con Calcoflúor e hibridada contra la sonda 16Sr DNA de *Wolbachia*. Imágenes tomadas de las películas S1 y S2 que muestran la reconstrucción de los cortes en Z obtenidos por microscopía confocal de *S. cerevisiae* W303 infectada con *Wolbachia* (*wSc*W303) hibridada con la sonda 16S rDNA de *Wolbachia* y teñida con calcoflúor.

Observamos la presencia de los cuerpos bacterianos en la levadura infectada por microscopía electrónica de transmisión (Figura 13). En cultivos de 14 días, las levaduras control *Sc*W303 (Figura 13a), tienen una membrana intacta pero sin organelos

distinguibles; es decir, perdieron la mayoría de las estructuras mitocondriales probablemente porque las células se encuentran en fase estacionaria tardía.

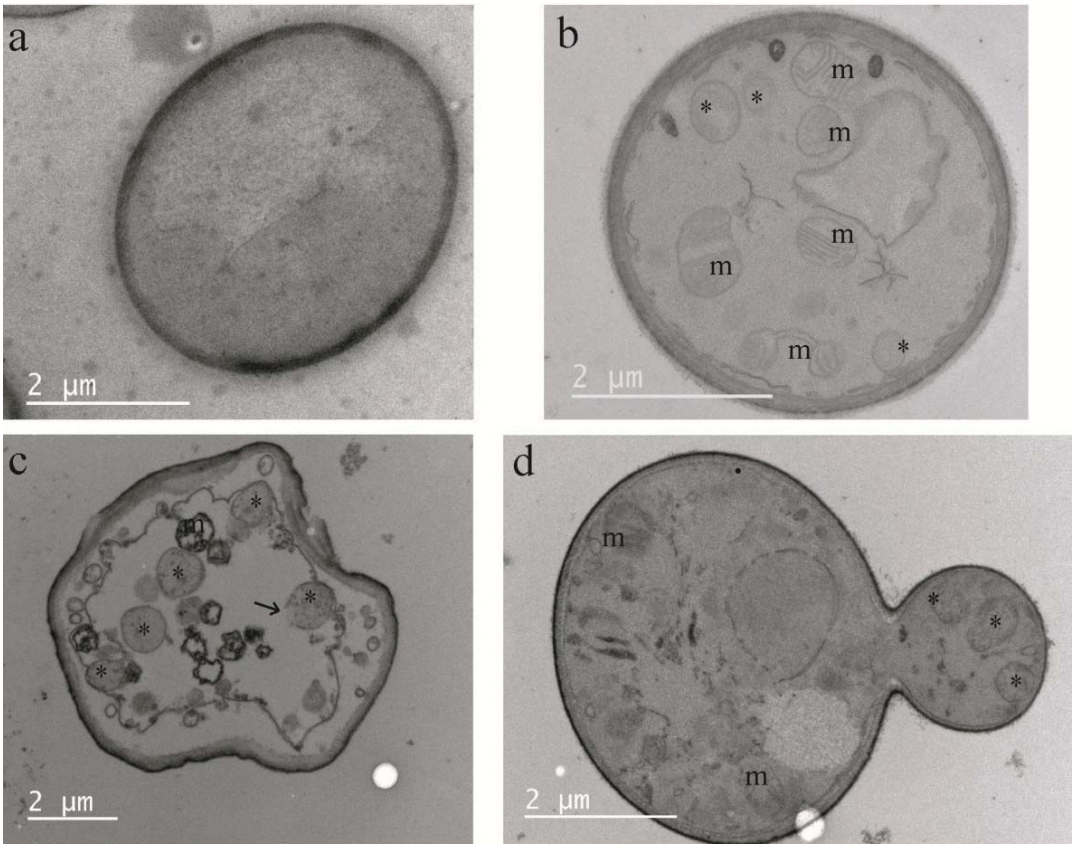

Figura 13. Microscopía Electrónica de Transmisión de *Sc*W303 y w*Sc*W303. Las imágenes de microscopía electrónica de transmisión confirman la ubicación intracelular de cuerpos parecidos a bacterias. Se tomaron imágenes de cultivos de 14 días con (a) *Sc*W303 y (b-d) *wSc*W303. Las imágenes muestran la presencia de cuerpos similares a bacterias (BLB: Bacteria-like-bodies) (*) que no están presentes en las levaduras control (a) y mitocondrias (m) cuyas crestas se pueden identificar fácilmente.

En cambio, la levadura *wSc*W303 mostró otra morfología. En la mayoría de las células, (ej. 13b) la membrana estaba intacta y podían observarse mitocondrias (M) y cuerpos bacterianos (*) dentro de la levadura. Esta tinción nos permite observar las crestas mitocondriales permitiéndonos apreciar la diferencia entre las mitocondrias y las bacterias. Otras levaduras en la muestra *wSc*W303 exhibieron membranas dañadas (ej. Figura 13c), conservando parcialmente las estructuras similares a las bacterias. La flecha en la figura 13c señala uno de los cuerpos bacterianos cuya membrana está dañada. Finalmente, encontramos algunas levaduras gemando, en las que se observan

los cuerpos bacterianos en la gema (Figura 13d). Esta población no apareció en los cultivos de la levadura control (Figura 13a). No podemos asegurar que sean bacterias aún, para esto necesitaríamos realizar una inmunotinción con oro acoplado a un anticuerpo primario contra *Wolbachia*. Además de la ausencia de estos cuerpos en las levaduras control, podemos comparar la morfología de las bacterias con la reportada por otros autores y son muy parecidas (Figura 1, Figura 13).

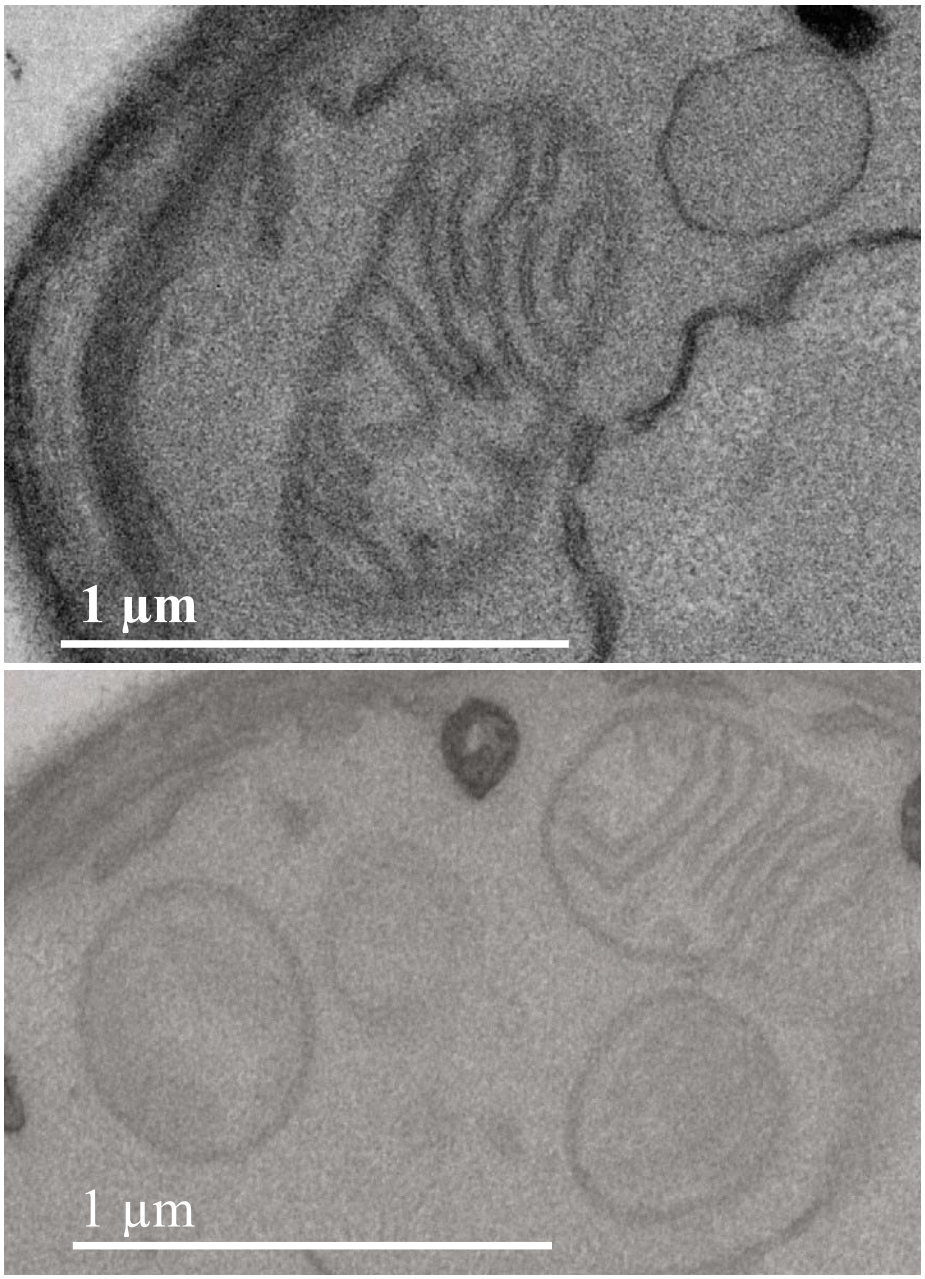

Figura 14. Acercamientos de fotografías tomada por Microscopía Electrónica de Transmisión de w*Sc*W303. Se emplearon cultivos de 14 días con *wSc*W303. Las imágenes muestran acercamientos de cuerpos similares a bacterias y mitocondrias cuyas crestas se pueden identificar fácilmente.

8.4.1 Evolución de la infección de *Wolbachia* en *S. cerevisiae* W303

Monitoreamos el efecto de *Wolbachia* en el crecimiento de la levadura durante 18 días y la cantidad de *Wolbachia* por célula de levadura a diferentes tiempos para determinar en qué momento teníamos mayor cantidad de *Wolbachia*.

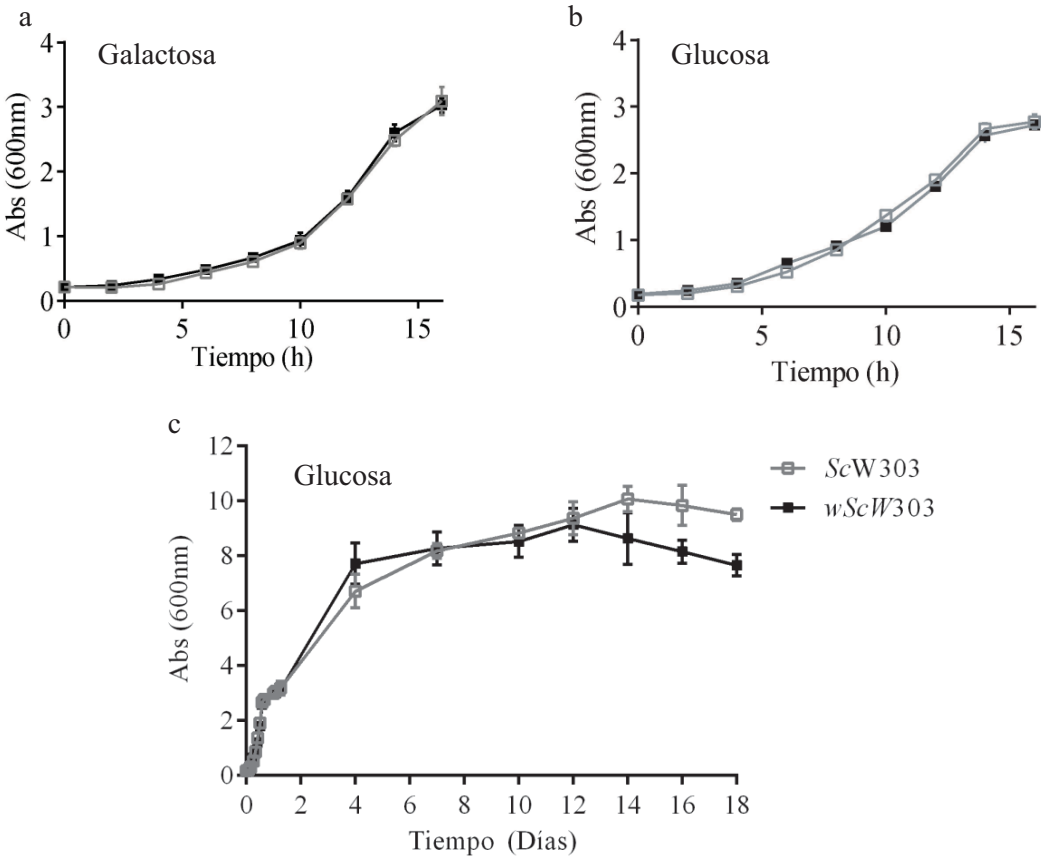

Figura 15. Crecimiento de *S. cerevisiae* infectada con *Wolbachia* utilizando como fuente de carbono galactosa y glucosa. Aumento de densidad óptica (600 nm) de *Sc*W303 (negro) y *wSc*W303 (gris) utilizando como fuente de carbono (a) galactosa y (b y c) glucosa. Se realizaron 3 mediciones de 3 experimentos independientes. Se graficó el promedio de estos ± desviación estándar.

Realizamos curvas de crecimiento determinando el aumento de la densidad óptica (D.O.) de cultivos de *Sc*W303 y *wSc*W303 utilizando glucosa y galactosa al 2% como fuentes de carbono (Figura 15a y b). Las cepas *Sc*W303 y *wSc*W303 exhibieron un crecimiento similar y monofásico usando galactosa como fuente de carbono, alcanzando la fase estacionaria a las 16 horas (Figura 15a). En medios con dextrosa, en la levadura control se observó un crecimiento bifásico debido a que en la fase diáuxica (10-12 horas) la levadura pasó de un metabolismo fermentativo a uno aeróbico. En la cepa *wSc*W303 se observó un mínimo adelanto de la fase diáuxica a 6 horas (Figura

15b). En el medio con dextrosa como fuente de carbono se observó una ligera disminución de la densidad óptica de los cultivos de la cepa no infectada a los 16 días, y a los 14 días para la cepa infectada (Figura 15c). La viabilidad celular se observó con el kit Baclight que tiñe todo el DNA presente en la muestra de verde mientras que el DNA de las células cuya integridad membranal está comprometida se tiñe de rojo. La supervivencia de las células bajó en las células infectadas después de 14 días de cultivo (Figura 16 a y b).

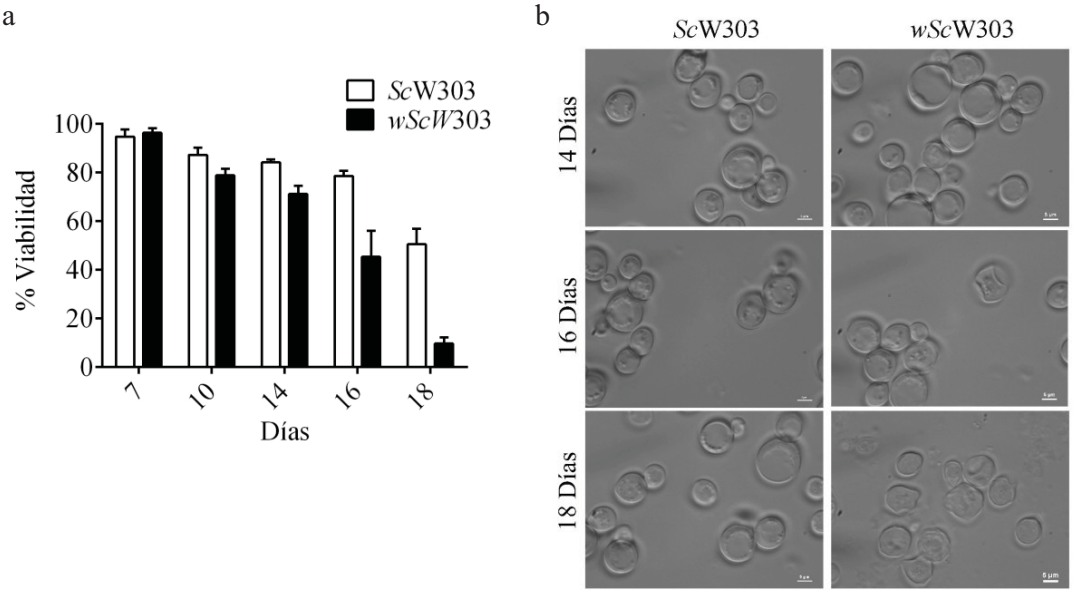

Figura 16. Efecto de *Wolbachia* sobre la viabilidad de *Saccharomyces cerevisiae* W303. (a) Viabilidad de los cultivos de levadura estimada con el kit de viabilidad celular Baclight. Se realizaron 3 mediciones de 3 experimentos independientes y se graficó su promedio ± desviación estándar. (b) Microfotografías de la levadura *Sc*W303 (primera columna) y *wSc*W303 (segunda columna) tomadas a 14, 16 y 18 días, que muestran la degradación de la membrana de la levadura infectada.

A los 14 días hay 84.19 ± 1.21 % y 71.20 ± 3.39 % de células vivas para *Sc*W303 y *wSc*W303, respectivamente. A los 16 días, la viabilidad de la levadura infectada disminuyó drásticamente (78.61 ± 2.06 % y 45.37 ± 10.77 % para *Sc*W303 y *wSc*W303). Finalmente, a los 18 días de cultivo ambas cepas presentaron alta mortandad (viabilidad de 50.57 ± 2.07 % y 9.66 ± 2.51 % para *Sc*W303 y *wSc*W303) por lo que decidimos no llevar los cultivos más allá de 14 días (Figura 16a). Las fotografías de las levaduras a estos tiempos muestran degradación de la membrana de las levaduras infectadas (Figura 16b).

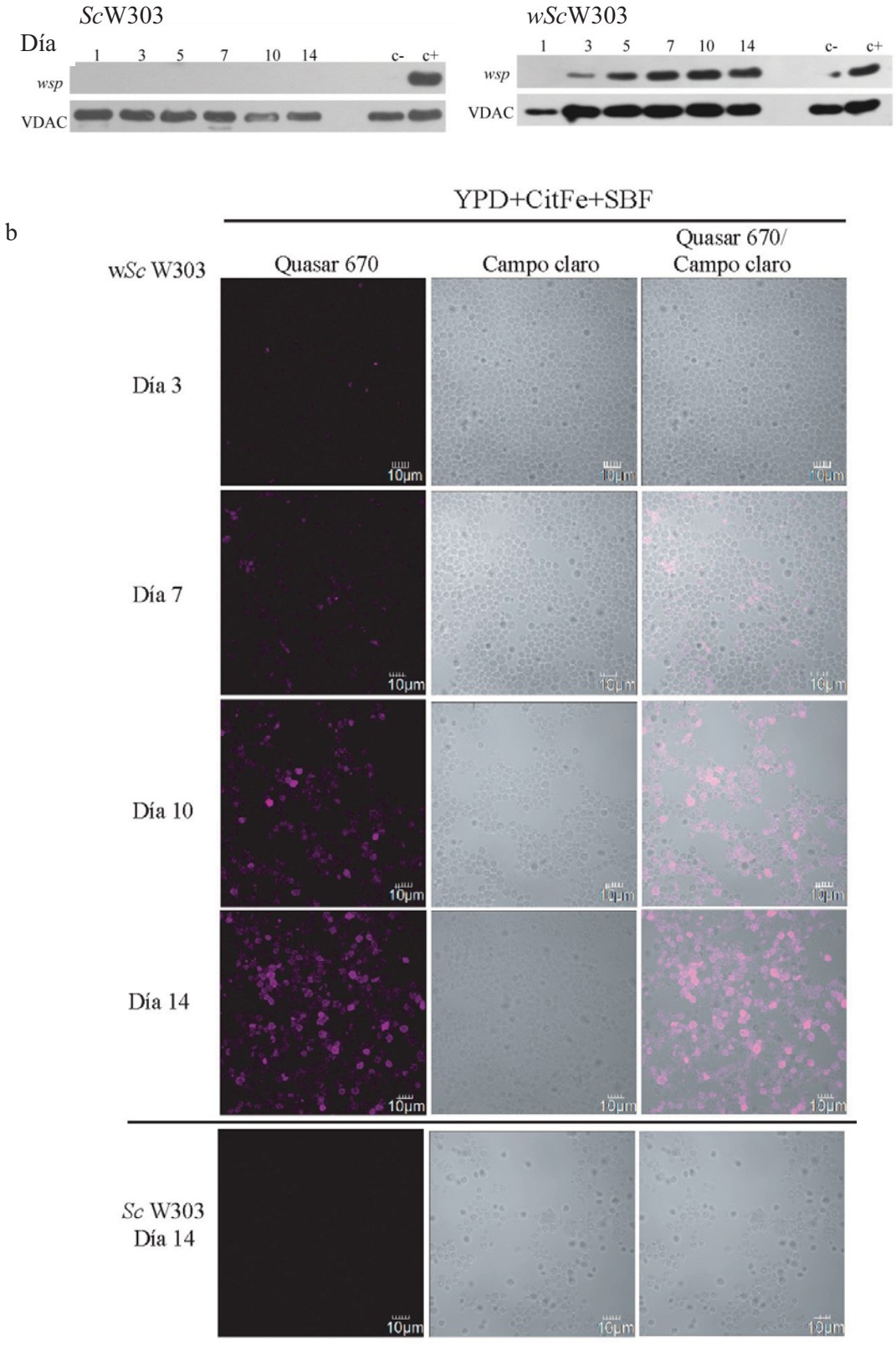

Figura 17. Evolución de la infección de *S. cerevisiae* W303 con *Wolbachia*. (a) Western Blot contra la proteína wsp de *Wolbachia* (proteína wsp detectada a 37 kDa); y contra VDAC

utilizado como control de carga (detectado a 25 kDa). *Sc*W303 levadura control, *wSc*W303 levadura infectada. Muestras tomadas a 1, 3, 5, 7, 10 y 14 días de cultivo en YPDS. (c-) *Sc*W303, (c+) W303 infectada en medio sólido (b) Imágenes obtenidas por microscopía confocal de *Sc*W303 levadura control, *wSc*W303 levadura infectada a diferentes días. En el primer carril se muestra la fluorescencia obtenida por la hibridación del gen 16S rDNA de *Wolbachia* con una sonda marcada con Quasar 670; el segundo carril muestra el campo claro y el tercer carril es una sobreposición de las imágenes, en la que se observa la sonda dentro de la línea celular.

Monitoreamos el aumento de *Wolbachia* en la levadura hasta 14 días por Western Blot (Figura 17a). El aumento gradual de la cantidad de *Wolbachia* (en función de la cantidad de proteína wsp detectada) se puede observar a partir del día 3 y aumentó considerablemente hasta el día 10 y 14. Se realizó la hibridación del gen 16S rDNA con una sonda marcada con Quasar a los mismos tiempos del cultivo y se observó una correlación en el aumento de fluorescencia del Quasar 670 entre 7 y 14 días (Figura 17b). La bacteria fue detectable a partir del día 7 y aumentó hasta el día 14.

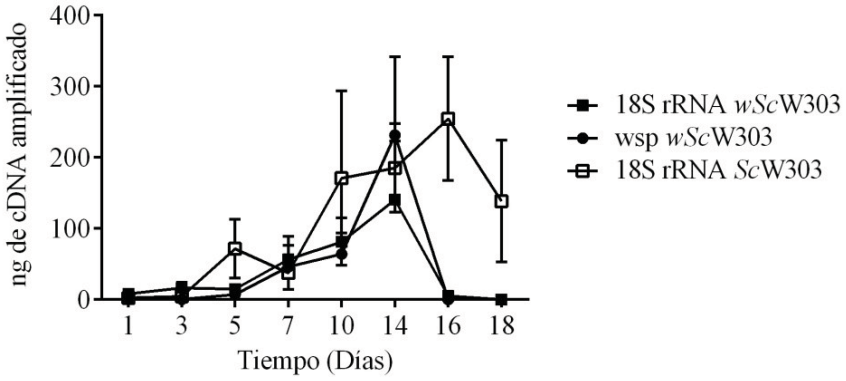

Figura 18. Viabilidad de *Wolbachia* durante la infección en *S. cerevisiae* W303. RT-qPCR para el transcrito del gen (□) 18S rRNA de la levadura control, (■) de la levadura infectada. y del transcrito del gen *wsp* de *Wolbachia* ●.

Para comprobar la viabilidad de la bacteria se realizó un RT-qPCR del gen wsp. Se utilizó como control el gen ribosomal 18S rRNA de la levadura. El transcrito bacteriano fue detectado a partir del día 3 y hasta el día 14 (Figura 18). Las bajas concentraciones de transcrito detectadas en los primeros días pueden deberse a que la actividad transcripcional de la levadura este opacando a la de la bacteria. Finalmente, a los 16 días, las cantidades de transcrito obtenido disminuyeron, probablemente debido a la muerte del hospedero y a la sensibilidad de *Wolbachia* a las condiciones de cultivo.

En una revisión de los métodos con los que se ha cuantificado a *Wolbachia* en líneas celulares (Tabla 5) se señala que lo más común es contar por microscopía la señal

de fluorescencia emitida por la bacteria. Los métodos empleados fueron tinción con SYTO 9 e hibridación con sondas marcadas (FISH). Únicamente la segunda es específica para *Wolbachia*. Al contar puntos marcados con la sonda o los cuerpos bacterianos presentes en las imágenes tomadas por microscopía electrónica de trasmisión, encontramos de 1 a 6 cuerpos bacterianos por levadura, aunque no todas las levaduras se encuentran infectadas (Figura 7) indicando que la transferencia no es perfecta.

Tabla 5. Densidad de la infección con *Wolbachia* de diferentes hospederos

Hospedero	**Método**	**Wb/célula**	**Rendimiento***	**Ref.**
Aedes albopictus C/wStr	Microscopía (SYTO)	50-100	**.85-1.7 *10^{10} w/L**	(Baldridge y cols., 2014)
Aedes albopictus Aa23	Microscopía (FISH)	40-65 (10-30 D)	**0.67-1.1 *10^{10} w/L**	(Khoo y cols., 2013)
Aedes, C7-C10B, C7-C10R	Microscopía (FISH)	10-60 (40-100 D)	**0.16-1.0 *10^{10} w/L**	(Khoo y cols., 2013)
Aedes albopictus C/wStr	Citometría de flujo	500 (6-10)	**8.3 *10^{10} w/L**	(Fallon, 2014)

*Cálculo basado en una cantidad de 10^6 células de Aa23 en una caja de 60 mm (Fallon, 2008).
** Considerando 2.4 x 10^9 levaduras/mL contado con la Cámara de Neubauer.
NR: No reportado, BB: Bead beater, Centrif.: Centrifugación

La utilización de las levaduras como hospederos nos da muchas ventajas sobre las líneas celulares. La primordial para nuestro trabajo es la facilidad de cultivo y el aumento en la cantidad de biomasa. El número de *Wolbachia* por levadura es menor que el número de *Wolbachia* por célula de insecto (Figura 13, Tabla 5), sin embargo la cantidad de levaduras que se obtienen de un cultivo de un matraz de un litro es mayor que el que se obtiene de células en un litro de cultivo de línea celular aumentando así el rendimiento de la bacteria. El cultivo de las líneas celulares, además, se realiza en cajas de Petri o frascos de Roux (para un litro son 17 Frascos de Roux de 225 cm^2) que deben incubarse en la cámara de CO_2 (volumen limitado) y que necesitan por lo menos 30 días para crecer. En cambio, la levadura se cultiva en matraces de un litro en una temperatura constante durante 14 días. La levadura se cultiva en YPD que cuesta menos

que el medio mínimo de Eagle suplementado. Al reducir y simplificar el material utilizado se reducen enormemente los costos del proyecto.

Finalmente, la levadura es más robusta que la célula de insecto, por lo que da una mayor protección contra cambios ambientales, cambios de pH, de concentración de oxígeno y de temperatura. Al ser capaces de infectar diversas levaduras tenemos acceso a una gran variedad de cepas y mutantes lo que ofrece la posibilidad de explorar los efectos de *Wolbachia* sobre su hospedero.

8.5 Actividad fermentativa de *Sc*W303 y *wSc*W303

En la curva de crecimiento utilizando glucosa como fuente de carbono (Figura 15b y c) puede observarse un pequeño desplazamiento de la fase diáuxica en la cepa *Sc*W303 infectada con *Wolbachia*. Si esto es cierto, entonces la fermentación de la levadura infectada debe estar aumentada en fases tempranas del crecimiento.

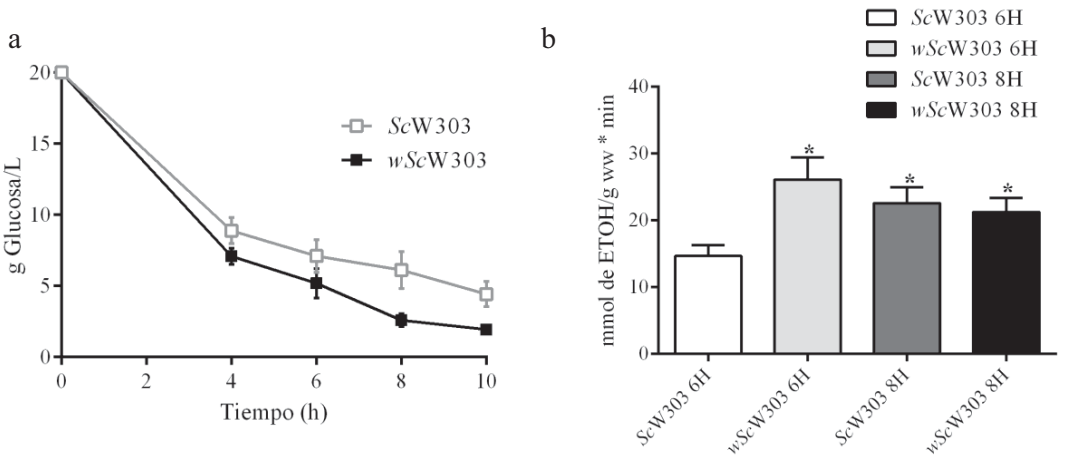

Figura 19. Fermentación en *S. cerevisiae* W303 infectada con *Wolbachia*. (a) Consumo de glucosa en cultivos de *Sc*W303 y *wSc*W303. (b) Actividad fermentativa de cultivos de *Sc*W303 y *wSc*W303 a 6 y 8 horas.Se realizaron 3 determinaciones en 3 experimentos independientes y se graficó el promedio de éstos ± desviación estándar. $P<0.05$.

Para comprobar que había un efecto en la fermentación de la levadura se cuantificó el consumo de glucosa que fue más lento en los cultivos de *Sc*W303 que en los cultivos de*wSc*W303: la cepa infectada consumió un poco más rápido la glucosa en el medio (Figura 19a). Los ensayos a diferentes tiempos indicaron que la fermentación aumentó en los cultivos infectados a las 6 horas con respecto al control (Figura 19b). A las 8 horas, la capacidad fermentativa de los controles aumentó, mientras que los de la levadura infectada disminuyeron. Es poco probable que *Wolbachia* haya consumido

directamente la glucosa, ya que no posee las enzimas glucolíticas necesarias, pero sí puede haber consumido el glicerol-3-fosfato, las hexosas fosfatadas o el ácido pirúvico generado por el hospedero como se ha propuesto (da Rocha Fernandes y cols., 2014; Voronin y cols., 2016). Otra posibilidad es que haya modificado el metabolismo del hospedero y éste consuma los sustratos a mayor velocidad.

8.6 Efecto de *Wolbachia* sobre la cadena respiratoria de *S cerevisiae*

Evaluamos la influencia de *Wolbachia* sobre la función mitocondrial de la levadura a 14 días de cultivo, donde la cantidad de *Wolbachia* fue significativa y a un día en donde la actividad mitocondrial debe ser óptima (Tabla 6).

Se observa una disminución en la velocidad de consumo de oxígeno en el estado III en la levadura control a los 14 días, lo que significa una pérdida de la capacidad respiratoria máxima, que se traduce en un CR menor. Este fenómeno no ocurrió en las levaduras infectadas de 14 días: el consumo de oxígeno en el estado III se mantuvo, lo que podría indicarnos que la actividad respiratoria de las mitocondrias del hospedero, agregada a la de la bacteria, le permite mantener por mayor tiempo una alta capacidad respiratoria, pero también el acoplamiento.

Tabla 6. Control respiratorio de *Sc*W303 y *wSc*W303

	Cepa	Estado IV*	Estado III**	CR
Día 1	*Sc*W303	25.2 ± 3.1	52.5 ± 6.8	2.1 ± 0.15
	*wSc*W303	27.4 ± 4.6	65.4 ± 9.0	2.4 ± 0.2
Día 14	*Sc*W303	22.6 ± 5.1	29.0 ± 6.3	1.3 ± 0.2
	*wSc*W303	34.3 ± 5.1	73.3 ± 11.1	2.1 ± 0.1

* Etanol
** ADP

Se determinó el consumo de oxígeno en los extractos de la levadura no infectada e infectada utilizando diferentes sustratos e inhibidores de la cadena transportadora de electrones para indirectamente elucidar si la respiración era de la mitocondria o de la bacteria (Figura 20). En el extracto *Sc*W303 de 14 días, el consumo de oxígeno fue semejante al de los extractos de un día, excepto para los valores obtenidos con NADH, que mostraron un consumo de oxígeno menor que en el de 1 día.

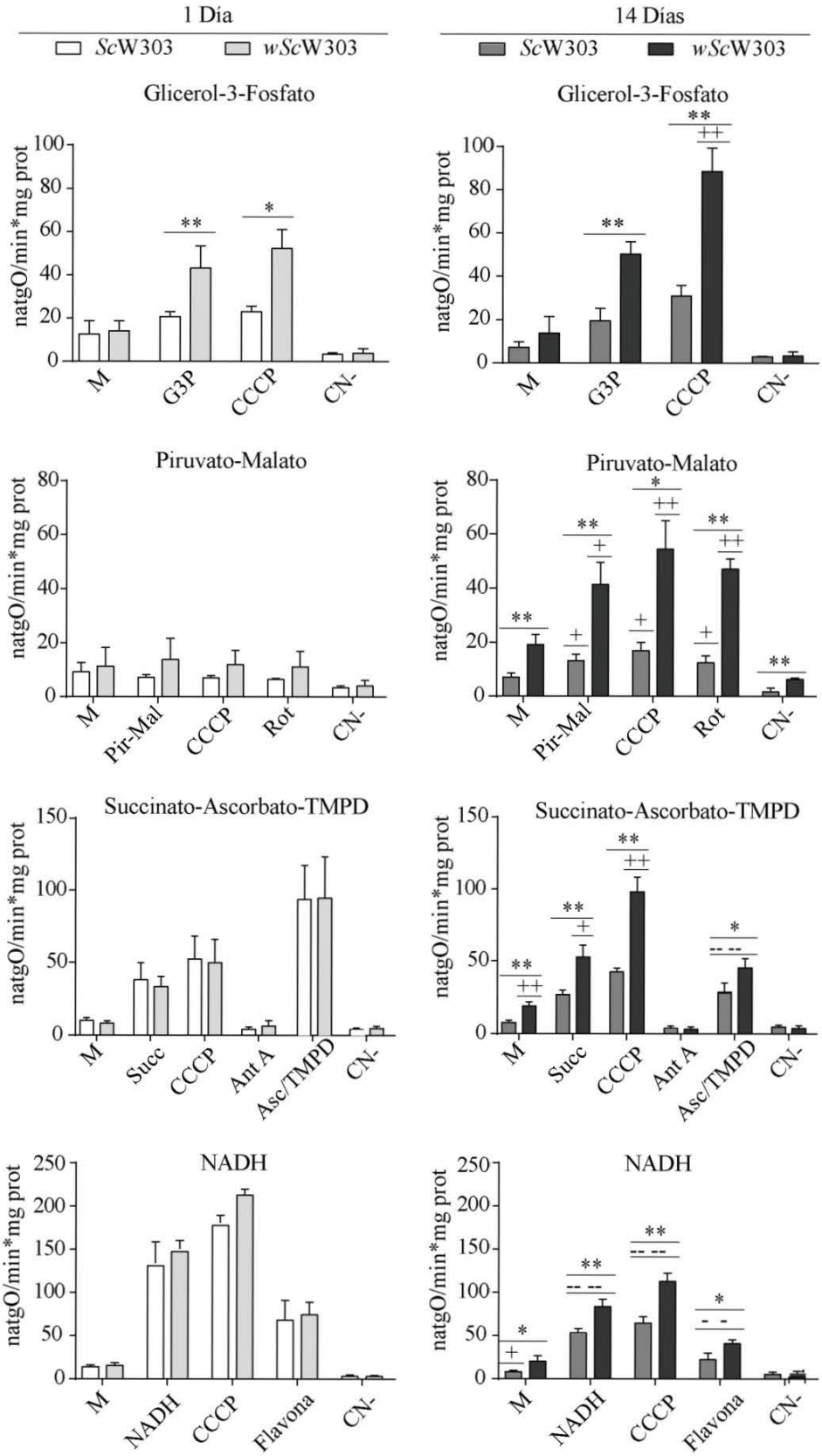

Figura 20. Consumo de oxígeno de la fracción mitocondrial de *S. cerevisiae* control o infectada con *Wolbachia* con uno y 14 días de cultivo. El consumo de oxígeno se determinó en un volumen final de 1.5 mL en un OROBOROS equipado con un electrodo de Clark. Se

utilizó una concentración de 5 mM de cada sustrato: glicerol-3-fosfato (G3P), piruvato-malato (PM), succinato (Succ). Donde se indica, se agregó: CCCP 0.5 μM, rotenona (Rot) 0.1 μM, antimicina A (Ant A) 0.1 μM, cianuro (CN^-) 1 mM o flavona 0.15 mM. Se añadieron 0.5 mg prot / mL de mitocondrias (M). Los datos representan la media ± SEM de n = 4. Prueba T * p <0.005, ** p <0.001 para *Sc*W303 contra la levadura *wSc*W303 en el mismo día. Prueba T - / + p <0.05 - - / ++ p <0.001 (-, disminución; +, aumento) para *Sc*W303 en el día uno frente al día 14 de cultivo o *wSc*W303 en el día uno frente al día 14 de cultivo.

En lo que se refiere al consumo de oxígeno del extracto mitocondria-*Wolbachia* de *wSc*W303, se afectó de diferentes maneras: El consumo de oxígeno utilizando Glicerol-3-fosfato se vió aumentado en la fracción de *wSc*W303 a 1 y 14 días. Utilizando piruvato-malato y succinato como sustratos: el consumo de oxígeno de la fracción mitocondria-bacteria de *wSc*W303 fue mayor al del extracto de *Sc*W303 en 14 días. Es de notar que al utilizar como sustrato piruvato-malato en los extractos de *Sc*W303 y *wSc*W303 de 1 día y *Sc*W303 de 14 días no se observó consumo de oxígeno; sin embargo, a los 14 días de cultivo de las levaduras infectadas aumentó el consumo de oxígeno. También observamos que al agregar rotenona no hubo inhibición de la respiración, indicando que un posible complejo I de *Wolbachia* no es responsable de este consumo. Utilizando NADH como sustrato, el consumo de oxígeno fue menor que el de las muestras con un día de cultivo (*wSc*W303) pero mayor que el del extracto de la levadura no infectada (*Sc*W303) de 14 días.

Por otra parte, el aumento en el consumo de oxígeno en los extractos de *wSc*W303, en mayor o menor grado, con todos los sustratos, fue todavía más claro ante la adición de CCCP, lo que indica un aumento de la capacidad respiratoria, pero también que tiene, un componente importante de acoplamiento. Todo indica que, o bien *Wolbachia* participa en la generación de energía, o favorece la generación de ésta por las mitocondrias del hospedero.

En los extractos de las levaduras infectadas se observó un patrón similar de consumo de oxígeno utilizando todos los sustratos, lo que indica que la cadena transportadora de electrones en las levaduras no infectadas e infectadas es la misma o semejante. Tratando de elucidar si los componentes de la CTE eran de bacterias o de levaduras, ensayamos la actividad de los complejos en geles de poliacrilamida nativos (BN-PAGE) y geles claros nativos de alta resolución (hr-CN-PAGE) (Figura 21).

Los pesos moleculares de los complejos respiratorios mitocondriales y bacterianos son diferentes (Tabla 2), por lo que al realizar la electroforesis en geles nativos esperábamos ver bandas diferentes en caso de que ambos organismos

expresasen su cadena respiratoria. Una levadura posee en promedio tres mitocondrias cuando se cultiva en un medio con glucosa como fuente de carbono. La levadura infectada posee entre 2 y 3 células de *Wolbachia* por levadura, y esperábamos por lo tanto ver una proporción que aproximase el 50% de proteínas mitocondriales con respecto a las de la bacteria.

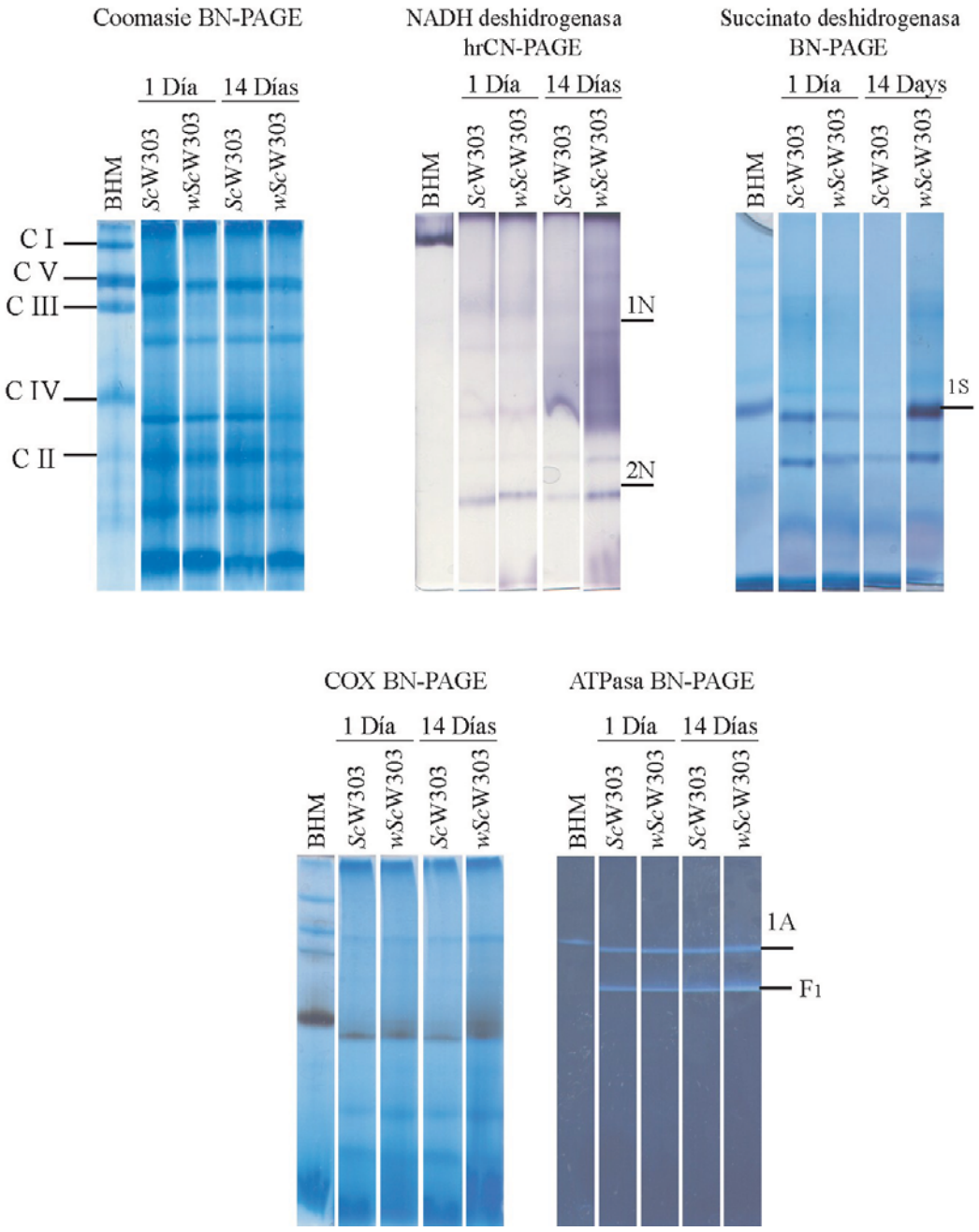

Figura 21. BN-PAGE y hrCN-PAGE de *Sc*W303 con y sin *Wolbachia* a 1 y 14 días. Electroforesis en geles nativos azules (BN) y claros de alta resolución (hrCN) de BHM (mitocondrias de corazón de bovino), *S. cerevisiae* *Sc*W303 y *S. cerevisiae* infectada con

Wolbachia (*wSc*W303) de uno y 14 días. Las bandas indicadas se secuenciaron y los resultados se encuentran en el Anexo C.

Las actividades de Complejo II, citocromo *c* oxidasa y ATPasa mostraron los mismos patrones de bandas, aunque con diferente intensidad, lo que sugiere que los únicos complejos respiratorios presentes eran los de levadura y que *Wolbachia* únicamente estaba modificando la expresión o actividad mitocondrial. Por otro lado, en el gel de actividad para NADH deshidrogenasa se observó una banda diferencial (1N) únicamente en los extractos de *wScW303* de 14 días. Esta banda, así como las de la actividad de succinato deshidrogenasa, citocromo *c* oxidasa y ATPasa se cortaron y se secuenciaron. La secuencia de las bandas de actividad (Indicadas en la Figura 21) 1N, 2N, 1S, mostró que todas las proteínas de CTE pertenecían a *S. cerevisiae*: no se encontraron proteínas de los complejos respiratorios de *Wolbachia*. Sólo en la banda secuenciada 1A correspondiente a actividad de ATPasa se detectaron las subunidades a y b de la subunidad F_1 de la ATPasa de *Wolbachia* (ver anexo C).

Los espectros diferenciales de las fracciones mitocondriales muestran una cantidad de citocromos *b* y *c* similares en *Sc*W303 y en *wSc*W303. Sin embargo, a los 14 días la cantidad de citocromos *a* de *Sc*W303 disminuyó drásticamente, mientras que la cantidad de citocromos *a* de *wSc*W303 se mantuvo constante (Figura 22, Tabla 7).

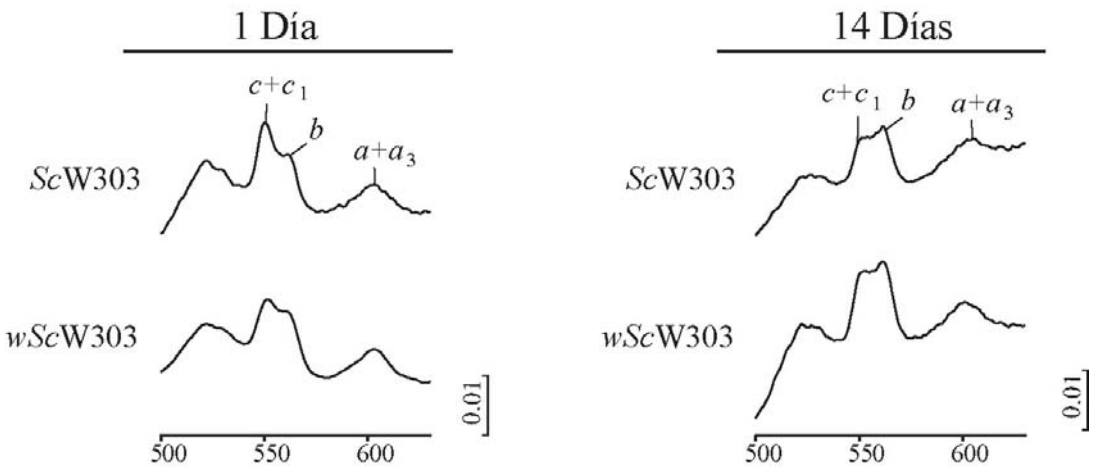

Figura 22. Espectros diferenciales de membranas de *Sc*W303 y *wSc*W303. 15 mg/mL de membranas de la fracción mitocondria-*Wolbachia* se resuspendieron en Tris-HCl 50 mM pH 7.4 en un volumen final de 200µL. Se realizaron barridos de 500 nm a 630 nm de una muestra reducida con hidrosulfito de sodio (ditionita) y se le restó una muestra oxidada con persulfato de amonio. Se observan los citocromos *c* (550 nm), *b* (560 nm) y *a* (604 nm).

Tabla 7. Concentración de citocromos (nmol/mg proteína) en la fracción mitocondria-*Wolbachia* de *Sc*W303 y *wSc*W303

	Citocromo $a + a_3$	Citocromo b	Citocromo $c + c_1$
*Sc*W303 1 D	1.61 ±0.25	3.78 ± 0.23	2.34 ± 0.65
*wSc*W303 1 D	1.54 ± 0.34	3.85 ± 0.42	2.19 ± 0.24
*Sc*W303 14 D	0.27 ± 0.18	3.18 ± 0.90	1.01 ± 0.99
*wSc*W303 14 D	1.14 ± 0.30	3.59 ± 1.37	2.05 ± 1.40

8.7 Cultivo de *Wolbachia* en diferentes cepas de *Saccharomyces cerevisiae* rho^0

Con el fin de probar si *Wolbachia* era capaz de consumir oxígeno, infectamos a *S. cerevisiae* W303 rho^0 (Figura 23). Primero, esta cepa resultó ser sensible al oxígeno, por lo que se cultivó en cajas de Petri, perdiendo la ventaja del volumen de cultivo en medios líquidos. Al realizar los controles de infección por *Wolbachia* (PCR, FISH y WB) nos percatamos de que la infección era muy débil y la infección se perdía al resembrar. Se intentó infectar la cepa *Sc*D723-10B rho^0, también con resultados negativos, a pesar de que la infección en *Sc*NB40 fue posible (Figura 7).

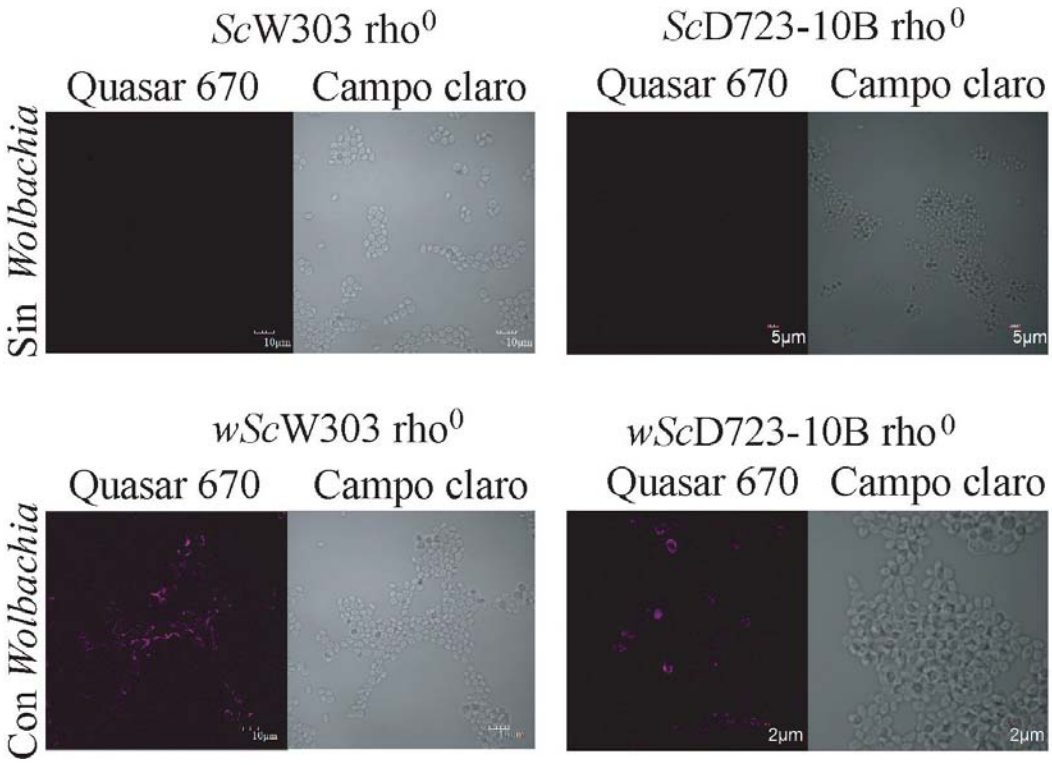

Figura 23. Infección de *S. cerevisiae* rho°. (a) FISH contra el gen 16S rDNA de *Wolbachia* en las cepas de *S. cerevisiae* W303 rho^{0,} y 723-10B rho^0 control e infectadas con *Wolbachia*. Serie

superior: levaduras control; serie inferior: levaduras infectadas con *Wolbachia*. La cantidad de Quasar 670 (rosa) indica la densidad de infección en cada cultivo.

A pesar de que la infección en las cepas rho^0 era muy baja y no se mantenía en el cultivo al resembrar las levaduras, se determinó el consumo de oxígeno en células completas y en extractos mitocondria/bacteria de la primera infección y no se observó consumo de oxígeno (Figura 24 a y b).

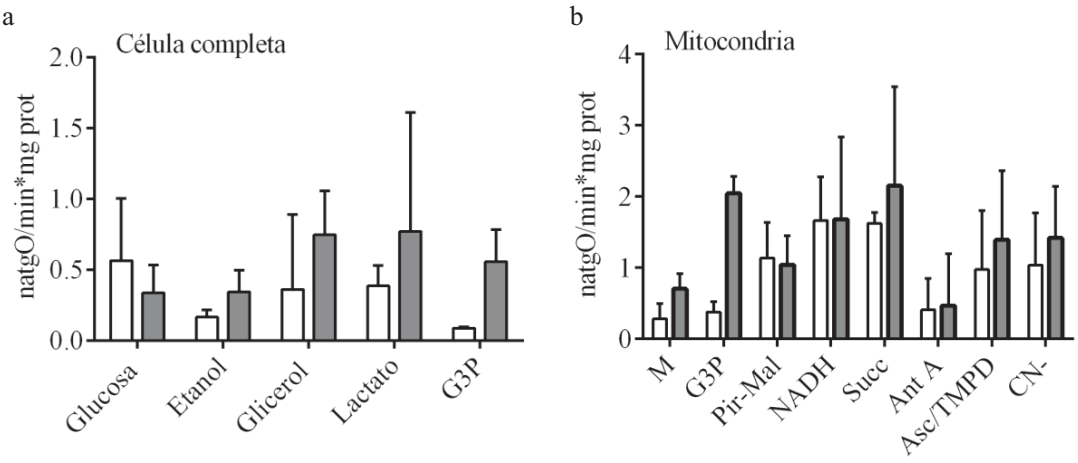

Figura 24. Consumo de oxígeno de la fracción mitocondrial de *S. cerevisiae* rho^0 control o infectada con *Wolbachia* con uno y 14 días de cultivo. El consumo de oxígeno se determinó en un volumen final de 1.5 mL en un OROBOROS equipado con un electrodo de Clark. Condiciones experimentales iguales a las empleadas en la Figura 20. Se añadieron 0.5 mg prot/mL de mitocondrias (M) o 50 mg de peso húmedo de levadura. Los datos representan la media ± SEM de n = 4. Prueba T * p <0.005,** p <0.001.

8.8 *Wolbachia* aislada no expresa una cadena respiratoria activa

Para eliminar separar a *Wolbachia* de las mitocondrias seguimos el protocolo descrito en la sección 7.23. Aislamos *Wolbachia* de cultivos de 50 a 100 mL de *Sc*W303 y *wSc*W303 (Figura 25). Se observaron dichas muestras en el microscopio electrónico de transmisión y se observó que en los controles, cuya biomasa era significativamente menor, se observaban pequeñas vesículas cuyo tamaño era inferior al esperado en la bacteria (Figura 25 a y b). En cambio, en las muestras aisladas a partir de *wSc*W303 se observaron numerosos cuerpos bacterianos, vesículas y fragmentos de mitocondrias (Figura 25 c, d y e). *Wolbachia* puede sobrevivir ex-vivo durante 7 días (Rasgon y cols., 2006) por lo que las muestras se incubaron a 27ºC en una incubadora de 5% CO_2 en MEM, 10% SBF, 100 μg/mL de anfotericina B de 48 a 96 horas (figura 25) con el fin de eliminar cualquier actividad mitocondrial remanente.

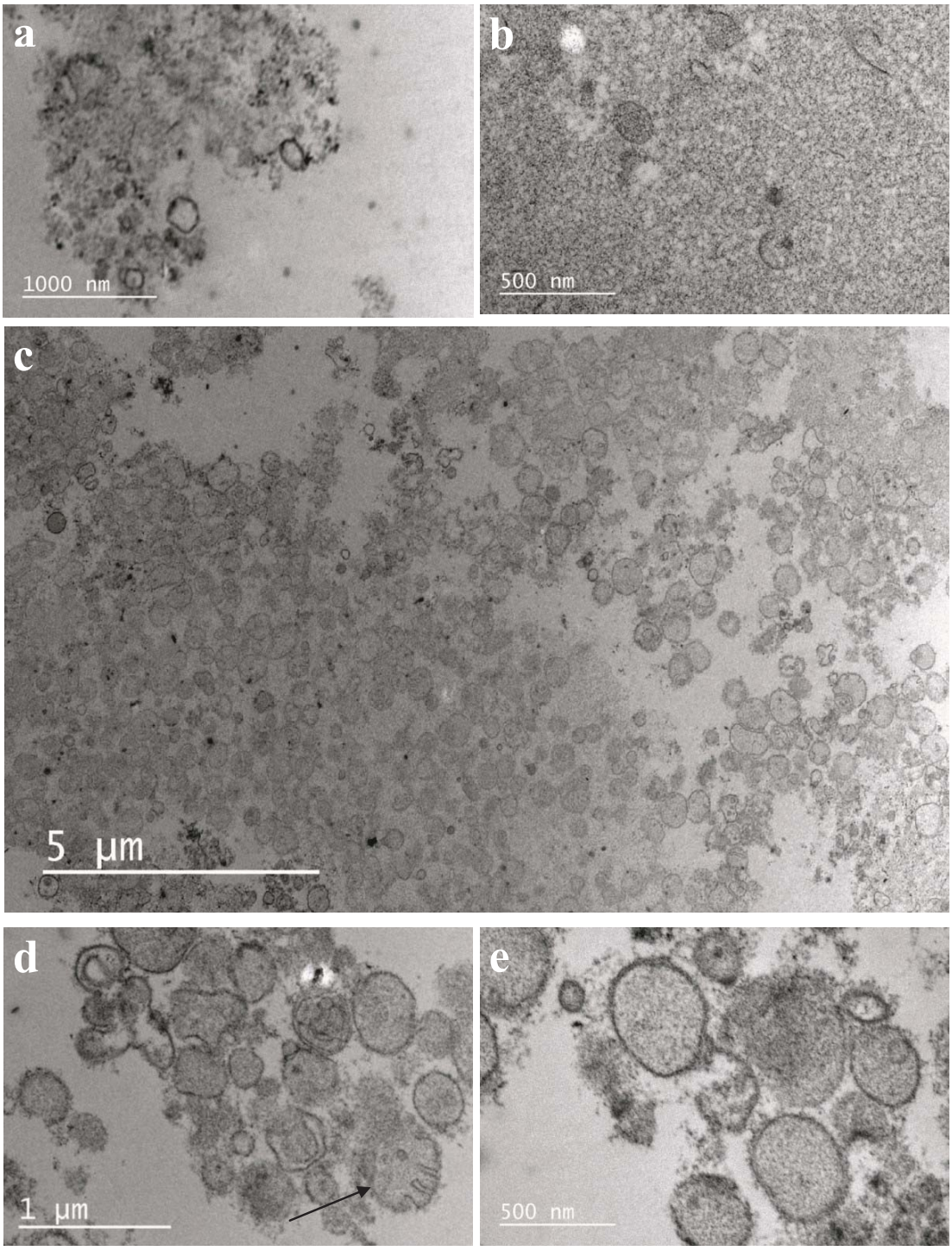

Figura 25. Microscopía Electrónica de Transmisión de la fracción con *Wolbachia* aisalda de *Sc*W303 y w*Sc*W303. Imágenes tomadas de la fracción aislada de *Sc*W303 (a) y (b) y de *wSc*W303 (c, d y e). En las imágenes tomadas a partir de la wScW303 podemos observar cuerpos bacterianos con doble membrana y mitocondrias degradas (flecha).

Después de 48 horas no se detectó respiración con piruvato, malato, glutamato, glicerol-3-fosfato, succinato o glucosa en células integras o permeabilizadas (Figura 26).

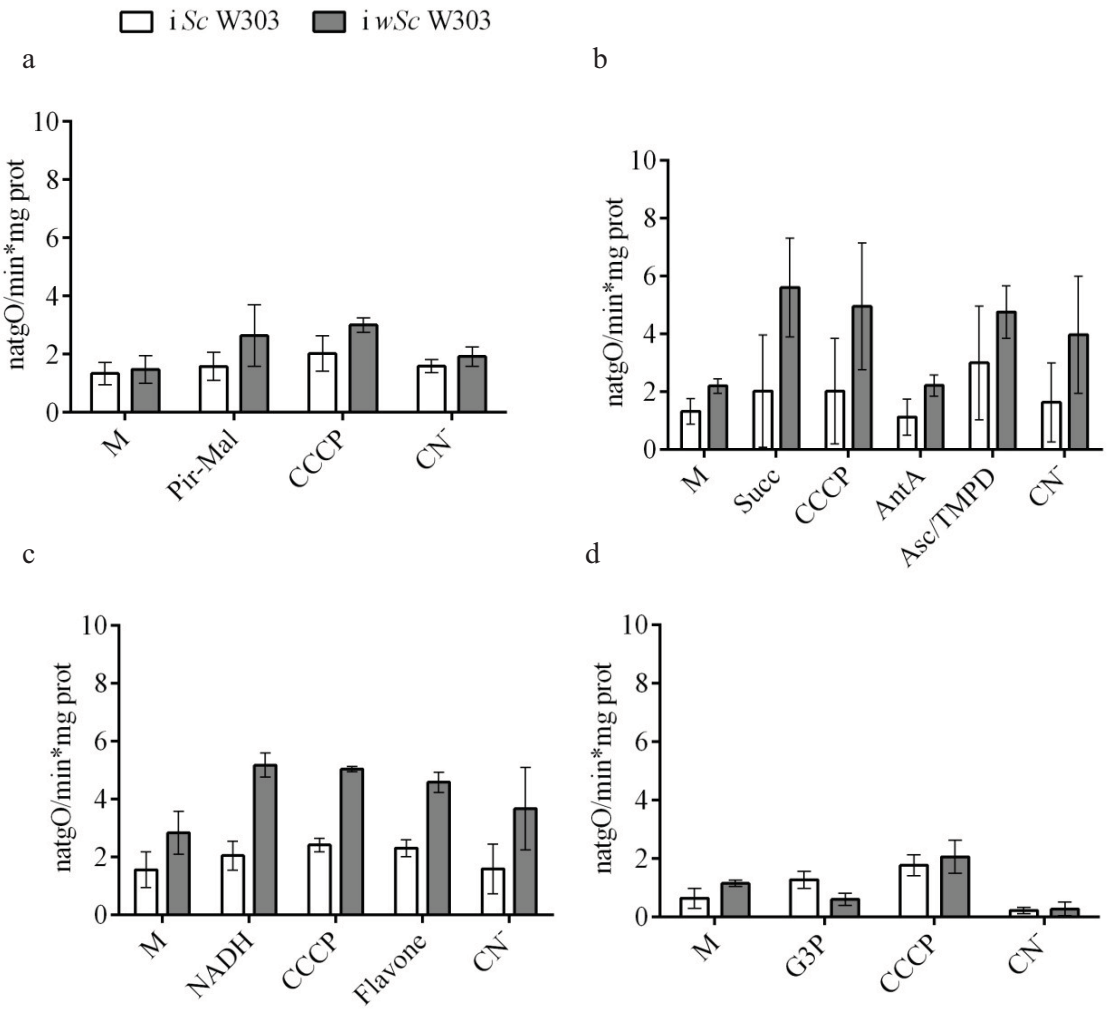

Figura 26. Consumo de oxígeno de *Wolbachia* aislada. Condiciones experimentales iguales a las empleadas en la Figura 19. i *Sc*W303: fracción que contiene a *Wolbachia* de *Sc*W303; i *wSc*W303: fracción que contiene a *Wolbachia* de *wSc*W303. Se añadieron 0.5 mg prot/ mL de bacteria. Los datos representan la media ± SEM de n = 4. Prueba T * p <0.005.

8.9 Hidrólisis de ATP por *Wolbachia* aislada

Se detectó la actividad ATPasa sensible a oligomicina en bacterias aisladas (Figura 27), lo que podría indicarnos que *Wolbachia* pueda captar de alguna manera el

ATP del hospedero y puede hidrolizarlo, tal vez para energizar sus sistemas de secreción SST2 o/y SST4.

Wolbachia es un endosimbionte obligado, y los dos últimos experimentos fueron realizados en bacteria aislada e incubada varios días en un medio extracelular, lo que podría significar que el metabolismo de *Wolbachia* puede ser diferente al observado en un medio intracelular.

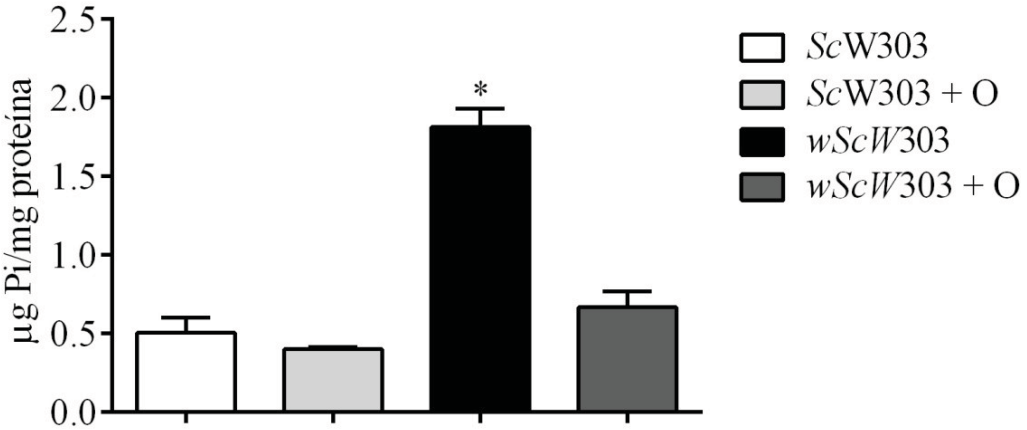

Figura 27. *Wolbachia* aislada hidroliza ATP. Se añadieron 0.05 mg prot/ mL de bacteria aislada de *wSc*W303 o la fracción equivalente a la bacteria *Sc*W303 en un volumen final de 100 µL. Dónde se indica (+O), se agregaron 3 µg/mL de oligomicina. Los datos representan la media ± SEM de n = 4. Prueba T * p <0.005.

8.10 *Wolbachia* aislada a partir de levaduras mantiene su capacidad infectiva pero no modifica el consumo de oxígeno de la línea celular.

Inoculamos una muestra de *Wolbachia* extraída de *wSc*W303 en la línea celular C6/C36 con el fin de observar si permanecía infectiva después de permanecer de dos a seis meses como endoparásito de levaduras. La línea celular C6/C36 es una línea celular derivada de *Aedes albopictus* (ATCC CRL-1660) que soporta el parasitismo de *Wolbachia* (Baldridge y cols., 2014). Preferimos la línea celular C6/C36 sobre la Aa23Tet, porque la primera jamás había sido expuesta a *Wolbachia* o a tetraciclina. La infección por *Wolbachia* se evaluó mediante tinción específica usando FISH (Figura 28, Película S3).

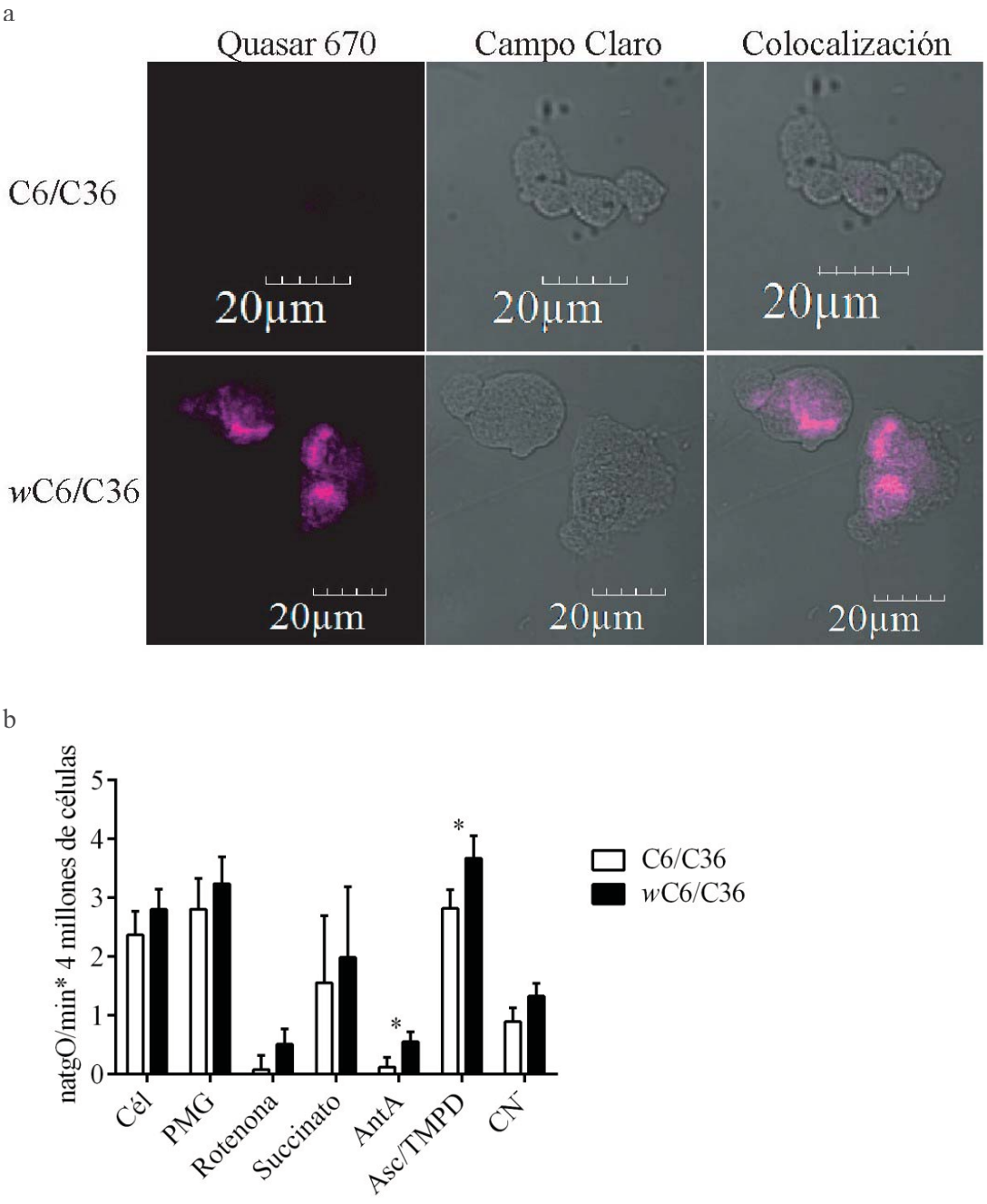

Figura 28. **Infección de C6/C36 por *Wolbachia*.** (a) FISH (Quasar 670-pink) de la línea celular *w*C6/C36. Las imágenes de luz / Quasar 670 muestran hibridación dentro de la línea celular infectada. La línea celular no infectada C6/C36 no tiene ninguna marca de hibridación. (b) Oximetría de la línea celular C6/C36 control y C6/C36 infectada con *Wolbachia w*AlbB. Las condiciones fueron similares a las empleadas en la figura 13. Se emplearon 4 millones de células por trazo. n=4, *p<0.05.

No se realizaron oximetrías comparando la línea celular Aa23 con Aa23tet, ya que la tetraciclina aumenta las actividades mitocondriales de los hospederos expuestos a ésta (Ballard y cols., 2007). Como la cepa C6/C36 nunca estuvo expuesta a *Wolbachia* o a tetraciclina se determinó el consumo de oxígeno en C6/C36 y la *w*C6/C36 y se encontraron diferencias significativas ($p<0.05$) (Figura 28b). Cabe destacar que el consumo de oxígeno es muy bajo a comparación con el obtenido en la fracción *Wolbachia*/mitocondria de levadura, pero congruente con lo reportado para otras líneas celulares (Loyola-Machado y cols., 2017). Este experimento realza la importancia de nuestro modelo sintético en donde se obtiene suficiente biomasa para lograr aislar tanto la fracción *Wolbachia*/mitocondria y evaluar el efecto sobre el metabolismo energético del hospedero, como a la bacteria aislada y poder evaluar su metabolismo aerobio.

9. DISCUSIÓN

El primer reto enfrentado en el proyecto para cumplir con el objetivo de estudiar el metabolismo aeróbico de *Wolbachia*, fue aumentar la cantidad de biomasa disponible para trabajar. Siguiendo los métodos empleados para cultivar otros endosimbiontes en medio axénicos, se intentó cultivar *Wolbachia* en medios ricos utilizando como medios base MEM, BHI y MM suplementados con aminoácidos, solutos compatibles, colesterol, catalasa, suero bovino fetal y eritrocitos de rata, borrego y humano. En esta etapa del proyecto encontramos que varios de estos medios pueden mantener a *Wolbachia* viva, pero no se reproduce y no hay aumento de la biomasa. Los resultados obtenidos no eran relevantes ya que Rasgon y cols., (2006) reportaron que *Wolbachia* podía sobrevivir afuera de un hospedero durante 7 días en MEM suplementado son SBF en una atmosfera de 5% de CO_2.

Wolbachia es una bacteria endosimbionte obligada comúnmente reportada en artrópodos y en nemátodos (Bandi y cols., 1999; Fenn y cols., 2004). En reportes recientes se ha detectado *Wolbachia* en humanos inmunocomprometidos (Chen y cols., 2015) y en plantas (Li y cols., 2017), demostrando que *Wolbachia* es una bacteria parásita con una gran facilidad de infección a nuevos hospederos por lo que sugerimos cultivar a *Wolbachia* como endobacteria en la levadura *Saccharomyces cerevisiae*.

En el área de biotecnología las endosimbiosis artificiales se han propuesto como microrreactores, en dónde una bacteria huésped produce un metabolito necesario para su hospedero y que a su vez es precursor de algún otro compuesto que el hospedero puede sintetizar y que por lo general tiene algún uso humano (Hosoda y cols., 2011a; Hosoda y cols., 2011b; Momeni y cols., 2011). Las endosimbiosis artificiales también se han propuesto como modelos para estudiar la evolución de organismos independientes a organelos celulares (Brenner y cols., 2008; French, 2017; Frey-Klett y cols., 2011; Mee y cols., 2012) y finalmente, se ha propuesto el uso de hospederos artificiales para el cultivo de endosimbiontes y endoparásitos obligados (Stewart, 2012).

Este trabajo es uno de los primeros en demostrar que el cultivo de endobacterias obligadas en hongos levaduriformes es posible. La facilidad en el cultivo y el manejo de la levadura puede aumentar la biomasa bacteriana obtenida facilitando el estudio del metabolismo de la bacteria y su interacción con el hospedero. Las levaduras son más robustas que las líneas celulares, por lo que se disminuyen los requerimientos nutricionales de los cultivos y se protege al endosimbionte contra cambios ambientales. Otra ventaja de la levadura utilizada es que son aerobias facultativas, es decir, pueden

crecer a altas concentraciones de oxígeno, en condiciones microaeróbicas o anaeróbicas dependiendo de lo que necesitemos y no requieren forzosamente de una incubadora de CO_2 (Baldridge y cols., 2014; Gasch, 2002; Gasch y cols., 2002; Khoo y cols., 2013) . Finalmente, todas las líneas celulares empleadas para cultivar a *Wolbachia* son adherentes, es decir están limitadas a crecer en la superficie de las cajas petri ó frascos de Roux. Las líneas celulares tienen un rendimiento de $3x10^6$ de células en 75 mL, mientras que un cultivo de 24 horas de *S. cerevisiae* tiene $9*10^7$ células por mL.

A pesar de que en esta tesis se presenta una propuesta novedosa, hay que recordar que el sistema *Wolbachia/S. cerevisiae* es un modelo artificial y por lo tanto las interacciones observadas pueden diferir de las que ocurren en la naturaleza. Además hay que ajustar las condiciones de cultivo dependiendo del huésped, del hospedero, de los posibles mecanismos de infección y del objetivo del experimento. *Escherichia coli* puede cultivarse como endoparásito de amoebas (Hosoda y cols., 2011a), y recientemente el grupo iGEM Marburg se ha dedicado a establecer una endosimbiosis artificial y cultivar la bacteria como endosimbionte de *S. cerevisiae.* (http://2016.igem.org/Team:Marburg/PEG_Method/Results) El objetivo primordial de este proyecto es hacer microbiorreactores para la producción de terpenoides con alto valor comercial como por ejemplo el limoneno. En este proyecto lograron introducir a *E. coli* en *S. cerevisiae* mediante una fusión entre la membrana del hospedero, quitando la pared celular con zimoliasa y la bacteria encapsulada en poli etilenglicol. Confirman la introducción de la bacteria a la levadura haciendo cortes en Z de la levadura teñida con calcoflúor y con *E. coli* marcada con una RFP (proteína roja fluorescente). En este caso aprovechan la facilidad de manejo de *E. coli*. Este proyecto fue descontinuado ya que, aunque lograron introducir la bacteria a la levadura, esta última lisó a *E. coli*, evitando una simbiosis estable. Lamentablemente no hay ningún artículo al respecto por lo que no hay métodos experimentales ni resultados de este evento. Esta reportado que los lisosomas de *S. cerevisiae* W303 generados como respuesta ante una invasión bacteriana lisan a *E. coli* y otras bacterias como *Xantamonas oryzae* y *Shigella flexneri*, (Yoon y cols., 2009) .

A diferencia de *E. coli*, a la fecha, no se ha logrado transformar a *Wolbachia* utilizando técnicas convencionales de biología molecular ni utilizando los sistemas de CRISPR-cas (datos no publicados de Thiem S., Proyecto MICL02352, Departamento de entomología, Universidad de Michigan), por lo que el uso de *Wolbachia* como bacteria endosimbionte en un microrreactor no sería práctico. Sin embargo, los resultados

presentes en esta tesis y aquellos reportados por el equipo Marburg pueden utilizarse con otras bacterias y levaduras, por ejemplo, se podrían utilizar con *Burkholderia sp*, que puede cultivarse ex-vivo, tiene mecanismos de transmisión horizontal y vertical y es capaz de adaptarse a la vida intracelular (Partida-Martinez y cols., 2005; Scherlach y cols., 2006).

Al igual que en las líneas celulares, dependiendo del linaje de las levaduras observamos diferentes densidades de infección. En esta tesis se utilizaron tres cepas diferentes de *Saccharomyces cerevisiae*: *Sc*BY, *Sc*W303 y *Sc*D273-10B. *Wolbachia* fue capaz de colonizar las cepas de *S. cerevisiae* W303 y D273-10B efectivamente mientras que la infección en la cepa BY fue menor. Las cepas que soportan la infección de *Wolbachia* respiran más y tienen una menor sensibilidad a especies reactivas de oxígeno (Gutierrez-Aguilar y cols., 2014; Montanari y cols., 2014). Montanari y cols. (2014) evalúan la capacidad de diferentes cepas de *S. cerevisiae* de formar colonias después de ser cultivadas en YPD. *Sc*W303 tiene un 100% de supervivencia después de cultivarse durante 30 días, mientras que *Sc*D273-10B tiene una supervivencia del 50% a los 5 días y el cultivo el incapaz de formar colonias después de 22 días de cultivo. En líneas celulares la infección por *Wolbachia* se reporta después de 15 y hasta 100 días de cultivo.

Cultivar a *Wolbachia* en levadura nos ha permitido publicar el primer artículo en dónde se evalúa la actividad metabólica de la bacteria aislada y su relación con el metabolismo del hospedero con experimentos bioquímicos y no solo evaluando la expresión diferencial de los genomas y los proteomas, los cuáles, nos sirvieron de referencia para desarrollar los experimentos (Uribe-Alvarez y cols., 2018). Además la levadura es más robusta que las líneas celulares, son más tolerantes al estrés ambiental como la temperatura, desecación, pH, antibióticos y osmóticos. estrés, etc. que las líneas celulares. Los medios utilizados son más baratos y al cultivarse en frascos de vidrio que se pueden esterilizar hay una gran reducción de material plástico empleado. La levadura puede crecer en aerobiosis por lo que la limitación de espacio ya no es un problema, sin embargo al fermentar también pueden cultivarse en micro y anaerobiosis en caso de ser necesario. Además, la infección de *S. cerevisiae* nos da la ventaja de que, dado que es una de las levaduras más estudiadas, hay bibliotecas mutantes completas disponibles, así se puede estudiar el propósito de la bacteria en su hospedero, eligiendo una levadura con una mutación que imita la condición de este y evaluando si la infección con *Wolbachia* revierte el efecto de la mutación.

En este trabajo buscamos estudiar la cadena transportadora de electrones de *Wolbachia* porque estudios previos sugieren que esta bacteria contribuye a la actividad respiratoria del hospedero e inclusive es capaz de sustituirla (Darby y cols., 2012; Darby y cols., 2014; Strubing y cols., 2010). *Wolbachia* es una α-proteobacteria filogenéticamente cercana a la mitocondria, por lo que la posibilidad de que remplazara o cooperara con la actividad respiratoria era una idea atractiva. En contraste el grupo del Dr. Sullivan describe a este endosimbionte como una bacteria con capacidades metabólicas limitadas, completamente dependiente del hospedero y sugiere que en vez de aportar energía directamente al hospedero, aporta únicamente grupos hemo y riboflavina(Pietri y cols., 2016).

Durante el análisis del genoma de la cepa *w*AlbB (Mavingui y cols., 2012) encontramos que *Wolbachia* carece de las subunidades *nuo*C y *nuo*D del Complejo I de la cadena transportadora de electrones (Anexo B). Estas subunidades son dos de las cuatro necesarias para la unión de la ubiquinona al complejo I (Figura 3) (Sazanov, 2015). Del complejo II, hace falta el gen *sdh*D que es necesario para la formación del sitio de unión a la ubiquinona. Del Complejo III únicamente hay un gen que corresponde a la proteína fierro-azufre (Mavingui y cols., 2012). Todas las subunidades necesarias para el funcionamiento del complejo IV y de la ATPasa (no posee subunidad inhibidora ζ) están presentes en el genoma. El genoma reportado para *w*AlbB tiene 1.29 Mpb y en general los genomas de *Wolbachia* de artrópodo tienen un tamaño de 1.4 Mpb, por lo existe la posibilidad de que el genoma no esté completo o que en la cepa *w*AlbB se hayan perdido algunos genes presentes en otras cepas (ver Anexo B). *Wolbachia* de *Culex pipientis* (Klasson y cols., 2008), que es la más parecida a *w*AlbB, posee todos los genes necesarios para sintetizar una cadena transportadora de electrones funcional (Anexo B). La recopilación de todos los posibles componentes de la cadena transportadora de electrones de diferentes grupos de *Wolbachia* se encuentra en la Figura 3 (Rosas-Lemus, 2016), sin embargo, estos varían enormemente de acuerdo a la especie de la cual se aisló *Wolbachia* (Anexo B). Debido a la información contrastante decidimos explorar si *Wolbachia* contribuye al consumo de oxígeno en el hospedero, si posee su propia CTE y si es capaz de consumir oxígeno.

En la fracción mitocondria-*Wolbachia* de levaduras infectadas observamos un aumento en el consumo de oxígeno y en el acoplamiento de la CTE a los 14 días. Aprovechando la diferencia en los pesos moleculares de estos pudimos definir que el aumento en el consumo de oxígeno a los 14 días en levaduras infectadas es

responsabilidad de la mitocondria y no de la bacteria. Esto coincide con lo observado en la microscopía electrónica de transmisión, en dónde las levaduras control no presentan mitocondrias mientras que en las levaduras infectadas éstos organelos están conservados. El aumento en el consumo de oxígeno por parte del hospedero puede ser resultado de la suplementación de nutrientes por parte de la bacteria como se observa para el SOPE (Primary endosymbiont of *Sytophilus oryzae)* del gorgojo de arroz (Heddi y cols., 1999; Heddi A, 1993); o puede ser una respuesta inespecífica del hospedero a la infección de la bacteria. Por lo tanto, la posibilidad de que *Wolbachia* esté donando riboflavina o grupos hemo a su hospedero artificial permanece latente y constituye una de nuestras principales perspectivas.

Finalmente aislamos *Wolbachia* aprovechando la capacidad que tiene de sobrevivir ex-vivo y ésta no presentó consumo de oxígeno bajo ninguna de las condiciones examinadas. Podemos concluir que *Wolbachia* no presenta CTE propia y por lo tanto no consume oxígeno. Estos resultados también cuestionan la propuesta de que *Wolbachia* pueda donar ATP al hospedero ya que a pesar de tener las vías de síntesis de nucleótidos, al no tener CTE no puede generar el gradiente necesario ´para fosforilar el ADP. Otro motivo por el cual esta teoría esta desacreditada es la falta de un mecanismo definido por el cual *Wolbachia* pueda donar ATP a la célula (Krause y cols., 1985; Winkler, 1976).

Dependiendo del experimento planeado, la metodología para aislar a *Wolbachia* puede modificarse. En nuestro caso, necesitábamos eliminar los fragmentos de mitocondria que podían dar falsos positivos en los experimentos de oximetría. El paso crítico de este protocolo es romper y centrifugar las células empleando medios suplementados con suero bovino fetal y mantener la esterilidad. Por ejemplo, para este experimento podemos filtrar las células por una membrana de 0.8 µm y deshacernos de la mayoría de las levaduras, pero como las levaduras crecen en microaerobiosis agregamos anfotericina B para evitarlo. Si usamos las bacterias obtenidas de la levadura para infectar otras levaduras, es necesario filtrar las células con una membrana de 0.45 µm para asegurar que no haya levadura. Si se agrega anfotericina B, es probable que afecte el crecimiento de la levadura receptora. Filtrar las células por membranas de 0.45 µm provoca que se pierda una gran cantidad de bacterias.

Wolbachia aislada no sobrevive en una atmósfera aerobia, por lo que podría especularse que necesita de la mitocondria para reducir la cantidad de oxígeno en su entorno (Potter y cols., 2016). También es más sensible a especies reactivas de oxígeno

que su hospedero y necesita una atmósfera con 5% CO_2 para sobrevivir ex-vivo (Fallon y cols., 2013). La posibilidad de que *Wolbachia* entre al citoplasma de hospedero para escapar del oxígeno atmosférico no excluye el hecho de que también utilice algún sustrato del hospedero como fuente de energía.

Actualmente se han liberado mosquitos infectados con *Wolbachia* en muchas partes del mundo; inhibe la transmisión de diferentes arboviruses (Brownlie y cols., 2009b; Hedges y cols., 2008; Hoffmann y cols., 2011; Moreira y cols., 2009; Mousson y cols., 2010; Pan y cols., 2012; Raquin y cols., 2015) modificando el metabolismo del hospedero y compitiendo por los nutrientes (colesterol y aminoácidos principalmente) disponibles en el hospedero. Se sabe ya que algunas cepas de *Wolbachia* (*w*MelPop acortan la vida de sus hospederos en un 50% y tienen efectos dañinos sobre ellos(McMeniman y cols., 2009), pero no se ha explorado cómo causa la muerte prematura, ni qué pasa con el metabolismo del hospedero. Hacen falta estudios para detectar los posibles efectos de la bacteria sobre el hospedero, en especial sobre su posible intercambio de material genético y proteínas y su facilidad para adaptarse a nuevos hospederos.

Con nuestros resultados y los de genomas obtenidos por otros grupos de investigación, podemos proponer que en vez de suministrar ATP al hospedero, *Wolbachia* absorbe el ATP de éste en forma de intermediarios fosforilados de la glucólisis (piruvato o fructosa-6-fosfato y la fructosa 1,6-difosfato por medio de un transportador de hexosas fosfato). Después, utilizando el ATP generado en la segunda fase de la glucólisis y el ciclo de Krebs, genera un potencial transmembranal utilizando la ATP sintasa de manera reversa (ninguna *Wolbachia* posee la subunidad inhibidora ζ de la ATPasa). Finalmente, este potencial transmembranal es utlizado para energizar los transportadores de aminoácidos (simportadores aa/H^+) ya que según los reportes de los genomas complementarios de *Wolbachia* y sus hospederos, no es capaz de sintetizar aminoácidos y debe de tomarlos forzosamente del hospedero.

Dado que no se encontraron aumentadas las proteínas propias de *Wolbachia*, no pareciera difícil que en su genoma existan factores capaces de interactuar, o bien con el genoma nuclear o mitocondrial de la levadura y modificar la expresión de algunos componentes implicados en el metabolismo energético.

10. CONCLUSIONES

En este trabajo se desarrolló un novedoso sistema de parasitismo artificial infectando a la levadura *S. cerevisiae* con el endosimbionte obligado *Wolbachia sp.* Las cepas W303 y D723-10B resultaron ser más susceptibles a la infección por *Wolbachia* que la cepa BY.

La infección con *Wolbachia* en las cepas W303 rho° y D723-10B rho° fue inestable, indicando la importancia en la integridad del genoma mitocondrial para la infección por *Wolbachia*.

La transferencia (vertical/horizontal) de *Wolbachia* en los cultivos de *S. cerevisiae* no es perfecta. En *wSc*W303, el 72 % del cultivo de levadura se encuentra infectado con un máximo de 6 bacterias por levadura.

Wolbachia secuestra el metabolismo de *S. cerevisiae* W303: A las 6 horas de cultivo, la actividad fermentativa de la levadura aumenta, provocando un aumento de biomasa y un adelanto en la fase diáuxica.

A 14 días de cultivo, la actividad respiratoria mitocondrial se ve anormalmente elevada en la levadura infectada. Finalmente, a los 16 días, las levaduras infectadas mueren abruptamente.

Durante la infección en la levadura, no se detectaron proteínas de la cadena transportadora de electrones de *Wolbachia*.

Se desarrolló un método para aislar a *Wolbachia* y se determinó que la bacteria aislada no consume oxígeno.

Bajo las condiciones probadas en esta tesis, *Wolbachia* no presenta una CTE y por lo tanto no parece ser capaz de generar energía para el hospedero.

11. PERSPECTIVAS

Wolbachia aumenta la tasa de respiración del hospedero infectado, sin embargo parece no contribuir con consumo de oxígeno. El análisis de los genomas del hospedero y del huésped sugieren que *Wolbachia* podría esta suplementando riboflavina y/o grupos hemos al hospedero, lo que provocaría un aumento en la actividad de la cadena transportadora de electrones. En nuestro grupo de investigación se propone infectar levaduras con mutaciones en las enzimas de las vías de síntesis de riboflavina para determinar si *Wolbachia* es capaz de revertir parcial o totalmente el efecto de dichas mutaciones. Las cepas de *S. cerevisiae* Δrib no crecen en medios sin riboflavina. Si la infección con *Wolbachia* pueda revertir este fenómeno sería un indicativo de que *Wolbachia* suplementa a su hospedero con riboflavina. Los grupos FMN y FAD+ de los complejos respiratorios de la levadura se sintetizan a partir de riboflavina, por lo que una cepa carente de la vía de síntesis de riboflavina tiene una respiración nula. Si *Wolbachia* suplementa estos grupos, la levadura Δrib podrá respirar y se podrá comprobar que *Wolbachia* puede suplementar con riboflavina al hospedero.

A pesar de que en esta tesis se encontró que *Wolbachia* no posee una CTE con la capacidad de suplementar ATP al hospedero, no se exploró el metabolismo de *Wolbachia*. Por lo que se propone medir el aumento en el potencial transmembranal al agregar diferentes sustratos, principalmente sustratos fosforilados, ya que *Wolbachia* carece de las primeras enzimas de la glucólisis y posee transportadores de hexosas fosfato; y piruvato que ha sido propuestos como el sustrato principal de *Wolbachia* según el análisis de los genomas reportados a la fecha. Después proponemos definir si la F_1F_0-ATPasa carece de la subunidad inhibidora ζ como se ha reportado para las α-proteobacterias endocelulares obligadas y que está de acuerdo con los genomas reportados. Posteriormente podemos analizar si en efecto la ATPasa puede hidrolizar el ATP para generar un potencial transmembranal que eventualmente puede utilizar para transportar aminoácidos, que, según todos los genomas reportados, *Wolbachia* es incapaz de sintetizar sus propios aminoácidos.

Los mecanismos de transmisión horizontal de *Wolbachia* están poco estudiados. Este año se publicó el primer reporte que indica que *Wolbachia* utiliza el sistema de endocitosis mediada por de clatrina de las líneas celulares. En nuestro laboratorio buscamos definir el mecanismo de transferencia horizontal de *Wolbachia* entre levaduras.

Wolbachia es capaz de manipular la endocitosis, el metabolismo y la longevidad de sus diferentes hospederos por lo que es de suma importancia explorar las modificaciones que provoca la infección con *Wolbachia* sobre las vías de señalización de rho GTPasas y mTor, responsables de proliferación, apoptosis y envejecimiento del hospedero. La activación o inhibición de estas vías de señalización puede evaluarse sencillamente con experimentos de proliferación y Western Blots contra las diferentes moléculas implicadas en las vías de señalización.

12. BIBLIOGRAFÍA.

Aguilar-Uscanga, B. y cols. (2003). "A study of the yeast cell wall composition and structure in response to growth conditions and mode of cultivation." Lett Appl Microbiol **37**(3): 268-274.

Ahmed, M. Z. y cols. (2016). "Evidence for common horizontal transmission of Wolbachia among butterflies and moths." BMC Evol Biol **16**(1): 118.

Akman, L. y cols. (2002). "Genome sequence of the endocellular obligate symbiont of tsetse flies, Wigglesworthia glossinidia." Nat Genet **32**(3): 402-407.

Alsmark, C. M. y cols. (2004). "The louse-borne human pathogen Bartonella quintana is a genomic derivative of the zoonotic agent Bartonella henselae." Proc Natl Acad Sci U S A **101**(26): 9716-9721.

Amuzu, H. E. y cols. (2016). "Wolbachia-Based Dengue Virus Inhibition Is Not Tissue-Specific in Aedes aegypti." PLoS Negl Trop Dis **10**(11): e0005145.

Andersson, S. G. y cols. (1998). "The genome sequence of Rickettsia prowazekii and the origin of mitochondria." Nature **396**(6707): 133-140.

Anraku, Y. (1987). Biochemistry and Molecular Biology of the Escherichia Coli Aerobic Respiratory Chain. Cytochrome Systems: Molecular Biology and Bioenergetics. Papa, S., Chance, B. yErnster, L. Boston, MA, Springer US**:** 565-574.

Anraku, Y. (1988). "Bacterial electron transport chains." Annu Rev Biochem **57**: 101-132.

Avrahami-Moyal, L. y cols. (2012). "Overexpression of PDE2 or SSD1-V in Saccharomyces cerevisiae W303-1A strain renders it ethanol-tolerant." FEMS Yeast Res **12**(4): 447-455.

Bakhtiari, N. y cols. (1999). "Structure/function of the beta-barrel domain of F1-ATPase in the yeast Saccharomyces cerevisiae." J Biol Chem **274**(23): 16363-16369.

Baldridge, G. D. y cols. (2014). "Proteomic profiling of a robust Wolbachia infection in an Aedes albopictus mosquito cell line." Mol Microbiol **94**(3): 537-556.

Ballard, J. W. y cols. (2007). "Tetracycline treatment influences mitochondrial metabolism and mtDNA density two generations after treatment in Drosophila." Insect Mol Biol **16**(6): 799-802.

Bandi, C. y cols. (1999). "Wolbachia genomes and the many faces of symbiosis." Parasitol Today **15**(11): 428-429.

Bandi, C. y cols. (2001). "Wolbachia in filarial nematodes: evolutionary aspects and implications for the pathogenesis and treatment of filarial diseases." Vet Parasitol **98**(1-3): 215-238.

Belda, E. y cols. (2012). "Metabolic networks of Sodalis glossinidius: a systems biology approach to reductive evolution." PLoS One **7**(1): e30652.

Berden, J. A. y cols. (1970). "The reaction of antimycin with a cytochrome b preparation active in reconstitution of the respiratory chain." Biochim Biophys Acta **216**(2): 237-249.

Bianciotto, V. y cols. (1996). "An obligately endosymbiotic mycorrhizal fungus itself harbors obligately intracellular bacteria." Appl Environ Microbiol **62**(8): 3005-3010.

Bianciotto, V. y cols. (2002). "Arbuscular mycorrhizal fungi: a specialised niche for rhizospheric and endocellular bacteria." Antonie Van Leeuwenhoek **81**(1-4): 365-371.

Bjorkholm, B. y cols. (2000). "Helicobacter pylori entry into human gastric epithelial cells: A potential determinant of virulence, persistence, and treatment failures." Helicobacter **5**(3): 148-154.

Blagrove, M. S. y cols. (2013). "A Wolbachia wMel transinfection in Aedes albopictus is not detrimental to host fitness and inhibits Chikungunya virus." PLoS Negl Trop Dis **7**(3): e2152.

Bradford, M. M. (1976). "A rapid and sensitive method for the quantitation of microgram quantities of protein utilizing the principle of protein-dye binding." Anal Biochem **72**: 248-254.

Brattig, N. W. y cols. (2004). "The major surface protein of Wolbachia endosymbionts in filarial nematodes elicits immune responses through TLR2 and TLR4." J Immunol **173**(1): 437-445.

Brenner, K. y cols. (2008). "Engineering microbial consortia: a new frontier in synthetic biology." Trends Biotechnol **26**(9): 483-489.

Brownlie, J. C. y cols. (2009a). "Evidence for metabolic provisioning by a common invertebrate endosymbiont, Wolbachia pipientis, during periods of nutritional stress." PLoS Pathog **5**(4): e1000368.

Brownlie, J. C. y cols. (2009b). "Symbiont-mediated protection in insect hosts." Trends Microbiol **17**(8): 348-354.

Buchner, P. (1965). "Endosymbiosis of Animals with Plant Microorganims." Mycologia **60**(2): 466-469.

Cabrera-Orefice, A. y cols. (2014). "The branched mitochondrial respiratory chain from Debaryomyces hansenii: components and supramolecular organization." Biochim Biophys Acta **1837**(1): 73-84.

Capaldi, R. A. (1990). "Structure and assembly of cytochrome c oxidase." Arch Biochem Biophys **280**(2): 252-262.

Caragata, E. P. y cols. (2013). "Dietary cholesterol modulates pathogen blocking by Wolbachia." PLoS Pathog **9**(6): e1003459.

Caragata, E. P. y cols. (2014). "Competition for amino acids between Wolbachia and the mosquito host, Aedes aegypti." Microb Ecol **67**(1): 205-218.

Carroll, J. y cols. (2003). "Analysis of the subunit composition of complex I from bovine heart mitochondria." Mol Cell Proteomics **2**(2): 117-126.

Cecchini, G. (2003). "Function and structure of complex II of the respiratory chain." Annu Rev Biochem **72**: 77-109.

Chang, H. H. y cols. (2015). "Complete Genome Sequence of "Candidatus Sulcia muelleri" ML, an Obligate Nutritional Symbiont of Maize Leafhopper (Dalbulus maidis)." Genome Announc **3**(1).

Chen, X. P. y cols. (2015). "Detection of Wolbachia genes in a patient with non-Hodgkin's lymphoma." Clin Microbiol Infect **21**(2): 182 e181-184.

Chiquete-Felix, N. y cols. (2009). "In guinea pig sperm, aldolase A forms a complex with actin, WAS, and Arp2/3 that plays a role in actin polymerization." Reproduction **137**(4): 669-678.

Chrostek, E. y cols. (2017). "Horizontal Transmission of Intracellular Insect Symbionts via Plants." Front Microbiol **8**: 2237.

da Rocha Fernandes, M. y cols. (2014). "The modulation of the symbiont/host interaction between Wolbachia pipientis and Aedes fluviatilis embryos by glycogen metabolism." PLoS One **9**(6): e98966.

Dale, C. y cols. (1999). "Sodalis gen. nov. and Sodalis glossinidius sp. nov., a microaerophilic secondary endosymbiont of the tsetse fly Glossina morsitans morsitans." Int J Syst Bacteriol **49 Pt 1**: 267-275.

Dale, C. y cols. (2006). "Molecular interactions between bacterial symbionts and their hosts." Cell **126**(3): 453-465.

Darby, A. C. y cols. (2012). "Analysis of gene expression from the Wolbachia genome of a filarial nematode supports both metabolic and defensive roles within the symbiosis." Genome Res **22**(12): 2467-2477.

Darby, A. C. y cols. (2014). "Integrated transcriptomic and proteomic analysis of the global response of Wolbachia to doxycycline-induced stress." ISME J **8**(4): 925-937.

Davies, K. M. y cols. (2012). "Structure of the yeast F1Fo-ATP synthase dimer and its role in shaping the mitochondrial cristae." Proc Natl Acad Sci U S A **109**(34): 13602-13607.

de Boer, W. y cols. (2004). "Collimonas fungivorans gen. nov., sp. nov., a chitinolytic soil bacterium with the ability to grow on living fungal hyphae." Int J Syst Evol Microbiol **54**(Pt 3): 857-864.

Degli Esposti, M. (1998). "Inhibitors of NADH-ubiquinone reductase: an overview." Biochim Biophys Acta **1364**(2): 222-235.

Degnan, P. H. y cols. (2005). "Genome sequence of Blochmannia pennsylvanicus indicates parallel evolutionary trends among bacterial mutualists of insects." Genome Res **15**(8): 1023-1033.

Dimijian, G. G. (2000). "Evolving together: the biology of symbiosis, part 1." Proc (Bayl Univ Med Cent) **13**(3): 217-226.

Dobson, S. L. y cols. (2002). "Characterization of Wolbachia host cell range via the in vitro establishment of infections." Appl Environ Microbiol **68**(2): 656-660.

Douglas, A. E. (2015). "Multiorganismal insects: diversity and function of resident microorganisms." Annu Rev Entomol **60**: 17-34.

Drose, S. y cols. (2008). "The mechanism of mitochondrial superoxide production by the cytochrome bc1 complex." J Biol Chem **283**(31): 21649-21654.

Dryer RL, T. A., Routh JI (1956). "The determination of phosphorus and phosphatase with N-phenyl-p-phenylendiamine." J Biol Chem **225**: 177-183.

Dubois, A. y cols. (2007). "Helicobacter pylori is invasive and it may be a facultative intracellular organism." Cell Microbiol **9**(5): 1108-1116.

Dutra, H. L. y cols. (2016). "Wolbachia Blocks Currently Circulating Zika Virus Isolates in Brazilian Aedes aegypti Mosquitoes." Cell Host Microbe.

Elliott, A. y cols. (2013). "Coxiella burnetii interaction with neutrophils and macrophages in vitro and in SCID mice following aerosol infection." Infect Immun **81**(12): 4604-4614.

Emelyanov, V. V. (2003). "Common evolutionary origin of mitochondrial and rickettsial respiratory chains." Arch Biochem Biophys **420**(1): 130-141.

Evans, O. y cols. (2009). "Increased locomotor activity and metabolism of Aedes aegypti infected with a life-shortening strain of Wolbachia pipientis." J Exp Biol **212**(Pt 10): 1436-1441.

Fallon, A. M. (2008). "Cytological properties of an Aedes albopictus mosquito cell line infected with Wolbachia strain wAlbB." In Vitro Cell Dev Biol Anim **44**(5-6): 154-161.

Fallon, A. M. (2014). "Flow cytometric evaluation of the intracellular bacterium, Wolbachia pipientis, in mosquito cells." J Microbiol Methods **107**: 119-125.

Fallon, A. M. y cols. (2013). "The oxidizing agent, paraquat, is more toxic to Wolbachia than to mosquito host cells." In Vitro Cell Dev Biol Anim **49**(7): 501-507.

Fenn, K. y cols. (2004). "Are filarial nematode Wolbachia obligate mutualist symbionts?" Trends Ecol Evol **19**(4): 163-166.

Foster, J. y cols. (2005). "The Wolbachia genome of Brugia malayi: endosymbiont evolution within a human pathogenic nematode." PLoS Biol **3**(4): e121.

French, K. E. (2017). "Engineering Mycorrhizal Symbioses to Alter Plant Metabolism and Improve Crop Health." Front Microbiol **8**: 1403.

Frey-Klett, P. y cols. (2011). "Bacterial-fungal interactions: hyphens between agricultural, clinical, environmental, and food microbiologists." Microbiol Mol Biol Rev **75**(4): 583-609.

Garcia-Trejo, J. J. y cols. (2016). "The Inhibitory Mechanism of the zeta Subunit of the F1FO-ATPase Nanomotor of Paracoccus denitrificans and Related alpha-Proteobacteria." J Biol Chem **291**(2): 538-546.

Gasch, A. P. (2002). "Yeast genomic expression studies using DNA microarrays." Methods Enzymol **350**: 393-414.

Gasch, A. P. y cols. (2002). "The genomics of yeast responses to environmental stress and starvation." Funct Integr Genomics **2**(4-5): 181-192.

Geier, B. M. y cols. (1995). "Kinetic properties and ligand binding of the eleven-subunit cytochrome-c oxidase from Saccharomyces cerevisiae isolated with a novel large-scale purification method." Eur J Biochem **227**(1-2): 296-302.

Genty, L. M. y cols. (2014). "Wolbachia infect ovaries in the course of their maturation: last minute passengers and priority travellers?" PLoS One **9**(4): e94577.

Gil, R. y cols. (2003). "The genome sequence of Blochmannia floridanus: comparative analysis of reduced genomes." Proc Natl Acad Sci U S A **100**(16): 9388-9393.

Glaser, R. L. y cols. (2010). "The native Wolbachia endosymbionts of Drosophila melanogaster and Culex quinquefasciatus increase host resistance to West Nile virus infection." PLoS One **5**(8): e11977.

Gornall, A. G. y cols. (1949). "Determination of serum proteins by means of the biuret reaction." J Biol Chem **177**(2): 751-766.

Green, D. E. y cols. (1959). "Studies on the elecron transport system. XIV. The isolation and properties of soluble cytochrome c1." Biochim Biophys Acta **31**(1): 34-46.

Gutierrez-Aguilar, M. y cols. (2014). "Effects of ubiquinone derivatives on the mitochondrial unselective channel of Saccharomyces cerevisiae." J Bioenerg Biomembr **46**(6): 519-527.

Hagerhall, C. (1997). "Succinate: quinone oxidoreductases. Variations on a conserved theme." Biochim Biophys Acta **1320**(2): 107-141.

Heddi, A. y cols. (1999). "Four intracellular genomes direct weevil biology: nuclear, mitochondrial, principal endosymbiont, and Wolbachia." Proc Natl Acad Sci U S A **96**(12): 6814-6819.

Heddi A, L. F., Nardon P (1993). "Effect of endocytobiotic bacteria on mitochondrial enzymatic activities in the weevil Sitophilus oryzae (Coleoptera: Curculionidae)." Insect Biochemistry and Molecular Biology **23**(3): 8.

Hedges, L. M. y cols. (2008). "Wolbachia and virus protection in insects." Science **322**(5902): 702.

Hoffman, M. T. y cols. (2010). "Diverse bacteria inhabit living hyphae of phylogenetically diverse fungal endophytes." Appl Environ Microbiol **76**(12): 4063-4075.

Hoffmann, A. A. y cols. (2011). "Successful establishment of Wolbachia in Aedes populations to suppress dengue transmission." Nature **476**(7361): 454-457.

Hosoda, K. y cols. (2011a). "Cooperative adaptation to establishment of a synthetic bacterial mutualism." PLoS One **6**(2): e17105.

Hosoda, K. y cols. (2011b). "Designing symbiosis." Bioeng Bugs **2**(6): 338-341.

Hughes, G. L. y cols. (2011). "Wolbachia infections are virulent and inhibit the human malaria parasite Plasmodium falciparum in Anopheles gambiae." PLoS Pathog **7**(5): e1002043.

Hughes, G. L. y cols. (2012). "Wolbachia strain wAlbB enhances infection by the rodent malaria parasite Plasmodium berghei in Anopheles gambiae mosquitoes." Appl Environ Microbiol **78**(5): 1491-1495.

Hussain, M. y cols. (2013). "Effect of Wolbachia on replication of West Nile virus in a mosquito cell line and adult mosquitoes." J Virol **87**(2): 851-858.

Ingledew, W. J. y cols. (1984). "The respiratory chains of Escherichia coli." Microbiol Rev **48**(3): 222-271.

Iturbe-Ormaetxe, I. y cols. (2011). "A simple protocol to obtain highly pure Wolbachia endosymbiont DNA for genome sequencing." J Microbiol Methods **84**(1): 134-136.

Iwata, S. (1998). "Structure and function of bacterial cytochrome c oxidase." J Biochem **123**(3): 369-375.

Iwata, S. y cols. (1998). "Complete structure of the 11-subunit bovine mitochondrial cytochrome bc1 complex." Science **281**(5373): 64-71.

Jeyaprakash, A. y cols. (2000). "Long PCR improves Wolbachia DNA amplification: wsp sequences found in 76% of sixty-three arthropod species." Insect Mol Biol **9**(4): 393-405.

Johnson, K. N. (2015). "The Impact of Wolbachia on Virus Infection in Mosquitoes." Viruses **7**(11): 5705-5717.

Johnston, K. L. y cols. (2010). "Lipoprotein biosynthesis as a target for anti-Wolbachia treatment of filarial nematodes." Parasit Vectors **3**: 99.

Jonckheere, A. I. y cols. (2012). "Mitochondrial ATP synthase: architecture, function and pathology." J Inherit Metab Dis **35**(2): 211-225.

Juarez, O. y cols. (2004). "The mitochondrial respiratory chain of Ustilago maydis." Biochim Biophys Acta **1658**(3): 244-251.

Kambris, Z. y cols. (2010). "Wolbachia stimulates immune gene expression and inhibits plasmodium development in Anopheles gambiae." PLoS Pathog **6**(10): e1001143.

Kang, S. W. y cols. (2009). "Symbiotic relationship between Microbacterium sp. SK0812 and Candida tropicalis SK090404." J Microbiol **47**(6): 721-727.

Kerscher, S. y cols. (2008). "The three families of respiratory NADH dehydrogenases." Results Probl Cell Differ **45**: 185-222.

Kerscher, S. y cols. (2001). "Exploring the catalytic core of complex I by Yarrowia lipolytica yeast genetics." J Bioenerg Biomembr **33**(3): 187-196.

Kerscher, S. J. y cols. (1999). "A single external enzyme confers alternative NADH:ubiquinone oxidoreductase activity in Yarrowia lipolytica." J Cell Sci **112 (Pt 14)**: 2347-2354.

Khoo, C. C. y cols. (2013). "Infection, growth and maintenance of Wolbachia pipientis in clonal and non-clonal Aedes albopictus cell cultures." Bull Entomol Res **103**(3): 251-260.

Klasson, L. y cols. (2008). "Genome evolution of Wolbachia strain wPip from the Culex pipiens group." Mol Biol Evol **25**(9): 1877-1887.

Kobialka, M. y cols. (2016). "Sulcia symbiont of the leafhopper Macrosteles laevis (Ribaut, 1927) (Insecta, Hemiptera, Cicadellidae: Deltocephalinae) harbors Arsenophonus bacteria." Protoplasma **253**(3): 903-912.

Krause, D. C. y cols. (1985). "Cloning and expression of the Rickettsia prowazekii ADP/ATP translocator in Escherichia coli." Proc Natl Acad Sci U S A **82**(9): 3015-3019.

Laemmli, U. K. (1970). "Cleavage of structural proteins during the assembly of the head of bacteriophage T4." Nature **227**(5259): 680-685.

Lamarque, D. y cols. (2003). "Pathogenesis of Helicobacter pylori infection." Helicobacter **8 Suppl 1**: 21-30.

Lamelas, A. y cols. (2011). "New clues about the evolutionary history of metabolic losses in bacterial endosymbionts, provided by the genome of Buchnera aphidicola from the aphid Cinara tujafilina." Appl Environ Microbiol **77**(13): 4446-4454.

Lange, C. y cols. (2002). "Crystal structure of the yeast cytochrome bc1 complex with its bound substrate cytochrome c." Proc Natl Acad Sci U S A **99**(5): 2800-2805.

Langworthy, N. G. y cols. (2000). "Macrofilaricidal activity of tetracycline against the filarial nematode Onchocerca ochengi: elimination of Wolbachia precedes worm death and suggests a dependent relationship." Proc Biol Sci **267**(1448): 1063-1069.

Lehninger (2013). Principles of Biochemistry. New York, W. H. FREEMAN.

Lehninger, A. L., David L. Nelson, and Michael M. Cox. (2000). Lehninger Principles of Biochemistry, New York: Worth Publishers.

Levine, M. M. (1987). "Escherichia coli that cause diarrhea: enterotoxigenic, enteropathogenic, enteroinvasive, enterohemorrhagic, and enteroadherent." J Infect Dis **155**(3): 377-389.

Li, S. J. y cols. (2017). "Plantmediated horizontal transmission of Wolbachia between whiteflies." ISME J **11**(4): 1019-1028.

Lo Nathan, C. M., Salati Emanuela, Bazzocchi Chiara, Bandi (2002). " How many Wolbachia supergroups exist?" Molecular Biology and Evolution **19**(3): 341–346.

Lopez-Madrigal, S. y cols. (2011). "Complete genome sequence of "Candidatus Tremblaya princeps" strain PCVAL, an intriguing translational machine below the living-cell status." J Bacteriol **193**(19): 5587-5588.

Loreto, E. L. y cols. (2016). "Risks of Wolbachia mosquito control." Science **351**(6279): 1273.

Loyola-Machado, A. C. y cols. (2017). "The Symbiotic Bacterium Fuels the Energy Metabolism of the Host Trypanosomatid Strigomonas culicis." Protist **168**(2): 253-269.

Lu, L. y cols. (2003). "Rsf1p, a protein required for respiratory growth of Saccharomyces cerevisiae." Curr Genet **43**(4): 263-272.

Lumini, E. y cols. (2007). "Presymbiotic growth and sporal morphology are affected in the arbuscular mycorrhizal fungus Gigaspora margarita cured of its endobacteria." Cell Microbiol **9**(7): 1716-1729.

Malke, H. (1964). "Production of Aposymbiotic Cockroaches by Means of Lysozyme." Nature **204**: 1223-1224.

Mason, T. L. y cols. (1973). "Cytochrome c oxidase from bakers' yeast. I. Isolation and properties." J Biol Chem **248**(4): 1346-1354.

Matthew, C. Z. y cols. (2005). "The rapid isolation and growth dynamics of the tsetse symbiont Sodalis glossinidius." FEMS Microbiol Lett **248**(1): 69-74.

Mavingui, P. y cols. (2012). "Whole-genome sequence of Wolbachia strain wAlbB, an endosymbiont of tiger mosquito vector Aedes albopictus." J Bacteriol **194**(7): 1840.

McCutcheon, J. P. y cols. (2009). "Origin of an alternative genetic code in the extremely small and GC-rich genome of a bacterial symbiont." PLoS Genet **5**(7): e1000565.

McCutcheon, J. P. y cols. (2012). "Extreme genome reduction in symbiotic bacteria." Nat Rev Microbiol **10**(1): 13-26.

McCutcheon, J. P. y cols. (2011). "An interdependent metabolic patchwork in the nested symbiosis of mealybugs." Curr Biol **21**(16): 1366-1372.

McLeod, M. P. y cols. (2004). "Complete genome sequence of Rickettsia typhi and comparison with sequences of other rickettsiae." J Bacteriol **186**(17): 5842-5855.

McMeniman, C. J. y cols. (2009). "Stable introduction of a life-shortening Wolbachia infection into the mosquito Aedes aegypti." Science **323**(5910): 141-144.

McMeniman, C. J. y cols. (2010). "A virulent Wolbachia infection decreases the viability of the dengue vector Aedes aegypti during periods of embryonic quiescence." PLoS Negl Trop Dis **4**(7): e748.

Mee, M. T. y cols. (2012). "Engineering ecosystems and synthetic ecologies." Mol Biosyst **8**(10): 2470-2483.

Melnikow, E. y cols. (2013). "A potential role for the interaction of Wolbachia surface proteins with the Brugia malayi glycolytic enzymes and cytoskeleton in maintenance of endosymbiosis." PLoS Negl Trop Dis **7**(4): e2151.

Metcalf, J. A. y cols. (2014). "Recent genome reduction of Wolbachia in Drosophila recens targets phage WO and narrows candidates for reproductive parasitism." PeerJ **2**: e529.

Mitchell, P. (1966). "Chemiosmotic coupling in oxidative and photosynthetic phosphorylation." Biol Rev Camb Philos Soc **41**(3): 445-502.

Momeni, B. y cols. (2011). "Using artificial systems to explore the ecology and evolution of symbioses." Cell Mol Life Sci **68**(8): 1353-1368.

Montanari, A. y cols. (2014). "Strain-specific nuclear genetic background differentially affects mitochondria-related phenotypes in Saccharomyces cerevisiae." Microbiologyopen **3**(3): 288-298.

Montecucco, C. y cols. (2001). "Living dangerously: how Helicobacter pylori survives in the human stomach." Nat Rev Mol Cell Biol **2**(6): 457-466.

Morales-Rios, E. y cols. (2010). "A novel 11-kDa inhibitory subunit in the F1FO ATP synthase of Paracoccus denitrificans and related alpha-proteobacteria." FASEB J **24**(2): 599-608.

Morales-Rios, E. y cols. (2015). "Structure of ATP synthase from Paracoccus denitrificans determined by X-ray crystallography at 4.0 A resolution." Proc Natl Acad Sci U S A **112**(43): 13231-13236.

Moreira, L. A. y cols. (2009). "A Wolbachia symbiont in Aedes aegypti limits infection with dengue, Chikungunya, and Plasmodium." Cell **139**(7): 1268-1278.

Moss, C. y cols. (2003). "Intracellular bacteria associated with the ascidian Ecteinascidia turbinata: phylogenetic and in situ hybridisation analysis." Marine Biology **143**(1): 99-110.

Moulder, J. W. (1991). "Interaction of chlamydiae and host cells in vitro." Microbiol Rev **55**(1): 143-190.

Mousson, L. y cols. (2010). "Wolbachia modulates Chikungunya replication in Aedes albopictus." Mol Ecol **19**(9): 1953-1964.

Mowery, P. C. y cols. (1977). "Inhibition of mammalian succinate dehydrogenase by carboxins." Arch Biochem Biophys **178**(2): 495-506.

Nakabachi, A. y cols. (2006). "The 160-kilobase genome of the bacterial endosymbiont Carsonella." Science **314**(5797): 267.

Noda, H. y cols. (2002). "In vitro cultivation of Wolbachia in insect and mammalian cell lines." In Vitro Cell Dev Biol Anim **38**(7): 423-427.

O'Neill, S. L. y cols. (1997). "In vitro cultivation of Wolbachia pipientis in an Aedes albopictus cell line." Insect Mol Biol **6**(1): 33-39.

Omsland, A. y cols. (2013). "Bringing culture to the uncultured: Coxiella burnetii and lessons for obligate intracellular bacterial pathogens." PLoS Pathog **9**(9): e1003540.

Omsland, A. y cols. (2014). "Chlamydial metabolism revisited: interspecies metabolic variability and developmental stage-specific physiologic activities." FEMS Microbiol Rev **38**(4): 779-801.

Osyczka, A. y cols. (2005). "Fixing the Q cycle." Trends Biochem Sci **30**(4): 176-182.

Pan, X. y cols. (2012). "Wolbachia induces reactive oxygen species (ROS)-dependent activation of the Toll pathway to control dengue virus in the mosquito Aedes aegypti." Proc Natl Acad Sci U S A **109**(1): E23-31.

Partida-Martinez, L. P. y cols. (2007a). "Rhizonin, the first mycotoxin isolated from the zygomycota, is not a fungal metabolite but is produced by bacterial endosymbionts." Appl Environ Microbiol **73**(3): 793-797.

Partida-Martinez, L. P. y cols. (2005). "Pathogenic fungus harbours endosymbiotic bacteria for toxin production." Nature **437**(7060): 884-888.

Partida-Martinez, L. P. y cols. (2007b). "Endosymbiont-dependent host reproduction maintains bacterial-fungal mutualism." Curr Biol **17**(9): 773-777.

Pena, A. y cols. (1977). "A novel method for the rapid preparation of coupled yeast mitochondria." FEBS Lett **80**(1): 209-213.

Pietri, J. E. y cols. (2016). "The rich somatic life of Wolbachia." Microbiologyopen **5**(6): 923-936.

Potter, M. y cols. (2016). "Monitoring Intracellular Oxygen Concentration: Implications for Hypoxia Studies and Real-Time Oxygen Monitoring." Adv Exp Med Biol **876**: 257-263.

Ramsay, R. R. y cols. (1981). "Reaction site of carboxanilides and of thenoyltrifluoroacetone in complex II." Proc Natl Acad Sci U S A **78**(2): 825-828.

Rao, R. U. y cols. (2002). "Brugia malayi: effects of antibacterial agents on larval viability and development in vitro." Exp Parasitol **101**(1): 77-81.

Raquin, V. y cols. (2015). "Native Wolbachia from Aedes albopictus Blocks Chikungunya Virus Infection In Cellulo." PLoS One **10**(4): e0125066.

Rasgon, J. L. y cols. (2006). "Survival of Wolbachia pipientis in cell-free medium." Appl Environ Microbiol **72**(11): 6934-6937.

Robinson, G. C. y cols. (2013). "The structure of F(1)-ATPase from Saccharomyces cerevisiae inhibited by its regulatory protein IF(1)." Open Biol **3**(2): 120164.

Rosas-Lemus, M., Uribe-Alvarez, C., Contreras-Zentella M., Luévano-Martínez, L.A., Chiquete-Félix, N., Espinosa-Simón, E. Muhlia-Almazán, A., Escamilla-Marván, E., Uribe-Carvajal, S. (2016). Oxygen: From Toxic Waste to potimal (Toxic) Fuel of Life.

Sabree, Z. L. y cols. (2009). "Nitrogen recycling and nutritional provisioning by Blattabacterium, the cockroach endosymbiont." Proc Natl Acad Sci U S A **106**(46): 19521-19526.

Salmanian, A. H. y cols. (2008). "Yeast of the oral cavity is the reservoir of Heliobacter pylori." J Oral Pathol Med **37**(6): 324-328.

Salzberg, S. L. y cols. (2009). "Genome sequence of the Wolbachia endosymbiont of Culex quinquefasciatus JHB." J Bacteriol **191**(5): 1725.

Saniee, P. y cols. (2013a). "Immunodetection of Helicobacter pylori-specific proteins in oral and gastric Candida yeasts." Arch Iran Med **16**(11): 624-630.

Saniee, P. y cols. (2013b). "Localization of H.pylori within the vacuole of Candida yeast by direct immunofluorescence technique." Arch Iran Med **16**(12): 705-710.

Sato, Y. y cols. (2010). "Detection of betaproteobacteria inside the mycelium of the fungus Mortierella elongata." Microbes Environ **25**(4): 321-324.

Sazanov, L. A. (2015). "A giant molecular proton pump: structure and mechanism of respiratory complex I." Nat Rev Mol Cell Biol **16**(6): 375-388.

Sazanov, L. A. y cols. (2006). "Structure of the hydrophilic domain of respiratory complex I from Thermus thermophilus." Science **311**(5766): 1430-1436.

Scientific, G. T. (2017). Growth and maintenance of insect cell lines USER GUIDE**:** 42.

Schagger, H. (2002). "Respiratory chain supercomplexes of mitochondria and bacteria." Biochim Biophys Acta **1555**(1-3): 154-159.

Schägger, H. (1994). Denaturing electrophoretic techniques. A Practical Guide to Membrane Protein Purification
Schagger, G. V. J. a. H. San Diego, California, Academic Press**:** 166.

Scherlach, K. y cols. (2006). "Antimitotic rhizoxin derivatives from a cultured bacterial endosymbiont of the rice pathogenic fungus Rhizopus microsporus." J Am Chem Soc **128**(35): 11529-11536.

Schneiker, S. y cols. (2007). "Complete genome sequence of the myxobacterium Sorangium cellulosum." Nat Biotechnol **25**(11): 1281-1289.

Schofield, M. M. y cols. (2015). "Identification and analysis of the bacterial endosymbiont specialized for production of the chemotherapeutic natural product ET-743." Environ Microbiol **17**(10): 3964-3975.

Schonbaum, G. R. y cols. (1971). "Specific inhibition of the cyanide-insensitive respiratory pathway in plant mitochondria by hydroxamic acids." Plant Physiol **47**(1): 124-128.

Shevchenko, A. y cols. (2006). "In-gel digestion for mass spectrometric characterization of proteins and proteomes." Nat Protoc **1**(6): 2856-2860.

Shih, K. M. y cols. (1998). "Culture of mosquito cells in Eagle's medium." In Vitro Cell Dev Biol Anim **34**(8): 629-630.

Shiny, C. y cols. (2009). "Serum antibody responses to Wolbachia surface protein in patients with human lymphatic filariasis." Microbiol Immunol **53**(12): 685-693.

Siavoshi, F. y cols. (2005a). "Helicobacter pylori endemic and gastric disease." Dig Dis Sci **50**(11): 2075-2080.

Siavoshi, F. y cols. (2005b). "Detection of Helicobacter pylori-specific genes in the oral yeast." Helicobacter **10**(4): 318-322.

Smith, A. E. y cols. (2000). "The mechanical properties of Saccharomyces cerevisiae." Proc Natl Acad Sci U S A **97**(18): 9871-9874.

Smith, P. M. y cols. (2012). "Reprint of: Biogenesis of the cytochrome bc(1) complex and role of assembly factors." Biochim Biophys Acta **1817**(6): 872-882.

Solmaz, S. R. y cols. (2008). "Structure of complex III with bound cytochrome c in reduced state and definition of a minimal core interface for electron transfer." J Biol Chem **283**(25): 17542-17549.

Steffens, G. C. y cols. (1987). "Cytochrome c oxidase is a three-copper, two-heme-A protein." Eur J Biochem **164**(2): 295-300.

Stenmark, P. y cols. (2003). "A prokaryotic alternative oxidase present in the bacterium Novosphingobium aromaticivorans." FEBS Lett **552**(2-3): 189-192.

Stepkowski, T. y cols. (2001). "Reduction of bacterial genome size and expansion resulting from obligate intracellular lifestyle and adaptation to soil habitat." Acta Biochim Pol **48**(2): 367-381.

Stewart, E. J. (2012). "Growing unculturable bacteria." J Bacteriol **194**(16): 4151-4160.

Stolpe, S. y cols. (2004). "The Escherichia coli NADH:ubiquinone oxidoreductase (complex I) is a primary proton pump but may be capable of secondary sodium antiport." J Biol Chem **279**(18): 18377-18383.

Storey, B. T. (1976). "Respiratory Chain of Plant Mitochondria: XVIII. Point of Interaction of the Alternate Oxidase with the Respiratory Chain." Plant Physiol **58**(4): 521-525.

Strubing, U. y cols. (2010). "Mitochondrial genes for heme-dependent respiratory chain complexes are up-regulated after depletion of Wolbachia from filarial nematodes." Int J Parasitol **40**(10): 1193-1202.

Sukumaran, S. K. y cols. (2003). "Entry and intracellular replication of Escherichia coli K1 in macrophages require expression of outer membrane protein A." Infect Immun **71**(10): 5951-5961.

Sun, F. y cols. (2005). "Crystal structure of mitochondrial respiratory membrane protein complex II." Cell **121**(7): 1043-1057.

Sun, X. Y. y cols. (2015). "Copper Tolerance and Biosorption of Saccharomyces cerevisiae during Alcoholic Fermentation." PLoS One **10**(6): e0128611.

Tamames, J. y cols. (2007). "The frontier between cell and organelle: genome analysis of Candidatus Carsonella ruddii." BMC Evol Biol **7**: 181.

Taylor, M. J. y cols. (1999). "Wolbachia bacteria of filarial nematodes." Parasitol Today **15**(11): 437-442.

Terradas, G. y cols. (2017). "The RNAi pathway plays a small part in Wolbachia-mediated blocking of dengue virus in mosquito cells." Sci Rep **7**: 43847.

Tortosa, P. y cols. (2008). "Chikungunya-Wolbachia interplay in Aedes albopictus." Insect Mol Biol **17**(6): 677-684.

Trumpower, B. L. (1990). "Cytochrome bc1 complexes of microorganisms." Microbiol Rev **54**(2): 101-129.

Tsukihara, T. y cols. (1996). "The whole structure of the 13-subunit oxidized cytochrome c oxidase at 2.8 A." Science **272**(5265): 1136-1144.

Unden, G. y cols. (1997). "Alternative respiratory pathways of Escherichia coli: energetics and transcriptional regulation in response to electron acceptors." Biochim Biophys Acta **1320**(3): 217-234.

Uribe-Alvarez, C. y cols. (2016). "Staphylococcus epidermidis: metabolic adaptation and biofilm formation in response to different oxygen concentrations." Pathog Dis **74**(1): ftv111.

Uribe-Alvarez, C. y cols. (2018). "Wolbachia pipientis grows in Saccharomyces cerevisiae evoking early death of the host and deregulation of mitochondrial metabolism." Microbiologyopen: e00675.

Uribe-Carvajal, S., Guerrero-Castillo, S., King-Diaz, B., Hennsen, B.L. (2008). "Allelochemicals targeting the phospholipid bilayer and the proteins of biological membranes." Allelopathy Journal **21**(1): 1-24

Vallenet, D. y cols. (2009). "MicroScope: a platform for microbial genome annotation and comparative genomics." Database (Oxford) **2009**: bap021.

Vieira-Silva, S. y cols. (2010). "The systemic imprint of growth and its uses in ecological (meta)genomics." PLoS Genet **6**(1): e1000808.

Voronin, D. y cols. (2016). "Glucose and Glycogen Metabolism in Brugia malayi Is Associated with Wolbachia Symbiont Fitness." PLoS One **11**(4): e0153812.

Walker, J. E. (1992). "The NADH:ubiquinone oxidoreductase (complex I) of respiratory chains." Q Rev Biophys **25**(3): 253-324.

Walker, T. y cols. (2011). "The wMel Wolbachia strain blocks dengue and invades caged Aedes aegypti populations." Nature **476**(7361): 450-453.

Watt, I. N. y cols. (2010). "Bioenergetic cost of making an adenosine triphosphate molecule in animal mitochondria." Proc Natl Acad Sci U S A **107**(39): 16823-16827.

Weiss, E. (1973). "Growth and physiology of rickettsiae." Bacteriol Rev **37**(3): 259-283.

Werren, J. H. (1997). "Biology of Wolbachia." Annu Rev Entomol **42**: 587-609.

Werren, J. H. y cols. (2008). "Wolbachia: master manipulators of invertebrate biology." Nat Rev Microbiol **6**(10): 741-751.

White, P. M. y cols. (2017). "Mechanisms of Horizontal Cell-to-Cell Transfer of Wolbachia spp. in Drosophila melanogaster." Appl Environ Microbiol **83**(7).

White, T. J., Bruns, T. Lee, S. J. W. T., Taylor, J. W. (1990). "Amplification and direct sequencing of fungal ribosomal RNA genes for phylogenetics." PCR protocols: a guide to methods and applications **18**(1): 315-322.

WHO, W. H. O. (2016). World Malaria Report 2016, License: CC BY-NC-SA 3.0 IGO**:** 186.

WHO, W. H. O. (2017). Dengue and severe Dengue Fact Sheet.

Winkler, H. H. (1976). "Rickettsial permeability. An ADP-ATP transport system." J Biol Chem **251**(2): 389-396.

Winner, H. I. (1969). "The transition from commensalism to parasitism." Br J Dermatol **81**: Suppl 1:62+.

Wittig, I. y cols. (2010). "Mass estimation of native proteins by blue native electrophoresis: principles and practical hints." Mol Cell Proteomics **9**(10): 2149-2161.

Wittig, I. y cols. (2006). "Blue native PAGE." Nat Protoc **1**(1): 418-428.

Wood, D. O. y cols. (2012). "Establishment of a replicating plasmid in Rickettsia prowazekii." PLoS One **7**(4): e34715.

Wu, D. y cols. (2006). "Metabolic complementarity and genomics of the dual bacterial symbiosis of sharpshooters." PLoS Biol **4**(6): e188.

Wu, M. y cols. (2004). "Phylogenomics of the reproductive parasite Wolbachia pipientis wMel: a streamlined genome overrun by mobile genetic elements." PLoS Biol **2**(3): E69.

Xia, D. y cols. (1997). "Crystal structure of the cytochrome bc1 complex from bovine heart mitochondria." Science **277**(5322): 60-66.

Yang, X. H. y cols. (1986). "Purification of a three-subunit ubiquinol-cytochrome c oxidoreductase complex from Paracoccus denitrificans." J Biol Chem **261**(26): 12282-12289.

Yankovskaya, V. y cols. (2003). "Architecture of succinate dehydrogenase and reactive oxygen species generation." Science **299**(5607): 700-704.

Yoon, J. y cols. (2009). "Characterization of antimicrobial activity of the lysosomes isolated from Saccharomyces cerevisiae." Curr Microbiol **59**(1): 48-52.

Yoshikawa, S. y cols. (1990). "Infrared evidence of cyanide binding to iron and copper sites in bovine heart cytochrome c oxidase. Implications regarding oxygen reduction." J Biol Chem **265**(14): 7945-7958.

Zannoni, D. (2008). Respiration in Archaea and Bacteria: Diversity of Prokaryotic Respiratory Systems, Springer Netherlands.

Zarco-Zavala, M. y cols. (2014). "The zeta subunit of the F1FO-ATP synthase of alpha-proteobacteria controls rotation of the nanomotor with a different structure." FASEB J **28**(5): 2146-2157.

Zendehdel, N. y cols. (2005). "Helicobacter pylori reinfection rate 3 years after successful eradication." J Gastroenterol Hepatol **20**(3): 401-404.

Zhang, Z. y cols. (1998). "Electron transfer by domain movement in cytochrome bc1." Nature **392**(6677): 677-684.

Zhou, W. y cols. (1998). "Phylogeny and PCR-based classification of Wolbachia strains using wsp gene sequences." Proc Biol Sci **265**(1395): 509-515.

Zhu, J. y cols. (2016). "Structure of mammalian respiratory complex I." Nature **536**(7616): 354-358.

Zickermann, V. y cols. (2000). "The NADH oxidation domain of complex I: do bacterial and mitochondrial enzymes catalyze ferricyanide reduction similarly?" Biochim Biophys Acta **1459**(1): 61-68.

Zickermann, V. y cols. (2015). "Structural biology. Mechanistic insight from the crystal structure of mitochondrial complex I." Science **347**(6217): 44-49.

Zouache, K. y cols. (2012). "Chikungunya virus impacts the diversity of symbiotic bacteria in mosquito vector." Mol Ecol **21**(9): 2297-2309.

12. Anexos

Anexo A. Abreviaturas

ANT	Translocador de adenin nucleótidos
AntA	Antimicina A
AOX	Oxidasa alterna
BN-PAGE	Electroforesis azul nativa en geles de poliacrilamida
BHI	Medio corazón-cerebro
BHM	Mitocondria de corazón de bovino
CCCP	Carbonilcianuro m-clorofenilhidrazona
CitFe	Citrato Férrico Amoniacal
CN-PAGE	Electroforesis clara nativa en geles de poliacrilamida
COX	Citocromo c oxidasa
CR	Control respiratorio
CTE	Cadena transportadora de electrones
DAB	3´,5´-diaminobencidina
DMSO	Dimetilsulfóxido
DO	Densidad óptica
DOC	Desoxicolato de sodio
EIM	Espacio Intermembranal
FAD	Flavinadenindinucleótido
FISH	Hibridación *in-situ* con sondas fluorescentes
FMN	Mononucleótido de flavina
G3P	Glicerol-3-fosfato
G6P	Gluoca-6-fosfato
hrCN-PAGE	Electroforesis clara nativa de alta resolución en geles de poliacrilamida
HEPES	Ácido (4-(2-hidroxietil)-1-piperazinaetanosulfónico
LM	n-dodecil-β-D-maltósido
M	Mitocondria
MAT	Matriz mitocondrial
Mbp	Millones de pares de bases

MEM	Medio Mínimo de Eagle
MES	Ácido 2-(N-morfolino) etanosulfónico
MM	Medio Mitsuhashi-Maramorosh
MMFeS	Medio líquido Mitsuhashi-Maramorosh/Suero bovino fetal/Citrato férrico amoniacal
MMFeSS	Medio sólido Mitsuhashi-Maramorosh/Suero bovino fetal/Citrato férrico amoniacal
NBT	Bromuro de nitro-azul de tetrazolio
NDH	NADH deshidrogenasa
NDH2	NADH deshidrogenasa tipo II
O2	Oxígeno
PDB	ProteinDatabank
PFK	Fosfofructocinasa
Pir-Mal	Piruvato-Malato
PK	PiruvatoCinasa
PTM	Potencial transmembranal
Q	Quinona
QH2	Quinol
ROS	Especies reactivas de oxígeno
Rot	Rotenona
SBF	Suero Bovino Fetal
*Sc*W303	*Saccharomyces cerevisiae* W303
Succ	Succinato
TEA	Trietanolamina
TEMED	N,N,N´,N´-tetrametiletilendiamina
UQ	Ubiquinona
VDAC	Canal de aniones dependientes de voltaje
*w*AlbB	*Wolbachia* de *Aedesalbopictus**w*AlbB
wBm	*Wolbachia* de *Brugiamalayi*
*wSc*W303	*Saccharomyces cerevisiae* W303 infectada con *Wolbachia*
YPD	Extracto de levadura/peptona/dextrosa
YPDS	Extracto de levadura/peptona/dextrosa/SBF/Citrato Férrico Amoniacal

Anexo B. Comparación de genomas de *Wolbachia* utilizando la base de datos

Genoscope/metabolism/metabolicprofiles.
URL: http://www.genoscope.cns.fr/agc/microscope/metabolism/metabolicprofil.php?submit=MicroCyc
Electron Transfer pathways

NADH:ubiquinona reductasa EC 1.6.5.3

Wolbachia endosymbiont of Culex quinquefasciatus Pel wPip not-predicted	Wolbachia endosymbiont of Drosophila ananassae predicted	Wolbachia endosymbiont of Drosophila simulans wHa predicted	Wolbachia endosymbiont of Drosophila simulans wNo not-predicted	Wolbachia endosymbiont TRS of Brugia malayi not-predicted	Wolbachia pipientis wAlbB PRJEA76855 not-predicted	Wolbachia pipientis wMel predicted	Wolbachia pipientis wRec predicted	Wolbachia sp. wRi predicted
WPa_0853 - nuoB WPa_0847 WPa_1018 WPa_0996 - nuoM WPa_0993 - nuoJ WPa_0852 - nuoA WPa_1096 - nuoH WPa_1004 - nuoF WPa_0995 - nuoL WPa_0854 - nuoC WPa_0588 - nuoE WPa_1008 - nuoI WPa_1094 - nuoG WPa_0997 - nuoN WPa_0994 - nuoK	WOLDAv1_3740001 - nuoD WOLDAv1_2530001 WOLDAv1_1470003 - nuoII WOLDAv1_80024 - nuoN WOLDAv1_10012 - nuoG WOLDAv1_3320003 - nuoE WOLDAv1_1820001 WOLDAv1_510012 (*pseudo*) WOLDAv1_80006 - nuoB WOLDAv1_10011 - nuoH WOLDAv1_3850001 - nuoD WOLDAv1_2590003 (*pseudo*) WOLDAv1_370001 - nuoD WOLDAv1_80005 - nuoA	wHa_10810 wHa_09400 - nuoC wHa_08200 - nuoI wHa_08100 - nuoM wHa_08070 - nuoJ wHa_00750 - nuoH wHa_09420 - nuoA wHa_09260 wHa_08170 - nuoF wHa_08090 - nuoL wHa_06880 wHa_06230 - nuoE wHa_09410 - nuoB wHa_09250 wHa_08110 - nuoN wHa_08080 - nuoK wHa_00760 - nuoG	wNo_06220 wNo_07440 - nuoB wNo_06990 - nuoF wNo_06910 - nuoL wNo_06530 - nuoH wNo_05030 wNo_09440 wNo_07430 - nuoC wNo_06930 - nuoN wNo_06900 - nuoK wNo_06520 - nuoG wNo_02890 - nuoE wNo_07450 - nuoA wNo_07020 - nuoI wNo_06920 - nuoM wNo_06890 - nuoJ	Wbm0621 - nuoN Wbm0376 Wbm0241 Wbm0594 Wbm0471 - nuoI Wbm0017 Wbm0623 Wbm0474 Wbm0242 - nuoB	WALBB_v1_1220006 - nuoK WALBB_v1_1220003 - nuoN WALBB_v1_540002 - nuoF WALBB_v1_420011 - nuoB WALBB_v1_20011 - nuoG WALBB_v1_1220005 - nuoL WALBB_v1_840005 WALBB_v1_500005 WALBB_v1_290006 - nuoE WALBB_v1_1220008 - nuoJ WALBB_v1_1220004 - nuoM WALBB_v1_540005 - nuoI WALBB_v1_420012 - nuoA WALBB_v1_20012 - nuoH	WD1122 - nuoC WD0159 - nuoH WD0968 - nuoM WD0965 - nuoJ WD0734 - nuoE WD1124 - nuoA WD0980 - nuoI WD1129 WD0967 - nuoL WD1123 - nuoB WD0160 - nuoG WD0976 WD0966 - nuoK	WRECv1_0186 - nuoH WRECv1_1079 - nuoB WRECv1_0924 - nuoN WRECv1_0920 - nuoK WRECv1_0663 - nuoE WRECv1_0024 WRECv1_1085 WRECv1_0936 - nuoI WRECv1_0922 - nuoM WRECv1_0919 - nuoJ WRECv1_0187 - nuoG WRECv1_1080 - nuoA WRECv1_0930 - nuoF WRECv1_0921 - nuoL	WRi_012970 - nuoA WRi_009290 - nuoI WRi_009150 - nuoN WRi_009120 - nuoK WRi_000920 WRi_012960 - nuoB WRi_007410 - nuoE WRi_013020 WRi_009140 - nuoM WRi_009110 - nuoJ WRi_012950 - nuoC WRi_009240 - nuoF WRi_009130 - nuoL WRi_003800 - nuoD

WALBB_v1_500005: putative monovalent cation/H+ antiporter
WALBB_v1_500005: NDUFA12 propio de eucariotes.

*w*AlbB carece de los genes de las subunidades nuoC y nuoD

Succinato deshidrogenasa EC 1.3.5.1

Wolbachia endosymbiont of Culex quinquefasciatus Pel wPip predicted	Wolbachia endosymbiont of Drosophila ananassae predicted	Wolbachia endosymbiont of Drosophila simulans wHa predicted	Wolbachia endosymbiont of Drosophila simulans wNo predicted	Wolbachia endosymbiont TRS of Brugia malayi predicted	Wolbachia pipientis wAlbB PRJEA76855 predicted	Wolbachia pipientis wMel predicted	Wolbachia pipientis wRec predicted	Wolbachia sp. wRi predicted
WPa_0580 - sdhB WPa_0681 - sdhA WPa_1068 - sdhC	WOLDAv1_40003 - sdhC WOLDAv1_890006 WOLDAv1_190003 - sdhA WOLDAv1_4010001 - sdhB	wHa_06170 - sdhB wHa_03380 - sdhA wHa_10200 - sdhC	wNo_02820 - sdhB wNo_02290 - sdhA wNo_06260 - sdhC	Wbm0486 Wbm0600 - sdhB Wbm0448 - sdhA	WALBB_v1_40023 - sdhC WALBB_v1_770009 - sdhA WALBB_v1_340006 - sdhB	WD1221 - sdhC WD0437 - sdhA WD0727 - sdhB	WRECv1_0449 - sdhA WRECv1_0656 - sdhB WRECv1_1182 - sdhC	WRi_007490 - sdhB WRi_003080 - sdhA WRi_012010 - sdhD WRi_012000 - sdhC

*w*AlbB carece del gen de la subunidad sdhC

Ubiquinol-Citocromo *c* reductasa EC 1.10.2.2

Wolbachia endosymbiont of Culex quinquefasciatus Pel wPip predicted	Wolbachia endosymbiont of Drosophila ananassae not-predicted	Wolbachia endosymbiont of Drosophila simulans wHa not-predicted	Wolbachia endosymbiont of Drosophila simulans wNo not-predicted	Wolbachia endosymbiont TRS of Brugia malayi not-predicted	Wolbachia pipientis wAlbB PRJEA76855 not-predicted	Wolbachia pipientis wMel predicted	Wolbachia pipientis wRec not-predicted	Wolbachia sp. wRi predicted
WPa_0735 - petC WPa_0734 - petB WPa_0952 - petA	WOLDAv1_40026 - petA	wHa_10030 - petA wHa_08940 - petC	wNo_03960 - petC wNo_05750 - petA	–	WALBB_v1_490025 - petA	WD1071 - petB WD1070 - petC WD1201 - petA	WRECv1_1159 - petA WRECv1_1025 - fbcH	WRi_011070 - petB WRi_011060 - petC WRi_011790 - petA

WALBB_v1_490025 – peta: ubiquinol-cytochrome c reductase, iron-sulfursubunit

*w*AlbB carece de los genes de las subunidades pet B y pet C

Citocromo *c* oxidasa EC 1.9.3.1

Wolbachia endosymbiont of Culex quinquefasciatus Pel wPip predicted	Wolbachia endosymbiont of Drosophila ananassae predicted	Wolbachia endosymbiont of Drosophila simulans wHa predicted	Wolbachia endosymbiont of Drosophila simulans wNo predicted	Wolbachia endosymbiont TRS of Brugia malayi predicted	Wolbachia pipientis wAlbB PRJEA76855 predicted	Wolbachia pipientis wMel predicted	Wolbachia pipientis wRec predicted	Wolbachia sp. wRi predicted
WPa_0082 - coxA WPa_1145 - coxC WPa_0083 - coxB	WOLDAv1_320009 - coxA WOLDAv1_230012 - coxC WOLDAv1_4060001 (*pseudo*) WOLDAv1_320010 - coxB	wHa_05340 - coxA wHa_00590 - coxC wHa_05350 - coxB	wNo_00390 - coxB wNo_08050 - coxC wNo_00400 - coxA	Wbm0698 Wbm0308 Wbm0307	WALBB_v1_670017 - ctaD WALBB_v1_670018 - ctaC WALBB_v1_1500007 - ctaE	WD0141 - coxC WD0301 - coxA WD0300 - coxB	WRECv1_0312 - ctaD WRECv1_0311 - coxB WRECv1_0175 - ctaE	WRi_004820 - coxA WRi_004830 - coxB WRi_001120 - coxC

Citocromo *bd* EC 1.10.3.-

Wolbachia endosymbiont of Culex quinquefasciatus Pel wPip not-predicted	Wolbachia endosymbiont of Drosophila ananassae predicted	Wolbachia endosymbiont of Drosophila simulans wHa predicted	Wolbachia endosymbiont of Drosophila simulans wNo not-predicted	Wolbachia endosymbiont TRS of Brugia malayi not-predicted	Wolbachia pipientis wAlbB PRJEA76855 not-predicted	Wolbachia pipientis wMel predicted	Wolbachia pipientis wRec predicted	Wolbachia sp. wRi predicted
–	WOLDAv1_1490001 - cydB	wHa_06280 - cydA wHa_06290 - cydB	–	–	–	WD0740 - cydA WD0741 - cydB	WRECv1_0670 - cydB	WRi_007350 - cydB WRi_007360 - cydA

*w*AlbB carece de los genes

Anexo C. Secuencias de genes amplificados

Wolbachia de la línea celular Aa23	Wsp691	GTTGAtCTCTTTAGTAGCTGATACTGTTTCTTTATTAAAACTAGCACCATAAGAACCAAAATAACGAGCACCAGCATA AAGCTTGATTTCTGGGGTTACATCATAACTAACACCAGCTTTTGCTTGATAAGCAAAACCAAATCCTTTTTGATCTTT AACTGCACTAGCTTCTGAAGGATTGCTGATATATGCTGCACCAACACCAACACCAACGTATGGAGTGATAGGCATAT CTTCAATCGCTATATCGTAATAAACGTTAACCAATCCTGAAAATACTGCCACACTGTTTGCAACAGTTGTTGGAGCAA ATGTTGCACCACCAACGTCGTTTTTGTTTAGTTGTGAGTAAAGTCCCTCAACATCAACCCTGATATCGTCCATTTTATA ACCAAATGCAGCACCACCAGCCATAAAAGATGCTTTTAAAGGATCATGAACTTCGGTTCCTTTTTTATATTCAATGCC GTCAATTCTTGTTTTAAAAGGTAAAACTTCACCATTATATTGCAAACGAACATAGTAGCTAGTTTCTTCATCACT
Wolbachia de la línea celular Aa23 gen *wsp*	Wsp81	NTNGCATANATGGTGAAGTTTTACCTTTTAAAACAAGAATTGACGGCATTGAATATAAAAAAGGAACCGAAGTTCAT GATCCTTTAAAAGCATCTTTTATGGCTGGTGGTGCTGCATTTGGTTATAAAATGGACGATATCAGGGTTGATGTTGAG GGACTTTACTCACAACTAAACAAAAACGACGTTGGTGGTGCAACATTTGCTCCAACAACTGTTGCAAACAGTGTGGC AGTATTTTCAGGATTGGTTAACGTTTATTACGATATAGCGATTGAAGATATGCCTATCACTCCATACGTTGGTGTTGG TGTTGGTGCAGCATATATCAGCAATCCTTCAGAAGCTAGTGCAGTTAAAGATCAAAAAGGATTTGGTTTTGCTTATCA AGCAAAAGCTGGTGTTAGTTATGATGTAACCCCAGAAATCAAGCTTTATGCTGGTGCTCGTTATTTTGGTTCTTATGG TGCTAGTTTTAATAAAGAAACAGTATCAGCTACTAAAGAGATCAACGTTCTTTACAGCGCTGTTGGTGCAGAAGCTG GA
*Sc*W303 infectada con *Wolbachia*, gen *wsp*	Wsp691	TTGANCTCTTTAGTAGCTGATACTGTTTCTTTATTAAAACTAGCACCATAAGAACCAAAATAACGAGCACCAGCATA AAGCTTGATTTCTGGGGTTACATCATAACTAACACCAGCTTTTGCTTGATAAGCAAAACCAAATCCTTTTTGATCTTT AACTGCACTAGCTTCTGAAGGATTGCTGATATATGCTGCACCAACACCAACACCAACGTATGGAGTGATAGGCATAT CTTCAATCGCTATATCGTAATAAACGTTAACCAATCCTGAAAATACTGCCACACTGTTTGCAACAGTTGTTGGAGCAA ATGTTGCACCACCAACGTCGTTTTTGTTTAGTTGTGAGTAAAGTCCCTCAACATCAACCCTGATATCGTCCATTTTATA ACCAAATGCAGCACCACCAGCCATAAAAGATGCTTTTAAAGGATCATGAACTTCGGTTCCTTTTTTATATTCAATGCC GTCAATTCTTGTTTTAAAAGGTAAAACTTCACCATTATATTGCAAACGAACATAGTAGCTAGTTTCTTCATCACTNAA TTNGNACNNA

*Sc*W303 infectada con *Wolbachia*, gen wsp	Wsp 81	TANATGGTGAAGTTTTACCTTTTAAAACAAGAATTGACGGCATTGAATATAAAAAAGGAACCGAAGTTCATGATCCT TTAAAAGCATCTTTTATGGCTGGTGGTGCTGCATTTGGTTATAAAATGGACGATATCAGGGTTGATGTTGAGGGACTT TACTCACAACTAAACAAAAACGACGTTGGTGGTGCAACATTTGCTCCAACAACTGTTGCAAACAGTGTGGCAGTATT TTCAGGATTGGTTAACGTTTATTACGATATAGCGATTGAAGATATGCCTATCACTCCATACGTTGGTGTTGGTGTTGG TGCAGCATATATCAGCAATCCTTCAGAAGCTAGTGCAGTTAAAGATCAAAAAGGATTTGGTTTTGCTTATCAAGCAA AAGCTGGTGTTAGTTATGATGTAACCCCAGAAATCAAGCTTTATGCTGGTGCTCGTTATTTTGGTTCTTATGGTGCTA GTTTTAATAAAGAAACAGTATCAGCTACTAAAGAGATCAACGTTCTTTACAGCGCTGTTGGTGCAGAAGCTGGANNA NNN
Saccharomyces cerevisiae W303 5.8S rRNA	ITS1	TTTGTTTTGGCAAGAGCATGAGAGCTTTTACTGGGCAAGAAGACAAGAGATGGAGAGTCCAGCCGGGCCTGCGCTTA AGTGCGCGGTCTTGCTAGGCTTGTAAGTTTCTTTCTTGCTATTCCAAACGGTGAGAGATTTCTGTGCTTTTGTTATAGG ACAATTAAAACCGTTTCAATACAACACACTGTGGAGTTTTCATATCTTTGCAACTTTTTCTTTGGGCATTCGAGCAAT CGGGGCCCAGAGGTAACAAACACAAACAATTTTATCTATTCATTAAATTTTTGTCAAAAACAAGAATTTTCGTAACT GGAAATTTTAAAATATTAAAAACTTTCAACAACGGATCTCTTGGTTCTCGCATCGATGAAGAACGCAGCGAAATGCG ATACGTAATGTGAATTGCAGAATTCCGTGAATCATCGAATCTTTGAACGCACATTGCGCCCCTTGGTATTCCAGGGGG CATGCCTGTTTGAGCGTCATTTCCTTCTCAAACATTCTGTTTGGTAGTGAGTGATACTCTTTGGAGTTAACTTGAAATT GCTGGCCTTTTCATTGGATGTTTTTTTTCCAAAGAGAGGTTTCTCTGCGTGCTTGAGGTATAATGCAAGTACGGTCGTT TTAgGTTTTACCAACTGCGGCTAATCTTTTTTTATACTGA
Saccharomyces cerevisiae W303 5.8S rRNA	ITS1	TTGTTCGCCTAGACGCTCTCTTCTTATCGATAACGTTCCAATACGCTCAGTATAAAAAAAGATTAGCCGCAGTTGGTA AAACCTAAAACGACCGTACTTGCATTATACCTCAAGCACGCAGAGAAACCTCTCTTTGGAAAAAAAACATCCAATGA AAAGGCCAGCAATTTCAAGTTAACTCCAAAGAGTATCACTCACTACCAAACAGAATGTTTGAGAAGGAAATGACGCT CAAACAGGCATGCCCCCTGGAATACCAAGGGGCGCAATGTGCGTTCAAAGATTCGATGATTCACGGAATTCTGCAAT TCACATTACGTATCGCATTTCGCTGCGTTCTTCATCGATGCGAGAACCAAGAGATCCGTTGTTGAAAGTTTTTAATAT TTTAAAATTTCCAGTTACGAAAATTCTTGTTTTTGACAAAAATTTAATGAATAGATAAAATTGTTTGTGTTTGTTACCT CTGGGCCCCGATTGCTCGAATGCCCAAAGAAAAAGTTGCAAAGATATGAAAACTCCACAGTGTGTTGTATTGAAACG GTTTTAATTGTCCTATAACAAAAGCACAGAAATCTCTCACCGTTTGGAATAGCAAGAAAGAAACTTACAAGCCTAGC AAGACCGCGCACTTAAGCGCAGGCCCGGCTGGACTCTCCATCTCTTGTCTTCTTGCCCAGTAAAAGCTCTCATGCTCT TGCCAAAACAAAAAAATCCATTTTCAAAATTATTAAATTTCTTTAATGATCCTTCCGCACGTC

D. Proteínas identificadas por MS

Proteinas Identificadas pos MS. Bandas cortadas a partir de geles CN or BN-PAGE. Bases de datos utilizadas, Uniprot Wolbachia wAlbB/S cerevisiae

1A: ATPasa

N	Unused	Total	% Cov	% Cov (50)	% Cov (95)	Accession	Name	Species	Pep(95%)
1	7.98	7.98	52.83	10.5	10.5	H0U0X5_WOLPI	ATP synthase subunit alpha	W pipientis wAlbB	9
2	6.62	6.62	70.9	33.1	33.1	H0U0S7_WOLPI	ATP synthase subunit beta	W pipientis wAlbB	16
3	2	2	44.7	1.76	1.76	H0U3S8_WOLPI	NADH-quinone oxidoreductase	W pipientis wAlbB	1

% Cov (95): The percentage of matching amino acids from identified peptides having confidence greater than or equal to 95% divided by the total number of amino acids in the sequence.

Accession: The accession number for the protein.

Name: The name of the protein.

Species: The species for this protein.
Peptides (95%): The number of distinct peptides having at least 95% confidence. Multiple modified and cleaved states of the same underlying peptide sequence are considered distinct

peptides because they have different molecular formulas. Multiple spectra of the same peptide, due to replicate acquisition or different charge states, only count once.

1N: NADH DH

N[a]	Unused	Total	% Cov	% Cov (50)	% Cov (95)	Accession	Name OS=Saccharomyces cerevisiae (strain ATCC 204508 / S288c)	Species	Pep(95%)
1	25.27	25.3	71.48	47.53	37.83	sp|P32316|ACH1_YEAST	Acetyl-CoA hydrolase	*S. cerevisiae*	18
2	23.85	23.9	47.13	34.26	33.74	sp|P07275|PUT2_YEAST	Delta-1-pyrroline-5-carboxylate dehydrogenase, mitochondrial	*S. cerevisiae*	19
3	23.76	23.8	62.03	47.85	47.85	sp|P06168|ILV5_YEAST	Ketol-acid reductoisomerase, mitochondrial	*S. cerevisiae*	17
4	22.24	22.2	79.15	74.91	56.89	sp|P04840|VDAC1_YEAST	Mitochondrial outer membrane protein porin 1	*S. cerevisiae*	17
5	18	18	54.06	25.94	22.97	sp|Q00711|SDHA_YEAST	Succinate dehydrogenase [ubiquinone] flavoprotein subunit, mitochondrial	*S. cerevisiae*	12
6	16.06	16.1	55.35	25.47	22.01	sp|P18239|ADT2_YEAST	ADP,ATP carrier protein 2	*S. cerevisiae*	10

7	14.54	14.5	36.47	28.95	27.07	sp|P21801|SDHB_YEAST	Succinate dehydrogenase [ubiquinone] iron-sulfur subunit, mitochondrial	*S. cerevisiae*	7
8	14	14	42.01	20.9	20.9	sp|P08417|FUMH_YEAST	Fumarate hydratase, mitochondrial	*S. cerevisiae*	16
9	12.05	12.1	34.73	29.58	29.58	sp|P23641|MPCP_YEAST	Mitochondrial phosphate carrier protein	*S. cerevisiae*	8
10	12	12	33.94	16.21	14.07	sp|P0CS90|HSP77_YEAST	Heat shock protein SSC1, mitochondrial O	*S. cerevisiae*	7
11	10.35	10.4	24.08	10.35	8.124	sp|P49095|GCSP_YEAST	Glycine dehydrogenase (decarboxylating), mitochondrial	*S. cerevisiae*	6
12	10.1	10.1	41.83	18.72	16.33	sp|P07251|ATPA_YEAST	ATP synthase subunit alpha, mitochondrial	*S. cerevisiae*	6
13	10.05	10.1	36.12	19.83	17.33	sp|P00890|CISY1_YEAST	Citrate synthase, mitochondrial	*S. cerevisiae*	7
14	10	10	37.27	27.64	27.64	sp|P33303|SFC1_YEAST	Succinate/fumarate mitochondrial transporter	*S. cerevisiae*	9
15	8.52	8.52	19.35	11.92	8.976	sp|Q01574|ACS1_YEAST	Acetyl-coenzyme A synthetase 1	*S. cerevisiae*	4
16	8	8	59.02	33.03	22.94	sp|Q12289|CRC1_YEAST	Mitochondrial carnitine carrier	*S. cerevisiae*	5
17	6.22	6.22	30.86	14.05	9.208	sp|P06208|LEU1_YEAST	2-isopropylmalate synthase	*S. cerevisiae*	4
18	6	6	41.67	9.762	9.762	sp|P16387|ODPA_YEAST	Pyruvate dehydrogenase E1 component subunit alpha, mitochondrial	*S. cerevisiae*	3
19	6	6	6.929	6.929	6.929	sp|P00401|COX1_YEAST	Cytochrome c oxidase subunit 1	*S. cerevisiae*	5
20	5.24	5.24	23.29	12.95	8.151	sp|P07342|ILVB_YEAST	Acetolactate synthase catalytic subunit, mitochondrial	*S. cerevisiae*	3
21	5.2	5.2	26.44	13.41	13.41	sp|P34227|PRX1_YEAST	Mitochondrial peroxiredoxin PRX1	*S. cerevisiae*	3
22	5.08	5.08	17.98	11.74	7.89	sp|Q07500|NDH2_YEAST	External NADH-ubiquinone oxidoreductase 2, mitochondrial	*S. cerevisiae*	3
23	4.78	4.78	50.64	23.16	15.01	sp|P16547|OM45_YEAST	Mitochondrial outer membrane protein OM45	*S. cerevisiae*	4
24	4.55	4.55	22.59	16.87	13.86	sp|P25619|HSP30_YEAST	30 kDa heat shock protein	*S. cerevisiae*	3
25	4.52	4.52	23.77	10.38	7.104	sp|P32473|ODPB_YEAST	Pyruvate dehydrogenase E1 component subunit beta, mitochondrial	*S. cerevisiae*	2
26	4.06	4.06	37.74	12.4	7.008	sp|P40495|LYS12_YEAST	Homoisocitrate dehydrogenase, mitochondrial	*S. cerevisiae*	3
27	4.03	4.03	22.61	8.967	8.967	sp|P32340|NDI1_YEAST	Rotenone-insensitive NADH-ubiquinone oxidoreductase, mitochondrial	*S. cerevisiae*	4
28	4	8.04	21.36	16.18	12.62	sp|P04710|ADT1_YEAST	ADP,ATP carrier protein 1	*S. cerevisiae*	5
29	4	4	19.36	3.329	3.329	sp|P33416|HSP78_YEAST	Heat shock protein 78, mitochondrial	*S. cerevisiae*	2
30	4	4	18.64	5.398	5.398	sp|P19414|ACON_YEAST	Aconitate hydratase, mitochondrial	*S. cerevisiae*	2
31	4	4	28.5	7.125	7.125	sp|Q12443|RTN2_YEAST	Reticulon-like protein 2	*S. cerevisiae*	2
32	4	4	27.71	11.45	11.45	sp|P00359|G3P3_YEAST	Glyceraldehyde-3-phosphate dehydrogenase 3	*S. cerevisiae*	3
33	4	4	62.71	16.95	16.95	sp|P07255|COX9_YEAST	Cytochrome c oxidase subunit 7A	*S. cerevisiae*	2

34	4	4	24.74	24.74	24.74	sp|Q96VH5|MIC10_YEAST	MICOS complex subunit MIC10	*S. cerevisiae*	2
35	3.1	3.1	21.7	2.86	2.86	sp|P20967|ODO1_YEAST	2-oxoglutarate dehydrogenase, mitochondrial	*S. cerevisiae*	3
36	3.02	3.02	17.41	6.009	3.39	sp|P32191|GPDM_YEAST	Glycerol-3-phosphate dehydrogenase, mitochondrial	*S. cerevisiae*	2
37	2.46	2.46	19.66	5.128	5.128	sp|P39522|ILV3_YEAST	Dihydroxy-acid dehydratase, mitochondrial	*S. cerevisiae*	2
38	2.26	2.26	24.45	9.82	2.405	sp|P09624|DLDH_YEAST	Dihydrolipoyl dehydrogenase, mitochondrial	*S. cerevisiae*	1
39	2.16	2.16	13.53	8.257	2.982	sp|P32335|MSS51_YEAST	Protein MSS51, mitochondrial	*S. cerevisiae*	1
40	2.15	2.15	23.23	7.407	3.367	sp|P40471|AYR1_YEAST	NADPH-dependent 1-acyldihydroxyacetone phosphate reductase	*S. cerevisiae*	1
41	2.08	2.08	30.18	10.06	5.03	sp|P47085|YJX8_YEAST	MEMO1 family protein YJR008W	*S. cerevisiae*	1
42	2.05	2.05	13.07	13.07	13.07	sp|P25613|ADY2_YEAST	Accumulation of dyads protein 2	*S. cerevisiae*	2
43	2.04	2.04	26.81	2.74	2.74	sp|P00830|ATPB_YEAST	ATP synthase subunit beta, mitochondrial	*S. cerevisiae*	1
44	2	4	16.57	11.45	11.45	sp|P00358|G3P2_YEAST	Glyceraldehyde-3-phosphate dehydrogenase 2	*S. cerevisiae*	4

2N: NADH DH

N	Unused	Total	% Cov	% Cov (50)	% Cov (95)	Accession	Name OS=Saccharomyces cerevisiae (strain ATCC 204508 / S288c)	Species	Pep(95%)
1	18.16	18.2	43.88	23.25	20.98	sp|P19882|HSP60_YEAST	Heat shock protein 60, mitochondrial	*S. cerevisiae*	9
2	16.06	16.1	34.05	18.98	18.98	sp|P00830|ATPB_YEAST	ATP synthase subunit beta, mitochondrial	*S. cerevisiae*	9
3	12.27	12.3	38.71	17.3	17.3	sp|Q12230|LSP1_YEAST	Sphingolipid long chain base-responsive protein LSP1	*S. cerevisiae*	7
4	12.04	12	27.68	13.15	13.15	sp|P0CS90|HSP77_YEAST	Heat shock protein SSC1, mitochondrial	*S. cerevisiae*	7
5	11.41	11.4	24.55	9.769	9.769	sp|P19414|ACON_YEAST	Aconitate hydratase, mitochondrial	*S. cerevisiae*	6
6	8.02	8.02	31.19	17.68	17.68	sp|P23641|MPCP_YEAST	Mitochondrial phosphate carrier protein	*S. cerevisiae*	5
7	8	8	26.86	14.24	14.24	sp|P25605|ILV6_YEAST	Acetolactate synthase small subunit, mitochondrial	*S. cerevisiae*	5
8	6	6	19.12	5.835	5.835	sp|P07213|TOM70_YEAST	Mitochondrial import receptor subunit TOM70	*S. cerevisiae*	4
9	6	6	29.29	24.24	24.24	sp|Q12335|PST2_YEAST	Protoplast secreted protein 2	*S. cerevisiae*	5
10	5.35	5.35	41.78	17.81	14.73	sp|P32602|SEC17_YEAST	Alpha-soluble NSF attachment protein	*S. cerevisiae*	3
11	4.95	4.95	18.08	11.9	8.238	sp|Q12363|WTM1_YEAST	Transcriptional modulator WTM1	*S. cerevisiae*	3
12	4.29	6.37	37.46	16.22	13.86	sp|P53252|PIL1_YEAST	Sphingolipid long chain base-responsive protein PIL1	*S. cerevisiae*	4
13	4.03	4.03	26.57	8.02	8.02	sp|P39676|FHP_YEAST	Flavohemoprotein	*S. cerevisiae*	4
14	4.01	4.01	17.06	5.688	5.688	sp|P07251|ATPA_YEAST	ATP synthase subunit alpha, mitochondrial	*S. cerevisiae*	2

15	4	4	41.39	11.89	11.89	sp|P05626|ATPF_YEAST	ATP synthase subunit 4, mitochondrial	*S. cerevisiae*	2
16	2.2	2.2	31.61	18.71	8.387	sp|P04037|COX4_YEAST	Cytochrome c oxidase subunit 4, mitochondrial	*S. cerevisiae*	1
17	2.05	2.05	18.18	16.67	16.67	sp|Q2V2P9|YD19A_YEAST	Uncharacterized protein YDR119W-A	*S. cerevisiae*	2
18	2.04	2.04	20	9.565	9.565	sp|Q12233|ATPN_YEAST	ATP synthase subunit g, mitochondrial	*S. cerevisiae*	1
19	2	2	29.5	4.969	4.969	sp|P33303|SFC1_YEAST	Succinate/fumarate mitochondrial transporter	*S. cerevisiae*	1
20	2	2	13.87	2.933	2.933	sp|P60010|ACT_YEAST	Actin	*S. cerevisiae*	1
21	2	2	29.41	9.15	9.15	sp|P00424|COX5A_YEAST	Cytochrome c oxidase polypeptide 5A, mitochondrial	*S. cerevisiae*	1

1S: Succinato DH

N	Unused	Total	% Cov	% Cov (50)	% Cov (95)	Accession	Name	Species	Pep(95%)
1	48.67	48.7	79.05	55.81	54.43	sp|P0CS90|HSP77_YEAST	Heat shock protein SSC1, mitochondrial	*S. cerevisiae*	42
2	44.71	44.7	71.85	45.37	45.37	sp|P19414|ACON_YEAST	Aconitate hydratase, mitochondrial	*S. cerevisiae*	49
3	34.2	34.2	54.9	39.34	38.99	sp|P19882|HSP60_YEAST	Heat shock protein 60, mitochondrial	*S. cerevisiae*	21
4	21.75	21.8	74.18	37.47	37.22	sp|P06168|ILV5_YEAST	Ketol-acid reductoisomerase, mitochondrial	*S. cerevisiae*	16
5	14.43	14.4	49.27	23.59	20.46	sp|P00890|CISY1_YEAST	Citrate synthase, mitochondrial	*S. cerevisiae*	10
6	8.39	8.39	50.53	24.03	22.61	sp|P04840|VDAC1_YEAST	Mitochondrial outer membrane protein porin 1	*S. cerevisiae*	6
7	8	8	41.7	11.13	11.13	sp|P46681|DLD2_YEAST	D-lactate dehydrogenase [cytochrome] 2, mitochondrial	*S. cerevisiae*	4
8	6.42	6.42	50.16	25.24	22.08	sp|Q07629|YD218_YEAST	Uncharacterized membrane protein YDL218W	*S. cerevisiae*	6
9	6.01	6.01	31.76	11.64	11.64	sp|P18239|ADT2_YEAST	ADP,ATP carrier protein 2	*S. cerevisiae*	3
10	4.44	4.44	41.76	8.166	8.166	sp|P32191|GPDM_YEAST	Glycerol-3-phosphate dehydrogenase, mitochondrial	*S. cerevisiae*	3
11	4.01	4.01	48.05	7.323	7.323	sp|P02992|EFTU_YEAST	Elongation factor Tu, mitochondrial	*S. cerevisiae*	2
12	4.01	4.01	27.09	3.688	3.688	sp|P15108|HSC82_YEAST	ATP-dependent molecular chaperone HSC82	*S. cerevisiae*	2
12	0	4	36.53	3.667	3.667	sp|P02829|HSP82_YEAST	ATP-dependent molecular chaperone HSP82	*S. cerevisiae*	2
13	3.72	3.72	17.11	7.224	5.703	sp|P54783|ALO_YEAST	D-arabinono-1,4-lactone oxidase	*S. cerevisiae*	2
14	2.05	2.05	39.92	6.262	2.74	sp|P00830|ATPB_YEAST	ATP synthase subunit beta, mitochondrial	*S. cerevisiae*	1
15	2	6	25.65	9.13	9.13	sp|P08679|CISY2_YEAST	Citrate synthase, peroxisomal	*S. cerevisiae*	3
16	2	2	38.72	2.385	2.385	sp|P07251|ATPA_YEAST	ATP synthase subunit alpha, mitochondrial	*S. cerevisiae*	1
17	2	2	28.28	2.187	2.187	sp|Q00711|SDHA_YEAST	Succinate dehydrogenase [ubiquinone] flavoprotein subunit,	*S. cerevisiae*	1

							mitochondrial		
17	0	2	17.98	2.208	2.208	sp|P47052|SDHX_YEAST	Succinate dehydrogenase [ubiquinone] flavoprotein subunit 2, mitochondrial	*S. cerevisiae*	1

1A: ATPase

N	Unused	Total	% Cov	% Cov (50)	% Cov (95)	Accession	Name	Species	Pep(95%)
1	45.71	45.7	81.1	59.27	52.84	sp|P07251|ATPA_YEAST	ATP synthase subunit alpha, mitochondrial	*S. cerevisiae*	39
2	34.95	35	85.91	71.43	66.54	sp|P00830|ATPB_YEAST	ATP synthase subunit beta, mitochondrial	*S. cerevisiae*	46
3	17	17	90.76	41.58	39.13	sp|P07257|QCR2_YEAST	Cytochrome b-c1 complex subunit 2, mitochondrial	*S. cerevisiae*	12
4	14.29	14.3	90.8	65.52	60.34	sp|P30902|ATP7_YEAST	ATP synthase subunit d, mitochondrial	*S. cerevisiae*	16
5	13.97	14	80.06	45.02	36.98	sp|P38077|ATPG_YEAST	ATP synthase subunit gamma, mitochondrial	*S. cerevisiae*	13
6	10.17	10.2	56.29	26.42	18.55	sp|P18239|ADT2_YEAST	ADP,ATP carrier protein 2	*S. cerevisiae*	8
7	8	8	60.18	20.13	14.44	sp|P07256|QCR1_YEAST	Cytochrome b-c1 complex subunit 1, mitochondrial	*S. cerevisiae*	7
8	6.88	6.88	37.54	20.71	20.71	sp|P07143|CY1_YEAST	Cytochrome c1, heme protein, mitochondrial	*S. cerevisiae*	4
9	6.46	6.46	48.56	10.49	7.783	sp|P00175|CYB2_YEAST	Cytochrome b2, mitochondrial	*S. cerevisiae*	3
10	6.06	6.06	91.94	91.94	91.94	sp|P21306|ATP5E_YEAST	ATP synthase subunit epsilon, mitochondrial	*S. cerevisiae*	7
11	6.04	6.04	64.66	31.1	31.1	sp|P04840|VDAC1_YEAST	Mitochondrial outer membrane protein porin 1	*S. cerevisiae*	7
12	6	6	55.45	20.79	20.79	sp|Q06405|ATPK_YEAST	ATP synthase subunit f, mitochondrial	*S. cerevisiae*	3
13	5.97	5.97	38.91	12.54	12.54	sp|P23641|MPCP_YEAST	Mitochondrial phosphate carrier protein	*S. cerevisiae*	4
14	5.9	5.9	83.02	24.06	24.06	sp|P09457|ATPO_YEAST	ATP synthase subunit 5, mitochondrial	*S. cerevisiae*	4
15	4.82	4.82	58.72	12.02	9.496	sp|Q12428|PRPD_YEAST	Probable 2-methylcitrate dehydratase	*S. cerevisiae*	3
16	4.4	4.4	68.03	27.05	21.72	sp|P05626|ATPF_YEAST	ATP synthase subunit 4, mitochondrial	*S. cerevisiae*	7
17	4.19	4.19	34.66	7.724	7.724	sp|P00890|CISY1_YEAST	Citrate synthase, mitochondrial	*S. cerevisiae*	4
18	4.03	4.03	42	9.2	4.8	sp|P00549|KPYK1_YEAST	Pyruvate kinase 1	*S. cerevisiae*	3
19	4	4	70.03	14.68	8.563	sp|Q12289|CRC1_YEAST	Mitochondrial carnitine carrier	*S. cerevisiae*	2
20	4	4	46.07	10.92	5.895	sp|P02994|EF1A_YEAST	Elongation factor 1-alpha	*S. cerevisiae*	2
21	4	4	23.13	4.375	4.375	sp|Q00711|SDHA_YEAST	Succinate dehydrogenase [ubiquinone] flavoprotein subunit, mitochondrial	*S. cerevisiae*	2
21	0	1.96	30.76	2.208	2.208	sp|P47052|SDHX_YEAST	Succinate dehydrogenase [ubiquinone] flavoprotein subunit 2, mitochondrial	*S. cerevisiae*	1

22	4	4	34.5	3.73	3.73	sp|P38248|ECM33_YEAST	Cell wall protein ECM33	*S. cerevisiae*	2
23	3.89	3.89	43.48	9.006	9.006	sp|P33303|SFC1_YEAST	Succinate/fumarate mitochondrial transporter	*S. cerevisiae*	4
24	3.68	3.68	58.65	9.774	9.774	sp|P21801|SDHB_YEAST	Succinate dehydrogenase [ubiquinone] iron-sulfur subunit, mitochondrial	*S. cerevisiae*	2
25	3.37	3.37	32.41	7.342	7.342	sp|P06168|ILV5_YEAST	Ketol-acid reductoisomerase, mitochondrial	*S. cerevisiae*	3
26	3.17	3.17	91.53	16.95	16.95	sp|P07255|COX9_YEAST	Cytochrome c oxidase subunit 7A	*S. cerevisiae*	2
27	3.1	3.1	30.28	5.505	5.505	sp|Q07500|NDH2_YEAST	External NADH-ubiquinone oxidoreductase 2, mitochondrial	*S. cerevisiae*	2
28	2.97	2.97	20.91	2.663	2.663	sp|P20967|ODO1_YEAST	2-oxoglutarate dehydrogenase, mitochondrial	*S. cerevisiae*	2
29	2.81	2.81	45.57	4.128	4.128	sp|P0CS90|HSP77_YEAST	Heat shock protein SSC1, mitochondrial	*S. cerevisiae*	3
30	2.03	2.03	64.38	45.63	45.63	sp|Q12165|ATPD_YEAST	ATP synthase subunit delta, mitochondrial	*S. cerevisiae*	5

% Cov (95): The percentage of matching amino acids from identified peptides having confidence greater than or equal to 95% divided by the total number of amino acids in the sequence.

Accession: The accession number for the protein.

Name: The name of the protein.

Species: The species for this protein.

Peptides (95%): The number of distinct peptides having at least 95% confidence. Multiple modified and cleaved states of the same underlying peptide sequence are considered distinct

peptides because they have different molecular formulas. Multiple spectra of the same peptide, due to replicate acquisition or different charge states, only count once.

Anexo E. Publicaciones.

a) Artículos publicados

1. **Uribe-Alvarez C**, Chiquete-Félix N, Morales-García L, Bohórquez-Hernández A, Delgado-Buenrostro NL, Vaca L, Peña A, Uribe-Carvajal S. (2018). *Wolbachia pipientis* grows in *Saccharomyces cerevisiae* evoking early death of the host and deregulation of mitochondrial metabolism. **Microbiology open. Accepted: May 15th.**

2. Olicón-Hernández DR, **Uribe-Alvarez C**, Uribe-Carvajal S, Pardo JP, Guerra-Sánchez G. (2017). Response of *Ustilagomaydis*against the stress caused by three polycationic chitin derivatives.Molecules; 22(12): 1-11.

3. Pavón N, Cabrera-Orefice A, Gallardo-Pérez JC, **Uribe-Alvarez C**, Rivero-Segura NA, Vazquez-Martínez ER, Cerbón M, Martínez-Abundis E, Torres-Narvaez JC, Martínez-Memije R, Roldán-Gómez FJ, Uribe-Carvajal S. (2017). In female rat heart mitochondria, oophorectomy results in loss of oxidative phosphorylation. Journal of Endocrinology. 232(2):221-235.

4. **Uribe-Alvarez C**, Chiquete-Félix N, Contreras-Zentella M, Guerrero-Castillo S, Peña A, Uribe-Carvajal S. (2016). *Staphylococcus epidermidis*: metabolic adaptation and biofilm formation in response to different oxygen concentrations. FEMS Pathogens and Disease. 74(1):1-15.

5. Rosas-Lemus M, **Uribe-Alvarez C**, Chiquete-Felix N, Uribe-Carvajal S. (2014). In *Saccharomyces cerevisiae* fructose-1,6-bisphosphate contributes to the Crabtree effect through closure of the mitochondrial unspecific channel. Archives of Biochemistry and Biophysics. 555-556:66-70.

6. Gutierrez-Aguilar M, López-Carbajal HM, **Uribe-Alvarez C**, Espinoza-Simón E, Rosas-Lemus M, Chiquete-Félix N, Uribe-Carvajal S. (2014). Effects of ubiquinone derivatives on the mitochondrial unselective channel of *Saccharomyces cerevisiae*.Journal of Bioenergetics and Biomembranes. 2014; 46(6):519-27.

c) Capítulo de libro

1. Mónica Rosas-Lemus, **Cristina Uribe-Alvarez**, Martha Contreras-Zentella, Luis Alberto Luévano-Martínez, Natalia Chiquete-Félix, N. Lilia Morales-García, Adriana Muhlia-Almazán, Edgardo Escamilla-Marván and Salvador Uribe-Carvajal. (2016). Oxygen: From Toxic Waste to Optimal (Toxic) Fuel of Life. Biochemistry, Genetics and Molecular Biology. "Free Radicals and Diseases", edited by Rizwan Ahmad, ISBN 978-953-51-2747-5, Print ISBN 978-953-51-2746-8, Published: October 26, 2016.

d) Divulgación

1. **Uribe-Alvarez C**, Chiquete-Félix N, 2017. Las enfermedades transmitidas por vectores y el potencial uso de *Wolbachia*, una bacteria endocelular obligada, para erradicarlas. Revista de divulgación de la Facultad de Medicina. 60(6):51-55.1.

2. Espinoza-Simón E, Rosas-Lemus M, Cabrera-Orefice A, **Uribe-Alvarez C**, Chiquete-Félix, Uribe-Carvajal S. 2014. Oxígeno, para bien y para mal. Revista de divulgación de la Facultad de Medicina. 57(6):57-60.

Received: 14 December 2017 | Revised: 15 May 2018 | Accepted: 15 May 2018

DOI: 10.1002/mbo3.675

ORIGINAL ARTICLE

WILEY MicrobiologyOpen Open Access

Wolbachia pipientis grows in *Saccharomyces cerevisiae* evoking early death of the host and deregulation of mitochondrial metabolism

Cristina Uribe-Alvarez[1]* | Natalia Chiquete-Félix[1]* | Lilia Morales-García[1] | Arlette Bohórquez-Hernández[2] | Norma Laura Delgado-Buenrostro[3] | Luis Vaca[2] | Antonio Peña[1] | Salvador Uribe-Carvajal[1]

[1]Depto. de Genética Molecular, Instituto de Fisiología Celular, Universidad Nacional Autónoma de México, Ciudad de México, México

[2]Depto. de Biología Celular y del Desarrollo, Instituto de Fisiología Celular, Universidad Nacional Autónoma de México, Ciudad de México, México

[3]Unidad de Biomedicina UBIMED, Facultad de Estudios Superiores Iztacala, Universidad Nacional Autónoma de México, Tlanepantla, Edo. de México, México

Correspondence
Antonio Peña and Salvador Uribe-Carvajal
Depto. de Genética Molecular, Instituto de Fisiología Celular, Universidad Nacional Autónoma de México, Ciudad de México, México.
Emails: apd@ifc.unam.mx; suribe@ifc.unam.mx

Funding information
Dirección General de Asuntos del Personal Académico, Universidad Nacional Autónoma de México, Grant/Award Number: IN204015 and IN2114; Consejo Nacional de Ciencia y Tecnología, Grant/Award Number: 239487 and 344726

Abstract

Wolbachia sp. has colonized over 70% of insect species, successfully manipulating host fertility, protein expression, lifespan, and metabolism. Understanding and engineering the biochemistry and physiology of *Wolbachia* holds great promise for insect vector-borne disease eradication. *Wolbachia* is cultured in cell lines, which have long duplication times and are difficult to manipulate and study. The yeast strain *Saccharomyces cerevisiae* W303 was used successfully as an artificial host for *Wolbachia w*AlbB. As compared to controls, infected yeast lost viability early, probably as a result of an abnormally high mitochondrial oxidative phosphorylation activity observed at late stages of growth. No respiratory chain proteins from *Wolbachia* were detected, while several *Wolbachia* F_1F_0-ATPase subunits were revealed. After 5 days outside the cell, *Wolbachia* remained fully infective against insect cells.

KEYWORDS

bioenergetics, endosymbiosis, oxidative phosphorylation, *Saccharomyces cerevisiae*, *Wolbachia pipientis*

1 | INTRODUCTION

Construction of artificial ecosystems mimicking symbiotic relationships have been proposed to study ecology and evolution of symbioses (Hosoda et al., 2011; Momeni, Chen, Hillesland, Waite, & Shou, 2011), to engineer microbial consortia (Brenner, You, & Arnold, 2008; French, 2017; Frey-Klett et al., 2011; Mee & Wang, 2012), and to host uncultivable bacteria (Stewart, 2012). Synthetic mutualism of species that do not interact naturally has been established in co-culture between bacteria, yeast, amoeba, alga, cell lines, and tissues (Buchsbaum & Buchsbaum, 1934; Hosoda & Yomo, 2011; Hosoda et al., 2011; Kubo et al., 2013; Lőrincz et al., 2010; Shou, Ram, & Vilar, 2007). Several bacterial endosymbionts have been found in yeast (Kang, Jeon, Hwang, & Park, 2009; Saniee & Siavoshi, 2015) as

*Cofirst authors.

well as in fungal hyphae and spores (Bertaux et al., 2003; Bianciotto et al., 2004; de Boer et al., 2004; Hoffman & Arnold, 2010; Lumini, Ghignone, Bianciotto, & Bonfante, 2006; Partida-Martinez & Hertweck, 2005; Sato et al., 2010). In this work, we cultured the obligate endosymbiont bacterium *Wolbachia* in an artificial host: the nonpathogenic yeast *Saccharomyces cerevisiae*.

Wolbachia pipientis is an exceedingly successful obligate endoparasite/endosymbiont in nematodes and arthropods (Taylor & Hoerauf, 1999; Werren, 1997; Werren, Baldo, & Clark, 2008). The size of the *Wolbachia* genome varies widely depending on the strain. Arthropod endoparasites have much larger genomes than nematode endosymbionts (Bandi, Slatko, & O'Neill, 1999; Darby et al., 2012; Foster et al., 2005; Klasson et al., 2008; Salzberg, Puiu, Sommer, Nene, & Lee, 2009; Wu et al., 2004). In regard to a possible aerobic metabolism, the *Wolbachia* from the plant hopper *Leodelphax stratellus* (*wStr*) is ten times more sensitive to paraquat than the insect host cell, suggesting that *wStr* does not possess the enzymes needed for reactive oxygen species (ROS) detoxification and thus it may be anaerobic or microaerophilic (Fallon, Kurtz, & Carroll, 2013). In contrast, eliminating *Wolbachia* with tetracycline in filaria, increases respiratory-chain gene expression in the host and causes an early death. This result, lead to the hypothesis that at least in filariae *Wolbachia* contributes as an energy generator for the host (Strübing, Lucius, Hoerauf, & Pfarr, 2010; Darby et al., 2012, 2014).

Culturing obligate intracellular bacteria is a challenge. Insect cells support *Wolbachia* growth, but culture times are long and cells are difficult to manipulate. Alternative systems such as mammalian blood have proven helpful to grow intracellular organisms such as *Sodalis* (Dale & Maudlin, 1999). However, *Wolbachia* did not seem to grow in blood and this was not pursued further (Result not-shown; see Methods). In contrast, *Saccharomyces cerevisiae* did support the growth of *Wolbachia* strain *w*AlbB.

As it can be extensively manipulated, *S. cerevisiae* is widely used as a model organism in biochemistry and molecular biology. In *S. cerevisiae*, it is possible to study processes such as the Crabtree effect observed in tumor cells (Diaz-Ruiz, Rigoulet, & Devin, 2011) and to model cell death in response to anoxia or ischemia/reperfusion (Stella, Burgos, Chapela, & Gamondi, 2011). In addition, it is used as a host to study DNA and RNA viral replication (Alves-Rodrigues, Galão, Meyerhans, & Díez, 2006), to identify and characterize bacterial effectors and toxins (Siggers & Lesser, 2008) and to analyze the function of heterologously expressed proteins such as the *Yarrowia lipolytica* and the mammalian brown-fat mitochondrial uncoupling proteins (UCPs) (Guerrero-Castillo et al., 2011). Thus, when it was observed that *Wolbachia* grew in *S. cerevisiae*, the system was characterized and the effects of *Wolbachia* infection on its host were analyzed.

Growing *Wolbachia* in insect cell cultures or in live hosts presents difficulties that have precluded detailed biochemistry and physiology studies (Baldridge et al., 2014; Khoo, Venard, Fu, Mercer, & Dobson, 2013). Here, we used the *S. cerevisiae* strain W303 as an alternative host for *Wolbachia* *w*AlbB and analyzed the host/endosymbiont system. Infected yeasts died earlier than controls. This probably resulted from an abnormally high mitochondrial oxidative phosphorylation activity observed at late stages of growth. Understanding *Wolbachia* and host-*Wolbachia* interactions holds great promise for medical, parasitological, and biotechnological applications.

2 | EXPERIMENTAL PROCEDURES

2.1 | Aa23 cell line maintenance

Aa23 cell line (*Aedes albopictus* infected with *w*AlbB) (O'Neill et al., 1997) was kindly donated by Professor Anne Fallon (U. Minnesota) and maintained in Eagle's minimal essential medium (MEM, Sigma Chemical Co. M0643). MEM was supplemented as indicated elsewhere (Shih, Gerenday, & Fallon, 1998). The medium was filter-sterilized (Millipore, 0.22 μm) and stored in 200 ml aliquots at 4°C. Prior to use, heat-inactivated fetal bovine serum (FBS; 30 min at 56°C) was added to a final concentration of 10% (Shih et al., 1998). The insect cell line was grown on True Line TR 4003 140 mm sterile petri dishes at 27°C in a 5% CO_2 atmosphere (ESCO CelCulture CO_2 incubator or in Corning culture flasks, Shanghai, China). Subcultures were performed in a 1:10 split at 90% confluence. A sample from this cell line was treated with tetracycline to eliminate *Wolbachia* infection (Aa23Tet) (Dobson, Marsland, Veneti, Bourtzis, & O'Neill, 2002).

2.2 | Cell viability assays

Viability of Aa23 cell line, *Wolbachia* or yeast was assessed using the BacLight live-dead staining kit (Molecular Probes, Carlsbad, CA). Ten microliters of cell suspension were stained according to the manufacturer suggested protocol and viewed in an epifluorescence NIKON microscope.

2.3 | Failed attempts to grow *Wolbachia* ex-vivo and a serendipitous finding

The original idea was to find a system where *Wolbachia* would grow ex-vivo. To do this, diverse protocols used for other endosymbionts such as *Sodalis* and *Coxiella* were followed (Dale & Maudlin, 1999; Omsland et al., 2009, 2013). It was found that some components did improve survival in isolated *Wolbachia*, even if we never observed substantial growth. Some of these agents were: (1) Trehalose and other compatible solutes such as mannitol, glycerol and sucrose, known to stabilize pollen (Crowe, Reid, & Crowe, 1996; Leslie, Israeli, Lighthart, Crowe, & Crowe, 1995) and isolated proteins (Sampedro & Uribe, 2004) (2) Actin, which supports binding and movements of some endosymbionts in vivo. (3) Catalase which deactivates hydrogen peroxide (Dale & Maudlin, 1999) and (4) Blood from large mammals, which has been used to grow *Sodalis* (Dale & Maudlin, 1999) and increases *Wolbachia* titers (Amuzu, Simmons, & McGraw, 2015; McMeniman, Hughes, & O'Neill, 2011). Human blood was also effective.

First, we tried growing *Wolbachia* using sheep blood. However, it was easily contaminated at the sites of extraction, so cultures

had to be discarded often. On one occasion we obtained positive *wsp* gene amplification from a yeast colony grown in one of the agar plates. Out of curiosity, we studied the host, which turned out to be *S. cerevisiae*. From this accidental finding we decided to test a known strain of *S. cerevisiae* as an alternative host. We learned that, in order to support growth of *Wolbachia*, yeast culture media needed to be supplemented with blood, which eventually was substituted with ammonium ferric citrate with excellent results and none of the contamination problems. Neither compatible solutes, nor catalase nor actin enhanced growth. The second addition needed was bovine fetal serum, which was present in all original growth media but not in yeast culture media. FBS was titrated and we ended up using 1%.

Among laboratory strains, infection was successful in W303 and NB40, while infection % in BY was milder (Figure 1). The *S. cerevisiae* strain W303-1A (MATα; ura3-1; trp1Δ 2; leu2-3,112; his3-11,15; ade2-1; can1-100) (Gutierrez-Aguilar et al., 2014), where *Wolbachia* was abundant at 10 days of infection was chosen for further experiments (See Results).

2.4 | *Wolbachia wAlbB* infection of the *Saccharomyces cerevisiae* W303 yeast strain (*wScW303*)

A first yeast infection was performed following a modified cell line infection protocol (Dobson et al., 2002). All procedures were performed under sterile conditions. The Aa23 cell line (containing *Wolbachia*) was grown in Corning cell culture flasks (225 cm^2) as described in (Shih et al., 1998). After 20 days of culture, cells were scrapped and concentrated by centrifugation at 3,000*g* for 5 min. For homogenization, ~1*10^7 cells were resuspended in 10 ml Eagles medium and vortexed for 10 min with (50% v/v) 3 mm sterile borosilicate glass beads (Rasgon, Gamston, & Ren, 2006). The homogenate was centrifuged at 3,000*g* for 10 min to remove unbroken cells. The supernatant was passed through a 2.7 μm syringe filter and the filtrate containing bacteria was centrifuged at 16,500*g* for 10 min. The pellet was resuspended in 2 ml of Mitsuhashi-Maramorosch medium (MM) supplemented with 1 mmol L^{-1} ammonium ferric citrate and 20% fetal bovine serum (FBS) (MM Fe FBS). In parallel, yeasts were

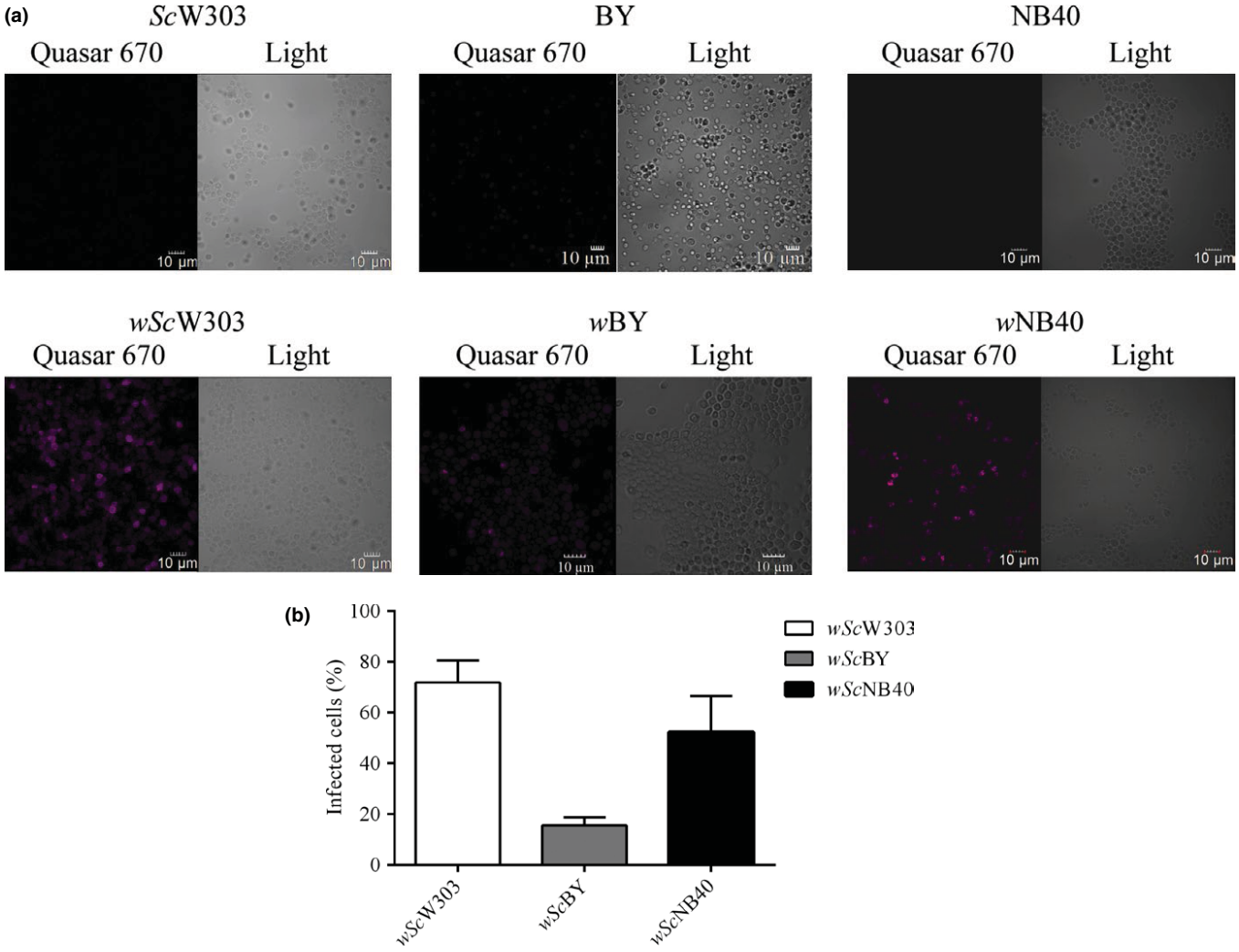

FIGURE 1 Infection of *Saccharomyces cerevisiae* with *Wolbachia*. (a) FISH using a *Wolbachia* 16S rDNA specific probe labeled with Quasar 670 (pink) was performed on 14 day old cultures of infected and control *S. cerevisiae strains* W303 (*Sc*W303), BY (*Sc*BY), and NB40 (*Sc*NB40) (b) After 14 days postinfection, the percentage of infected cells were counted as those with positive hybridization.

grown in a liquid YPD culture for 3 hr, harvested and centrifuged at 3,000*g* for 3 min. Culturing yeast in low oxygen environments prevents thickening of the cell wall (Aguilar-Uscanga & Francois, 2003; Smith et al., 2000; Avrahami-Moyal, Braun, & Engelberg, 2012). To induce contact between bacteria and yeast both bacteria (the whole 2 ml sample) and yeast (60 mg ww) were mixed and centrifuged at 2,500*g* for 1 hr at 20°C (Dobson et al., 2002). Bacteria-infected yeast were plated (all 2 ml) on a Petri dish containing MM supplemented with 1 mmol L^{-1} ammonium ferric citrate plus 25% v/v outdated human packaged erythrocytes and 2% agar (MM Fe-blood) and incubated at 27°C in a 5% CO_2 chamber (ESCO, Cell Culture CO_2 incubator, Singapore) for 14 days (Dale & Maudlin, 1999). Infection was confirmed by FISH and PCR. Infected yeast was transferred to a fresh agar plate every month for up to 6 months, then yeast was discarded and a new sample was used. Some aliquots were added with 40% glycerol, frozen and stored at −80°C, these samples have remained infective for nearly 10 months.

To transfer *Wolbachia* from yeast to yeast, slight modifications to the protocol were made: An aliquot of 100 µl of yeast taken from a glycerol-frozen sample or a loophole of infected yeast cells was diluted in 2 ml YPD Fe 20% FBS and plated in YPD Fe-blood agar plates, which were grown in 5% CO_2. After 14 days, all cells grown in a Petri dish were collected and washed by centrifugation at 3,000*g* for 3 min at 20°C with sterile water and the pellet was suspended in 10 ml MM. The suspension was vortexed for 10 min in the presence of 0.425–0.600 mm sterile borosilicate glass beads (60% v/v) to disrupt yeast cells (note that beads were smaller than those used for insect cell lines). Disrupted yeasts were centrifuged at 3,000*g* for 10 min and the supernatant was centrifuged again 3,000*g* for 10 min. The washed supernatant was filtered through different 0.8–0.65–0.45 µm syringe filters. Again, we used filters with smaller pores than those used for cell lines due to the small size of yeast cells. The last filtrate was centrifuged at 16,500*g* for 10 min. The pellet (~60 mg ww) was suspended in 2 ml MM Fe FBS and used to infect yeast from 3-h cultures as described above. The yeast–bacterium mixture was plated in a YPD Fe agar plate and incubated at 27°C with 5% CO_2 for at least 7 days. Infection was evaluated using FISH and PCR.

2.5 | Culture and maintenance of *w*AlbB-infected *Saccharomyces cerevisiae* W303

Infected *S. cerevisiae* strains were kept in YPD plus 1 mmol L^{-1} ammonium ferric citrate agar plates. When transferring to liquid medium, a loophole from the desired strain was suspended in 100 ml of sterile YPDS and incubated at 28°C, 130 rpm for 48 hr. Precultures were decanted in one liter YPDS and incubated at the same conditions for up to 14 days. When transferring from solid to solid media, a loophole of yeast was suspended in 1 ml YPD supplemented with 1 mmol L^{-1} ammonium ferric citrate plus 20% FBS and plated on YPD agar. A cell passage every 2–3 weeks was performed in order to maintain the infection. When it was desired to eliminate *Wolbachia* from yeast, tetracycline 30 µg/ml was added five consecutive times to the medium as passages were performed (Dobson et al., 2002).

2.6 | *Wolbachia w*AlbB infection of the C6C36 *Aedes albopictus* cell line

To determine whether *Wolbachia* cells retained its infective ability after all treatments, *Wolbachia* were isolated from *S. cerevisiae* grown in liquid YPD Fe 1% FBS and they were tested for infection against a C6C36 insect cell line.

2.7 | *Wolbachia* surface protein (*wsp*) gene PCR identification

The *Wolbachia wsp* gene was amplified using the following primers: *wsp* 81F (5′ TGGTCCAATAAGTGATGAAGAAAC 3′) and *wsp* 691R (5′ AAAAATTAAACGCTACTCCA 3′) (Braig, Zhou, Dobson, & O'Neill, 1998) in a 25 µl reaction volume using recombinant Taq DNA polymerase (Thermo Fisher Scientific). PCR amplification was performed as reported elsewhere (Braig et al., 1998; Xi, Khoo, & Dobson, 2006). The PCR product was electrophoresed on a 1% agarose gel and stained with ethidium bromide. PCR product was purified using a GeneJET PCR purification Kit (Thermo Fisher Scientific) and sequenced in the Molecular Biology Unit at the Institute of Cellular Physiology, UNAM.

2.8 | Fluorescence in-situ hybridization (FISH)

Wolbachia 16S rDNA oligonucleotide probe labeled with Quasar 670 dye (λ_{em}647, λ_{ex}670) W1, 5′-AATCCGGCCGARCCGACCC-3′ was used for FISH assays (Heddi, Grenier, Khatchadourian, Charles, & Nardon, 1999). One milliliter of the desired culture was centrifuged at 3,000*g* for Aa23, C6C36 and yeast, and 18,500*g* for purified *Wolbachia* for 5 min. Protocol was followed as reported elsewhere (Genty, Bouchon, Raimond, & Bertaux, 2014). Samples were viewed in a FluoView FV-1,000 Olympus confocal microscope, NA 1.4 with a 100X objective. Images were analyzed with the FV-Viewer Olympus software.

2.9 | Z-cut images for cell reconstruction

Fourteen day old infected and noninfected yeast samples were visualized with a Olympus-FV1000 or FV-3000 microscopes. Z-cut images were reconstructed using Imaris 7.2.1 and Image J software. Calcofluor-white (0.05 mmol L^{-1} in 20% DMSO-20 mmol L^{-1} Bicine Buffer) was used to stain fungus cell wall.

2.10 | Antibodies

Primary antibodies: Mouse monoclonal Anti-*Wolbachia* Surface Protein NR-31029 was from BEI Resources, NIAID, NIH. Mouse monoclonal Anti-VDAC was from Abcam. Secondary antibody: HRP

coupled Anti-mouse antibody from Jackson ImmunoResearch (West Grove, PA).

2.11 | Western blot

A loophole from yeast grown in solid media was suspended in 200 µl of water; otherwise, 200 µl from liquid culture samples were centrifuged at 3,000*g* for 5 min and washed twice in water. The pellet was solubilized in 200 µl RIPA buffer (25 mmol L^{-1} Tris•HCl pH 7.6, 150 mmol L^{-1} NaCl, 1% NP-40, 1% sodium deoxycholate, 0.1% SDS) supplemented with protease inhibitors 1 mmol L^{-1} PMSF (Sigma-Aldrich) and Complete protease inhibitor cocktail (Roche-CO-RO) as recommended by the abcam protocol. Samples were lysed in a Sonics VibraCell sonicator (Sonics & materials, Inc., Newtown, CT) at 80% amplitude for 10 s and left under agitation in a Multi-Vortex V-32 (Biosan, Riga, Latvia) for 30 min at 4°C. Samples were centrifuged at 15,160*g* for 5 min. The supernatant was recovered and protein concentration was measured by Bradford in a PolarStar Omega (BMG labtech, Ortenberg, Germany) [(Bradford, 1976) #64]. Samples were diluted in a 4X buffer (500 mmol L^{-1} Tris, pH 6.8, 10% glycerol, 10% SDS, 0.05% beta-mercapto-ethanol, and 0.01% bromophenol blue) and boiled for 5 min. SDS/PAGE was performed in 10% polyacrylamide gels and electrotransferred to poly(vinylidenedifluoride) membranes as reported elsewhere (Chiquete-Felix et al., 2009). Membranes were blocked with 5% Blotto nonfat dry milk in TBS-T (50 mmol L^{-1} Tris, 104 mmol L^{-1} NaCl, pH 7.6, 0.1% Tween 20) for 1 hr, and incubated overnight at 4°C with the primary antibody. Membranes were washed with TBS-T and incubated at 37°C for 1 hr with secondary antibody. Membranes were washed again and the bands were developed by chemiluminescence using an ECL kit (Amersham Biosciences, GE, Healthcare) (Chiquete-Felix et al., 2009). PVDF membranes were stripped as indicated by abcam protocol using a mild-stripping buffer, blocked with 5% Blotto nonfat dry milk in TBS-T and reprobed with a different antibody as indicated.

2.12 | Transmission electron microscopy of *wSc*W303

Infection was assessed by transmission electron microscopy (TEM) following a protocol from (Sun et al., 2015). Briefly, 500 µl of cells were harvested from 100 ml cultures of infected and uninfected *Saccharomyces cerevisiae* cultures form the first unintentional infection (*wSc*) at 10 days and *wSc*W303 of fourteen days. Yeast and *Wolbachia* samples were washed twice in distilled water at 740 g for 5 min for yeast and 23400 g for 10 min for bacteria in an Eppendorff Centrifuge 5415C. Samples were fixed in 2% $KMnO_4$ at 4°C overnight. Next day, samples were washed for 15 min with deionized water six times and dehydrated with sequential 10-minute washes with 50%, 70%, 80%, 90% ethanol and three washes with 100% ethanol. Samples were washed with ethanol-propanone (1: 1) for 8 min, then with anhydrous propanone for 5 min, then with propanone-EPON 821 (3: 1) for 1 hr and left in propanone-EPON 821 (1 : 3) overnight. Next day, samples were concentrated and resuspended in propanone-EPON 821 (1: 1) for 1 hr. Then, samples were concentrated again and left in resin for 24 hr. Then they were incubated for 12 hr at 37°C and then further incubated for 36 hr at 60°C. Resins were cut into 70 nm slices on an ultra-microtome (Ultracut Reicheit-jung) and observed in a JEOL JEM-1200 EXII electron microscope. Data were processed using Gatan Digital Micrograph Software.

2.13 | Mitochondrial (or Mitochondria/*Wolbachia* mixture) isolation

Yeast were centrifuged at 3,000*g* for 5 min, washed twice in water and resuspended in MES-mannitol buffer (5 mmol L^{-1} MES, 0.6 mol L^{-1} mannitol, 0.1% BSA pH 6.8 adjusted with triethanolamine). Yeast were disrupted using a Bead Beater cell homogenizer (Biospec Products, OK, USA, final volume 50 ml) with 0.425–0.6 mm glass beads during three 20 s pulses separated by 40 s resting periods in ice (Uribe, Rangel, Espínola, & Aguirre, 1990). The homogenate was differentially centrifuged to isolate mitochondria similar to described in (Peña, Piña, Escamilla, & Piña, 1977). Briefly, cells were centrifuged at 1,100*g* for 5 min. The supernatant was centrifuged at 9,798*g* for 10 min and the pellet was resuspended in MES-mannitol buffer and centrifuged at 3,000*g* for 5 min. Finally, the supernatant was centrifuged at 17,500*g* for 10 min. The resulting pellet was resuspended in minimal volume and protein concentration was measured by Biuret (Gornal, 1957) using a Beckman Coulter spectrophotometer at 540 nm.

2.14 | Oxymetry

Mitochondrial high resolution respirometry was assessed in an Oroboros oxygraph (Oroboros Intrs Corp, Innsbruck, Austria) using 5 mmol L^{-1} MES, 0.6 mol L^{-1} mannitol pH 6.8, 10 mmol L^{-1} KCl and 4 mmol L^{-1} Pi at 30°C. Final volume in the closed chamber was 1.5 ml with a protein concentration of 0.5 mg prot/ml. Bacterial protein concentration of 0.5 mg prot/ml was used. The trace was started by the addition of 5 mmol L^{-1} of the indicated substrate: glycerol-3-phosphate, ethanol, NADH, pyruvate-malate, succinate, glutamine or glutamate. For Complex IV evaluation, 5 mmol L^{-1} ascorbate (pH 7.6)- 0.05 mmol L^{-1} TMPD was used (Uribe, Ramirez, & Peña, 1985). Respiratory control was measured using 0.5 µl/ml ethanol to induce state II respiration and 1 mmol L^{-1} ADP to induce the phosphorylated state (Uribe et al., 1985). Respiratory chain inhibitors were used in the following concentrations: 0.1 µmol L^{-1} rotenone, 0.15 mmol L^{-1} flavone, 0.1 µmol L^{-1} antimycin A, and 2 mmol L^{-1} cyanide (Uribe et al., 1985).0.5 µmol L^{-1} CCCP was added as an uncoupler. Data were analyzed using the Oroboros Lab software.

2.15 | Electrophoretic techniques and in-gel activities

Blue native gel electrophoresis (BN-PAGE) and high-resolution clear native electrophoresis (hrCN-PAGE) were performed as in (Wittig,

Braun, & Schägger,2006; Wittig, Karas, & Schägger, 2007). Whole cells were solubilized with 2 mg dodecylmaltoside/mg protein plus 1 mmol L^{-1} PMSF and Complete protease inhibitor cocktail (Roche-CO-RO) and shaken for 30 min at 4°C. Membranes were centrifuged at 23,680*g* at 4°C for 1 hr. Protein concentration in the supernatants was determined by Bradford (1976). Between 0.1 and 0.15 mg of protein were loaded in 5%–15% polyacrylamide gradient gels. When hr-CN PAGE electrophoresis was performed 0.01% Lauryl maltoside and 0.05% sodium deoxycholate were added to the cathode buffer [(Wittig et al., 2007) #69]. Gels were run for about an hour at 15 mA/gel in a Bio-rad electrophoresis chamber. In-gel NADH-NBT oxido-reductase (100 μg protein), succinate-NBT oxido-reductase (150 μg protein), cytochrome *c* oxidase (100 μg protein), and in-gel ATPase (100 μg protein) activities were done as reported previously (Uribe-Alvarez et al., 2016). 20 μg protein of solubilized Bovine Heart Mitochondria (BHM) were loaded in each gel as controls.

2.16 | LC-MALDI-MS/MS

Indicated bands from hr-CN PAGE or BN-PAGE were enzymatically digested, separated on a HPLC EkspertnanoLC 425 (Eksigent, Redwood City CA) and analyzed in a MALDI-TOF/TOF 4800 Plus mass spectrometer (ABSciex, Framingham MA) (Shevchenko, Tomas, Havli, Olsen, & Mann, 2006) in the Unidad de Genómica, Proteómica y Metabolómica, CINVESTAV-IPN. Generated MS/MS spectra were compared using Protein Pilot software v. 4.0 (ABSciex, Framingham MA) against the *Saccharomyces cerevisiae* ATCC 204508 database (downloaded of Uniprot, 6721 protein sequences) and *Wolbachia* genus database (downloaded of Uniprot, 47781 protein sequences) using Paragon algorithm.

3 | RESULTS

3.1 | At the expense of its own viability, the artificial host *Saccharomyces cerevisiae* W303 supports growth of *Wolbachia* *w*AlbB

To study *Wolbachia* (*w*AlbB) large biomass yields plus a host that is easy to manipulate are needed. After testing different alternatives (see Methods), it was discovered that different *S. cerevisiae* strains were susceptible to infection and supported active *Wolbachia* proliferation. At 14 days of infection, *Wolbachia* grew efficiently in *S. cerevisiae* strains W303 (*Sc*W303) and NB40 (*Sc*NB40), while strain BY (*Sc*BY) supported only a weak infection (Figure 1a). After 14 days the percentage of infected cells counted by FISH using probes against the *Wolbachia* 16S rDNA was 71.8% ± 8.7% for *Sc*W303 and 52.3% ± 14.3% for *Sc*NB40, while in *Sc*BY less than 20% cells were positive for FISH (Figure 1b). Strain *Sc*W303 was chosen for further studies. *Sc*W303 maintains high rate of oxidative phosphorylation regardless of the carbon source, it is highly resistant to oxidative stress (Ocampo, Liu, Schroeder, Shadel, & Barrientos, 2012) and it has a weak cell wall (Avrahami-Moyal et al., 2012). Strains used in this study are detailed in Table S1.

3.2 | Proliferation of *Wolbachia* in *Sc*W303 was further confirmed using different independent methods as follows (Figure 2)

3.2.1 | PCR of the *Wolbachia* outer surface protein gene (*wsp*)

Both the Aa23 cell line (Figure 2a) and infected *S. cerevisiae* (*wSc*W303) (Figure 2b) amplified 650 bp fragments exhibiting sequences 100% identical to the surface protein of the *Wolbachia* endosymbiont of *Aedes albopictus* (NCBI database: KC242223.1) (Table S2). PCR amplification bands were not observed in the tetracycline-treated Aa23 cell line (Figure 2a, Aa23 Tet) and in the noninfected yeast (Figure 2b, *Sc*W303). Tetracycline used continuously in cell cultures is reported to kill *Wolbachia* (Dobson et al., 2002).

3.2.2 | Western Blot analysis detected *Wolbachia* wsp in *S. cerevisiae*

In the Aa23 cell line, a ~37 kDa protein corresponding to the *Wolbachia* Surface protein (wsp) was revealed with anti wsp antibodies (Bei resources, NIH, MD) (Figure 2c, Aa23). This band disappeared after growth in the presence of tetracycline (Aa23 Tet). VDAC (Voltage dependent anionic channel) protein was used as a loading control. In non–infected yeast wsp was not detected, (Figure 2c, *Sc*W303), while in infected yeast the wsp western blot signal was first detected at day 3 and increased gradually up to day 10, remaining stable until day 14 (Figure 2c, *wSc*W303). (For images of original Western Blots, see Figure S1a). When tetracycline was added to the medium, the wsp signal decreased, disappearing by day 10 (Figure S1b, *wSc*W303Tet).

3.2.3 | Normal growth and early death were observed in infected *S. cerevisiae*

During the first 12 days of culture, growth curves of infected *wSc*W303 were similar to the controls (Figure 3a). Then, beginning at day 14, *wSc*W303 absorbance decreased. Cell wall degradation (Figure S2) and viability staining (Figure 3b) confirmed that *wSc*W303 viability was rapidly lost during the late stages of the stationary phase, from 14 to 18 days of culture.

In addition, during growth the transcriptional activity of both *S. cerevisiae* 18S rRNA and the *Wolbachia wsp* were tested. Transcription was high in *S. cerevisiae* from the first day, decreased at day fourteen and became negligible at days 16 and 18 (Figure 3c). In contrast, transcription of the *wsp* from *Wolbachia* became detectable only after 3 days, increased exponentially until day 10 and remained constant until day 14. Then, at days 16 and 18, transcription decreased abruptly (Figure 3c). Transcription data in the *Wolbachia/S. cerevisiae* system indicated that *Wolbachia* activity grew later than *S. cerevisiae*, reaching a maximum at 10 days. Later, beginning at 14 days both transcription activities decreased abruptly in parallel with the death of the host.

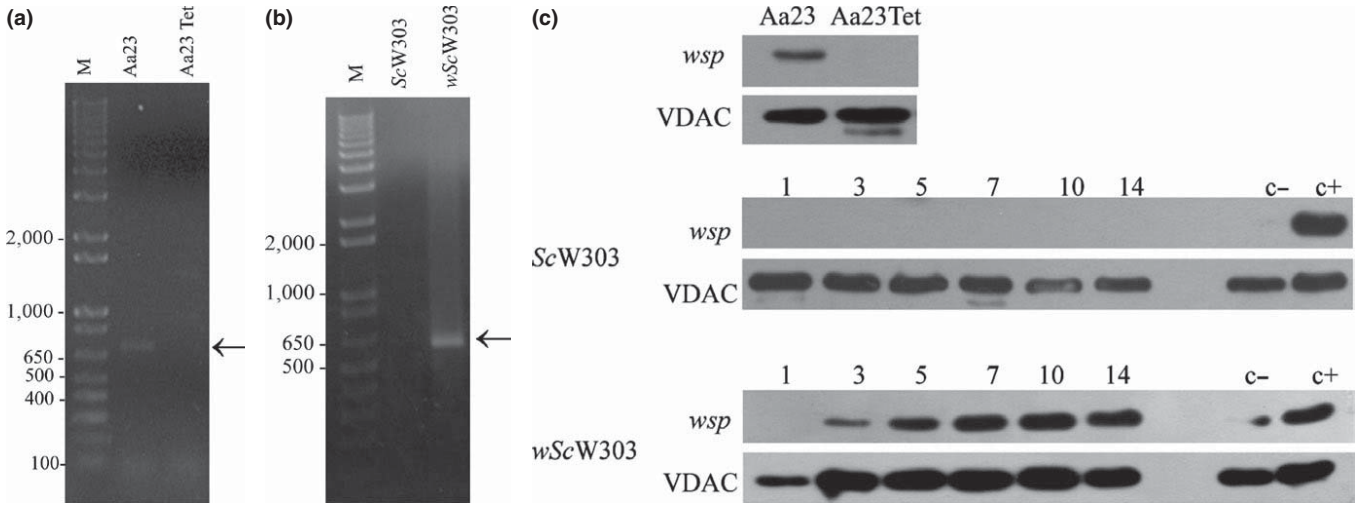

FIGURE 2 Detection of *Wolbachia* in *Saccharomyces cerevisiae* W303. (a) Agarose gel electrophoresis of the *wsp* PCR products predicted as a ~600 bp band in the Aa23 cell line. Lanes: M, Invitrogen 1 kb plus DNA ladder; Aa23, infected cell line; Aa23 Tet, noninfected cell line. (b) Agarose gel electrophoresis of the *wsp* PCR products for *S. cerevisiae*. Lanes: M, Invitrogen 1 kb plus DNA ladder; *Sc*W303, uninfected original yeast; *wSc*W303, infected yeast. (c) Western blot against the wsp and VDAC proteins. First row, first lane Aa23 infected cell line and second lane Aa23Δw tetracycline-cured cell line. Yeast samples were taken at 1, 3, 5, 7, 10, and 14 days postinfection. A positive control was taken from a 20 day YPD-2% agar culture infected-*wSc*W303. Negative control was a noninfected sample *Sc*W303

3.2.4 | Yeast cell/endosymbiont images were observed by staining *S. cerevisiae* with Calcofluor white and *w*AlbB with Quasar 670

Both the western blot and the RT-PCR experiments suggested that *Wolbachia* grew in the presence of *S. cerevisiae* becoming abundant at days 10–14. In order to determine whether *Wolbachia* was inside yeast, samples from infected and noninfected yeast cells from 14-day old cultures were hybridized using a *Wolbachia* specific 16S rDNA probe labeled with Quasar-670 (FISH). Then, the yeast cell wall was stained with Calcofluor white (Figure 4, Movie S1, Movie S2), Staining of the *S. cerevisiae* cell wall allowed observation of labeled bacteria inside yeast. Figure 4 shows that the Quasar-670 label was detectable only in *wSc*W303 and not in *Sc*W303. Merge of the Calcofluor, Quasar-670 and Clear field (Light) images show bacteria are inside the cell (Figure 4). Tridimensional reconstructions of z-cuts performed in a *wSc*W303 sample show the intracellular location of different bacteria (movies S1 and S2). In the periphery of movies S1 and S2, few independent bacterial labels were detected, which we speculate, may come from bacteria inside heavily deteriorated host cells whose cell wall was not stained by Calcofluor (movies S1 and S2).

3.2.5 | TEM images detected *Wolbachia* inside *S. cerevisiae*

Transmission electron microscopy images further suggested the intracellular location of *Wolbachia*. Cultures of 10 and 14 days of control and infected *S. cerevisiae* were analyzed. In infected yeast cells (Figure 5b–f, g), bacteria-like bodies (Figure 5, labeled *) that are not present in the uninfected yeast (Figure 5a and d) can be observed. At 10 days both infected and noninfected yeast present mitochondria, which can be identified by the presence of inner membrane cristae (Figure 5, labeled m). In contrast 14 day-old cultures of *Sc*W303 lost most mitochondrial structures, which suggest that these organelles are dysfunctional probably because cells are in late stationary phase. In contrast, 14 days-old infected *wSc*W303 show *Wolbachia* plus mitochondria where the typical cristae pattern may be observed, suggesting abnormal preservation of mitochondria in infected yeast (Figure 5e–g). In *wSc*W303 cultures, we can observe different cell images: most cells had an intact plasma membrane and contained mitochondria and bacteria-like bodies inside (Figure 5e). Other cells exhibited damaged membranes but the bacteria like structures were still present (Figure 5f). Among the whole population, we found some budding yeast, where bacteria-like bodies can be seem concentrated in the bud (Figure 5g). None of the latter populations was found in control *Sc*W303 cultures.

3.2.6 | *Wolbachia*-infected yeast retained high mitochondrial oxidative phosphorylation activity for abnormally long periods

A possible mechanism for the early death of infected yeast was explored in our infected *Sc*W303/*w*AlbB system. This system exhibited an abnormal preservation of mitochondria (Figure 5), so it was logical to explore aerobic metabolic activity. The relationship between *Wolbachia* and aerobic metabolism in the host is a matter of controversy. Some authors have proposed that these endo-cellular organisms possess an aerobic metabolism that contributes to overall activity (Strübing et al., 2010) while others suggest that *Wolbachia* optimizes aerobic metabolism by supplying heme groups for respiratory complexes (Darby et al., 2012; Fallon, Baldridge, Carroll, &

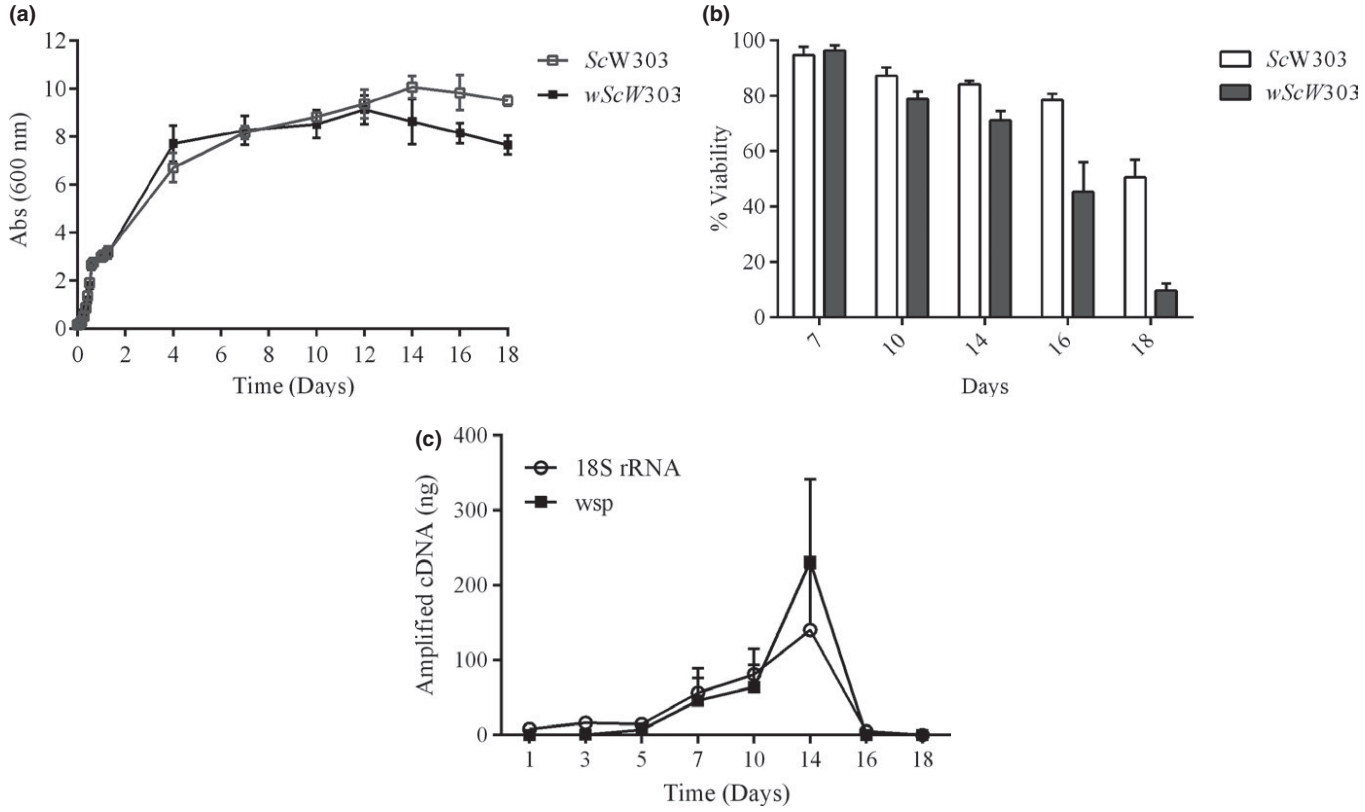

FIGURE 3 *S. cerevisiae* growth, viability, and transcriptional activity in the absence and presence of *Wolbachia*. (a) Growth curves of *Sc*W303 and *wSc*W303 grown in YPDS at 30°C, 130 rpm for 18 days. (b) Yeast cell viability in different days of culture quantified by microscopy with the BacLight viability kit. (c) Amplification of the *wsp* gene of *Wolbachia* and the 18S rRNA gene of *S. cerevisiae* of samples taken at different days of culture

Kurtz, 2014; Foster et al., 2005; Heddi et al., 1999; Strübing et al., 2010). Thus, we decided to evaluate oxidative phosphorylation activities in our system, which preserved mitochondrial structure beyond the stationary phase (Figure 5).

When isolation of *Wolbachia* was attempted, it was found that the bacterium and mitochondria migrated together (Baldridge et al., 2014; Uribe et al., 1985). Thus, it was decided to characterize oxidative phosphorylation activity in the mitochondria/*Wolbachia* mixture and then determine the contribution of each entity using different bioenergetics techniques. The rate of oxygen consumption was measured using ethanol as a substrate (Table 1). We isolated the mitochondria/*Wolbachia* fraction from either one-day cultures

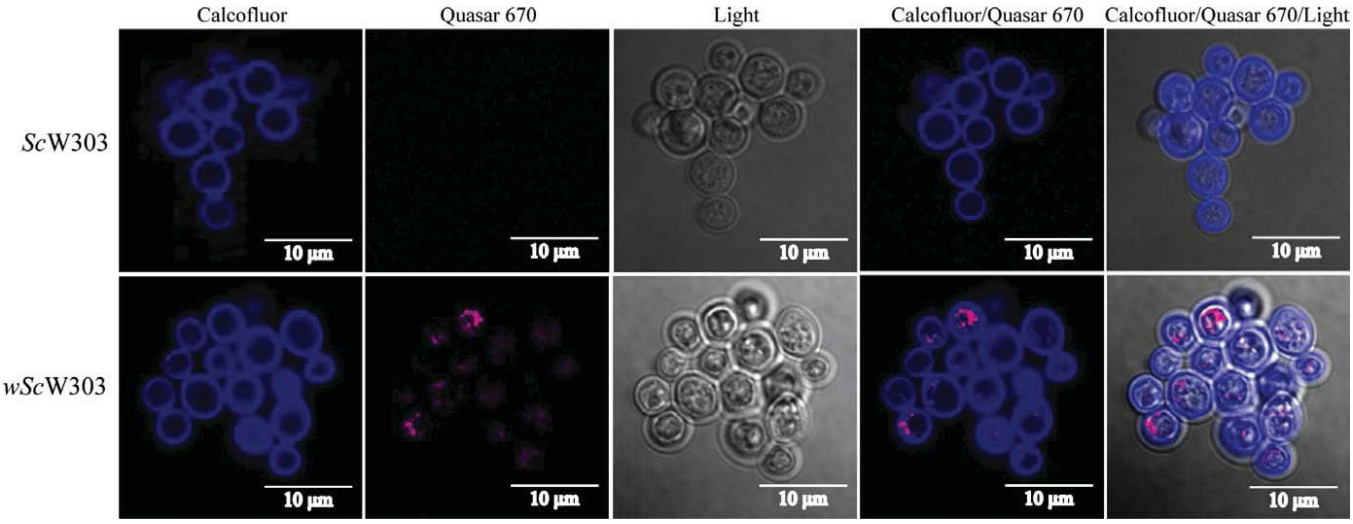

FIGURE 4 *Wolbachia* in calcofluor-labeled *S. cerevisiae*. Infected (*wSc*W303) and noninfected (*Sc*W303) *S. cerevisiae* cells were hybridized with the 16S rDNA *Wolbachia* probe (Quasar 670, pink). Then, the yeast cell wall was stained with calcofluor-white (Calcofluor, blue) to confirm the endosymbiosis. Merge images are shown to evaluate the presence of *Wolbachia* inside yeast

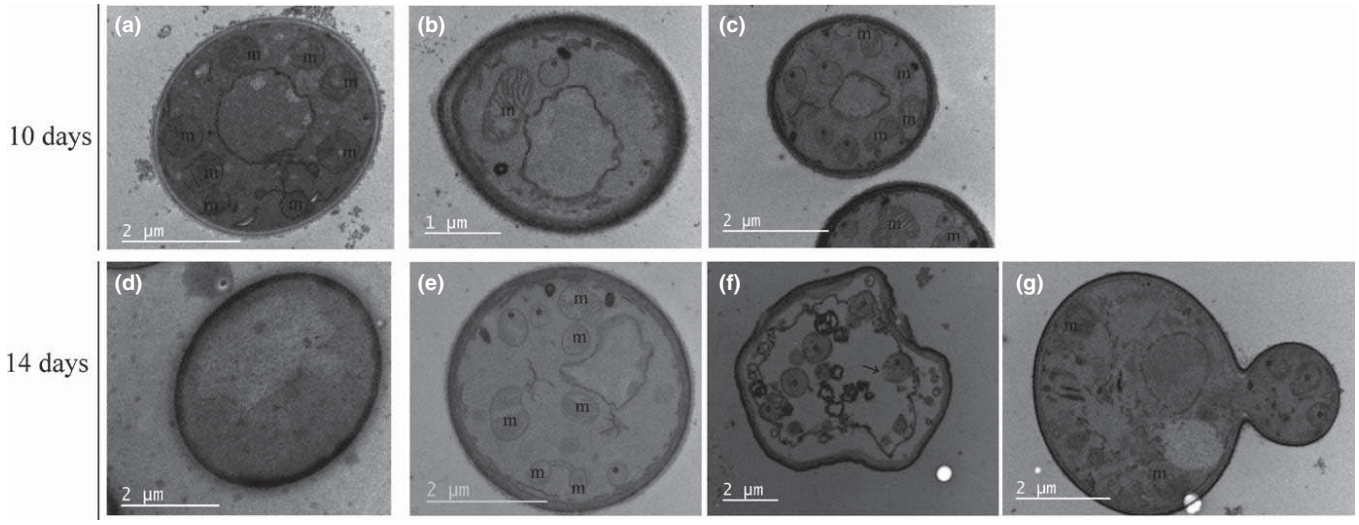

FIGURE 5 Electron microscopy images of infected and noninfected *Saccharomyces cerevisiae* at different times of incubation. Transmission electron microscopy images confirm the intracellular location of *Wolbachia*. 10-day images were taken with uninfected (a) *Sc* and infected (b–c) *wSc*; 14 day-old images were taken with (d) *Sc*W303 and (e–g) *wSc*W303. Images show the presence of bacteria-like bodies (*) that are not present in uninfected yeast and mitochondria (m) whose cristae can be easily identified

TABLE 1 Oxygen consumption rates of mitochondrial fractions from 1 and 14 day-old cultures of *Wolbachia*-infected (*wSc*W303) and noninfected (*Sc*W303) *Saccharomyces cerevisiae* cells

	State IV (natgO/min*mg prot)	State III (natgO/min*mg prot)	RCIII/IV
1 Day *Sc*W303	25.2 ± 3.1	52.5 ± 6.8	2.1 ± 0.15
1 Day *wSc*W303	27.4 ± 4.6	65.4 ± 9.0	2.4 ± 0.2
14 Days *Sc*W303	22.6 ± 5.1	29.0 ± 6.3	1.3 ± 0.2
14 Days *wSc*W303	34.2 ± 5.1	73.3 ± 11.1	2.1 ± 0.1

Reaction mixture: 0.6 mol L^{-1} mannitol, 5 mmol L^{-1} MES, pH 6.8, 4 mmol L^{-1} Pi, 10 mmol L^{-1} KCl. As substrate, 5 mmol L^{-1} ethanol. For state III, 1 mmol L^{-1} ADP.

where there are very few *Wolbachia* cells or from 14-day cultures, where *Wolbachia* numbers were high (Table 1). In one-day cultures from *Sc*W303 and *wSc*W303 respiratory activities were very similar. However, at 14 days the rates of oxygen consumption and respiratory controls (RC) were widely different as follows: In noninfected yeast, both the rate of oxygen consumption and respiratory control decreased at the expense of state 3 inhibition, while in contrast, *wSc*W303 retained high rates of oxygen consumption plus high respiratory controls, i.e. in 14-day old *Wolbachia*-infected yeast exhibited high oxidative phosphorylation activity, consistent with the presence of mitochondria observed by TEM in the infected cells (Table 1).

3.2.7 | In the presence of *Wolbachia* the activity of different mitochondrial respiratory complexes was preserved

In the isolated mitochondria/*Wolbachia* mixture, we tested specific substrates for each respiratory chain complex/enzyme (Table S3). In one-day cultures the rates of oxygen consumption were similar in infected and noninfected *S. cerevisiae* (Figure 6). In aged mitochondria from noninfected yeast, external NADH dehydrogenase (NDH2e, Pyruvate-Malate), succinate dehydrogenase (Succinate) and Complex IV (Ascorbate-TMPD) activities were strongly diminished. In contrast, in the 14 day-old mitochondrial fractions from *Wolbachia*-infected cells, respiratory activities in the presence of glycerol-3-phosphate, pyruvate-malate, and succinate were increased in comparison to 1-day cultures. Since *S. cerevisiae* does not have complex I and pyruvate-malate dependent respiration was insensitive to rotenone, redox activity was most likely from the mitochondrial NDH2 and not a bacterial complex I. Succinate oxidation was completely inhibited by antimycin A, indicating the absence of an alternative oxidase. Complex IV and NADH-dependent oxygen consumption rates were still decreased as compared to mitochondria from one-day cultures (Figure 6). Other respiratory substrates, namely glutamate and glutamine, which are used by Rickettsia (Winkler & Turco, 1988) where assayed and they did not support oxygen consumption. The respiratory activities measured indicate that the mitochondria/*Wolbachia* fractions from the infected and noninfected yeast consume the same substrates and are inhibited by the same respiratory chain inhibitors.

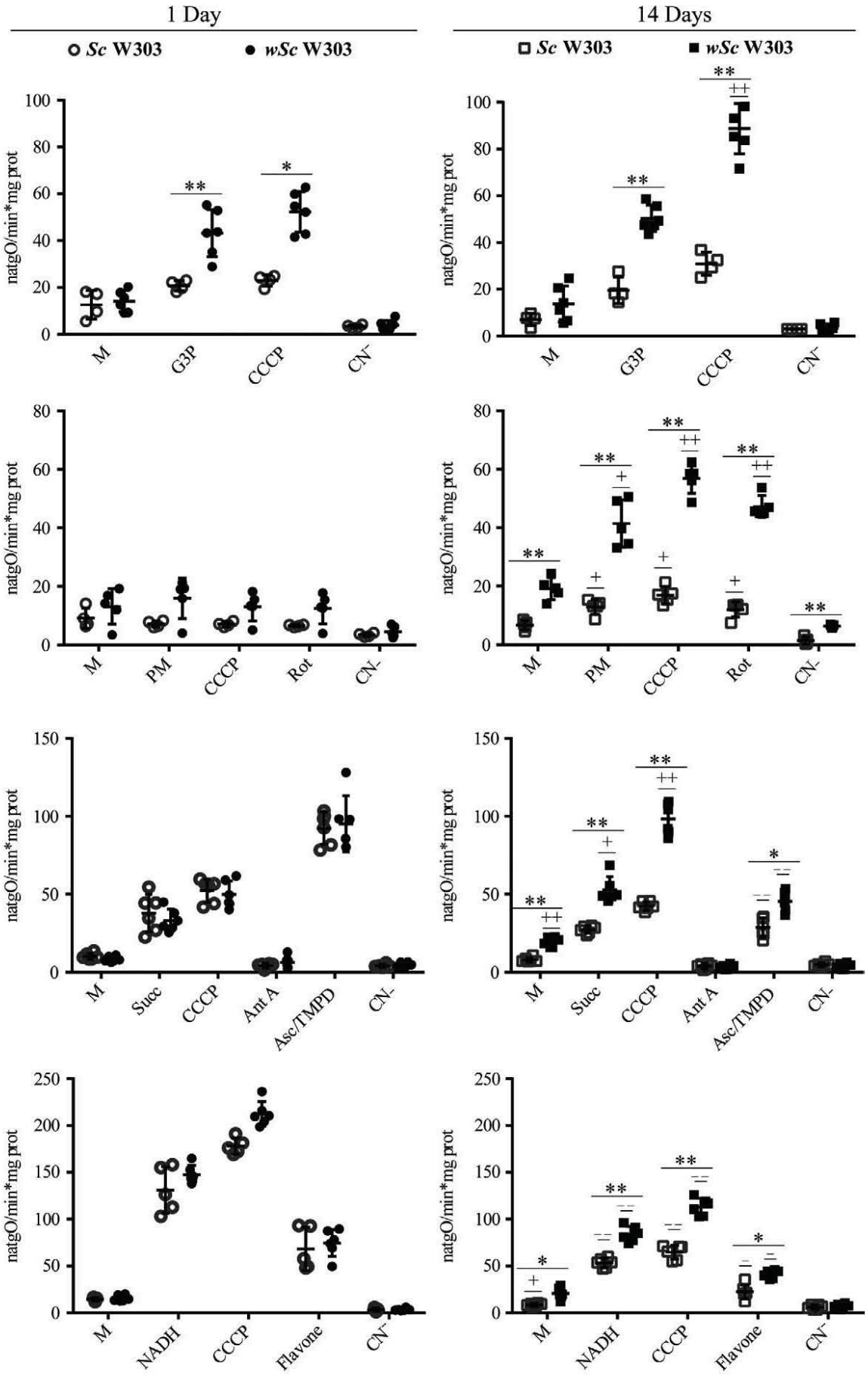
1 Day
14 Days
Sc W303
wSc W303
natgO/min*mg prot
M
G3P
CCCP
CN-
PM
Rot
Succ
Ant A
Asc/TMPD
NADH
Flavone

FIGURE 6 *Wolbachia*–mediated effects on the oxygen consumption activity of isolated yeast mitochondria. High-resolution respirometry. 1 day-old cultures of noninfected (1 Day *Sc*W303) and infected (1 Day *wSc*W303) yeast and 14 day-old cultures of noninfected (14 Days *Sc*W303) and infected (14 Days *wSc*W303) yeast. 5 mmol L^{-1} from each substrate was added as indicated: glycerol-3-phosphate (G3P), NADH, pyruvate-malate (Pyr-Mal), succinate (Succ), and ascorbate-TMPD (Asc/TMPD). Where indicated, 0.5 μmol L^{-1} CCCP, 0.1 μmol L^{-1} rotenone (Rot), 0.1 μmol L^{-1} antimycin A (Ant A), 1 mmol L^{-1} cyanide (CN-), and 0.15 mmol L^{-1} flavone. 0.5 mg prot/ml of mitochondria (M) were added. Data represent mean ± SEM. T test $^{*}p < .005$, $^{**}p < .001$ for *Sc*W303 versus *wSc*W303 yeast on the same day. *T* test $^{-/+}p < .05$ $^{--/++}p < .001$ ($^{-}$, decrease; $^{+}$, increase) for *Sc*W303 in day one versus day 14 cultures or *wSc*W303 in day one versus day 14 cultures

3.2.8 | Under the experimental conditions tested, infected *wSc*W303 oxygen consumption activity was mitochondrial

The experiments above suggested that either *Wolbachia* has the exact same electron transport chain as mitochondria or *Wolbachia* respiratory proteins may be damaged when the mitochondria/*Wolbachia* fraction is isolated and exposed to oxygen.

To explore this possibility further, we measured in-gel activities in the mitochondria/bacterium fraction. As eukaryote and prokaryote respiratory complexes I, II, III, and IV have different molecular masses the contribution from each organism to a given activity would be easily detected by native gel electrophoresis. The in-gel activities for each complex from infected and noninfected yeast from 1 and 14 day-old cultures were analyzed and, in all cases, activities were detected only at MWs corresponding to the mitochondrial enzymes (Table S3, Figure 7) suggesting that in the artificial *Sc*W303/*w*AlbB system and under the specific conditions of growth reported here, *Wolbachia* did not express any functional respiratory chain proteins. The above results suggest that mitochondria were responsible for all the observed oxygen consumption activity. Still, one NADH dehydrogenase (Table S4) was weakly expressed making it impossible to conclude on whether different *Wolbachia* strains may be aerobic or not.

3.2.9 | F_1F_0-ATPase subunits from *Wolbachia* were detected in *wSc*W303

In the in gel ATPase activity from the mitochondria/*Wolbachia* isolate no differential bands were observed. This was expected as the proposed MWs are similar for of both ATPases: 543 kDa for the eukaryote *S. cerevisiae* and 530 kDa for prokaryotes *Escherichia coli* and *Paracoccus denitrificans* (Bakhtiari, Lai-Zhang, Yao, & Mueller, 1999; Jonckheere, Smeitink, & Rodenburg, 2012; Morales-Rios, Montgomery, Leslie, & Walker, 2015; Robinson et al., 2013; Schagger, 2002). However, the ATPase activity band (Figure 7A1, Table S4) sequence exhibited a mixture of yeast and *Wolbachia* ATPase proteins. BN and hrCN-PAGE results indicate that if *Wolbachia* expresses any electron transport chain proteins (still a possibility), under our experimental conditions their concentration was negligible when compared to the mitochondrial proteins and to its own F_1F_0-ATPase.

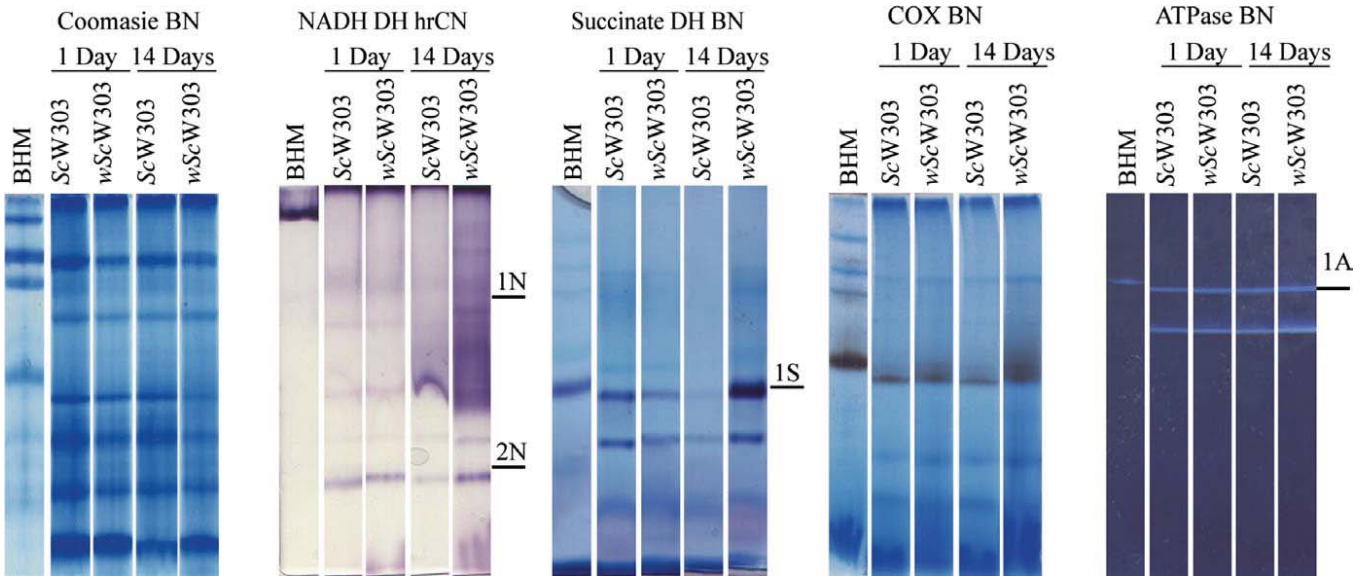

FIGURE 7 *Wolbachia*–mediated effects on the activity of each mitochondrial respiratory complex. BN-PAGE Coomassie-stained gel of *Sc*W303 and *wSc*W303 cells harvested at one and 14 days. In gel NADH-NBT oxido-reductase, succinate dehydrogenase, cytochrome *c* oxidase and ATPase enzyme activities in hrCN-PAGE or BN-PAGE, from 14 day old culture of *wSc*W303. Bands 1N, 2N, 1S, and 1A were sequenced (Table S4). Bovine heart mitochondria (BHM) were used as a control

3.2.10 | *Wolbachia* remains infective against insect cell lines

After being cultured in a yeast cell, the question arose on whether *Wolbachia* remained viable and infective when isolated. To test this, we extracted *Wolbachia* from *wSc*W303, incubated it in isolation for 5 days and then infected a C6C36 insect cell line which was previously reported to support bacterial infection (Baldridge et al., 2014). Aged *Wolbachia* infection was successful as assessed by specific staining using FISH (Figure 8 Movie S3).

4 | DISCUSSION

Growing obligate endosymbionts in cell lines yields low biomass at high costs (Baldridge et al., 2014; Khoo et al., 2013). To circumvent this problem, we built a synthetic host–endosymbiont system by artificially infecting the commonly used yeast *Saccharomyces cerevisiae* strain W303 with *Wolbachia* *w*AlbB from *A. albopictus* (Figures 1–5, Movies S1–S2). Culturing *Wolbachia* in yeast allowed us to study the complex relationship between the host and the bacterium. Using *S. cerevisiae* as an artificial host confers benefits such as a high resistance to changing environments (Gasch, 2002; Gasch & Werner-Washburne, 2002), use of inexpensive liquid cultures and most importantly, the ease of manipulating and genetically engineering the host cell. Following our approach, it may be possible to construct other synthetic parasite-mutualistic systems for obligate endosymbionts. Our system requirements for a successful infection were: supplementing YPD with iron and bovine fetal serum, plus low speed agitation of the nonbaffled Erlenmeyer flask and keeping the temperature between 28 and 30°C. These adjustments resulted in successful yeast infection and considerable *Wolbachia* yields in 14 days as compared with available methods that need up to 100 days. Even if the *Saccharomyces*/*Wolbachia* system is only a model of the interactions that occur in a naturally infected eukaryote cell, its manageability is outstanding and it may yield results that are not possible in cell lines.

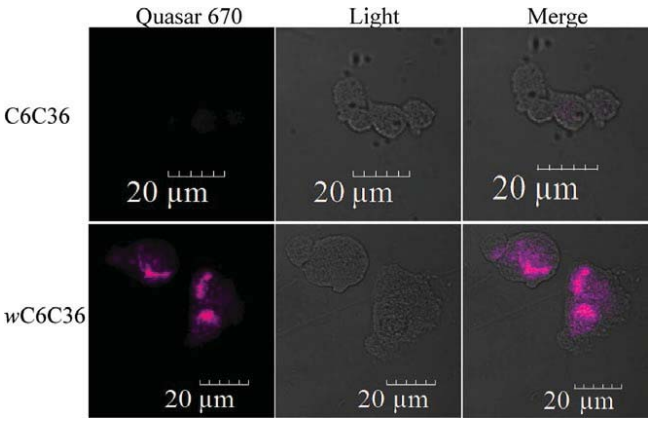

FIGURE 8 *Wolbachia* remains infective after being cultured in *S. cerevisiae*. FISH (Quasar 670-pink) of the *w*C6C36 cell line. Light/Quasar images show hybridization only inside the infected cell line. The noninfected cell line C6C36 does not have any of the pink hybridization mark identified as *Wolbachia*

Since *Wolbachia* is an alpha-proteobacterium closely related to mitochondria, it seemed likely that the aerobic metabolic machinery of *Wolbachia* might mimic, enhance, or supplement the respiratory activity from the host. (Strübing et al., 2010). However, under our conditions, *Wolbachia* respiratory chain proteins were not detectable, instead, we found an increase in host mitochondrial activity. Another obligate endosymbiont, the *Sytophilus oryzae* Principal Endosymbiont (SOPE), has also been reported to increase the mitochondrial activity in the host, probably by providing nutrients such as riboflavin (Heddi, Lefebvre, & Nardon, 1993; Heddi et al., 1999). Several authors suggest that *Wolbachia* provides riboflavin or heme groups to their arthropod and nematode hosts (Brownlie et al., 2009; Darby et al., 2012; Foster et al., 2005; Wu et al., 2009). This may vary with strains as *Wolbachia* from *Brugia malayi* (*wBm)* contains complete sets of riboflavin, heme and nucleotide biosynthesis genes the filarial host lacks (Darby et al., 2012; Foster et al., 2005; Klasson et al., 2008; Wu et al., 2004). In return, the host provides amino acid, proteins and a safe, stable environment (Brownlie et al., 2009; Darby et al., 2012; Foster et al., 2005; Wu et al., 2009). The possibility that *Wolbachia*, behaves as SOPE, donating riboflavin or heme groups to the host may be explored in auxotrophic yeast mutants. *S. cerevisiae* libraries have a mutant for almost every enzyme on the riboflavin and heme synthesis pathways e.g. *S. cerevisiae* genome database (https://www.yeastgenome.org/).

Under the conditions tested here, expression of *Wolbachia* electron transport proteins was not detected. The reported *Wolbachia pipientis* *w*AlbB genome (Mavingui et al., 2012) shows that some respiratory complex subunits are missing, e.g. *nuo*C and *nuo*D for a functional complex I (Sazanov, 2015); yet other *Wolbachia* sequenced genomes contain all the genes necessary for a functional electron transport chain (Klasson et al., 2008), so maybe under different growth conditions, hosts and *Wolbachia* strains, bacterial respiratory proteins may be detected. It is suggested that other *Wolbachia* strains should be tested in order to determine whether some consume oxygen.

In our hands, *Wolbachia* infection resulted in activation of mitochondria beyond the stationary growth phase. It may be speculated that such activation constitutes an advantage for *Wolbachia* either due to quenching of oxygen in the cytoplasm (Rosas-Lemus et al., 2016) or because *Wolbachia* needs high ATP that an active mitochondria provides (Potter, Badder, Hoade, Johnston, & Morten, 2016). It has already been suggested by experiments using paraquat that *Wolbachia* sensitivity to free radicals is higher than that of the host (Fallon et al., 2013) and it cannot survive outside a host cell unless it is kept in a 5% CO_2 atmosphere (Rasgon et al., 2006). Also, high agitation speeds, which would increase oxygen concentrations, lead to loss of the *Wolbachia* infection (Result not shown). Thus, it is possible that *Wolbachia* enters the cytoplasm to hide from high atmospheric oxygen and then it optimizes cell metabolism to both, use host metabolites and find low cytoplasmic oxygen concentrations.

Avoidance, i.e. hiding from oxygen, is a common behavior in oxyconformers (Rosas-Lemus et al., 2016). In air, oxygen saturation concentration is ~21% (200 μmol L^{-1}) while intracellular oxygen concentration ranges between 13.2% and 14% (126–133 μmol L^{-1}) for rhabdomyosarcoma (RD) cells (Potter et al., 2016) or HEK293T cells (Abcam, 2016). When cells are exposed to lower ambient oxygen, intracellular oxygen concentration is also decreased: HEK293T cells exposed to 6% oxygen (50 μmol L^{-1}) have an intracellular oxygen concentration below 2% (19 μmol L^{-1}) (Abcam, 2016); RD cells exposed to 10% or 5% ambient oxygen reduce their intracellular oxygen concentration to 5.4% and 2.1% respectively (Potter et al., 2016). In addition, there is an intracellular oxygen gradient in the area surrounding the mitochondria in rat heart and hepatocytes, where oxygen concentration ranges between 3 (Gnaiger, 2003) and 6 μmol L^{-1} (Jones & Kennedy, 1982; Tamura, Oshino, Chance, & Silver, 1978). Thus, a mitochondrion-containing host such as cell lines and yeast would probably provide the endosymbiont with a microaerobic environment. The mechanism for the increase in host mitochondrial activity needs to be defined.

In conclusion, we describe the infection of *S. cerevisiae* strain W303 by *Wolbachia w*AlbB. Infection led to premature death of the host and to an abnormal pattern of oxygen consumption. Further experiments using other yeast and other *Wolbachia* strains are needed to further explore oxidative phosphorylation patterns in the host/endosymbiont relationship. This system holds a large potential for different evaluations of biochemical and genetical processes in *Wolbachia*. Large biofermentors may be used to yield large amounts of biomass as required for different genomics and proteomics studies.

ACKNOWLEDGMENTS

Aa23 cell line was kindly donated by Dr. Ann Fallon from the University of Minnesota. The wsp antibody was a kind gift from Bei resources. CUA is a CONACYT PhD fellow enrolled in the Biochemistry PhD Program at UNAM. LMG is a CONACYT PhD fellow enrolled in the Biomedical Sciences PhD Program at UNAM. We received technical help from the Molecular Biology, the Microscopy and the Computation Units at IFC, UNAM. MALDI-TOF sequencing was performed by E. Ríos Castro from the Unidad de Genómica, Proteómica y Metabolómica, CINVESTAV-IPN, R Méndez-Franco, M. Contreras-Zentella, N.S. Sánchez and M. Calahorra are recognized for their technical assistance. M. Rigoulet, A. Devin (U-Bordeaux), D. González-Halphen, and G. Dreyfus-Cortés (IFC, UNAM) critically read the manuscript.

CONFLICT OF INTEREST

None declared.

REFERENCES

Abcam. (2016). ab197245 intracellular oxygen concentration assay. Retrieved from http://www.abcam.com/ps/products/197/ab197245/documents/ab197245%20Intracellular%20Oxygen%20Concentration%20Assay%20protocol%20v4%20(website).pdf.

Aguilar-Uscnaga, B., & Francois, J. M. (2003). A study of the cell wall composition and structure in response to growth conditions and mode of cultivation. *Letters in Applied Microbiology*, *37*(3), 268–274. https://doi.org/10.1046/j.1472-765X.2003.01394.x

Alves-Rodrigues, I., Galão, R. P., Meyerhans, A., & Díez, J. (2006). *Saccharomyces cerevisiae*: A useful model host to study fundamental biology of viral replication. *Virus Research*, *120*(1–2), 49–56. https://doi.org/10.1016/j.virusres.2005.11.018

Amuzu, H. E., Simmons, C. P., & McGraw, E. A. (2015). Effect of repeat human blood feeding on *Wolbachia* density and dengue virus infection in *Aedes aegypti*. *Parasit Vectors*, *8*, 246. https://doi.org/10.1186/s13071-015-0853-y

Avrahami-Moyal, L., Braun, S., & Engelberg, D. (2012). Overexpression of PDE2 or SSD1-V in *Saccharomyces cerevisiae* W303-1A strain renders it ethanol-tolerant. *FEMS Yeast Research*, *12*(4), 447–455. https://doi.org/10.1111/j.1567-1364.2012.00795.x

Bakhtiari, N., Lai-Zhang, J., Yao, B., & Mueller, D. M. (1999). Structure/function of the beta-barrel domain of F1-ATPase in the yeast *Saccharomyces cerevisiae*. *Journal of Biological Chemistry*, *274*(23), 16363–16369. https://doi.org/10.1074/jbc.274.23.16363

Baldridge, G. D., Baldridge, A. S., Witthuhn, B. A., Higgins, L., Markowski, T. W., & Fallon, A. M. (2014). Proteomic profiling of a robust *Wolbachia* infection in an *Aedes albopictus* mosquito cell line. *Molecular Microbiology*, *94*(3), 537–556. https://doi.org/10.1111/mmi.12768

Bandi, C., Slatko, B., & O'Neill, S. L. (1999). *Wolbachia* genomes and the many faces of symbiosis. *Parasitol Today*, *15*(11), 428–429. https://doi.org/10.1016/S0169-4758(99)01543-4

Bertaux, J., Schmid, M., Prevost-Boure, N. C., Churin, J. L., Hartmann, A., Garbaye, J., & Frey-Klett, P. (2003). In situ identification of intracellular bacteria related to *Paenibacillus* spp. in the mycelium of the ectomycorrhizal fungus *Laccaria* bicolor S238N. *Applied and Environment Microbiology*, *69*(7), 4243–4248. https://doi.org/10.1128/AEM.69.7.4243-4248.2003

Bianciotto, V., Genre, A., Jargeat, P., Lumini, E., Becard, G., & Bonfante, P. (2004). Vertical transmission of endobacteria in the arbuscular mycorrhizal fungus Gigaspora margarita through generation of vegetative spores. *Applied and Environment Microbiology*, *70*(6), 3600–3608. https://doi.org/10.1128/AEM.70.6.3600-3608.2004

de Boer, W., Leveau, J. H., Kowalchuk, G. A., Gunnewiek, P. J. K., Abeln, E. C., Figge, M. J., … van Veen, J. A. (2004). *Collimonas fungivorans* gen. nov., sp. nov., a chitinolytic soil bacterium with the ability to grow on living fungal hyphae. *International Journal of Systematic and Evolutionary Microbiology*, *54*(Pt 3), 857–864. https://doi.org/10.1099/ijs.0.02920-0

Bradford, M. M. (1976). A rapid and sensitive method for the quantification of microgram quantities of protein utilizing the principle of protein-dye binding. *Veterinary Parasitology*, *98*(1–3), 215–238.

Braig, H. R., Zhou, W., Dobson, S. L., & O'Neill, S. L. (1998). Cloning and characterization of a gene encoding the major surface protein of the bacterial endosymbiont *Wolbachia pipientis*. *Journal of Bacteriology*, *180*(9), 2373–2378.

Brenner, K., You, L., & Arnold, F. H. (2008). Engineering microbial consortia: A new frontier in synthetic biology. *Trends in Biotechnology*, *26*(9), 483–489. https://doi.org/10.1016/j.tibtech.2008.05.004

Brownlie, J. C., Cass, B. N., Riegler, M., Witsenburg, J. J., Iturbe-Ormaetxe, I., McGraw, E. A., & O'Neill, S. L. (2009). Evidence for metabolic provisioning by a common invertebrate endosymbiont, *Wolbachia pipientis*, during periods of nutritional stress. *PLoS Pathogens*, *5*(4), e1000368.

Buchsbaum, R., & Buchsbaum, M. (1934). An artificial symbiosis. *Science*, *80*(2079), 408–409.

Chiquete-Felix, N., Hernández, J. M., Méndez, J. A., Zepeda-Bastida, A., Chagolla-López, A., & Mujica, A. (2009). In guinea pig sperm, aldolase

A forms a complex with actin, WAS, and Arp2/3 that plays a role in actin polymerization. *Reproduction*, *137*(4), 669–678. https://doi.org/10.1530/REP-08-0353

Crowe, L. M., Reid, D. S., & Crowe, J. H. (1996). Is trehalose special for preserving dry biomaterials? *Biophysical Journal*, *71*(4), 2087–2093. https://doi.org/10.1016/S0006-3495(96)79407-9

Dale, C., & Maudlin, I. (1999). Sodalis gen. nov. and *Sodalis glossinidius* sp. nov., a microaerophilic secondary endosymbiont of the tsetse fly Glossina morsitans morsitans. *International Journal of Systematic Bacteriology*, *49* (Pt 1), 267–275. https://doi.org/10.1099/00207713-49-1-267

Darby, A. C., Armstrong, S. D., Bah, G. S., Kaur, G., Hughes, M. A., Kay, S. M., … Tanya, V. N. (2012). Analysis of gene expression from the *Wolbachia* genome of a filarial nematode supports both metabolic and defensive roles within the symbiosis. *Genome Research*, *22*(12), 2467–2477. https://doi.org/10.1101/gr.138420.112

Darby, A. C., Gill, A. C., Armstrong, S. D., Hartley, C. S., Xia, D., Wastling, J. M., & Makepeace, B. L. (2014). Integrated transcriptomic and proteomic analysis of the global response of *Wolbachia* to doxycycline-induced stress. *ISME Journal*, *8*(4), 925–937. https://doi.org/10.1038/ismej.2013.192

Diaz-Ruiz, R., Rigoulet, M., & Devin, A. (2011). The Warburg and Crabtree effects: On the origin of cancer cell energy metabolism and of yeast glucose repression. *Biochimica et Biophysica Acta*, *1807*(6), 568–576. https://doi.org/10.1016/j.bbabio.2010.08.010

Dobson, S. L., Marsland, E. J., Veneti, Z., Bourtzis, K., & O'Neill, S. L. (2002). Characterization of *Wolbachia* host cell range via the in vitro establishment of infections. *Applied and Environment Microbiology*, *68*(2), 656–660. https://doi.org/10.1128/AEM.68.2.656-660.2002

Fallon, A. M., Baldridge, G. D., Carroll, E. M., & Kurtz, C. M. (2014). Depletion of host cell riboflavin reduces *Wolbachia* levels in cultured mosquito cells. *In Vitro Cellular & Developmental Biology – Animal*, *50*(8), 707–713. https://doi.org/10.1007/s11626-014-9758-x

Fallon, A. M., Kurtz, C. M., & Carroll, E. M. (2013). The oxidizing agent, paraquat, is more toxic to *Wolbachia* than to mosquito host cells. *In Vitro Cellular & Developmental Biology – Animal*, *49*(7), 501–507. https://doi.org/10.1007/s11626-013-9634-0

Foster, J., Ganatra, M., Kamal, I., Ware, J., Makarova, K., Ivanova, N., … Vincze, T. (2005). The *Wolbachia* genome of *Brugia malayi*: Endosymbiont evolution within a human pathogenic nematode. *PLoS Biology*, *3*(4), e121. https://doi.org/10.1371/journal.pbio.0030121

French, K. E. (2017). Engineering mycorrhizal symbioses to alter plant metabolism and improve crop health. *Frontiers in Microbiology*, *8*, 1403. https://doi.org/10.3389/fmicb.2017.01403

Frey-Klett, P., Burlinson, P., Deveau, A., Barret, M., Tarkka, M., & Sarniguet, A. (2011). Bacterial-fungal interactions: Hyphens between agricultural, clinical, environmental, and food microbiologists. *Microbiology and Molecular Biology Reviews*, *75*(4), 583–609. https://doi.org/10.1128/MMBR.00020-11

Gasch, A. P. (2002). Yeast genomic expression studies using DNA microarrays. *Methods in Enzymology*, *350*, 393–414. https://doi.org/10.1016/S0076-6879(02)50976-9

Gasch, A. P., & Werner-Washburne, M. (2002). The genomics of yeast responses to environmental stress and starvation. *Functional & Integrative Genomics*, *2*(4–5), 181–192. https://doi.org/10.1007/s10142-002-0058-2

Genty, L. M., Bouchon, D., Raimond, M., & Bertaux, J. (2014). *Wolbachia* infect ovaries in the course of their maturation: Last minute passengers and priority travellers? *PLoS ONE*, *9*(4), e94577. https://doi.org/10.1371/journal.pone.0094577

Gnaiger, E. (2003). Oxygen conformance of cellular respiration. In R. C. Roach, P. D. Wagner, & P. H. Hackett (Eds.), *Hypoxia: Through the lifecycle* (pp. 39–55). Boston, MA: Springer. https://doi.org/10.1007/978-1-4419-8997-0

Gornal, A. G. (1957). Spectrophotometric and turbidimetric methods for mesuring proteins III: Biuret method. *Methods in Enzymology*, *3*, 447–454.

Guerrero-Castillo, S., Araiza-Olivera, D., Cabrera-Orefice, A., Espinasa-Jaramillo, J., Gutiérrez-Aguilar, M., Luévano-Martínez, L. A., … Uribe-Carvajal, S. (2011). Physiological uncoupling of mitochondrial oxidative phosphorylation. Studies in different yeast species. *Journal of Bioenergetics and Biomembranes*, *43*(3), 323–331. https://doi.org/10.1007/s10863-011-9356-5

Gutierrez-Aguilar, M., López-Carbajal, H. M., Uribe-Alvarez, C., Espinoza-Simón, E., Rosas-Lemus, M., Chiquete-Félix, N., & Uribe-Carvajal, S. (2014). Effects of ubiquinone derivatives on the mitochondrial unselective channel of Saccharomyces cerevisiae. *Journal of Bioenergetics and Biomembranes*, *46*(6), 519–527. https://doi.org/10.1007/s10863-014-9595-3

Heddi, A., Grenier, A. M., Khatchadourian, C., Charles, H., & Nardon, P. (1999). Four intracellular genomes direct weevil biology: Nuclear, mitochondrial, principal endosymbiont, and *Wolbachia*. *Proceedings of the National Academy of Sciences of the United States of America*, *96*(12), 6814–6819. https://doi.org/10.1073/pnas.96.12.6814

Heddi, A., Lefebvre, F., & Nardon, P. (1993). Effect of endocytobiotic bacteria on mitochondrial enzymatic activities in the weevil *Sitophilus oryzae* (Coleoptera: Curculionidae). *Insect Biochemistry and Molecular Biology*, *23*(3), 8.

Hoffman, M. T., & Arnold, A. E. (2010). Diverse bacteria inhabit living hyphae of phylogenetically diverse fungal endophytes. *Applied and Environment Microbiology*, *76*(12), 4063–4075. https://doi.org/10.1128/AEM.02928-09

Hosoda, K., Suzuki, S., Yamauchi, Y., Shiroguchi, Y., Kashiwagi, A., Ono, N., … Yomo, T. (2011). Cooperative adaptation to establishment of a synthetic bacterial mutualism. *PLoS ONE*, *6*(2), e17105. https://doi.org/10.1371/journal.pone.0017105

Hosoda, K., & Yomo, T. (2011). Designing symbiosis. *Bioengineered Bugs*, *2*(6), 338–341. https://doi.org/10.4161/bbug.2.6.16801

Jonckheere, A. I., Smeitink, J. A., & Rodenburg, R. J. (2012). Mitochondrial ATP synthase: Architecture, function and pathology. *Journal of Inherited Metabolic Disease*, *35*(2), 211–225. https://doi.org/10.1007/s10545-011-9382-9

Jones, D. P., & Kennedy, F. G. (1982). Intracellular oxygen supply during hypoxia. *American Journal of Physiology*, *243*(5), C247–C253. https://doi.org/10.1152/ajpcell.1982.243.5.C247

Kang, S. W., Jeon, B. Y., Hwang, T. S., & Park, D. H. (2009). Symbiotic relationship between *Microbacterium* sp. SK0812 and *Candida tropicalis* SK090404. *The Journal of Microbiology*, *47*(6), 721–727. https://doi.org/10.1007/s12275-009-0146-2

Khoo, C. C. H., Venard, C. M. P., Fu, Y., Mercer, D. R., & Dobson, S. L. (2013). Infection, growth and maintenance of *Wolbachia pipientis* in clonal and non-clonal *Aedes albopictus* cell cultures. *Bulletin of Entomological Research*, *103*(3), 251–260. https://doi.org/10.1017/S0007485312000648

Klasson, L., Walker, T., Sebaihia, M., Sanders, M. J., Quail, M. A., Lord, A., … Sinkins, S. P. (2008). Genome evolution of *Wolbachia* strain wPip from the *Culex pipiens* group. *Molecular Biology and Evolution*, *25*(9), 1877–1887. https://doi.org/10.1093/molbev/msn133

Kubo, I., Hosoda, K., Suzuki, S., Yamamoto, K., Kihara, K., Mori, K., & Yomo, T. (2013). Construction of bacteria-eukaryote synthetic mutualism. *Biosystems*, *113*(2), 66–71. https://doi.org/10.1016/j.biosystems.2013.05.006

Leslie, S. B., Israeli, E., Lighthart, B., Crowe, J. H., & Crowe, L. M. (1995). Trehalose and sucrose protect both membranes and proteins in intact bacteria during drying. *Applied and Environment Microbiology*, *61*(10), 3592–3597.

Lőrincz, Z., Preininger, É., Kósa, A., Pónyi, T., Nyitrai, P., Sarkadi, L., … Gyurján, I. (2010). Artificial tripartite symbiosis involving a green alga (*Chlamydomonas*), a bacterium (*Azotobacter*) and a fungus

(*Alternaria*): Morphological and physiological characterization. *Folia Microbiologica (Praha)*, *55*(4), 393–400. https://doi.org/10.1007/s12223-010-0067-9

Lumini, E., Ghignone, S., Bianciotto, V., & Bonfante, P. (2006). Endobacteria or bacterial endosymbionts? To be or not to be. *New Phytologist*, *170*(2), 205–208. https://doi.org/10.1111/j.1469-8137.2006.01673.x

Mavingui, P., Moro, C. V., Tran-Van, V., Wisniewski-Dyé, F., Raquin, V., Minard, G., … Lozano, L. (2012). Whole-genome sequence of *Wolbachia* strain wAlbB, an endosymbiont of tiger mosquito vector *Aedes albopictus*. *Journal of Bacteriology*, *194*(7), 1840. https://doi.org/10.1128/JB.00036-12

McMeniman, C. J., Hughes, G. L., & O'Neill, S. L. (2011). A *Wolbachia* symbiont in *Aedes aegypti* disrupts mosquito egg development to a greater extent when mosquitoes feed on nonhuman versus human blood. *Journal of Medical Entomology*, *48*(1), 76–84. https://doi.org/10.1603/ME09188

Mee, M. T., & Wang, H. H. (2012). Engineering ecosystems and synthetic ecologies. *Molecular BioSystems*, *8*(10), 2470–2483. https://doi.org/10.1039/c2mb25133g

Momeni, B., Chen, C. C., Hillesland, K. L., Waite, A., & Shou, W. (2011). Using artificial systems to explore the ecology and evolution of symbioses. *Cellular and Molecular Life Sciences*, *68*(8), 1353–1368. https://doi.org/10.1007/s00018-011-0649-y

Morales-Rios, E., Montgomery, M. G., Leslie, A. G., & Walker, J. E. (2015). Structure of ATP synthase from *Paracoccus denitrificans* determined by X-ray crystallography at 4.0 A resolution. *Proceedings of the National Academy of Sciences of the United States of America*, *112*(43), 13231–13236. https://doi.org/10.1073/pnas.1517542112

Ocampo, A., Liu, J., Schroeder, E. A., Shadel, G. S., & Barrientos, A. (2012). Mitochondrial respiratory thresholds regulate yeast chronological life span and its extension by caloric restriction. *Cell Metabolism*, *16*(1), 55–67. https://doi.org/10.1016/j.cmet.2012.05.013

Omsland, A., Cockrell, D. C., Howe, D., Fischer, E. R., Virtaneva, K., Sturdevant, D. E., … Heinzen, R. A. (2009). Host cell-free growth of the Q fever bacterium *Coxiella burnetii*. *Proceedings of the National Academy of Sciences of the United States of America*, *106*(11), 4430–4434. https://doi.org/10.1073/pnas.0812074106

Omsland, A., Cockrell, D. C., Howe, D., Fischer, E. R., Virtaneva, K., Sturdevant, D. E., … Heinzen, R. A. (2013). Bringing culture to the uncultured: *Coxiella burnetii* and lessons for obligate intracellular bacterial pathogens. *PLoS Pathogens*, *9*(9), e1003540. https://doi.org/10.1371/journal.ppat.1003540

O'Neill, S. L., M Pettigrew, M., Sinkins, S. P., Braig, H. R., Andreadis, T. G., & Tesh, R. B. (1997). In vitro cultivation of *Wolbachia pipientis* in an *Aedes albopictus* cell line. *Insect Molecular Biology*, *6*(1), 33–39. https://doi.org/10.1046/j.1365-2583.1997.00157.x

Partida-Martinez, L. P., & Hertweck, C. (2005). Pathogenic fungus harbours endosymbiotic bacteria for toxin production. *Nature*, *437*(7060), 884–888. https://doi.org/10.1038/nature03997

Peña, A., Piña, M. Z., Escamilla, E., & Piña, E. (1977). A novel method for the rapid preparation of coupled yeast mitochondria. *FEBS Letters*, *80*(1), 209–213.

Potter, M., Badder, L., Hoade, Y., Johnston, I. G., & Morten, K. J. (2016). Monitoring intracellular oxygen concentration: Implications for hypoxia studies and real-time oxygen monitoring. *Advances in Experimental Medicine and Biology*, *876*, 257–263. https://doi.org/10.1007/978-1-4939-3023-4

Rasgon, J. L., Gamston, C. E., & Ren, X. (2006). Survival of *Wolbachia pipientis* in cell-free medium. *Applied and Environment Microbiology*, *72*(11), 6934–6937. https://doi.org/10.1128/AEM.01673-06

Robinson, G. C., Bason, J. V., Montgomery, M. G., Fearnley, I. M., Mueller, D. M., Leslie, A. G., & Walker, J. E. (2013). The structure of F(1)-ATPase from *Saccharomyces cerevisiae* inhibited by its regulatory protein IF(1). *Open Biology*, *3*(2), 120164. https://doi.org/10.1098/rsob.120164

Rosas-Lemus, M., Uribe-Alvarez, C., Contreras-Zentella, M., Luévano-Martínez, L.A., Chiquete-Félix, N., Espinosa-Simón, E., … Uribe-Carvajal, S. (2016). Oxygen: from toxic waste to optimal (Toxic) fuel of life. In Free Radicals and Diseases. InTech.

Salzberg, S. L., Puiu, D., Sommer, D. D., Nene, V., & Lee, N. H. (2009). Genome sequence of the *Wolbachia* endosymbiont of *Culex quinquefasciatus* JHB. *Journal of Bacteriology*, *191*(5), 1725. https://doi.org/10.1128/JB.01731-08

Sampedro, J. G., & Uribe, S. (2004). Trehalose-enzyme interactions result in structure stabilization and activity inhibition. The role of viscosity. *Molecular and Cellular Biochemistry*, *256–257*(1–2), 319–327. https://doi.org/10.1023/B:MCBI.0000009878.21929.eb

Saniee, P., & Siavoshi, F. (2015). Endocytotic uptake of FITC-labeled anti-*H. pylori* egg yolk immunoglobulin Y in Candida yeast for detection of intracellular *H. pylori*. *Frontiers in Microbiology*, *6*, 113.

Sato, Y., Narisawa, K., Tsuruta, K., Umezu, M., Nishizawa, T., Tanaka, K., … Ohta, H. (2010). Detection of betaproteobacteria inside the mycelium of the fungus Mortierella elongata. *Microbes and Environments*, *25*(4), 321–324. https://doi.org/10.1264/jsme2.ME10134

Sazanov, L. A. (2015). A giant molecular proton pump: Structure and mechanism of respiratory complex I. *Nature Reviews Molecular Cell Biology*, *16*(6), 375–388. https://doi.org/10.1038/nrm3997

Schagger, H. (2002). Respiratory chain supercomplexes of mitochondria and bacteria. *Biochimica et Biophysica Acta*, *1555*(1–3), 154–159. https://doi.org/10.1016/S0005-2728(02)00271-2

Shevchenko, A., Tomas, H., Havli, J., Olsen, J. V., & Mann, M. (2006). In-gel digestion for mass spectrometric characterization of proteins and proteomes. *Nature Protocols*, *1*(6), 2856–2860.

Shih, K. M., Gerenday, A., & Fallon, A. M. (1998). Culture of mosquito cells in Eagle's medium. *In Vitro Cellular & Developmental Biology – Animal*, *34*(8), 629–630. https://doi.org/10.1007/s11626-996-0010-1

Shou, W., Ram, S., & Vilar, J. M. (2007). Synthetic cooperation in engineered yeast populations. *Proceedings of the National Academy of Sciences of the United States of America*, *104*(6), 1877–1882. https://doi.org/10.1073/pnas.0610575104

Siggers, K. A., & Lesser, C. F. (2008). The yeast *Saccharomyces cerevisiae*: A versatile model system for the identification and characterization of bacterial virulence proteins. *Cell Host & Microbe*, *4*(1), 8–15. https://doi.org/10.1016/j.chom.2008.06.004

Smith, A. E., Zhang, Z., Thomas, C. R., Moxham, K. E., & Middelberg, A. P. (2000). The mechanical properties of Saccharomyces cerevisiae. *Proceedings of the National Academy of Sciences of the United States of America*, *97*(18), 9871–9874.

Stella, C., Burgos, I., Chapela, S., & Gamondi, O. (2011). Ischemia–reperfusion: A look from yeast mitochondria. *Current Medicinal Chemistry*, *18*(23), 3476–3484. https://doi.org/10.2174/092986711796642553

Stewart, E. J. (2012). Growing unculturable bacteria. *Journal of Bacteriology*, *194*(16), 4151–4160. https://doi.org/10.1128/JB.00345-12

Strübing, U., Lucius, R., Hoerauf, A., & Pfarr, K. M. (2010). Mitochondrial genes for heme-dependent respiratory chain complexes are up-regulated after depletion of *Wolbachia* from filarial nematodes. *International Journal for Parasitology*, *40*(10), 1193–1202. https://doi.org/10.1016/j.ijpara.2010.03.004

Sun, X. Y., Zhao, Y., Liu, L. L., Jia, B., Zhao, F., Huang, W. D., & Zhan, J. C. (2015). Copper tolerance and biosorption of *Saccharomyces cerevisiae* during alcoholic fermentation. *PLoS ONE*, *10*(6), e0128611. https://doi.org/10.1371/journal.pone.0128611

Tamura, M., Oshino, N., Chance, B., & Silver, I. A. (1978). Optical measurements of intracellular oxygen concentration of rat heart in vitro. *Archives of Biochemistry and Biophysics*, *191*(1), 8–22. https://doi.org/10.1016/0003-9861(78)90062-0

Taylor, M. J., & Hoerauf, A. (1999). *Wolbachia* bacteria of filarial nematodes. *Parasitology Today*, *15*(11), 437–442. https://doi.org/10.1016/S0169-4758(99)01533-1

Uribe, S. A., Ramirez, J. O., & Peña, A. N. (1985). Effects of beta-pinene on yeast membrane functions. *Journal of Bacteriology*, *161*(3), 1195–1200.

Uribe, S., Rangel, P. A., Espínola, G. L., & Aguirre, G. A. (1990). Effects of cyclohexane, an industrial solvent, on the yeast *Saccharomyces cerevisiae* and on isolated yeast mitochondria. *Applied and Environment Microbiology*, *56*(7), 2114–2119.

Uribe-Alvarez, C., Chiquete-Félix, N., Contreras-Zentella, M., Guerrero-Castillo, S., Peña, A., & Uribe-Carvajal, S. (2016). *Staphylococcus epidermidis*: Metabolic adaptation and biofilm formation in response to different oxygen concentrations. *Pathogens and Disease*, *74*(1), ftv111. https://doi.org/10.1093/femspd/ftv111

Werren, J. H. (1997). Biology of *Wolbachia*. *Annual Review of Entomology*, *42*, 587–609. https://doi.org/10.1146/annurev.ento.42.1.587

Werren, J. H., Baldo, L., & Clark, M. E. (2008). *Wolbachia*: Master manipulators of invertebrate biology. *Nature Reviews Microbiology*, *6*(10), 741–751. https://doi.org/10.1038/nrmicro1969

Winkler, H. H., & Turco, J. (1988). Rickettsia prowazekii and the host cell: entry, growth and control of the parasite. *Current Topics in Microbiology and Immunology*, *138*, 81–107.

Wittig, I., Braun, H. P., & Schägger, H. (2006). Blue native PAGE. *Nature Protocols*, *1*(1), 418–428. https://doi.org/10.1038/nprot.2006.62

Wittig, I., Karas, M., & Schägger, H. (2007). High resolution clear native electrophoresis for in-gel funtional assays and fluorescence studies of membrane protein complexes. *Molecular & Cellular Proteomics: MCP*, *6*(7), 1215–1225. https://doi.org/10.1074/mcp.M700076-MCP200

Wu, B., Novelli, J., Foster, J., Vaisvila, R., Conway, L., Ingram, J., … Slatko, B. (2009). The heme biosynthetic pathway of the obligate *Wolbachia* endosymbiont of *Brugia malayi* as a potential anti-filarial drug target. *PLoS Neglected Tropical Diseases*, *3*(7), e475. https://doi.org/10.1371/journal.pntd.0000475

Wu, M., Sun, L. V., Vamathevan, J., Riegler, M., Deboy, R., Brownlie, J. C., … Wiegand, C. (2004). Phylogenomics of the reproductive parasite *Wolbachia pipientis* wMel: A streamlined genome overrun by mobile genetic elements. *PLoS Biology*, *2*(3), E69. https://doi.org/10.1371/journal.pbio.0020069

Xi, Z., Khoo, C. C., & Dobson, S. L. (2006). Interspecific transfer of *Wolbachia* into the mosquito disease vector *Aedes albopictus*. *Proceedings. Biological sciences Royal Society*, *273*(1592), 1317–1322. https://doi.org/10.1098/rspb.2005.3405

SUPPORTING INFORMATION

Additional supporting information may be found online in the Supporting Information section at the end of the article.

How to cite this article: Uribe-Alvarez C, Chiquete-Félix N, Morales-García L, et al. *Wolbachia pipientis* grows in *Saccharomyces cerevisiae* evoking early death of the host and deregulation of mitochondrial metabolism. *MicrobiologyOpen*. 2018;e675. https://doi.org/10.1002/mbo3.675

molecules

MDPI

Article

Response of *Ustilago maydis* against the Stress Caused by Three Polycationic Chitin Derivatives

Dario Rafael Olicón-Hernández [1], Cristina Uribe-Alvarez [2], Salvador Uribe-Carvajal [2], Juan Pablo Pardo [3] and Guadalupe Guerra-Sánchez [1,*]

1 Instituto Politécnico Nacional, Escuela Nacional de Ciencias Biológicas, Departamento de Microbiología, Prolongación de Carpio y Plan de Ayala S/N, Col. Sto. Tomas, Del, Miguel Hidalgo, CP 11340 Ciudad de México, Mexico; magnadroh@hotmail.com

2 Universidad Nacional Autónoma de México, Instituto de Fisiología Celular, Circuito exterior S/N, Ciudad Universitaria, CP 04510 Ciudad de México, Mexico; curibe@email.ifc.unam.mx (C.U.-A.); suribe@ifc.unam.mx (S.U.-C.)

3 Universidad Nacional Autónoma de México, Facultad de Medicina, Departamento de Bioquímica, Circuito exterior S/N, Ciudad Universitaria, CP 04510 Ciudad de México, Mexico; pardov@bq.unam.mx

* Correspondence: lupegs@hotmail.com; Tel.: +52-55-5729-6000 (ext. 62339)

Received: 10 August 2017; Accepted: 13 October 2017; Published: 7 December 2017

Abstract: Chitosan is a stressing molecule that affects the cells walls and plasma membrane of fungi. For chitosan derivatives, the action mode is not clear. In this work, we used the yeast *Ustilago maydis* to study the effects of these molecules on the plasma membrane, focusing on physiologic and stress responses to chitosan (CH), oligochitosan (OCH), and glycol-chitosan (GCH). Yeasts were cultured with each of these molecules at 1 mg·mL^{-1} in minimal medium. To compare plasma membrane damage, cells were cultivated in isosmolar medium. Membrane potential ($\Delta\psi$) as well as oxidative stress were measured. Changes in the total plasma membrane phospholipid and protein profiles were analyzed using standard methods, and fluorescence-stained mitochondria were observed. High osmolarity did not protect against CH inhibition and neither affected membrane potential. The OCH did produce higher oxidative stress. The effects of these molecules were evidenced by modifications in the plasma membrane protein profile. Also, mitochondrial damage was evident for CH and OCH, while GCH resulted in thicker cells with fewer mitochondria and higher glycogen accumulation.

Keywords: chitosan; oligochitosan; glycol-chitosan; *Ustilago maydis*; stress response

1. Introduction

Ecological niches for fungi are numerous and varied. In nature, fungi can be found as saprophytic agents, as pathogenic or phytopathogenic parasites, as communities (mycorrhiza), or as symbionts [1]. Thus, fungi are exposed to different environmental stress conditions such as variations in pH, temperature, osmolarity, toxins, and natural or synthetic compounds that could damage their structure or disrupt their metabolism and yet, they survive [2]. Stress in fungi may be an external biotic or abiotic condition that interferes with optimal growth parameters and generates physiological responses [3]. These defense responses may involve overexpression of genes related to carbohydrate metabolism [4], the production of structural proteins [5], modifications in cell wall or membrane composition [6,7], changes in cell integrity [4], and the production of reactive oxygen species (ROS) [8]. One of the advantages of studying stress responses in fungi is that they are excellent models of eukaryotic responses against external or internal factors which could also be observed in plants and animals; indeed, very conserved defense mechanisms exist [9].

Chitosan (CH) elicits a strong stress response in fungi. It is a polycationic semi-natural carbohydrate with an average molecular weight of 50 kDa, constituted by the aminated sugars glucosamine (<90%) and *N*-acetyl glucosamine (>10%) [10]. The main source of chitosan is their extraction from chitin from insects and crustaceans; however, it also is an important constituent of green algae, yeasts, protozoa, as well as the cell walls of some fungi and used in the fabrication of environmentally friendly antimicrobial agents [11]. In this context, it was reported that CH and its derivatives are able to inhibit bacteria, fungi, and viruses that can generate diseases from the clinical and environmental point of view, mainly by boosting the immune systems of humans, animals, and plants, interfering with the normal metabolism of the pathogens, destroying cellular structures [12–14]. In acidic pH, the CH amino groups are protonated and thus, CH is polycationic. It is used to produce different antimicrobial agents [15], such as oligochitosan (OCH) and glycol-chitosan (GCH), also polycationic in nature, which are applied in different industries and research activities. The OCH (MW around 5 kDa) is smaller than chitosan [16], while GCH is produced by etherification of chitosan and ethylene glycol and is used in bio-gel fabrication [12]. In contrast to CH, which is soluble only at an acid pH, both OCH and GCH are soluble at pH 7.0. The polycationic nature of these compounds allows strong interactions with different fungal structures such as the cell wall, membrane lipids, proteins, and nucleic acids, probably triggering a stress response [17]. In eukaryotic cells, chitosan and its derivatives promote morphological mechanical alterations [15], increased ROS concentration [18,19], mitochondrial dysfunction [20], decreased metabolic processes [21], decreased septation, increased spore mitoses [22], and overexpression of genes related to oxidative stress [23]. Fungi react to these polycations through proteins involved in plasma membranes, respiration, ATP production, and mitochondrial organization. In *Neurospora crassa,* the generation of reactive oxygen species, cellular energy, and cellular membrane homeostasis was affected by chitosan [21].

Ustilago maydis is a basidiomycete and an ustilaginal fungus used as a model species in several biochemical and physiological studies. Due to its accessible genome, easy handling, ability to grow in defined media by budding and formation of compact colonies on plates, *U. maydis* is considered an ideal fungal model for cell and molecular biology studies [24]. We have previously described the effects of CH, OCH, and GCH on the development and morphology of *Ustilago maydis* [15]. Here, we characterize the response of *U. maydis* to each of these polycationic compounds and conclude that each chitosan derivative triggers a specific stress-like response in *U. maydis*.

2. Results

2.1. Growth of U. maydis at Different Osmolarities: Effects of CH, OCH, and GCH

In hypo-osmotic medium, CH inhibits the growth of *U. maydis*, while OCH and GCH have no effects [15]. Here, when culturing the cells in an isosmotic medium, the same inhibition pattern was observed (Figure 1), i.e., OCH and GCH did not exhibit any effect, while CH fully inhibited *U. maydis* growth.

2.2. Cell Membrane Permeability Changes in U. maydis upon Addition of CH, OCH or GCH

Since osmotic support to *U. maydis* did not prevent the chitosan effect, it was decided to determine whether the plasmatic membrane was intact. For this, the transmembrane electrical potential ($\Delta\psi$) in the cell was estimated using a cyanine derivative [25]; 2 $\mu g \cdot mL^{-1}$ of chitosan decreased $\Delta\psi$ by more than 50%. Higher concentrations further decreased $\Delta\psi$ (Figure 2I). The presence of different polycation compounds (OCH) and (GCH) did not produce changes in this physiological parameter (Figure 2II,III).

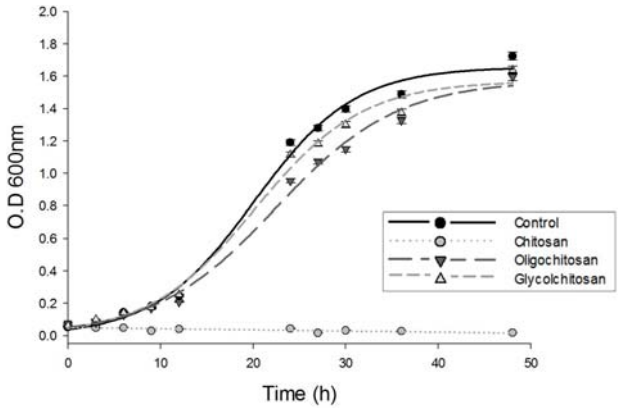

Figure 1. Growth of *Ustilago maydis* in minimal medium and in the presence of chitosan, oligochitosan or glycol-chitosan. Each agent was added to a final concentration of 1 mg·mL^{-1}. Growth was measured as an increase in optical density at 600 nm.

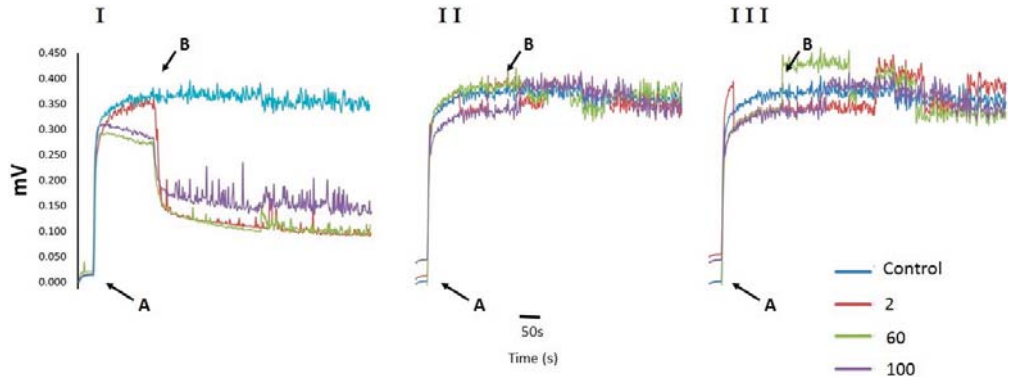

Figure 2. Changes in Δψ in response to different concentrations of CH, OCH or CGH. All concentrations are expressed in μg·mL^{-1}. The numbers correspond to each antifungal tested, (**I**) CH; (**II**) OCH; (**III**) GCH. Additions were: A = cells; B = Antifungal. *U. maydis*, 25 mg wet weight.

2.3. Determination of ROS Released by U. maydis as a Response to CH, OCH or GCH

The production/presence of ROS was measured directly (Amplex Red® method) and indirectly (catalase activity) after treatment with the different polycation compounds. During growth, the control cells produced 3.13 nmol H_2O_2 min^{-1} mg wet weight^{-1}, and the catalase-specific activity was 1.87 U mg protein^{-1}, indicating that some hydrogen peroxide is formed under the physiological conditions and normal growth. Cells treated with chitosan produced considerably less ROS (0.11 nmol H_2O_2 min^{-1} mg of cell wet weight^{-1}) and showed a catalase activity of 0.56 U mg of protein^{-1}. This is associated with immediate and total CH-mediated cell destruction [15]. The OCH treatment produced a statistically significant increase in ROS (16.6 nmol H_2O_2 min^{-1} mg of cell wet weight^{-1} and catalase activity of 7.97 U mg of protein^{-1}), which means that it produced a greater amount of ROS compared to the other treatments. Cells grown in GCH did not show any differences in terms of ROS production (5.75 nmol H_2O_2 min^{-1} mg of cell wet weight^{-1} and 2.19 U mg of protein^{-1}) compared to the control cells; this was corroborated by the results of Tukey´s test (Figure 3).

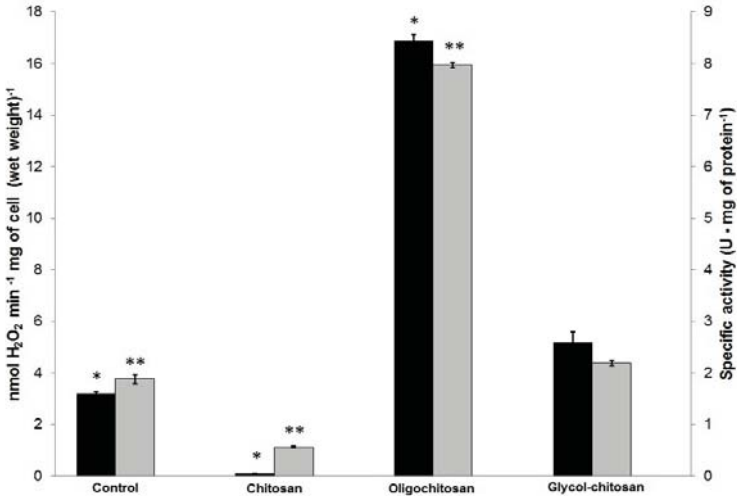

Figure 3. Quantification of ROS production by *Ustilago maydis* grown in the presence of CH, OCH or GCH. H_2O_2 production as measured with Amplex red® (■) and catalase activity (■). Cells were incubated in minimal medium for 24 h at 128 rpm and the indicated antifungal agent was added at 1 mg·mL^{-1}. Significance was evaluated by one-way ANOVA analysis and Tukey test ($p < 0.05$). The experiments were performed in triplicate ($n = 3$). * and ** indicate significant difference in H_2O_2 production and catalase activity, respectively, compared to control cells.

2.4. CH-, OCH-, or GCH-Mediated Damage of the Mitochondrial Structure in U. maydis

Damages in the mitochondrial structure were observed by the use of Mitotracker green® (Invitrogen/Thermo Fisher Scientific, Waltham, MA, USA) via fluorescence microscopy. In all cases, background fluorescence was observed, but specific regions were stained with greater intensity when mitochondria were present, especially in the control cells (Figure 4A2). The mitochondrial staining of cells with CH and OCH (Figure 4B2,C2) showed irregular fluorescence distribution, suggesting high damage. Cells incubated in the presence of GCH exhibited a lower fluorescence intensity than the control cells (Figure 4D2), suggesting mitochondria loss.

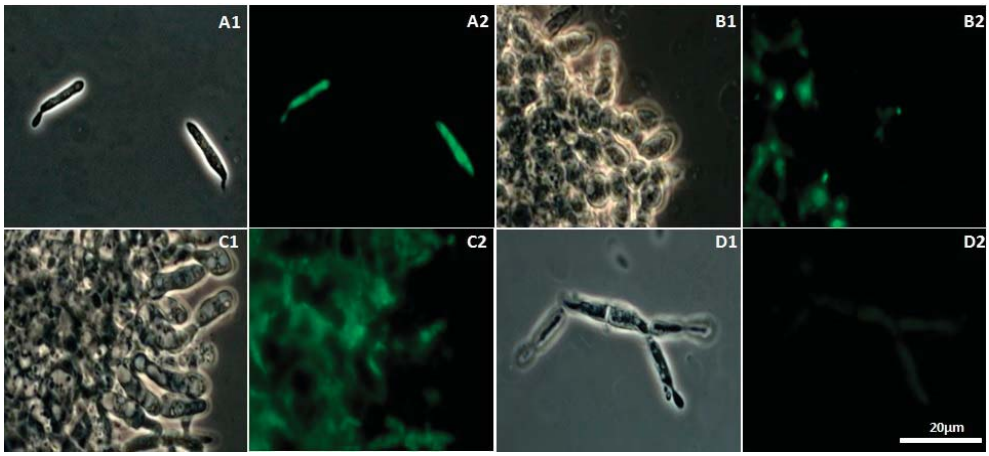

Figure 4. Phase contrast (1) and fluorescence (2) microscopy of *U. maydis* stained with MitoTracker® Green FM. An Eclipse E800 fluorescent microscope (Nikon Instruments Inc., Melville, NY, USA) with a fluorescein filter was used. The cells were growth in MM with the different treatment in a concentration of 1 mg mL^{-1}. The intensity of the signal is according with the presence of the mitochondrial proteins. **A** = Control; **B** = Chitosan; **C** = Oligochitosan; **D** = Glycol-chitosan. Time of incubation of 24 h.

2.5. Chitin Derivatives Modify Total Phospholipid Contents

As shown in Table 1, the phospholipid contents of the membrane fraction of yeast grown in the presence of chitin derivates were statistically decreased. The greatest decrease (44.72%) was induced by oligochitosan, followed by glycol-chitosan with an approximated decrease by 17.78% compared to the control. There was no data for chitosan, due to its inhibitory effect on yeast growth.

Table 1. Total phospholipid concentration (mM phospholipids g of cells^{-1}) in the membrane fraction of *U. maydis* growth under antifungal treatments.

Antifungal Tested (1mg·mL^{-1})	Total Phospholipid Concentration (mM Phospholipids g of Cells^{-1} Wet Weight)
Control	4.54 ± 0.035 [a]
Chitosan	ND
Oligochitosan	2.51 ± 0.12 [b]
Glycol-chitosan	3.76 ± 0.043 [c]

ND = Not determined. Different letters (a, b and c) indicate significant difference in one-way ANOVA evaluated by Tukey test ($p < 0.05$). The experiments were performed in triplicate ($n = 3$).

2.6. SDS-PAGE Analysis of U. maydis Membrane Proteins in the Absence and Presence of CH, OCH or GCH

The SDS-PAGE analysis (Figure 5) was performed to observe the modification in the protein profile caused by the addition of chitin derivatives. In CH-treated cells, the decrease in the intensity of a band near 100 kDa, suggested as the electrophoretic mark of the plasma membrane H ± ATPase (band A) [26], was observed. The samples treated with OCH exhibited the largest changes, presenting a more intense protein band at approximately 90 kDa (band C), 57 kDa (Band D), and 14 kDa (band E). The A band was not neatly distinguished as observed in the control cells. Cells grown in glycol–chitosan showed a well-delimited band A, with greater banding intensity in a protein of near 83 kDa (Band G).

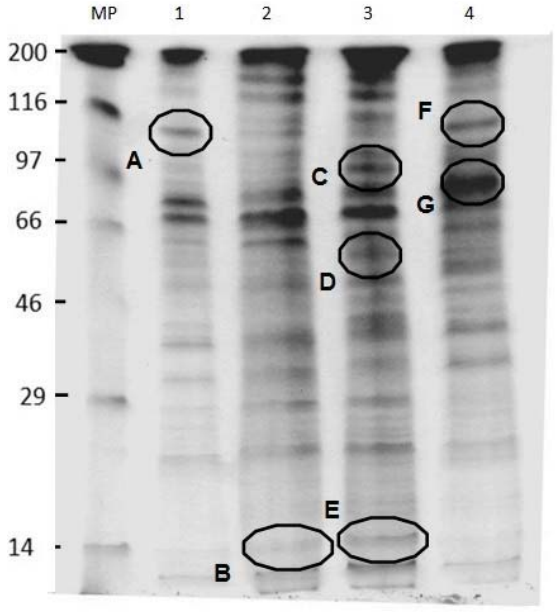

Figure 5. SDS-PAGE of the membrane fraction of *U. maydis* after the different antifungal treatments. Oligochitosan and glycol–chitosan were added at 1 mg·mL^{-1}. Chitosan was added at 10 μg·mL^{-1} due to the effect on cell growth. MW= Molecular weight marker (KDa); 1 = Control cell without antifungals; 2 = Cells treated with chitosan; 3 = Cells treated with oligochitosan; 4 = Cells treated with glycol–chitosan. Squares indicate differences in the bands pattern.

2.7. Effects of CH, OCH or GCH on the Accumulation of Glycogen by U. maydis

In response to stress, bacteria and yeasts accumulate glycogen. The cells cultured in the presence of GCH accumulated glycogen as compared to the control (Figure 6A). No glycogen was detected by PAS staining of cells with CH and OCH (data not shown). Interestingly, cells with GCH showed an increased size compared to the control (Figure 6B). This abnormal glycogen accumulation suggests that metabolic changes may be activated to use the GCH as fuel storage, which induces cell thickening.

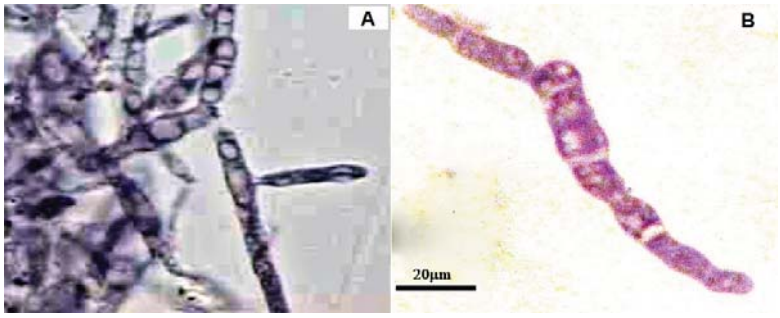

Figure 6. PAS staining of *U. maydis* in the presence of GCH. A 1 mg·mL^{-1} of each antifungal compound was added. The positive schiff reaction was demonstrated by the presence of the purple compound derivate of the interaction between the basic fuchsin with aldehydes sugars. (**A**) = Control; (**B**) = Glycol-chitosan (100×).

3. Discussion

Adverse external conditions trigger the stress defense response that comprises diverse metabolic modifications needed for survival [27]. In *U. maydis*, different chitin derivatives prompted different responses. As our results show, high osmolarity did not modify the effects of the different derivatives tested, indicating that the findings observed for the fungus do not solely result from osmotic stress [15]. This observation stands in contrast to the evidence reported by Zakrzewska et al. [28], who observed that 1M sorbitol protected *Saccharomyces cerevisiae* cells against chitosan. The authors state that the high-osmolarity glycerol pathway is crucial to establish fungal sensibility to chitosan. In this regard, *U. maydis* does exhibit important differences in the activation and control of this pathway, which would explain its sensitivity to chitosan, even in an isosmolar environment [28,29]. As reported before, chitosan promotes has a complete inhibitory effect on *Ustilago maydis* as a consequence of the interaction between specific sites in the plasma membrane and protonated free amino groups, constituting the main change of the polymer [15]. The modifications in cell permeability explain the depletion of the membrane potential and are consistent with observations in *Rhizopus stolonifer* at a chitosan concentration of 2000 µg·mL^{-1} [15,30]. However, in a non-susceptible model, such as *Candida albicans*, the effect of chitosan on the plasma membrane is completely the opposite: Peña et al. [31] described hyperpolarization of the cell membrane of *C. albicans* due to an alignment of internal charges with a subsequent increase in potential membrane when the yeast was in the presence of low chitosan concentrations [31]. Thus, it is evident that the effects of chitosan vary depending on the model [32]. In this study, OCH and GCH did not affect the plasma membrane potential.

There is evidence of an enhancement of oxygen consumption in *R stolonifer*, *C. albicans*, and *U. maydis* by chitosan and oligochitosan [15,31,33]. This modification of the rate of oxygen consumption could be due to an increased use of ATP, involved in energy-depended defense against these polymers, or to the generation of reactive oxygen species [31]. Oxidative stress in the presence of OCH has previously been described in macrophages, plant cells, and fungi [16,18,34]. In the last case, it was proposed that chitin derivatives inhibited proteins involved in the generation of reducing power for the neutralization of intracellular ROS, such as glutathione S-transferase-4 [34]. Our results do not indicate whether the formation of ROS is part of the oligochitosan antifungal effect or simply a response to

the stress generated by these molecules. On the other hand, the addition of CH and OCH seems to disorganize the mitochondrial structure without affecting its function. In contrast, in *U. maydis*, GCH does affect mitochondrial function. Previously, we described the reduction in the oxygen consumption rate in *U. maydis* in the presence of GCH [15]. In the present work, we corroborated the affectation of the mitochondria by GCH; this result is consistent with the decrease in respiration in *U. maydis* by the addition of glycol-chitosan, which has been described previously [15]. We believe this is the first report on the mitochondrial effects of GCH.

In the presence of chitin derivatives, the responses of *U. maydis*, modifying its lipid, protein, and carbohydrate composition, are part of a global survival mechanism. The OCH modified the total phospholipids and, to a lesser extent, so did GCH. Additionally, the protein profile was modified by the presence of each of the compounds used. The stressors may interact with the plasma membrane and produce different signals that up-regulate different membrane proteins. The modification of the protein concentration and protein functionality during CH stress has been described for *R. stolonifer*, where the amount of membrane proteins decreases to about 50%, as well as the activity of H + ATPase [35]. Under several stress conditions, fungi are able to modify the composition of their cell membrane, accumulate glycogen as a secondary energy source, and express, overexpress, and/or repress several genes for kinases, enzymes, transcriptional factors, detoxification systems, and mediators of apoptosis [36–41]. In fungi, chitin derivatives increased proteins for ergosterol synthesis, actin cytoskeleton organization, protein *N*-glycosylation, endocytosis, cell wall formation, and carbohydrate metabolism [28]. Previously, it has been demonstrated that chitosan produces a fungal stress response, involving a large number of genes mediated by the action of common stress transcription factors in yeast, such as Msn2p and Msn4p [42]. It is therefore possible that in *U. maydis*, the same factors are involved in the stress response to CH, OCH, and GCH.

Our results demonstrated that chitosan and its derivatives produce stress responses in *U. maydis*; these responses are significantly different depending on the characteristics of the molecule. Further experiments are necessary to establish the mode of action of these polycationic compounds and the stress response they elicit in fungi.

4. Materials and Methods

4.1. Reagents and Solutions

Low molecular weight chitosan (deacetylation degree (DD) $\geq$ 85%, MW 50–190 kDa), oligochitosan (chitosan oligosaccharide lactate, DD > 90%, average MW 5 kDa), and glycol chitosan (DD $\geq$ 60%, average MW 250 kDa) were purchased from Sigma-Aldrich (St. Louis, MO, USA). The stock solutions of CH, OCH, and GCH were prepared according to our previously published protocol [15]. All chemical compounds and solvents were analytical grade.

4.2. Growth in Isosmolar Medium

Ustilago maydis ATCC 201384 FB2 was grown in minimal medium (1% glucose, 0.3% potassium nitrate, and salt solution, pH 5.6), individually or in the presence of 1 mg CH, OCH, or GCH per mL. To establish an isosmolar environment, 400 mM sorbitol was added. This isosmolar medium was prepared considering the intracellular potassium concentration and its counter anions of the model yeast *Saccharomyces cerevisiae* [43]. Cells were cultured at 28 °C under agitation at 130 rpm for 48 h. Growth was measured by the changes in optical density at 600 nm.

4.3. Transmembrane Potential

Yeasts of *U. maydis* were cultured in YPD (1% yeast extract, 0.15% ammonium nitrate, 0.25% bacto peptone, 1% glucose, pH 6.8) for 24 h under the condition previously described [15]. Biomass was centrifuged at 3000× *g* for 10 min and diluted to 50% (*w/v*) with distilled water; 10-µL samples were used. The membrane potential was estimated by following the changes in fluorescence of a 0.25 mM

cyanine solution at 540–590 nm, according to the protocol previously described by Peña et al. [25]. Increasing concentrations of each chitosan derivative (from 2 to 100 $\mu g \cdot \mu L^{-1}$) were added after 50 s and the effects on the transmembrane potential were monitored.

4.4. H_2O_2 Production Measured by the Amplex Red® Method

Cells were cultured (24 h/130 rpm/28 °C) in minimal media and with or without 1 mg polycation mL^{-1}. The cells were collected by centrifugation and a 50% (*w/v*) cell suspension was prepared with sterilized water. Subsequently, 20-µL aliquots were placed into an ELISA 100-well plate with 50 µL of reaction mixture (0.1 units mL^{-1} horseradish peroxidase, 100 units mL^{-1} superoxide dismutase, 10 µM Amplex red® (Thermo Fisher Scientific, Waltham, MA, USA), 0.6 M mannitol, and 5 mM MES) and the volume was adjusted to 100 µL. The mixture was incubated at room temperature for 5 min. The formation of the fluorescence derivative (resorufin) as a consequence of the release of H_2O_2 was measured in a PolarStar OMEGA detector (571–585 nm), using the OMEGA control software (Ortenberg, Germany); the results were interpolated against a calibration curve [44]. The data are reported as nmol of H_2O_2 per min per mg wet weight of cells.

4.5. Catalase Activity

We also used *U. maydis* to measure catalase in cells grown in the absence or presence of each chitosan derivative. Cells were collected by centrifugation and mechanically disrupted in 0.1 M phosphate buffer (pH 7), using 0.5 mm glass beads. Subsequently, 100 µL of the supernatant were taken and added to 1.5 mL phosphate buffer. After this, 1 mL of 5 mM hydrogen peroxide was added and catalase activity was measured by the decrease in absorbance at 240 nm after 10 min. Protein was quantified by the Lowry method [45]. The specific activity of catalase is reported as units per mg protein. One unit is defined as the amount of enzyme necessary to reduce the absorbance at a rate of 0.1 units per mL per minute [46].

4.6. Mitochondrial Staining

Ustilago maydis was grown in minimal medium supplemented with 1 $mg \cdot mL^{-1}$ of each compound for 24 h, under the conditions described before. Cell suspension aliquots of 1 mL were incubated in the presence of 25 nM Mitotracker green® (Invitrogen/Thermo Fisher Scientific, Waltham, MA, USA) for 30 min at 37 °C. Untreated cells were used as control. Fluorescent mitochondria were observed in phase contrast microscopy with a fluorescein filter (494–520 nm) [47].

4.7. Total Phospholipid Quantification

The membrane fraction of *U. maydis* grown in the presence of each compound at a concentration of 1 $mg \cdot mL^{-1}$ for 24 hours at 28 °C was obtained by fractional centrifugation, as described in our previous publication [15]. For the quantification of total phospholipids, a commercial kit was used (Spinreact, Spain). Phospholipid concentration was determined by comparing the absorbance against a standard containing 300 $mg \cdot dL^{-1}$ of total phospholipids. The results were expressed in mM phospholipids g of $cells^{-1}$ (wet weight).

4.8. SDS-PAGE of the Membrane Fraction

Cells were incubated for 24 h on a shaker in the presence of each compound at 1 $mg \cdot mL^{-1}$, with the exception of CH, which was added at 10 $\mu g \cdot mL^{-1}$. The membrane fraction was obtained and the Lowry method was used to determine the protein concentration. Samples with ≈30 µg of protein were mixed with 4× loading buffer (0.5 M Tris pH 6.8; 10% SDS; 15% β-mercaptoethanol, 25% glycerol, and 0.1 $mg \cdot mL^{-1}$ bromophenol blue) and analyzed on 10% SDS-PAGE; staining and de-staining were performed with Coomassie Blue and acetic acid–methanol–water (1:2:10) solution, respectively.

4.9. Glycogen Accumulation and PAS Staining

Ustilago maydis was fixed with 0.6% periodic acid solution for 10 min at room temperature. The sample was washed with distilled water and mixed with Schiff's reagent (leucobasic fuchsin) for 30 min. Subsequently, the samples were washed three times with 10% sodium metabisulfite-1 N HCl for 1 min. Samples were rinsed with an ethanol-xylene mixture, mounted on a slide with synthetic resin, and observed in an optical microscope, denoting a purple color in the case of glycogen presence.

Acknowledgments: Special thanks to Escuela Nacional de Ciencias Biológicas of Instituto Politécnico Nacional; Facultad de medicina and Instituto de Fisiología Celular of Universidad Nacional Autónoma de México for the support for carrying out this work. This research received financial support from CONACyT projects No. 256520 and 254904; DGAPA-PAPIIT project IN222117 and IPN-SIP-ENCB projects No. 20141521, No. 20160999 and No. 20170864. The first author was recipient of a Ph.D. fellowship provided by CONACyT (No. 231581). For the publication as an open access article, this research had financial support by CONACyT project No. 256520 and 254904; grants CONACyT 239587 and DGAPA-PAPIIT IN204015 to SUC.

Author Contributions: D.R.O.-H. and G.G.-S. conceived and designed the experiments; J.P.P. designed isosmolar media experiments; D.R.O.-H. performed the experiments; C.U.-A. and S.U.-C. performed ROS quantification; S.U.-C. and C.U.-A. contributed reagents and analysis tools; D.R.O.-H. and G.G.-S. wrote the paper; J.P.P. and S.U.-C. reviewed and corrected the document.

Conflicts of Interest: The authors declare no conflict of interest. The founding sponsors had no role in the design of the study; in the collection, analyses, or interpretation of data; in the writing of the manuscript, and in the decision to publish the results.

References

1. Martin, F.; Cullen, D.; Hibbett, D.; Pisabarro, A.; Spatafora, J.W.; Baker, S.E.; Grigoriev, I.V. Sequencing the fungal tree of life. *New Phytol.* **2011**, *190*, 818–821. [CrossRef] [PubMed]
2. Lackner, D.H.; Schmidt, M.W.; Wu, S.; Wolf, D.A.; Bähler, J. Regulation of transcriptome, translation, and proteome in response to environmental stress in fission yeast. *Genome Biol.* **2012**, *13*, R25. [CrossRef] [PubMed]
3. Ortiz-Urquiza, A.; Keyhani, N.O. Stress response signaling and virulence: Insights from entomopathogenic fungi. *Curr. Genet.* **2015**, *61*, 239–249. [CrossRef] [PubMed]
4. Gasch, A.P. Comparative genomics of the environmental stress response in ascomycete fungi. *Yeast* **2007**, *24*, 961–976. [CrossRef] [PubMed]
5. Tesei, D.; Marzban, G.; Zakharova, K.; Isola, D.; Selbmann, L.; Sterflinger, K. Alteration of protein patterns in black rock inhabiting fungi as a response to different temperatures. *Fungal Biol.* **2012**, *116*, 932–940. [CrossRef] [PubMed]
6. Francois, J.M.; Formosa, C.; Schiavone, M.; Pillet, F.; Martin-Yken, H.; Dague, E. Use of atomic force microscopy (afm) to explore cell wall properties and response to stress in the yeast saccharomyces cerevisiae. *Curr. Genet.* **2013**, *59*, 187–196. [CrossRef] [PubMed]
7. Gunde-Cimerman, N.; Plemenitaš, A.; Buzzini, P. Changes in lipids composition and fluidity of yeast plasma membrane as response to cold. In *Cold-Adapted Yeasts: Biodiversity, Adaptation Strategies and Biotechnological Significance*; Buzzini, P., Margesin, R., Eds.; Springer: Berlin/Heidelberg, Germany, 2014; pp. 225–242.
8. Lushchak, V.I. Adaptive response to oxidative stress: Bacteria, fungi, plants and animals. *Comp. Biochem. Physiol. Part C Toxicol. Pharmacol.* **2011**, *153*, 175–190. [CrossRef] [PubMed]
9. Hernández-Oñate, M.A.; Herrera-Estrella, A. Damage response involves mechanisms conserved across plants, animals and fungi. *Curr. Genet.* **2015**, *61*, 359–372.
10. Dash, M.; Chiellini, F.; Ottenbrite, R.M.; Chiellini, E. Chitosan—A versatile semi-synthetic polymer in biomedical applications. *Prog. Polym. Sci.* **2011**, *36*, 981–1014. [CrossRef]
11. Bautista-Baños, S.; Hernández-Lauzardo, A.N.; Velázquez-del Valle, M.G.; Hernández-López, M.; Ait Barka, E.; Bosquez-Molina, E.; Wilson, C.L. Chitosan as a potential natural compound to control pre and postharvest diseases of horticultural commodities. *Crop Prot.* **2006**, *25*, 108–118.
12. Vinsova, J.; Vavrikova, E. Chitosan derivatives with antimicrobial, antitumour and antioxidant activities—A review. *Curr. Pharma. Des.* **2011**, *17*, 3596–3607. [CrossRef]

13. Benhabiles, M.S.; Salah, R.; Lounici, H.; Drouiche, N.; Goosen, M.F.A.; Mameri, N. Antibacterial activity of chitin, chitosan and its oligomers prepared from shrimp shell waste. *Food Hydrocoll.* **2012**, *29*, 48–56. [CrossRef]
14. Raafat, D.; Sahl, H.-G. Chitosan and its antimicrobial potential—A critical literature survey. *Microb. Biotechnol.* **2009**, *2*, 186–201. [CrossRef] [PubMed]
15. Olicón-Hernández, D.R.; Hernández-Lauzardo, A.N.; Pardo, J.P.; Peña, A.; Velázquez-del Valle, M.G.; Guerra-Sánchez, G. Influence of chitosan and its derivatives on cell development and physiology of Ustilago maydis. *Int. J. Biol. Macromol.* **2015**, *79*, 654–660.
16. Ma, Z.; Yang, L.; Yan, H.; Kennedy, J.F.; Meng, X. Chitosan and oligochitosan enhance the resistance of peach fruit to brown rot. *Carbohydr. Polym.* **2013**, *94*, 272–277. [CrossRef] [PubMed]
17. Gupta, K.; Dey, A.; Gupta, B. Plant polyamines in abiotic stress responses. *Acta Physiol. Plant.* **2013**, *35*, 2015–2036. [CrossRef]
18. Liu, L.; Zhou, Y.; Zhao, X.; Wang, H.; Wang, L.; Yuan, G.; Asim, M.; Wang, W.; Zeng, L.; Liu, X.; et al. Oligochitosan stimulated phagocytic activity of macrophages from blunt snout bream (megalobrama amblycephala) associated with respiratory burst coupled with nitric oxide production. *Dev. Comp. Immunol.* **2014**, *47*, 17–24. [CrossRef] [PubMed]
19. Xu, J.; Zhao, X.; Wang, X.; Zhao, Z.; Du, Y. Oligochitosan inhibits phytophthora capsici by penetrating the cell membrane and putative binding to intracellular targets. *Pestic. Biochem. Physiol.* **2007**, *88*, 167–175. [CrossRef]
20. Lopez-Moya, F.; Colom-Valiente, M.F.; Martinez-Peinado, P.; Martinez-Lopez, J.E.; Puelles, E.; Sempere-Ortells, J.M.; Lopez-Llorca, L.V. Carbon and nitrogen limitation increase chitosan antifungal activity in neurospora crassa and fungal human pathogens. *Fungal Biol.* **2015**, *119*, 154–169. [CrossRef] [PubMed]
21. Martinez, L.R.; Mihu, M.R.; Tar, M.; Cordero, R.J.B.; Han, G.; Friedman, A.J.; Friedman, J.M.; Nosanchuk, J.D. Demonstration of antibiofilm and antifungal efficacy of chitosan against candidal biofilms, using an in vivo central venous catheter model. *J. Infect. Dis.* **2010**, *201*, 1436–1440. [CrossRef] [PubMed]
22. Cota-Arriola, O.; Cortez-Rocha, M.O.; Rosas-Burgos, E.C.; Burgos-Hernández, A.; López-Franco, Y.L.; Plascencia-Jatomea, M. Antifungal effect of chitosan on the growth of aspergillus parasiticus and production of aflatoxin b1. *Polym. Int.* **2011**, *60*, 937–944. [CrossRef]
23. Xing, K.; Zhu, X.; Peng, X.; Qin, S. Chitosan antimicrobial and eliciting properties for pest control in agriculture: A review. *Agron. Sustain. Dev.* **2015**, *35*, 569–588. [CrossRef]
24. Dean, R.; Van Kan, J.A.L.; Pretorius, Z.A.; Hammond-Kosack, K.E.; Di Pietro, A.; Spanu, P.D.; Rudd, J.J.; Dickman, M.; Kahmann, R.; Ellis, J.; et al. The top 10 fungal pathogens in molecular plant pathology. *Mol. Plant Pathol.* **2012**, *13*, 414–430. [CrossRef] [PubMed]
25. Peña, A.; Uribe, S.; Pardo, J.P.; Borbolla, M. The use of a cyanine dye in measuring membrane potential in yeast. *Arch. Biochem. Biophys.* **1984**, *231*, 217–225.
26. Hernández, A.; Cooke, D.T.; Clarkson, D.T. In vivo activation of plasma membrane h+-atpase hydrolytic activity by complex lipid-bound unsaturated fatty acids in *Ustilago maydis*. *Eur. J. Biochem.* **2002**, *269*, 1006–1011.
27. Shor, E.; Perlin, D.S. Coping with stress and the emergence of multidrug resistance in fungi. *PLoS Pathog.* **2015**, *11*, e1004668. [CrossRef] [PubMed]
28. Zakrzewska, A.; Boorsma, A.; Delneri, D.; Brul, S.; Oliver, S.G.; Klis, F.M. Cellular processes and pathways that protect saccharomyces cerevisiae cells against the plasma membrane-perturbing compound chitosan. *Eukaryot. Cell.* **2007**, *6*, 600–608. [CrossRef] [PubMed]
29. Krantz, M.; Becit, E.; Hohmann, S. Comparative genomics of the hog-signalling system in fungi. *Curr. Genet.* **2006**, *49*, 137–151. [CrossRef] [PubMed]
30. Hernández-Lauzardo, A.N.; Vega-Pérez, J.; Velázquez-del Valle, M.G.; Sánchez, N.S.; Peña, A.; Guerra-Sánchez, G. Changes in the functionality of plasma membrane of rhizopus stolonifer by addition of chitosan. *J. Phytopathol.* **2011**, *159*, 563–568.
31. Pena, A.; Sanchez, N.S.; Calahorra, M. Effects of chitosan on candida albicans: Conditions for its antifungal activity. *BioMed Res. Int.* **2013**, *2013*, 15. [CrossRef] [PubMed]
32. Palma-Guerrero, J.; Lopez-Jimenez, J.A.; Pérez-Berná, A.J.; Huang, I.C.; Jansson, H.B.; Salinas, J.; Villalaín, J.; Read, N.D.; Lopez-Llorca, L.V. Membrane fluidity determines sensitivity of filamentous fungi to chitosan. *Mol. Microbiol.* **2010**, *75*, 1021–1032. [CrossRef] [PubMed]

33. Alfaro-Gutiérrez, I.C.; Guerra-Sánchez, M.G.; Hernández-Lauzardo, A.N.; Velázquez-del Valle, M.G. Morphological and physiological changes on rhizopus stolonifer by effect of chitosan, oligochitosan or essential oils. *J. Phytopathol.* **2014**, *162*, 723–730.
34. Lopez-Moya, F.; Kowbel, D.; Nueda, M.J.; Palma-Guerrero, J.; Glass, N.L.; Lopez-Llorca, L.V. Neurospora crassa transcriptomics reveals oxidative stress and plasma membrane homeostasis biology genes as key targets in response to chitosan. *Mol. BioSyst.* **2016**, *12*, 391–403. [CrossRef] [PubMed]
35. García-Rincón, J.; Vega-Pérez, J.; Guerra-Sánchez, M.G.; Hernández-Lauzardo, A.N.; Peña-Díaz, A.; Velázquez-Del Valle, M.G. Effect of chitosan on growth and plasma membrane properties of rhizopus stolonifer (ehrenb.:Fr.) vuill. *Pestic. Biochem. Physiol.* **2010**, *97*, 275–278.
36. Cannon, R.D.; Lamping, E.; Holmes, A.R.; Niimi, K.; Tanabe, K.; Niimi, M.; Monk, B.C. Candida albicans drug resistance—Another way to cope with stress. *Microbiology* **2007**, *153*, 3211–3217. [CrossRef] [PubMed]
37. Kroll, K.; Pähtz, V.; Kniemeyer, O. Elucidating the fungal stress response by proteomics. *J. Proteom.* **2014**, *97*, 151–163. [CrossRef] [PubMed]
38. Smith, D.A.; Morgan, B.A.; Quinn, J. Stress signalling to fungal stress-activated protein kinase pathways. *FEMS Microbiol. Lett.* **2010**, *306*, 1–8. [CrossRef] [PubMed]
39. Hayes, B.M.E.; Anderson, M.A.; Traven, A.; van der Weerden, N.L.; Bleackley, M.R. Activation of stress signalling pathways enhances tolerance of fungi to chemical fungicides and antifungal proteins. *Cell. Mol. Life Sci.* **2014**, *71*, 2651–2666. [CrossRef] [PubMed]
40. Kim, J.H.; Campbell, B.C.; Yu, J.; Mahoney, N.; Chan, K.L.; Molyneux, R.J.; Bhatnagar, D.; Cleveland, T.E. Examination of fungal stress response genes using saccharomyces cerevisiae as a model system: Targeting genes affecting aflatoxin biosynthesis by aspergillus flavus link. *Appl. Microbiol. Biotechnol.* **2005**, *67*, 807–815. [CrossRef] [PubMed]
41. Freitas, F.Z.; Virgilio, S.; Cupertino, F.B.; Kowbel, D.J.; Fioramonte, M.; Gozzo, F.C.; Glass, N.L.; Bertolini, M.C. The SEB-1 transcription factor binds to the STRE motif in Neurospora crassa and regulates a variety of cellular processes including the stress response and reserve carbohydrate metabolism. *G3 Genes Genomes Genet.* **2016**, *6*, 1327–1343. [CrossRef] [PubMed]
42. Zakrzewska, A.; Boorsma, A.; Brul, S.; Hellingwerf, K.J.; Klis, F.M. Transcriptional response of saccharomyces cerevisiae to the plasma membrane-perturbing compound chitosan. *Eukaryot. Cell* **2005**, *4*, 703–715. [CrossRef] [PubMed]
43. Navarrete, C.; Petrezsélyová, S.; Barreto, L.; Martínez, J.L.; Zahrádka, J.; Ariño, J.; Sychrová, H.; Ramos, J. Lack of main k+ uptake systems in saccharomyces cerevisiae cells affects yeast performance in both potassium-sufficient and potassium-limiting conditions. *FEMS Yeast Res.* **2010**, *10*, 508–517. [CrossRef] [PubMed]
44. Guerrero-Castillo, S.; Cabrera-Orefice, A.; Vázquez-Acevedo, M.; González-Halphen, D.; Uribe-Carvajal, S. During the stationary growth phase, yarrowia lipolytica prevents the overproduction of reactive oxygen species by activating an uncoupled mitochondrial respiratory pathway. *Biochim. Biophys. Acta* **2012**, *1817*, 353–362. [CrossRef] [PubMed]
45. Lowry, O.H.; Rosebrough, N.J.; Farr, A.L.; Randall, R.J. Protein measurement with the folin phenol reagent. *J. Biol. Chem.* **1951**, *193*, 265–275. [PubMed]
46. Li, Y.; Schellhorn, H.E. Rapid kinetic microassay for catalase activity. *J. Biomol. Tech. JBT* **2007**, *18*, 185–187. [PubMed]
47. Pham, C.D.; Yu, Z.; Sandrock, B.; Bölker, M.; Gold, S.E.; Perlin, M.H. *Ustilago maydis* rho1 and 14-3-3 homologues participate in pathways controlling cell separation and cell polarity. *Eukaryot. Cell* **2009**, *8*, 977–989. [CrossRef] [PubMed]

Sample Availability: Samples of the compounds chitosan, oligochitosan and glycol-chitosan are not available from the authors.

In female rat heart mitochondria, oophorectomy results in loss of oxidative phosphorylation

Natalia Pavón[1,*], Alfredo Cabrera-Orefice[2,*], Juan Carlos Gallardo-Pérez[3], Cristina Uribe-Alvarez[2], Nadia A Rivero-Segura[4], Edgar Ricardo Vazquez-Martínez[4], Marco Cerbón[4], Eduardo Martínez-Abundis[5], Juan Carlos Torres-Narvaez[1], Raúl Martínez-Memije[6], Francisco-Javier Roldán-Gómez[7] and Salvador Uribe-Carvajal[2]

[1]Departamento de Farmacología, Instituto Nacional de Cardiología Ignacio Chávez, México, Mexico
[2]Departamento de Genética Molecular, Instituto de Fisiología Celular, Universidad Nacional Autónoma de México, México D.F., Mexico
[3]Departamento de Bioquímica, Instituto Nacional de Cardiología Ignacio Chávez, México, Mexico
[4]Unidad de Investigación en Reproducción Humana, Instituto Nacional de Perinatología-Facultad de Química UNAM, México D.F., Mexico
[5]División Académica Multidisciplinaria de Comalcalco, Universidad Juárez Autónoma de Tabasco, México, Mexico
[6]Departamento de Instrumentación Electromecánica, Instituto Nacional de Cardiología Ignacio Chávez, Tlalpan DF, México, Mexico
[7]Departamento de Consulta externa, Instituto Nacional de Cardiología Ignacio Chávez, México, Mexico
*(N Pavón and A Cabrera-Orefice contributed equally to this work)

Correspondence should be addressed to N Pavón
Email
pavitonat@yahoo.com.mx

Journal of Endocrinology

Abstract

Oophorectomy in adult rats affected cardiac mitochondrial function. Progression of mitochondrial alterations was assessed at one, two and three months after surgery: at one month, very slight changes were observed, which increased at two and three months. Gradual effects included decrease in the rates of oxygen consumption and in respiratory uncoupling in the presence of complex I substrates, as well as compromised Ca^{2+} buffering ability. Malondialdehyde concentration increased, whereas the ROS-detoxifying enzyme Mn^{2+} superoxide dismutase (MnSOD) and aconitase lost activity. In the mitochondrial respiratory chain, the concentration and activity of complex I and complex IV decreased. Among other mitochondrial enzymes and transporters, adenine nucleotide carrier and glutaminase decreased. 2-Oxoglutarate dehydrogenase and pyruvate dehydrogenase also decreased. Data strongly suggest that in the female rat heart, estrogen depletion leads to progressive, severe mitochondrial dysfunction.

Key Words
- estrogens
- heart mitochondria
- oophorectomy
- estrogen receptors
- gender

Journal of Endocrinology (2017) **232**, 221–235

Introduction

Estrogens (17β-estradiol, estrone and progesterone) control diverse reproductive system functions. Their participation in other physiological processes such as cognition (Sherwin 1999), cardiovascular function (Stevenson 2000), immunity (Ahmed *et al.* 1999) and bone and mineral metabolism (Compston 2001) has been reported. Thus, estrogens are considered pleiotropic hormones. Estrogens enter the nucleus after being internalized by estrogen receptors α and β (ERα and ERβ) (Hall *et al.* 2001). In the myocardium, non-genomic pathways involving plasma membrane-bound ERs that activate protein kinase-mediated

http://joe.endocrinology-journals.org
DOI: 10.1530/JOE-16-0161

Published by Bioscientifica Ltd.

signaling cascades have been described (Sugden & Clerk 1998, Nuedling *et al.* 1999). Each estrogen receptor is codified by a unique gene (Giguere *et al.* 1998), which possesses the characteristic functional domains of the steroid/thyroid hormone superfamily of nuclear receptors (Matthews & Gustafsson 2003).

ERα and ERβ are widely distributed. ERα is expressed primarily in the uterus, liver, kidneys and heart, whereas ERβ is expressed primarily in the ovaries, prostate, lungs, gastrointestinal tract, bladder and hematopoietic and central nervous systems. Both receptors are co-expressed in mammary glands, epididymis, thyroid, adrenals, bone and some brain regions (Orshal & Khalil 2004, Mendoza-Garcés *et al.* 2011, Knowlton & Lee 2012). In addition, both receptors have been found in mitochondria, where their functions seem to be different and even antagonistic (Pedram *et al.* 2006, Psarra & Sekeris 2008, Yang *et al.* 2009). In brain mitochondria, estrogens modulate mitochondrial functions such as oxidative phosphorylation (Wang *et al.* 2001, Duckles *et al.* 2006) and Ca^{2+} uptake (Nilsen & Diaz Brinton 2003). In mouse heart, estrogens increase mitochondrial respiratory complex IV activity (Hsieh *et al.* 2006). In monkeys and in MCF-7 human breast cancer cells, estrogens may regulate mitochondrial biogenesis and size (Irwin *et al.* 2008, Rosario *et al.* 2008). However, in rats, this response has not been observed (Mattingly *et al.* 2008).

We used oophorectomized rats as a model to study estrogenic depletion. In adipose tissue mitochondria, oophorectomy decreases oxidative capacity and antioxidant defenses (Nadal-Casellas *et al.* 2011), as well as complex IV (COX) and pyruvate dehydrogenase (PDH) activities in whole-brain mitochondria (Irwin *et al.* 2011). However, these changes have not been fully explored in heart mitochondria. Estrogen receptors have been reported in the mitochondrial inner membrane and matrix of neurons, primary cardiomyocytes, murine hippocampus cell lines and human heart cells, whereas for other steroids, such as progesterone, receptors have been found only in the outer membrane (Dai *et al.* 2013).

We observed that oophorectomy affects heart mitochondrial functions such as oxygen consumption, Ca^{2+} uptake, transmembrane potential and the expression of different mitochondrial oxidative phosphorylation-related proteins; in castrated male rats, these results are not observed (Pavón *et al.* 2012). Thus, it was decided to evaluate the post-oophorectomy time-dependent evolution of heart mitochondria function.

Materials and methods

All experiments were conducted in agreement with ethical rules and guides from the Instituto Nacional de Cardiología, México (Record N°14-865).

Animals

Sixty Wistar female rats (3 weeks old) were used in the experiments. These were randomly assigned to one of two groups: control (Ctrl, intact rats) and oophorectomized (Cast). In addition, the latter were subdivided in three groups of twenty, to be analyzed at 1st, 2nd and 3rd month after surgery. Oophorectomy was performed in three-week-old animals under pentobarbital anesthesia. After surgery, rats were housed in our animal colony and maintained under controlled light/darkness cycles (12 h each) with water and rodent chow *ad libitum*.

Isolation of heart mitochondria

Rats were killed with sodium pentobarbital (100 mg/kg i.p.), and the heart was obtained. Heart tissue was incubated for 10 min with 2 mg/g of proteinase K (Sigma, P6556). Digested samples were centrifuged at 11,951.9 ***g***, and the resulting pellet was homogenized in 125 mM KCl, 1 mM EDTA, 10 mM Tris, pH 7.3 (Pavón *et al.* 2012) and centrifuged again at 478.1 ***g***, to pellet debris. From the supernatant, mitochondria were separated by differential centrifugation. Protein concentration was determined by the Bradford method (Bradford 1976).

Oxygen consumption measurements

It was assayed polarographically with a Clark electrode at 25°C. Reaction medium was 125 mM KCl, 3 mM phosphate, 2 mM $MgCl_2$, 10 mM HEPES, pH 7.3. Either 10 mM succinate + 5 µg/mL rotenone or 5 mM glutamate + 5 mM malate were added as respiratory substrates. 300 µM ADP was added to induce the phosphorylating state (state 3) as described in Pavón and coworkers (Pavón *et al.* 2012). Mitochondria were added to a final concentration of 0.5 mg prot/mL; final volume was 1.5 mL. Respiratory control (RC) was calculated as

http://joe.endocrinology-journals.org
DOI: 10.1530/JOE-16-0161

Published by Bioscientifica Ltd.

the quotient between the rate of oxygen consumption in state 3 (ADP-stimulated respiration) and the rate in state 4 (after ADP pulse is entirely phosphorylated and respiration shifts to resting state).

Calcium uptake

Mitochondrial Ca^{2+} uptake was measured spectrophotometrically at 675–685 nm (dual wavelength mode) at room temperature using the indicator Arsenazo III as described by Janssen and Helbing (1991). Briefly, 10 mM succinate, 5 µg/mL rotenone, 100 µM $CaCl_2$, 50 µM Arsenazo III, 100 µM ADP and 2 mg of mitochondrial protein were added to 2.9 mL 125 mM KCl, 3 mM phosphate, 10 mM HEPES, pH 7.3.

Enzyme activities

Citrate synthase (CS) was measured at 412 nm (ε = 13.6 mM/cm) in a reaction mixture containing 0.023 mg/mL acetyl-CoA, 0.1 mM DTNB (5,5′-dithio-bis-2-nitrobenzoic acid), 0.25 mM oxaloacetate, 0.05% Triton X-100 and 10 mM Tris–HCl, pH 8; mitochondria 0.03 mg prot/mL. CS activity was used for normalization of enzyme activities (Davies *et al.* 2001, Barrientos *et al.* 2009, Schwarzer *et al.* 2013). NADH:decylubiquinone oxidoreductase (complex I) activity was measured by following the fluorescence changes of NADH at 460 nm using SET buffer (250 mM sucrose, 0.2 mM EDTA and 50 mM Tris, pH 7.2), 0.155 mM NADH, 0.077 mM decylubiquinone, 10 µM antimycin A, 0.05% Triton X-100 and 0.5 mg prot/mL mitochondria (Barrientos *et al.* 2009). Rotenone (10 µM) was added to inhibit complex I and remaining inhibitor-insensitive activities were subtracted to the data. Succinate:DCPIP oxidoreductase (complex II) activity was measured spectrophotometrically at 590 nm (ε = 15.96 mM/cm) in SET buffer, 100 µM DCPIP, 10 mM succinate, 10 µM antimycin A, 5 µM rotenone and 0.5 mg prot/mL mitochondria (Barrientos *et al.* 2009). An OMEGA microplate reader was used to determine CS and complexes I and II activities; final volume per well was 200 µL. Complex IV activity was measured as cyanide-sensitive oxygen consumption in the presence of 5 mM ascorbate, 1 µM TMPD (tetramethyl-phenylenediamine), 10 µM antimycin A and 0.5 mg prot/mL mitochondria (Barrientos *et al.* 2009). NaCN (1 mM) was added to inhibit respiration at the end of each trace. Pyruvate dehydrogenase (PDH) and 2-oxoglutarate dehydrogenase (2-OGDH) activities were measured as in Cooney and coworkers (Cooney *et al.* 1981) with slight modifications using 125 mM KCl, 10 mM phosphate, 10 mM Tris/HCl, 5 mM $MgCl_2$, 0.05% Triton X-100, 2 mM NAD^+, 0.63 mM CoA, 1 mM TPP, 1 mM DTT, 1 mM PMSF, 10 µM rotenone, pH 7.4; mitochondria 0.5 mg prot/mL. The reaction was started with either 10 mM pyruvate or 10 mM 2-oxoglutarate. Reduction of NAD^+ (ε = 6.22 mM/cm) was followed in a DW2000 AMINCO OLIS spectrophotometer at 340 nm. Aconitase activity was measured as in Hausladen & Fridovich (1994). Mitochondria were solubilized by adding 0.05% Triton X-100 in 25 mM phosphate, pH 7.2. Then, 0.6 mM $MnSO_4$ and 10 mM citrate were added to the reaction mixture. The formation of cis-aconitate was measured at 240 nm.

Malondialdehyde by capillary zone electrophoresis

Malondialdehyde was determined as in Claeson and coworkers (Claeson *et al.* 2000). Briefly, 2 mg mitochondria were washed with methanol (1:1), centrifuged at 16,000 ***g*** for 15 min and filtered through a 0.22 µm nitrocellulose membrane. Samples were diluted (1:10) with 0.1 M NaOH and analyzed in a P/ACE MDQ (Beckman Coulter). Capillary tube was preconditioned with 0.1 M NaOH/10 min, distilled water/10 min and finally with 10 mM borate + 0.5 mM CTAB, pH 9 buffer. Separation was performed at −25 kV/4 min and absorbance was followed at 267 nm.

Western blot

Mitochondria were powdered in liquid nitrogen and dissolved in RIPA lysis buffer (PBS 1×, 1% IGEPAL NP40, 0.1% SDS and 0.05% sodium deoxycholate, pH 7.2) plus 5 mM protease inhibitor cocktail (Roche). Protein samples (40 µg) were re-suspended in loading buffer plus 5% β-mercaptoethanol and separated under denaturing conditions. Electrophoretic transfer to PVDF membranes (BioRad) was followed by overnight immunoblotting at 4°C with 1:500 diluted primary antibodies (Santa Cruz) against complex I subunit ND1; complex IV subunit COX4; ATP synthase subunit 5B (beta); adenine nucleotide translocator; pyruvate dehydrogenase subunit E1α; 2-oxoglutarate dehydrogenase; succinate dehydrogenase subunit C or glutaminase. Bands were revealed with secondary antibodies conjugated with horseradish peroxidase (Santa Cruz). The signal was detected by chemiluminescence using an ECL-Plus system (Amersham Bioscience). Densitometry was performed using the Scion Image Software (Scion; MD, USA) and normalized against its respective loading control.

http://joe.endocrinology-journals.org
DOI: 10.1530/JOE-16-0161

Published by Bioscientifica Ltd.

Blue native polyacrylamide gel electrophoresis (BN-PAGE) and in-gel enzymatic activities

BN-PAGE was performed as described by Schägger (2001). Briefly, mitochondrial pellet was re-suspended in sample buffer (750 mM aminocaproic acid, 25 mM imidazole, pH 7.0) and solubilized with 2 mg *n*-dodecyl-β-D-maltoside (lauryl maltoside, LM)/mg prot at 4°C for 30 min and centrifuged at 60,000 ***g***; 4°C/25 min. Supernatants were loaded into 4–12% (w/v) polyacrylamide gradient gels. After electrophoresis, in-gel NADH oxidoreductase (NDH) and cytochrome *c* oxidase (COX) activities were performed as in Zerbetto and coworkers (Zerbetto *et al*. 1997). BN-gels not subjected to in-gel activities, were stained with Coomassie blue G-250 (Wittig *et al*. 2007). Densitometry was done using the ImageJ (1.49v) software (NIH) and normalized against its respective loading control.

Superoxide dismutase (MnSOD) activity

MnSOD activity was determined in non-denaturing gels. Solubilized mitochondria (200 µg) were loaded into 10% polyacrylamide gels. After electrophoresis, gels were incubated in 0.5 mg/mL nitrotetrazolium blue (NTB) for 30 min and then in 28 mM TEMED, 36 mM potassium phosphate, 0.28 mM riboflavin, pH 7.8, in the darkness for 10 min. Activities were revealed by exposure to UV light for 10 min. A standard curve was performed using a serial dilution (2.5, 5, 10, 15, 30 and 60 ng) of MnSOD from bovine erythrocytes (Sigma Chemical Co.). Activities were calculated as in Pérez-Torres and coworkers (Pérez-Torres *et al*. 2009).

Statistical analysis

Student's *t*-test for unpaired data was used to compare the baseline variables of the groups. ANOVA test was employed and when a significant *F* was obtained, a Newman–Keuls post-test was used to find intergroup differences. A $P<0.05$ was considered statistically significant. For statistical analysis, we used Prism 5.0 software.

Results

Strong evidence indicates that estrogens control mitochondrial functions. Blood vessel mitochondria from oophorectomized rats (Cast) exhibit a delay in respiration that disappears upon estradiol administration (Duckles *et al*. 2006). Thus, we explored functional alterations in rat heart mitochondria at one, two and three months after oophorectomy.

Oxygen consumption measurements were performed to analyze the progressive effect of castration on rat heart mitochondrial oxidative phosphorylation (OXPHOS) system (Table 1). Respiratory substrates used were succinate or glutamate–malate. Succinate-dependent oxygen consumption and respiratory controls (RC) were similar in oophorectomized (Cast) groups and in non-oophorectomized controls (Table 1 and Supplementary Fig. 1, see section on supplementary data given at the end of this article). By contrast, in the presence of glutamate–malate, respiratory coupling gradually decreased from the 1st month after surgery, whereas state 4 increased up to two times (Table 1 and

Table 1 Oxygen consumption and respiratory controls in isolated heart mitochondria from control (Ctrl) and castrated (Cast) female rats at different times after surgery.

	+ Glutamate–malate			+ Succinate–rotenone		
Condition	State 4	State 3	RC	State 4	State 3	RC
1st month						
Ctrl	36 ± 10	178 ± 42	5.2 ± 1.2	54 ± 9	153 ± 31	2.8 ± 0.2
Cast	56 ± 8	192 ± 36	3.4 ± 0.5*	70 ± 8	186 ± 35	2.7 ± 0.6
2nd month						
Ctrl	32 ± 6	152 ± 23	4.8 ± 1.1	71 ± 23	190 ± 36	2.8 ± 0.8
Cast	92 ± 19**	164 ± 27	1.9 ± 0.6***	70 ± 14	172 ± 19	2.5 ± 0.5
3rd month						
Ctrl	33 ± 6	165 ± 16	5.1 ± 1.1	49 ± 13	141 ± 29	3.0 ± 0.9
Cast	62 ± 13*	96 ± 16**	1.6 ± 0.4***	54 ± 19	157 ± 40	3.1 ± 0.9

Oxygen consumption was measured at 25°C, incubating mitochondria in 1.5 mL of a medium containing 125 mM KCl, 3 mM phosphate, 2 mM $MgCl_2$, 10 mM HEPES, pH 7.3 and either 5 mM glutamate + 5 mM malate or 10 mM succinate + 5 µg/mL rotenone as substrates. To induce phosphorylating state (state 3), 300 µM ADP was added to the reaction chamber. Mitochondrial respiratory control (RC) is defined as the ratio between the rate of oxygen consumption in phosphorylating and non-phosphorylating states (RC = state 3/state 4). Values of oxygen consumption are expressed as ngAO/min.mg prot. Data of six independent experiments are shown as the mean ± S.D. *$P<0.05$, **$P<0.01$ and ***$P<0.001$ with respect to each Ctrl value.

http://joe.endocrinology-journals.org
DOI: 10.1530/JOE-16-0161

Published by Bioscientifica Ltd.

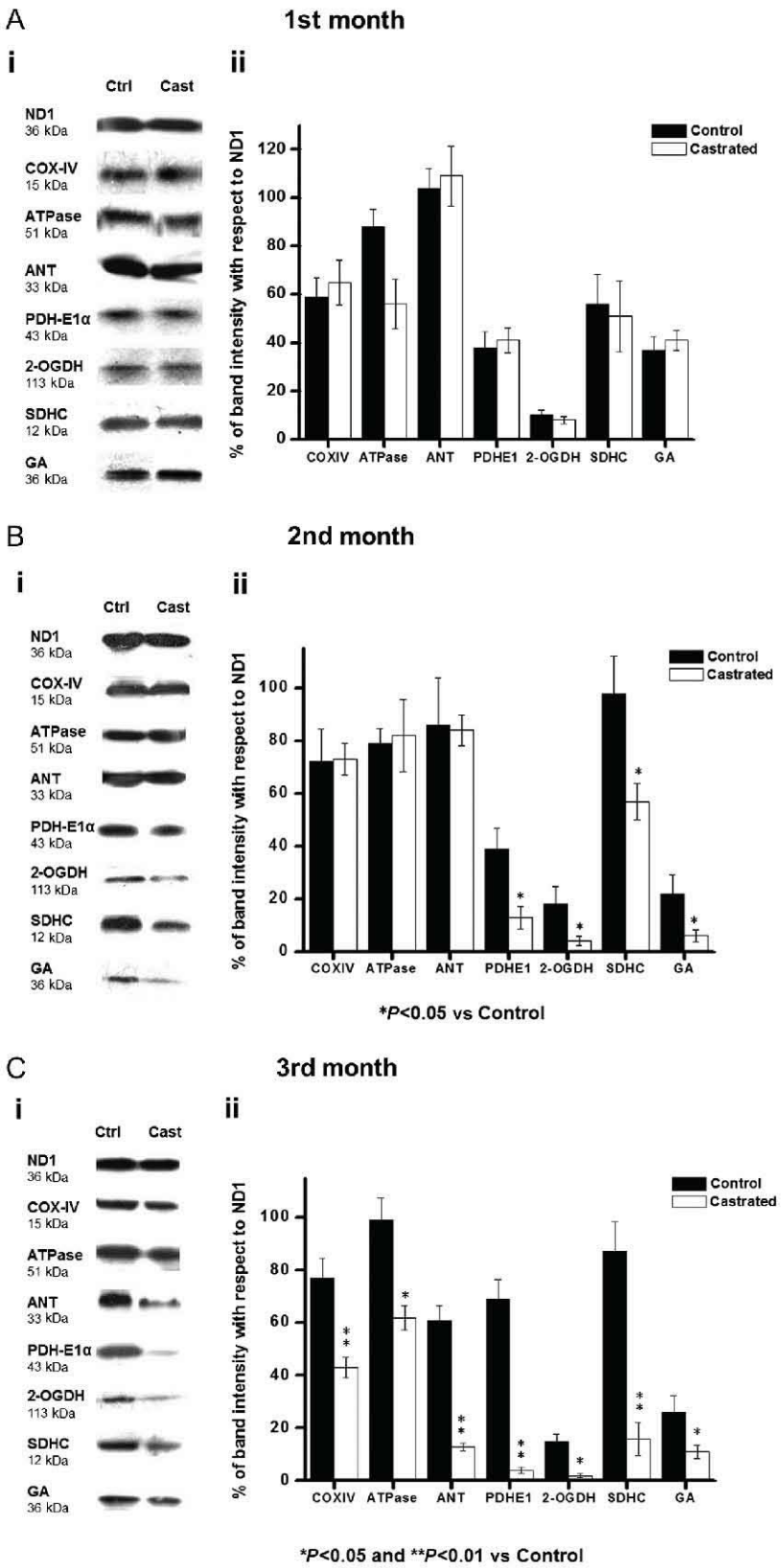

Figure 1
Progressive mitochondrial protein contents modifications during the first three months after oophorectomy. Panel A, one month; panel B, two months; panel C, third month after castration. Left panels (i) western blot analysis of proteins from intact (Ctrl) and castrated (Cast) female rat mitochondria. ND1, NADH ubiquinone oxidoreductase (complex I); COX IV, cytochrome *c* oxidase subunit 4; ATPase, ATP synthase subunit 5B (beta); ANT, adenine nucleotide translocase; PDH-E1α, pyruvate dehydrogenase subunit E1; 2-OGDH, α-ketoglutarate dehydrogenase; SDHC, succinate dehydrogenase subunit B; GA, glutaminase. Right panels (ii), variations in protein contents compared to the control ND1. Representative blots and data from three independent experiments; $*P<0.05$ and $**P<0.01$.

Journal of Endocrinology

http://joe.endocrinology-journals.org
DOI: 10.1530/JOE-16-0161

Published by Bioscientifica Ltd.

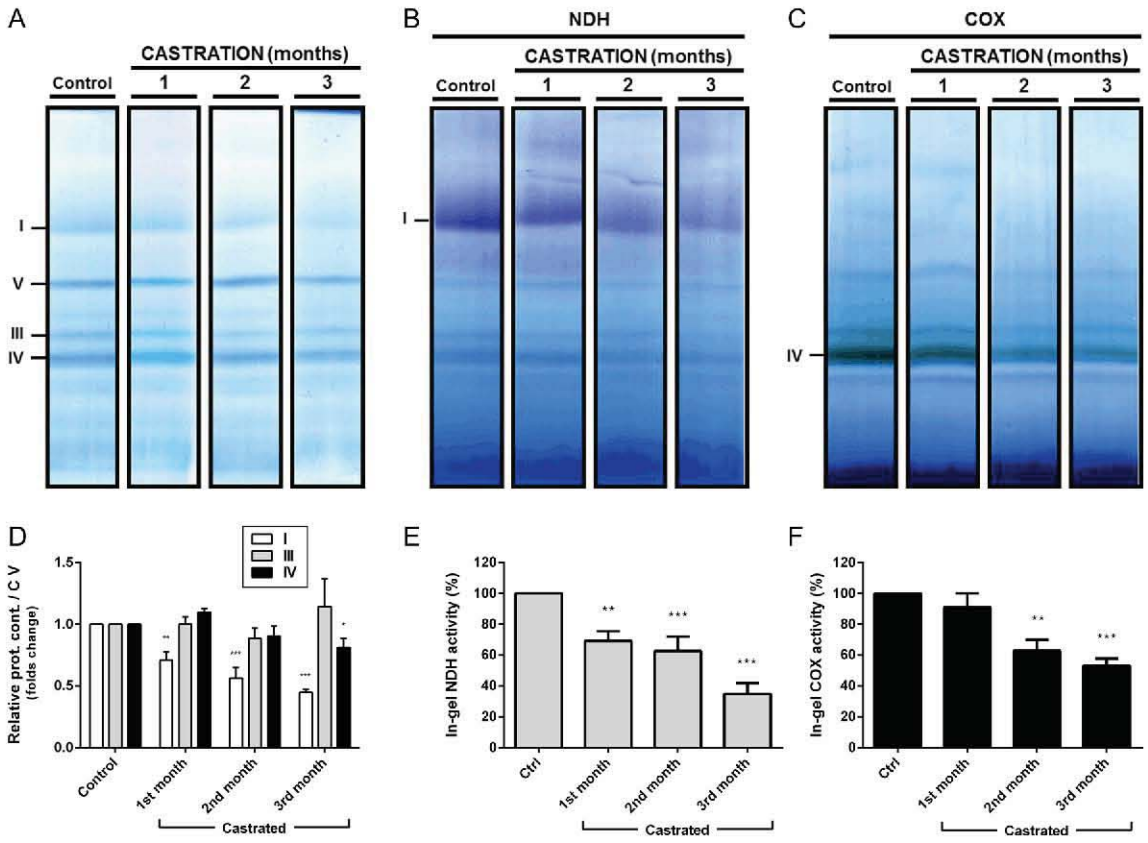

Figure 2

Progressive effects of castration on heart mitochondrial OxPhos complexes I, III, IV and V from female rats. Lanes are from control (Ctrl) and 1-, 2- and 3-month castrated rat heart mitochondrial samples. Isolated mitochondria were solubilized with lauryl-maltoside (LM) 2 mg/mg protein before electrophoretic separation. (A) Different samples were resolved by BN-PAGE in a 4–12% polyacrylamide gradient gel and were subjected to Coomassie staining. (B) In-gel NADH dehydrogenase activity (NDH); 1 mM NADH and 0.5 mg/mL Nitrotetrazolium blue chloride (NTB). (C) In-gel cytochrome *c* oxidase activity (COX); 0.04% diaminobenzidine and 0.02% cytochrome *c*. (D, E and F) Densitometry analysis of different protein bands from panels A (complexes I, III, IV and V), B (complex I in-gel activity (NDH)) and C (complex IV in-gel activity (IV)), respectively; $*P<0.05$, $**P<0.01$, $***P<0.01$. Representative figures from 3 independent gels. Respiratory chain complexes of interest are marked as I and IV. ATP synthase (V) was used as loading control. A full colour version of this figure is available at http://dx.doi.org/10.1530/JOE-16-0161.

Supplementary Fig. 1). At the 3rd month after surgery, state 3 decreased near to half (Table 1). These results suggested a dysfunction of complex I, which is highly sensitive to stress and can be regulated by estrogens (Chen *et al*. 2009).

Previously, in rats tested at the 4th month after castration, we detected changes in different mitochondrial OXPHOS-related proteins such as cytochrome *c* oxidase, ATP synthase, adenine nucleotide translocase (ANT), pyruvate dehydrogenase subunit 1 (PDH-E1α), 2-oxoglutarate dehydrogenase (2-OGDH), succinate dehydrogenase subunit C (SDHC) and glutaminase (GA). These data led to measure the activity and contents of these proteins at different times after oophorectomy (Fig. 1).

At the 1st month, Cast rats showed similar contents of mitochondrial OXPHOS-related proteins as those of Ctrl (Fig. 1A). Then, at 2nd and 3rd months, some of these proteins gradually changed their expression (Fig. 1B and C). For example, at the 2nd month, there was a perceptible decrease in 2-OGDH, SDHC and GA (Fig. 1B) and later on the decrease was more evident (from 0.5 to 5 times approximately) for most proteins, particularly for PDH (Fig. 1C). Besides, it was of interest to determine if these low levels of protein expression correlated with changes in OXPHOS complexes function; therefore, these enzymes were explored.

The amount of complexes I, III, IV and V was determined by BN-PAGE (Fig. 2A). After oophorectomy, a progressive decrease in complex I was observed (Fig. 2A) and evidenced further by densitometry (Fig. 2D). At the 3rd month, a slight decrease in complex IV content was also present (Fig. 2A and D). As there are only subtle changes in the amount of complexes III and V (Fig. 2A

Published by Bioscientifica Ltd.

Table 2 Effect of castration on the mitochondrial enzyme activities at different times (months) after surgery.

Enzyme	Condition	Activity (%)	Activity (%)/CS activity (%)
Citrate synthase	Control	100 ± 10[a]	
	Castrated		
	1st month	95 ± 9	
	2nd month	90 ± 12	
	3rd month	85 ± 12	
Complex I	Control	100 ± 6[b]	1
	Castrated		
	1st month	90 ± 6	0.95
	2nd month	62 ± 10**	0.69**
	3rd month	31 ± 8***	0.36***
Complex II	Control	100 ± 13[c]	1
	Castrated		
	1st month	94 ± 15	0.99
	2nd month	83 ± 5	0.92
	3rd month	84 ± 16	0.98
Complex IV	Control	100 ± 13[d]	1
	Castrated		
	1st month	91 ± 21	0.96
	2nd month	50 ± 12**	0.56**
	3rd month	47 ± 8***	0.55***
Pyruvate dehydrogenase	Control	100 ± 14[e]	1
	Castrated		
	1st month	94 ± 12	0.99
	2nd month	54 ± 10**	0.60**
	3rd month	10 ± 2***	0.12***
2-Oxoglutarate dehydrogenase	Control	100 ± 12[f]	1
	Castrated		
	1st month	102 ± 10	1.07
	2nd month	48 ± 6***	0.53***
	3rd month	30 ± 4***	0.35***

100% of activity corresponds to: [a]444.13 ± 43.9 nmol DTNB/min·mg prot; [b]627.2 ± 54.6 nmol NADH/min·mg prot; [c]141.6 ± 18.9 nmol DCPIP/min·mg prot; [d]620 ± 83.3 ngAO/min·mg prot; [e]34.5 ± 4.7 nmol NADH/min·mg prot; [f]121.8 ± 14.4 nmol NADH/min·mg prot. Activities were measured at room temperature (~25°C). In PDH, OGDH and complex II determinations, rotenone 10 µM was added to prevent the oxidation of the NADH or reverse electron transfer by complex I. Data from three-six independent experiments. $^{**}P<0.01$, $^{***}P<0.001$ with respect to each control value.

and D), the last one was used as loading control. Only one control (1st month) is shown in Fig. 2 as no differences were observed throughout the three months (data not shown). Furthermore, in-gel activities for complexes I (Fig. 2B) and IV (Fig. 2C) decreased as post-castration time increased. Once again, densitometry analysis confirmed the differences in both NDH (Fig. 2E) and COX (Fig. 2F) activities at two and three months after castration.

Individual activities of the enzymes that decreased after oophorectomy were determined to verify our findings. Citrate synthase (CS) activity was almost the same at different post-castration times; only a slight decrease at the 3rd month was detected (Table 2). Therefore, to discard the effects of different yield or stability of mitochondria on enzyme activities, data were also normalized to their respective CS activities. Complex I activity decreased as post-oophorectomy time increased in a similar way as observed by in-gel staining (Table 2). In addition, complex II activity did not change in any case (Table 2). The activities of complexes III and V were not determined as their respective relative contents did not change (Fig. 2A). PDH and 2-OGDH activities were also determined spectrophotometrically. At the 1st month after oophorectomy, no differences were found in enzyme activities, although beginning on the 2nd month, both

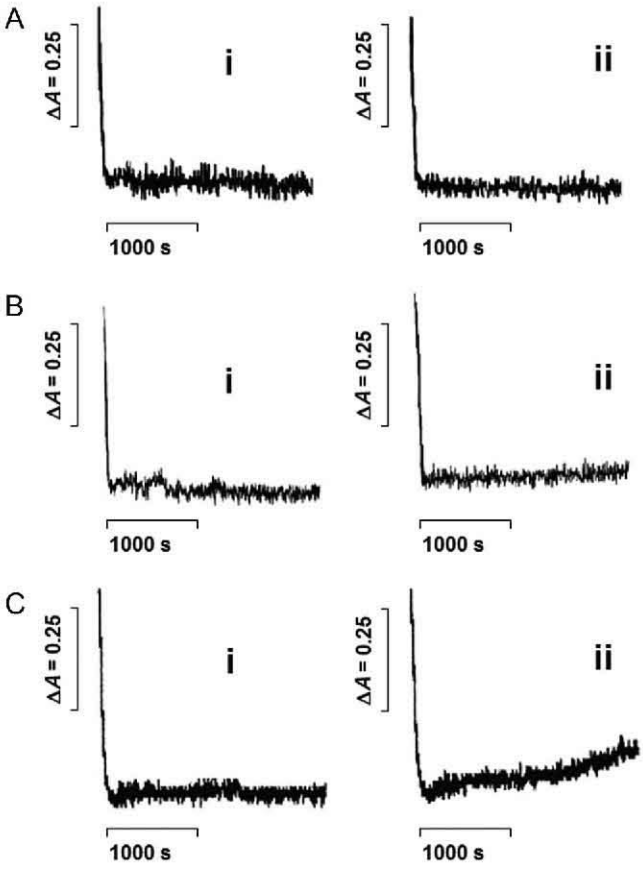

Figure 3
Effect of castration on Ca^{2+} transport by heart mitochondria isolated from female rats at different castration times. Mitochondrial protein (2 mg) was added to 3 mL of a medium containing 125 mM KCl, 10 mM succinate, 10 mM HEPES, 3 mM phosphate, 100 µM ADP, 100 µM $CaCl_2$, 5 µg rotenone and 50 µM arsenazo III. Arsenazo III absorbance changes were followed at 675–685 nm; room temperature. Panel A, trace (i) shows intact female mitochondria from 1 month; trace (ii) shows castrated female mitochondria from 1 month; panel B trace (i) shows intact female mitochondria from 2 months; trace (ii) shows castrated female mitochondria from 2 months; panel C trace (i) shows intact female mitochondria from 3 months; trace (ii) shows castrated female mitochondria from 3 months. Representative traces from 10 independent experiments.

http://joe.endocrinology-journals.org
DOI: 10.1530/JOE-16-0161

Published by Bioscientifica Ltd.

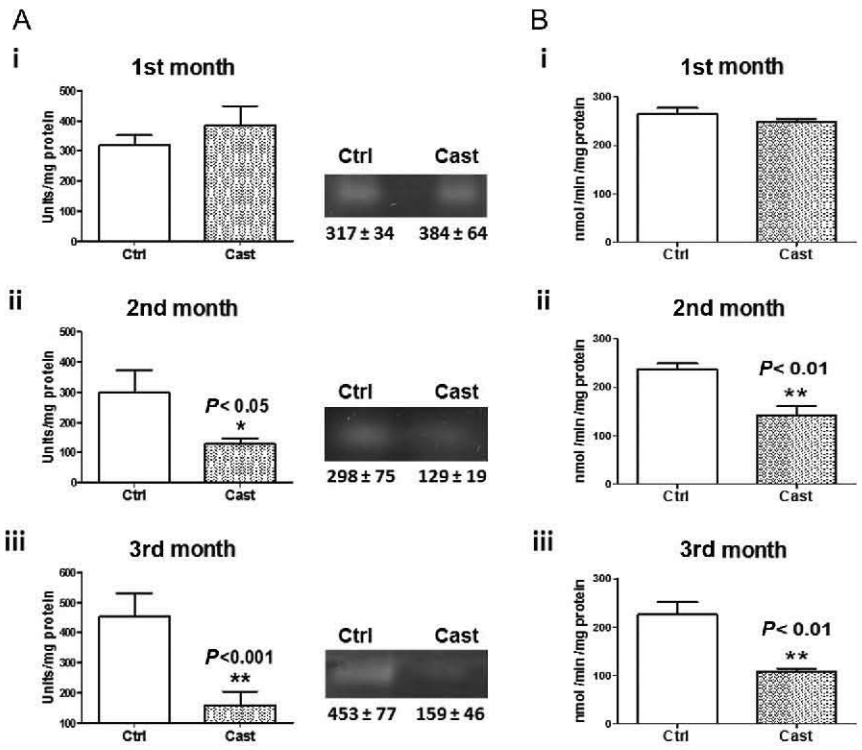

Figure 4
Superoxide dismutase (MnSOD) and aconitase activities in heart mitochondria from control and castrated female rats. Panel A figure (i) shows MnSOD activity in heart mitochondria from control (Ctrl) and castrated (Cast) rats after 1st month; figure (ii) shows MnSOD activity in Ctrl and Cast rats at the 2nd month; figure (iii) shows MnSOD activity in Ctrl and Cast at the 3rd month. Representative figures from 5 independent gels; images are representative of 10 separate experiments. Panel B trace (i) shows aconitase activity in Ctrl and Cast heart mitochondria at the 1st month; trace (ii) shows aconitase activity at the 2nd month and trace (iii) shows aconitase activity at the 3rd month. The results are expressed as the mean ± S.D. from 10 different experiments. Unpaired *t*-test was used for statistical analysis. $*P<0.05$, $**P<0.01$.

decreased (Table 2). This was more evident at the 3rd month after surgery where PDH activity decreased almost 10 times and 2-OGDH almost 3 times (Table 2).

Ca^{2+} overaccumulation is considered as another effect of oophorectomy on mitochondria (Pavón *et al.* 2012). Therefore, it was interesting to study whether this parameter changed in heart mitochondria. As Fig. 3A shows, at 1st month, there was no difference between Ctrl (trace i) and Cast (trace ii). At the 2nd month, a minimal difference was present (Fig. 3B, i and ii). Nonetheless, 3rd month Cast mitochondria exhibited a mild loss in the capacity to retain Ca^{2+} (Fig. 3C). After 45 min, these mitochondria released about a 30% of Ca^{2+} (Fig. 3C).

Heart mitochondria are equipped with effective ROS scavenging systems. Dysfunctions in these systems are directly related to cardiovascular disease (Matthews & Gustafsson 2003, Nilsen & Diaz Brinton 2003, Orshal & Khalil 2004, Psarra & Sekeris 2008, Irwin *et al.* 2011). Earlier observations have evidenced the influence of estrogens on the expression and function of antioxidant proteins such as MnSOD (Baños *et al.* 2005*a*,*b*). These evidences raise the possibility of oxidative damage in Cast rats. To test if this condition was present, MnSOD and aconitase activities were quantified (Fig. 4 panels A, B) and malondialdehyde levels were measured (Fig. 5). In regard to MnSOD activity, it was found that at the 1st month after oophorectomy, there were no differences between Ctrl and Cast groups (Fig. 4A, i). However, at the 2nd month, activity was lower in Cast group, which was statistically significant (Fig. 4, ii). This difference in MnSOD activity was even more obvious at the 3rd month (Fig. 4, iii).

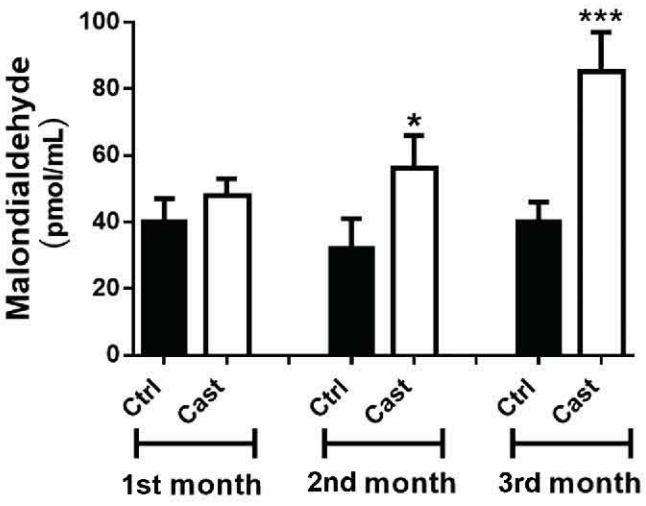

Figure 5
Lipoperoxidation expressed as malondialdehyde generation in heart mitochondria from Ctrl and Cast female rats. The results are expressed as mean ± S.D. for 10 different samples per group analyzed. 2 mg of protein were used and malondialdehyde was separated at –25 kV/4 min at 267 nm. Results were expressed as pmol/mL. $*P<0.05$, $***P<0.001$.

http://joe.endocrinology-journals.org
DOI: 10.1530/JOE-16-0161

Published by Bioscientifica Ltd.

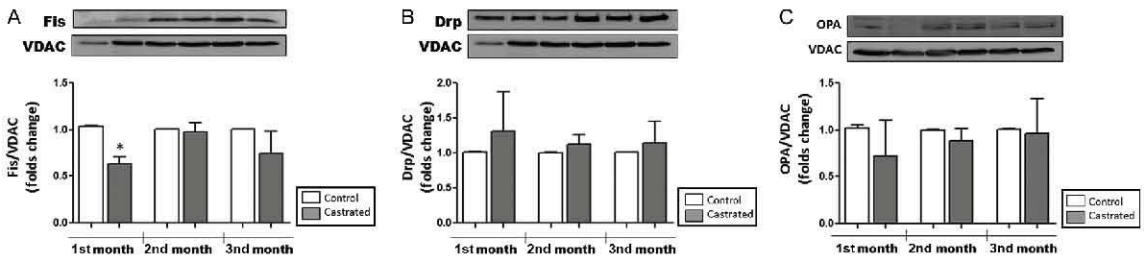

Figure 6
Western blot detection of proteins Fis-1, Drp-1 and OPA-1. Panel A shows content of Fis-1 in each experimental group; Panel B shows the content of Drp-1 and Panel C, OPA-1 content. In all cases, 30 μg of each sample were loaded per lane. VDAC was used as loading control. Bars represent mean ± S.E.M. of 3 independent experiments; *$P<0.05$.

In a previous study, we found evidence that estrogens may control the expression of some proteins involved in OXPHOS (Pavón *et al*. 2012). Thereby, a dysfunction in the respiratory chain should also involve the overproduction of ROS. These ROS would inactivate enzymes containing iron–sulfur centers, e.g. aconitase and complexes I, II and III. Aconitase inactivation is an appropriate marker of the superoxide production on the matrix side (Muller *et al*. 2004). No differences were detected at the 1st month (Fig. 4B, i), whereas inhibition was present from the 2nd month (40%) (Fig. 4B, ii) and increased during the 3rd month (54%) (Fig. 4B, iii). Thus, higher production of ROS or defective detoxification mechanisms will damage lipids, proteins and DNA. An indicator of oxidative damage is malondialdehyde (MDA), whose level increased in the Cast group beginning at the 2nd month and becoming even higher at the 3rd month (Fig. 5).

All previous data indicated that oophorectomy leads to dysfunctional mitochondria and increased levels of oxidative damage. Both effects have also been implicated in abnormal mitochondrial dynamics (fusion and fission) (Ong & Hausenloy 2010, Wohlgemuth *et al*. 2014). In an effort to determine if oophorectomy is associated with mitochondrial dynamics, we measured the expression of the fission-associated proteins Fis-1 and Drp-1, the fusion-associated protein OPA-1 and the apoptosis-related proteins Bcl-2 and Bax. Figure 6 shows no significant changes in the expression of the dynamic-related proteins at any time after castration. In fact, only Fis-1 decreased at the first month, but increased back to Ctrl levels at the second and third month. In addition, we found a decrease in expression of Bcl-2 after the first month of castration, whereas an increase was detected at the third month (Fig. 7).

Mitochondrial dysfunction can result from a decrease in protein content (Chen *et al*. 2004, 2009) and activity of OXPHOS enzymes (Stirone *et al*. 2005). These may affect the important functions for the cell (e.g. Ca^{2+} uptake, metabolite transport, and so forth) and mitochondrial biogenesis (Mattingly *et al*. 2008). All such changes would presumably lead to a decrease in metabolites oxidation. Under our experimental conditions, it is probable that most of them were present and higher at the 3rd month after oophorectomy.

Discussion

After the 1st month post-oophorectomy, isolated mitochondria in the presence of glutamate–malate exhibited a slight decrease in respiratory coupling compared to the controls (Table 1). At the 2nd and 3rd months, respiratory coupling in Cast groups was almost 40% and a decrease in complex I content and activity was detected (Fig. 2A, B, Tables 1 and 2). By contrast, using succinate–rotenone, respiratory activities and coupling

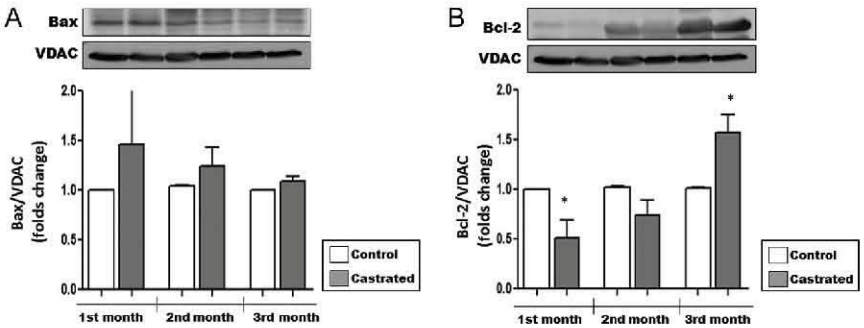

Figure 7
Western blot detection of proteins Bax and Bcl-2. Panel A shows the content of Bax in each experimental group. Panel B shows content of Bcl-2 in each experimental group. VDAC was used as loading control. Bars represent mean ± S.E.M. of 3 independent experiments; *$P<0.05$.

http://joe.endocrinology-journals.org
DOI: 10.1530/JOE-16-0161

Published by Bioscientifica Ltd.

were not different between Ctrl and Cast groups at any time after surgery. Individual complex II activities normalized to CS were not affected in Cast groups (Table 2) even if SDHC subunit expression decreased ~40% (Fig. 1). COX IV and ATPase β subunits decreased, suggesting a general decrease in OXPHOS-related proteins. A decrease in complex IV content (~85%) and activity (~55%) was observed, whereas complexes III and V were constant (Fig. 2 and Table 2).

Although the amount and activity of complex IV decreased, electron flux through complexes I and II was not limited. In complex I-dependent respiration, flux control mostly lies on complexes I and III, whereas in complex II-dependent respiration, control lies on complexes III and IV (Bianchi *et al.* 2004). The stoichiometry for complexes I:II:III:IV is 1:1.5:3:6–7, respectively (Schägger & Pfeiffer 2001); thus, a partial decrease in complexes II and IV contents would not be expected to modify respiratory activity as would for instance, complex I deficiency. After oophorectomy, complex IV activity decreased up to 300 ngAO/min·mg prot (~50% of the V_{max}); nevertheless, this value was still higher than the control respiratory rate in state 3 (Table 1). Thus, in Cast samples, succinate oxidation would not decrease as complex IV is still in excess compared to the other three complexes. Conversely, in the NADH–O_2 reaction, glutamate and malate were oxidized through different pathways to produce NADH and feed the respiratory chain via complex I. That is, electron flux was mostly limited by complex I. In addition to the gradual loss of complex I contribution (Fig. 2 and Table 2), we found a lower activity in two of NAD-dependent dehydrogenases from the Krebs cycle: PDH and 2-OGDH (Fig. 1 and Table 2), which must have limited even further the rate of electron transfer through this pathway. Further studies are required to explore these individual pathways in heart mitochondria after oophorectomy.

Furthermore, it has been described that the transcription of the mRNA encoding for complex I subunits ND1, NDUFS7 and NDUFS8 might be regulated by estrogens (Too *et al.* 1999, Noguchi *et al.* 2002, Chen *et al.* 2009). Thus, in the absence of estrogens, a decrease in complex I content and activity would be expected as observed here (Fig. 2A and B). Remarkably, expression of subunit ND1 did not change after castration (Fig. 1). ND1 is a mitochondrial DNA-encoded protein, whereas NDUFS7 and NDUFS8 are codified by nuclear genes (Chen *et al.* 2009). The last two subunits are associated with each other and are also known to be part of the catalytic site for ubiquinone (Sánchez-Caballero *et al.* 2016). We have not analyzed yet the expression of nuclear-encoded subunits, which are probably more susceptible to estrogenic regulation than the mitochondrial-encoded proteins as other nuclear proteins were clearly downregulated after oophorectomy (e.g. SDHC, COX IV, GA and PDH-E1α) (Fig. 1). For instance, GA expression is upregulated via estrogen-related receptor alpha (ERRα during cell differentiation (Huang *et al.* 2016)). Estrogen receptors are known to play a crucial role in the transcriptional control of mitochondrial function and energy metabolism (Hsieh *et al.* 2006, Huang *et al.* 2016).

Inability to regulate matrix solutes is among the first alterations in damaged mitochondria. Here, Cast mitochondria exhibited dysfunction in Ca^{2+} accumulation at the 3rd month after surgery (Fig. 3C). The inability of isolated heart mitochondria to hold Ca^{2+} and its further release may be due to MPTP activation and transmembrane potential depletion, a condition fully achieved at the 4th month (Hunter *et al.* 2012, Pavón *et al.* 2012). Different stress conditions such as ischemia, hypoxia, oxidative stress and cytotoxic drugs were identified as inducers of MPTP. A link between estrogen deficiency and MPTP activation is suggested, but then again, the mechanism remains obscure.

Cardiac mitochondria exist in two functionally distinct populations: subsarcolemmal mitochondria (SSM) and interfibrillar mitochondria (IFM) (Palmer *et al.* 1977). SSM are released by tissue homogenization leaving behind skinned myocytes; the liberation of IFM from skinned myocytes requires a brief exposure to a protease. Aging (Fujioka *et al.* 2011, Suh *et al.* 2003) and caloric restriction (Hofer *et al.* 2009) studies have shown that age-related decline in mitochondrial capacity affects IFM, whereas SSM located beneath the plasma membrane remain unaffected. Changes in morphology and disposition in IFM without estrogens were reported previously (Zhai *et al.* 2000); the SSM population was not studied by these authors. Based on these observations, it would be very interesting to determine whether changes occur only in the IFM population.

Moreover, it has been described that oxidative stress in Cast mitochondria and antioxidant systems, such as MnSOD, depends on estrogens (Baños *et al.* 2005*a*,*b*, Pedram *et al.* 2006, Bellanti *et al.* 2013). Thus, estrogen loss probably impairs SOD activity increasing ROS (Borras *et al.* 2007), as in fact we found (Figs 4 and 5). ROS damaged aconitase and increased malondialdehyde. Also, key enzymes involved in mitochondrial bioenergetics, such as 2-oxoglutarate dehydrogenase (OGDH), were

http://joe.endocrinology-journals.org
DOI: 10.1530/JOE-16-0161

Published by Bioscientifica Ltd.

probably affected by ROS (Gibson *et al*. 2000, Starkov *et al*. 2004, Martin *et al*. 2005).

In regard to the possibility of disequilibrium in apoptosis, we evaluated the expression of two members of the Bcl-2 protein family, which regulate apoptosis. We measured Bax, which is a pro-apoptotic protein and Bcl-2 that is an anti-apoptotic protein. Although Bax remained constant, Bcl-2 levels decreased at the 1st month after castration and then increased at the 3rd month (Fig. 7). However, no increase in apoptosis was observed (data not shown).

Our findings provide an important overview of the cardioprotective effect of estrogens on mitochondrial bioenergetics and dynamics. At menopause, the decrease in estrogens may contribute to cardiac vulnerability by playing important roles in intracellular energy and redox-dependent intracellular signaling. Mitochondrial contents have to adapt to cellular growth rate and meet cell requirements. In this landscape, estrogens could orchestrate a comprehensive cardiac transcriptional program including use of substrates, production and transport of ATP and modulation of antioxidant enzymes (Noguchi *et al*. 2002, Baños *et al*. 2005*a*,*b*, Klinge 2008). Estrogen levels in rats vary and seem to affect mitochondrial functions. In rats, it is known that steroidogenesis by testes or ovaries are reactivated at 30–45 days of postnatal life (Banu & Aruldhas 2002) reaching their maximum levels of estrogens at puberty at 10 weeks of age (Ojeda *et al*. 2007). To avoid hormonal influences and isolate estrogen depletion-related damage, three-week-old rats were used. Our animals will not be exposed to estrogens in their lifetime unless these are provided exogenously. Thus, our model is not exactly equivalent to menopause.

Sexual hormones affect diverse non-reproductive tissues including immune, central nervous and skeletal systems, as well as cells from liver, skin and kidneys (Smith *et al*. 1994, Carani *et al*. 1997, Kovats 2012, 2015, Koss *et al*. 2015, Khalid & Krum 2016, Khan & Ansar Ahmed 2016). There is a variety of biological effects, many of which bear no clear relationship to their primary reproductive functions. Particularly in rodents, estrogens have many actions that may affect the body weight and adiposity independently of feeding patterns, including energy expenditure, gastrointestinal function, basal metabolism, growth and body composition. For example, estrogen deprivation decreases triiodothyronine (Thomas *et al*. 1986). Thyroid hormones and estrogens exhibit overlapping functions and cross-modulate genes involved in reproduction and sexual behavior (Vasudevan *et al*. 2001). On the other hand, estrogens prevent hypertension by modulating the renin–angiotensin–aldosterone system (RAAS), acting not only on the kidney, heart and vasculature but also on the central nervous system (Sullivan 2008, Sandberg & Ji 2012, O'Donnell *et al*. 2014). Estrogens also modulate pituitary growth hormone (GH) secretion and signaling (Sinha *et al*. 1979, Kerrigan & Rogol 1992, Baik *et al*. 2011, Fernández-Pérez *et al*. 2013). Thus, after menopause or oophorectomy, a precipitous decline in insulin levels and sensitivity is present, parallels an increase in fat mass and elevations in circulating inflammatory markers, low-density lipoproteins (LDL), triacylglycerols and fatty acids, i.e. estrogen deprivation leads to metabolic syndrome (Pfeilschifter *et al*. 2002, Sites *et al*. 2002, Carr 2003, Toth *et al*. 2006). Estrogens have also been linked to cholecystokinin, increasing its satiation action (Asarian & Geary 2006). Low estrogen levels promote increased body weight and adiposity (Mauvais-Jarvis *et al*. 2013). This was also observed in our experimental groups (1st month Ctrl 75 ± 10 g vs Cast 85 ± 13 g; 2nd month Ctrl 109 ± 14 g vs Cast 137 ± 14 g; 3rd month Ctrl 216 ± 21 g vs Cast 269 ± 13 g).

Our study evaluated the progression of the oophorectomy-evoked changes in cardiac mitochondrial OXPHOS functions. These modifications were fully established only after three months of castration and not at 2 weeks as in mitochondria from other organs (Li *et al*. 2009, Cavalcanti-de-Albuquerque *et al*. 2014). These effects clearly mimic those observed in human menopause (Barrett-Connor 2013). Thus, our data provide strong evidence in favor of estrogen substitution therapy (Al-Safi & Santoro 2014, Whayne & Mukherjee 2015).

Surgical castration is generally favored as a model of menopause. However, 4-vinylcyclohexene diepoxide (VCD) has been recently proposed to reproduce 'menopausal conditions' as it destroys preantral ovarian follicles preserving ovaries (Hoer *et al*. 2001, Mayer *et al*. 2002). VCD increases markers of oxidative damage and inflammation (in liver and kidney) and also caspases 9 and 3 and other side effects (Abolaji *et al*. 2016). In heart, these secondary effects have not been discarded, so, we advocate surgery over VCD as a model to study estrogen depletion.

In conclusion, in rat heart mitochondria, estrogen deprivation gradually leads to (a) decreased contents and function of aerobic metabolism-related proteins such as complex I, complex IV, ATPase-b, ANT, PDH-E1α, 2KGDH, SDHC and GA; (b) impaired mitochondrial

http://joe.endocrinology-journals.org
DOI: 10.1530/JOE-16-0161

Published by Bioscientifica Ltd.

Ca^{2+} transport; (c) decreased ROS-detoxifying enzyme activities and (d) increased lipoperoxidation (MDA). By contrast, it is suggested that fusion and fission were not affected, as only small and reversible changes in proteins Fis-1, Drp-1 and OPA-1 were detected (Fig. 6). In addition, mitochondrial biogenesis probably was not affected as CS activity did not change after castration (Table 2). All oophorectomy effects were progressive; at month 1, some were hardly detectable and gradually became more evident at months 2 and 3. Our evidence suggests that estrogens regulate mitochondrial function (Hall *et al*. 2001, Duckles *et al*. 2006, Pedram *et al*. 2006, Psarra & Sekeris 2008, Yang *et al*. 2009), probably through transcriptional changes (Orshal & Khalil 2004, Klinge 2008, Mattingly *et al*. 2008) that lead to loss of OXPHOS.

Supplementary data

This is linked to the online version of the paper at http://dx.doi.org/10.1530/JOE-16-0161.

Declaration of interest

The authors declare that there is no conflict of interest that could be perceived as prejudicing the impartiality of the research reported.

Funding

Partially funded by PAPIIT/UNAM (Grant IN204015) and CONACyT (Grant 239487). This work is part of Project 14-865 Instituto Nacional de Cardiología.

Acknowledgements

The authors would like to thank Eréndira Reyes Camacho for her technical assistance and Dr Verónica Guarner for her valuable assistance and helpful discussions. A C O, C U A and N A R S are CONACyT fellows.

References

Abolaji AO, Tolovai PE, Odeleye TD, Akinduro S, Teixeira Rocha JB & Farombi EO 2016 Hepatic and renal toxicological evaluations of an industrial ovotoxic chemical 4-vinylcyclohexene diepoxide, in both sexes of Wistar rats. *Environmental Toxicology and Pharmacology* **13** 28–40. (doi:10.1016/j.etap.2016.05.010)

Ahmed SA, Hissong BD, Verthelyi D, Donner K, Becker K & Karpuzoglu-Sahin E 1999 Gender and risk of autoimmune diseases: possible role of estrogenic compounds. *Environmental Health Perspectives* **107** 681–686. (doi:10.1289/ehp.99107s5681)

Al-Safi ZA & Santoro N 2014 Menopausal hormone therapy and menopausal symptoms. *Fertility and Sterility* **101** 905–915. (doi:10.1016/j.fertnstert.2014.02.032)

Asarian L & Geary N 2006 Modulation of appetite by gonadal steroid hormones. *Philosophical Transactions of the Royal Society of London. Series B, Biological Sciences* **361** 1251–1263. (doi:10.1098/rstb.2006.1860)

Baik M, Yu JH & Hennighausen L 2011 Growth hormone-STAT5 regulation of growth hepatocellular carcinoma and liver metabolism. *Annals of the New York Academy of Sciences* **1229** 29–37. (doi:10.1111/j.1749-6632.2011.06100.x)

Banu KS & Aruldhas MM 2002 Sex steroids regulate TSH-induced thyroid growth during sexual maturation in Wistar rats. *Experimental and Clinical Endocrinology and Diabetes* **110** 37–42. (doi:10.1055/s-2002-19993)

Baños G, Medina-Campos ON, Maldonado PD, Zamora J, Pérez I, Pavón N & Pedraza-Chaverrí J 2005*a* Antioxidant enzymes in hypertensive and hypertriglyceridemic rats: effect of gender. *Clinical and Experimental Hypertension* **27** 45–57. (doi: 10.1081/ceh-200044255)

Baños G, Medina-Campos ON, Maldonado PD, Zamora J, Pérez I, Pavón N & Pedraza-Chaverrí J 2005*b* Activities of antioxidant enzymes in two stages of pathology development in sucrose-fed rats. *Canadian Journal of Physiology and Pharmacology* **83** 278–286. (doi:10.1139/y05-013)

Barrett-Connor E 2013 Menopause, atherosclerosis, and coronary artery disease. *Current Opinion in Pharmacology* **13** 186–191. (doi:10.1016/j.coph.2013.01.005)

Barrientos A, Fontanesi F & Díaz F 2009 Evaluation of the mitochondrial respiratory chain and oxidative phosphorylation system using polarography and spectrophotometric enzyme assays. *Current Protocols in Human Genetics* Chapter 19, Unit 19.3. (doi:10.1002/0471142905.hg1903s63)

Bellanti F, Matteo M, Rollo T, De Rosario F, Greco P, Vendemiale G & Serviddio G 2013 Sex hormones modulate circulating antioxidant enzymes: impact of estrogen therapy. *Redox Biology* **1** 340–346. (doi:10.1016/j.redox.2013.05.003)

Bianchi C, Genova ML, Parenti Castelli G & Lenaz G 2004 The mitochondrial respiratory chain is partially organized in a supercomplex assembly: kinetic evidence using flux control analysis. *Journal of Biological Chemistry* **279** 36562–36569. (doi:10.1074/jbc.M405135200)

Borras C, Gambini J & Vina J 2007 Mitochondrial oxidant generation is involved in determining why females live longer than males. *Frontiers in Bioscience* **12** 1008–1013. (doi:10.2741/2120)

Bradford MM 1976 A rapid and sensitive method for the quantitation of microgram quantities of protein utilizing the principle of protein-dye binding. *Analytical Biochemistry* **72** 248–254. (doi:10.1016/0003-2697(76)90527-3)

Carani C, Qin K, Simoni M, Faustini-Fustini M, Serpente S, Boyd J, Korach KS & Simpson ER 1997 Effect of testosterone and estradiol in a man with aromatase deficiency. *New England Journal of Medicine* **337** 91–95. (doi:10.1056/NEJM199707103370204)

Carr MC 2003 The emergence of the metabolic syndrome with menopause. *Journal of Clinical Endocrinology and Metabolism* **88** 2404–2411. (doi:10.1210/jc.2003-030242)

Cavalcanti-de-Albuquerque JPA, Salvador CI, Lopes ME, Jardim-Messeder D, Werneck-de-Castro JPS, Galina A & Carvalho DP 2014 Role of estrogen on skeletal muscle mitochondrial function in ovariectomized rats: a time course study in different fiber types. *Journal of Applied Physiology* **116** 779–789. (doi:10.1152/japplphysiol.00121.2013)

Chen JQ, Delannoy M, Cooke C & Yager DJ 2004 Mitochondrial localization of ERα and ERβ in human MCF7 cells. *American Journal of Physiology: Endocrinology and Metabolism* **286** E1011–E1022. (doi:10.1152/ajpendo.00508.2003)

Chen JQ, Cammarata PR, Baines CP & Yager JD 2009 Regulation of mitochondrial respiratory chain biogenesis by estrogens/estrogen receptors and physiological, pathological and pharmacological implications. *Biochimica et Biophysica Acta* **1793** 1540–1570. (doi:10.1016/j.bbamcr.2009.06.001)

Claeson K, Aberg T & Karlberg B 2000 Free malondialdehyde determination in rat brain tissue by capillary zone electrophoresis:

http://joe.endocrinology-journals.org
DOI: 10.1530/JOE-16-0161

Published by Bioscientifica Ltd.

evaluation of two protein removal procedures. *Journal of Chromatography B: Biomedical Applications* **740** 87–92. (doi:10.1016/S0378-4347(00)00030-X)

Compston JE 2001 Sex steroids and bone. *Physiological Reviews* **81** 419–447.

Cooney GJ, Taegtmeyer H & Newsholme EA 1981 Tricarboxylic acid cycle flux and enzyme activities in the isolated working rat heart. *Biochemical Journal* **200** 701–703. (doi:10.1042/bj2000701)

Dai Q, Shah AA, Garde RV, Yonish BA, Zhang L, Medvitz NA, Miller SE, Hansen EL, Dunn CN & Price TM 2013 A truncated progesterone receptor (PR_M) localizes to the mitochondrion and controls cellular respiration. *Molecular Endocrinology* **27** 741–753. (doi:10.1210/me.2012-1292)

Davies SM, Poljak A, Duncan MW, Smythe GA & Murphy MP 2001 Measurements of protein carbonyls, orthoand meta-tyrosine and oxidative phosphorylation complex activity in mitochondria from young and old rats. *Free Radical Biology and Medicine* **31** 181–190. (doi:10.1016/S0891-5849(01)00576-7)

Duckles SP, Krause DN, Stirone C & Procaccio V 2006 Estrogen and mitochondria: a new paradigm for vascular protection? *Molecular Interventions* **6** 26–35. (doi:10.1124/mi.6.1.6)

Fernández-Pérez L, Guerra B, Díaz-Chico JC & Flores-Morales A 2013 Estrogens regulate the hepatic effects of growth hormone, a hormonal interplay with multiple fates. *Frontiers in Endocrinology* **3** 66. (doi:10.3389/fendo.2013.00066)

Fujioka H, Moghaddas S, Murdock GD, Lesnefsky JE, Tandler B & Hoppel LC 2011 Decreased cytochrome c oxidase subunit VIIa in aged rat heart mitochondria: immunocytochemistry. *Anatomical Record* **294** 1825–1833. (doi:10.1002/ar.21486)

Gibson GE, Park LC, Sheu KF, Blass JP & Calingasan NY 2000 The alpha-ketoglutarate dehydrogenase complex in neurodegeneration. *Neurochemistry International* **36** 97–112. (doi:10.1016/S0197-0186(99)00114-X)

Giguere V, Tremblay A & Tremblay GB 1998 Estrogen receptor beta: re-evaluation of estrogen and antiestrogen signaling. *Steroids* **63** 335–339. (doi:10.1016/S0039-128X(98)00024-5)

Hall MJ, Couse FJ & Korach SK 2001 The multifaceted mechanisms of estradiol and estrogen receptor signaling. *Journal of Biological Chemistry* **276** 36869–36872. (doi:10.1074/jbc.R100029200)

Hausladen A & Fridovich I 1994 Superoxide and peroxynitrite inactivate aconitases, but nitric oxide does not. *Journal of Biological Chemistry* **269** 29405–29408.

Hoer PB, Devine PJ, Hu X, Thompson KE & Sipes IG 2001 Ovarian toxicity of 4-vinylcyclohexene diepoxide: a mechanistic model. *Toxicologic Pathology* **29** 91–99. (doi:10.1080/019262301301418892)

Hofer T, Servais S, Seo AY, Marzetti E, Hiona A, Upadhyay SJ, Wohlgemuth SE & Leewenburgh C 2009 Bioenergetics and permeability transition pore opening in heart subsarcolemmal and interfibrillar mitochondria: effects of aging and lifelong calorie restriction. *Mechanisms of Ageing and Development* **130** 297–307. (doi:10.1016/j.mad.2009.01.004)

Hsieh YC, Yu HP, Suzuki T, Choudhry MA, Schwacha MG, Bland KI & Chaudry IH 2006 Upregulation of mitochondrial respiratory complex IV by estrogen receptore-(beta) is critical for inhibiting mitochondrial apoptotic signaling and restoring cardiac functions following trauma-hemorrhage. *Journal of Molecular and Cellular Cardiology* **41** 511–521. (doi:10.1016/j.yjmcc.2006.06.001)

Huang T, Liu R, Fu X, Yao D, Yang M, Liu Q, Lu WW, Wu C & Guan M 2016 Aging reduces an ERRalpha-directed mitochondrial glutaminase expression suppressing glutamine anaplerosis and osteogenic differentiation of mesenchymal stem cells. *Stem Cells* [in press]. (doi:10.1002/stem.2470)

Hunter CJ, Machijas MA & Korzick HD 2012 Age dependent reductions in mitochondrial respiration are exacerbated by calcium in the female heart. *Gender Medicine* **9** 197–206. (doi:10.1016/j.genm.2012.04.001)

Irwin RW, Yao J, Hamilton RT, Cadenas E, Brinton RD & Nilsen J 2008 Progesterone and estrogen regulate oxidative metabolism in brain mitochondria. *Endocrinology* **149** 3167–3175. (doi:10.1210/en.2007-1227)

Irwin RW, Syeda SS, Hamilton RT, Cardenas E & Brinton RD 2011 Medroxyprogesterone acetate antagonizes estrogen up-regulation of brain mitochondrial function. *Endocrinology* **152** 556–567. (doi:10.1210/en.2010-1061)

Janssen JW & Helbing AR 1991 Arsenazo III: an improvement of the routine calcium determination in serum. *European Journal of Clinical Chemistry and Clinical Biochemistry* **29** 197–201.

Kerrigan JR & Rogol AD 1992 The impact of gonadal steroid hormone action on growth hormone secretion during childhood and adolescence. *Endocrine Reviews* **13** 281–298. (doi:10.1210/er.13.2.281)

Khalid AB & Krum SA 2016 Estrogen receptors alpha and beta in bone. *Bone* **87** 130–135. (doi:10.1016/j.bone.2016.03.016)

Khan D & Ansar Ahmed S 2016 The immune system is a natural target for estrogen action: opposing effects of estrogen in two prototypical autoimmune diseases. *Frontiers in Immunology* **3** 73–93. (doi:10.3389/fimmu.2015.00635)

Klinge MC 2008 Estrogenic control of mitochondrial function and biogenesis. *Journal of Cellular Biochemistry* **105** 1342–1351. (doi:10.1002/jcb.21936)

Knowlton AA & Lee RA 2012 Estrogen and the cardiovascular system. *Pharmacology and Therapeutics* **135** 54–70. (doi:10.1016/j.pharmthera.2012.03.007)

Koss WA, Lloyd MM, Sadowski RN, Wise LM & Juraska JM 2015 Gonadectomy before puberty increases the number of neurons and glia in the medial prefrontal cortex of female, but not male, rats. *Developmental Psychobiology* **57** 305–312. (doi:10.1002/dev.21290)

Kovats S 2012 Estrogen receptors regulate an inflammatory pathway of dendritic cell differentiation: mechanisms and implications for immunity. *Hormones and Behavior* **62** 254–262. (doi:10.1016/j.yhbeh.2012.04.011)

Kovats S 2015 Estrogen receptors regulate innate immune cells and signaling pathways. *Cellular Immunology* **294** 63–69. (doi:10.1016/j.cellimm.2015.01.018)

Li S, Li S, Hydery T, Juan Y, Lin WY, Kogan B, Mannikarottu A, Leggett RE, Schule C & Levin RM 2009 The effect of 2- and 4-week ovariectomy on female rabbit urinary bladder function. *Urology* **74** 691–696. (doi:10.1016/j.urology.2009.02.068)

Martin E, Rosenthal RE & Fiskum G 2005 Pyruvate dehydrogenase complex: metabolic link to ischemic brain injury and target ofoxidative stress. *Journal of Neuroscience Research* **79** 240–247. (doi:10.1002/jnr.20293)

Matthews J & Gustafsson A-J 2003 Estrogen signaling: a subtle balance between ERα and ERβ. *Molecular Interventions* **3** 281–292. (doi:10.1124/mi.3.5.281)

Mattingly KA, Ivanova MM, Riggs KA, Wickramasinghe NS, Barch MJ & Klinge CM 2008 Estradiol stimulates transcription of Nuclear Respiratory Factor-1 and increases mitochondrial biogenesis. *Molecular Endocrinology* **22** 609–622. (doi:10.1210/me.2007-0029)

Mauvais-Jarvis F, Clegg DJ & Henever AL 2013 The role of estrogens in control of energy balance and glucose homeostasis. *Endocrine Reviews* **34** 309–338. (doi:10.1210/er.2012-1055)

Mayer LP, Pearsall NA, Christian PJ, Devine PJ, Payne CM, McCuskey MK, Marion SL, Sipes IG & Hoyer PB 2002 Long-term effects of ovarian follicular depletion in rats by 4-vinylcyclohexene diepoxide. *Reproductive Toxicology* **16** 775–781. (doi:10.1016/S0890-6238(02)00048-5)

Mendoza-Garcés L, Mendoza-Rodríguez CA, Jiménez-Trejo F, Picazo O, Rodríguez MC & Cerbón M 2011 Differential expression of estrogen receptors in two hippocampal regions during the estrous cycle of the rat. *Anatomical Record* **294** 1913–1919. (doi:10.1002/ar.21247)

http://joe.endocrinology-journals.org
DOI: 10.1530/JOE-16-0161

Published by Bioscientifica Ltd.

Muller FL, Liu Y & Van Remmen H 2004 Complex III releases superoxide to both sides of the inner mitochondrial membrane. *Journal of Biological Chemistry* **279** 49064–49073. (doi:10.1074/jbc.M407715200)

Nadal-Casellas A, Proenza AM, Liadó I & Gianotti M 2011 Effects of ovariectomy and 17β-estradiol replacement on rat brown adipose tissue mitochondrial function. *Steroids* **76** 1051–1056. (doi:10.1016/j.steroids.2011.04.009)

Nilsen J & Diaz Brinton R 2003 Mechanism of estrogen-mediated neuroprotection: regulation of mitochondrial calcium and Bcl-2 expression. *PNAS* **100** 2842–2847. (doi:10.1073/pnas.0438041100)

Noguchi S, Nakatsuka M, Asagiri K, Habara T, Takate M, Konishi H & Kudo T 2002 Bisphenol A stimulates NO synthesis through a non-genomic estrogen receptor-mediated mechanism in mouse endothelial cells. *Toxicology Letters* **303** 29–34. (doi:10.1016/S0378-4274(02)00252-7)

Nuedling S, Kahlert S, Loebbert K, Meyer R, Vetter H & Grohe C 1999 Differential effects of 17β-estradiol on mitogen-activated protein kinase pathways in rat cardiomyocytes. *Federation of European Biochemical Societies Letters* **454** 271–276. (doi:10.1016/S0014-5793(99)00816-9)

O'Donnell E, Floras SJ & Harvey PJ 2014 Estrogen status and the renin angiotensin aldosterone system. *American Journal of Physiology: Regulatory, Integrative and Comparative Physiology* **307** R498–R500. (doi:10.1152/ajpregu.00182.2014)

Ojeda NB, Grigore D, Robertson EB & Alexandder BT 2007 Estrogen protects against increased blood pressure in postpubertal female growth restricted offspring. *Hypertension* **50** 679–685. (doi:10.1161/HYPERTENSIONAHA.107.091785)

Ong BS & Hausenloy JD 2010 Mitochondrial morphology and cardiovascular disease. *Cardiovascular Research* **88** 16–29. (doi:10.1093/cvr/cvq237)

Orshal MJ & Khalil R 2004 Gender, sex hormones and vascular tone. *American Journal of Physiology: Regulatory, Integrative and Comparative Physiology* **286** R233–R249. (doi:10.1152/ajpregu.00338.2003)

Palmer JW, Tandler B & Hoppel CL 1977 Biochemical properties of subsarcolemmal and interfibrillar mitochondria isolated from rat cardiac muscle. *Journal of Biological Chemistry* **252** 8731–8739.

Pavón N, Martínez-Abundis E, Hernández L, Gallardo-Pérez JC, Alvarez-Delgado C, Cerbón M, Pérez-Torres I, Aranda A & Chávez E 2012 Sexual hormones: effects on cardiac and mitochondrial activity after ischemia-reperfusion in adult rats. Gender difference. *Journal of Steroid Biochemistry and Molecular Biology* **132** 135–146. (doi:10.1016/j.jsbmb.2012.05.003)

Pedram A, Razandi M, Wallace CD & Levin RE 2006 Functional estrogen receptors in the mitochondria of breast cancer cells. *Molecular Biology of the Cell* **17** 2125–2137. (doi:10.1091/mbc.E05-11-1013)

Pérez-Torres I, Roque P, El Hafidi M, Diaz-Diaz E & Baños G 2009 Association of renal damage and oxidative stress in a rat model of metabolic syndrome. Influence of gender. *Free Radical Research* **43** 761–771. (doi:10.1080/10715760903045296)

Pfeilschifter J, Koditz R, Pfohl M & Schatz H 2002 Changes in proinflammatory cytokine activity after menopause. *Endocrine Reviews* **23** 90–119. (doi:10.1210/edrv.23.1.0456)

Psarra AM & Sekeris CE 2008 Steroid and thyroid hormone receptors in mitochondria. *International Union of Biochemistry and Molecular Biology Life* **60** 210–223. (doi:10.1002/iub.37)

Rosario GX, D'Souza SJ, Manjramkar DD, Parmar V, Puri CP & Sachvedra G 2008 Endometrial modifications during earl pregnancy in bonnet monkeys (Macaca radiata). *Reproduction Fertility and Development* **20** 281–294. (doi:10.1071/RD07152)

Sánchez-Caballero L, Guerrero-Castillo S & Nijtmans L 2016 Unraveling the complexity of mitocondrial complex I assembly: a dynamic process. *Biochimica et Biophysica Acta* **1857** 980–990. (doi:10.1016/j.bbabio.2016.03.031)

Sandberg K & Ji H 2012 Sex differences in primary hypertension. *Biology of Sex Differences* **3** 7. (doi:10.1186/2042-6410-3-7)

Schägger H 2001 Respiratory chain supercomplexes. *International Union of Biochemistry and Molecular Biology Life* **52** 119–128. (doi:10.1080/15216540152845911)

Schägger H & Pfeiffer K 2001 The ratio of oxidative phosphorylation complexes I-V in bovine heart mitochondria and the composition of respiratory chain supercomplexes. *Journal of Biological Chemistry* **276** 37861–37867.

Schwarzer M, Schrepper A, Amorim PA, Osterholt M & Doenst T 2013 Pressure overload differentially affects respiratory capacity in interfibrillar and subsarcolemmal mitochondria. *American Journal of Physiology: Heart and Circulatory Physiology* **304** H529–H537. (doi:10.1152/ajpheart.00699.2012)

Sherwin BB 1999 Can estrogen keep your smart? Evidence from clinical studies. *Journal of Psychiatry and Neuroscience* **24** 315–321.

Sinha YN Wicker MA, Salocks CB & Vanderlaan WP 1979 Gonadal regulation of prolactin and growth hormone secretion in the mouse. *Biology of Reproduction* **21** 473–481. (doi:10.1095/biolreprod21.3.763-s)

Sites CK, Toth MJ, Cushman M, L'Hommedieu GD, Tchernof A, Tracy RP & Poehlman ET 2002 Menopause-related differences in inflammation markers and their relationship to body fat distribution and insulin-stimulated glucose disposal. *Fertility and Sterility* **77** 128–135. (doi:10.1016/S0015-0282(01)02934-X)

Smith EP, Boyd J, Frank G, Takahashi H, Cohen RM, Specker B, Williams TC, Lubahn DB & Korach KS 1994 Estrogen resistance caused by a mutation in the estrogen-receptor gene in a man. *New England Journal of Medicine* **331** 1056–1061. (doi:10.1056/NEJM199410203311604)

Starkov AA, Fiskum G, Chinopoulos C, Lorenzo BJ, Browne SE, Patel MS & Beal MF 2004 Mitochondrial alpha-ketoglutarate dehydrogenase complex generates reactive oxygen species. *Journal of Neuroscience* **24** 7779–7788. (doi:10.1523/JNEUROSCI.1899-04.2004)

Stevenson JC 2000 Cardiovascular effects of estrogens. *Journal of Steroid Biochemistry and Molecular Biology* **74** 387–393. (doi:10.1016/S0960-0760(00)00117-5)

Stirone C, Duckles SP, Krause DN & Procaccion V 2005 Estrogen increases mitochondrial efficiency and reduces oxidative stress in cerebral blood vessels. *Molecular Pharmacology* **68** 959–965. (doi:10.1124/mol.105.014662)

Sugden PH & Clerk A 1998 Stress-responsive mitogen-activated protein kinases (c-Jun N-terminal kinases and p38 mitogen-activated protein kinases) in the myocardium. *Circulation Research* **83** 345–352. (doi:10.1161/01.RES.83.4.345)

Suh JH, Health SH & Hagen TM 2003 Two subpopulations of mitochondria in the aging rat heart display heterogenous levels of oxidative stress. *Free Radical Biology and Medicine* **35** 1064–1072. (doi:10.1016/S0891-5849(03)00468-4)

Sullivan JC 2008 Sex and the renin-angiotensin system: inequality between the sexes in response to RAS stimulation and inhibition. *American Journal of Physiology: Regulatory, Integrative and Comparative Physiology* **294** R1220–R1226. (doi:10.1152/ajpregu.00864.2007)

Thomas DK, Storlien LH, Bellingham WP & Gillette K 1986 Ovarian hormone effects on activity, glucoregulation and thyroid hormone in the rat. *Physiology and Behavior* **36** 567–573. (doi:10.1016/0031-9384(86)90332-X)

Too CK, Giles A & Wilkinson M 1999 Estrogen stimulates expression of adenine nucleotide translocator ANT1 messenger RNA in female rat hearts. *Molecular and Cellular Endocrinology* **25** 161–167. (doi:10.1016/S0303-7207(99)00002-7)

Toth MJ, Sites CK & Matthews DE 2006 Role of ovarian hormones in the regulation of protein metabolism in women: effects of menopausal status and hormone replacement therapy. *American Journal of Physiology: Endocrinology and Metabolism* **291** E639–E646. (doi:10.1152/ajpendo.00050.2006)

Vasudevan N, Davidovka G, Zhu YS, Koibuchi N, Chin WW & Ptaff D 2001 Differential interaction of estrogen receptor and thyroid

http://joe.endocrinology-journals.org
DOI: 10.1530/JOE-16-0161

Published by Bioscientifica Ltd.

hormone receptor isoforms on the rat oxytocin receptor promoter leads to differences in transcriptional regulation. *Neuroendocrinology* **74** 309–324. (doi:10.1159/000054698)

Wang J, Green PS & Simpkins JW 2001 Estradiol protects against ATP depletion, mitochondrial membrane potential decline and the generation of reactive oxygen species induced by 3-nitropropionic acid in SK-N-SH human neuroblastoma cells. *Journal of Neurochemistry* **77** 804–811. (doi:10.1046/j.1471-4159.2001.00271.x)

Whayne TF Jr & Mukherjee D 2015 Women, the menopause, hormone replacement therapy and coronary heart disease. *Current Opinion in Cardiology* **30** 432–438. (doi:10.1097/HCO.0000000000000157)

Wittig I, Karas M & Schägger H 2007 High resolution clear native electrophoresis for in-gel functional assays and fluorescence studies of membrane protein complexes. *Molecular and Cellular Proteomics* **6** 1215–1225. (doi:10.1074/mcp.M700076-MCP200)

Wohlgemuth SE, Calvani R & Marzetti E 2014 The interplay between autophagy and mitochondrial dysfunction in oxidative stress-induced cardiac aging and pathology. *Journal of Molecular and Cellular Cardiology* **71** 62–70. (doi:10.1016/j.yjmcc.2014.03.007)

Yang HS, Sarkar NS, Liu R, Pérez JE, Wang X, Wen Y, Yan JL & Simpkins WJ 2009 Estrogen receptor β as a mitochondrial vulnerability factor. *Journal of Biological Chemistry* **284** 9540–9548. (doi:10.1074/jbc.M808246200)

Zerbetto E, Vergani L & Dabbeni-Sala F 1997 Quantification of muscle mitochondrial oxidative phosphorylation enzymes via histochemical staining of blue native polyacrylamide gels. *Electrophoresis* **18** 2059–2064. (doi:10.1002/elps.1150181131)

Zhai P, Eurell TE, Cotthaus R, Jeffery EH, Bahr JM & Gross DR 2000 Effect of estrogen on global myocardial ischemia-reperfusion injury in female rats. *American Journal of Physiology: Heart and Circulatory Physiology* **279** H2766–H2775.

Received in final form 15 November 2016
Accepted 21 November 2016
Accepted Preprint published online 21 November 2016

http://joe.endocrinology-journals.org
DOI: 10.1530/JOE-16-0161

Published by Bioscientifica Ltd.

FEMS Pathogens and Disease, 74, 2016, ftv111

doi: 10.1093/femspd/ftv111
Advance Access Publication Date: 25 November 2015
Research Article

RESEARCH ARTICLE

Staphylococcus epidermidis: metabolic adaptation and biofilm formation in response to different oxygen concentrations

Cristina Uribe-Alvarez[1], Natalia Chiquete-Félix[1], Martha Contreras-Zentella[2], Sergio Guerrero-Castillo[3], Antonio Peña[1] and Salvador Uribe-Carvajal[1,*]

[1]Department of Molecular Genetics, Instituto de Fisiología Celular, Universidad Nacional Autónoma de México, 04510, México DF, México, [2]Department of Cellular and Developmental Biology, Instituto de Fisiología Celular, Universidad Nacional Autónoma de México, 04510, México DF, México and [3]Nijmegen Center for Mitochondrial Disorders, Radboud University Medical Center, 6525 GA Nijmegen, the Netherlands

*Corresponding author: Department of Molecular Genetics, Instituto de Fisiología Celular, Cdad Universitaria, Apdo Postal 70-472, Coyoacán, 04510 México, México. Tel: +5255-56225632; Fax: +5255-56225630; E-mail: suribe@ifc.unam.mx

One sentence summary: Biofilm formation by Staphylococcus epidermidis is enhanced in anaerobic conditions. Many enzymes are expressed as oxygen becomes low, which can be considered as possible therapeutic targets.

Editor: Tom Coenye

ABSTRACT

Staphylococcus epidermidis has become a major health hazard. It is necessary to study its metabolism and hopefully uncover therapeutic targets. Cultivating *S. epidermidis* at increasing oxygen concentration [O_2] enhanced growth, while inhibiting biofilm formation. Respiratory oxidoreductases were differentially expressed, probably to prevent reactive oxygen species formation. Under aerobiosis, *S. epidermidis* expressed high oxidoreductase activities, including glycerol-3-phosphate dehydrogenase, pyruvate dehydrogenase, ethanol dehydrogenase and succinate dehydrogenase, as well as cytochromes *bo* and *aa3*; while little tendency to form biofilms was observed. Under microaerobiosis, pyruvate dehydrogenase and ethanol dehydrogenase decreased while glycerol-3-phosphate dehydrogenase and succinate dehydrogenase nearly disappeared; cytochrome *bo* was present; anaerobic nitrate reductase activity was observed; biofilm formation increased slightly. Under anaerobiosis, biofilms grew; low ethanol dehydrogenase, pyruvate dehydrogenase and cytochrome *bo* were still present; nitrate dehydrogenase was the main terminal electron acceptor. KCN inhibited the aerobic respiratory chain and increased biofilm formation. In contrast, methylamine inhibited both nitrate reductase and biofilm formation. The correlation between the expression and/or activity or redox enzymes and biofilm-formation activities suggests that these are possible therapeutic targets to erradicate *S. epidermidis*.

Keywords: *Staphylococcus epidermidis*; biofilms; anaerobiosis; pathogenicity; therapeutic target; opportunistic

Received: 11 September 2015; **Accepted:** 23 November 2015

INTRODUCTION

Staphylococcus epidermidis is a coagulase-negative saprophytic inhabitant of the outer skin layers where it excludes pathogenic bacteria such as *S. aureus* (Otto 2009; Cogen *et al*. 2010). Regretfully, when *S. epidermidis* is introduced into tissues by needle punctures or surgical wounds, it becomes a major health hazard as it forms biofilms on catheters or prosthesis forcing their removal (Gristina 1987; Raad, Alrahwan and Rolston 1998). Among coagulase-negative staphylococci-caused prosthetic valve infective endocarditis, *S. epidermidis* is found in 82% cases (Mack *et al*. 2013). Also in 30%–43% implant perioperative infections (Zimmerli, Trampuz and Ochsner 2004) and in 50%–70% catheter-related infections (von Eiff, Peters and Heilmann 2002).

In spite of its growing importance as a human pathogen, the metabolism of *S. epidermidis* has not been fully characterized. Also, the signals that promote biofilm formation are poorly understood, although it is known that stress triggers the expression of proteins that bind cells together and enhance resistance to antiseptics, antibiotics and host defenses (Cramton *et al*. 2001; Vuong and Otto 2002; Kostakioti, Hadjifrangiskou and Hultgren 2013). To optimize treatment, *S. epidermidis* metabolism and biofilm-forming activity have to be understood (Vuong and Otto 2002).

Staphylococcus epidermidis is a facultative anaerobe, i.e. it can survive in a wide range of [O_2]. This bacterium thrives on human skin, where [O_2] ranges from 2% to 5% (Peyssonnaux *et al*. 2008) and also in ischemic/anoxic tumors and abscesses where [O_2] is zero (Atkuri *et al*. 2007; Wiese *et al*. 2012). *Staphylococcus epidermidis* biofilm-forming activity increases as [O_2] decreases (Cramton *et al*. 1999, 2001; Cotter, O'Gara and Casey 2009; Cotter *et al*. 2009). Indeed, production of biofilm-associated molecules such as the cell adhesion-promoting, extracellular polysaccharide β-1,6-linked glucosaminoglycan is enhanced at low [O_2] (Cramton *et al*. 1999). Anaerobic growth increases biofilm formation in both *S. aureus* and *S. epidermidis* (Cramton *et al*. 2001; Fuchs *et al*. 2007; Cotter *et al*. 2009).

Bacteria contain branched respiratory chains with multiple terminal oxidases that work at different [O_2] (Anraku 1988). These alternative pathways allow survival in adverse and changing environments (Nakano *et al*. 1997; Mukhopadhyay *et al*. 2002; Gandhi and Chikindas 2007; Desriac *et al*. 2013). In this regard, the closely related *S. aureus* modifies its respiratory chain as [O_2] varies (Taber and Morrison 1964; Artzatbanov and Petrov 1990; Fuchs *et al*. 2007; Gotz and Mayer 2013; Hammer *et al*. 2013). Thus, it was hypothesized that the adaptation of both the response to [O_2] and the propensity to form biofilms are related. The emerging pathological importance of *S. epidermidis* led us to analyze its oxidative phosphorylation machinery as well as the generation of biofilms when grown under aerobic, microaerobic or anaerobic conditions. Such knowledge may uncover different therapeutic targets as it has in other research efforts (Gordon *et al*. 2010; Hurdle *et al*. 2011; Kim *et al*. 2013).

MATERIALS AND METHODS

Materials

Brij 58, Ethylenediaminetetraacetic acid (EDTA), glycerol-3-phosphate, glycerol, horse heart cytochrome c, methyl-viologen, lead (II) nitrate, NAD^+, NADH, ATP, n-dodecyl β-D-maltoside, nitrotetrazolium blue chloride (NBT), phenylmethylsulfonyl fluoride (PMSF), sodium deoxycholate, sodium dithionite, sodium dodecyl sulfate, Gram Stain Kit and trizma base were from Sigma Co (St Louis, MO). Ethanol, magnesium sulfate, potassium nitrate, potassium cyanide, potassium carbonate, potassium hydroxide, sodium phosphate, sodium bicarbonate and succinic acid were from JT Baker (Center Valley, PA). TSB medium, 3,3′-Diaminobenzidine tetrahydrochloride hydrate (DAB) and digitonin were from Fluka (Taufenkirchen, Germany). Ammonium persulfate, acrylamide and Bis N,N´-Methylene-bis-acrylamide were from BioRad (Richmond, CA). Imidazol and ξ-aminocaproic were from MP (Santa Ana, CA). Glucose and ammonium sulfate were from Merck (Kenilworth, NJ); Tryptone was from Difco (Sparks, MD); yeast extract was from Bioxon; and PCR Master mix (2X) was from Thermo Scientific (Whaltham, MA).

Bacterial strain and growth

Staphylococcus epidermidis ATCC 12228 was donated by Dr Juan Carlos Cancino Díaz (Instituto Politécnico Nacional). Bacteria were grown in LB medium at 27°C under aerobic (*Ae*) conditions under shaking (250 rpm) unless otherwise specified; under microaerobic (μA) conditions (5% CO_2 atmosphere, static); and under anaerobic (*An*) conditions generated with GazPak EZ anaerobe pouch in a sealed acrylic chamber (static). Pre-cultures were grown in TSB for 24 h at 37°C, 250 rpm. A 1:15 dilution in LB was made in a sterile 100-well TrueLine Honeycomb Cell Culture Plate and grown at 27°C. Absorbance at 600 nm was measured every 3 h in a Bioscreen C spectrophotometer (Growth Curves, USA). To induce cytochrome *bd* expression, *S. epidermidis* was grown in G-medium (Hanson, Srinivasan and Halvorson 1963) with 0.8% casein hydrolysate, 0.32% L-Glutamic acid, 0.21% D-L alanine and 0.12% asparagine under μA for 48 h (Escamilla *et al*. 1987).

DNA extraction, *mutS* and *yqiL* amplification

DNA extraction was performed with a Quick-gDNA MiniPrep from Zymo Research. *mutS* and *yqiL* genes were amplified by PCR using a PCR Master Mix (Life technologies) containing *Taq* polymerase. Oligonucleotides used to amplify a mismatch repair protein *mutS* were as follows:

mutS − *F*3 (GATATAAGAATAAGGGTTGTGAA
and
mutS − R3 GTAATCGTCTCAGTTATCATGTT)

which amplified a 412-bp fragment (Thomas *et al*. 2007). Acetyl coenzyme A acetyltransferase *yqiL* oligonucleotides were as follows:

yqiL − *F*2 (CACGCATAGTATTAGCTGAAG)
and
yqiL − R2 (CTAATGCCTTCATCTTGAGAAATAA)

which amplified a 416-bp fragment (Wang *et al*. 2003). Both PCR assays involved an initial denaturation at 94°C for 5 min, 35 cycles of 94°C for 1 minute, 55°C for 40 s and 72°C for 40 s; and a final extension of 72°C for 5 min. PCR amplification products were subjected to electrophoresis in 1% agarose gels and ethidium bromide staining.

Biofilm detection

Staphylococcus epidermidis pre-cultures and cultures were performed as indicated previously. After incubation in 300 μL for

6, 12, 24 or 30 h in Costar 96 well plates, each well was gently washed three times with 200 μL phosphate-buffered saline (PBS), dried and stained with 1% crystal violet for 15 min. Plates were rinsed with PBS three more times, and bound crystal violet was solubilized in 200 μL ethanol-acetone (80:20 v/v). Optical density at 600 nm (OD_{600}) was determined in a Polar Star Omega (BMG Labtech) microplate reader (Okajima *et al.* 2006). To evaluate the effect of different respiratory chain inhibitors, cyanide or methylamine was added to the microplate at the beginning of the assay.

Bovine heart mitochondria

Beef heart mitochondria (BHM) obtained as in Löw and Vallin (1963) were a gift from Dr Marietta Tuena (IFC, UNAM). These were used as activity standards for different mitochondrial respiratory enzymes and for ATPase (Wittig, Braun and Schagger 2006; Wittig, Karas and Schagger 2007).

Cell membrane isolation

All procedures were conducted at 4°C. Cells were centrifuged at 10 000 × *g* for 10 min and washed with isolation buffer (50 mM Tris-HCl pH 7.4). The pellet was suspended in isolation buffer plus 1mM EDTA and 1 mM PMSF. Cells were disrupted by five passages through a French Press at 4000 psi (SLM Aminco). The suspension was centrifuged at 10 000 × *g* for 20 min to remove unbroken cells; the supernatant was centrifuged at 200 000 × *g* for 90 min (Niebisch and Bott 2003). The membrane pellet was resuspended and homogenized in isolation buffer plus 1mM PMSF. Protein was quantified by Bradford, frozen at −70°C and stored until further use.

Spectral analysis of cytochromes

Cell membranes from 24-h cultures grown in LB media at 27°C were suspended in 50 mM Tris-HCl buffer (pH 7.4) plus 30% (v/v) glycerol, frozen with liquid nitrogen in 2 mm light path cuvettes and analyzed in an Olis DW2000 spectrophotometer. Differential spectra from 400 to 700 nm were obtained from dithionite-reduced minus persulfate-oxidized and dithionite + CO-reduced minus dithionite-reduced membranes.

Nitrate reductase activity

Cells grown under *Ae*, μ*A* or *An* conditions were sonicated three times 30 s with 10 s rests and centrifuged at 10 000 × *g* for 10 min to remove unbroken cells. Methyl-viologen oxidation by nitrate reductase of the cytosolic membrane extracts was recorded at 546 nm in an Aminco-Olis DW 2000 spectrophotometer. Samples (10 μg protein) were assayed in 50 mM potassium phosphate (pH 7) with 0.2 mM methyl viologen previously reduced with 2.9 mM sodium dithionite. The reaction was started with 5 mM potassium nitrate (Kern and Simon 2009). Specific activities were calculated using an extinction coefficient of 19.5 mM^{-1} cm^{-1}. When indicated, methylamine was added at the beginning of the assay (Franco, Cárdenas and Fernández 1984; McCarty and Bremner 1992).

Electrophoretic techniques and in-gel activities

Clear native gel electrophoresis (CN-PAGE) was performed according to Wittig and Schagger (2005) and Wittig, Karas and Schagger (2007). Isolated membranes from *S. epidermidis* and BHM were solubilized with 1% Brij 58 and 0.5 mg lauryl maltoside/mg protein respectively and shaken for 1 h at 4°C. Membranes were centrifuged at 100 000 × *g* at 4°C for 30 min. Supernatants protein concentration was determined by Bradford and 0.1–0.3 mg protein per well was loaded on 4–12% polyacrylamide gradient gels. When clear native electrophoresis was performed, 0.01% Lauryl maltoside and 0.05% sodium deoxycholate were added to the cathode buffer as in Wittig, Karas and Schagger (2007). Gels were run for an hour at 15 mA/gel in a Bio-rad electrophoresis chamber.

In-gel NADH:NBT oxidoreductase activity (120 μg protein for *S. epidermidis* and 20 μg protein for BHM) was determined by incubating the native gels in 10 mM Tris (pH 7.0), 0.5 mg nitrotetrazolium blue chloride (NBT)/mL and 1 mM NADH. In-gel succinate:NBT oxidoreductase activity (120 μg protein for *S. epidermidis* and 100 μg protein for BHM) was determined by incubating the native gels in 10 mM Tris (pH 7.0), 0.5 mg nitrotetrazolium blue chloride (NBT)/mL and 1 mM succinate. In-gel cytochrome *c* oxidase activity (150 μg protein for *S. epidermidis* and 20 μg protein for BHM) was determined using diaminobenzidine (Wittig, Karas and Schagger 2007). In-gel ATPase activity (200 μg *S. epidermidis* protein and 100 μg BHM protein) was measured by incubating the CN-gel in 35 mM Tris with 270 mM glycine (pH 8.4) for an hour, then 0.2% $Pb(NO_3)_2$, 14 mM $MgSO_4$ and 8 mM ATP were added (Wittig, Karas and Schagger 2007).

Glycerol-3-phosphate dehydrogenase activity

Activity was measured in lysates from cells grown in different [O_2] in fresh 33 mM ammonium sulfate, 100 mM carbonate-bicarbonate buffer, 1 mM NAD^+ (pH 7.0) and 100 mM of glycerol-3-phosphate as substrate. Final solution was adjusted to pH 9.0 with KOH or HCl. Absorbance change for NADH was measured at 340 nm and specific activities were calculated (Burton 1955; Van Eys, Nuenke and Patterson 1959).

Mass spectrometry

From the CN-PAGE gel, the indicated bands were excised and in-gel digested with trypsin. Peptides were analyzed by liquid chromatography tandem mass spectrometry (LC-MS/MS) a in a Q-exactive mass spectrometer (Thermo Fisher Scientific) equipped at the front end with a nano-flow high-performance liquid chromatography system Agilent1200s (Wessels *et al.* 2013). Peptides were separated in a 100 μm ID PicoTip emitter column filled with 3 μm C18 reverse phase silica beads using 30 min linear gradients of 5%–35% acetonitrile with 0.1% formic acid. The mass spectrometer operated in a Top 20 dependent, positive ion mode switching automatically between MS and MS/MS. Full scan MS mode (400–1400 m z^{-1}) was operated at a resolution of 70 000 with automatic gain control target of 1 × 10^6 ions and a maximum ion transfer of 20 ms. Raw files were analyzed by MaxQuant software (version 1.5). Spectra were searched against the *S. epidermidis* database with additional sequences of known contaminants and reverse decoy with a strict FDR of 0.01. Trypsin was selected as the protease with two missed cleavages allowed. Dynamic modifications included N-terminal acetylation and oxidation of methionine. Cystein carbamidomethylation was set as fixed modification.

Oxymetry

Staphylococcus epidermidis grown under *Ae*, μ*A* or *An* conditions were resuspended in 10 mM Hepes pH 7.4. Protein

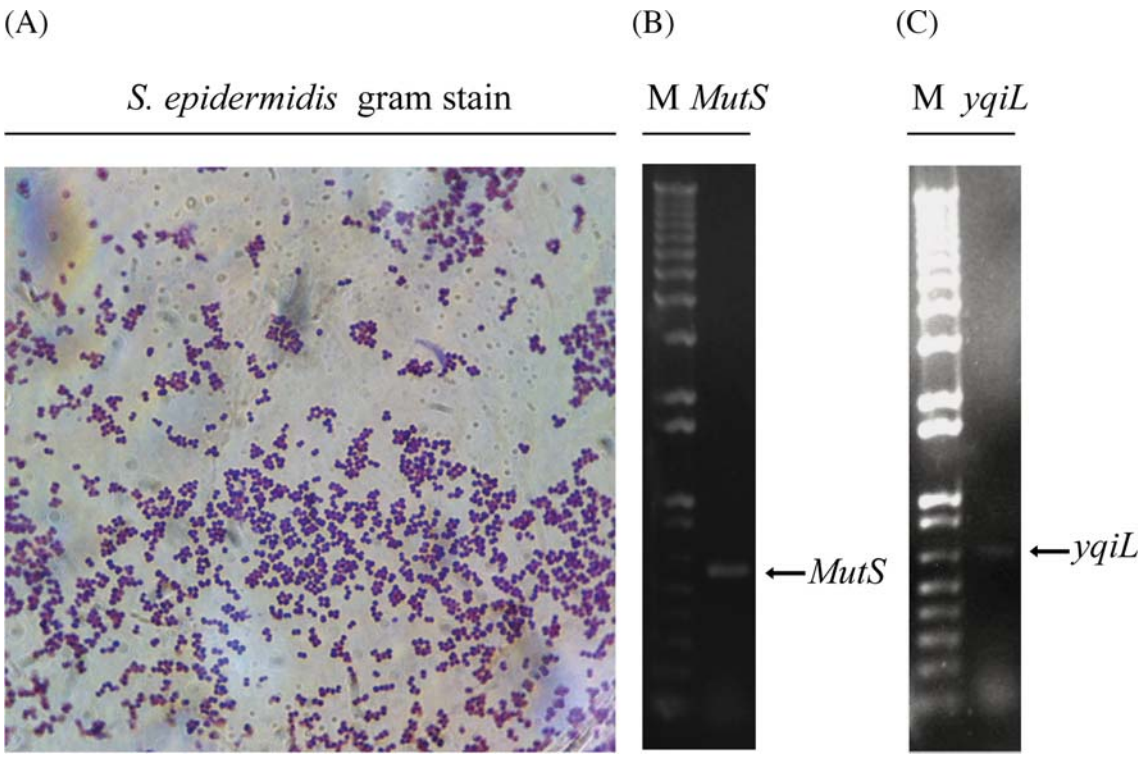

Figure 1. Characterization of *S. epidermidis* ATCC 12228. (**A**) Gram stain was performed using a kit from Sigma diagnostics HT90-A. Image shows Gram-positive cocci in clusters, diplococci and cocci. (**B**) Staphylococcus *epidermidis*-specific gene amplification. 1: 1kb plus marker, Invitrogen. 2: PCR product of DNA mismatch repair protein oligonucleotides (mutS) of 412 pb C. Staphylococcus *epidermidis* specific gene amplification. 1: 1kb plus marker, Invitrogen. 2: PCR product of Acetyl coenzyme A acetyltransferase (yqiL) of 416 pb.

concentration was determined by Biuret in a Beckman Coulter spectrophotometer at 540 nm. Oxygen consumption by cells was assessed in an oxygen meter model 782 (Warner/Strathkelvin Instruments) with a Clark type electrode in a 1 mL water-jacketed chamber at 30°C. Approximately 5 mg mL^{-1} of cells were added to the chamber. Reaction was started by the addition of 10 μM of ethanol (Guerrero-Castillo *et al.* 2009). Data were analyzed using the 782 Oxygen System Software (Warner/Strathkelvin Instruments). Different concentrations of cyanide were used as a respiratory chain inhibitor in order to block oxygen consumption.

Statistics

Results are expressed as mean ± standard deviation from at least four individual experiments to which Tukey´s test was applied. Significance levels and number of experiments were specified under each figure.

RESULTS

Staphylococcus epidermidis adaptability to different [O_2] is illustrated by the plasticity of the respiratory chain and the variations in biofilm formation. Under the microscope, *S. epidermidis* ATCC 12228 colonies formed typical clusters (Fig. 1A). The identity of *S. epidermidis* ATCC 12228 was confirmed by amplifying DNA oligonucleotides from the mismatch repair protein (*mutS*) (Fig. 1B, first gel) and from acetyl coenzyme A acetyltransferase (*yqiL*) (Fig. 1B, second gel). (Wang *et al.* 2003; Thomas *et al.* 2007)

Bacterial growth and biofilm formation at different [O_2]. The adaptability of *S. epidermidis* to different [O_2] was analyzed in cultures under atmospheric oxygen, with (*Ae*) or without agitation, under μA or under *An* conditions (Fig. 2A). In the absence of agitation, at all [O_2] tested, cells grew to a similar density reaching the stationary phase at 24–27 h. In contrast, under agitation at atmospheric [O_2] (*Ae*) the stationary phase was reached within half the time (Fig. 2A).

Even though *S. epidermidis* ATCC 12228 is considered a low-virulence, low-biofilm forming strain, we were able to detect biofilm formation (Fazly Bazzaz *et al.* 2014). In this strain, biofilm-generation decreased as [O_2] increased (Fig. 2B). In *Ae* cells with agitation, biofilms were hardly detectable and they increased slightly in cells subjected to *Ae*-without shaking. Biofilms were large in μA and *An* samples (Fig. 2B). Thus, in *S. epidermidis* increasing [O_2] stimulated growth while inhibiting biofilm formation. i.e. at low oxygen concentration, biofilm formation was high, suggesting that low [O_2] contributes to bacterial virulence (Gristina 1987; Raad, Alrahwan and Rolston 1998).

Detection of Oxidative Phosphorylation-related proteins in S. epidermidis grown at different [O_2]. The adaptive response of *S. epidermidis* to different [O_2] implies handling [O_2] and phosphorylating ADP. Thus, we evaluated the composition of the respiratory chain and the expression of F_1F_0-ATPase. Solubilized plasma membranes from *Ae*, μA or *An* cells were subjected to clear native PAGE, and protein bands were revealed by Coomassie blue staining (Fig. 3A). These samples were used to measure in-gel NADH dehydrogenase (Fig. 3B), succinate dehydrogenase (Fig. 3C) and ATPase (Fig. 3D) activities. In all cases, BHM were used as a positive control (Fig. 3 BHM lanes). BHM bands were labeled according to the migration and activity patterns reported for each complex (I, V, III, IV and II) (Fig. 3A BHM) (Schagger and von Jagow 1991; Wittig, Braun and Schagger 2006; Wittig, Karas and Schagger 2007). I for NADH dehydrogenase activity from complex I, V for ATPase activity of complex V and II for succinate dehydrogenase activity of complex II. Bands corresponding to

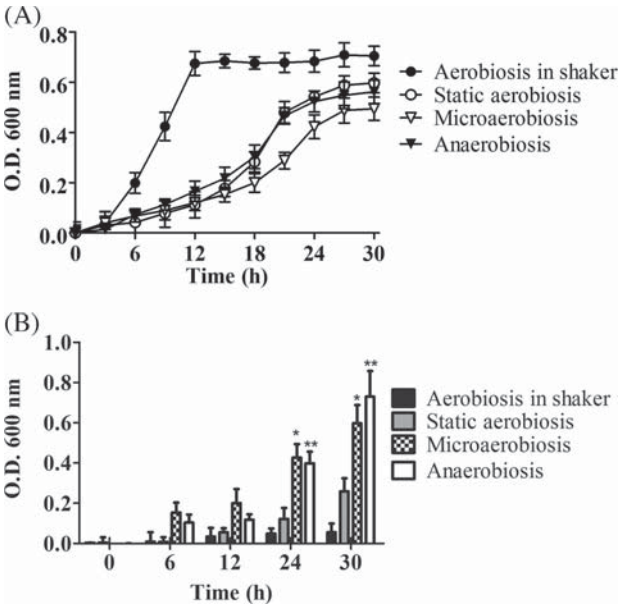

Figure 2. *Staphylococcus epidermidis* growth and biofilm formation under different aeration conditions. **(A)** Growth curves of *S. epidermidis* at 27°C at aerobic (atmosphere oxygen level) with and without shaking, microaerobic (5% CO_2) and anaerobic environment. Absorption at 600 nm was measured in a Bioscreen C spectrophotometer. Data shown are mean ± S.D. from $n = 18$. **(B)** Staphylococcus *epidermidis* biofilm formation at 6, 12, 24 or 30 h. Solubilized crystal violet was measured at 600 nm using a Polar Star Omega (BMG Labtech) microplate reader. Tukey´s comparison test showed significant difference ($^*P < 0.05$) between biofilm formation in microaerobic and anaerobic conditions between 6 and 24 and 30 h. After 6 h, a significant biofilm formation difference ($^*P < 0.05$) was found between aerobic conditions with and without shaking and microaerobic and anaerobic conditions. No difference was observed between oxygen-limited conditions at all times, $n = 6$.

BHM respiratory complexes III and IV are also indicated although no complex III or IV activities were detected in *S. epidermidis* (result not shown). *Staphylococcus epidermidis* cells grown at different [O_2] exhibited different protein bands (Fig. 3A, *S. epidermidis* lanes) that were further analyzed for oxidoreductase and ATPase activities.

NADH dehydrogenase in-gel activity (Fig. 3B) in BHM complex I was detected at 1000 kDa NADH dehydrogenase activity band (Fig. 3B, BHM band I) (Wittig, Braun and Schagger 2006; Wittig, Karas and Schagger 2007). For *S. epidermidis* grown in *Ae*, four NADH dehydrogenase activity bands of lower molecular weight were observed (Fig. 3B lane *S. epidermidis Ae*). In *μA* or *An* cells, these bands were either not observed (N1) or were much lighter (N2, N3 and N4) (Fig. 3B, lanes *S. epidermidis Ae*, *μA* and *An*).

Complex II succinate dehydrogenase activity from BHM was detected as a single 130 kDa band (Fig. 3C, BHM, band II) (Wittig, Braun and Schagger 2006). In *S. epidermidis*, one succinate dehydrogenase activity band was detected in *Ae* grown cells and was practically lost under O_2-limiting conditions (Fig. 3A and C, lanes *S. epidermidis Ae*, *μA* and *An*).

Cytochrome *c* oxidase in-gel activity was detected in BHM membranes as a single band (results not shown) corresponding to complex IV, MW 200 kDa (Wittig, Braun and Schagger 2006). No oxidase activity was detected in *S. epidermidis* even when adding up to 300 *μ*g of protein (results not shown). Thus, in agreement with others (Taber and Morrison 1964), it is concluded that cytochrome c oxidase is not present in *S. epidermidis*.

The ATPase activity assay revealed a strong band in the BHM sample (Fig. 3D, BHM, band V). *Staphylococcus epidermidis Ae* exhibited two ATPase activity bands (Fig. 3D, *Ae*, bands A1 and A2 while *μA* and *An* revealed only one band (Fig. 3D *μA* and *An* bands). Taken together, the above data indicate that in *S. epidermidis* oxidative-phosphorylation-related activities increased in cells grown at higher [O_2].

Identification of in-gel activity bands by mass spectroscopy: Bands exhibiting the tested oxidoreductase or ATPase activities (Fig. 3), i.e. bands N1, N2, N3, N4, S1 and A1 were identified by LC-MS/MS and were matched against all *S. epidermidis* protein entries of the NCBI database (Table 1). Band N1 sequencing revealed, among other proteins, an aerobic glycerol-3-phosphate dehydrogenase, a NADH dehydrogenase-like protein (SE_0635) and a glycine decarboxylase complex. Band N2 contained the pyruvate dehydrogenase complex (PDC), constituted by

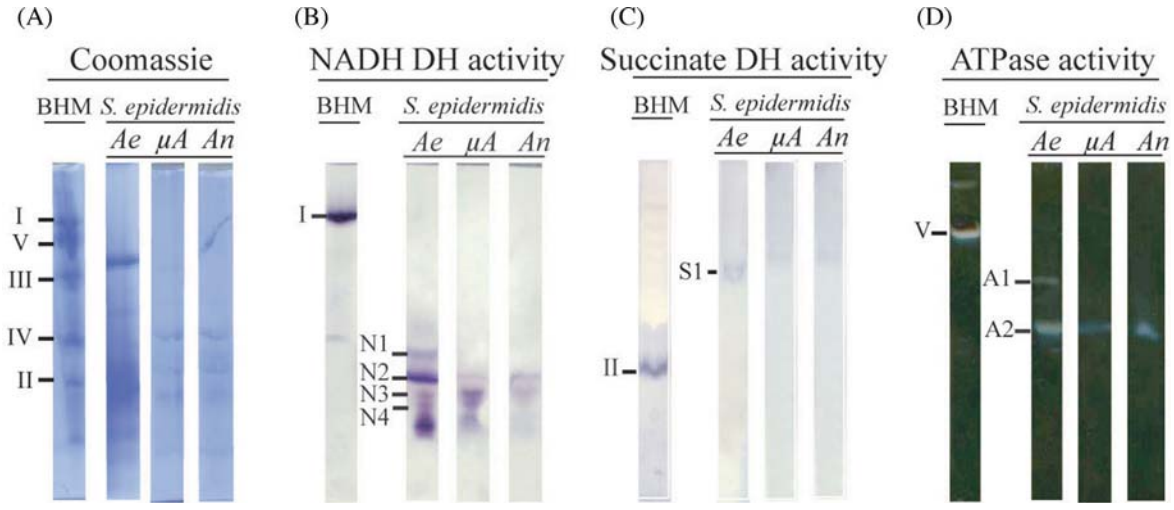

Figure 3. *Staphylococcus epidermidis* membrane protein electrophoretic analysis. Oxidoreductase in-gel activities from *S. epidermidis* membranes grown in different [O_2] were evaluated. BHM was solubilized with Lauryl maltoside. Staphylococcus *epidermidis* membranes were obtained from cultures grown under: (*Ae*) aerobic conditions, (*μA*) microaerobic conditions, (*An*) anaerobic conditions. **(A)** Solubilisates were resolved by CN-PAGE in a 4%–12% polyacrylamide gradient gel and stained with Coomasie. **(B)** In-gel NADH-NBT activity: BHM revealed complex I band **(I)** and *S. epidermidis* aerobic grown membranes revealed four bands labeled as N1, N2, N3 and N4. **(C)** In-gel Succinate-NBT activity: BHM band II corresponds to complex II. Band S1 of *S. epidermidis* was present only in aerobic growth conditions. **(D)** In-gel ATPase activity: BHM Band V corresponds to complex V. *S. epidermidis* ATPase activity was labeled as bands A1 and A2.

Table 1. Analyzed proteins by LC/MS-MS protein sequencing from a Coomassie stained CN-PAGE gel.

Band	Protein name or BLAST homology	NCBI database number	Peptides	MW (kDa)	PEP
N1	Aerobic glycerol-3-phosphate dehydrogenase (*S. epidermidis* ATCC 12228)	gi|81842889	27	62.3	4.62^{-211}
	NADH dehydrogenase-like protein SE_0635	gi|695605246	3	43.86	2.02^{-10}
	Glycine decarboxylase subunit 1	gi|81674491	6	49.96	5.8^{-48}
	Glycine decarboxylase subunit 2	gi|81674492	4	56.4	5.72^{-11}
N2	Dihydrolipoamide dehydrogenase (E3)	gi|721492590	21	49.7	0
	Pyruvate dehydrogenase E1 component subunit β	gi|81674992	21	35.29	1.07^{-167}
	Pyruvate dehydrogenase E1 component subunit α	gi|81674993	12	41.33	1.63^{-222}
	Dihydrolipoamide acetyltransferase component (E2)	gi|694237422	10	46.22	1.08^{-52}
	Glycerol-3-phosphate dehydrogenase	gi|81674534	19	36.12	6.54^{-36}
	Malate:quinone oxidoreductase	gi|721493807	9	56.35	2.51^{-29}
N3	Dihydrolipoamide dehydrogenase	gi|721492590	21	49.7	0
	NADH dehydrogenase-like protein SE_0635	gi|695605246	5	43.86	1.35^{-16}
	Lactate dehydrogenase, partial	gi|520977789	3	32.54	5.04^{-11}
N4	Alcohol dehydrogenase	gi|721493754	13	37.8	9.40^{-225}
	Glyceraldehyde-3-phosphate dehydrogenase	gi|81675183	7	36.2	3.96^{-57}
	Lactate dehydrogenase, partial	gi|520977789	3	36.19	3.39^{-25}
S1	Succinate dehydrogenase/fumarate reductase, flavoprotein subunit	gi|721492636	29	65.631	9.83^{-102}
	Succinate dehydrogenase	gi|721492637	9	31.43	0
	Putative succinate dehydrogenase, cytochrome *b556* subunit	gi|291319172	1	20.2	6.22^{-8}
	cytochrome *aa3* quinol oxidase, subunit I (*S. caprae*)	gi|242348990	10	75.38	$1.37E^{-97}$
	cytochrome *aa3* quinol oxidase, subunit II (*S. caprae*)	gi|242348991	7	42.7	$6.04E^{-76}$
A1	ATP synthase subunit alfa	gi|81170377	22	54.7	0
	ATP synthase subunit beta	gi|81170379	35	55.6	0
	ATP synthase subunit delta	gi|488441919	11	16.8	5.52^{-147}
	ATP synthase subunit gamma	gi|81842668	10	31.94	2.68^{-97}
	ATP synthase F1, epsilon subunit	gi|691218402	4	14.09	3.48^{-73}
	ATP synthase subunit b	gi|81842667	3	19.47	1.07^{-26}

pyruvate dehydrogenase, dihydrolipoamide acetyltranferase and dihydrolipoamide dehydrogenase, a glycerol-3-phosphate dehydrogenase, and a malate:quinone oxidoreductase; band N3 also contained enzymes from the PDC, a partial lactate dehydrogenase (LDH) and the NADH dehydrogenase-like protein (SE_0635) found in the N1 band; in N4 proteins included alcohol dehydrogenase, glyceraldehyde-3-phosphate dehydrogenase, a partial LDH (Table 1). Aerobic glycerol-3-phosphate dehydrogenase (SE_0979 MW = 62.3 kDa) from the N1 band is the one with highest number of peptides identified and the least error. Previous work in isolating glycerol-3-phosphate dehydrogenase from Escherichia *coli* (Schryvers, Lohmeier and Weiner 1978) and data from the crystal structure (Yeh, Chinte and Du 2008) indicate that the aerobic glycerol-3-phosphate dehydrogenase works as a dimeric enzyme, so it is possible that in *S. epidermidis* glycerol-3-phosphate dehydrogenase is also a dimer that feeds electrons directly to the respiratory chain. NADH dehydrogenase-like protein (SE_0635 MW = 43.86 kDa identified in bands N1 and N3 with a very low peptide count and a high posterior error (PEP) may be a type 2 NADH:quinone oxidoreductase (NDH-2), which is a single 50 kDa subunit protein with FAD as a non-covalently bound cofactor (Schurig-Briccio *et al.* 2014). Bacterial complex I weighs 500–600 kDa depending on the bacterium under study (Young, Jaworowski and Poulis 1978; Young *et al.* 1982; Bergsma, Van Dongen and Konings 2008; Baradaran *et al.* 2013). The *S. epidermidis* genome shows no other NADH dehydrogenases (NC_004461.1). As reported for *S. aureus* (Schryvers, Lohmeier and Weiner 1978), bacterial respiratory complex I was absent in *S. epidermidis*. Unrelated to oxidoreductase activity, we found glycine decarboxylase, a membrane-bound complex that catalyzes the oxidative decarboxylation of glycine.

Both N2 and N3 bands (Table 1) contain the PDC. PDC contains multiple copies of all three enzymatic components: pyruvate dehydrogenase E1 components α (Q8CPN3) and β (Q8CPN2) and dihydrolipoamide acetyltransferase E2 (Q8CTW0), and dihydrolipoamide dehydrogenase E3 (GenBank: KGY36148.1). The PDC decarboxylates pyruvate into acetyl-CoA that participates in the citric acid cycle and feeds the electron transport chain. Band N2 also revealed a malate:quinone oxidoreductase. The malate:quinone oxidoreductase complex oxidizes malate to oxaloacetate donating its electrons to quinone. This complex is absent in mammalians, which makes it a potential drug target. Bands N3 and N4 revealed the presence of an LDH. LDH from *Lactobacillus casei* is a dimeric 70 kDa enzyme (Padgaonkar and Nadkarni 1980). Finally, band N4 has an alcohol dehydrogenase, reported to be a dimeric enzyme of approximately 80 kDa (Hammes-Schiffer and Benkovic 2006).

Band S1 sequence revealed a succinate dehydrogenase/fumarate reductase flavoprotein subunit (SE_0841, MW = 66 kDa). The much larger mass observed here suggests that we isolated the whole succinate dehydrogenase complex (SDC), including succinate dehydrogenase cytochrome *b*-558 (SE_0840, MW 23.67 kDa) and succinate dehydrogenase iron–sulfur protein subunit (SE_0842, MW 31.4 kDa). The complex may also be interacting with other proteins. In *Bacillus subtilis*, the CN-PAGE in-gel activity band for succinate dehydrogenase is reported at 301 kDa because a complex with nitrate reductase may be formed (Sousa *et al*. 2013). In *Wolinella succinogenes* and in *E. coli*, the SDC is crystallized as a dimeric enzyme (Lancaster and Kroger 2000; Cecchini *et al*. 2002). Also, SDC might be in a complex with one or two small hydrophobic polypeptides that anchor the enzyme to the membrane and are required for electron transfer to quinone (Hederstedt 1980, 1986). In band S1, an additional cytochrome *aa3* quinol oxidase was found.

No activity was found when trying to measure in-gel activities with cytochrome *c* as electron donor, which was expected as electrons are donned directly from ubiquinol to oxidases.

The A1 band was F_1F_0-ATPase as confirmed by finding F_1 subunits alfa, beta, delta, gamma and epsilon, plus the F_0 subunit b (Table 1). The number of bands detected may vary depending on the detergent, although the *Ae* grown cells have stronger bands and probably more activity. Comparison with the literature indicates that digitonin-solubilized *B. subtilis* membranes contained three ATPase activity bands at MW = 487, 277 and 187 kDa. (Sousa *et al*. 2013).

Glycerol-3-phosphate dehydrogenase activity. Aerobic glycerol-3-phosphate dehydrogenase was identified as the most prominent protein in band N1, and in-gel activities indicate that it is highly inhibited as $[O_2]$ decreases. Thus, we decided to test its activity in extracts from *S. epidermidis* grown at different $[O_2]$ (Fig. 4). As expected, glycerol-3-phosphate dehydrogenase activity was much higher in *Ae* grown cells and decreased dramatically in under oxygen-limiting conditions (Fig. 4).

The respiratory chain terminal oxidases from S. epidermidis are differentially expressed at different $[O_2]$. In order to increase our understanding of the adaptability of *S. epidermidis* to $[O_2]$, it was decided to analyze the terminal electron acceptors in the respiratory chain, considering that, while the different O_2-dependent oxidases reduce O_2, anaerobic respiratory chains contain enzymes that use fumarate, nitrite, nitrate or DMSO as final electron acceptors (Haddock and Jones 1977).

Differential absorbance spectra of membrane extracts obtained at 77 K indicated that in the respiratory chain from *S. epidermidis* grown at different $[O_2]$, *b*-type cytochrome peaks were observed at 426–427 nm and 555–557 nm; *a*-type cytochromes

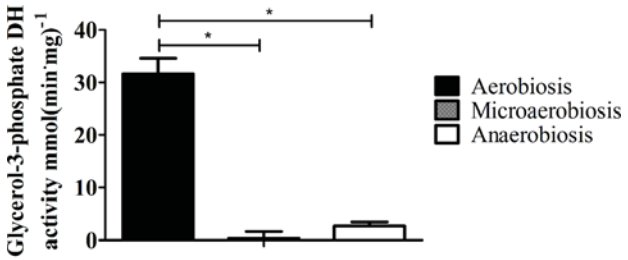

Figure 4. Glycerol-3-phosphate dehydrogenase activities from *S. epidermidis* grown at different oxygen concentrations. NADH absorbance change was measured at 340 nm and specific activities were calculated for extracts from *Ae*, μ*A* and *An* cells. Glycerol-3-phoshate dehydrogenase activity was much higher in aerobic cell growth conditions than in oxygen-limited growth conditions. Tukey's comparison test showed G-3-PDH activity difference between the aerobic and microaerobic grown cells and aerobic and anaerobic grown cells. Significance is $^*P < 0.05$.

were observed as a shoulder at 441–451 and peak at 604 nm. The absence of a peak at 630 nm in all samples is indicative of the lack of a *d*-type cytochrome. The absence of shoulders at 417 and 550 nm indicates the lack of *c*-cytochromes (Fig. 5). When $[O_2]$ was restricted, i.e. at μ*A* or *An*, complete loss of *a*-type cytochromes (*aa3*) (shoulders at 441 and 451 nm and peak at 604 nm) and a decrease in *b*-type cytochromes were observed (peaks at 427 and 557 nm) (Fig. 5). The detection of a small amount of cytochrome *b* in the anaerobic sample is in contrast with a report where complete loss of cytochromes was observed in *S. epidermidis* grown in anaerobic conditions for 16 h (Jacobs and Conti 1965) and in agreement with Frerman and White (1967) where the presence of cytochromes *b* and *o* is reported. The lack of cytochrome *c* confirmed the absence of cytochrome oxidase and in turn, the lack of cytochromes *d* confirmed the absence of *bd*-cytochromes (Fig. 5) as has been reported by others (Taber and Morrison 1964).

To further analyze the respiratory chain terminal oxidases from *S. epidermidis* grown at different $[O_2]$, CO-dithionite-reduced minus dithionite-reduced difference spectra were obtained from *Ae* or μ*A* membranes (Fig. 6) These spectra have an absorbance maximum at 417 nm, and smaller peaks at 545 and 575 nm together with valleys at 430 and 554 nm which are indicative of presence of a CO complex with cytochrome *o* (Fig. 6). Thus, it may be concluded that cytochrome *bo* was present in both *Ae* and μ*A S. epidermidis* (Frerman and White 1967)

Although *S. aureus* and *S. epidermidis* have *cydAB* genes, cyt *bd* has not been found by spectroscopy (Taber and Morrison 1964; Jacobs and Conti 1965). This may be due to an insufficient expression of *cydAB* genes. In all cases only *b*-type cytochromes were observed (Fig 6). In *S. epidermidis* cytochrome *d* was absent in μ*A* cells (Fig. 6) or in those grown in the presence of KCN (results not shown). Thus, in *S. epidermidis* both μ*A* and *Ae* cells express *o*-type cytochromes, while an *a*-type cytochrome was expressed in *Ae* cells.

Staphylococcus epidermidis grown under anaerobic conditions increases expression of nitrate reductase. Anaerobically grown *S. epidermidis* expresses nitrate reductase (Kucera, Dadak and Dobry 1983). In our hands, nitrate reductase activity in *An* was 0.215 ± 0.017 mmol(min·mg)$^{-1}$ protein. Then, in μ*A* it decreased to 0.085 ± 0.01 mmol(min·mg)$^{-1}$ protein. In *Ae* cells, nitrate reductase activity decreased further, to 0.015 ± 0.012 mmol(min·mg)$^{-1}$ protein, 14 times less than in *An* (Fig. 7). Thus, when under *An*, *S. epidermidis* expressed nitrate reductase to substitute oxygen with nitrate as a terminal electron acceptor.

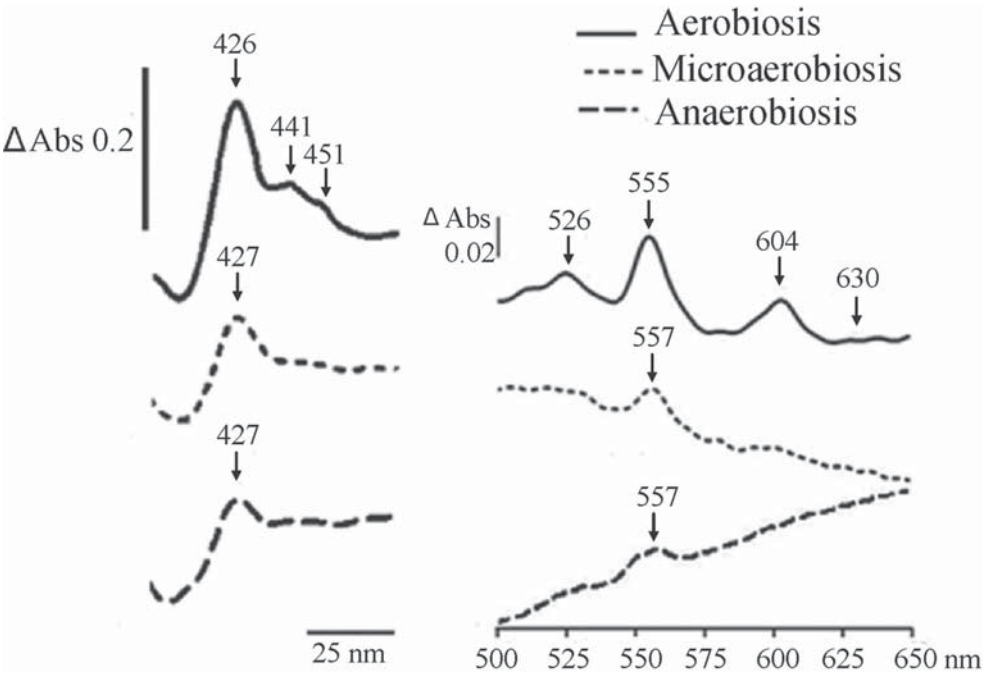

Figure 5. Difference spectra (dithionite-reduced minus persulfate-oxidized) of membranes from cells cultured under different [O_2]: (——) *Ae*, (- - -) μA, (– – –) *An*. Spectra were recorded at 77 K. Membrane protein from 24 h-grown cells in LB medium were adjusted to 15 mg/ml. *b*-type cytochromes can be observed at 426–427 nm and at 555–557 nm in all conditions, *a*-type cytochromes can be observed as a shoulder at 441–451 and peak at 604 nm in membranes obtained from aerobic grown cells. In all samples, *c*-cytochrome shoulders at 417 and 550 nm are absent as well as the *d*-type cytochrome peak at 630 nm.

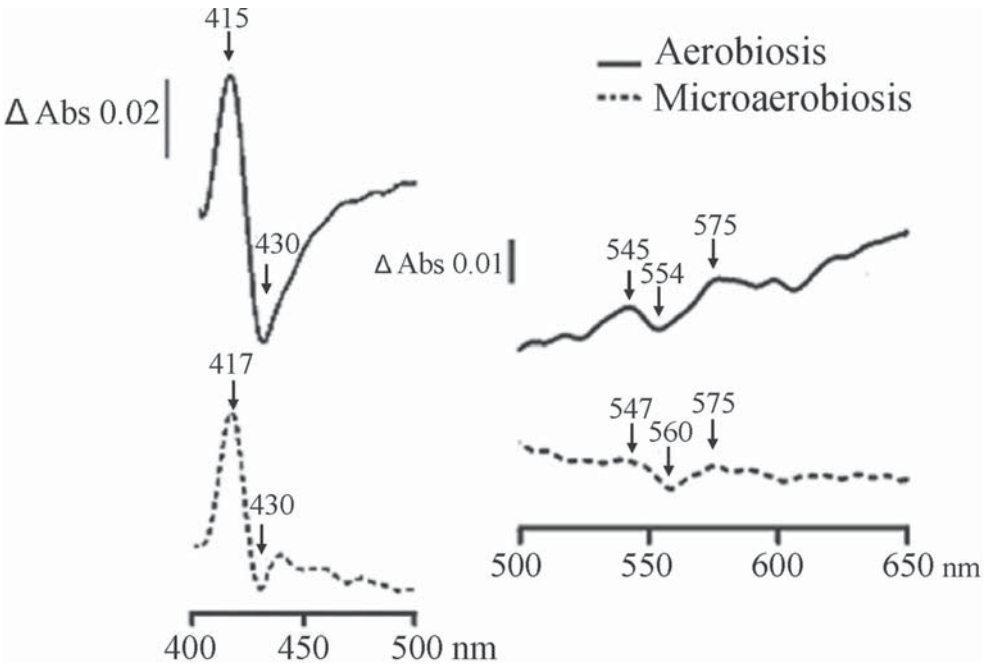

Figure 6. CO Difference spectra (CO + dithionite-reduced minus dithionite-reduced) of membranes from cells cultured under different conditions: (——) *Ae*, (- - -) μA, (– – –) *An*. Spectra were recorded at 77 K. Membrane protein from 24 h grown cells in LB medium were adjusted to 15 mg/ml. A CO complex resembling that of cytochrome *o* with the Söret peak at 417 nm and peaks at 545 and 575 nm and troughs at 430 and 560–554 nm can be observed. In both conditions, there is a small peak at 592 nm with a shoulder at 445 indicating the presence of an a-type cytochrome.

Cyanide inhibits oxygen consumption and promotes biofilm formation in S. epidermidis. After evaluating the respiratory chain electron acceptors available, we decided to test if mimicking an anaerobic environment by inhibiting the cytochromes *aa3* and *bo* with cyanide would increase biofilm formation. Oxygen consumption in aerobic cells was completely inhibited with 200 μM of cyanide (Fig. 8A). Then biofilm formation was evaluated in the same concentrations of cyanide in cultures grown to 24 or 30 h. At 24 h biofilm formation promotion by cyanide was suggested but not clear. However, at 30 h we observed an increase in the biofilm formation as we exposed *S. epidermidis* to increasing concentrations of cyanide reaching 0.50 ± 0.04 which is close to the

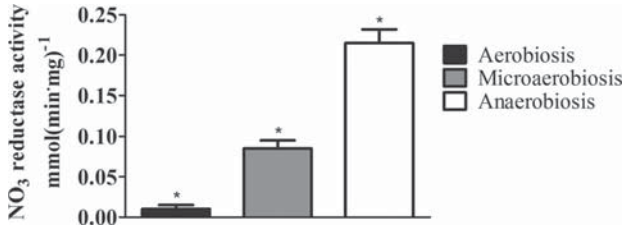

Figure 7. Nitrate reductase activity of *S. epidermidis* grown at different oxygen concentrations. Nitrate reductase activity was measured by means of methylviologen oxidation, which was previously reduced by 2.9 mM of sodium dithionite. Reaction was monitored at 546 nm. Data shown are mean ± S.D. from $n = 4$. Tukey´s comparison test showed significant differences (*$P < 0.05$) between all conditions.

0.59 ± 0.09 obtained in microaerobic conditions. At 24 h, no significant differences in biofilm formation were observed (Fig. 8B).

Methylamine inhibits nitrate reductase activity and biofilm formation in S. epidermidis ATCC 12228. Methylamine is reported to inhibit nitrate reductase activity at 150 mM. We measured nitrate reductase of *S. epidermidis* grown in microaerobic conditions using different concentrations of methylamine (Fig. 8C) and found that at 10 mM methylamine nitrate reductase activity was fully inhibited. Afterwards, biofilm formation was evaluated in cells grown in microaerobic conditions and in the presence of different methylamine concentrations and a decrease in biofilm formation was observed at (Fig. 8D). Microaerobic conditions were used and not anaerobic conditions, because under anaerobic conditions bacteria would be unable to grow (result not shown). This is explained by the lack of oxygen for cytochromes and the inhibition of nitrate reductase.

As *S. epidermidis* gains pathogenic importance it becomes necessary to study its metabolic adaptations to different environmental conditions. Our results provide an image of the plasticity of the *S. epidermidis* respiratory chain. Branched respiratory chains from pathogens may contain therapeutic targets. For instance, *S. epidermidis* expresses an MQO complex, a *bo* cytochrome and a nitrate reductase not found in mammals. Several known inhibitors of *bo* cytochrome (Meunier *et al.* 1995) and nitrate reductase (Magalon *et al.* 1998; Moreno-Vivian *et al.* 1999; Gates *et al.* 2003) might prevent *S. epidermidis* colonization of tissues or prosthetic devices.

DISCUSSION

O_2 is the final electron acceptor in aerobic oxidative phosphorylation, which is the main source of ATP. Bacteria sense substrates and environmental conditions adjusting their metabolism to optimize ATP yields and minimize production of toxic O_2 partial-reduction molecules known collectively as reactive oxygen

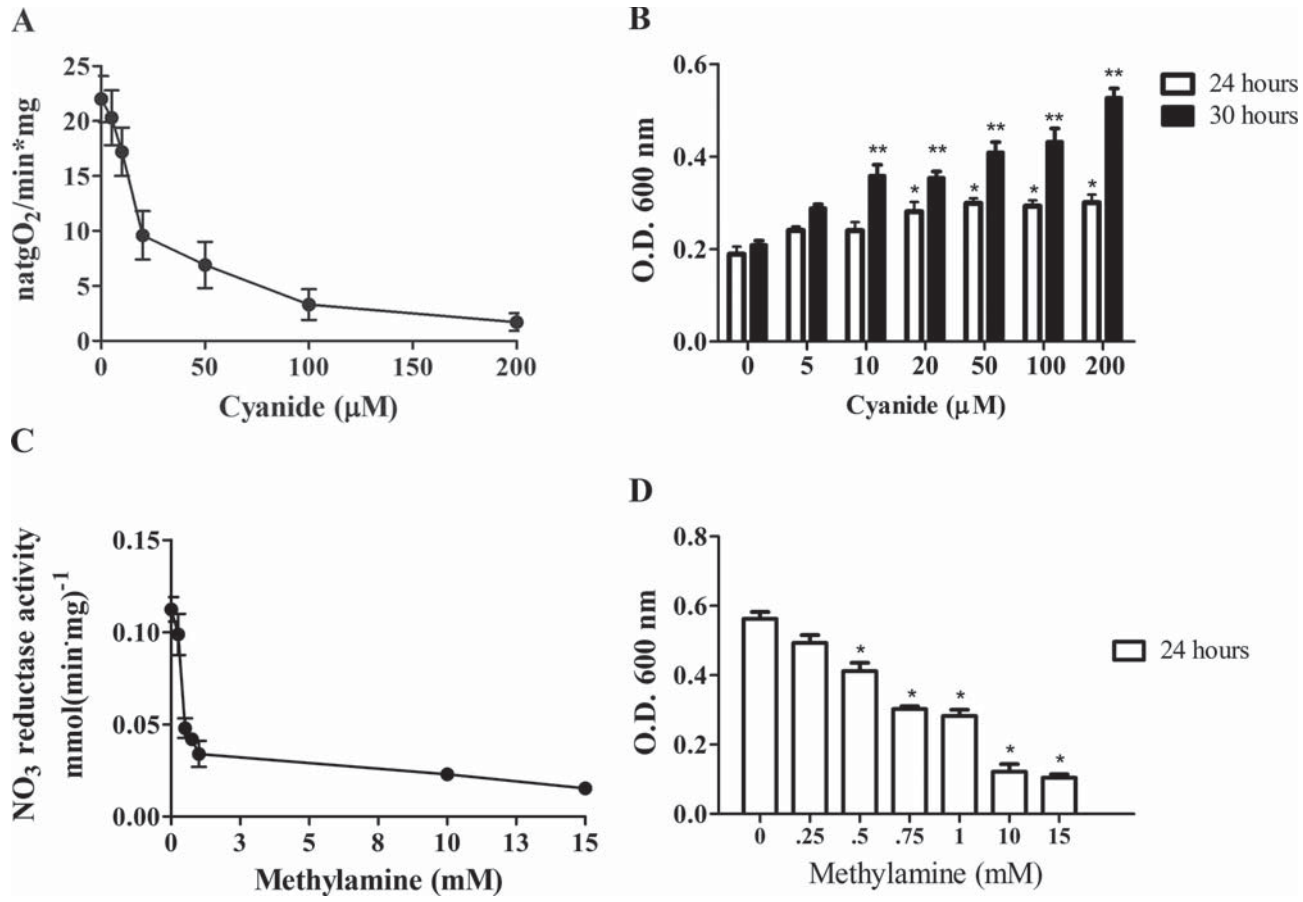

Figure 8. Effect of cyanide or methylamine on *S. epidermidis:* rate of O_2 consumption or biofilm formation. (**A**) KCN-mediated inhibition of O_2 consumption by *S. epidermidis* grown under *Ae* conditions.. Data are mean ± SD from $n = 4$. (**B**) Biofilm formation by *S. epidermidis* cultures at 24 and 30 h in *Ae* and in the presence of KCN as in A. Significance (*$P < 0.01$). (**C**) Inhibition of nitrate reductase activity by methylamine in μA- *S. epidermidis*. Data are mean ± SD from $n = 4$. (**D**) Biofilm formation in 24-h cultures grown in LB medium in μA conditions and in the presence of methylamine as in C. Significant difference (*$P < 0.01$) between 0 and 0.5 mM methylamine at 24 h of growth, $n = 6$. For oxymetry, inhibitors were added directly to the reaction mixture, while in biofilm-forming assays these were present throughout the culture.

species. Among these adaptations, most prokaryotes are able to differentially express the components in their highly branched respiratory chains developing different electron transport pathways (Anraku 1988). Different terminal oxidases are expressed in response to the availability of electron acceptors in the medium, e.g. when O_2 is available it is chosen as the preferred electron acceptor (Unden and Bongaerts 1997). In anaerobic atmospheres, respiratory chains use other final electron acceptors such as nitrate, nitrite, fumarate or DMSO, which upon reduction do not provide as much energy as O_2 (Unden and Bongaerts 1997).

In some unicellulars including *Staphylococci*, different [O_2] may trigger biofilm formation (Xu *et al*. 1998; Gomez, Hontoria and Gonzalez-Lopez 2002). Other factors affecting biofilm formation are temperature, osmolarity, pH and iron concentrations (Otto 2008). Also hydrophobic surfaces provide an anchor for bacterial association (Hall-Stoodley and Stoodley 2005). Biofilms protect cells against environmental hazards and are a source of pyogenic emboli. *Staphylococcus epidermidis* increases its biofilm-forming activity when grown under anaerobiosis, probably through the expression of exopolysaccharide PIA, teichoic acids and proteins needed for biofilm maturation (Otto 2008). Here, as [O_2] was increased, biofilm formation was inhibited. When respiratory enzymes that use oxygen as electron acceptor were inhibited with cyanide (Fig. 8A) in an effort to mimic anaerobic conditions, biofilm formation increased (Fig. 8B). In contrast, when nitrate reductase activity was inhibited by methylamine (Fig. 8C) in a μA conditions and the cell was forced to use whatever O_2 was available, biofilm formation was reduced (Fig. 8D). These data suggest that expression of different respiratory chains may be tightly related to the decision the cell makes to form biofilms.

In *Staphyloccocci*, electrons flow from different dehydrogenases to menaquinone (Gotz and Mayer 2013). Bacterial respiratory chains can contain different cytochrome *c* oxidases or quinol oxidases and oxidoreductases that are expressed depending on growth conditions. Cyt *bo* expression increases in non-fermentable sources and it decreases in fermentable sources (Escamilla *et al*. 1987); cytochrome *bd* has a high affinity for O_2 and it is induced in microaerobic conditions, meanwhile cytochrome *bo* has a lower oxygen affinity and is typically induced in high [O_2]; cytochrome aa_3 is induced in high [O_2] (Shepherd and Poole 2013). *Staphylococcus aureus* expresses cytochrome *bo,* cytochrome *aa3* (qoxABCD) and possibly a cytochrome *bd* oxidase (CydAB) (Gotz and Mayer 2013), but only cytochromes *o* and *a*- have been detected by spectrophotometry (Taber and Morrison 1964). The gene cluster encoding cytochrome *bo* oxidase has not been identified so its existence is in doubt (Hammer *et al*. 2013). *Staphylococci* lack *c*-type cytochromes such as *c*-549 and *c*-554 (Faller, Götz and Schleifer 1980; Gotz and Mayer 2013).

Using data reported here, we propose a model where the branched respiratory chain of *S. epidermidis* is modified by growth at different [O_2]. The enzymes under consideration include soluble enzymes (white circles) donating their electrons to NADH dehydrogenase type II, (NDH2) (green circle) which in turn donates electrons to menaquinone (yellow circle); other membrane dehydrogenases donating electrons to menaquinone (green circles) and terminal electron acceptors, which may be O_2 dependent (blue circles) or O_2 independent (orange circle) (Fig. 9). In aerobic grown cells (*Ae*) (Fig. 9A), menaquinone receives electrons directly from a large number of membrane dehydrogenases including glycerol-3-phosphate dehydrogenase, succinate dehydrogenase, the menaquinone oxidase complex, LDH and an NDH2, which in turn receives electrons from at least two soluble enzymes: alcohol dehydrogenase and the PDC. In mitochondria LDH and glycerol-3-phosphate dehydrogenase do not donate electrons to the respiratory chain, yet in bacteria they are membrane-bound enzymes transferring their electrons directly to ubiquinol (Barnes and Kaback 1970; Lascelles 1978; Doig *et al*. 1999; Modun and Williams 1999; Dym *et al*. 2000; Delgado *et al*. 2001; Fuller *et al*. 2011). From menaquinone, electrons are transferred to one of two terminal O_2-dependent oxidases, namely, cytochrome *bo* and cytochrome aa_3.

When [O_2] decreases in the growth medium, the composition of the *S. epidermidis* respiratory chain composition changes. In microaerobic grown cells (μA) (Fig. 9B), soluble enzymes alcohol dehydrogenase and pyruvate dehydrogenase activities remain. Among membrane dehydrogenases, glycerol 3-phosphate dehydrogenase and succinate dehydrogenase become non-detectable, while NDH2, lactate DH and the MQO complex do not seem to change. Among the final electron-acceptors, cytochrome aa_3 disappears, cytochrome *bo* decreases, and an O_2-independent nitrate reductase is expressed at low levels (Fig. 9B). In anaerobic grown cells (*An*) (Fig. 9C), dehydrogenases do not change, while cytochrome *bo* almost disappears. The most striking characteristic of the *An* cell was the high expression of nitrate reductase as the anaerobic final electron acceptor of the respiratory chain. The lack of complexes III and IV is in agreement with the notion that in *Staphylococci* electrons flow from different dehydrogenases to menaquinone and from menaquinone to different quinol oxidases, e.g. *S. epidermidis* ATCC 12228 grown in aerobic conditions contains two main cytochromes: *cyt bo* and *cyt aa3* and this is similar to the reported respiratory chain from *S. aureus* (Taber and Morrison 1964).

The spectra we obtained suggest the presence of cytochromes *aa3* and *bo*. However, the genome shown only one *qox*ABCD operon, and thus there are no genes for *bo* cytochromes. A possible explanation for our data may be that a promiscuous assembly of cytochrome *c* oxidase apo-proteins with hemes *b* and *o* occurred, where a *bo* cytochrome replaced heme *aa3*. Under specific culture conditions, bacterial oxidases may be assembled promiscuously accepting a different heme group to that present on its original structure. Examples of these substitutions have been described previously (Matsushita *et al*. 1992; Puustinen *et al*. 1992; Peschek *et al*. 1995; Sakamoto, Handa and Sone 1997; Azarkina *et al*. 1999; Contreras-Zentella *et al*. 2003). Even though we did not observe absorption bands characteristics of the cytochrome *d* at 630 nm, proteins that form the Cytochrome *d* ubiquinol oxidase are reported in the Uniprot databank (SE0785, SE 0784). The possibility that there is a similar promiscuous substitution of heme groups has to be considered. Previous reports on *Pseudomonas aeruginosa* that encodes a cyanide-insensitive oxidase (*CioAB*), which is homologous to the Cytochrome *bd* oxidase (*CydAB*) of *E. coli*, indicate that there is a substitution of *b*-type cytochromes instead of *d*-type cytochromes and this prevents the detection of an absorption peak at 630 nm (Cooper, Tavankar and Williams 2003). Furthermore, in *Campylobacter jejuni* the *cydAB* genes reported in the genome apparently encode a cyanide-resistant oxidase that does not have a *d*-type cytochrome (Jackson *et al*. 2007). The oxidoreductases we proposed (Fig. 9) were sought in the Uniprot proteome database. We did find expression of proteins exhibiting each of the activities detected here (Table 2). In addition, we found in the proteome some oxidoreductases, namely Glycerol dehydrogenase (SE0235) and Cytochrome *d* ubiquinol oxidase-like proteins I (SE0784) and II (SE0785) that were not detected in our experiments.

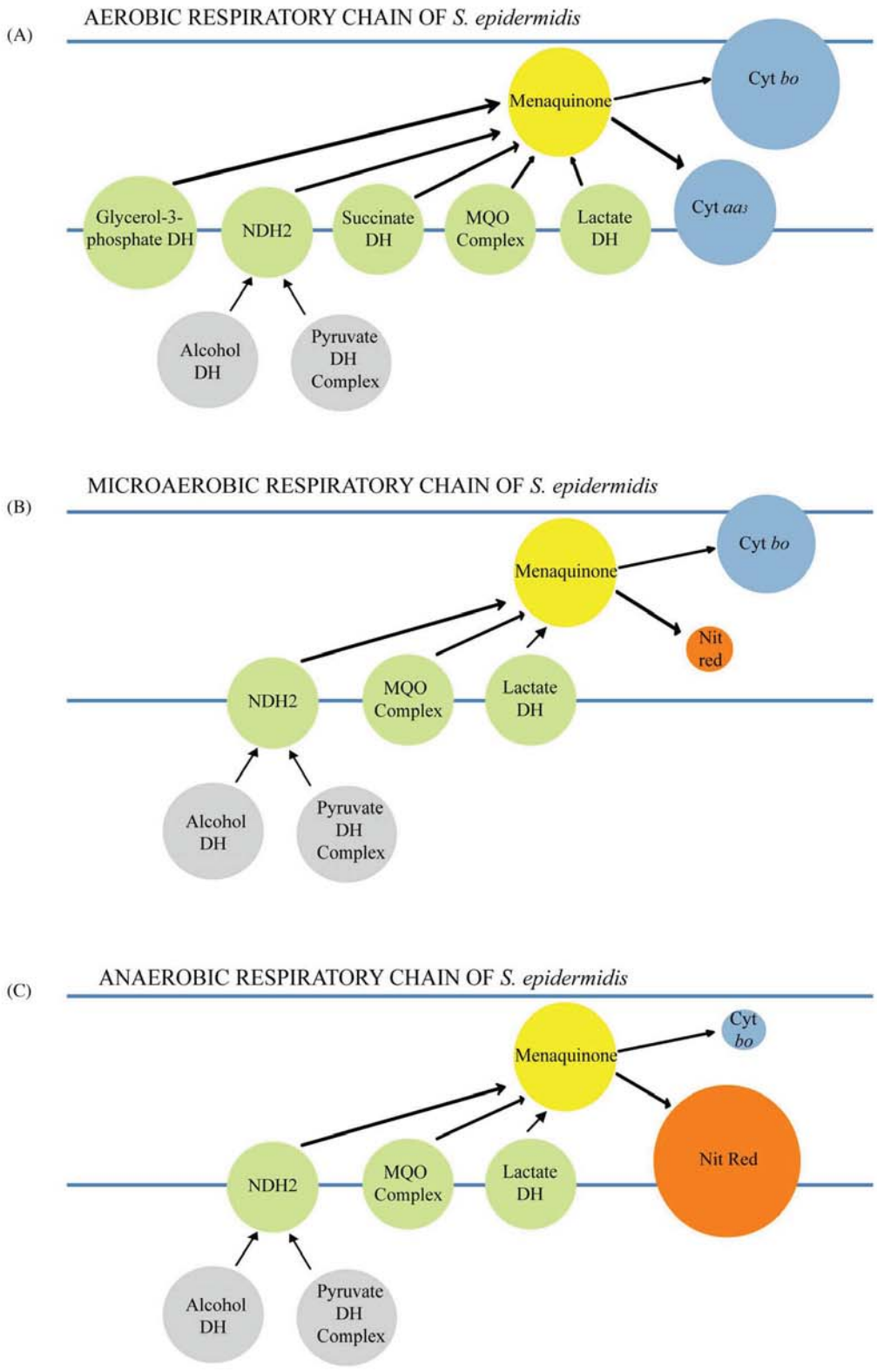

Figure 9. Proposed models of the *S. epidermidis* respiratory chain in response to [O_2] during growth. Color code: soluble enzymes (gray), membrane dehydrogenases (green); menaquinone (yellow); O_2-dependent terminal electron acceptors (blue) or O_2-independent acceptors (orange). (**A**) In aerobic (*Ae*) grown cells menaquinone receives electrons from glycerol-3-phosphate dehydrogenase, succinate dehydrogenase, the menaquinone oxidase complex, LDH or a NDH2, which receives electrons from at least two soluble enzymes: alcohol dehydrogenase and the PDC. From menaquinone, electrons are transferred to one of two terminal O_2-dependent oxidases, namely, cytochrome *bo* and Cytochrome *aa3*. (**B**) In μA, soluble enzymes (alcohol dehydrogenase and pyruvate dehydrogenase) remain. Glycerol 3-phosphate dehydrogenase and succinate dehydrogenase become non-detectable, while NDH2, lactate DH and the MQO complex do not change. Cytochrome *aa3* disappears, cytochrome *bo* decreases, and an O_2-independent nitrate reductase is expressed at low levels. (**C**) In anaerobic (*An*) conditions, dehydrogenases do not change, cytochrome *bo* almost disappears and nitrate reductase is highly expressed.

Table 2. Possible correspondence between oxidoreductase activities detected here and oxidoreductases found in the Uniprot proteome database.

Oxidoreductases found in the proteome database	Detected here by LC-MS and/or enzymatic activities	Uniprot Databank Accession number
Glycerol dehydrogenase	No	SE0235
Glyceraldehyde-3-phosphate dehydrogenase	Yes	SE0557, SE1361
NADH dehydrogenase	Yes	SE0635, SE2333
Alcohol dehydrogenase	Yes	SE0375
D,L-Lactate dehydrogenase	Yes	SE2074, SE2145
Succinate dehydrogenase	Yes	SE0841, SE0842
Succinate dehydrogenase cytochrome b-558	Yes	SE0840
Glycerol-3-phosphate dehydrogenase	Yes	SE0979
Malate dehydrogenase	Yes	SE0461
Probable quinol oxidase	Yes	SE0756, SE0757, SE0758, SE0759
Cytochrome d ubiquinol oxidase like protein	No	SE0784, SE0785
Respiratory nitrate reductase	Yes	SE1972, SE1973, SE1974, SE1975

Non-pathogenic staphylococcal species such as the ATCC12228 encode a pyocyanin- and cyanide-insensitive cytochrome *bd* quinol oxidase, while pathogenic species, such as *S. aureus* encode a sensitive variant; yet, in our hands no *bd* cytochrome was found (Voggu *et al.* 2006). Even when *S. epidermidis* was grown in a non-fermentable carbon source medium in the presence of 1 mM of KCN cytochrome *bd* was not present. The glycerol-3-phosphate dehydrogenase from *S. epidermidis* is more active than other bacteria used in biotechnology for glycerol degradation (Holmberg *et al.* 1990; Yazdani and Gonzalez 2007; da Silva, Mack and Contiero 2009). The PDC enzymes we found on membranes are usually reported as cytoplasmic enzymes, but they were also found in the membrane fraction of *Mycoplasma pneumonia* (Dallo *et al.* 2002) and Rhodospirillum *rubrum* (Luderitz and Klemme 1977).

Knowledge on how branched respiratory chains provide survival capabilities to cells can help identify specific respiratory chain inhibitors that can be used as therapeutic targets in human infections. Even though we are suggesting that the enzymes that are expressed at low oxygen concentrations may be therapeutic targets, we do not know exactly how they act during biofilm maturation. Previous studies state that anaerobic conditions increase polysaccharide gene expression in staphylococci (Cramton *et al.* 2001). Interestingly, methylamine was an effective inhibitor of the *S. epidermidis* nitrate reductase, the main final-electron acceptor present during microaerobic or anaerobic growth, and by consequence reduced biofilm formation. The high adaptability of *S. epidermidis* plays an important role in its pathogenicity and this has to be analyzed thoroughly. Already, the large effects of $[O_2]$ on biofilm formation and on the respiratory chain composition of *S. epidermidis* suggest preventive and therapeutic strategies against this bacterium.

ACKNOWLEDGEMENTS

Ramón Méndez, Martha Calahorra and Norma Sánchez provided technical assistance for this project.

FUNDING

Partially funded by grants CONACYT 239487 and UNAM-DGAPA-PAPIIT IN204015 to SUC. CUA is a CONACYT fellow enrolled in the Biochemistry PhD program at UNAM.

Conflict of interest. None declared.

REFERENCES

Anraku Y. Bacterial electron transport chains. *Annu Rev Biochem* 1988;**57**:101–32.

Artzatbanov V, Petrov VV. Branched respiratory chain in aerobically grown *Staphylococcus aureus*—oxidation of ethanol by cells and protoplasts. *Arch Microbiol* 1990;**153**: 580–4.

Atkuri KR, Herzenberg LA, Niemi AK, *et al.* Importance of culturing primary lymphocytes at physiological oxygen levels. *P Natl Acad Sci USA* 2007;**104**:4547–52.

Azarkina N, Siletsky S, Borisov V, *et al.* A cytochrome bb'-type quinol oxidase in *Bacillus subtilis* strain 168. *J Biol Chem* 1999;**274**:32810–7.

Baradaran R, Berrisford JM, Minhas GS, *et al.* Crystal structure of the entire respiratory complex I. *Nature* 2013;**494**: 443–8.

Barnes EM, Jr, Kaback HR. Beta-galactoside transport in bacterial membrane preparations: energy coupling via membrane-bounded D-lactic dehydrogenase. *P Natl Acad Sci USA* 1970;**66**:1190–8.

Bergsma J, Van Dongen MB, Konings WN. Purification and characterization of NADH dehydrogenase from *Bacillus subtilis*. *Eur J Biochem* 1982;**128**:151–7.

Burton RM. Glycerol dehydrogenase from Aerobacter aerogenes. In: Colowick SP, Kaplan NO (eds). *Methods in Enzymology* Vol. 1 in [59] pp. 397–400. NY: Academic Press, 1955.

Cecchini G, Schroder I, Gunsalus RP, *et al.* Succinate dehydrogenase and fumarate reductase from *Escherichia coli*. *Biochim Biophys Acta* 2002;**1553**:140–57.

Cogen AL, Yamasaki K, Sanchez KM, *et al.* Selective antimicrobial action is provided by phenol-soluble modulins derived from *Staphylococcus epidermidis*, a normal resident of the skin. *J Invest Dermatol* 2010;**130**:192–200.

Contreras-Zentella M, Mendoza G, Membrillo-Hernandez J, *et al.* A novel double heme substitution produces a functional bo3 variant of the quinol oxidase aa3 of *Bacillus cereus*. Purification and paratial characterization. *J Biol Chem* 2003;**278**:31473–8.

Cooper M, Tavankar GR, Williams HD. Regulation of expression of the cyanide-insensitive terminal oxidase in *Pseudomonas aeruginosa*. *Microbiology* 2003;**149**:1275–84.

Cotter JJ, O'Gara JP, Casey E. Rapid depletion of dissolved oxygen in 96-well microtiter plate *Staphylococcus epidermidis* biofilm assays promotes biofilm development and is influenced

by inoculum cell concentration. *Biotechnol Bioeng* 2009;**103**: 1042–7.

Cotter JJ, O'Gara JP, Mack D, *et al*. Oxygen-mediated regulation of biofilm development is controlled by the alternative sigma factor sigma(B) in *Staphylococcus epidermidis*. *Appl Environ Microb* 2009;**75**:261–4.

Cramton SE, Gerke C, Schnell NF, *et al*. The intercellular adhesion (ica) locus is present in *Staphylococcus aureus* and is required for biofilm formation. *Infect Immun* 1999;**67**: 5427–33.

Cramton SE, Ulrich M, Gotz F, *et al*. Anaerobic conditions induce expression of polysaccharide intercellular adhesin in *Staphylococcus aureus* and *Staphylococcus epidermidis*. *Infect Immun* 2001;**69**:4079–85.

da Silva GP, Mack M, Contiero J. Glycerol: a promising and abundant carbon source for industrial microbiology. *Biotechnol Adv* 2009;**27**:30–9.

Dallo SF, Kannan TR, Blaylock MW, *et al*. Elongation factor Tu and E1 beta subunit of pyruvate dehydrogenase complex act as fibronectin binding proteins in *Mycoplasma pneumoniae*. *Mol Microbiol* 2002;**46**:1041–51.

Delgado ML, O'Connor JE, Azorin I, *et al*. The glyceraldehyde-3-phosphate dehydrogenase polypeptides encoded by the *Saccharomyces cerevisiae* TDH1, TDH2 and TDH3 genes are also cell wall proteins. *Microbiology* 2001;**147**:411–7.

Desriac N, Broussolle V, Postollec F, *et al*. *Bacillus cereus* cell response upon exposure to acid environment: toward the identification of potential biomarkers. *Front Microbiol* 2013;**4**: 284.

Doig P, de Jonge BL, Alm RA, *et al*. *Helicobacter pylori* physiology predicted from genomic comparison of two strains. *Microbiol Mol Biol R* 1999;**63**:675–707.

Dym O, Pratt EA, Ho C, *et al*. The crystal structure of D-lactate dehydrogenase, a peripheral membrane respiratory enzyme. *P Natl Acad Sci USA* 2000;**97**:9413–8.

Escamilla JE, Ramírez R, Del Arenal IP, *et al*. Expression of cytochrome oxidases in *Bacillus cereus*: effects of oxygen tension and carbon source. *J Gen Microbiol* 1987;**133**:3549–55.

Faller AH, Götz F, Schleifer KH. Cytochrome-patterns of Staphylococci and Micrococci and their taxonomic implications. Zentralblatt für Bakteriologie: I. Abt. Originale C: Allgemeine, angewandte und ökologische. *Mikrobiologie* 1980;**1**:26–39.

Fazly Bazzaz BS, Jalalzadeh M, Sanati M, *et al*. Biofilm formation by *Staphylococcus epidermidis* on foldable and rigid intraocular lenses. *Jundishapur J Microbiol* 2014;**7**:e10020.

Franco AR, Cárdenas J, Fernández E. Ammonium (methylammonium) is the co-represor of nitrate reductase in *Chlamydomonas reinhardii*. *FEBS Lett* 1984;**176**:453–6.

Frerman FE, White DC. Membrane lipid changes during formation of a functional electron transport system in *Staphylococcus aureus*. *J Bacteriol* 1967;**94**:1868–74.

Fuchs S, Pane-Farre J, Kohler C, *et al*. Anaerobic gene expression in *Staphylococcus aureus*. *J Bacteriol* 2007;**189**:4275–89.

Fuller JR, Vitko NP, Perkowski EF, *et al*. Identification of a lactate-quinone oxidoreductase in *Staphylococcus aureus* that is essential for virulence. *Front Cell Infect Microbiol* 2011;**1**:19.

Gandhi M, Chikindas ML. Listeria: a foodborne pathogen that knows how to survive. *Int J Food Microbiol* 2007;**113**:1–15.

Gates AJ, Hughes RO, Sharp SR, *et al*. Properties of the periplasmic nitrate reductases from *Paracoccus pantotrophus* and *Escherichia coli* after growth in tungsten-supplemented media. *FEMS Microbiol Lett* 2003;**220**:261–9.

Gomez MA, Hontoria E, Gonzalez-Lopez J. Effect of dissolved oxygen concentration on nitrate removal from groundwater using a denitrifying submerged filter. *J Hazard Mater* 2002;**90**:267–78.

Gordon O, Vig Slenters T, Brunetto PS, *et al*. Silver coordination polymers for prevention of implant infection: thiol interaction, impact on respiratory chain enzymes, and hydroxyl radical induction. *Antimicrob Agents Ch* 2010;**54**:4208–18.

Gotz F, Mayer S. Both terminal oxidases contribute to fitness and virulence during organ-specific *Staphylococcus aureus* colonization. *MBio* 2013;**4**:e00976–13.

Gristina AG. Biomaterial-centered infection: microbial adhesion versus tissue integration. *Science* 1987;**237**:1588–95.

Guerrero-Castillo S, Vazquez-Acevedo M, Gonzalez-Halphen D, *et al*. In *Yarrowia lipolytica* mitochondria, the alternative NADH dehydrogenase interacts specifically with the cytochrome complexes of the classic respiratory pathway. *Biochim Biophys Acta* 2009;**1787**:75–85.

Haddock BA, Jones CW. Bacterial respiration. *Bacteriol Rev* 1977;**41**:47–99.

Hall-Stoodley L, Stoodley P. Biofilm formation and dispersal and the transmission of human pathogens. *Trends Microbiol* 2005;**13**:7–10.

Hammer ND, Reniere ML, Cassat JE, *et al*. Two heme-dependent terminal oxidases power *Staphylococcus aureus* organ-specific colonization of the vertebrate host. *MBio* 2013;**4**:8873–94.

Hammes-Schiffer S, Benkovic SJ. Relating protein motion to catalysis. *Annu Rev Biochem* 2006;**75**:519–41.

Hanson RS, Srinivasan VR, Halvorson HO. Biochemistry of sporulation. I. Metabolism of acetate by vegetative and sporulating cells. *J Bacteriol* 1963;**85**:451–60.

Hederstedt L. Cytochrome b reducible by succinate in an isolated succinate dehydrogenase-cytochrome b complex from *Bacillus subtilis* membranes. *J Bacteriol* 1980;**144**:933–40.

Hederstedt L. Molecular properties, genetics, and biosynthesis of *Bacillus subtilis* succinate dehydrogenase complex. *Methods Enzymol* 1986;**126**:399–414.

Holmberg C, Beijer L, Rutberg B, *et al*. Glycerol catabolism in *Bacillus subtilis*: nucleotide sequence of the genes encoding glycerol kinase (glpK) and glycerol-3-phosphate dehydrogenase (glpD). *J Gen Microbiol* 1990;**136**:2367–75.

Hurdle JG, O'Neill AJ, Chopra I, *et al*. Targeting bacterial membrane function: an underexploited mechanism for treating persistent infections. *Nat Rev Microbiol* 2011;**9**:62–75.

Jackson RJ, Elvers KT, Lee LJ, *et al*. Oxygen reactivity of both respiratory oxidases in *Campylobacter jejuni*: the cydAB genes encode a cyanide-resistant, low-affinity oxidase that is not of the cytochrome bd type. *J Bacteriol* 2007;**189**:1604–15.

Jacobs NJ, Conti SF. Effect of hemin on the formation of the cytochrome system of anaerobically grown *Staphylococcus epidermidis*. *J Bacteriol* 1965;**89**:675–9.

Kern M, Simon J. Periplasmic nitrate reduction in *Wolinella succinogenes*: cytoplasmic NapF facilitates NapA maturation and requires the menaquinol dehydrogenase NapH for membrane attachment. *Microbiology* 2009;**155**:2784–94.

Kim JH, Haff RP, Faria NC, *et al*. Targeting the mitochondrial respiratory chain of Cryptococcus through antifungal chemosensitization: a model for control of non-fermentative pathogens. *Molecules* 2013;**18**:8873–94.

Kostakioti M, Hadjifrangiskou M, Hultgren SJ. Bacterial biofilms: development, dispersal, and therapeutic strategies in the dawn of the postantibiotic era. *Cold Spring Harb Perspect Med* 2013;**3**:a010306.

Kucera I, Dadak V, Dobry R. The distribution of redox equivalents in the anaerobic respiratory chain of Paracoccus denitrificans. *Eur J Biochem* 1983;**130**:359–64.

Lancaster CR, Kroger A. Succinate: quinone oxidoreductases: new insights from X-ray crystal structures. *Biochim Biophys Acta* 2000;**1459**:422–31.

Lascelles J. sn-Glycerol-3-phosphate dehydrogenase and its interaction with nitrate reductase in wild-type and hem mutant strains of *Staphylococcus aureus*. *J Bacteriol* 1978;**133**:621–5.

Löw H, Vallin I. Succinate-linked Diphosphopyridine nucleotide reduction in Submitochondrial particles. *Biochim Biophys Acta* 1963;**69**:361–74.

Luderitz R, Klemme JH. Isolation and characterization of a membrane-bound pyruvate dehydrogenase complex from the phototrophic bacterium *Rhodospirillum rubrum* (author's transl). *Z Naturforsch C* 1977;**32**:351–61.

McCarty GW, Bremner JM. Inhibition of assimilatory nitrate reductase activity in soil by glutamine and ammonium analogs. *P Natl Acad Sci USA* 1992;**89**:5834–6.

Mack D, Davies AP, Harris LG, *et al*. Biomaterials associated infection. In: Fintan Moriarty SAJZT, Busscher HJ (eds). *Immunological Aspects and Antimicrobial Strategies. Chapter 2. Staphylococcus Epidermidis in Biomaterial-Associated Infections*. New York: Springer, 2013, 25–56.

Magalon A, Rothery RA, Lemesle-Meunier D, *et al*. Inhibitor binding within the NarI subunit (cytochrome bnr) of *Escherichia coli* nitrate reductase A. *J Biol Chem* 1998;**273**:10851–6.

Matsushita K, Ebisuya H, Ameyama M, *et al*. Change of the terminal oxidase from cytochrome a1 in shaking cultures to cytochrome o in static cultures of *Acetobacter aceti*. *J Bacteriol* 1992;**174**:122–9.

Meunier B, Madgwick SA, Reil E, *et al*. New inhibitors of the quinol oxidation sites of bacterial cytochromes bo and bd. *Biochemistry* 1995;**34**:1076–83.

Modun B, Williams P. The staphylococcal transferrin-binding protein is a cell wall glyceraldehyde-3-phosphate dehydrogenase. *Infect Immun* 1999;**67**:1086–92.

Moreno-Vivian C, Cabello P, Martinez-Luque M, *et al*. Prokaryotic nitrate reduction: molecular properties and functional distinction among bacterial nitrate reductases. *J Bacteriol* 1999;**181**:6573–84.

Morgan DJ, Sazanov LA. Three-dimensional structure of respiratory complex I from *Escherichia coli* in ice in the presence of nucleotides. *Biochim Biophys Acta* 2008;**1777**:711–8.

Mukhopadhyay R, Rosen BP, Phung LT, *et al*. Microbial arsenic: from geocycles to genes and enzymes. *FEMS Microbiol Rev* 2002;**26**:311–25.

Nakano MM, Dailly YP, Zuber P, *et al*. Characterization of anaerobic fermentative growth of *Bacillus subtilis*: identification of fermentation end products and genes required for growth. *J Bacteriol* 1997;**179**:6749–55.

Niebisch A, Bott M. Purification of a cytochrome bc-aa3 supercomplex with quinol oxidase activity from *Corynebacterium glutamicum*. Identification of a fourth subunity of cytochrome aa3 oxidase and mutational analysis of diheme cytochrome c1. *J Biol Chem* 2003;**278**:4339–46.

Okajima Y, Kobayakawa S, Tsuji A, *et al*. Biofilm formation by *Staphylococcus epidermidis* on intraocular lens material. *Invest Ophthalmol Vis Sci* 2006;**47**:2971–5.

Otto M. Staphylococcal biofilms. *Curr Top Microbiol Immunol* 2008;**322**:207–28.

Otto M. *Staphylococcus epidermidis*–the 'accidental' pathogen. *Nat Rev Microbiol* 2009;**7**:555–67.

Padgaonkar VA, Nadkarni GB. Effect of heavy water on structure-function relationship of lactate dehydrogenase from *Lactobacillus casei*. *Indian J Biochem Biophys* 1980;**17**:272–5.

Peschek GA, Alge D, Fromwald S, *et al*. Transient accumulation of heme O (cytochrome o) in the cytoplasmic membrane of semi-anaerobic *Anacystis nidulans*. Evidence for oxygenase-catalyzed heme O/A transformation. *J Biol Chem* 1995;**270**:27937–41.

Peyssonnaux C, Boutin AT, Zinkernagel AS, *et al*. Critical role of HIF-1alpha in keratinocyte defense against bacterial infection. *J Invest Dermatol* 2008;**128**:1964–8.

Puustinen A, Morgan JE, Verkhovsky M, *et al*. The low-spin heme site of cytochrome o from *Escherichia coli* is promiscuous with respect to heme type. *Biochemistry* 1992;**31**:10363–9.

Raad I, Alrahwan A, Rolston K. *Staphylococcus epidermidis*: emerging resistance and need for alternative agents. *Clin Infect Dis* 1998;**26**:1182–7.

Sakamoto J, Handa Y, Sone N. A novel cytochrome b(o/a)3-type oxidase from *Bacillus stearothermophilus* catalyzes cytochrome c-551 oxidation. *J Biochem* 1997;**122**:764–71.

Schagger H, von Jagow G. Blue native electrophoresis for isolation of membrane protein complexes in enzymatically active form. *Anal Biochem* 1991;**199**:223–31.

Schryvers A, Lohmeier E, Weiner JH. Chemical and functional properties of the native and reconstituted forms of the membrane-bound, aerobic glycerol-3-phosphate dehydrogenase of *Escherichia coli*. *J Biol Chem* 1978;**253**:783–8.

Schurig-Briccio LA, Yano T, Rubin H, *et al*. Characterization of the type 2 NADH: menaquinone oxidoreductases from *Staphylococcus aureus* and the bactericidal action of phenothiazines. *Biochim Biophys Acta* 2014;**1837**:954–63.

Shepherd M, Poole RK. Bacterial respiratory chains. In: Roberts GCK (ed.). *Encyclopedia of Biophysics*. European Biophysical Societies' Association (EBSA). Berlin, Heidelberg: Springer-Verlag, 2013, DOI: 10.1007/978-3-642-16712-6.

Sousa PM, Videira MA, Santos FA, *et al*. The bc:caa3 supercomplexes from the Gram positive bacterium *Bacillus subtilis* respiratory chain: a megacomplex organization? *Arch Biochem Biophys* 2013;**537**:153–60.

Taber HW, Morrison M. Electron transport in Staphylococci. properties of a particle preparation from exponential phase *Staphylococcus aureus*. *Arch Biochem Biophys* 1964;**105**:367–79.

Thomas JC, Vargas MR, Miragaia M, *et al*. Improved multilocus sequence typing scheme for *Staphylococcus epidermidis*. *J Clin Microbiol* 2007;**45**:616–9.

Unden G, Bongaerts J. Alternative respiratory pathways of *Escherichia coli*: energetics and transcriptional regulation in response to electron acceptors. *Biochim Biophys Acta* 1997;**1320**:217–34.

Van Eys J, Nuenke BJ, Patterson MK, Jr. The nonprotein component of alpha-glycerophosphate dehydrogenase. Physical and chemical properties of the crystalline rabbit muscle enzyme. *J Biol Chem* 1959;**234**:2308–13.

Voggu L, Schlag S, Biswas R, *et al*. Microevolution of cytochrome bd oxidase in Staphylococci and its implication in resistance to respiratory toxins released by Pseudomonas. *J Bacteriol* 2006;**188**:8079–86.

von Eiff C, Peters G, Heilmann C. Pathogenesis of infections due to coagulase-negative staphylococci. *Lancet Infect Dis* 2002;**2**:677–85.

Vuong C, Otto M. *Staphylococcus epidermidis* infections. *Microbes Infect* 2002;**4**:481–9.

Wang XM, Noble L, Kreiswirth BN, *et al*. Evaluation of a multilocus sequence typing system for *Staphylococcus epidermidis*. *J Med Microbiol* 2003;**52**:989–98.

Wessels HJ, Vogel RO, Lightowlers RN, *et al.* Analysis of 953 human proteins from a mitochondrial HEK293 fraction by complexome profiling. *PLoS One* 2013;**8**:e68340.

Wiese M, Gerlach RG, Popp I, *et al.* Hypoxia-mediated impairment of the mitochondrial respiratory chain inhibits the bactericidal activity of macrophages. *Infect Immun* 2012;**80**:1455–66.

Wittig I, Braun HP, Schagger H. Blue native PAGE. *Nat Protoc* 2006;**1**:418–28.

Wittig I, Karas M, Schagger H. High resolution clear native electrophoresis for in-gel functional assays and fluorescence studies of membrane protein complexes. *Mol Cell Proteomics* 2007;**6**:1215–25.

Wittig I, Schagger H. Advantages and limitations of clear-native PAGE. *Proteomics* 2005;**5**:4338–46.

Xu KD, Stewart PS, Xia F, *et al.* Spatial physiological heterogeneity in *Pseudomonas aeruginosa* biofilm is determined by oxygen availability. *Appl Environ Microb* 1998;**64**:4035–9.

Yazdani SS, Gonzalez R. Anaerobic fermentation of glycerol: a path to economic viability for the biofuels industry. *Curr Opin Biotechnol* 2007;**18**:213–9.

Yeh JI, Chinte U, Du S. Structure of glycerol-3-phosphate dehydrogenase, an essential monotopic membrane enzyme involved in respiration and metabolism. *P Natl Acad Sci USA* 2008;**105**:3280–5.

Young IG, Jaworowski A, Poulis MI. Amplification of the respiratory NADH dehydrogenase of *Escherichia coli* by gene cloning. *Gene* 1978;**4**:25–36.

Zimmerli W, Trampuz A, Ochsner PE. Prosthetic-joint infections. *N Engl J Med* 2004;**351**:1645–54.

Archives of Biochemistry and Biophysics 555–556 (2014) 66–70

Contents lists available at ScienceDirect

Archives of Biochemistry and Biophysics

journal homepage: www.elsevier.com/locate/yabbi

In *Saccharomyces cerevisiae* fructose-1,6-bisphosphate contributes to the Crabtree effect through closure of the mitochondrial unspecific channel

Mónica Rosas-Lemus, Cristina Uribe-Alvarez, Natalia Chiquete-Félix, Salvador Uribe-Carvajal *

Department of Molecular Genetics, Inst. de Fisiología Celular, Universidad Nacional Autónoma de México, Mexico

ARTICLE INFO

Article history:
Received 25 March 2014
and in revised form 16 May 2014
Available online 9 June 2014

Keywords:
Fructose-1,6-bisphosphate
Glucose-6-phosphate
Crabtree effect
Mitochondria
Saccharomyces cerevisiae
Permeability transition

ABSTRACT

In *Saccharomyces cerevisiae* addition of glucose inhibits oxygen consumption, i.e. *S. cerevisiae* is Crabtree-positive. During active glycolysis hexoses-phosphate accumulate, and probably interact with mitochondria. In an effort to understand the mechanism underlying the Crabtree effect, the effect of two glycolysis-derived hexoses-phosphate was tested on the *S. cerevisiae* mitochondrial unspecific channel ($_{Sc}$MUC). Glucose-6-phosphate (G6P) promoted partial opening of $_{Sc}$MUC, which led to proton leakage and uncoupling which in turn resulted in, accelerated oxygen consumption. In contrast, fructose-1,6-bisphosphate (F1,6BP) closed $_{Sc}$MUC and thus inhibited the rate of oxygen consumption. When added together, F1,6BP reverted the mild G6P-induced effects. F1,6BP is proposed to be an important modulator of $_{Sc}$MUC, whose closure contributes to the "Crabtree effect".

Introduction

In "Crabtree positive" yeast, the addition of glucose both increases glycolysis and inhibits the rate of oxygen consumption [1,2]. It has been proposed that glucose addition induces a rapid metabolic switch from a gluconeogenic/respiratory metabolism to a fermentative mode [3]. The Crabtree effect and the Warburg effect are different in that the Crabtree effect is immediate and reversible, while the Warburg effect is established at longer times, after the expression of different proteins that lead to its irreversibility. Both phenomena have been observed in tumor cells [1]. The Crabtree effect is triggered by different metabolic signals [2,4,5]. Among these is the accumulation of the glycolytic intermediaries glucose-6-phosphate (G6P)[1] [6–10 mM], and fructose-1,6-bisphosphate (F1,6BP) [5–10 mM] [6–8]. Glycolysis-derived accumulation of hexoses-phosphate complements other known signaling molecules such as fructose-2,6-biphosphate [9].

The Crabtree effect is observed in tumor cells [10,11], highly proliferating non-tumor cells [11], some yeast species [12] and some bacteria [13]. In regard to the mechanism underlying the Crabtree effect, a competition between glycolysis and oxidative phosphorylation for ADP or Pi has been proposed [14–16]. The mechanism underlying the Crabtree effect is still elusive, although inhibition of complex III and complex IV by F1,6BP has been reported [17].

Most Crabtree positive cells accumulate F1,6BP and G6P, which seem to modulate both glycolysis and oxidative phosphorylation [17–19]. Indeed, G6P and F6P activate the mitochondrial respiratory complex III, while F1,6BP inhibits the activity of both complex III and IV [17].

In the yeast *Saccharomyces cerevisiae*, oxidative phosphorylation is strongly regulated by the mitochondrial unspecific channel ($_{Sc}$MUC) [20,21]. MUCs have been observed in animals, plants and yeast [22,23]. MUCs opening, known as the permeability transition (PT), allows the passage of molecules up to 1.5 kDa [23–27], which results in mitochondrial swelling, transmembrane potential depletion and even rupture of the outer membrane [28]. It has been suggested that PT is physiological and reversible and that its main function is to eliminate cations or to partially uncouple the respiratory chain to prevent ROS overproduction [22,24,29–31]. ATP, low Pi and the rapid flow of electrons through the respiratory chain promote opening of $_{Sc}$MUC [20,32,33], while Pi, Ca^{2+} and Mg^{2+} close it [26].

In order to determine the mechanism by which G6P and F1,6BP control mitochondrial metabolism and whether these molecules contribute to the Crabtree effect, their effects of these hexoses-phosphate on $_{Sc}$MUC were tested. It was observed that G6P opens $_{Sc}$MUC while F1,6BP closes it. When added together, the F1,6BP effect dominated. We propose that the closing of the $_{Sc}$MUC by F1,6BP inhibits the rate of oxygen consumption in the resting state

* Corresponding author. Fax: +52 55 5622 5630.
E-mail address: suribe@ifc.unam.mx (S. Uribe-Carvajal).

[1] *Abbreviations used:* $_{Sc}$MUC, *S. cerevisiae* mitochondrial unspecific channel; G6P, glucose-6-phosphate; F1,6BP, fructose-1,6-bisphosphate; PT, permeability transition; CCCP, carbonyl cyanide 3-chlorophenylhydrazone.

http://dx.doi.org/10.1016/j.abb.2014.05.027
0003-9861/

through the tight coupling of mitochondria, i.e. F1,6BP is a Crabtree effect promoter.

Material and methods

Materials

All chemicals were of the highest purity commercially available. Fructose-1,6-bisphosphate, MES, mannitol, triethanolamine, safranine-O, trizma-base, dextrose, carbonyl cyanide 3-chlorophenylhydrazone (CCCP) and glucose-6-phosphate, were from Sigma–Aldrich Co. (St. Louis, MO), $(NH_4)_2SO_4$, D-lactic acid and ethanol were from J.T. Baker S.A. de C.V. (Xalostoc, México), yeast extract and gelatin peptone were from Bioxon Dickinson, S.A. de C.V. (Cuautitlán Izcalli, México), KH_2PO_4, KCl, and phosphoric acid were from Química Suastes S.A. de C.V. (Tlahuac, México), BSA type V was from Research Organics (Cleveland, OH).

Growth conditions

An industrial strain of baker's yeast "yeast foam" (YF) and the *Kluyveromyces lactis* strain 12/8 were used [34]. A 75 mL preculture in YPD (1% yeast extract, 2% gelatin peptone, 2% dextrose) was maintained for 8 h at 30 °C under agitation at 250 rpm. Subsequently, the pre-culture was added to 1L of YPLac (1% yeast extract, 1% gelatin peptone, 0.12% $(NH_4)_2SO_4$, 0.1% KH_2PO_4 and 2% lactic acid, pH = 5.5) and incubated overnight. The cells were washed twice with distilled water by centrifugation in a F14 6x250y Sorvall rotor at 3800×*g* for 5 min.

Isolation of mitochondria

Mitochondria were obtained by homogenization and differential centrifugation [35]. Briefly, cells were suspended 50% w/v in mitochondrial buffer (0.6 M mannitol, 5 mM MES pH 6.8 TEA) plus 0.1% BSA and were homogenized in a Bead Beater using 0.5 mm glass beads [36]. The homogenate was centrifuged in a F21-8x50y Sorvall rotor at 1017×*g* for 5 min. Then the supernatant was recovered and centrifuged at 10,700×*g* for 10 min. The pellet was suspended in mitochondrial buffer containing BSA, and centrifuged at 3600×*g* for 5 min. The supernatant was recovered and centrifuged at 17,000×*g* for 10 min. The resulting pellet was suspended in a small volume of mitochondrial buffer (without BSA) and protein was determined by biuret [37].

Oxygen uptake

The rate of oxygen consumption was measured in resting state (State IV), in phosphorylating conditions (State III) and in the presence of the uncoupler CCCP (State U). We used a Strathkelvin Oximeter model 782 (Warner/Strathkelvin Instruments) with a Clark type electrode immersed in a 1 ml chamber with a water bath (PolyScience model 9000, USA) at 30 °C. The reaction mixture was 0.6 M mannitol, 5 mM MES, pH 6.8 (TEA), 10 mM KCl and 2 μl/ml ethanol. Pi concentrations used are indicated in the legends of the figures and tables. Mitochondrial protein concentration was 0.25 mg/ml.

Mitochondrial swelling

The K^+-mediated mitochondrial swelling was determined at room temperature. The reaction mixture was 0.3 M mannitol, 5 mM MES, pH 6.8 (TEA) and 2 μl/ml, ethanol. Swelling was started with 20 mM KCl as indicated. The absorbance changes were measured at 540 nm in a DW 2000 Aminco spectrophotometer in split mode equipped with a magnetic stirrer [38].

Transmembrane potential

The $\Delta\Psi$ was determined spectrophotometrically using a DW2000 Aminco spectrophotometer in dual mode. The reaction mixture was 0.6 M mannitol, 5 mM MES pH 6.8, 10 mM KCl, 2 μl/ml ethanol and 15 μM safranine-O. Absorbance changes were followed at 511–533 nm [39].

Results and discussion

G6P increases, while F1,6BP inhibits the rate of oxygen consumption through direct inhibition of the cytochrome complexes III and IV [17]. However, a possible additional effect on $_{Sc}$MUC has not been explored. The opening of $_{Sc}$MUC accelerates oxygen consumption through uncoupling of oxidative phosphorylation [20,24,25,40]. By contrast, when $_{Sc}$MUC is closed, oxygen consumption decreases [41]. Therefore, it was decided to explore in isolated yeast mitochondria the effect of G6P and F1,6BP on the rate of oxygen consumption (Table 1).

G6P was tested at concentrations of 2–20 mM in mitochondria where the $_{Sc}$MUC was fully open (0.1 mM Pi), partially open (1 mM Pi) or fully closed (4 mM Pi). When $_{Sc}$MUC was fully open, G6P had no effects (Results not shown). In mitochondria with partially closed $_{Sc}$MUC, G6P increased the rate of oxygen consumption in the resting state IV while the uncoupled state was mildly accelerated only at the highest concentrations tested. These effects led to a mild decrease in the U/IV quotient (Table 1). In the conditions where $_{Sc}$MUC was fully closed, only the highest concentrations of G6P resulted in a small increase in state IV respiration, while the uncoupled rate did not change significantly. Thus, a small decrease in the U/IV quotient was observed at the highest G6P concentrations tested (Table 1). In all cases, the effects of G6P on the phosphorylating state III were similar to those observed in the uncoupled state (Result not shown). The results suggest that at the tested concentrations, G6P has a mild uncoupling effect.

F1,6BP was tested at concentrations of 2–20 mM under conditions where $_{Sc}$MUC was fully open (0.1 mM Pi) or fully closed (4 mM Pi) (Table 2). In mitochondria with an open $_{Sc}$MUC, F1,6BP inhibited both state IV and the uncoupled state, increasing the U/IV from 1.0 in the totally uncoupled control to 2.0 at 6 mM. In mitochondria with a closed $_{Sc}$MUC, F1,6BP also decreased the rates of respiration both in state IV and in the uncoupled state. The U/IV remained constant up to 6 mM F1,6BP, and it decreased at 10 and 20 mM F1,6BP (Table 2). The decrease in the rate of oxygen consumption in state IV respiration and the increase in the U/IV quotient indicated that F1,6BP is a coupling agent. Thus, the oxygen consumption results (Tables 1 and 2) indicate that G6P and F1,6BP are $_{Sc}$MUC effectors, and that while the former is a mild uncoupler, the latter is an efficient coupling agent even at low concentrations.

When $_{Sc}$MUC is open, mitochondria swell upon K^+ addition. Thus, to further investigate whether G6P and F1,6BP modulate $_{Sc}$MUC, swelling was measured. As expected from the oxygen consumption results, G6P had no effect on the opening of $_{Sc}$MUC (Result not shown). However, in the presence of a partially closed $_{Sc}$MUC (1 mM Pi) a slight rate of swelling was observed which increased mildly at higher G6P concentrations (Fig. 1A). In mitochondria where the $_{Sc}$MUC was closed, K^+-mediated swelling was not observed and G6P did not have any effects (Fig. 1B).

The data in Table 2 suggest that F1,6BP is a coupling agent. To determine whether this effect may be related to $_{Sc}$MUC, we added increasing concentrations of F1,6BP to mitochondria with open

Table 1
Effect of G6P on the rate of oxygen consumption under conditions where the $_{Sc}$MUC is partially closed (1 mM Pi) or completely closed (Pi 4 mM).

Pi	G6P (mM)	State IV natgO(min*mgprot)$^{-1}$	Uncoupled state natgO(min*mgprot)$^{-1}$	U/IV
1 mM ($_{Sc}$MUC partially closed)	0	132 ± 17.0	210 ± 19.8	1.6
	2	138 ± 19.8	198 ± 36.8	1.4
	4	150 ± 31.1	212 ± 39.6	1.4
	6	160 ± 11.3	214 ± 14.1	1.3
	10	194 ± 19.8	262 ± 14.1	1.3
	20	234 ± 14.1	280 ± 11.3	1.2
4 mM ($_{Sc}$MUC closed)	0	162.9 ± 28.8	310.0 ± 45.4	1.9
	2	170.8 ± 5.25	278.8 ± 32.9	1.6
	4	196.7 ± 23.5	318.2 ± 23.6	1.6
	6	212.0 ± 18.3	333.9 ± 21.6	1.6
	10	208.7 ± 7.8	326.6 ± 11.0	1.6
	20	231.2 ± 16.5	332.8 ± 40.7	1.4

Reaction mixture: 0.6 M mannitol, 5 mM MES pH 6.8 (TEA), 2 µl ethanol/mL, 10 mM KCl and Pi as indicated. Glucose-6-phosphate (G6P) as indicated. Mitochondria (250 µg prot./mL). The uncoupled state was generated using CCCP (1.5 µM).

Table 2
Effect of F1,6BP on the rate of oxygen consumption under conditions where the $_{Sc}$MUC is opened (Pi 0.1 mM) or closed (Pi 4 mM).

Pi	F1,6BP (mM)	State IV natgO(min*mg prot)$^{-1}$	Uncoupled state natgO(min*mg prot)$^{-1}$	U/IV
0.1 mM ($_{Sc}$MUC open)	0	328.4 ± 29.0	339.2 ± 24.0	1.0
	2	167.6 ± 21.3	257.9 ± 46.0	1.5
	4	143.3 ± 27.3	263.2 ± 25.0	1.8
	6	129.4 ± 4.9	254.0 ± 43.0	2.0
	10	142.2 ± 12.5	276.7 ± 66.0	1.9
	20	140.6 ± 21.7	250.4 ± 46.0	1.8
4 mM ($_{Sc}$MUC closed)	0	240.7 ± 21.1	452.5 ± 40.3	1.9
	2	214.2 ± 5.1	408.0 ± 48.5	1.9
	4	229.0 ± 19.4	422.2 ± 57.9	1.8
	6	208.3 ± 24.6	385.9 ± 8.8	1.8
	10	194.1 ± 24.4	357.3 ± 56.0	1.8
	20	192.7 ± 27.6	334.7 ± 28.3	1.7

Reaction mixture as in Table 1, except F1,6BP as indicated.

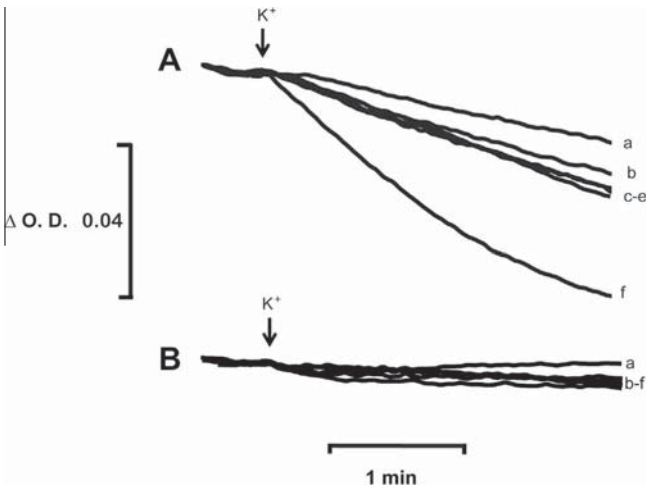

Fig. 1. Effects of G6P on mitochondrial swelling. Reaction mixture: 0.3 M mannitol, 5 mM MES pH 6.8 (TEA), 2 µL ethanol/mL, mitochondria 250 µg prot./mL, and Pi as indicated. Swelling was measured spectrophotometrically at 540 nm. The arrow indicates the addition of 20 mM KCl. (A) Pi 1 mM. (B) Pi 4 mM. G6P (mM) was: a, 0; b, 2; c, 4; d, 6; e, 10; f, 20.

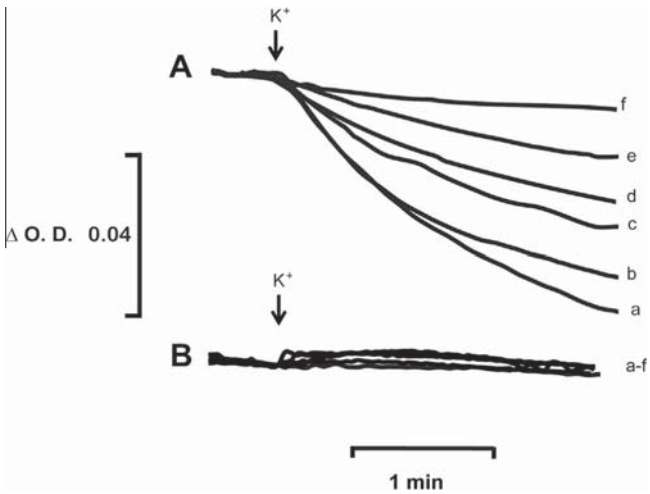

Fig. 2. Effects of F1,6BP on mitochondrial swelling. Reaction mixture as in Fig 1 except (A) Pi 0.1 mM. (B) Pi 4 mM. At the arrow 20 mM KCl was added. G6P (mM) was: a, 0; b, 0.25; c, 0.5; d, 1; e, 2; f, 4.

$_{Sc}$MUC (0.1 mM Pi). In the absence of F1,6BP, mitochondrial swelling was large and rapid (Fig. 2A). Then, as the F1,6BP concentration increased, swelling decreased, becoming negligible at concentrations of 4 mM and above (Fig. 2A trace f). At 4 mM Pi, where $_{Sc}$MUC was closed, no swelling was detected neither in the control nor at any F1,6BP concentration (Fig 2B). Both oxygen consumption and mitochondrial swelling experiments indicate that F1,6BP promotes closure of $_{Sc}$MUC, leading to coupling of oxidative phosphorylation.

The transmembrane potential decreases upon opening of $_{Sc}$MUC [25], and thus the effect of G6P and F1,6BP on this parameter was also tested. In mitochondria with partially closed $_{Sc}$MUC, G6P depleted the already-low transmembrane potential (Fig. 3A). Under conditions where $_{Sc}$MUC was closed, different concentrations of G6P decreased the transmembrane potential (Fig. 3B). When assaying F1,6BP effects on mitochondria with fully open $_{Sc}$MUC (Fig. 4A), the transmembrane potential increased with

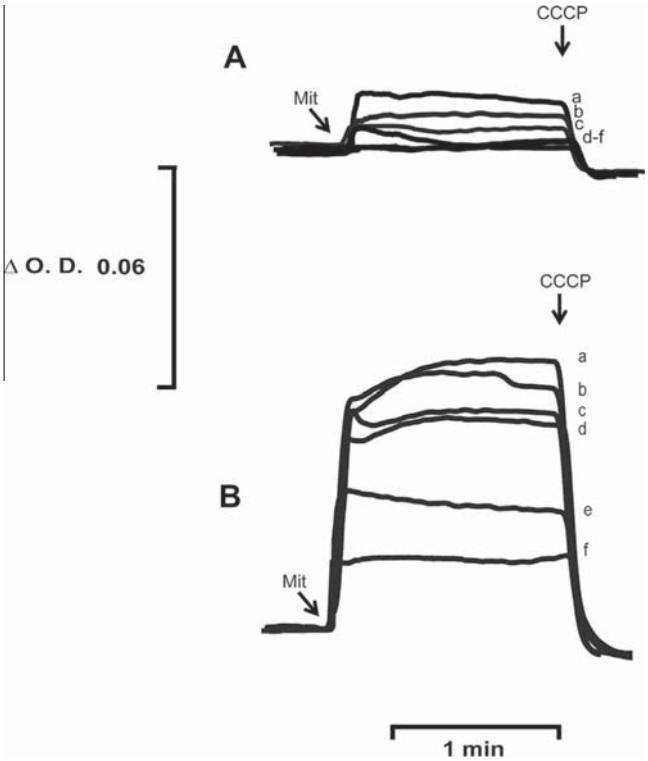

Fig. 3. Effects of G6P on the mitochondrial transmembrane potential. Reaction mixture as in Table 1 (except 15 μM safranin-O), 10 mM KCl and Pi as indicated. (A) Pi 1 mM, (B) Pi 4 mM. G6P (mM) as follows: a, 0; b, 2; c, 4; d, 6; e, 10; f, 20. Where indicated, mitochondria (250 μg prot./mL) or CCCP (1.5 μM) were added.

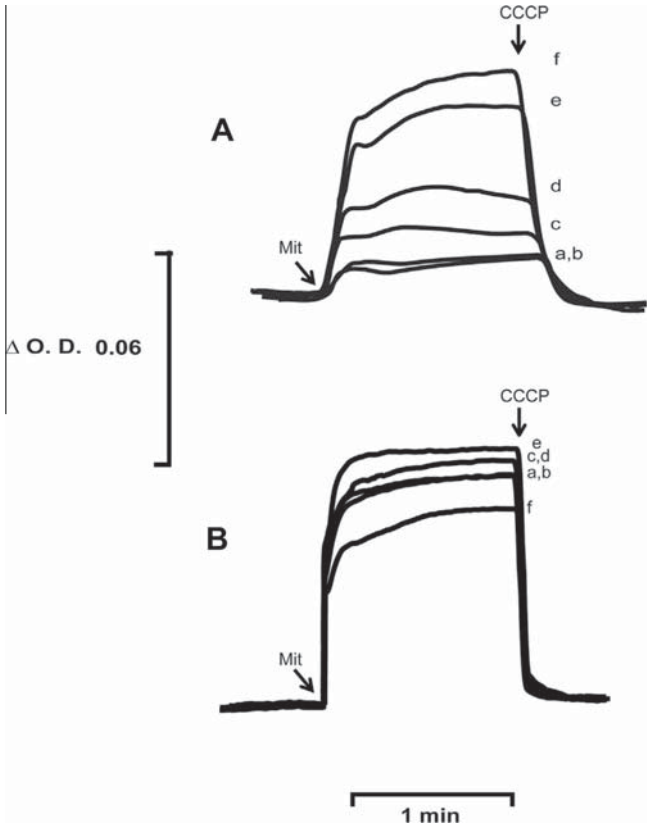

Fig. 4. Effects of F1,6BP on the transmembrane potential. Reaction mixture as in Fig. 3, except (A) Pi 0.1 mM and (B) Pi 4 mM. F1,6BP (mM) was: a, 0; b, 2; c, 4; d, 6; e, 10; f, 20. Mitochondria (250 μg prot./mL), CCCP (1.5 μM).

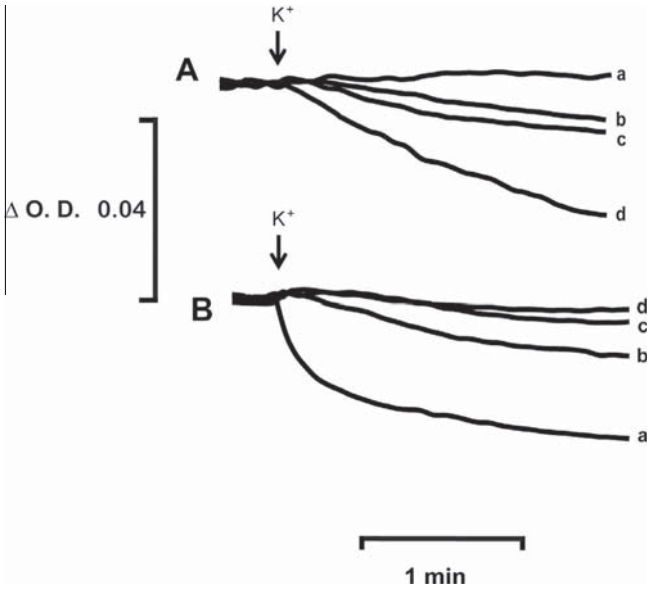

Fig. 5. Effects of competition between F1,6BP and G6P on mitochondrial swelling. Reaction mixture: as in Fig. 1. Pi as indicated. (A) Pi 0.1 mM, 2 mM F1,6BP. G6P (mM) was: a, 0; b, 4; c, 10; d, 20. (B) Pi 1 mM, 10 mM G6P. F1,6BP (mM) was a, 0; b, 0.5; c, 4; d,10.

increasing F1,6BP concentrations, reaching the highest value at 10 mM (Fig. 4A, trace e) and 20 mM (Fig. 4A trace f). Under closed $_{Sc}$MUC conditions, a biphasic effect was observed, where a slight hyperpolarization was detected at 6 (Fig. 4B trace d) and 10 mM (Fig. 4B trace e) whereas a modest decrease in the transmembrane potential was observed at 20 mM F1,6BP (Fig. 4B trace f).

Both phosphate hexoses tested here seem to induce opposite effects. G6P is a mild uncoupler, probably opening $_{Sc}$MUC, while F1,6BP has a strong coupling effect that probably results from closing $_{Sc}$MUC. As both molecules are accumulated simultaneously during active glycolysis, it was decided to test which of their effects predominates when both are present.

To close $_{Sc}$MUC even at low Pi (0.1 mM), 2 mM F1,6BP was added. Under these conditions K^+ addition did not induce swelling (Fig. 5A, trace a). Then, increasing G6P concentrations promoted swelling, reaching a maximum at 20 mM G6P. The opposite experiment was performed under partially closed $_{Sc}$MUC conditions (1 mM Pi) and in the presence of 10 mM G6P, where a slight swelling was promoted by K^+ addition. Then, at increasing F1,6BP concentrations inhibition of swelling was observed, suggesting that the $_{Sc}$MUC-closing effect of F1,6BP was much stronger than the $_{Sc}$MUC-opening effect of G6P.

Thus, we propose that the two hexose-phosphates known to accumulate during active glycolysis are effectors of the $_{Sc}$MUC. G6P is a mild uncoupler working through the opening $_{Sc}$MUC while F1,6BP has stronger coupling properties that probably result in $_{Sc}$MUC closure. The effect of the hexose-phosphate derivatives tested here was observed at lower concentrations than those needed to inhibit respiration.

In mammalians, the mitochondrial permeability transition triggers cell death programs while in turn, a persistently closed MUC results in resistance to apoptosis. Indeed, in rat liver, overexpressed hexokinase seems to interact directly with mitochondria, maintaining MUC in a closed state and thus inhibiting cell death [40–42]. F1,6BP promoted $_{Sc}$MUC closure, therefore inhibiting the permeability transition. In addition, a closed $_{Sc}$MUC inhibits apoptosis and promotes unregulated cell growth, indicating that there

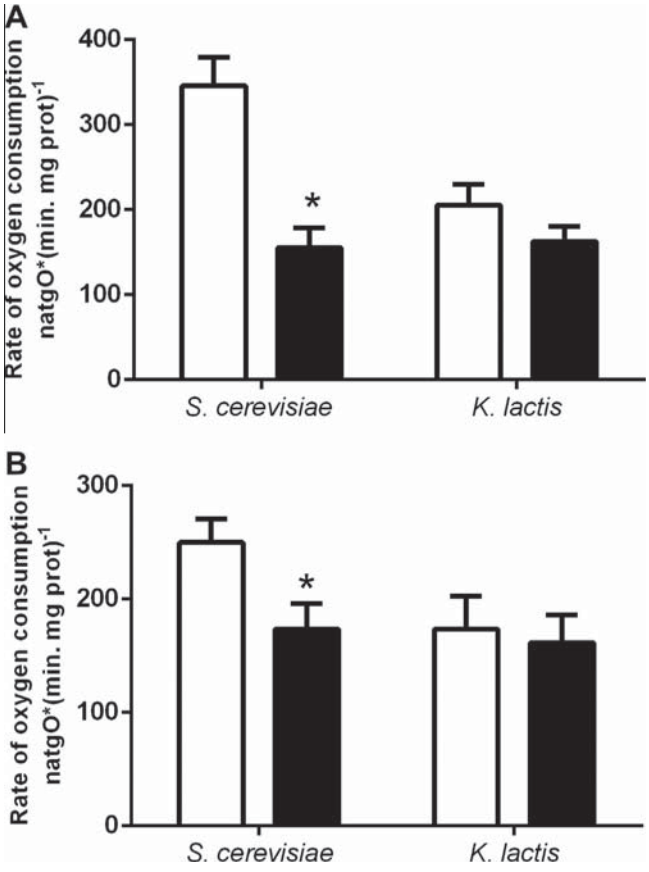

Fig. 6. Effect of F1,6BP on the rate of oxygen consumption of isolated mitochondria from *S. cerevisiae* or *K. lactis*. Reaction mixture as in Table 2, except (A) Pi 0.1 mM; (B) Pi 1 mM. F1,6BP was absent (empty bars) or 10 mM (black bars).*Differences are statistically significant $P < 0.01$, based on ANOVA tukey's multiple comparison test.

may be a causal relationship between tumor cell immortalization and F1,6P accumulation.

If the F1,6BP-mediated inhibition of oxygen consumption by *S. cerevisiae* were related to the Crabtree effect, then Crabtree-negative yeasts should not be inhibited. To test this, we compared the effect of 10 mM F1,6BP on mitochondria isolated from either *S. cerevisiae* or from the Crabtree negative yeast *Kluyveromyces lactis* [43]. As expected from the results shown in Table 2, F1,6BP inhibited the rate of oxygen consumption in mitochondria from *S. cerevisiae* at both 0.1 mM (Fig. 6A) and 1.0 mM Pi (Fig. 6B). By contrast, in mitochondria from *K. lactis*, F1,6BP did not have any effects on the rate of oxygen consumption at either phosphate concentration (Fig. 6). These results strongly support the notion that F1,6BP is a key metabolite that signals closure of $_{Sc}$MUC, triggering the Crabtree effect. Indeed, upon glucose addition, F1,6BP rises to 5–10 mM, which is much higher than the concentration of 0.5 mM F1,6BP needed to maintain $_{Sc}$MUC in a closed state [7]. Furthermore, at 5 mM F1,6BP, additional mitochondrial effects are observed, such as inhibition of complex III and IV activities in the resting state IV. Further studies are needed in order to elucidate the physiological role of maintaining $_{Sc}$MUC closed and dissect its likely relationship with the Crabtree effect.

Acknowledgments

M.R.L. and C.U.A. are CONACYT fellows enrolled in the Biochemistry PhD program at UNAM. Partially funded by PAPIIT-DGAPA/UNAM (grant IN202612). The authors thank Dr. Roberto Coria and Dr. Rocío Navarro for the kind donation of the *K. lactis* 12/8 strain. Dr. Diego González Halphen critically read the manuscript and participated in discussion of the data.

References

[1] R. Diaz-Ruiz, M. Rigoulet, A. Devin, Biochim. Biophys. Acta 1807 (2011) 568–576.
[2] A. Devin, L. Dejean, B. Beauvoit, C. Chevtzoff, N. Averet, O. Bunoust, M. Rigoulet, J. Biol. Chem. 281 (2006) 26779–26784.
[3] J.M. Thevelein, S. Hohmann, Trends Biochem. Sci. 20 (1995) 3–10.
[4] B. Beauvoit, M. Rigoulet, O. Bunoust, G. Raffard, P. Canioni, B. Guerin, Eur. J. Biochem. 214 (1993) 163–172.
[5] N. Averet, H. Aguilaniu, O. Bunoust, L. Gustafsson, M. Rigoulet, J. Bioenerg. Biomembr. 34 (2002) 499–506.
[6] N. Averet, V. Fitton, O. Bunoust, M. Rigoulet, B. Guerin, Mol. Cell. Biochem. 184 (1998) 67–79.
[7] C. Stefan, U. Sauer, FEMS Yeast Res. 11 (2011) 263–272.
[8] J.R. Ernandes, C. De Meirsman, F. Rolland, J. Winderickx, J. de Winde, R.L. Brandao, J.M. Thevelein, Yeast 14 (1998) 255–269.
[9] J. Francois, E. Van Schaftingen, H.-G. Hers, Eur. J. Biochem. 145 (1984) 187–193.
[10] H.G. Crabtree, Biochem. J. 23 (1929) 536–545.
[11] E.F. Greiner, M. Guppy, K. Brand, J. Biol. Chem. 269 (1994) 31484–31490.
[12] A. Merico, P. Sulo, J. Piškur, C. Compagno, FEBS J. 274 (2007) 976–989.
[13] I. Mustea, T. Muresian, Cancer 20 (1967) 1499–1501.
[14] D.H. Koobs, Science 178 (1972) 127–133.
[15] R.L. Veech, J.W. Lawson, N.W. Cornell, H.A. Krebs, J. Biol. Chem. 254 (1979) 6538–6547.
[16] S. Rodriguez-Enriquez, O. Juarez, J.S. Rodriguez-Zavala, R. Moreno-Sanchez, Eur. J. Biochem. 268 (2001) 2512–2519.
[17] R. Diaz-Ruiz, N. Averet, D. Araiza, B. Pinson, S. Uribe-Carvajal, A. Devin, M. Rigoulet, J. Biol. Chem. 283 (2008) 26948–26955.
[18] D.H. Huberts, B. Niebel, M. Heinemann, FEMS Yeast Res. 12 (2012) 118–128.
[19] R. Diaz-Ruiz, S. Uribe-Carvajal, A. Devin, M. Rigoulet, Biochim. Biophys. Acta 1796 (2009) 252–265.
[20] B. Guerin, O. Bunoust, V. Rouqueys, M. Rigoulet, J. Biol. Chem. 269 (1994) 25406–25410.
[21] S. Manon, X. Roucou, M. Guerin, M. Rigoulet, B. Guerin, J. Bioenerg. Biomembr. 30 (1998) 419–429.
[22] S. Uribe-Carvajal, L.A. Luevano-Martinez, S. Guerrero-Castillo, A. Cabrera-Orefice, N.A. Corona-de-la-Pena, M. Gutierrez-Aguilar, Mitochondrion 11 (2011) 382–390.
[23] P. Bernardi, Physiol. Rev. 79 (1999) 1127–1155.
[24] R.A. Haworth, D.R. Hunter, Arch. Biochem. Biophys. 195 (1979) 460–467.
[25] V. Castrejon, C. Parra, R. Moreno, A. Pena, S. Uribe, Arch. Biochem. Biophys. 346 (1997) 37–44.
[26] V. Perez-Vazquez, A. Saavedra-Molina, S. Uribe, J. Bioenerg. Biomembr. 35 (2003) 231–241.
[27] V. Castrejon, A. Pena, S. Uribe, J. Bioenerg. Biomembr. 34 (2002) 299–306.
[28] P. Bernardi, M. Forte, Novartis Found. Symp. 287 (2007) 157–164 (discussion 164–159).
[29] M. Crompton, Biochem. J. 341 (1999) 233–249.
[30] J.J. Lemasters, A.L. Nieminen, T. Qian, L.C. Trost, S.P. Elmore, Y. Nishimura, R.A. Crowe, W.E. Cascio, C.A. Bradham, D.A. Brenner, B. Herman, Biochim. Biophys. Acta 1366 (1998) 177–196.
[31] A.P. Halestrap, Nature 430 (2004). 1 p following 983.
[32] S. Manon, M. Guerin, Biochem. Mol. Biol. Int. 44 (1998) 565–575.
[33] E. Fontaine, O. Eriksson, F. Ichas, P. Bernardi, J. Biol. Chem. 273 (1998) 12662–12668.
[34] R. Navarro-Olmos, L. Kawasaki, L. Dominguez-Ramirez, L. Ongay-Larios, R. Perez-Molina, R. Coria, Mol. Biol. Cell 21 (2010) 489–498.
[35] A. Pena, M.Z. Pina, E. Escamilla, E. Pina, FEBS Lett. 80 (1977) 209–213.
[36] S. Uribe, J. Ramirez, A. Pena, J. Bacteriol. 161 (1985) 1195–1200.
[37] A.G. Gornall, C.J. Bardawill, M.M. David, J. Biol. Chem. 177 (1949) 751–766.
[38] S. Prieto, F. Bouillaud, D. Ricquier, E. Rial, Eur. J. Biochem. 208 (1992) 487–491.
[39] K.E. Akerman, M.K. Wikstrom, FEBS Lett. 68 (1976) 191–197.
[40] C. Fiek, R. Benz, N. Roos, D. Brdiczka, Biomembranes 688 (1982) 429–440.
[41] M. Gutierrez-Aguilar, X. Perez-Martinez, E. Chavez, S. Uribe-Carvajal, Arch. Biochem. Biophys. 494 (2010) 184–191.
[42] H. Azoulay-Zohar, A. Israelson, S. Abu-Hamad, V. Shoshan-Barmatz, Biochem. J. 377 (2004) 347–355.
[43] N. Mates, K. Kettner, F. Heidenreich, T. Pursche, R. Migotti, G. Kahlert, E. Kuhlisch, K.D. Breunig, W. Schellenberger, G. Dittmar, B. Hoflack, T.M. Kriegel, Mol. Cell. Proteomics 13 (2014) 860–875.

J Bioenerg Biomembr (2014) 46:519–527
DOI 10.1007/s10863-014-9595-3

Effects of ubiquinone derivatives on the mitochondrial unselective channel of *Saccharomyces cerevisiae*

Manuel Gutiérrez-Aguilar · Helga M. López-Carbajal · Cristina Uribe-Alvarez · Emilio Espinoza-Simón · Mónica Rosas-Lemus · Natalia Chiquete-Félix · Salvador Uribe-Carvajal

Received: 15 June 2014 / Accepted: 25 November 2014 / Published online: 3 December 2014

Abstract Ubiquinone derivatives modulate the mammalian mitochondrial Permeability Transition Pore (PTP). Yeast mitochondria harbor a similar structure: the respiration- and ATP-induced *Saccharomyces cerevisiae* Mitochondrial Unselective Channel ($_{Sc}$MUC). Here we show that decylubiquinone, a well-characterized inhibitor of the PTP, suppresses $_{Sc}$MUC opening in diverse strains and independently of respiratory chain modulation or redox-state. We also found that naturally occurring derivatives such as hexaprenyl and decaprenyl ubiquinones lacked effects on the $_{Sc}$MUC. The PTP-inactive ubiquinone 5 (Ub_5) promoted the $_{Sc}$MUC-independent activation of the respiratory chain in most strains tested. In an industrial strain however, Ub_5 blocked the protection elicited by dUb. The results indicate the presence of a ubiquinone-binding site in the $_{Sc}$MUC.

Keywords Ubiquinone analogues · Mitochondria · Permeability transition pore · Yeast

Abbreviations

dUb	Decylubiquinone
dVO_4	Decavanadate
$\Delta\psi$	Mitochondrial transmembrane potential
FCCP	Carbonyl cyanide *p*-trifluoro-methoxyphenyl-hydrazone
Cyclosporine A	CsA
PTP	Mitochondrial permeability transition pore
$_{Sc}$MUC	*Saccharomyces cerevisiae* mitochondrial unselective channel
Ub_5	Ubiquinone 5
Ub_{30}	Hexaprenylquinone
Ub_{50}	Decaprenylquinone

M. Gutiérrez-Aguilar (✉)
Dalton Cardiovascular Research Center, University of Missouri-Columbia, 134 Research Park Dr, Columbia, MO 65211, U.S.A
e-mail: gutierrezaguilarm@missouri.edu

H. M. López-Carbajal · C. Uribe-Alvarez · E. Espinoza-Simón · M. Rosas-Lemus · N. Chiquete-Félix · S. Uribe-Carvajal
Department of Molecular Genetics, Instituto de Fisiología Celular, Universidad Nacional Autónoma de México, UNAM, Mexico City, Mexico

Introduction

The mitochondrial permeability transition can be defined as the rise in unselective conductance to ions and metabolites triggered by the opening of an unidentified non-selective pore (Brenner and Moulin 2012). In mammalian mitochondria, the permeability transition pore (PTP) depletes the protonmotive force and exhibits a molecular mass cutoff of up to 1.5 kDa (Bernardi 2013). The *Saccharomyces cerevisiae* Mitochondrial Unselective Channel ($_{Sc}$MUC) is probably an equivalent of the PTP (Uribe-Carvajal et al. 2011).

The biochemistry and physiopathology of the PTP has been studied *ad extenso*. Most hypotheses suggest that this pore opens irreversibly during several disease states, inducing a collapse in mitochondrial homeostasis (for a review, see Di Lisa and Bernardi 2006). In contrast, PTP transient opening or flickering has also been proposed to regulate Ca^{2+} homeostasis in mitochondria (Ichas and Mazat 1998). Less is known in terms of the molecular composition of the PTP; earlier models proposing that the Adenine Nucleotide Translocator and the Voltage Dependent Anion Channel could form the PTP have not successfully passed genetic tests (reviewed in Bonora et al. 2014). When the mitochondrial phosphate carrier is deleted, this results in changes in the properties of both, the PTP (Kwong et al. 2014) and the $_{Sc}$MUC (Gutiérrez-Aguilar et al. 2010) likely by controlling inorganic phosphate

(Pi) availability in mitochondria. However, a moderate change in the expression levels of the Pi carrier does not impact the Ca^{2+}-induced PTP (Gutiérrez-Aguilar et al. 2014). Up to now, Cyclophilin D (CypD) and mitochondrial Complex I are the only widely accepted modulators of the PTP (Giorgio et al. 2010; Di Lisa et al. 2011; Li et al. 2012). Topical studies suggest that CypD regulates F_1F_0-ATP synthase. In addition, the purified dimeric enzyme from both mouse and *S. cerevisiae* mitochondria forms a multiple conductance channel with PTP-like behavior (Giorgio et al. 2013; Carraro et al. 2014). This has led to propose that the unselective pores observed in yeast and higher eukaryotes are equivalent structures that form at the interface of two F_0 sectors of ATP synthase and that the F_0 sector may play an important role in PTP formation (Bernardi 2013; Bonora et al. 2013).

The $_{Sc}$MUC probably participates in energy surplus dissipation processes (Prieto et al. 1995). Although the $_{Sc}$MUC and the mammalian PTP present similar molecular exclusion properties, it was earlier proposed that the $_{Sc}$MUC could be hardly considered a yeast counterpart of the PTP (Manon et al. 1998). Since *S. cerevisiae* lacks a mitochondrial Ca^{2+}-uniporter (Uribe et al. 1992), Ca^{2+} does not activate the $_{Sc}$MUC unless *S. cerevisiae* mitochondria are incubated in the presence of the Ca^{2+} ionophore ETH129 (Yamada et al. 2009; Carraro et al. 2014). In regard to similarities in their properties, $_{Sc}$MUC and PTP are both regulated by ADP, octylguanidine, Mg^{2+}, Pi, mercurials and mastoparan (Uribe-Carvajal et al. 2011). Indeed it has been suggested that MUCs are conserved throughout the eukaryotic domain (for reviews see Azzolin et al. 2010; Bernardi and Von Stockum 2012).

Different ubiquinone analogues seem to interact with mammalian mitochondria on a specific site. Then, depending on the analogue substituent, PTP may be activated, unaffected or inhibited (Walter et al. 2000). In addition, since ubiquinones are natural ligands of respiratory complexes I, II and III, certain analogues can also interfere with respiration thus making difficult to detect off-site effects (Walter et al. 2000). Here we aimed to determine whether ubiquinone analogues modulate the $_{Sc}$MUC. This is interesting as *S. cerevisiae* mitochondria lack respiratory complex I. Our results show that known PTP inhibitors modulate $_{Sc}$MUC activity and support the notion of a conserved ubiquinone-binding site on the channel.

Materials and methods

Materials

All chemicals were reagent grade. dUB, Ub_5, Ub_{30}, Ub_{50}, Mannitol, MES, ethanol, safranine-O, $CaCl_2$, $MgCl_2$, ADP, FCCP and bovine serum albumin type V were from Sigma Chem Co. (St. Louis, MO). All other reagents were of the highest purity commercially available.

Industrial and laboratory yeast strains

A commercial strain of the baker's yeast *S. cerevisiae* (La Azteca) was purchased from a local bakery. The industrial strain Yeast Foam (YF) was obtained from a previous collaboration (Díaz-Ruiz et al. 2008). The laboratory strains were BY4741 (BY) (*MATa; his3 Δ1; leu2 Δ0; met15 Δ0; ura3 Δ)* and W303 (*MATα; ura3-1; trp1Δ 2; leu2-3,112; his3-11,15; ade2-1; can1-100*).

Isolation of Yeast Mitochondria

For experiments in Figs. 1, 2A, B, C, 3, 4B and 5, an industrial strain of *S. cerevisiae* (La Azteca) was used. Cells (40 g) were suspended and incubated in a rich liquid medium under aeration (3 L/min) for 16 h, washed, suspended in distilled water and starved overnight under aeration (de Kloet et al. 1961). Cells were washed by centrifugation three times and suspended in 0.6 M mannitol, 5 mM MES, 0.1 % bovine serum albumin, pH 6.8 adjusted with triethanolamine (TEA). Cells were disrupted using a Braun cell-homogenizer and 0.45 mm diameter glass beads. Mitochondria were isolated by differential centrifugation in a SS34 rotor (Sorvall) (Cortés et al. 2000). Protein concentration was determined by a biuret method. For experiments in Figs. 2D and 4, the strains YF, W303 and BY were also used. The *S. cerevisiae* industrial strain Yeast Foam (YF) was subcultured 8 hours in YPD and cultured in YPLac until reaching an optical density of 3.0-3.5. The *S. cerevisiae* laboratory strains W303 and BY were subcultured in YPD for 24 hours and cultured in of YPLac for 24 hours. All cultures were grown under constant agitation (250 rpm) at 30 °C. Mitochondria were isolated from the YF, W303 and BY strains after spheroplast homogenization and differential centrifugation (for detailed protocols see Gutiérrez-Aguilar et al. 2010).

Oxygen consumption

The rate of oxygen consumption was measured in the resting state (State 4) and in the phosphorylating state (State 3) using an YSI model 5,300 oxygraph equipped with a Clark-Type electrode at room temperature in a 1.5 mL chamber containing mitochondria at a final concentration of 0.5 mg protein/mL. Samples were suspended in respiration buffer (0.6 M mannitol, 5 mM MES pH 6.8 (TEA) plus 5 μL/mL 96 % ethanol as respiratory substrate, unless indicated otherwise). The concentrations of Pi and K^+ used are indicated under each figure. Stock solutions were 1.0 M $MgCl_2$, 2.0 M KCl, and either 1.0

or 0.1 M PO_4^{3-} buffer, pH 6.8 (TEA) and 20 mM dUb, Ub_5, Ub_{30}, Ub_{50}.

Transmembrane potential (Δψ)

The Δψ was determined using 10 μM safranine-O, following the absorbance changes at 511–533 nm in a DW2000 Aminco spectrophotometer in dual mode (Akerman and Wikström 1976). At the end of each trace, Δψ was collapsed by adding 6 μM FCCP.

Mitochondrial swelling

The K^+-mediated swelling of mitochondria was measured as described before (Castrejón et al. 2002). Typically, coupled isolated mitochondria are impermeable to K^+. However, when the $_{Sc}$MUC opens, it allows unselective transport of externally added K^+ along with anions present in the medium, resulting in the transport of osmotically active species. This will result in the transport of water towards the mitochondrial matrix following swelling of the organelles, which is optically measured as a decrease in light scattering of isolated mitochondria in suspension. Swelling buffer, containing 0.3 M mannitol, 5 mM MES, pH 6.8 (TEA), plus 5 μL/mL ethanol or NADH was used to promote swelling under energized conditions. Swelling was promoted by adding 20 mM KCl where indicated by an arrow. The absorbance changes were measured at 540 nm in a DW2 Aminco spectrophotometer in split mode equipped with a magnetic stirrer. Sample volume was kept constant at 4 mL of respiration buffer. Mitochondrial concentration was 0.5 mg protein/mL.

NADH:NAD^+ ratio determination

In order to determine whether the increase in alcohol dehydrogenase activity led to an increase in the percentage of reduced NADH, we made a NADH concentration curve, which we used to determine the amount of NADH present in samples incubated in the presence of increasing ethanol. Then, the 100 % percent NADH concentration was evaluated after adding 3 μM sodium dithionite, which was prepared within one hour (Quinlan et al. 2013). NADH absorbance was read at 340 nm in a Varian 50 Bio-UV/Vis spectrophotometer.

Results

In isolated mitochondria, dUb inhibits opening of the $_{Sc}$MUC

The ubiquinone derivative dUb closes the PTP in mitochondria from different cell lines and mammalian sources (Walter et al. 2000; Devun et al. 2010). With this in mind, we decided to assess whether other ubiquinone derivatives also regulate $_{Sc}$MUC opening (Fig. 1A). We first monitored oxygen consumption of isolated *S. cerevisiae* mitochondria from the industrial strain La Azteca under control conditions where the $_{Sc}$MUC is typically closed by high phosphate (Fig. 1B, "c"). Under these conditions, the respiration rate of isolated mitochondria remained low. Respiration was significantly increased when phosphate was decreased, indicating opening of $_{Sc}$MUC (Fig. 1B, "0"). This high respiration rate phenotype was gradually attenuated with dUb in a concentration-dependent manner (Fig. 1B "10" to "30"). We next wanted to assess if the protective effects of dUb on respiration were derived from a direct interaction with the respiratory chain (Fig. 1C). To address this possibility we tested the effects of increasing amounts of dUb in mitochondria incubated with the uncoupler FCCP. Under these conditions, dUb failed to decrease the respiration rate of isolated mitochondria suggesting that the protection was not at the level of the respiratory chain. The $_{Sc}$MUC can be regulated by fluctuations in the NADH:NAD^+ ratio (Bradshaw and Pfeiffer 2013). This is of particular relevance as *S. cerevisiae* lacks respiratory complex I, which has been proposed to regulate PTP opening (Li et al. 2012). To further address if dUb regulates the $_{Sc}$MUC through modifications of the NADH dehydrogenase activity, we performed state 4 oxygen consumption experiments in the presence of increasing concentrations of ethanol (which generates NADH), in the absence and presence of dUb (Fig. 1D). As expected, increasing concentrations of ethanol enhanced the rate of respiration, being maximal at 20 mM ethanol. The presence of dUb under these conditions resulted in a decreased state four respiration, reaching significance at 20 mM ethanol. Further Lineweaver-Burk processing of these results suggests that dUb behaves as a non-competitive inhibitor of NADH-linked respiration and further implying that the dUb effects on $_{Sc}$MUC activity are not related to NADH:NAD^+ ratio fluctuations (Fig. 1E). Furthermore, the NADH:NAD^+ ratio did not change in any of the ethanol concentrations tested (result not shown); this probably indicates that alcohol dehydrogenase is much slower than NADH dehydrogenase activities and thus it cannot affect the NADH reduction percentage.

Opening of the $_{Sc}$MUC prevents energized mitochondria from building up a stable Δψ (Gutiérrez-Aguilar et al. 2010). With this in mind, we tested the effects of dUb on the Δψ of isolated mitochondria from La Azteca strain under the same conditions as those used for oxygen consumption. The results show that in the presence of high phosphate, mitochondria are able to sustain a high, constant and FCCP-sensitive Δψ (Fig. 2A trace a). Decreasing phosphate in the incubation media resulted in a fast drop in Δψ, indicative of $_{Sc}$MUC opening. This Δψ reading was not sensitive to further

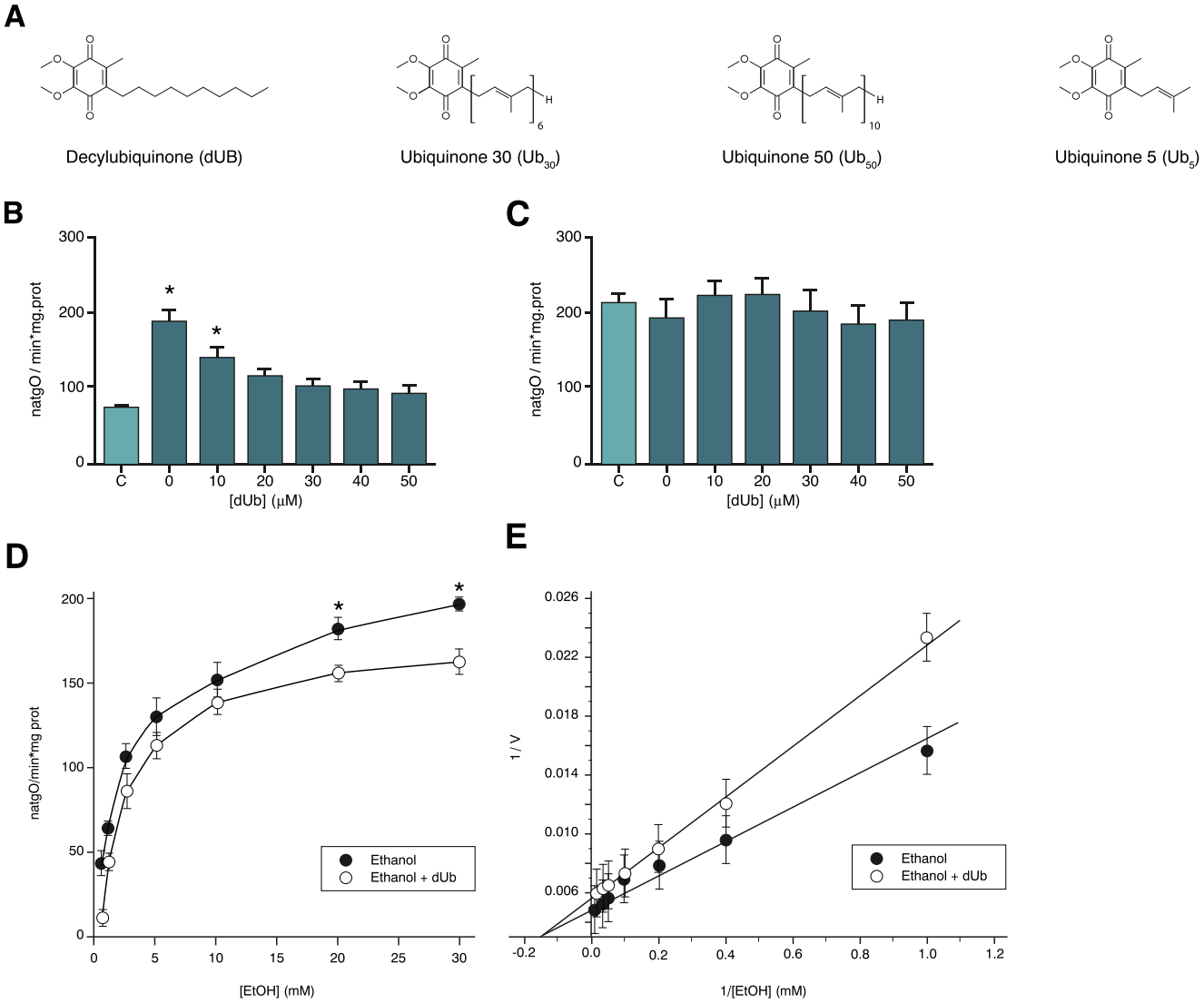

Fig. 1 Ubiquinone derivatives used in this study and effects of dUb on the rates of oxygen consumption in closed/open $_{Sc}$MUC conditions in mitochondria isolated from *S. cerevisiae* La Azteca strain. Chemical structures in (**A**) represent the ubiquinone derivatives used in this study. For panels B-E, experimental conditions were: 0.6 M Mannitol, 5 mM MES, pH 6.8, 20 mM KCl, pH 6.8 (TEA), 5 μL ethanol /mL. To obtain the uncoupled state respiration, 6 μM FCCP was added in the experiments on panel C. Measurements were conducted in a water-jacketed chamber (30 °C) connected to an oxymeter interfaced to a computer. Rates of oxygen consumption are expressed in natoms gram O (min.mg prot)$^{-1}$. Isolated mitochondria were used at a final concentration of 0.5 mg prot/mL. Bars in both B and C were: "C"=4 mM Pi, no dUb, 0=0.4 mM Pi no dUb, 10=0.4 mM Pi plus 10 μM dUb, 20=0.4 mM Pi plus 20 μM dUb, 30=0.4 mM Pi plus 30 μM dUb, 40=0.4 mM Pi plus 40 μM dUb, 50=0.4 mM Pi plus 50 μM dUb. In (**D**), oxygen uptake in open MUC (0.4 mM Pi) condition was evaluated in the presence (●) or absence (○) of 30 μM dUb. Rates of respiration were calculated at different ethanol concentrations (0.5 mM, 1 mM, 2.5 mM, 5 mM, 10 mM, 20 mM, 30 mM) with and without dUb added. (**E**) Lineweaver-Burk plot from data presented in (**D**), which indicates a non-competitive inhibition of dUb. Each point represents the mean of three experiments±Standard Deviation. *P<0.05 vs. "C"

addition of FCCP (Fig. 2A trace b). Under this condition, increasing dUb resulted in the gradual buildup of a $\Delta\psi$ Fig. 2A traces c to h), reaching maximal values at 50 and 100 μM dUb (Fig. 2A traces g, h).

A typical parameter used to measure $_{Sc}$MUC (and PTP) activity is the swelling resulting from opening of the pore (Castrejón et al. 2002). Mitochondria suspended in buffer with ethanol as respiratory substrate and high levels of phosphate were not sensitive to K^+-induced swelling (Fig. 2B trace a). Isolated mitochondria in the presence of ethanol plus low phosphate levels rapidly swelled following K^+ addition (Fig. 2B trace b). Then increasing levels of dUb, attenuated mitochondrial swelling confirming a direct inhibition of the $_{Sc}$MUC (Fig. 2B traces c-h). The experiments above show that dUb closed the $_{Sc}$MUC in the presence of 0.4 mM phosphate. However, all experiments were performed in the presence of ethanol as respiratory substrate. Ethanol reduces NAD^+ to $NADH+H^+$, which in turn is reoxidized by the internal

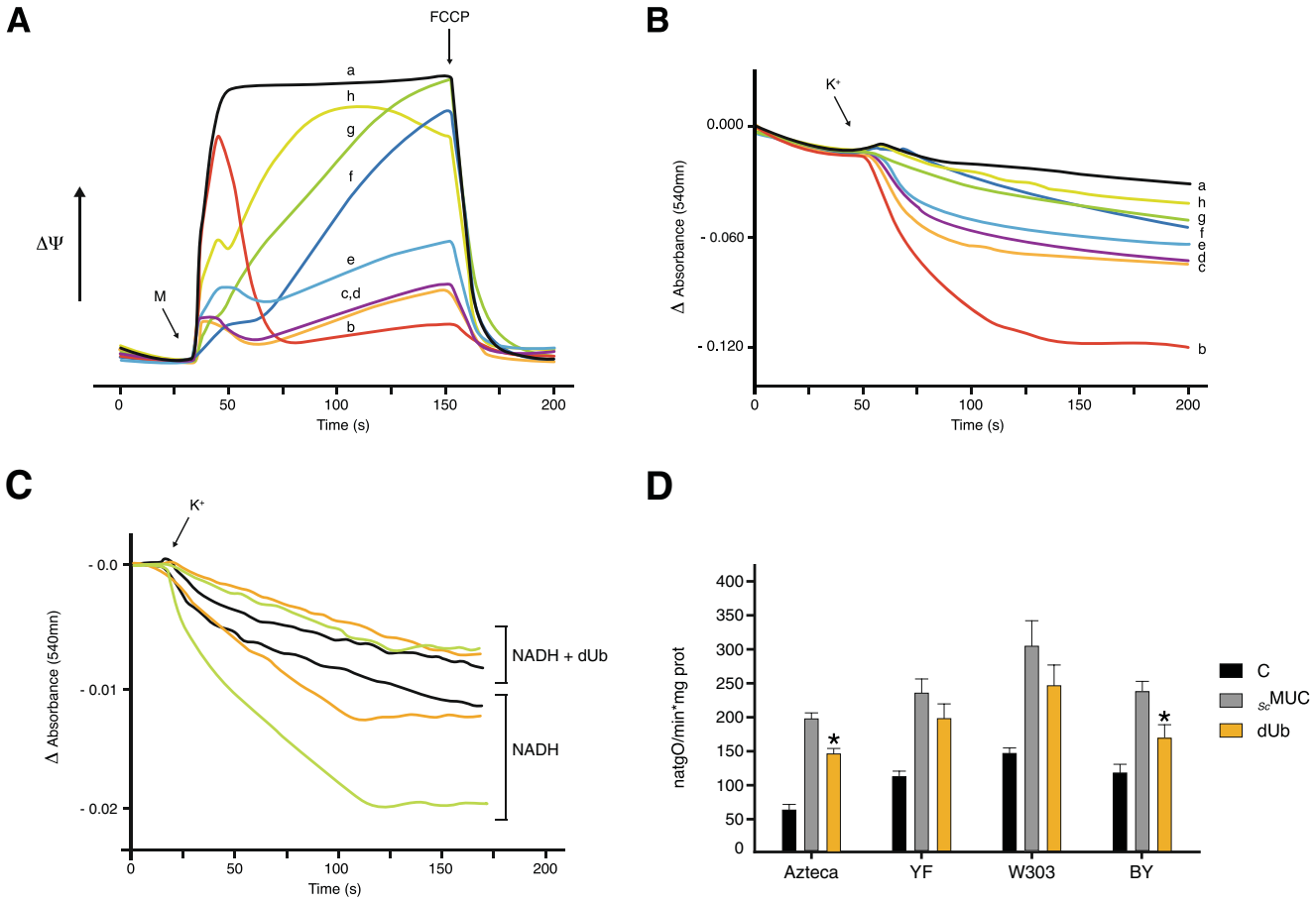

Fig. 2 Effect of dUb on the (**A**) Δψ and (**B**) swelling of mitochondria isolated from different industrial and laboratory strains of *S. cerevisiae*. Experimental conditions: As in Fig. 1 except in (**A**), 10 μM safranine-O. Traces in both (**A**) and (**B**) were: a=4 mM Pi, no dUb, b=0.4 mM Pi no dUb, c=0.4 mM Pi plus 10 μM dUb, d=0.4 mM Pi plus 20 μM dUb, e=0.4 mM Pi plus 30 μM dUb, f=0.4 mM Pi plus 40 μM dUb, g=0.4 mM Pi plus 50 μM dUb, h=0.4 mM Pi plus 100 μM dUb. Mitochondria (M) were added at the arrow. Representative experiment from n=3. For the experiments detailed in (**C**), externally added NADH was used instead of ethanol to energize mitochondria in the presence of 0.4 mM Pi being 0 mM NADH (black traces), 1 mM NADH (yellow traces) and 2 mM NADH (green traces) in the absence or presence of 30 μM dUb as indicated. Representative experiment from n=3. In (**D**), data are presented as oxygen uptake rate in natgO (min*mg prot)$^{-1}$. Bars labeled "C" represent the oxygen uptake rate in the presence of 4 mM phosphate. Bars labeled "dUb" represent the oxygen uptake rate in the presence of 30 μM dUb. Please refer to section "Industrial and laboratory yeast strains" for information of the strains used in these experiments. Each bar represents the mean of three independent experiments±Standard Error. *P<0.05 vs. values of "$_{Sc}$MUC" labeled bars

NADH dehydrogenase. In our hands the redox state of the pyridine nucleotides did not vary under these conditions. Nonetheless, it has been reported that increased NADH:NAD$^+$ ratios and/or high respiratory rates can result in $_{Sc}$MUC or PTP opening (Leverve and Fontaine 2001; Manon 1999; Manon et al. 1998). To determine whether dUb inhibited $_{Sc}$MUC opening in the presence of increasing NADH, we directly added NADH to isolated mitochondria (Fig. 2C). As expected, at 1 and 2 mM, NADH promoted $_{Sc}$MUC opening as indicated by an increase in mitochondrial swelling (Fig. 2C, "NADH" traces). In contrast, in the presence of 30 μM dUb swelling was prevented regardless of the NADH addition (Fig. 2C, "NADH+dUb" traces). Thus it may be concluded that the effect of dUb is independent of the purine nucleotide pool redox state.

Early studies assessing the regulation and transport properties of the $_{Sc}$MUC concluded that industrial and laboratory strains of *S. cerevisiae* presented a mitochondrial pore with different effector sensitivities (Manon et al. 1998). These differences were later proposed to be context-specific and were abolished under appropriate experimental conditions (Bradshaw and Pfeiffer 2013). In mammalian mitochondria, cell type-dependent differential response to ubiquinone derivatives has been reported (Devun et al. 2010). With this in mind, we assessed the sensitivity of different industrial and laboratory strains of *S. cerevisiae* to dUb (Fig. 2D). We performed state 4 oxygen uptake rate experiments on the industrial strains La Azteca and Yeast Foam (YF) and the laboratory W303 and BY strains. As expected, conditions leading to closure of the $_{Sc}$MUC induced a typical-baseline oxygen uptake rate phenotype in isolated mitochondria from

all strains (Fig. 2D, black bars). In the presence of low phosphate loads ($_{Sc}$MUC), oxygen consumption was enhanced (Fig. 2D, gray bars). In agreement with Fig. 1A, addition of 30 μM dUb reduced the oxygen uptake rate in the industrial and laboratory strains (Fig. 2D, yellow bars). The effect was $_{Sc}$MUC-specific and concentration-dependent as confirmed with Δψ and swelling experiments performed in the laboratory W303 and BY strains (results not shown).

Effects of naturally occurring ubiquinones on the $_{Sc}$MUC of industrial and laboratory strains

Based on our results showing that dUb-induced $_{Sc}$MUC closure does not depend on a potential interaction of the ubiquinone derivative with the respiratory chain, we next wanted to assess whether naturally occurring ubiquinones such as hexaprenyl (Ub_{30}) and decaprenyl quinone (Ub_{50}) could potentially influence $_{Sc}$MUC activity in addition to its physiological role in the respiratory chain (Fig. 3). We performed Δψ experiments on isolated mitochondria from the industrial strain La Azteca under control conditions where we detected a high and stable Δψ (Fig. 3A, trace a). As shown before, opening of the $_{Sc}$MUC led to a decrease in Δψ (Fig. 3A, trace b). Increasing concentrations of Ub_{30} (10–100 μM) did not confer any potential protection on the $_{Sc}$MUC-dependent Δψ decrease (Fig. 3A, traces c-f). Oxygen consumption experiments in the presence of Ub_{30} under the same experimental conditions resulted in no protection against $_{Sc}$MUC-mediated increase in the oxygen consumption rate (not shown). We measured Δψ of isolated mitochondria from La Azteca strain in the presence of Ub_{50} (Fig. 3B). Although we occasionally measured weak, concentration-independent increases in Δψ (see Fig. 3B, trace d), oxygen consumption experiments evidenced lack of Ub_{50} protection against $_{Sc}$MUC-dependent increase in respiration (not shown).

Ub_5 does not modulate the $_{Sc}$MUC

We decided to test whether Ub_5, which has been reported to behave as a PTP-inactive derivative, could modulate the $_{Sc}$MUC in isolated mitochondria from the industrial and laboratory strains of *S. cerevisiae* used in this study. Consequently, we measured state 4 oxygen uptake rates of isolated mitochondria from La Azteca YF, W303 and BY strains under control conditions (C), where oxygen uptake rates were low (Fig. 4A, black bars) and in the presence of low phosphate loads, which trigger $_{Sc}$MUC opening (Fig. 4A, gray bars). Addition of 200 μM Ub_5 under $_{Sc}$MUC conditions had no effects on the uptake rates of mitochondria from La Azteca strain. Conversely, Ub_5 increased oxygen uptake rates ~2-3 fold under $_{Sc}$MUC conditions in the YF, W303 and BY strains (Fig. 4A, white bars). Further oxygen uptake experiments in the presence of high phosphate loads (closed $_{Sc}$MUC) resulted in a concentration-dependent increase in mitochondrial respiration mediated by Ub_5 in all strains (Fig. 4B). The increase in oxygen uptake was significantly lower in La Azteca strain (Fig. 4B, ●). Such effects in the oxygen uptake of all strains were $_{Sc}$MUC-independent, given Ub_5 failed to modulate Δψ on isolated mitochondria from all strains in the presence of either low or high phosphate loads (not shown).

Ub_5 suppresses dUb protective effects in La Azteca strain

While dUb promoted closure of $_{Sc}$MUC, Ub_5 did not exhibit measurable $_{Sc}$MUC-related effects in La Azteca strain. Therefore, to determine if Ub_5 could still bind (but not

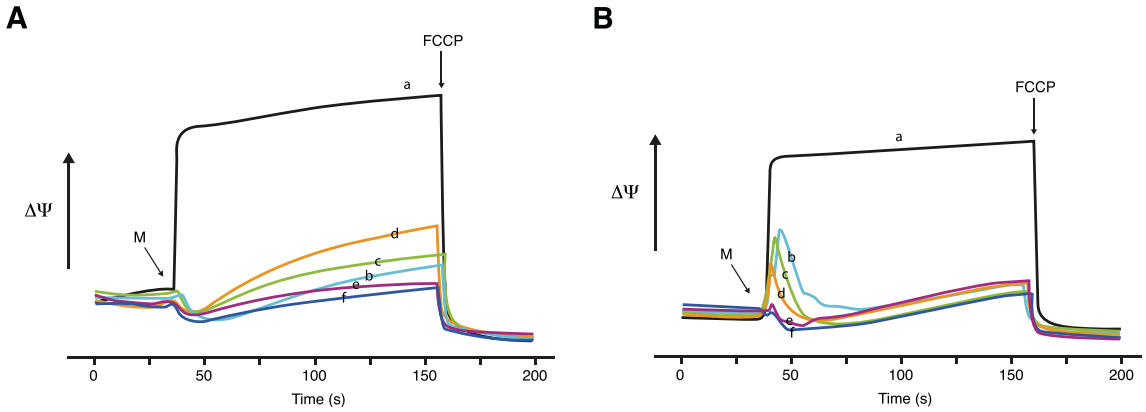

Fig. 3 Effects of Ub_{30} and Ub_{50} on the Δψ of isolated mitochondria of *S. cerevisiae* La Azteca strain. Experimental conditions were as in Fig. 2. Traces in (**A**) were: a=4 mM Pi, no Ub_{30}, b=0.4 mM Pi, no Ub_{30}, c=0.4 mM Pi plus 10 μM Ub_{30}, d=0.4 mM Pi plus 30 μM Ub_{30}, e=0.4 mM Pi plus 50 μM Ub_{30}, f=0.4 mM Pi plus 100 μM Ub_{30}. Traces in (**B**) were: a=4 mM Pi, no Ub_{50}, b=0.4 mM Pi, no Ub_{50}, c=0.4 mM Pi plus 10 μM Ub_{50}, d=0.4 mM Pi plus 30 μM Ub_{50}, e=0.4 mM Pi plus 50 μM Ub_{50}, f=0.4 mM Pi plus 100 μM Ub_{50}. Mitochondria (M) were added at the arrow. Representative experiment from $n=3$

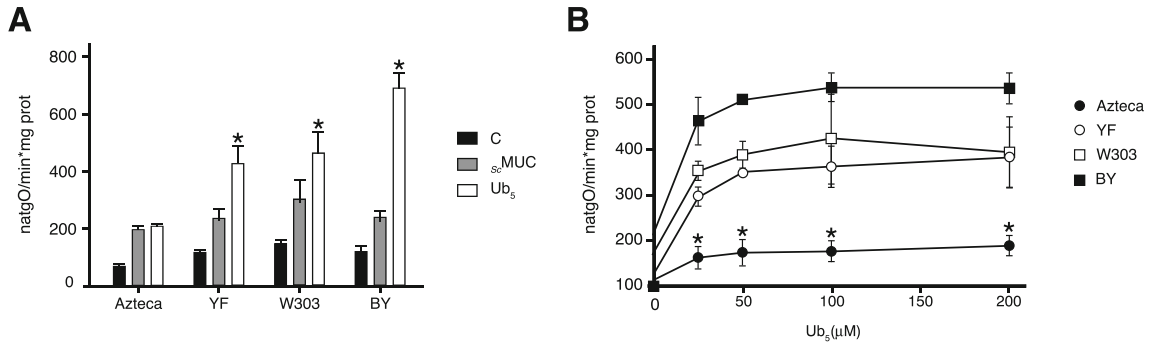

Fig. 4 Effects of Ub_5 on the oxygen uptake rates of mitochondria isolated from different industrial and laboratory strains of *S. cerevisiae*. Experimental conditions: As in Fig. 2. A, B=oxygen uptake rates. Bars labeled "$_{Sc}$MUC" represent oxygen uptake rates in the presence of 0.4 mM phosphate. Bars labeled "C" represent percent oxygen uptake rates in the presence of 4 mM phosphate. Bars labeled "Ub_5" represent percent oxygen uptake rates in the presence of 200 μM Ub_5. Please refer to section "Industrial and laboratory yeast strains" for information of the strains used in these experiments. Each bar represents the mean of three independent experiments±Standard Deviation. *P<0.05 vs. values of "$_{Sc}$MUC" labeled bars. In (**B**), oxygen uptake rates were evaluated with increasing concentrations of Ub_5 using isolated mitochondria from La Azteca (●), YF (○), W303 (□), and by (■) strains. Data are presented as oxygen uptake rate in natgO (min*mg prot)$^{-1}$. Rates of respiration were calculated at different Ub5 concentrations (0 μM, 25 μM, 50 μM, 100 μM, 200 μM). Each value represents the mean of three independent experiments±Standard Deviation. *P<0.05 vs. values of YF, W303 and BY strains

modulate) the $_{Sc}$MUC in this strain, we designed a competition protocol measuring the rate of oxygen consumption in the presence of dUb and increasing concentrations of Ub_5 (Fig. 5). At 0.4 mM Pi, addition of 50 μM dUb promoted the return to a basal rate. Further additions of Ub_5 from 25 to 200 μM increased oxygen consumption similarly to uncoupled rates (Fig. 5A). These results were confirmed with Δψ experiments under the same conditions. At 4 mM Pi, Δψ values were high and stable but low at 0.4 mM Pi. Δψ values returned to high values at 0.4 mM Pi plus 50 μM dUb. Then, in the presence of increasing Ub_5 concentrations Δψ values decreased again (Fig. 5B). These results indicate that dUb-mediated closure of $_{Sc}$MUC was reverted by Ub_5, suggesting that these ubiquinone derivatives compete for the same binding site.

Discussion

The PTP-modulating effects of ubiquinone analogues have been proposed to be downstream from the regulatory role of CypD (Basso *et al.* 2005). Fontaine et al. (1998) previously proposed that the ubiquinone effect-site was respiratory

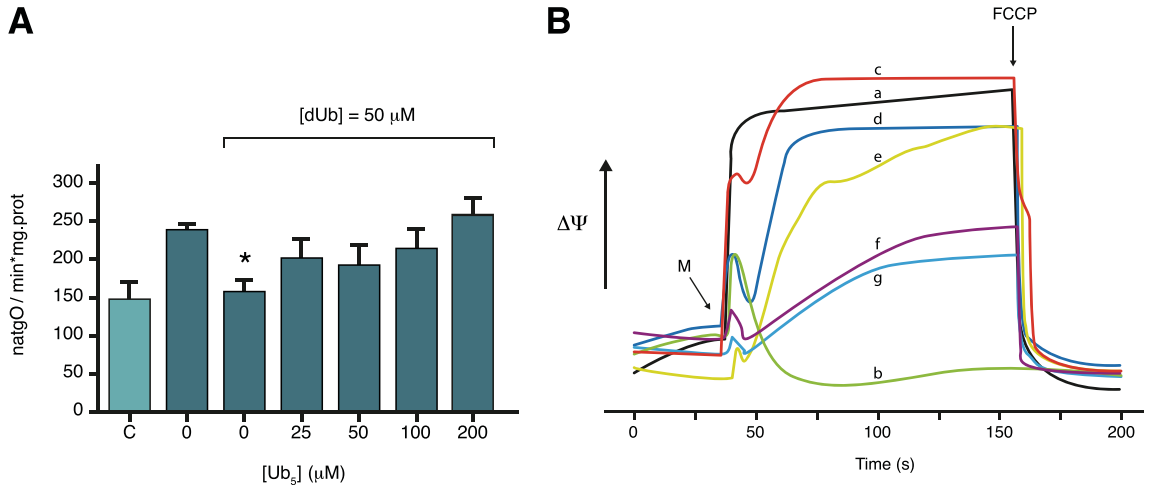

Fig. 5 Combined effects of dUb and Ub_5 on the rates of oxygen consumption and Δψ of mitochondria isolated from *S. cerevisiae* La Azteca strain. Experimental conditions: As in Fig. 2. A=oxygen consumption, B=Δψ. Bars in A were: "C"=4 mM Pi, no Ub_5 or dUb, 0=0.4 mM Pi no Ub_5 or dUb, 25=0.4 mM Pi plus 25 μM Ub_5, 50=0.4 mM Pi plus 50 μM Ub_5, 100=0.4 mM Pi plus 100 μM Ub_5, 200=0.4 mM Pi plus 200 μM Ub_5. Where indicated, 50 μM dUb was present in the reaction mixture. Each point represents the mean of three experiments±Standard Deviation. *P<0.05 vs. C. Traces in B were: a=4 mM Pi, no Ub_5, b=0.4 mM Pi and no Ub_5, c=0.4 mM Pi and no Ub_5, d=0.4 mM Pi plus 25 μM Ub_5 e=0.4 mM Pi plus 50 μM Ub_5, f=0.4 mM Pi plus 100 μM Ub_5, g=0.4 mM Pi plus 200 μM Ub_5. For traces c-g, 50 μM dUb was present in the reaction mixture. Mitochondria (M) were added where indicated by an arrow. Representative experiment from n=3

complex I. It is important to note that these analogues present divergent modulating properties depending on the ubiquinone side chain (Walter et al. 2002). In addition such divergent properties are cell line-specific (Devun et al. 2010). This implies that PTPs (and probably the $_{Sc}$MUC) may present context-specific accessory components. Indeed, (Li et al. 2012) proposed that rotenone-mediated inhibition of complex I may be even more protective against PTP opening than CsA as long as CypD levels do not exceed those of discrete complex I subunits. Manon (1999) also concluded that $_{Sc}$MUC activity is strictly dependent on respiratory chain activity. These data suggest that MUCs are likely modulated by the pyridine nucleotide redox state. In fact, Hunter and Haworth (1979) were the first to report NADH-induced PTP inhibition indicating that the PTP remained closed upon inhibition of complex I with rotenone or through the regulation of the NADH:NAD^+ ratio using β-hydroxybutyrate and acetoacetate. Ubiquinone derivatives regulate the PTP downstream of mitochondrial CypD, strongly indicating that these molecules bind directly to the pore or to another regulatory factor (Basso et al. 2005). Since the $_{Sc}$MUC is probably not regulated by the yeast mitochondrial Cyclophilin (Cpr3), but is still sensitive to ubiquinone derivatives, the $_{Sc}$MUC and the PTP still present conserved characteristics. To this, the utilization of *S. cerevisiae* as a model to understand the PTP constitutes a powerful genetic tool to unveil the molecular componentry of the $_{Sc}$MUC as recently proposed by Carraro et al. (2014). Here, we provide evidence supporting the notion that the $_{Sc}$MUC presents a conserved ubiquinone-sensitive site and that the effects of ubiquinone derivatives are independent of the presence of mitochondrial complex I, which is naturally absent in our yeast model. We also show that dUb blocks the $_{Sc}$MUC, like the PTP, in a similar concentration range. Then we confirm that the effects of dUb are not related to the regulation of the mitochondrial respiration nor changes in the matrix NADH:NAD^+ ratio, which are also known pore effectors (Leverve and Fontaine 2001). This suggests that respiration-induced $_{Sc}$MUC opening and dUb-mediated $_{Sc}$MUC closure likely occur through unrelated mechanisms.

We finally show that although the PTP-inactive Ub_5 counteracts the effects of dUb on the $_{Sc}$MUC of La Azteca strain, this derivative also strongly activates $_{Sc}$MUC-independent respiration in several yeast strains tested. To this, the Ub_5-mediated increase in respiration has also been reported for the laboratory CEN.PK2–1C strain of *S. cerevisiae* (James et al. 2005). Although the cause for such divergent phenotype between La Azteca and the rest of the strains tested is unknown and is subject of further research in our laboratory, adaptive evolution could account for the differences monitored herein, where close to 22 % of the total transcripts detected in industrial strains do not match annotated sequences for laboratory strains (Varela et al. 2005). We have discussed this possibility for the strain-specific differences in $_{Sc}$MUC activity reported before (Uribe-Carvajal et al. 2011).

Altogether, our results suggest that ubiquinone analogues can regulate the $_{Sc}$MUC as seen with the mammalian PTP. Consequently, ubiquinone analogues may bind to a conserved/discrete site and its lateral chain may be involved in the gating of the $_{Sc}$MUC as well as the PTP. This likely explains why ubiquinone derivatives with disparate side chains have similar properties on the PTP and the $_{Sc}$MUC. The results presented here also imply that ubiquinone analogues display its permeability-modulating effects in a complex I-independent context.

Acknowledgments M.G.-A. is currently supported by an American Heart Association Midwest Affiliate Postdoctoral Fellowship (13POST14060013). HLC is a CONACyT fellow enrolled in the Ms. Sc. Biochemistry program at UNAM. CUA, EGS and MRL are CONACyT fellows enrolled in the Ph. D. Biochemistry program at UNAM. Partially funded by DGAPA/PAPIIT Project IN202612. We acknowledge the technical assistance of Ramón Mendez. Mariana Valenzuela kindly helped to build the figures.

References

Akerman KE, Wikström MK (1976) Safranine as a probe of the mitochondrial membrane potential. FEBS Lett 68:191–197

Azzolin L, Von Stockum S, Basso E et al (2010) The mitochondrial permeability transition from yeast to mammals. FEBS Lett 584: 2504–2509

Basso E, Fante L, Fowlkes J et al (2005) Properties of the permeability transition pore in mitochondria devoid of Cyclophilin D. J Biol Chem 280:18558–18561

Bernardi P (2013) The mitochondrial permeability transition pore: a mystery solved? Front Physiol 4:95

Bernardi P, Von Stockum S (2012) The permeability transition pore as a Ca^{2+} release channel: new answers to an old question. Cell Calcium 52:22–27

Bonora M, Bononi A, De Marchi E et al (2013) Role of the c subunit of the F_O ATP synthase in mitochondrial permeability transition. Cell Cycle 12:674–683

Bonora M, Wieckowski MR, Chinopoulos C, et al. (2014) Molecular mechanisms of cell death: central implication of ATP synthase in mitochondrial permeability transition. Oncogene. doi:doi:10.1038/onc.2014.96

Bradshaw PC, Pfeiffer DR (2013) Characterization of the respiration-induced yeast mitochondrial permeability transition pore. Yeast 30: 471–483

Brenner C, Moulin M (2012) Physiological roles of the permeability transition pore. Circ Res 111:1237–1247

Carraro M, Giorgio V, Sileikytė J, et al. (2014) Channel Formation by Yeast F-ATP Synthase and the Role of Dimerization in the Mitochondrial Permeability Transition. J Biol Chem 289:15980–15985

Castrejón V, Peña A, Uribe S (2002) Closure of the yeast mitochondria unselective channel (YMUC) unmasks a Mg^{2+} and quinine sensitive K^+ uptake pathway in *Saccharomyces cerevisiae*. J Bioenerg Biomembr 34:299–306

Cortés P, Castrejón V, Sampedro JG, Uribe S (2000) Interactions of arsenate, sulfate and phosphate with yeast mitochondria. Biochim Biophys Acta 1456:67–76

de Kloet S, van Wermeskerken R, Koningsberger VV (1961) Studies on protein synthesis by protoplasts of *Saccharomyces carlsbergensis*. I. The effect of ribonuclease on protein synthesis. Biochim Biophys Acta 47:138–143

Devun F, Walter L, Belliere J et al (2010) Ubiquinone analogs: a mitochondrial permeability transition pore-dependent pathway to selective cell death. PLoS ONE 5:e11792

Díaz-Ruiz R, Averet N, Araiza D, Pinson B, Uribe-Carvajal S, Devin A et al (2008) Mitochondrial oxidative phosphorylation is regulated by fructose 1,6-bisphosphate. A possible role in Crabtree effect induction? J Biol Chem 283:26948–26955

Di Lisa F, Bernardi P (2006) Mitochondria and ischemia-reperfusion injury of the heart: fixing a hole. Cardiovasc Res 70:191–199

Di Lisa F, Carpi A, Giorgio V, Bernardi P (2011) The mitochondrial permeability transition pore and cyclophilin D in cardioprotection. Biochim Biophys Acta 1813:1316–1322

Fontaine E, Eriksson O, Ichas F, Bernardi P (1998) Regulation of the permeability transition pore in skeletal muscle mitochondria. Modulation By electron flow through the respiratory chain complex I. J Biol Chem 273:12662–12668

Giorgio V, Soriano ME, Basso E et al (2010) Cyclophilin D in mitochondrial pathophysiology. Biochim Biophys Acta 1797:1113–1118

Giorgio V, Von Stockum S, Antoniel M et al (2013) Dimers of mitochondrial ATP synthase form the permeability transition pore. Proc Natl Acad Sci U S A 110:5887–5892

Gutiérrez-Aguilar M, Douglas DL, Gibson AK et al (2014) Genetic manipulation of the cardiac mitochondrial phosphate carrier does not affect permeability transition. J Mol Cell Cardiol 72:316–325

Gutiérrez-Aguilar M, Pérez-Martínez X, Chávez E, Uribe-Carvajal S (2010) In *Saccharomyces cerevisiae*, the phosphate carrier is a component of the mitochondrial unselective channel. Arch Biochem Biophys 494:184–191

Hunter DR, Haworth RA (1979) The Ca^{2+}-induced membrane transition in mitochondria. I. The protective mechanisms. Arch Biochem Biophys 195:453–459

Ichas F, Mazat JP (1998) From calcium signaling to cell death: two conformations for the mitochondrial permeability transition pore. Switching from low- to high-conductance state. Biochim Biophys Acta 1366:33–50

James AM, Cochemé HM, Smith RAJ, Murphy MP (2005) Interactions of mitochondria-targeted and untargeted ubiquinones with the mitochondrial respiratory chain and reactive oxygen species. Implications for the use of exogenous ubiquinones as therapies and experimental tools. J Biol Chem 280:21295–21312

Kwong JQ, Davis J, Baines CP et al (2014) Genetic deletion of the mitochondrial phosphate carrier desensitizes the mitochondrial permeability transition pore and causes cardiomyopathy. Cell Death Differ 21(8):1209–1217

Leverve XM, Fontaine E (2001) Role of substrates in the regulation of mitochondrial function in situ. IUBMB Life 52(3–5):221–229

Li B, Chauvin C, De Paulis D et al (2012) Inhibition of complex I regulates the mitochondrial permeability transition through a phosphate-sensitive inhibitory site masked by cyclophilin D. Biochim Biophys Acta 1817:1628–1634

Manon S (1999) Dependence of yeast mitochondrial unselective channel activity on the respiratory chain. Biochim Biophys Acta 1410:85–90

Manon S, Roucou X, Guérin M et al (1998) Characterization of the yeast mitochondria unselective channel: a counterpart to the mammalian permeability transition pore? J Bioenerg Biomembr 30:419–429

Prieto S, Bouillaud F, Rial E (1995) The mechanism for the ATP-induced uncoupling of respiration in mitochondria of the yeast *Saccharomyces cerevisiae*. Biochem J 307(Pt 3):657–661

Quinlan CL, Peresvoshchikova IV, Hey-Mogensen M, Orr AL, Brand MD (2013) Sites of reactive oxygen species generation by mitochondria oxidizing different substrates. Redox Biol 1:304–312

Uribe S, Rangel P, Pardo JP (1992) Interactions of calcium with yeast mitochondria. Cell Calcium 13:211–217

Uribe-Carvajal S, Luévano-Martínez LA, Guerrero-Castillo S et al (2011) Mitochondrial unselective channels throughout the eukaryotic domain. Mitochondrion 11:382–390

Varela C, Cárdenas J, Melo F, Agosin E (2005) Quantitative analysis of wine yeast gene expression profiles under winemaking conditions. Yeast 22:369–383

Walter L, Miyoshi H, Leverve X et al (2002) Regulation of the mitochondrial permeability transition pore by ubiquinone analogs. a progress report. Free Radic Res 36:405–412

Walter L, Nogueira V, Leverve X et al (2000) Three classes of ubiquinone analogs regulate the mitochondrial permeability transition pore through a common site. J Biol Chem 275:29521–29527

Yamada A, Yamamoto T, Yoshimura Y et al (2009) Ca^{2+}-induced permeability transition can be observed even in yeast mitochondria under optimized experimental conditions. Biochim Biophys Acta 1787: 1486–1491

Provisional chapter

Oxygen: From Toxic Waste to Optimal (Toxic) Fuel of Life

Mónica Rosas-Lemus, Cristina Uribe-Alvarez1,
Martha Contreras-Zentella,
Luis Alberto Luévano-Martínez,
Natalia Chiquete-Félix, N. Lilia Morales-García,
Adriana Muhlia-Almazán,
Edgardo Escamilla-Marván and
Salvador Uribe-Carvajal

Additional information is available at the end of the chapter

Abstract

Some 2.5 billion years ago, the great oxygenation event (GOE) led to a 10^5-fold rise in atmospheric oxygen [O_2], killing most species on Earth. In spite of the tendency to produce toxic reactive oxygen species (ROS), the highly exergonic reduction of O_2 made it the ideal biological electron acceptor. During aerobic metabolism, O_2 is reduced to water liberating energy, which is coupled to adenosine triphosphate (ATP) synthesis. Today, all organisms either aerobic or not need to deal with O_2 toxicity. O_2-permeant organisms need to seek adequate [O_2], for example, aquatic crustaceans bury themselves in the sea bottom where O_2 is scarce. Also, the intestinal lumen and cytoplasm of eukaryotes is a microaerobic environment where many facultative bacteria or intracellular symbionts hide from oxygen. Organisms such as plants, fish, reptiles and mammals developed O_2-impermeable epithelia, plus specialized external respiratory systems in combination with O_2-binding proteins such as hemoglobin or leg-hemoglobin control [O_2] in tissues. Inside the cell, ROS production is prevented by rapid O_2 consumption during the oxidative phosphorylation (OxPhos) of ATP. When ATP is in excess, OxPhos becomes uncoupled in an effort to continue eliminating O_2. Branched respiratory chains, unspecific pores and uncoupling proteins (UCPs) uncouple OxPhos. One last line of resistance against ROS is deactivation by enzymes such as super oxide dismutase and catalase. Aerobic organisms profit from the high energy released by the reduction of O_2, while at the same time they need to avoid the toxicity of ROS.

Keywords: oxygen, ROS, oxidative stress, oxyconformers, oxyregulators, adaptative metabolism

1. At the beginning, all life was anaerobic

The early Earth atmosphere contained high [H_2], [NH_3] and [CH_4], while [O_2] was less than 10^{-5} the present atmospheric level (PAL) [1,2]. All life forms were anaerobic [3,4]. Early redox reactions involved electron donors such as H_2, CO_2 or HS [5,6], while electron acceptors were sulfur and NO_3 [7]. Eukaryotes were present before O_2 rose [8,9] and contained anaerobic mitochondrion-like organelles [10,11].

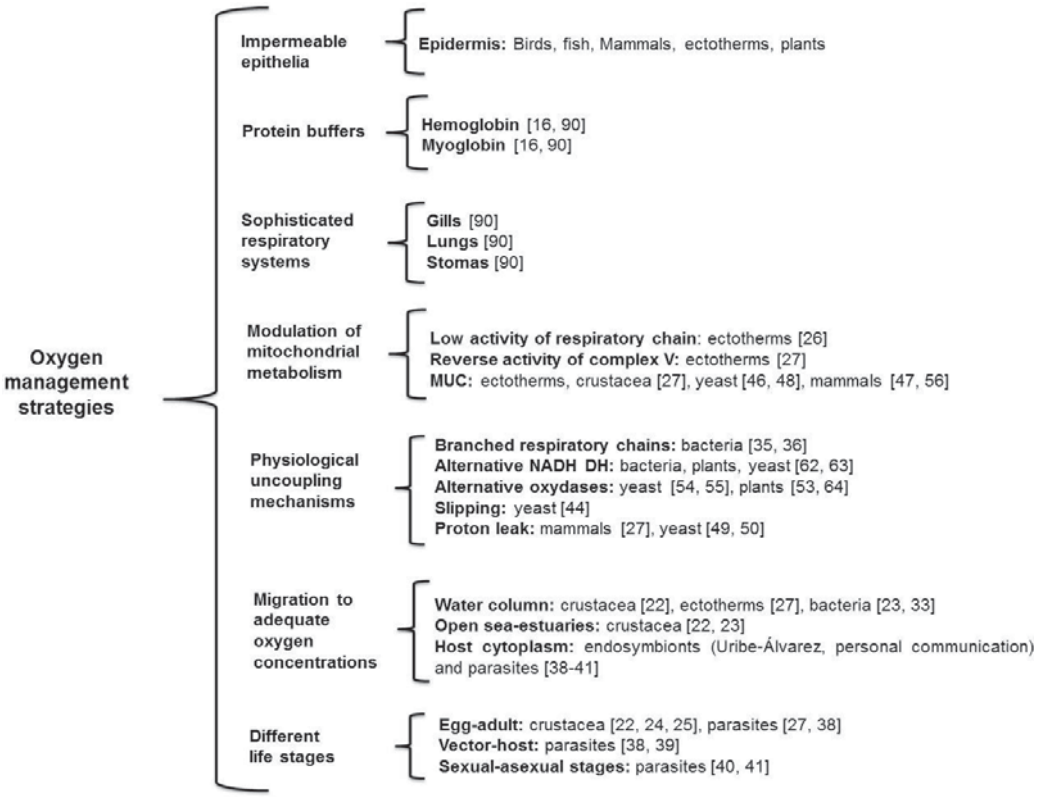

Figure 1. Oxygen management strategies in different organisms. Organisms need to adapt to the O_2 concentration in the environment. Therefore, either they move to environments with adequate O_2 or they engineer different mechanisms to process O_2 at varying rates (electron transport chain (ETC) activity, mitochondrial unspecific channels (MUC), uncoupling proteins (UCPs). Additionally, oxyregulators have developed O_2-excluding mechanisms such as impermeable epithelia, external respiratory systems (lungs, gills, stomas) and O_2-transporting proteins (hemoglobin, myoglobin).

Environment	O_2 concentration (μM)	References
Atmosphere	1000m ASL 256.0 Sea level 1028.0	[88]
Alveoles	143.0	[89]
Arteries	123.0 *Hb bound 120.5* *Not bound 2.5*	[89] [90]
Capillaries	130.0	[89]
Interstitial fluid	55.0	[89]
Tissue cells	31.0	[89]
Veins	59.0	[89]
Mitochondria	Minimal for coupling 0.1 Minimal reported 20.0	[91]
Distilled water	223.0	[92]
Sea water	Surface 198-397.0 250.0 MOZ < 20.0	[93] [34] [94]
Estuaries	Surface 375.0 Bottom 62.5	[95] [96]

Oxygen concentrations reported were modified from partial pressures to micromolar concentration (μM) using Henry's law at 310.15K ASL (above sea level).

Table 1. Oxygen concentrations in different environments.

2. The massive increase in [O_2] and the need to counteract its toxicity

Approximately 2.5 billion years ago, the great oxygenation event (GOE) was precipitated by both geological processes [12] and by the photosynthetic activity of cyanobacteria [13,14]. Today, O_2 is the preferred electron acceptor used by facultative microorganisms and the only one used by aerobes. The highly exergonic reduction of O_2 provided the energy needed for the development of multicellular organisms. In addition, the high energy of activation required for O_2 reduction ensures that this reaction occurs mostly through catalyzed reactions. For instance, oxidases bind their substrate tightly, preventing the liberation of reactive oxygen species (ROS) [15]. At low concentrations, ROS are useful as signaling molecules, while at higher concentrations ROS damage and kill cells. Cells need much less [O_2] than what is found in the atmosphere and thus, to prevent ROS production internal O_2 is kept at a low level [16]. Cells have developed two mechanisms to deal with surplus O_2: (1) avoiding it and (2) rapidly reducing it. Furthermore, cellular O_2 is found mostly bound to proteins such as hemoglobin, leg-hemoglobin and myoglobin. Early oxy-conformer organisms are permanent to O_2, and thus, at different stages in their life cycle, they have to migrate to microaerobic or anaerobic

spaces (**Table 1**) to cope with variations in O_2. More evolved oxyregulator organisms from fish to mammals enveloped themselves in an O_2-impermeable epithelium, while at the same time developing highly specialized systems that control tissue [O_2] (**Figure 1**). Oxyconformers and oxyregulators display different strategies to manage O_2-by-product toxicity (**Figure 1**).

In oxyconformers, all cells are exposed to environmental [O_2]. O_2-permeable organisms do have O_2 transport proteins and intracellular O_2-binding proteins, but in addition, they need to implement diverse strategies to deal with changing O_2. These include searching for microaerophilic or anaerobic environments. Arthropoda, the most abundant and widely distributed phylum on Earth, are oxyconformers [17]; it comprises subphyla Chelicerata (spiders), Myriapoda (centi- and millipedes), Hexapoda (Insects) and Crustacea, all of them protected by an exoskeleton. Nonaquatic insects possess a hard waterproof cuticle and branched invaginated tubules forming a specialized respiratory structure that works well at constant [O_2]. Aquatic organisms, including most of the crustacea, are exposed to highly variant [O_2], which may be 26 times lower than in the atmosphere [18,19]. In water, [O_2] varies with temperature, depth, mechanical aeration and tidal movements. Only few invertebrates (Plathelmynthes, Nematoda, Molluska, Anellida and Sypuncula) have been thoroughly studied in regard to their mechanisms to deal with fluctuating [O_2] [20,21]. Remarkably, very few studies on Crustacea are available.

In order to control the release of ROS oxyconformers reduce aerobic activity during hypoxia/anoxia cycles, marine crustaceans display different responses to hypoxia/anoxia. To avoid hyperoxygenated or anoxic waters, crustaceans migrate between open sea and coastal lagoons (**Figure 2**), or migrate vertically through the water column to flee the O_2 minimum zone (OMZ) and into [O_2] compatible with their metabolic needs [22,23]. Some shrimp species, such as the burrowing thalassinids *Upogebia major* and *Callianasa japonica,* which commonly inhabit the extremely hypoxic or even anoxic intertidal flats, can reduce their respiratory rate in dugout burrows, surviving up to 5 h of anoxia for *U. major* and 19 h for *C. japonica* [24]. *Artemia franciscana* is well known for its high tolerance to anoxia; the embryos of this species survive without O_2 for years through the complete depression of their metabolic rates [25,26]. Metabolic rate depression is also observed in ectotherms, which lower their mitochondrial activity in function of temperature adjusting their O_2 consumption machinery accordingly [27]. However, it is not clear how mitochondria from oxyconformers respond to hypoxia, how respiratory activity adapts to reduced metabolic rates and how the cellular redox balance and energetic homeostasis are preserved [28,29].

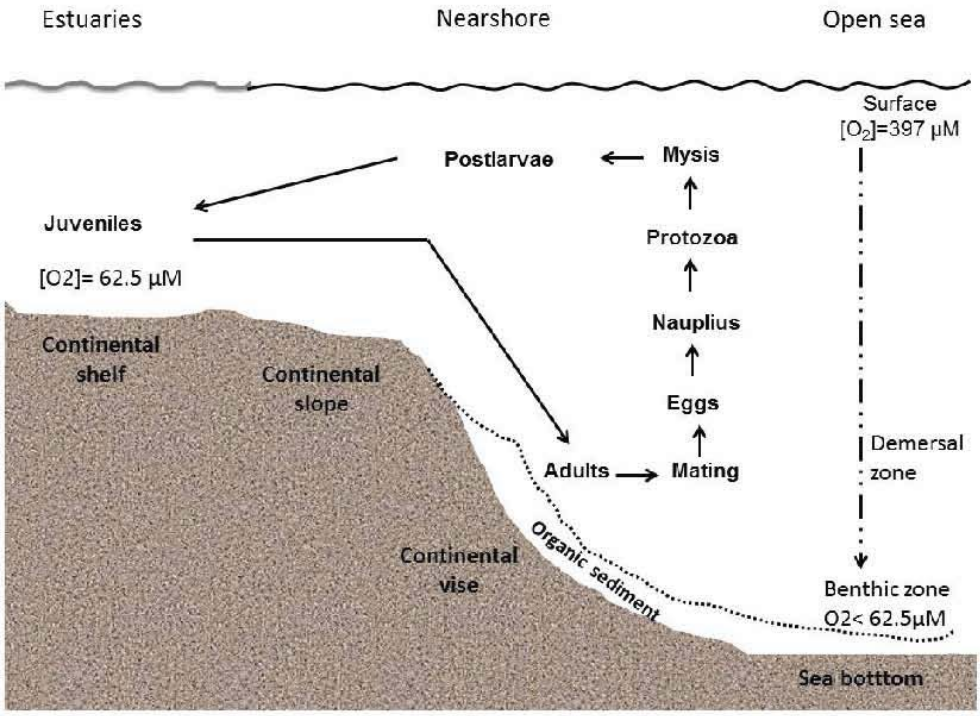

Figure 2. Migration of shrimp during their life cycle. Shrimp spend most of their life in the open sea, where they mate and lay eggs which hatch and undergo different larval stages (Nauplius, Protozoa, Mysis). Once in the postlarval stage, they travel to estuaries where they mature reaching the juvenile stage, and burying themselves in the sand for long periods. Once maturity is reached, they begin the cycle again returning to the open sea. This migration pattern takes shrimp to waters with widely different O_2 concentrations.

Among unicellular organisms, diverse yeast species can survive at almost any [O_2]. *Saccharomyces cerevisiae* can thrive at very low [O_2] through fermentation, although it does possess a facultative aerobic metabolism. The anaerobic metabolism of *S. cerevisiae, D. hansenii* and other yeast species is the basis for the fermentation industry of bread, wine and cheese. For example, during wine fermentation, *S. cerevisiae* produces large amounts of ethanol, while *D. hansenii* produces volatile products conferring the characteristic aroma of wine [30]. Also, *S. cerevisiae* participates in cheese fermentation, whereas *D. hansenii* protects against other filamentous fungi during ripening [31,32]. Yeast and other organisms have developed diverse systems to detoxify oxygen through physiological uncoupling and these are discussed later.

Many bacteria are facultative. Among these, *Escherichia coli* is a very illustrative representative that may thrive both in microaerobic environments such as the intestinal lumen and in the external environment in a wide range of [O_2]. Bacteria respond to environmental [O_2] variations or other conditions such as the need to fixate N_2 [33,34] by varying the composition of their branched respiratory chains (**Figure 3A**), which vectorially transport from 0 to 10 protons, as many as those in orthodox respiratory chains [35,36]. Still, when motile, bacteria will swim toward environments containing the ideal [O_2].

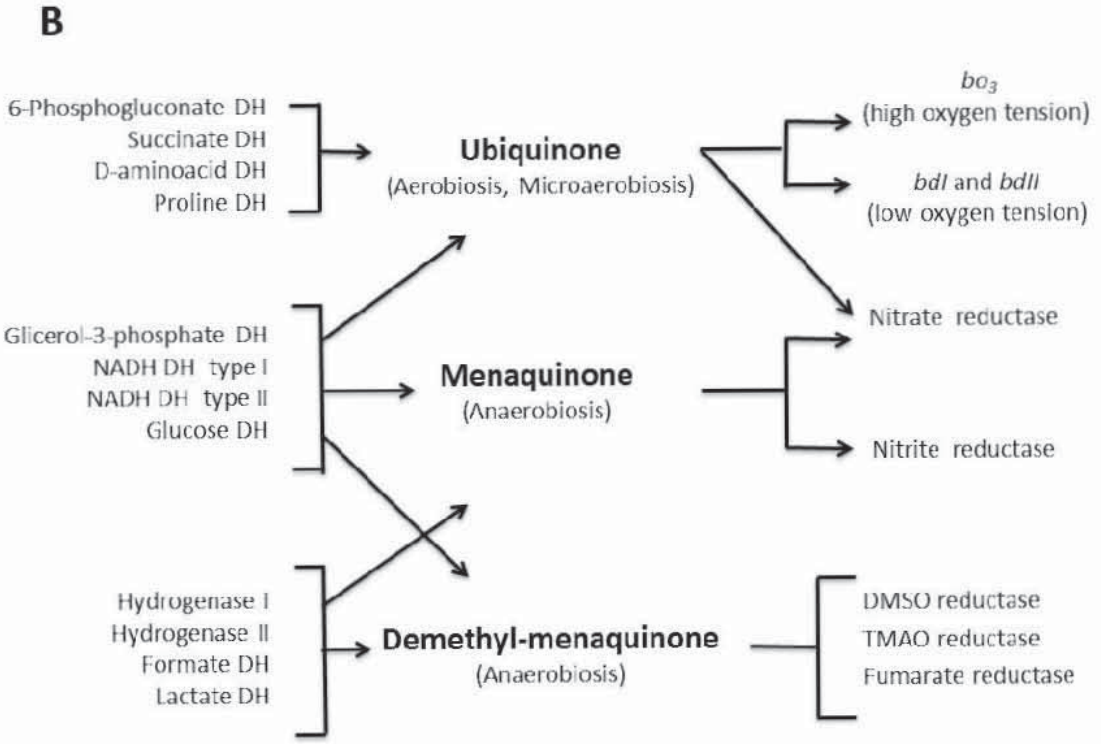

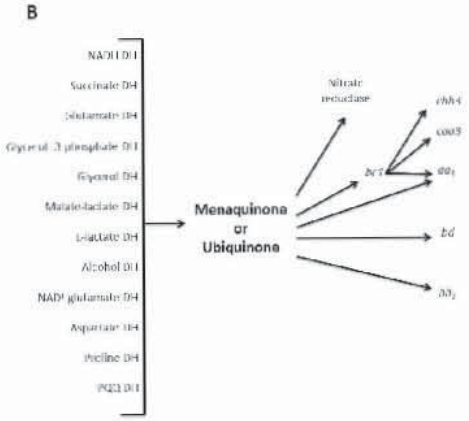

Figure 3. Diversity of bacterial respiratory chains at different [O_2]. **A**. The respiratory chain from *Escherichia coli* during aerobiosis, micro-aerobiosis and anaerobiosis. Modified from [35,36]. Ubiquinone is expressed at high [O_2] and NADH DH type II is overexpressed as compared to the NADH DH type I, which in turn is expressed at low [O_2]. The major final oxidase is cytochrome *bo*. During anaerobiosis, the respiratory chain in *Escherichia coli* succinate dehydrogenase is not expressed, whereas fumarate reductase or nitrate reductase may be the final electron acceptors. **B**. Hypothetical respiratory chain of *Wolbachia pipientis* constructed from BLAST and genome sequences reported in [76,77]. At high [O_2] cytochrome, bc1 and different cytochrome oxidases are expressed. Under microaerobic conditions, cytochrome *bd* is expressed. Then, under anaerobiosis, nitrate reductase is expressed.

Obligate endosymbionts, such as *R. prowazekii*, *Wolbachia sp.* or *Sodalis*, live in cytoplasmic vacuoles of multicellular organisms. The cytoplasm is a microaerophilic environment equip-

ped with O_2-consuming organelles and ROS-detoxifying enzymes. Remarkably, most endosymbionts contain a respiratory chain that at least in the case of *Wolbachia* seems to aid host mitochondria to deplete intracellular O_2 (**Figure 3B**).

Many parasites exhibit various life-cycle stages, which have different sensitivities to ROS engineered to endure attacks from macrophages. *Leishmania sp.* undergoes a relatively simple life cycle with two stages: the flagellated mobile promastigote living in the gut of the sand fly vector and the intracellular amastigote within phagolysosomal vesicles of the vertebrate host macrophage [37]. Promastigotes contain respiratory complexes I, II, III and IV, while it is not clear whether amastigotes possess an oxidative phosphorylation (OxPhos) machinery. Strikingly, amastigotes exhibit a succinate-dependent, uncoupler-sensitive transmembrane potential. Differences in sensitivity to oxidants are also observed between them, *in vitro*, promastigotes are more resistant to H_2O_2 than amastigotes [38].

In the bloodstream, *Trypanosoma cruzi* trypomastigotes contain high complex II and III activities. Interestingly, cytochrome *c* oxidase (COX) activity decreases creating an "electron bottleneck" that favors an increase in electron leakage, thus overproducing ROS. The oxidative preconditioning provided by this mechanism confers protection to bloodstream trypomastigotes against ROS liberated by the host immune system. These changes in mitochondrial activity, during the *T. cruzi* life cycle, are probably a key metabolic adaptation for survival in different hosts [39].

Malarial parasites are vulnerable to oxidative stress during their intraerythrocyte life stages. They contain the canonical respiratory chain (complex I, II, III and IV) plus an alternative electron transport pathway. Moreover, malarial mitochondria coordinate the biosynthesis of pyrimidine, heme and coenzyme Q [40]. *Plasmodium falciparum* possesses genes for two different superoxide dismutases (SOD), a cytosolic, Fe^{2+}-dependent, (SOD-1) expressed throughout the intraerythrocytic life of the parasite. The second, SOD-2, is mitochondrial and possesses a reminiscent apicoplast-targeting sequence. The host immune response to malaria involves phagocytosis and the production of nitric oxide and ROS that end up contributing to the pathology of the disease [41].

Regardless the organism studied, cytoplasmic [O_2] can vary widely, so damage control is needed at two levels. Either O_2 is reduced independently of adenosine triphosphate (ATP) production in a process known as physiological uncoupling, or the ROS-handling enzymes are activated. We shall briefly describe only physiological uncoupling as many reviews on ROS-handling enzymes, such as superoxide dismutase and catalase are found elsewhere [42,43].

3. Physiological uncoupling as an O_2-depleting mechanism and prevents ROS production

Both in oxyconformers and in oxyregulators, once O_2 enters the cell it has to be reduced at a high rate. When ATP is needed the respiratory chain rapidly catalyzes this reduction. When

there is energy surplus, O_2 consumption has to be uncoupled from ATP synthesis with the aim of preventing ROS overproduction [44]. A review on the physiological uncoupling mechanisms observed in mitochondria from different species of yeasts has been published recently [45]. Yeast mitochondrial uncoupling mechanisms may be (a) proton sinks, such as the mitochondrial unspecific channels [46–48] and the uncoupling protein (UCP) [49,50], or (b) nonpumping redox alternative enzymes found in branched respiratory chains [51–55].

(a). Proton sinks: The opening of the mitochondrial permeability transition pore (MPTP) leads to mitochondrial uncoupling and to the activation of signaling events leading to apoptosis [56], which was first detected in mammalian mitochondria as a response to the disruption of intracellular calcium homeostasis. In crustaceans subjected to hypoxia, mitochondrial functions are downregulated [57,58,20] and there is an anoxia-triggered intracellular increase in both calcium and phosphate, while ATP production is inhibited, probably as a result of the opening of a MPTP. In *Artemia franciscana* [26] and in the ghost shrimp *Lepidophthalmus louisianensis* [59], the proteins needed to form the MPTP are present. However, whether these crustaceans possess MPTPs is to be defined. Both in crustacean mitochondria and in other known hypoxia-tolerant invertebrates (mussels, oysters, and cnidarians among others), the role of a putative MPTP is an interesting question. AQ3

(b). Branched respiratory chains: Bacteria do not exhibit a permeability transition. This seems to be a mitochondrial trait. Instead, bacteria (and many mitochondria) exhibit branched respiratory chains. Indeed, different species of mitochondria may exhibit from none to three alternative enzymes. In contrast, bacteria may contain as much as twenty electron entry ports and as many exits. Thus, in most prokaryotes, branched respiratory chains seem to be the mechanism of choice to maintain a high rate of O_2 consumption, while adjusting ATP production to the energy requirements of the cell. In this regard, the bioenergetic efficiency for each entry point is defined as the stoichiometry of H^+ pumped per e^- traveling through the respiratory chain [60]. In addition, terminal oxidases are remarkably varied and their active site orientation, to the cytoplasm or to the periplasm determines their pumping efficiency [36].

Alternative oxidoreductases is the term designating all components of the respiratory chain different to the usual complexes I through IV. Most alternative oxidoreductases lack proton-pumping activity and may coexist with, or substitute for the respiratory proton-pumping complexes. Alternative enzymes catalyze the rapid, uncoupled flow of electrons towards O_2. Alternative NADH dehydrogenases may either substitute for (*S. cerevisiae*) or coexist with (bacteria, plants and diverse fungi) complex I [61,62].

Alternative oxidases (AOXs) catalyze the oxidation of ubiquinol to quinone and the reduction of O_2 to H_2O in the absence of proton translocation [53]. Although highly represented among plants, fungi and protist species, animal AOXs have been predicted to exist only in Molluska, Nematoda and Chordata [63]. Recently, the number of phyla that probably possess AOX has increased including Placozoa, Porifera, Cnidaria, Annelida, Echinodermata, Hemichordata and Chordata. In some marine vertebrates, such as sipunculids, annelids (*Nereis pelagica,* and *Arenicola marina)* and in bivalves (*Arctica islandica),* AOX has been detected [64–66]. However, there are no confirmed reports for AOX in mitochondria from crustaceans [51]. In different plant and animal species, cells lacking AOX show an increased susceptibility to death due to

H_2O_2, hypoxia and pathogens [67]. The ultimate decoupling of electron flow occurs when NADH dehydrogenases act in concert with alternative oxidases. The yeast *Yarrowia lipolytica* is a strict aerobic organism for which several biotechnological applications have been developed, such as in the cheese fermentation, obtention of extracellular enzymes [68], production of organic acids [69] and interconversion of fatty acids and alkenes [70]. In *Y. lipolytica,* metabolism occurs in a complex network between compartments, such as peroxisomes, endoplasmic reticulum, lipid bodies and mitochondria [69]. Mitochondria play an important role in ATP production, as well as in the maintenance of the NADH/NAD^+ redox ratio [71]. The respiratory chain is composed of the classic complexes: I, II, III and IV, one alternative NADH dehydrogenase external (NADH2) [72] and two isoforms of AOX [73]. During the logarithmic growth phase, NADH2 interacts with supercomplexes III–IV channeling the electrons to oxygen, while pumping protons at both complex III and IV [74]. In contrast, during the stationary growth phase, electrons are directly transferred from alternative NDH2 to AOX, thus uncoupling oxidative phosphorylation and decreasing the production of ROS [54,55]. This is a very illustrative example, which suggests that physiological uncoupling systems are present in all living organisms. Furthermore, in *Y. lipolytica,* both proton sinks and branched chains are observed [50,54].

Bacterial cytochrome-containing oxidases are many. These enzymes are differentially expressed in response to different oxygen concentrations and on whether an organism is an obligate aerobic or a facultative species. In addition, oxidases may coexist depending on the species under study and they may play different roles in the cell [75]. In *E. coli*, different oxidases are expressed depending on [O_2]. At high O_2, bo3 is expressed, while at low O_2, bd cytochromes are observed. Furthermore, *E. coli* is capable of growth under anaerobiosis, using respiratory chains reminiscent of the early Earth that use ubiquinone, menaquinone or demethylmenaquinone to donate electrons to enzymes that use terminal acceptors different to O_2 (**Figure 3A**) [35,36]. Branched respiratory chains provide the possibility of consuming O_2 without producing ATP. In the yeast *Y. lipolytica*, in the bacterium *E. coli* and probably in the Rickettsial *Wolbachia sp*., the arrangement of the respiratory chain varies such that when [O_2] is high, or ATP is needed, high proton pumping efficiency is observed. In contrast, factors such as arrival to the stationary phase or microaerophilic conditions probably trigger overexpression of the alternative NADH dehydrogenase and/or the AOX leading to the futile reduction of O_2 [61]. A possible arrangement of the respiratory chain of *Wolbachia* sp is illustrated (**Figure 3B**) where a large number of possible electron-donating enzymes reduce menaquinone or ubiquinone that in turn reduce final electron-accepting enzymes that are expressed according to the presence of O_2 in the cytoplasm of the host [76,77].

4. N-fixating bacteria are a special case

Nitrogen-fixating bacteria may be facultative as *Klebsiella pneumonia* or strict aerobics as *Azotobacter vinelandii* or *Gluconobacter diazotrophicus*. As they contain fragile, oxygen-sensitive nitrogen-fixating enzymes that need to be protected, these bacteria have developed many strategies to detoxify [O_2]. Thus, in N-fixating bacteria, both N-reductases and different

oxidases are expressed: *A. vinelandii* contains a highly active respiratory chain and is able to adjust the expression of its three oxidases to a wide range of [O_2]. Among these, cytochrome *bd* has high O_2 affinity (KmO_2= 5 μM) and becomes active during N fixation [15,78–80]. Indeed, during N fixation the H^+/O index is low, at 1 [81]. In *Ga. diazotrophicus* different periplasmic membrane enzymes such as glucose-, acetaldehyde- or ethanoldehydrogenases reduce a quinone, which in turn donates its electrons to two different oxidases, *ba* which is coupled to ATP synthesis and bb_3 which is not coupled, but its role is to deplete O_2 in the vicinity of nitrogen reductases [82].

5. ROS detoxification

In spite of the production-prevention mechanisms outlined earlier, ROS may reach high concentrations, for example, during ischemia-reperfusion. The last line of defense is detoxification. Enzymes such as superoxide dismutases (SODs) and catalases deactivate ROS. SODs have been grouped on the basis of the metal cofactor, which can be Fe, Mn, Ni or Cu/Zn [83]. The Fe-SODs are mostly found in microaerophiles and anaerobes. Microorganisms in aerobic environments prefer Mn-SOD [84]. Catalase dismutates hydrogen peroxide to water plus O_2 [85]. Several genes capable of H_2O_2 dismutation evolved from ancestral genomes. The most abundant was heme-containing enzymes spread among bacteria, Archaea and Eukarya [86].

AQ4

In *Clostridium acetobutylicum*, a strict anaerobic that survives little time when exposed to O_2, no catalases are found [87], and a function has yet to be found for the annotated SODs.

6. Conclusion

During the early paleoproterozoic period, a massive death toll resulted from a 10^5 times rise in atmospheric O_2. In order to survive, organisms had to learn to cope with O_2 toxicity while profiting from the large energy release coupled to its reduction. Several O_2-management strategies are revised here. Among these is hiding away from O_2, moving to adequate O_2 concentrations or excluding O_2 with impermeable epithelia. Once O_2 enters the cell, other mechanisms are designed to handle it. Its reactivity is controlled by O_2-quenching proteins or by rapidly reducing it with specific oxidases. In order to avoid side reactions, the rate of reduction had to be kept at optimal pace, independently of ATP production and thus several mechanisms of physiological uncoupling of oxidative phosphorylation evolved. Physiological uncoupling was achieved either by opening proton sinks or by using O_2 independently of the proton gradient. Today, these mechanisms are expressed in many cells. Proton sinks include unspecific channels and uncoupling proteins, while proton gradient-independent consumption of O_2 involved alternative oxido-reductases found in the branched respiratory chains of fungi, plants and arthropods. In spite of the function of all these O_2-management machines, O_2 can still react unspecifically to form ROS, which destroy the cell through processes such as aging, apoptosis or necrosis. Once formed, ROS may still be eliminated by enzymes such as

SOD and catalase, which are reviewed elsewhere [43] O_2 is a great source of energy for the cell, but its high toxicity has to be dealt with, through mechanisms that we are only beginning to understand.

Acknowledgements

Authors thank Ramón Méndez-Franco for technical assistance. Partially funded by the PAPIIT program and DGAPA/UNAM (grant IN202612). MRL, NLMG and CUA are CONACYT fellows enrolled in the Biochemistry Graduate Program at UNAM.

Declaration of Interest. The authors do not have any interests to disclose.

Author details

Mónica Rosas-Lemus[1], Cristina Uribe-Alvarez1[1], Martha Contreras-Zentella[2], Luis Alberto Luévano-Martínez[3], Natalia Chiquete-Félix[1], N. Lilia Morales-García[1], Adriana Muhlia-Almazán[4], Edgardo Escamilla-Marván[2] and Salvador Uribe-Carvajal[1*]

*Address all correspondence to: suribe@ifc.unam.mx

AQ2

1 Department of Molecular Genetics, Institute of Cellular Physiology, UNAM, CDMX, México

2 Department of Biochemistry and Structural Biology, Institute of Cellular Physiology, UNAM, CDMX, México AQ1

3 Department of Biochemistry, Institute of Chemistry, U de Sao Paulo, Sao Paulo, SP, Brazil

4 Laboratory of Bioenergetics and Molecular Genetics CIAD, Hermosillo, Sonora, México

References

[1] Lane N. Oxygen the molecule that made the world. Oxford: Oxford University Press; 2002. p. 384.

[2] Sessions AL, Doughty DM, Welander PV, Summons RE, Newman DK. The continuing puzzle of the great oxidation event. Current Biology. 2009;19(14):R567–74.

[3] Pavlov AA, Kasting JF. Mass-independent fractionation of sulfur isotopes in Archean sediments: strong evidence for an anoxic Archean atmosphere. Astrobiology. 2002;2(1): 27–41.

[4] Martin W, Rotte C, Hoffmeister M, Theissen U, Gelius-Dietrich G, Ahr S, et al. Early cell evolution, eukaryotes, anoxia, sulfide, oxygen, fungi first (?), and a tree of genomes revisited. IUBMB Life. 2003;55(4–5):193–204.

[5] Nisbet EG, Sleep NH. The habitat and nature of early life. Nature. 2001;409(6823):1083–91.

[6] Martin W, Muller M. The hydrogen hypothesis for the first eukaryote. Nature. 1998;392(6671):37–41.

[7] Castresana J, Saraste M. Evolution of energetic metabolism: the respiration-early hypothesis. Trends in Biochemical Sciences. 1995;20(11):443–8.

[8] Gray MW. Evolution of organellar genomes. Current Opinion in Genetics & Development. 1999;9(6):678–87.

[9] Kurland CG, Andersson SG. Origin and evolution of the mitochondrial proteome. Microbiology and Molecular Biology Reviews. 2000;64(4):786–820.

[10] Hellemond JJv, Klei Avd, Weelden SHv, Tielens AGM. Biochemical and evolutionary aspects of anaerobically functioning mitochondria. Philosophical Transactions of the Royal Society of London Series B: Biological Sciences. 2003;358(1429):205–15.

[11] Mentel M, Martin W. Energy metabolism among eukaryotic anaerobes in light of Proterozoic ocean chemistry. Philosophical Transactions of the Royal Society of London Series B, Biological Sciences. 2008;363(1504):2717–29.

[12] Hayes JM, Waldbauer JR. The carbon cycle and associated redox processes through time. Philosophical Transactions of the Royal Society B: Biological Sciences. 2006;361(1470):931–50.

[13] Holland HD. The oxygenation of the atmosphere and oceans. Philosophical Transactions of the Royal Society of London Series B, Biological Sciences. 2006;361(1470):903–15.

[14] Golblatt C, Lenton TM, Watson AJ. Bistability of atmospheric oxygen and the Great Oxidation. Nature. 2006;443(7112):683–6.

[15] Poole RK, D'Mello R, Hill S, Ioannidis N, Leung D, Wu G. The oxygen reactivity of bacterial respiratory haemoproteins: oxidases and globins. Biochimica et Biophysica Acta. 1994;1187(2):226–31.

[16] Hinton HE. Respiratory systems of insect egg shells. Annual review of entomology. 1969;14:343–68.

[17] Hochachka PW, Somero GN. Biochemical adaptation: mechanism and process in physiological evolution. United States Of America: Oxford University Press; 2002. 467 p.

[18] Hill RW, Wyse GA, Anderson M. Animal physiology. MA, USA: Sinauer Associates Inc. Publishers; 2004. p. 770.

[19] Abele D. Toxic oxygen: the radical life-giver. Nature. 2002;420(6911):27.

[20] Martinez-Cruz O, Calderon de la Barca AM, Uribe-Carvajal S, Muhlia-Almazan A. The function of mitochondrial F(O)F(1) ATP-synthase from the whiteleg shrimp *Litopenaeus vannamei* muscle during hypoxia. Comparative Biochemistry and Physiology Part B, Biochemistry & Molecular Biology. 162(4):107–12.

[21] Müller M, Mentel M, van Hellemond JJ, Henze K, Woehle C, Gould SB, et al. Biochemistry and evolution of anaerobic energy metabolism in eukaryotes. Microbiology and Molecular Biology Reviews. 2012;76(2):444–95.

[22] Dall W, Hill BJ, Rothlisberg PC, Sharples DJ. The biology of the Penaeidae. Advances in Marine Biology; 1990. pp 489, 27. CSIRO Marine Laboratories, P.O. Box 120, Cleveland, Qld. 4163, Australia 1990.

[23] Ekau W, Auel H, Pörtner HO, Gilbert D. Impacts of hypoxia on the structure and processes in pelagic communities (zooplankton, macro-invertebrates and fish). Biogeosciences. 2010;7(5):1669–99.

[24] Mukai H, Koike I. Behavior and respiration of the Burrowing Shrimps Upogebia major (de Haan) and Callianassa japonica (de Haan). Journal of Crustacean Biology. 1984;4(2): 191–200.

[25] Clegg J. Embryos of Artemia franciscana survive four years of continuous anoxia: the case for complete metabolic rate depression. Journal of Experimental Biology. 1997;200(3):467–75.

[26] Menze MA, Hutchinson K, Laborde SM, Hand SC. Mitochondrial permeability transition in the crustacean *Artemia franciscana*: absence of a calcium-regulated pore in the face of profound calcium storage. American Journal of Physiology – Regulatory, Integrative and Comparative Physiology. 2005;289(1):R68–76.

[27] Galli GJ, Richards J. Mitochondria from anoxia-tolerant animals reveal common strategies to survive without oxygen. Journal of Comparative Physiology B. 2014;184(3):285–302.

[28] Strahl J, Dringen R, Schmidt MM, Hardenberg S, Abele D. Metabolic and physiological responses in tissues of the long-lived bivalve Arctica islandica to oxygen deficiency. Comparative Biochemistry and Physiology Part A, Molecular & Integrative Physiology. 2011;158(4):513–9.

[29] Buttemer WA, Abele D, Costantini D. From bivalves to birds: oxidative stress and longevity. Functional Ecology. 2010;24(5):971–83.

[30] Rosi I, Vinella M, Domizio P. Characterization of beta-glucosidase activity in yeasts of oenological origin. The Journal of Applied Bacteriology. 1994;77(5):519–27.

[31] Roostita R, Fleet GH. Growth of yeasts in milk and associated changes to milk composition. International Journal of Food Microbiology. 1996;31(1–3):205–19.

[32] Eliskases-Lechner F, Ginzinger W, Rohm H, Tschager E. Raw milk flora affects composition and quality of Bergkäse. 1. Microbiology and fermentation compounds. Lait. 1999;79(4):385–96.

[33] Baracchini O, Sherris JC. The chemotactic effect of oxygen on bacteria. The Journal of Pathology and Bacteriology. 1959;77(2):565–74.

[34] Ulloa O, Canfield DE, DeLong EF, Letelier RM, Stewart FJ. Microbial oceanography of anoxic oxygen minimum zones. Proceedings of the National Academy of Sciences of the United States of America. 2012;109(40):15996–6003.

[35] Ingledew WJ, Poole RK. The respiratory chains of *Escherichia coli*. Microbiological Reviews. 1984;48(3):222–71.

[36] Unden G, Bongaerts J. Alternative respiratory pathways of *Escherichia coli*: energetics and transcriptional regulation in response to electron acceptors. Biochimica et Biophysica Acta. 1997;1320(3):217–34.

[37] Chakraborty B, Biswas S, Mondal S, Bera T. Stage specific developmental changes in the mitochondrial and surface membrane associated redox systems of *Leishmania donovani* promastigote and amastigote. Biochemistry Biokhimiia. 2010;75(4):494–518.

[38] Van Assche T, Deschacht M, da Luz RA, Maes L, Cos P. Leishmania-macrophage interactions: insights into the redox biology. Free Radical Biology & Medicine. 2011;51(2):337–51.

[39] Gonçalves RL, Barreto RF, Polycarpo CR, Gadelha FR, Castro SL, Oliveira MF. A comparative assessment of mitochondrial function in epimastigotes and bloodstream trypomastigotes of *Trypanosoma cruzi*. Journal of Bioenergetics and Biomembranes. 2011;43(6):651–61.

[40] Krungkrai J. The multiple roles of the mitochondrion of the malarial parasite. Parasitology. 2004;129(Pt 5):511–24.

[41] Muller S. Redox and antioxidant systems of the malaria parasite *Plasmodium falciparum*. Molecular Microbiology. 2004;53(5):1291–305.

[42] McCord JM, Keele BB, Jr., Fridovich I. An enzyme-based theory of obligate anaerobiosis: the physiological function of superoxide dismutase. Proceedings of the National Academy of Sciences of the United States of America. 1971;68(5):1024–7.

[43] D'Autreaux B, Toledano MB. ROS as signalling molecules: mechanisms that generate specificity in ROS homeostasis. Nature Reviews Molecular Cell Biology. 2007;8(10):813–24.

[44] Kadenbach B. Intrinsic and extrinsic uncoupling of oxidative phosphorylation. Biochimica et Biophysica Acta. 2003;1604(2):77–94.

[45] Guerrero-Castillo S, Araiza-Olivera D, Cabrera-Orefice A, Espinasa-Jaramillo J, Gutierrez-Aguilar M, Luevano-Martinez LA, et al. Physiological uncoupling of mitochondrial oxidative phosphorylation. Studies in different yeast species. Journal of Bioenergetics and Biomembranes. 2011;43(3):323–31.

[46] Manon S, Roucou X, Guerin M, Rigoulet M, Guerin B. Characterization of the yeast mitochondria unselective channel: a counterpart to the mammalian permeability transition pore? Journal of Bioenergetics Biomembranes. 1998;30(5):419–29.

[47] Bernardi P. The mitochondrial permeability transition pore: a mystery solved? Frontiers in Physiology. 2013;4:95.

[48] Uribe-Carvajal S, Luevano-Martinez LA, Guerrero-Castillo S, Cabrera-Orefice A, Corona-de-la-Pena NA, Gutierrez-Aguilar M. Mitochondrial unselective channels throughout the eukaryotic domain. Mitochondrion. 2011;11(3):382–90.

[49] Nicholls DG, Rial E. A history of the first uncoupling protein, UCP1. Journal of Bioenergetics and Biomembranes. 1999;31(5):399–406.

[50] Luevano-Martinez LA, Moyano E, de Lacoba MG, Rial E, Uribe-Carvajal S. Identification of the mitochondrial carrier that provides Yarrowia lipolytica with a fatty acid-induced and nucleotide-sensitive uncoupling protein-like activity. Biochimica et Biophysica Acta. 2010;1797(1):81–8.

[51] McDonald AE, Vanlerberghe GC, Staples JF. Alternative oxidase in animals: unique characteristics and taxonomic distribution. Journal of Experimental Biology. 2009;212(Pt 16):2627–34.

[52] McDonald AE, Vanlerberghe GC. Alternative oxidase and plastoquinol terminal oxidase in marine prokaryotes of the Sargasso Sea. Gene. 2005;349:15–24.

[53] Vanlerberghe GC, McIntosh L. Alternative oxydase: from gene to function. Annual Review of Plant Physiology and Plant Molecular Biology. 1997;48:703–34.

[54] Guerrero-Castillo S, Cabrera-Orefice A, Vazquez-Acevedo M, Gonzalez-Halphen D, Uribe-Carvajal S. During the stationary growth phase, Yarrowia lipolytica prevents the overproduction of reactive oxygen species by activating an uncoupled mitochondrial respiratory pathway. Biochimica et Biophysica Acta. 2012;1817(2):353–62.

[55] Cabrera-Orefice A, Chiquete-Felix N, Espinasa-Jaramillo J, Rosas-Lemus M, Guerrero-Castillo S, Pena A, et al. The branched mitochondrial respiratory chain from *Debaryomyces hansenii*: components and supramolecular organization. Biochimica et Biophysica Acta. 2013;1837(1):73–84.

[56] Bernardi P. Mitochondrial transport of cations: channels, exchangers, and permeability transition. Physiological Reviews. 1999;79(4):1127–55.

[57] Kwast KE, Hand SC. Acute depression of mitochondrial protein synthesis during anoxia: contributions of oxygen sensing, matrix acidification, and redox state. The Journal of Biological Chemistry. 1996;271(13):7313–9.

[58] Eads BD, Hand SC. Mitochondrial mRNA stability and polyadenylation during anoxia-induced quiescence in the brine shrimp Artemia franciscana. The Journal of Experimental Biology. 2003;206(Pt 20):3681–92.

[59] Holman JD, Hand SC. Metabolic depression is delayed and mitochondrial impairment averted during prolonged anoxia in the ghost shrimp, *Lepidophthalmus louisianensis* (Schmitt, 1935). Journal of Experimental Marine Biology and Ecology. 2009;376(2):85–93.

[60] Borisov VB, Murali R, Verkhovskaya ML, Bloch DA, Han H, Gennis RB, et al. Aerobic respiratory chain of *Escherichia coli* is not allowed to work in fully uncoupled mode. Proceedings of the National Academy of Sciences. 2011;108(42):17320–4.

[61] Kerscher SJ. Diversity and origin of alternative NADH:ubiquinone oxidoreductases. Biochimica et Biophysica Acta (BBA) - Bioenergetics. 2000;1459(2â€“3):274–83.

[62] Büschges R, Bahrenberg G, Zimmermann M, Wolf K. Nadh: Ubiquinone oxidoreductase in obligate aerobic yeasts. Yeast. 1994;10(4):475–9.

[63] McDonald A, Vanlerberghe G. Branched mitochondrial electron transport in the Animalia: presence of alternative oxidase in several animal phyla. IUBMB Life. 2004;56(6):333–41.

[64] Tschischka K, Abele D, Portner HO. Mitochondrial oxyconformity and cold adaptation in the polychaete *Nereis pelagica* and the bivalve *Arctica islandica* from the Baltic and White Seas. The Journal of Experimental Biology. 2000;203(Pt 21):3355–68.

[65] Buchner T, Abele D, Portner HO. Oxyconformity in the intertidal worm *Sipunculus nudus*: the mitochondrial background and energetic consequences. Comparative Biochemistry and Physiology Part B, Biochemistry & Molecular Biology. 2001;129(1):109–20.

[66] Hildebrandt TM, Grieshaber MK. Three enzymatic activities catalyze the oxidation of sulfide to thiosulfate in mammalian and invertebrate mitochondria. FEBS Journal. 2008;275(13):3352–61.

[67] Vanlerberghe GC, Robson CA, Yip JY. Induction of mitochondrial alternative oxidase in response to a cell signal pathway down-regulating the cytochrome pathway prevents programmed cell death. Plant Physiology. 2002;129(4):1829–42.

[68] Beckerich JM, Boisrame-Baudevin A, Gaillardin C. Yarrowia lipolytica: a model organism for protein secretion studies. International Microbiology: The Official Journal of the Spanish Society for Microbiology. 1998;1(2):123–30.

[69] Otto C, Holz M, Barth G. Production of Organic Acids by *Yarrowia lipolytica*. In: Barth G, editor. *Yarrowia lipolytica*: Biotechnological Applications. Berlin, Heidelberg: Springer Berlin Heidelberg; 2013. p. 137–49.

[70] Darvishi Harzevili F. *Yarrowia lipolytica*: An Overview. In: Biotechnological Applications of the Yeast *Yarrowia lipolytica*. Cham: Springer International Publishing; 2014. p. 1–16.

[71] Kerscher S, Dröse S, Zwicker K, Zickermann V, Brandt U. *Yarrowia lipolytica*, a yeast genetic system to study mitochondrial complex I. Biochimica et Biophysica Acta (BBA) – Bioenergetics. 2002;1555(1–3):83–91.

[72] Kerscher SJ, Okun JG, Brandt U. A single external enzyme confers alternative NADH:ubiquinone oxidoreductase activity in *Yarrowia lipolytica*. Journal of Cell Science. 1999;112(Pt 14):2347–54.

[73] Medentsev AG, Arinbasarova AY, Golovchenko NP, Akimenko VK. Involvement of the alternative oxidase in respiration of *Yarrowia lipolytica* mitochondria is controlled by the activity of the cytochrome pathway. FEMS Yeast Research. 2002;2(4):519–24.

[74] Guerrero-Castillo S, Vazquez-Acevedo M, Gonzalez-Halphen D, Uribe-Carvajal S. In *Yarrowia lipolytica* mitochondria, the alternative NADH dehydrogenase interacts specifically with the cytochrome complexes of the classic respiratory pathway. Biochimica et Biophysica Acta. 2009;1787(2):75–85.

[75] Cook GM, Poole RK. Oxidase and periplasmic cytochrome assembly in *Escherichia coli* K-12: CydDC and CcmAB are not required for haem-membrane association. Microbiology. 2000;146(Pt 2):527–36.

[76] Wu M, Sun LV, Vamathevan J, Riegler M, Deboy R, Brownlie JC, et al. Phylogenomics of the reproductive parasite Wolbachia pipientis wMel: a streamlined genome overrun by mobile genetic elements. PLoS Biology. 2004;2(3):E69.

[77] Klasson L, Walker T, Sebaihia M, Sanders MJ, Quail MA, Lord A, et al. Genome evolution of Wolbachia strain wPip from the *Culex pipiens* group. Molecular Biology and Evolution. 2008;25(9):1877–87.

[78] Haddock BA, Jones CW. Bacterial respiration. Bacteriological Reviews. 1977;41(1):47–99.

[79] Jones K. Acetilene reduction by mats of blue-green algae in sub-tropical grassland: possible contribution by other micro-organisms. New Phytologist. 1977;78(2):437–40.

[80] Ng TCN, Laheri AN, Maier RJ. Cloning, sequencing, and mutagenesis of the cytochrome c4 gene from *Azotobacter vinelandii*: characterization of the mutant strain and a proposed new branch in the respiratory chain. Biochimica et Biophysica Acta (BBA) – Bioenergetics. 1995;1230(3):119–29.

AQ7

[81] Bertsova YV, Bogachev AV, Skulachev VP. Two NADH:ubiquinone oxidoreductases of *Azotobacter vinelandii* and their role in the respiratory protection. Biochimica et Biophysica Acta. 1998;1363(2):125–33.

[82] González PJ, Correia C, Moura I, Brondino CD, Moura JJG. Bacterial nitrate reductases: molecular and biological aspects of nitrate reduction. Journal of Inorganic Biochemistry. 2006;100(5â€“6):1015–23.

[83] Whittaker MM, Whittaker JW. A glutamate bridge is essential for dimer stability and metal selectivity in manganese superoxide dismutase. The Journal of Biological Chemistry. 1998;273(35):22188–93.

[84] Cannio R, Fiorentino G, Morana A, Rossi M, Bartolucci S. Oxygen: friend or foe? Archaeal superoxide dismutases in the protection of intra- and extracellular oxidative stress. Frontiers in Bioscience: A Journal and Virtual Library. 2000;5:D768–79.

[85] Klotz MG, Loewen PC. The molecular evolution of catalatic hydroperoxidases: evidence for multiple lateral transfer of genes between prokaryota and from bacteria into eukaryota. Molecular Biology and Evolution. 2003;20(7):1098–112.

[86] Zamocky M, Furtmuller PG, Obinger C. Evolution of catalases from bacteria to humans. Antioxidants & Redox Signaling. 2008;10(9):1527–48.

[87] Nölling J, Breton G, Omelchenko MV, Makarova KS, Zeng Q, Gibson R, et al. Genome sequence and comparative analysis of the solvent-producing bacterium *Clostridium acetobutylicum*. Journal of Bacteriology. 2001;183(16):4823–38.

[88] Peacock AJ. ABC of oxygen: oxygen at high altitude. British Medical Journal. 1998;317(7165):1063–6.

[89] Hall JE, Guyton AC. Unit VII Respiration. In: Hall J, editor. Textbook of Medical Physiology. 12. Philadelphia, PA, USA: Elsevier; 2012.

[90] Popel AS. Theory of oxygen transport to tissue. Critical Reviews in Biomedical Engineering. 1989;17(3):257–321.

[91] Wilson DF, Rumsey WL, Green TJ, Vanderkooi JM. The oxygen dependence of mitochondrial oxidative phosphorylation measured by a new optical method for measuring oxygen concentration. The Journal of Biological Chemistry. 1988;263(6): 2712–8.

[92] Geng M, Duan Z. Prediction of oxygen solubility in pure water and brines up to high temperatures and pressures. Geochimica et Cosmochimica Acta. 2010;74(19):5631–40.

[93] Chapelle G, Peck LS. Amphipod crustacean size spectra: new insights in the relationship between size and oxygen. Oikos. 2004;106(1):167–75.

[94] Beman JM, Carolan MT. Deoxygenation alters bacterial diversity and community composition in the ocean's largest oxygen minimum zone. Nature Communications. 2013;4:2705.

AUTHOR QUERIES

AQ1	The affiliation section has been edited as per style. Kindly check whether it is done appropriately.
AQ2	Please provide full first name for the author: N. Lilia Morales-García.
AQ3	The sentence " First detected in mammalian mitochondria as a response to the disruption of intracellular calcium homeostasis..." has been edited for better clarity. Kindly check.
AQ4	Repeated text "Catalase dismutates hydrogen peroxide to..." have been deleted. Kindly check.
AQ5	Please check the publisher name for correctness in Ref. [18].
AQ6	Duplicate entry of Ref. [20] has been deleted and text citations changed accordingly. Please check.
AQ7	Please provide the name of the editors for Ref. [70].

[95] Borsuk ME, Stow CA, Luettich Jr RA, Paerl HW, Pinckney JL. Modelling oxygen dynamics in an intermittently stratified estuary: estimation of process rates using field data. Estuarine, Coastal and Shelf Science. 2001;52(1):33–49.

[96] Engle V, Summers JK. Refinement, validation, and application of a benthic condition index for Northern Gulf of Mexico estuaries. Estuaries. 1999;22(3):624–35.

Las enfermedades transmitidas por vectores y el potencial uso de *Wolbachia*, una bacteria endocelular obligada, para erradicarlas

Cristina Uribe-Álvarez[a], *Natalia Chiquete Félix*[a]

Resumen

Según la Organización Mundial de la Salud (OMS), 17% de las enfermedades infecciosas reportadas en el mundo son transmitidas por vectores artrópodos. Una alternativa para bloquear la transmisión es infectar a los vectores con una bacteria endocelular llamada *Wolbachia*. Diferentes investigaciones han demostrado que *Wolbachia* acorta la vida del mosquito, aumenta su resistencia ante la infección de algunos virus como dengue, Zika y chikungunya, y provoca incompatibilidad citoplasmática, por lo que al liberar mosquitos machos infectados con *Wolbachia* en una población de hembras no infectadas los productos no son viables, disminuyendo drásticamente la población total**.** En el presente artículo se incluye una descripción general de las enfermedades infecciosas más comunes transmitidas por vectores así como una revisión del uso de *Wolbachia* como una posible herramienta para controlar su propagación.

Palabras clave: Wolbachia*, enfermedades transmitidas por vector, dengue, malaria, endosimbiosis.*

[a]Departamento de Genética Molecular. Instituto de Fisiología Celular. Universidad Nacional Autónoma de México.
Correspondencia: Cristina Uribe-Ávarez.
Correo electrónico: curibe@email.ifc.unam.mx
Recibido 31-julio-2017. Aprobado: 02-oct-2017.

Vector-borne diseases and the potential use of *Wolbachia*, an obligate endocellular bacterium, to eradicate them

Abstract

According to the World and Health Organization (WHO), 17% of the worldwide reported infectious diseases are vector-borne. One alternative for blocking the transmission of these infectious agents is to infect the vectors with the endocellular bacterium *Wolbachia*. Several studies have shown that *Wolbachia* shortens mosquitos' lifespan and increases their resistance to some virus like Dengue, Zika or Chikungunya. *Wolbachia* also causes cytoplasmic incompatibility, so, when *Wolbachia*-infected male mosquitoes are released

among an uninfected female population, the production of an offspring is not viable and the mosquito population decreases drastically. This article includes an overview of the most common vector-borne infectious diseases as well as a review of the use of *Wolbachia* as a possible tool for controlling the spread of vector-borne diseases.

Key words: Wolbachia, *vector-borne diseases, dengue, malaria, endosymbiosis.*

A nivel mundial, las enfermedades trasmitidas por vectores registran altas tasas de morbilidad y mortalidad. Según la OMS, las enfermedades *airborne (arthropod-borne)* representan 17% del total de las enfermedades infecciosas en el mundo, con 1,000 millones de casos y un millón de defunciones anuales[1]. Se conoce como vector biológico a cualquier organismo vivo capaz de transportar y trasmitir un patógeno a otro organismo. Los vectores biológicos más comunes son los insectos hematófagos que al alimentarse de la sangre de un portador infectado, ingieren microorganismos patógenos que posteriormente inoculan a otro individuo **(tabla 1)**. De acuerdo con el agente causal, las enfermedades pueden contagiarse entre humanos o de animales (reservorios, **tabla 1**) a humanos. Un reservorio es un organismo que aloja microorganismos patógenos que pueden causar una enfermedad contagiosa y que, al ser difíciles de controlar, pueden provocar epidemias[1].

Dos de las enfermedades con mayor relevancia epidemiológica son la malaria y el dengue. La malaria es causada por los protozoarios *Plasmodium falciparum, P. vivax, P. ovale y P. malariae* y se transmite por la picadura de mosquitos del género *Anopheles* **(tabla 1)**. Entre los años 2001 a 2016, la OMS reportó 6.8 millones de muertes por su causa[2]. En 2015, se reportaron 212 millones de casos de malaria, de los que 429 mil pacientes fallecieron; de ellos, 70% eran niños menores de 5 años[1].

Actualmente, la enfermedad transmitida por vector con mayor crecimiento mundial es el dengue. Al igual que el virus del dengue, el del Zika, el chikungunya y la fiebre amarilla son transmitidos por los mosquitos *Aedes aegypti* y *Aedes albopticus*. Se estima que hay de 100 a 390 millones de casos de dengue al año, de los cuales 50,000 ingresan a un hospital, y 1,250 mueren[3]. Otros ejemplos de enfermedades transmitidas por vectores son la leishmaniasis cutánea y visceral, que se transmite por los mosquitos flebótomos; la enfermedad de Chagas, transmitida por chinches (triatomas); la enfermedad del sueño o tripanosomiasis africana, transmitida por la mosca tsé-tsé, etc. **(tabla 1)**. La peste bubónica es causada por la bacteria *Yersinia pestis*, que tiene como reservorio a las ratas y se transmite al humano por medio de picaduras de pulgas. A lo largo de la historia, se han registrado tres grandes pandemias de peste en el mundo: la primera, conocida como la peste de Justiniano en el siglo VI, que terminó con la vida de ~25 millones de personas en el Imperio Bizantino; la segunda, conocida como la peste negra que fue la causante de la muerte de un tercio de la población Europea en el siglo XIV (~75 millones de personas); y la tercera pandemia, que comenzó en China en el siglo XIX dónde aproximadamente 12 millones de personas murieron[4].

Estas enfermedades, también llamadas enfermedades tropicales desatendidas u olvidadas afectan en su mayoría a países del tercer mundo. El calentamiento global, la facilidad de desplazamiento en el mundo y la urbanización no planificada han propiciado el aumento de su incidencia en países del primer mundo (Australia, Europa y Estados Unidos), provocando un aumento en gastos médicos e impulsando la búsqueda de estrategias efectivas para combatir dichas enfermedades. Las diferentes alternativas propuestas incluyen la generación de vacunas, que tienen un proceso de desarrollo lento, aunado a las complicaciones para transportarlas y aplicarlas; la exterminación de los vectores con insecticidas, que podría causar un desequilibrio ecológico difícil de calcular y la posibilidad de infectar a los vectores con una bacteria llamada *Wolbachia*[5].

WOLBACHIA SP. Y SU INTERACCIÓN CON ARTRÓPODOS

Wolbachia es una α-proteobacteria endocelular obligada que coloniza las células germinales del mosquito hembra asegurando su transmisión vertical (la madre la hereda a su progenie). Esta bacteria disminuye la propagación de enfermedades me-

Tabla 1. Enfermedades transmitidas por vectores

	Vector	Reservorio	Enfermedad
	Mosquitos (*Aedes* y *Anopheles*)	Humanos y primates	Virus del dengue, Zika, chikungunya, fiebre amarilla, filariásis linfática (*B. Malayi*, *W. Bancrofti*, *B. timori*), Malaria/ paludismo (*Plasmodium* sp.)
	Mosquitos (*Phlebotomus*)	Humanos, primates, marsupiales, roedores y animales domésticos	Leishmaniasis (*Leishmania* sp.)
	Triatomas	Humanos, marsupiales, ratas, ratones y animales domésticos	Tripanosomiasis americana o enfermedad de Chagas (*Trypanosoma cruzi*)
	Mosca tsé-tsé	Humanos, animales domésticos, gacelas, antílopes	Tripanosomiasis africana o enfermedad del sueño (*Trypanosoma brucei*)
	Mosca negra	Humanos	Oncocercosis o ceguera de río (*Onchocerca volvulus*)
	Pulga	Humanos, roedores, animales domésticos	Peste bubónica y peste neumónica (*Yersinia pestis*)
	Garrapata	Humanos, vacas ovejas, cabras, avestruces, roedores	Fiebre de las Montañas Rocosas (*Rickettsia rickettsii*), fiebre hemorrágica de Crimea-Congo, enfermedad de Lyme (*Borrelia burgdorferi*), encefalitis, etc.

Los mosquitos del género *Aedes y Anopheles* son los vectores de enfermedades mejor conocidos. Sin embargo, las garrapatas, las moscas, las pulgas y los triatominos también son vectores de diferentes enfermedades infecciosas. Además de funcionar como hospederos, los humanos funcionamos como reservorio de todas estas enfermedades.

Figura 1. *Wolbachia* disminuye la vida media del mosquito y lo protege contra la infección de virus de Dengue, Zika y Chikungunya

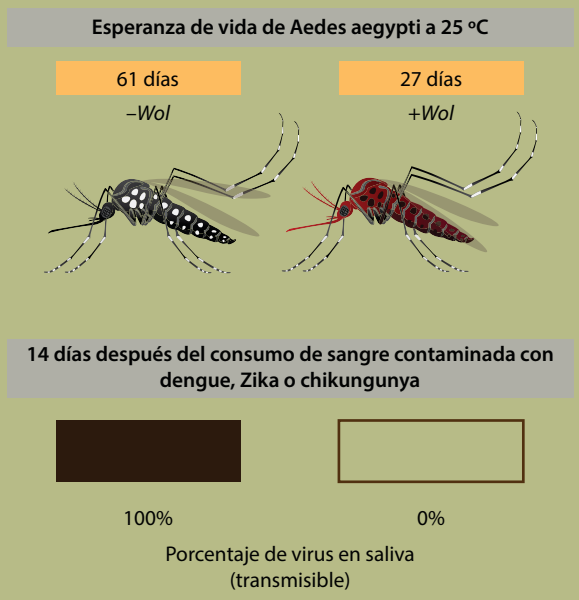

Después de 14 días de haber ingerido sangre infectada con diversos arbovirus, el mosquito infectado con *Wolbachia* no presenta virus en las glándulas salivales y, por lo tanto, no puede transmitir los agentes infecciosos. Además, *Wolbachia* (*wMelPop*) reduce la vida media de *Aedes aegipty* en un 50%. Fuente: Caragat et al., 2016, y McMeniman, 2009.

diante diversos mecanismos que incluyen acortar la vida media del mosquito, esterilizar a la población y bloquear la infección[6-10].

Los mosquitos machos no son hematófagos, únicamente las hembras deben alimentarse con sangre para poder poner huevos fértiles. En caso de ingerir sangre de un organismo contaminado, los parásitos patógenos entran al intestino del mosquito y se replican numerosas veces antes de infectar las glándulas salivales y poder transmitir la enfermedad. Este periodo, llamado de incubación extrínseca, dura entre 8 y 12 días para el virus del dengue[7] y entre 10 y 24 días para las diferentes especies de *Plasmodium*[5]. Un mosquito hembra vive entre 40 y 50 días a una temperatura de 25 °C, lo que implica que más de la mitad de su vida podrá ser contagioso[6,7]. El grupo del Dr. Scott O´ Neill en Australia, entre otros, ha demostrado que *Wolbachia (w*MelPop*)* aislada de la mosca de la fruta *Drosophila melanogaster* e introducida en *Aedes aegypti* acorta la vida media del mosquito en un 50%. La reducción en la longevidad de las hembras ha resultado en una disminución significativa en la transmisión de dengue[7] **(figura 1)**.

La segunda manera en la que *Wolbachia* puede disminuir la transmisión del dengue y la malaria reside en que, tanto en líneas celulares como en mosquitos, su presencia impide la colonización por otros patógenos, es decir, no comparte a su hospedero. En los mosquitos se ha observado que *Wolbachia* confiere protección contra la colonización del insecto por *Plasmodium,* virus del Dengue, del Nilo, de Chikungunya y de Zika evitando que dichas enfermedades se propaguen[8] **(figura 1)**. El mecanismo por el que *Wolbachia* inhibe la colonización del patógeno no está claro, pero se piensa que puede estar preactivando las vías de señalización del receptor tipo Toll y quinasas Jun N-terminal (JNK), que inducen la autofagia y aumentan las especies reactivas de oxígeno para defender al hospedero contra las infecciones por virus ARN.

Además, el mosquito posee unas proteínas de reconocimiento de peptidoglicanos (PGRP-LE y PGRP-LC, *peptidoglycan recognition proteins*) que reconocen peptidoglicanos de las paredes bacterianas. *Wolbachia* provoca la sobreexpresión de estas proteínas aumentando la respuesta inmune del hospedero y predisponiéndolo a defenderse de cualquier patógeno. La activación crónica de PGRP-LE puede llevar a un estado inflamatorio del hospedero que acorte su tiempo de vida media[9].

También parece ser que *Wolbachia* y el patógeno compiten por los nutrientes esenciales del hospedero: ni *Wolbachia* ni los arbovirus pueden producir colesterol y aminoácidos por sí mismos, por lo que deben competir por los provenientes de la célula hospedera[6,9,10].

Wolbachia también puede prevenir la propagación del virus causando incompatibilidad citoplásmica. Este fenómeno consiste en una modificación en el ácido desoxirribonucleico (ADN) del mosquito infectado con *Wolbachia* que provoca que los machos infectados únicamente puedan tener

una descendencia viable si se aparean con hembras infectadas **(figura 2)**. Las hembras infectadas tienen productos viables sin importar si el mosquito macho está infectado o no[6,10]. La estrategia propuesta para erradicar a las enfermedades de transmisión por vectores consiste en liberar una población de mosquitos machos infectados con *Wolbachia* en una zona no endémica de *Wolbachia* (las hembras no tendrán *Wolbachia*), lo que promovería una forma de esterilización de los mosquitos que culmina en la muerte de la mayoría de la progenie y en una disminución de la población total de mosquitos.

Desde el año pasado en China, Australia, Colombia, Estados Unidos y en algunos países de Asia se han liberado mosquitos infectados con *Wolbachia* (*wMelPop*) en diferentes zonas endémicas de dengue. A la fecha los resultados han sido positivos y se ha observado la disminución de casos reportados de la enfermedad. Sin embargo, los virus son conocidos por su capacidad para mutar velozmente y adaptarse a medios hostiles o a la presencia de tratamientos antivirales. Creemos que es necesario realizar una mayor cantidad de estudios en el área para poder sacar mayor provecho de *Wolbachia* como una herramienta para controlar las enfermedades transmitidas por vectores, que son tan comunes en nuestro país. ●

Figura 2. Resultados de la cruza de mosquitos infectados con *Wolbachia* (rojo)

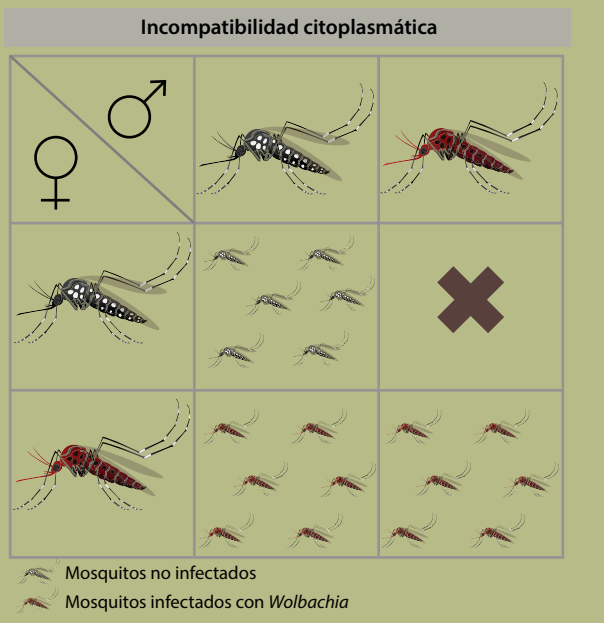

Wolbachia causa incompatibilidad citoplasmática por lo que no hay descendencia entre un macho infectado con *Wolbachia* y una hembra no infectada. En cambio, si la hembra está infectada con *Wolbachia* toda la progenie heredará a la bacteria, independientemente de si el macho está infectado o no.

Para obtener más información sobre este tema, consulte:

- Organización Mundial de la Salud: http://www.who.int/es/
- World Mosquito Program: http://www.eliminatedengue.com/program

REFERENCIAS

1. World Health Organization [portal en internet]. Vector Borne Diseases. [Actualizado: octubre de 2016]. Geneva, Switzerland. Disponible en: http://www.who.int/mediacentre/factsheets/fs387/en/
2. World Health Organization. World Malaria Report 2016. Geneva: WHO. ISBN 978-92-4-151171-1. Disponible en: https://goo.gl/BgU6NY
3. Bhatt S, Gething PW, Brady OJ, Messina JP, Farlow AW, Moyes CL et.al. The global distribution and burden of dengue. Nature. 2013;496:504-7. doi:10.1038/nature12060.
4. Dennis, DT, Gage KL, Gratz N, Poland JD, and Tikhomirov E. *Plague Manual. Epidemiology, Distribution, surveillance and Control.* Geneva, Switzerland: World Health Organization; 1999. 172 pp.
5. World Health Organization. A global brief on vector borne diseases. Document number: WHO/DCO/WHD/2014.1. Geneva, Switzerland; 2014. 56 pp.
6. Walker T, Moreira LA. Can Wolbachia be used to control malaria? Mem Inst Oswaldo Cruz [Internet]. 2011;106(Suppl 1):212-7.
7. McMeniman CJ, Lane RV, Cass BN, Fong AWC, Sidhu M, Wang YF, et al. Stable Introduction of a Life-Shortening *Wolbachia* Infection into the Mosquito *Aedes aegypti.* Science. 2009;323(5910):141-4.
8. Caragata EP, Dutra HL, Moreira LA. Inhibition of Zika virus by *Wolbachia* in *Aedes aegypti*. Microbcell. 2016; 3(7):293-5.
9. Maistrenko OM, Serga SV, Vaiserman AM, Kozeretska IA. Effect of Wolbachia Infection on Aging and Longevity-Associated Genes in Drosophila. En: Vaiserman AM, Moskalev AA, Pasyukova EG (editores). Life Extension: Lessons from Drosophila (Healthy Ageing and Longevity). Switzerland: Springer; 2015.
10. Werren JH, Baldo L, Clark ME. Wolbachia: master manipulators of invertebrate biology. Nature reviews. Microbiology. 2008;6:741-51.

Oxígeno, para bien y para mal

Emilio Espinoza Simón[a], Mónica Rosas Lemus[a], Alfredo Cabrera Orefice[a], Cristina Uribe Álvarez[a], Natalia Chiquete Félix[a], Salvador Uribe Carvajal[a]

El oxígeno ayuda a aprovechar la energía de los nutrientes, sin embargo, también produce especies reactivas de oxígeno (ERO), que en exceso, reaccionan con las moléculas del organismo y las destruyen. Esto provoca envejecimiento y, eventualmente, la muerte. Las diferentes especies biológicas han evolucionado para regular la formación de las ERO. La alimentación y el estilo de vida ejercen una fuerte influencia sobre la capacidad del organismo para lidiar con las ERO.

Desde su aparición hace 3,500 millones de años, los seres vivos proliferaron y se diversificaron hasta que hace 2,000 millones de años la concentración de oxígeno atmosférico aumentó 100,000 veces, lo que indujo la extinción de alrededor del 80% de las especies biológicas. Este aumento se debió a la actividad de las cianobacterias fotosintéticas cuya actividad metabólica libera oxígeno como subproducto y a la toxicidad de los derivados parcialmente reducidos del oxígeno que se conocen como ERO.

A partir de las especies que sobrevivieron a la oxigenación masiva de la atmósfera se desarrollaron los organismos aerobios. Es decir, células que utilizan al oxígeno como aceptor de electrones, lo que libera grandes cantidades de energía en un proceso conocido como respiración aerobia. La cadena respiratoria aerobia se localiza en la membrana plasmática de las bacterias o en la membrana interna mitocondrial de los eucariontes.

La fosforilación oxidativa mitocondrial resulta del acoplamiento entre 2 procesos **(figura 1)**. Primero, la cadena respiratoria bombea protones al espacio extramembranal usando la energía del flujo de electrones desde diversos donadores hasta el oxígeno, este proceso genera un "gradiente" de protones, es decir una diferencia de sus concentraciones a cada lado de la membrana. Luego el complejo V o adenosintrifosfato (ATP) sintetasa libera la energía almacenada en el gradiente de protones para la fosforilación, es decir la síntesis de ATP, a partir de una molécula de adenosindifosfato (ADP) y un fosfato. La cadena respiratoria acepta equivalentes reductores de diversos sustratos como el nicotinamida adenindinucleótido reducido (NADH) y el flavín adenin dinucleótido reducido ($FADH_2$). El nicotinamida adenindinucleótido (NAD^+) es reducido a NADH por diversas enzimas entre las que se encuentran algunas del ciclo de Krebs, como

[a]Laboratorio 305 Oriente. Departamento de Genética Molecular. Instituto de Fisiología Celular. UNAM. México, DF.

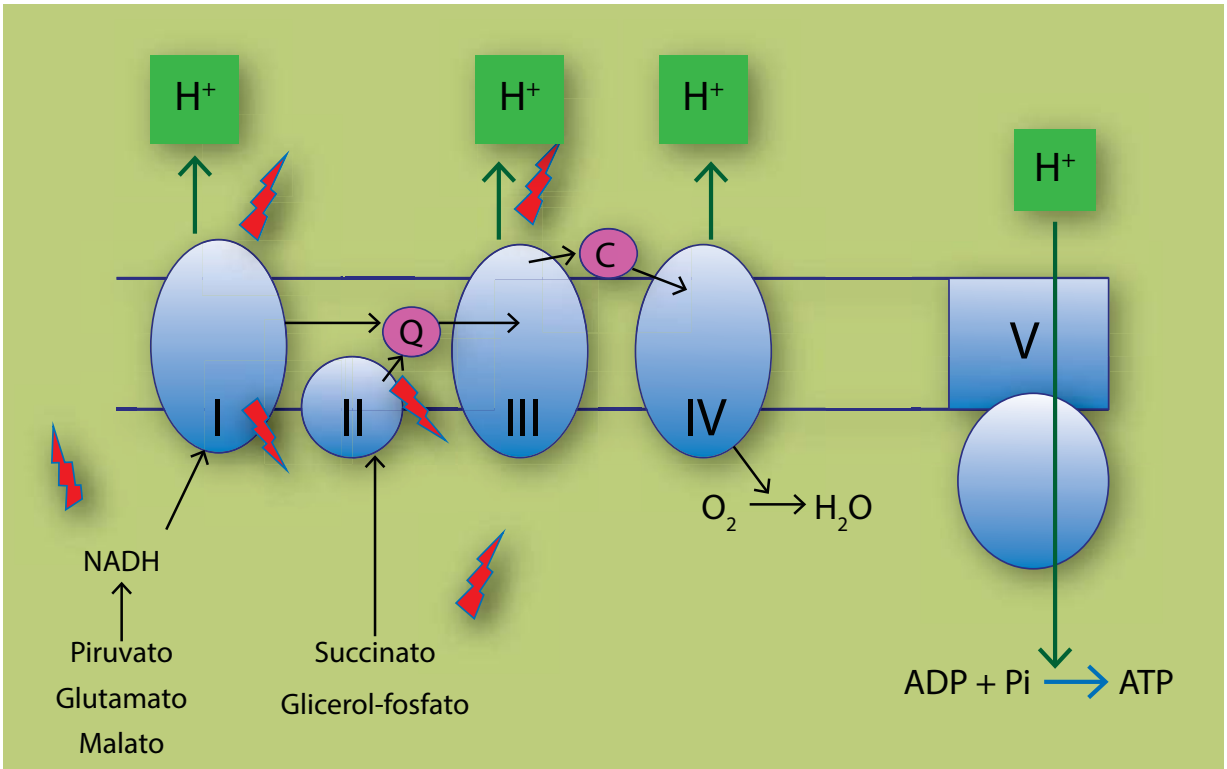

Figura 1. Estructura de la cadena respiratoria mitocondrial de mamíferos donde se muestra el flujo de electrones entre los intermediarios del ciclo de Krebs y la cadena respiratoria (flechas negras) hasta reducir al oxígeno obteniendo agua; el bombeo de protones hacia el espacio intermembranal (arriba) por los complejos I, III y IV y el regreso a la matriz mitocondrial a través del complejo V (complejos en azul) para energizar la síntesis de ATP (flechas verdes). La fuga de radicales libres proviene de diversas fuentes (flechas rojas) como las deshidrogenasas dependientes de NADH, los complejos I, II y III y la glicerol fosfato dehidrogenasa. La coenzima Q y el citocromo c (círculos rosa) transportan electrones entre los complejos de la cadena.

la piruvato deshidrogenasa, la alfa-ceto glutarato deshidrogenasa y la malato deshidrogenasa; luego el NADH es oxidado en el complejo I (NADH: coenzima Q óxido-reductasa). El $FADH_2$ proviene de la succinato dehidrogenasa o de la glicerol fosfato deshidrogenasa y alimenta al complejo II (FADH2: coenzima Q óxido-reductasa). Los electrones captados en los complejos I y II son cedidos a través de la coenzima Q al complejo III (coenzima Q: citocromo c óxido-reductasa) y luego, a través del citocromo C al complejo IV (citocromo-oxidasa). El complejo IV reduce al oxígeno para producir agua.

El flujo de electrones es ilustrado con flechas negras **(figura 1)**. Los electrones arrastran protones y 3 de los complejos respiratorios (I, III y IV) aprovechan la liberación de energía de las óxido-reducciones catalizadas para bombear los protones al espacio intermembranal y así almacenar la energía en forma de un gradiente de protones (**figura 1**, flechas y cuadros verdes). Los protones fluyen de regreso al interior mitocondrial a través de la ATP sintetasa o complejo V liberando energía que se usa para sintetizar ATP **(figura 1)**.

La eficiencia del metabolismo aerobio es unas 15 veces mayor que la del metabolismo anaerobio y por ello, los organismos que generaron un metabolismo aerobio pudieron crecer y llegaron a dominar la Tierra. Sin embargo, esa eficiencia tiene un elevado precio. Durante la respiración se generan radicales libres (especies químicas con electrones desaparea-

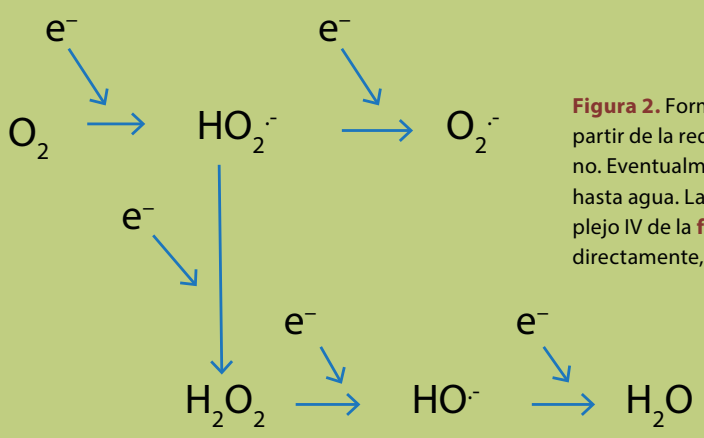

Figura 2. Formación de radicales libres de oxígeno a partir de la reducción parcial de la molécula de oxígeno. Eventualmente, las ERO se detoxifican al reducirse hasta agua. La citocromo oxidasa mitocondrial (complejo IV de la **figura 1**) reduce el oxígeno hasta agua directamente, sin pasar por estos intermediarios.

dos) que pueden reaccionar inespecíficamente con el oxígeno del medio y generar ERO (**figura 1**, flechas rojas).

Las ERO, que también son radicales libres, reaccionan rápidamente con los lípidos formando malondialdehido y 4-hidroxinonenal, oxidan las bases del DNA formando 8- hidroxiguanosina, además de carbonilar, nitrar y glutationilar a las proteínas. Estas modificaciones eventualmente conducen a la muerte celular.

Las principales ERO son el ion superóxido ($O_2^{\cdot-}$), el ion hidroperóxido (HOO^-) y el ion hidroxilo (HO^-), además del peróxido de hidrógeno (H_2O_2) que no es un radical libre pero es muy reactivo. Su génesis por introducción de electrones individuales provenientes de radicales libres se muestra en la **figura 2**.

Los organismos, lo mismo una bacteria que un humano, necesitan defenderse de las ERO. Las defensas son de 2 tipos: el primero es la desactivación de las ERO catalizada por enzimas como la superóxido-dismutasa (SOD), la catalasa y el sistema de la glutatión-peroxidasa/reductasa. La SOD convierte al radical superóxido en peróxido de hidrógeno, mientras que la catalasa transforma al peróxido de hidrógeno en agua. Estas 2 reacciones deben estar estrechamente coordinadas. Por ejemplo, en humanos la SOD se codifica en el cromosoma 21; si hay 3 cromosomas 21, en lugar de 2, se expresa un exceso de SOD que produce tanto peróxido de hidrógeno que la catalasa no logra eliminarlo y daña a las células. El sistema de la glutatión peroxidasa/reductasa usa al glutatión, un tripéptido antioxidante que contiene cisteína.

La glucólisis anaerobia genera 2 moléculas de ATP por glucosa consumida, mientras que la combinación de glucólisis con fosforilación oxidativa genera entre 36 y 38 moléculas de ATP por glucosa.

El segundo mecanismo de protección consiste en abatir la formación intracelular de las ERO. La aceleración de la velocidad del paso de electrones por la cadena respiratoria abate la producción de las ERO mediante 2 mecanismos: disminuye la concentración de oxígeno en la célula y elimina rápidamente a los radicales libres, antes de que puedan participar en reacciones inespecíficas.

Las mitocondrias, paradójicamente parecen ser la clave del manejo de las ERO. Si bien la cadena respiratoria mitocondrial produce una gran cantidad de radicales libres, es también gracias a la actividad de la cadena respiratoria mitocondrial que se evita que esos radicales libres se combinen con oxígeno y se produzcan ERO.

En humanos, las ERO tienen un papel relevante en procesos tan variados como el síndrome de Down (trisomía 21), la gangrena, el daño postis-

Foto: Tsutomu Takasu

El ejercicio regular, físico y muy probablemente intelectual y la ingesta de antioxidantes polifenólicos incrementan la biogénesis y la respiración mitocondrial en tejido nervioso, adiposo y muscular. En modelos animales se observó que la biogénesis y la función mitocondrial neuronal de la descendencia son beneficiadas por la práctica constante de ejercicio.

químico, cerebral o miocárdico, el envejecimiento fisiológico de los organismos y las enfermedades neurodegenerativas.

En pacientes con la enfermedad de Parkinson se observó una actividad deficiente del complejo I mitocondrial en la sustancia nigra, mientras que en la enfermedad de Huntington existe una baja actividad del complejo II en el cerebro de pacientes en etapas avanzadas y en la corteza temporal de pacientes con síndrome de Alzheimer se observa deficiencia del complejo III.

Diversos estudios demostraron que el ejercicio regular, físico y muy probablemente intelectual y la ingesta de antioxidantes polifenólicos incrementan la biogénesis y la respiración mitocondrial en tejido nervioso, adiposo y muscular en sujetos obesos, diabéticos y sanos. En modelos animales se observó que la biogénesis y la función mitocondrial neuronal de la descendencia son beneficiadas por la práctica constante de ejercicio. Asimismo, la restricción calórica preserva la función mitocondrial promoviendo la biogénesis mitocondrial y mejorando la eficiencia bioenergética.

El elixir de la juventud es el propio sudor. Conforme acumulamos años, es necesario luchar (en el gimnasio y en la pista de atletismo) por formar biomasa muscular y mantener el metabolismo aerobio funcionando. Así se producirán más mitocondrias y se evitará el daño inducido por las ERO. En este sentido, se ha demostrado que aún cuando un sujeto físicamente activo no necesariamente viva más tiempo, su calidad de vida será muy superior al que es sedentario. Evitar el exceso en la ingesta en alimentos también ayuda a aumentar la población mitocondrial. ●

BIBLIOGRAFÍA

Gregory MA, Gill DP, Petrella RJ. Brain health and exercise in older adults. Curr Sport Med Rep. 2013;12(4):256-71.

Lane N. Oxygen: the molecule that made the world. Oxford: Oxford University Press; 2003.

Sena LA, Chandel NS. Physiological roles of mitochondrial reactive oxygen species. Mol Cell. 2012;48(2):158-67.

Toledo FG, Goodpaster BH. The role of weight loss and exercise in correcting skeletal muscle mitochondrial abnormalities in obesity, diabetes and aging. Moll Cell Endocrinol. 2013;379(1-2):30-4.